VNIVERSITAT DE VALÈNCIA

Ph.D. program in Biomedicine and Biotechnology

Study of the Role of Telomeres in Ovarian Aging and Female Dysfunction or Infertility

International Ph.D. Thesis

Author:

Lucía Chico Sordo

Under the supervision of:

Dr. Sonia Herraiz Raya (co-director)

Dr. María Elisa Varela Sanz (co-director)

Dr. Irene Cervelló Alcaraz (tutor)

Valencia, January 2025

VNIVERSITAT DE VALÈNCIA

Dña. Sonia Herraiz Raya, Doctora en Biología, Investigadora Principal del grupo de Reactivación Ovárica y Preservación de la Fertilidad en Fundación IVI (FIVI), y miembro del grupo de Investigación en Medicina Reproductiva del Instituto de Investigación Sanitaria La Fe.

CERTIFICA:

Que la presente memoria, titulada ***"Study of the Role of Telomeres in Ovarian Aging and Female Dysfunction or Infertility"***, corresponde al trabajo realizado bajo su dirección por Dña. Lucía Chico Sordo, para su presentación como Tesis Doctoral en el Programa de Doctorado de Biomedicina y Biotecnología de la Universitat de València.

Y para que conste firma el presente certificado en Valencia, a 20 de enero del 2025.



Fdo. Dra. Sonia Herraiz Raya

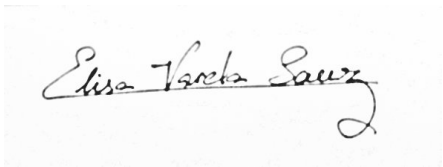
VNIVERSITAT DE VALÈNCIA

Dña. María Elisa Varela Sanz, Doctora en Ciencias Biológicas, Investigadora Principal del grupo de Telómeros y Telomerasa en Reproducción en Fundación IVI (FIVI), miembro del grupo de Investigación en Medicina Reproductiva del Instituto de Investigación Sanitaria La Fe, y Tutora Honorífica de la Universidad Rey Juan Carlos.

CERTIFICA:

Que la presente memoria, titulada ***"Study of the Role of Telomeres in Ovarian Aging and Female Dysfunction or Infertility"***, corresponde al trabajo realizado bajo su dirección por Dña. Lucía Chico Sordo, para su presentación como Tesis Doctoral en el Programa de Doctorado de Biomedicina y Biotecnología de la Universitat de València.

Y para que conste firma el presente certificado en Valencia, a 20 de enero del 2025.



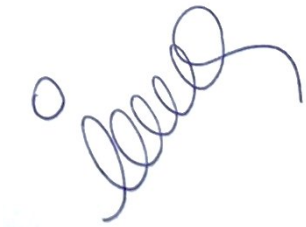
Fdo. Dra. María Elisa Varela Sanz

Dña. Irene Cervelló Alcaraz, Doctora en Biología, Investigadora Miguel Servet del Instituto de Salud Carlos III, Investigadora Principal del grupo de Células Madre y Bioingeniería en Fundación IVI (FIVI), y Coordinadora del laboratorio de FIVI.

CERTIFICA:

Que la presente memoria, titulada ***"Study of the Role of Telomeres in Ovarian Aging and Female Dysfunction or Infertility"***, corresponde al trabajo realizado íntegramente bajo su tutorización por Dña. Lucía Chico Sordo, para su presentación como Tesis Doctoral en el Programa de Doctorado de Biomedicina y Biotecnología de la Universitat de València.

Y para que conste firma el presente certificado en Valencia, a 20 de enero del 2025.



Fdo. Dra. Irene Cervelló Alcaraz

The herein Ph.D. thesis work was carried out at the facilities of IVI Foundation – La Fe Health Research Institut (Valencia, Spain), and the laboratories of the Gynecology and Obstetrics area of the Department of Medical Specialties and Public Health of the Faculty of Health Sciences of the Universidad Rey Juan Carlos (Alcorcón, Madrid). In addition, the study was done in the collaboration with the Assisted Human Reproduction Unit of the Hospital Universitario y Politécnico La Fe of Valencia, the Obstetrics and Gynecology Department of the Hospital Clínico San Carlos of Madrid, the Gynecology Department of the Hospital General Universitario of Valencia, and the Assisted Reproduction and Fertility Clinic IVI Madrid located in Aravaca.
This work was supported by a grant from the Health Research and Development Strategy from Carlos III Health Institute (AES ISCIII, PI20/00252). Lucía Chico Sordo obtained a predoctoral health research grant (PFIS, FI19/00008) financed by the ISCIII to develop the herein doctoral thesis. The International Mention in this doctoral thesis was possible through the international research stay at the University of Yale (New Haven, Connecticut, United States) and funding by ISCIII (M-AES, MV22-00065).

El presente trabajo de tesis doctoral ha sido realizado en las instalaciones de Fundación IVI – Instituto de Investigación Sanitaria La Fe (Valencia, España), y los laboratorios del área de Ginecología y Obstetricia del Departamento de Especialidades Médicas y Salud Pública de la Facultad de Ciencias de la Salud de la Universidad Rey Juan Carlos (Alcorcón, Madrid). Además, el estudio se realizó en colaboración con la Unidad de Reproducción Humana Asistida del Hospital Universitario y Politécnico La Fe de Valencia, el Servicio de Obstetricia y Ginecología del Hospital Clínico San Carlos de Madrid, el Servicio de Ginecología del Hospital General Universitario de Valencia, y la Clínica de Reproducción Asistida y Fertilidad IVI Madrid ubicada en Aravaca.
El estudio ha sido financiado a través de la convocatoria de ayudas de proyectos de investigación en salud, correspondiente a la Acción Estratégica en Salud del Instituto de Investigación Sanitaria Carlos III (AES ISCIII, PI20/00252). La doctoranda obtuvo un contrato predoctoral de formación en investigación en salud (PFIS, FI19/00008) financiado por el ISCIII para llevar a cabo el desarrollo de la presente tesis doctoral. Este mismo organismo público, ISCIII, financió la estancia en el extranjero mediante una ayuda para la movilidad de personal investigador contratado en el marco de la AES (M-AES, MV22-00065) que hace posible la obtención de la Mención Internacional en esta tesis doctoral.

ACKNOWLEDGEMENTS

Esta sección de la tesis se destina a dar las gracias a todos aquellos que de una manera u otra habéis formado parte de este proceso. En mi caso, también hay alguna disculpa escondida, porque durante este tiempo ha habido momentos malos y buenos, y estoy segura que en muchos de ellos no he mostrado mi mejor versión. Solo por haber decidido seguir ahí a pesar de los momentos difíciles, ya os habéis ganado mi primer “GRACIAS”.

Gracias a mis directoras y tutora de tesis por ser una fuente de inspiración femenina en la ciencia. Gracias Sonia, por tu disponibilidad siempre para resolver preguntas teóricas o sobre técnicas, tus conocimientos en este campo me han regalado tiempo, un lujo hoy en día y algo tremendamente valioso durante una tesis. Gracias Elisa, por haberme hecho enfrentarme a un desafío de este tamaño, sin duda sé mucho más que la Lucía de hace cinco años, y no me refiero solo a telómeros. Pero especialmente gracias por tu positividad ante todos los retos que han surgido, por tu paciencia en los cálculos para hacer diluciones, por enseñarme que existe una persona que puede disfrutar más que yo la Navidad, y sobre todo por haber formado un equipo de trabajo tan maravilloso. Gracias Irene, por tu disponibilidad para cualquier duda y por tu buena energía, incluso cuando todo iba a contrarreloj.

Gracias a otra persona importante durante todo este tiempo y gran mentor, Juancho. Primero porque me has enseñado a comprender lo importante que es investigar una enfermedad silenciosa y subestimada como la endometriosis. Y segundo, gracias por tu confianza plena en mí y en mis ideas, esa libertad me ha hecho crecer de manera indescriptible a nivel profesional.

Gracias a mis compañeras de laboratorio, volvería a pasar por todo esto porque conoceros y trabajar con vosotras ha hecho que todo merezca la pena. Lo he dicho muchas veces y lo repetiré, al laboratorio me trajo la ciencia, pero fuisteis vosotras las que hicisteis que me quedara. A Isa Córdova, por tu predisposición a echarme siempre una mano en lo que necesitaba, incluido cuando el día se hace cuesta arriba y solo un café te ayuda a remontar. Mis inicios en la clínica recogiendo muestras fueron mucho más fáciles contigo allí. A Isa Cuadrado, porque eres luz allá donde vas. Gracias amiga, por confiar en mi juicio y tu fe ciega en mis decisiones, por tu energía tan positiva, por celebrar mis logros como si fueran tuyos, por preguntar ¿vamos a la Lata? cuando intuías que algo no iba bien, y por demostrarnos que en Murcia no llueve nunca. A Marta, por saber siempre qué decir cuando me faltaban fuerzas, por los momentos que estando en el ordenador pasabas por detrás y tocándome el hombro me rescatabas de mis pensamientos, por nuestras charlas infinitas de cualquier tema, por los momentos de lágrimas por anécdotas varias, por estar en todo y llegar siempre a todo, y por ser tan práctica. Créeme cuando te digo que no te librarás de mí. Por último, gracias a Alba,

te admiro no solo por quién has sido y eres ahora, también por en quién te vas a convertir. Esta tesis sin ti no habría sido posible, me diste la mano desde el principio y no la soltaste, eso me salvó en muchas ocasiones. Gracias por tu valioso tiempo, por escucharme sin importar el dónde ni el cuándo, por pensar conmigo, por ayudarme siempre, por revisar todo a conciencia, por ser mi compañera de teatrillos, y sin duda gracias por tus clases de andaluz para que la comunicación entre nosotras fluya. Aunque siendo sinceras, con reírnos ya nos entendíamos.

A Valencia le estoy tremendamente agradecida, sobre todo por las personas que me ha permitido conocer.

Durante mi etapa en Education, muchas gracias a María Martínez, Luz, Carles, Coque, Paco, Loreto, y Helena. Especial mención a mi Pauli, que desde el primer día confió en mí, gracias por tu alegría que hace que renueve energía cada vez que nos vemos. Gracias a Miguel Tablado y María Delgado, no solo por recordar el nombre de mi pueblo, sino por hacerme sentir orgullosa de haber iniciado mi andadura en IVI en vuestro equipo.

A Fundación IVI, gracias por ser ese gran equipo que acoge con los brazos abiertos a tantos novatos ilusionados con la ciencia. Gracias a Nico y Marcos, porque recuerdo muchas veces ese día que me citasteis en un despacho para decirme que habíais pensado en mí para una beca de doctorado con Fundación. Gracias a ese día esta tesis hoy es una realidad. Y gracias por vuestra amabilidad, profesionalidad, y cercanía. Gracias a todos los demás, Horten, Patri Díaz-Gimeno, Paco, Amparo, Ali, Jessi, y Rober, colaborar con vosotros siempre ha sido un placer, gracias por vuestra amabilidad y paciencia. Especial mención a Patri Sebastián, tu energía positiva es tan contagiosa como tu risa, gracias por aparecer y ser salvavidas de esta tesis. A Majo, Pepi, y Ana Corachán, gracias por contestar siempre mis dudas y mensajes desesperados.

Gracias a la UAGI, los presentes y los que habéis formado parte de ella, no solo por los recordatorios de deadlines que recibía como agua de mayo, sino también por vuestra inmensa ayuda y siempre acogedora amabilidad. Gracias Davinia, Alba, Regina, Elena, Alfredo, Dago, Guille, Víctor, y Juanma.

Gracias a Mónica Romeu, que cogió las riendas del proyecto cuando la esperanza fallaba y no lo soltó. Tu profesionalidad, coraje y energía han hecho posible esta tesis.

Pero especialmente gracias a aquellos que han seguido de cerca todas mis aventuras y desventuras, siendo testigos de mis inoportunas y accidentadas anécdotas, y recordándome que lo importante es reírse de todas ellas. Ellos son Noe, María Gil, Vicent, Nando, Antonio, y Leo. Gracias Noe, por haber formado parte de este proyecto con tu integridad profesional, pero sobre todo como amiga, porque incluso cuando estás remando a contracorriente siempre

consigues sacar fuerzas para ayudarnos a los demás a no encallar. Gracias María, me quedo con tu talento musical, las ganas de vivir que contagias, tu alegría en cada momento, tu acento british, pero sobre todo quiero darte las gracias por haber sido mi cable a tierra al otro lado del charco. Gracias a Vicent, por tu complicidad, por tus abrazos reconfortantes, y por alegrarte siempre de verme. Gracias a Leo, aunque no lo recuerdes fuiste la primera persona que conocí en Fundación, y te aseguro que no me imaginé lo mucho que acabaría admirándote. Eres sabiduría, templanza, y el toque perfecto de humor que tanto bien hace.

Gracias a ellas, Ire, María Luisa, y Ro. Estaré eternamente agradecida a la vida por habernos juntado. Gracias Ire, por todo lo compartido en episodios anteriores, en el presente y el futuro. Me hace muy feliz haber evolucionado tanto junto a ti, con personas como tú no importa el final porque solo el camino ya merece la pena. Gracias a María Luisa, el primer día que llegaste a Education presentándote como mi becaria nunca me pude imaginar lo que llegarías a ser en mi vida. Gracias por ser siempre ese rayito de luz en la oscuridad. Gracias Ro, que lo que juntó la grabación de un vídeo en el laboratorio de Andro no lo separe nadie. Adoro tus sabios consejos, nuestra amistad y tu hospitalidad, pero sobre todo gracias por ser el espejo en el que me quiero mirar.

A Madrid también le doy las gracias, por acogerme y ser casa a pesar de no ser descendiente de dos generaciones de madrileños. Te agradezco enormemente las personas que me has permitido conocer.

Gracias a todo el personal de IVI Madrid que me acompañaron durante las largas jornadas de reclutamiento. Especialmente gracias al equipo de Andro (Sor, Ana, Martita, María y Mery), sin duda sois mi sitio favorito, fuisteis casa y cercanía cuando más lo necesitaba. Gracias Mery, no solo por tus raíces belviseñas, también por responder siempre con un sí rotundo a los planes, por preocuparte de que todo vaya bien, y por descubrirnos Mercado de Motores como punto de encuentro. Gracias a Alberto Pacheco, por tu alegría al verme, por tus performances de Grease, y sobre todo por ayudarme siempre a llevar a cabo mis ideas científicas. Gracias a Lucía Sánchez, por orientarme de múltiples maneras sobre mí futuro, pero sobre todo por quedarte para verlo en primera persona. Gracias a los que también formaron parte de este equipo, Jai y Fati. Gracias Jai, por aguantarme con mis miles de dudas nada más llegar al laboratorio, pero sobre todo gracias por empujarme siempre a avanzar en mi carrera profesional. A Fati solo le puedo dar las gracias por ser como es, porque personas reales, transparentes, y cercanas como tú no hay muchas, pero yo he tenido la suerte de conocerte a ti.

Gracias al equipo de la URJC, a todos y cada uno de ellos que han hecho de mi día a día una serie televisiva de las que te mantiene enganchada temporada tras temporada. Gracias a

Rosa, Virgi, Davi, José, Gema, Nines, Abdul, y Alex. Gracias a Miguel, si me tengo que cortar un dedito que no me duela, puedes estar tranquilo porque te salvas. Tus lecciones de cultura general, tu tan necesaria ayuda, y tus visitas diarias, sin duda eran un aliciente para ir al laboratorio. Nos vemos donde Rafita. A Almu gracias por la terapia gratuita, los cafés de desahogo, tus iniciativas, y por tu ayuda siempre que te necesitamos (que han sido muchas veces). Por último, gracias a Antonio, ese pasillo sin ti, sin tus chistes y sin tus comentarios no sería lo mismo.

No me puedo olvidar de los grandes profesionales que han trabajado en este proyecto como si fuera propio. Ellos son Nacho Cristóbal, Javi Mazario, y José Montans. Gracias Nacho, por tu amabilidad, por recibirme siempre con una sonrisa, por echarme una mano en lo que he necesitado, y por ofrecerme siempre un café cuando me veías al borde del colapso. Gracias a Javi, llegaste cuando más te necesitábamos con todos tus conocimientos sobre microscopía, gracias a ellos este trabajo tiene tantos resultados e imágenes preciosas. Perdón por haberte dado tanto la lata. Y gracias a José Montans, por sacarnos siempre un hueco, y por la rigurosidad en todo lo que haces.

A la gente de siempre, que lleva tantos años a mi vera, muchas gracias por seguir aquí. Gracias Carol, esta tesis existe porque tuve la gran suerte de empezar en la ciencia contigo. Eres un día soleado en pleno mes de febrero, de esos que te transmiten la sensación de que la primavera se acerca. Estaré eternamente en deuda contigo a nivel personal y profesional. Gracias a Jesús, Ana Asenjo, Anita, Mario, y Javi Pecero, saber que profesionales como vosotros lideran el campo de la ciencia e investigación me deja muy tranquila. Gracias a María, mi compañera de aventuras en la barra, me considero tremendamente afortunada de que la vida me haya permitido coincidir contigo. Las desavenencias del día a día son menos dolorosas con gente al lado como tú.

A mi equipo de La Puebla, Lucía, Aurora, Elena, María y Laura, muchas gracias. Sin duda, hoy soy doctora gracias a vosotras. El instituto nos juntó, nuestros caminos tomaron diferentes direcciones, pero aun así nos prometimos ser testigo de la vida de todas. A mi Luci, millones de gracias por tu plena confianza en mí y mis capacidades, porque si no fuera por ti no habría conseguido esto. Muchas veces pienso: ¡menos mal qué estás tú!. Te prometo que seguiré avanzando y que lo verás sentada justamente a mi lado. Gracias a Auro, por lo orgullosa que te sientes de mí, pero sobre todo por hacérmelo saber.

A mi equipo de Belvís, María, Selene, Alba, Laura, Jero, Carlota, Marta, Paloma, e Isra. Gracias por los fines de semana de desconexión en el pueblo, de aventuras y planes, de cafés y verderolas, y por hacerme sentir orgullosa de ser de allí. A ti, María, gracias por ser mi compañera de aventuras desde la infancia, por compartir siempre la mitad de las alegrías y

las penas, por tus ingeniosos comentarios, por ver la vida siempre desde el lado más amable. En definitiva, gracias por ser como eres.

Gracias a Jorge, por tu apoyo incondicional durante tantos años cuando la tesis doctoral era para mí una meta muy lejana.

To my friends from Yale, thank you for existing. Without a doubt, my American adventure was worth it because of you. Thanks to my favorite people, Mert, Ipek, and David. Thank you, Mert and Ipek, for your kindness, for suggesting plans, and for making me feel at home thousands of miles away from home. We will continue to enjoy many trips together, I promise you. A David muchas gracias por ser una persona tan bonita con energía tan positiva. Pero especialmente gracias por tu pasión por la ciencia, por seguir apostando por este camino a pesar de los obstáculos. Tú no lo sabes, pero reúnes todos los requisitos para triunfar en la investigación. To Mel, thank you for all those days in the lab, together we are a great team. Thanks to you, Le, our conversations always renew my energy. I'm waiting for you in Spain with thousands of places that I would love you to visit. Thanks also to Sinem, your energetic personality can only attract good things. Thank you to Emre Seli for allowing me to be part of your wonderful team. Thanks to Pete, living with you during that time was, without a doubt, a gift that life gave me. Por último, gracias al grupo de españoles, Mar, Pablo, Diego, Maleni, y Nira, gracias por hacer las maletas y alejaros de casa para perseguir el sueño de la investigación. Estados Unidos no es consciente de los grandes profesionales que tiene allí trabajando.

Gracias a Jesús, por llegar, pero sobre todo por quedarte y no abandonarme en el camino a pesar de las dificultades. Gracias por tu paciencia, por tu admiración, por ser tan diferente a mí, y por enseñarme tantas cosas. Y gracias por la gente que ha llegado a mi vida de tu mano, Cris, Juanan, Leyla, Jacoba, y Carlos, siempre dispuestos a una quedada para desconectar de la rutina y los obstáculos, y siempre atentos a cuál será mi siguiente paso.

Muchas gracias a mi familia, mis tíos y primos, Alfredo, Ori, Jose, Feli, Felipe, Almudena, David, Marco, Sergio, Mario, Andrés, y Víctor. Os volvería a elegir siempre. Es difícil encontrar una familia que reúna tantas cosas buenas, y vosotros lo tenéis todo. Me siento tremendamente orgullosa de ser parte de esta familia hospitalaria, feliz, y divertida. Gracias por confiar en mí y mi labor en la ciencia, sobre todo a mi tío Alfredo.

A mis abuelos, Amor, Tea, Teodoro, y Antonio, muchas gracias por ser un referente de superación. Vuestro amor incondicional, vuestras historias, experiencias, enseñanzas y sabiduría sin duda me han ayudado a ser quien soy. Pero sobre todo muchas gracias por vuestro tiempo, tiempo de calidad que me ha permitido crear tantos recuerdos especiales que nunca olvidaré.

A mis hermanos, Aitor y Abdón, muchas gracias. La forma tan peculiar que tenéis de afrontar la vida, reíros de las adversidades, y comeros el mundo, es una fuente de inspiración.

Por último, y muy importante, gracias a mis padres. Esta tesis es vuestra. No puedo dedicaros unas palabras sin emocionarme, porque literalmente os debo todo, y debería besar el suelo que pisáis como dicen los abuelos. Gracias por sacrificaros para que hoy yo pueda estar aquí defendiendo esta tesis, por hacer vuestros todos mis logros, pero también mis fracasos. Gracias a mi padre por su templanza y calma en los momentos difíciles, por ese humor tan característico, y por ser ejemplo de resiliencia cuando vienen mal dadas. Gracias a mi madre por su energía y personalidad arrolladora, por su afán de superación día a día, y por ser un ejemplo de que no importa ni el dónde, ni el cuándo, ni el cómo, que todo es posible si te lo propones. Gracias de verdad, os quiero.

Gracias a todas las personas que de una manera u otra creen en la ciencia, y apuestan por ella, sobre todo aquellas personas que de forma voluntaria acceden a participar en proyectos de investigación. No debemos olvidarnos de que el progreso y bienestar de la sociedad no sería posible sin ciencia.

No puedo acabar esta sección sin recurrir a una de mis escritoras favoritas, Jane Austen, en su novela *Sentido y Sensibilidad*: “No es lo que tenemos en la vida, sino a quién tenemos, lo que nos hace felices”.

TABLE OF CONTENTS

ACKNOWLEDGEMENTS....iii

ABBREVIATIONS AND ACRONYMS....xv

LIST OF FIGURES....xxi

LIST OF TABLES....xxiii

RESUMEN EXTENDIDO EN ESPAÑOL....25

1 INTRODUCTION....51

1.1 Reproductive senescence in women....51

1.1.1 The ovary....51

1.1.1.1 Endocrinology....52

1.1.1.2 Oogenesis and folliculogenesis....54

1.1.1.3 Ovarian reserve....58

1.1.2 Current landscape: female infertility and assisted reproduction technologies....62

1.2 Biological aging: telomeres....64

1.2.1 Hallmarks of aging....64

1.2.2 Telomere biology....67

1.2.3 Shelterin complex and telomerase....68

1.2.4 Telomere dysfunction and diseases....70

1.3 Telomere dynamics and female infertility....71

1.3.1 Ovarian telomere parameters....71

1.3.2 Telomeres and fertility-related cellular mechanisms....72

1.3.3 Telomere-related reproductive disorders....73

2 HYPOTHESIS....77

3 OBJECTIVES....81

3.1 Main objective....81

3.2 Secondary objectives....81

4 MATERIALS & METHODS....85

4.1 Study design 85
4.1.1 Project 1: “Understanding the implication of the telomere pathway in ovarian aging and dysfunction/infertility” 85
4.1.1.1 Project design 85
4.1.1.2 Summary of techniques and objectives to be achieved 86
4.1.1.3 Approval of the Ethics Committee 87
4.1.2 Project 2: “Effects of COVID-19 in the telomere biology of granulosa cells and in fertility as well as in IVF outcomes” 87
4.1.2.1 Project design 87
4.1.2.2 Summary of techniques and objectives to be achieved 88
4.1.2.3 Approval of the Ethics Committee 88
4.2 Sample collection and processing 90
4.2.1 Blood samples 90
4.2.1.1 Collection 90
4.2.1.2 Serum sample processing 90
4.2.1.3 Peripheral blood mononuclear cells isolation 90
4.2.2 Ovarian samples 92
4.2.2.1 Collection 92
4.2.2.2 Paraffin-embedded tissue, histological sections, and deparaffinization 93
4.2.2.3 Ovarian freezing, histological sections, and washing 94
4.2.3 Granulosa cell samples 95
4.2.3.1 Ovarian stimulation and oocyte retrieval 95
4.2.3.2 Isolation of granulosa cells 96
4.3 Hormone levels measurements 96
4.4 Reproductive and medical parameters 97
4.4.1 Medical history and lifestyle habits 97
4.4.2 Fertility outcomes 97
4.4.3 Serum SARS-CoV-2 antibody test and COVID-19 symptoms score 97

4.5 Telomere parameters....98
4.5.1 Telomerase activity....98
4.5.1.1 Cell lysate preparation....98
4.5.1.2 PCR....99
4.5.1.3 Running acrylamide gel....101
4.5.2 Telomere length....102
4.5.2.1 qFISH....102
4.5.2.2 Image acquisition and analysis....104
4.5.3 Culture conditions for Jurkat cells....107
4.6 Hematoxylin & Eosin Staining....108
4.7 Ovarian fibrosis....109
4.7.1 Masson's trichrome staining....109
4.7.2 Expression of TGF-β1, COL1A1 and, COL3A1 genes....109
4.7.2.1 RNA isolation....110
4.7.2.2 cDNA synthesis....110
4.7.2.3 RT-qPCR....111
4.8 Proteomic assessment of ovary samples....112
4.8.1 Sample preparation....112
4.8.2 Sample preparation for library generation....113
4.8.3 SP3 sample preparation....113
4.8.4 LC-MS/MS analysis for library construction, DDA, and SWATH....113
4.8.4.1 Spectral Library Generation....113
4.8.4.2 Mass Spectrometry....114
4.8.4.3 SWATH Mode....114
4.8.5 Data analysis....114
4.8.5.1 Peptide and protein identification....114
4.8.5.2 Spectral library construction and SWATH data processing....114
4.8.5.3 Normalization....115

4.9 Statistical analysis 115
4.9.1 General statistical analysis 115
5 RESULTS 119
5.1 Characterization of age-dependent female reproductive decay 119
5.1.1 Baseline characteristics of the study population and hormonal levels 120
5.1.2 Telomere analysis 124
5.1.2.1 Analysis of systemic telomere status 124
5.1.2.2 Analysis of reproductive telomere status 125
5.1.2.3 Systemic telomere length as a biomarker of ovarian aging 141
5.1.2.4 Analysis of telomerase activity in the ovary 144
5.1.3 Ovarian fibrosis 145
5.1.4 Proteomic analysis 147
5.1.5 Summary of findings in this section 153
5.2 Study of telomere parameters in lower ovarian reserve cases 153
5.2.1 Baseline characteristics of the study population and hormonal levels 153
5.2.2 Telomere analysis 155
5.2.2.1 Analysis of systemic telomere status 155
5.2.2.2 Analysis of ovarian telomere status 155
5.2.2.3 Analysis of telomerase activity in the ovary 161
5.2.3 Summary of findings in this section 162
5.3 Impact of pregnancy on ovarian telomere dynamics 162
5.3.1 Baseline characteristics of the study population and hormonal levels 162
5.3.2 Telomere analysis 163
5.3.2.1 Analysis of systemic telomere status 164
5.3.2.2 Analysis of ovarian telomere status 165
5.3.2.3 Analysis of telomerase activity in the ovary 171
5.3.3 Summary of findings in this section 172
5.4 Impact of COVID-19 disease on reproduction and the telomere pathway 173

5.4.1 Baseline characteristics of the study population and hormonal levels 173
5.4.2 Telomere length in GCs obtained during oocyte retrieval 174
5.4.3 Fertility outcomes: oocyte retrieval and maturation rate 177
5.4.4 Summary of findings in this section 179
6 DISCUSSION 183
6.1 Characterization of age-dependent female reproductive aging 183
6.1.1 Endocrine parameters 183
6.1.2 Telomere parameters 185
6.1.2.1 Systemic aging 185
6.1.2.2 Ovarian aging 186
6.1.2.3 Telomerase activity in the ovary 195
6.1.3 Ovarian fibrosis 196
6.1.4 Proteomic analysis of the ovary 197
6.2 Study of telomere parameters in lower ovarian reserve cases 199
6.2.1 Endocrine parameters 200
6.2.2 Telomere parameters 200
6.2.2.1 Systemic analysis 200
6.2.2.2 Ovarian analysis 201
6.3 Impact of pregnancy on ovarian telomere dynamics 203
6.3.1 Endocrine parameters 204
6.3.2 Telomere parameters 205
6.3.2.1 Systemic analysis 205
6.3.2.2 Ovarian analysis 205
6.4 Impact of COVID-19 disease on reproduction and the telomere pathway 207
7 CONCLUSIONS 213
8 REFERENCES 215
9 Appendices 246
9.1 Appendix A. Approval of the Ethics Committee 246

9.2 Appendix B. Fiji software macro for FISH quantification. 256
9.2.1 Macro 1 256
9.2.2 Macro 2 262
9.3 Appendix C. Supplemental material result 5.1. 264
9.4 Appendix D. Supplemental material result 5.2. 272
9.5 Appendix E. Supplemental material result 5.3. 274
9.6 Appendix F. Supplemental material result 5.4. 278
9.7 Appendix G. Scientific contributions. 280
9.8 Appendix H. Complete scientific papers by the student as first author. 286

ABBREVIATIONS AND ACRONYMS

%long	Percentage of Long Telomeres
%short	Percentage of Short Telomeres
°C	Degrees Celsius
µg	Microgram
µL	Microliter
µm	Micrometer (Micron)
1n	Haploid (One Set of Chromosomes)
1PB	First Polar Body
2n	Diploid (Two Sets of Chromosomes)
2PB	Second Polar Body
2PN	Two Pronuclei (Indicator of Normal Fertilization)
A	Adenine
a.u.	Arbitrary Units of Fluorescence Intensity
ACN	Acetonitrile
ADN	Ácido Desoxirribonucleico
AF	Antral Follicle
AFC	Antral Follicle Count
AL4A1	Delta-1-Pyrroline-5-Carboxylate Dehydrogenase
ALT	Alternative Lengthening of Telomeres
AMH	Anti-Müllerian Hormone
ANOVA	Analysis of Variance
APS	Ammonium Persulfate
ARN	Ácido Ribonucleico
ART	Assisted Reproduction Technologies
ATM	Serine-Protein Kinase
BCP	1-Bromo-3-Chloropropane
BMI	Body Mass Index
bp	Base Pairs
BSA	Bovine Serum Albumin
C	Cytosine
CALM3	Calmodulin 3
CAT	Clot Activator Tubes
CCs	Cumulus Cells
cDNA	Complementary Deoxyribonucleic Acid
CHAPS	3-((3-Cholamidopropyl) Dimethylammonio)-1-Propanesulfonate
Clpp	Caseinolytic Peptidase P
CNIO	Centro Nacional De Investigaciones Oncológicas
CO_2	Carbon Dioxide
COC	Oocyte-Cumulus Complex
COL1A1	Collagen Type I Alpha 1

COL3A1	Collagen Type III Alpha 1
COVID-19	Coronavirus Disease 2019
Cq	Quantification Cycle (Threshold Cycle in qPCR)
CUL1	Cullin-1
Cy3	Fluorochrome (emits in orange-red spectrum)
Cy5	Fluorochrome (emits in the far-red spectrum)
DAPI	DNA Stain (4',6-Diamidino-2-Phenylindole)
dATP	Deoxyadenosine Triphosphate
DCq	Delta Quantification Cycle (qPCR data analysis)
dCTP	Deoxycytidine Triphosphate
DDA	Data-Dependent Acquisition
DEPC	Diethylpyrocarbonate
DEPs	Differentially Expressed Proteins
dGTP	Deoxyguanosine Triphosphate
DMEM	Dulbecco's Modified Eagle's Medium
DNA	Deoxyribonucleic Acid
dNTP	Deoxynucleotide Triphosphates
DTT	Dithiothreitol
dTTP	Deoxythymidine Triphosphate
E2	Estrogen/Estradiol
EDTA	Ethylenediaminetetraacetic Acid
Eff	Amplification Efficiency
EGTA	Ethylene Glycol- Bis(2-Aminoethylether)-N,N,N',N'-Tetraacetic Acid
ELISA	Enzyme-Linked Immunosorbent Assay
ESHRE	European Society Of Human Reproduction And Embriology
EVPL	Envoplakin
FBS	Fetal Bovine Serum
FDR	False Discovery Rate
FF	Follicular Fluid
FISH	Fluorescence In Situ Hybridization
FIV	Fecundación *In Vitro*
FSH	Follicle-Stimulating Hormone
G	Guanine
G2	Cell Cycle's Growth 2 Phase
GAPDH	Glyceraldehyde-3-Phosphate Dehydrogenase (Housekeeping Gene)
GCP	Good Clinical Practice
GCs	Granulosa Cells
GGT5	Glutathione Hydrolase 5 Proenzyme
GnRH	Gonadotropin-Releasing Hormone
GV	Germinal Vesicle

GVBD	Germinal Vesicle Breaks Down
H	Hydrogen
h	Hour
H&E	Hematoxylin And Eosin
H_2O	Water
HA	Hyaluronic Acid
hCG	Recombinant Human Chorionic Gonadotropin
HCl	Chloride Acid
HCSC	Hospital Clínico San Carlos
HGUV	Hospital General Universitario de Valencia
hMG	Human Menopausal Gonadotropin
HNP	Hospital Nacional de Parapléjicos
HPOA	Hypothalamic-Pituitary-Ovary Axis
HT-qFISH	High-Throughput Quantitative Fluorescence In Situ Hybridization
HUPHM	Hospital Universitario Puerta de Hierro Majadahonda
HUPLF	Hospital Universitario y Politécnico La Fe
IAA	Iodoacetamide
IBM	International Business Machines (software like SPSS)
IC	Internal Control
ICF	Inform Consent Form
IgG	Immunoglobulin G
IgM	Immunoglobin M
IRB	Institutional Review Board
IU	International Unit
IVF	In Vitro Fertilization
kb	Kilobase (1000 base pairs of DNA/RNA)
KCl	Potassium Chloride
LC-MS/MS	Liquid Chromatography Tandem Mass Spectrometry
LDHB	L-lactate Dehydrogenase B Chain
LH	Luteinizing Hormone
M	Middle-Aged Women or Unit M (Molar = Mol/L)
M-	Middle-Aged Women with Low AMH
M+	Middle-Aged Women with High AMH
MARCS	Myristoylated Alanine Rich C Kinase Substrate
Mfn1	Mitofusin 1
$MgCl_2$	Magnessium Chloride
MI	Metaphase I
MII	Metaphase II
min	Minute
mIU	Milli-International Unit
mL	Milliliter
mm	Millimeter

mM	Millimolar (Mmol/L)
mm^2	Square Millimiters
mm^3	Cubic Millimeters
Mpreg	Middle-Aged Pregnant Women
MRP	MARCKS-Related Protein
n	Sample Size, Number of Subjects or Replicates
Na	Sodium
NA	Numerical Aperture or Not Applicable
Na_2HPO_4	Disodium Hydrogen Phosphate
NaCl	Sodium Chloride
NaH_2PO_4	Sodium Dihydrogen Phosphate
ng	Nanogram
O	Oxygen
OCT	Optimal Cutting Temperature
P	Perimenopausal or Phosphate
P-	Perimenopausal Women with Low AMH
p.c.	Post-conception
P+	Perimenopausal Women with High AMH
P4	Progesterone
PBMCs	Peripheral Blood Mononuclear Cells
PBS	Phosphate Buffered Saline
PC1	Principal Component 1
PC2	Principal Component 2
PCA	Principal Component Analysis
PCOS	Polycystic Ovary Syndrome
PCR	Polymerase Chain Reaction
pg	Picogram
PGCs	Primordial Germ Cells
PMSF	Phenylmethylsulfonyl Fluoride
PN	Pronuclei
PNA	Peptide Nucleic Acid
POF	Premature Ovarian Failure
POI	Premature or Primary Ovarian Insufficiency
POR	Poor Ovarian Response
POSEIDON	Patient-Oriented Strategies Encompassing Individualized Oocyte Number
POT1	Protection of Telomeres 1
Q1	First Quartile
Q3	Third Quartile
qFISH	Quantitative Fluorescence In Situ Hybridization
r	Pearson’s Correlation Coefficient
R^2	Coefficient of Determination

RAP1	Repressor Activator Protein 1
rFSH	Recombinant Follicle-Stimulating Hormone
rho	Spearman's Rank Correlation Coefficient
RNA	Ribonucleic Acid
ROI	Region of Interest
ROS	Reactive Oxygen Species
RPMI	Roswell Park Memorial Institute
RSMN	Small Nuclear Ribonucleoprotein-Associated Protein
RT	Room Temperature
RT-qPCR	Reverse Transcription Quantitative PCR
SARS-CoV-2	Severe Acute Respiratory Syndrome Coronavirus 2 (Causes COVID-19)
SBKG	Subtract Background
SD	Standard Deviation
sec	Second
SMAI	Microscopy And Image Analysis Service
SP3	Single-Pot Solid-Phase-Enhanced Sample Preparation
SWATH	Sequential Window Acquisition of All Theoretical Spectra
SYBR	Fluorescent Dye that Binds Double-Stranded DNA in qPCR
T	Thymine
TA	Telomerase Activity
TBE	Tris-Borate-EDTA Buffer
TBS	Tris Buffer Saline
TCs	Theca Cells
Tel-Cy3	Telomeric Probe Labelled with Cy3 Dye
tels	Telomeres
TEMED	N,N,N',N'-Tetramethyl Ethylenediamine
TERC	Telomerase Ribonucleic Acid Component
TERT	Telomerase Reverse Transcriptase
TGF-β1	Transforming Growth Factor Beta 1
TIN2	TRF1 and TRF2-Interacting Nuclear Factor 2
TL	Telomere Length
T-loop	Telomeric Loop Structure that Protects Chromosomes Ends
TMPRSS2	Transmembrane Serine Protease 2
TPP1	TINT1/PTOP1/PIP1; encoded by the gene ACD
TRAP	Telomerase Repeated Amplification Protocol
TRF1	Telomeric Repeat-Binding Factor 1
TRF2	Telomeric Repeat-Binding Factor 2
TTAGGG	Telomeric Repeat Sequence in Humans
t-test	Student's T-Test
U	Uracil
U test	Mann-Whitney U Test (Nonparametric Test)

UK	United Kingdom
USA	United States of America
vs.	Versus (used for comparisons)
x g	Relative Centrifugal Force
Y	Young
Y-	Young Women with Low AMH
Y+	Young Women with High AMH
Ypreg	Young Pregnant Women

LIST OF FIGURES

Figure 1. Hypothalamic-pituitary-ovarian axis and hormone levels during menstrual cycles. 53

Figure 2. Oogenesis process. 56

Figure 3. Folliculogenesis process. 57

Figure 4. Ovarian reserve declines during a woman's life. 60

Figure 5. Hallmarks of aging. 65

Figure 6. End replication problem. 67

Figure 7. Telomeres and the shelterin complex. 69

Figure 8. General projects outline. 89

Figure 9. Cell number counting using the Neubauer chamber. 92

Figure 10. Ovarian cortex processing. 95

Figure 11. Representative images of ovarian follicles by FISH. 106

Figure 12. Representative images of ovarian follicles by H&E. 108

Figure 13. Analysis of the levels of AMH, FSH, LH, E2, and P4 with age. 123

Figure 14. Telomere qFISH in PBMCs. 124

Figure 15. Analysis of telomere parameters in PBMCs in Y, M, and P women. 125

Figure 16. Telomere qFISH in ovarian stroma. 126

Figure 17. Analysis of telomere parameters in oocytes of Y and M women. 130

Figure 18. Analysis of telomere parameters in GCs during folliculogenesis. 133

Figure 19. Analysis of telomere parameters in primordial GCs in Y and M groups. 135

Figure 20. Analysis of telomere parameters in primary GCs in Y and M groups. 137

Figure 21. Analysis of telomere parameters in TCs in Y and M groups. 141

Figure 22. Telomere length of PBMCs and ovarian cell populations. 142

Figure 23. Telomere parameters with significant correlation in PBMCs and the ovary. 144

Figure 24. Analysis of telomerase activity in ovarian samples from women of Y, M, and P groups. 145

Figure 25. Fibrotic area in the ovary of Y, M, and P groups. 146

Figure 26. Proteomic profiling of the ovary in Y, M, and P groups. 148

Figure 27. Ovarian proteomic changes in age groups.....149

Figure 28. Volcano plot showing pairwise comparisons of protein expression levels between age groups.....150

Figure 29. Parallel plots highlight ATM, CUL1, CALM3, and LDHB protein expression tendency throughout age groups. 151

Figure 30. Analysis of telomere parameters in oocytes from M+ and M- women. 157

Figure 31. Analysis of telomere parameters in M+ and M- groups.....159

Figure 32. Analysis of telomere parameters in TCs from M+ and M- women. 160

Figure 33. Analysis of telomerase activity in ovarian samples from women classified by age and AMH.....161

Figure 34. Analysis of telomere parameters in PBMCs from pregnant and non-pregnant women. 164

Figure 35. Analysis of telomere parameters in oocytes from pregnant and non-pregnant women. 167

Figure 36. Analysis of telomere parameters in GCs from pregnant and non-pregnant women. 168

Figure 37. Analysis of telomere parameters in TCs from pregnant and non-pregnant women. 170

Figure 38. Analysis of telomerase activity in ovarian samples from pregnant and non-pregnant women. 172

Figure 39. Analysis of telomere length by HT-qFISH in GCs in control and COVID-19 patients. 175

Figure 40. Analysis of telomere parameters in GCs. 176

Figure 41. Analysis of telomere parameters in GCs and PBMCs from control and mild COVID groups.....177

Figure 42. Analysis of fertility outcomes in controls and COVI groups. 178

LIST OF TABLES

Table 1. Paraffin-embedded protocol. 94

Table 2. Deparaffinization protocol. 94

Table 3. Hormone commercial kits. 96

Table 4. Lysis buffer recipe. 98

Table 5. Primer sequences used in the TRAP assay. 99

Table 6. Elongation master mix recipe. 99

Table 7. 10X Stock elongation buffer recipe 100

Table 8. Amplification master mix recipe. 100

Table 9. 10X Stock TRAP buffer. 101

Table 10. Telomere FISH hybridization solution recipe. 104

Table 11. cDNA synthesis thermal cycler protocol. 110

Table 12. Primer sequences. 111

Table 13. RT-qPCR thermal cycler protocol. 111

Table 14. RT-qPCR quantification parameters detailed. 112

Table 15. Recipe for lysis buffer used in proteomic analysis. 112

Table 16. Characteristics of the study population classified by age. 121

Table 17. Ovarian stroma telomere parameters in groups based on age. 127

Table 18. Oocyte telomere parameters during folliculogenesis. 128

Table 19. Secondary GCs telomere parameters in groups based on age. 138

Table 20. TCs telomere parameters during folliculogenesis. 139

Table 21. Parameters of correlations between TL in kb of PBMCs and different ovarian cell populations. 143

Table 22. Fibrosis-related gene expression (DCq) in groups based on age. 147

Table 23. DEPs from p-value adjusted statistical analysis. 152

Table 24. Baseline characteristics and hormonal parameters of the study population classified by age and AMH levels. 154

Table 25. PBMCs telomere parameters in groups based on age and AMH levels. 155

Table 26. Stroma telomere parameters in groups based on age and AMH divisions. 156

Table 27. GCs telomere parameters in middle-aged women classified by AMH. 157

Table 28. Baseline characteristics and hormonal parameters of the study population classified by age and pregnancy. 163

Table 29. Stroma telomere parameters in pregnant and non-pregnant women. 166

Table 30. GCs telomere parameters in middle-aged pregnant and non-pregnant women. . 169

Table 31. TCs telomere parameters in young pregnant and non-pregnant women. 171

Table 32. Baseline characteristics of the COVID-19 study population. 174

RESUMEN EXTENDIDO EN ESPAÑOL

INTRODUCCIÓN

1. Senescencia reproductiva femenina

El término senescencia reproductiva se refiere a la disminución progresiva de la reserva ovárica y de la función hormonal en la mujer, que lleva a la desaparición de la menstruación y la incapacidad de concebir de manera natural. El principal motivo reside en que la mujer, a diferencia del hombre, nace con un número limitado de gametos que con la edad se irá agotando, sumado a la pérdida de la calidad de estos gametos.

A) EL OVARIO: ENDOCRINOLOGÍA, OVOGÉNESIS, FOLICULOGÉNESIS, Y RESERVA OVÁRICA

Las células germinales femeninas, los ovocitos, se originan en los ovarios durante el desarrollo embrionario. Los ovarios son los órganos centrales del sistema reproductivo femenino, encargados tanto de la producción de ovocitos, como de la síntesis y liberación de las hormonas sexuales femeninas. Estos órganos pareados están ubicados en la cavidad pélvica, uno a cada lado del útero. En ellos se desarrollan dos procesos claves para la vida reproductiva de una mujer, la ovogénesis y la foliculogénesis, ambos orquestados hormonalmente por el eje hipotálamo-hipófisis-ovario.

Durante el desarrollo embrionario de la mujer, las células germinales primordiales migran desde el saco vitelino hasta establecerse en las crestas genitales o gonadales. Una vez allí, se inicia el proceso de ovogénesis. Las células germinales primordiales se dividen mitóticamente y se diferencian en ovogonias. Las ovogonias continúan dividiéndose mitóticamente hasta iniciar la meiosis y dar lugar al ovocito primario. El ovocito permanece detenido en el estadio de profase de la primera división meiótica. Alrededor de él, se dispone una capa de células somáticas del ovario conocidas como células de la granulosa. Conjuntamente, el ovocito primario y las células de la granulosa forman la estructura funcional conocida como folículo ovárico primordial. La doctrina básica en biología reproductiva sostiene que la mujer nace con un número fijo finito de folículos primordiales, y, por tanto, de ovocitos.

Con la llegada de la pubertad y el establecimiento de los ciclos menstruales, se retoman la ovogénesis y la foliculogénesis en el ovario. Las fluctuaciones en los niveles hormonales que tienen lugar durante el ciclo menstrual de una mujer están destinadas al crecimiento folicular, la maduración del ovocito, la ovulación y la preparación del endometrio para albergar al futuro

embrión. Por tanto, cuando en una mujer se inician los ciclos menstruales, los folículos primordiales que habían permanecido quiescentes en el ovario hasta ese momento empiezan a desarrollarse. Los folículos primordiales formados únicamente por el ovocito y una capa de células de la granulosa se desarrollan a folículo primario, donde las células de la granulosa cambian su morfología alargada a otra más cuboidal. Estas comienzan a multiplicarse, aumentando en número y formando capas concéntricas alrededor del ovocito en el estadio de folículo secundario. En los estadios de folículo primario y secundario, las células del estroma ovárico próximas a las células de la granulosa adquieren una conformación especial, conocidas como células de la teca que participan activamente en la regulación hormonal. A continuación, entre las múltiples capas de células de la granulosa empiezan a formarse pequeños huecos que se llenan de líquido hasta unirse en una sola cavidad conocida como antro folicular. Los folículos ováricos con un gran antro se denominan folículos antrales. Este crecimiento ocurre como respuesta al incremento de la hormona foliculoestimulante o FSH por parte de la adenohipófisis. Las células de la granulosa en respuesta liberan una gran cantidad de estrógenos. Aproximadamente hacia la mitad del ciclo menstrual, se produce un pico en los niveles de la hormona luteinizante o LH que desencadena la ruptura del folículo ovárico, y la liberación del ovocito hacia las trompas de Falopio. Es en este momento donde se retoma el proceso de ovogénesis, y el ovocito continúa con la meiosis dividiendo su dotación cromosómica. Como resultado de esta división desigual del ovocito primario se generan un ovocito secundario haploide y un primer corpúsculo polar haploide. A su vez, el ovocito secundario alcanza el estadio de metafase II de la meiosis esperando a la fecundación para completar el proceso. Si la fecundación tiene lugar, el segundo corpúsculo polar será liberado.

Este proceso se repite continuamente durante la vida reproductiva de la mujer, desde la menarquia hasta la menopausia. Teniendo en cuenta que la mujer nace con un número finito de ovocitos, conocido como reserva ovárica, esta se irá agotando gradualmente. Cuando la reserva ovárica es muy baja, la mujer alcanza el periodo de menopausia donde pierde su capacidad reproductiva. La reserva ovárica puede evaluarse de forma indirecta mediante los niveles de FSH, el recuento de folículos antrales, o los niveles de hormona antimulleriana, también denominada AMH. Concretamente esta hormona es liberada por folículos pre-antrales y antrales pequeños. Los tres parámetros ofrecen información indirecta sobre la reserva ovárica de una mujer. Concretamente, niveles elevados de FSH, un bajo recuento de folículos antrales, y/o bajos niveles de AMH son indicativos de una baja reserva ovárica.

B) INFERTILIDAD FEMENINA

En la actualidad, por diversos motivos, las mujeres son madres a edades más avanzadas. Son muchos los casos de mujeres que cuando deciden ser madres no pueden cumplir sus

deseos genésicos, y se ven obligadas a recurrir a técnicas de reproducción asistida para conseguirlo. Tomando como premisa el hecho de que la reserva ovárica disminuye con la edad, a edades más avanzadas las probabilidades de ser madre disminuyen notablemente. Además, no solo se ve mermado el número de ovocitos, sino también su calidad. Esto se debe a que durante muchos años los ovocitos permanecen arrestados en profase I de la meiosis, siendo susceptibles a factores tanto endógenos como exógenos que pueden dañar su integridad.

2. Envejecimiento biológico: telómeros

A) SELLOS O MARCAS DE ENVEJECIMIENTO

En el último siglo, gracias a los múltiples avances en salud pública y medicina, la esperanza de vida se ha incrementado notablemente. El envejecimiento implica un proceso progresivo degenerativo que involucra numerosos cambios a nivel celular y molecular, los cuales causan un deterioro funcional de tejidos y órganos. Este proceso está ligado a la aparición de determinadas enfermedades como patologías cardiovasculares, enfermedades neurodegenerativas como el Alzheimer o el Parkinson, y cáncer. Entre los múltiples cambios que implica el envejecimiento, se pueden definir doce sellos o marcas científicamente reconocidos: inestabilidad genómica, acortamiento telomérico, alteraciones epigenéticas, pérdida de la proteostasis, desregulación de la sensibilización a nutrientes, disfunción mitocondrial, senescencia celular, agotamiento de células madre, comunicación intracelular alterada, alteración del proceso de macro-autofagia, inflamación crónica, y disbiosis. Todos ellos están interconectados, aparecen gradualmente con el paso de los años, su acentuación acelera el proceso de envejecimiento, y su ralentización o incluso detención mediante intervenciones terapéuticas podría detener el proceso de envejecimiento.

B) ACORTAMIENTO TELOMÉRICO, COMPLEJO SHELTERINA Y TELOMERASA

Uno de estos sellos del envejecimiento es el acortamiento telomérico. Los telómeros son estructuras finales de los extremos cromosómicos, formadas por la consecución repetitiva de la secuencia nucleotídica 5'TTAGGG3'. Esta secuencia no codifica para ninguna proteína, y su función es la protección del ADN cromosómico. Es decir, los cromosomas en todos sus extremos tienen largas secuencias teloméricas, las cuales se acortan gradualmente en las divisiones celulares. Esto ocurre debido al problema de replicación y la estructura de doble hélice del ADN. Cuando una célula se divide, las cadenas complementarias de ADN se separan para ser replicadas. La complementaria a una de las cadenas, conocida como cadena líder, se sintetiza de forma continua por una enzima polimerasa en sentido 5' > 3'. Sin embargo, la otra cadena, denominada cadena retardada, se replica de manera discontinua mediante la unión de cebadores y la síntesis de los fragmentos de Okazaki. Esto ocurre

porque la polimerasa necesita un extremo 3' libre para añadir nucleótidos. Por tanto, la replicación de esa cadena retardada mediante la síntesis de los fragmentos de Okazaki necesita de una ADN ligasa que una los fragmentos entre sí. El extremo 5' terminal de la cadena retardada no puede ser replicado debido a una falta de espacio para la unión de un nuevo cebador que origine otro fragmento de Okazaki. Es decir, inevitablemente, durante las divisiones celulares se produce un acortamiento telomérico.

Por este motivo, los telómeros son biomarcadores fidedignos del proceso de envejecimiento. Cuando una célula posee un determinado número de telómeros críticamente cortos, esta entra en senescencia y posterior apoptosis como mecanismo de protección del organismo. Sin embargo, existen mecanismos destinados a la protección del telómero, y su recuperación para combatir este acortamiento. Los propios telómeros en sí adquieren una conformación en bucle (denominado *T-loop*) para su propia protección, además se unen a un complejo proteico conocido como shelterina que también lo protege. Pero en el caso de que estos mecanismos protectores no sean suficientes, algunas células poseen actividad telomerasa. Se trata de una enzima ribonucleica capaz de añadir secuencias teloméricas *de novo*. Esto es posible gracias a que esta enzima posee actividad de transcriptasa reversa, y un componente de ARN molde de la secuencia telomérica. La actividad telomerasa la poseen las células germinales, células madre y células tumorales. Concretamente también se ha detectado actividad telomerasa en algunas células somáticas como las células de la granulosa ováricas.

C) DISFUNCIÓN TELOMÉRICA Y ENFERMEDADES

Como se ha explicado anteriormente, el acortamiento telomérico es una de las causas de la senescencia celular. Una acumulación de células senescentes junto con una capacidad de regeneración tisular mermada por el incremento de la edad, aumenta la susceptibilidad a la aparición de determinadas enfermedades. Entre las más frecuentes y estudiadas destaca el cáncer, dado que las células tumorales se caracterizan por una profunda inestabilidad genómica y una elevada actividad telomerasa. Sin embargo, otras enfermedades como la fibrosis pulmonar o el Alzheimer, ambas con elevadas incidencias en la población envejecida, o progerias como el síndrome de Hutchinson-Gilford, también se han relacionado directamente con defectos a nivel telomérico.

En los últimos cinco años, una enfermedad respiratoria conocida como COVID-19, producida por el coronavirus o SARS-CoV-2, también se ha vinculado con el envejecimiento. Está ampliamente documentado que, en individuos mayores, esta infección respiratoria cursa con graves síntomas. Sin embargo, no solo afecta a pacientes de edades avanzadas, sino a toda la población. La relación de causa y efecto entre la COVID-19 y el acortamiento telomérico está siendo analizada, ya que alteraciones en la ruta telomérica hacen al individuo más

susceptible a la infección y hacen más dificil su recuperación, aunque también se ha observado un mayor acortamiento telomérico en los pacientes en los que esta enfermedad ha cursado con mayor gravedad. La COVID-19 genera un ambiente de hipoxia en el individuo, aumentando el estrés oxidativo, y con ello la producción de especies reactivas de oxígeno, las cuales dañan directamente a los telómeros.

3. Dinámicas teloméricas e infertilidad femenina

El acortamiento telomérico no se ha asociado únicamente con enfermedades propias del envejecimiento como las anteriormente mencionadas, sino también con la infertilidad. Contextualizando, en las mujeres una edad avanzada se asocia con una caída de la reserva ovárica, es decir, una pérdida en el número de ovocitos, así como una caída en la calidad de los mismos. Por tanto, teniendo en cuenta que el acortamiento telomérico está también asociado al avance de la edad, la alteración de este podría afectar directamente al estado o capacidad reproductiva femenina.

El ovario tiene actividad telomerasa, concretamente en las células germinales y las células de la granulosa. Estas últimas necesitan actividad telomerasa para responder a las altas demandas de divisiones celulares que acontecen durante la foliculogénesis. Sin embargo, diferentes trabajos apuntan a una menor actividad telomerasa con la edad, lo que supondría una mayor tasa de acortamiento telomérico, y una menor capacidad para su recuperación. Estos hallazgos pueden tener consecuencias directamente relacionadas con la fertilidad de la mujer. Por ejemplo, el aumento de aneuploidías en mujeres de edad avanzada. Las aneuploidías, definidas como alteraciones en el número de cromosomas, pueden originarse por ineficiencia en el proceso de recombinación o alteraciones en la segregación cromosómica. Entre las causas de una segregación cromosómica alterada destacan los defectos en el huso acromático, la falta de cohesión entre las cromátidas, o un ensamblaje erróneo de los microtúbulos y los cinetocoros. Concretamente, está descrito que los telómeros pueden estar implicados tanto en la recombinación (formación del ramillete o *bouquet* para el encuentro de los cromosomas homólogos), como en la segregación correcta.

La teoría del envejecimiento reproductivo fundamentada en el acortamiento telomérico de los ovocitos, fue desarrollada por Keefe y colaboradores en el 2006. Esta teoría apunta a un deterioro telomérico en los ovocitos de mujeres mayores por dos razones principales. En primer lugar, hipotetiza que los ovocitos destinados a ser ovulados a edades más tardías son aquellos fruto de múltiples divisiones durante el desarrollo prenatal. Es decir, la selección de los ovocitos para la ovulación ocurriría de manera cronológica, de forma que los ovocitos ovulados a edades jóvenes han sufrido menores divisiones celulares durante el periodo fetal en comparación con los ovocitos ovulados a edades más tardías. En segundo lugar, durante

todo el tiempo que esos ovocitos permanecen detenidos en la meiosis I en el ovario, sufren y acumulan daños. Un ejemplo podría ser el daño telomérico directo por especies reactivas de oxígeno.

La relación entre los parámetros teloméricos y alteraciones reproductivas como la insuficiencia ovárica prematura, o el síndrome de ovario poliquístico ha sido analizada por múltiples grupos. Concretamente, se ha estudiado la longitud telomérica en células de la granulosa recogidas durante la obtención de ovocitos en los ciclos de fecundación *in vitro*. También se han analizado los parámetros teloméricos en células mononucleares de sangre periférica o leucocitos, con el objetivo de explorar su potencial papel como biomarcadores teloméricos de lo que ocurre en el ovario. No obstante, el análisis telomérico y su relación con la edad no ha sido estudiado en el propio tejido ovárico humano, y en las subpoblaciones celulares que lo componen.

HIPÓTESIS

Teniendo en cuenta que el acortamiento de los telómeros es un sello distintivo del envejecimiento y que el ovario es uno de los primeros órganos en sufrir senescencia temprana, la hipótesis de este trabajo es que el mantenimiento defectuoso de los telómeros en el ovario, podría conducir a la disfunción ovárica, incluyendo la disminución de la reserva ovárica. Además de la disfunción ovárica, la biología de los telómeros del ovario también puede verse alterada durante condiciones transitorias como el embarazo o la COVID-19, a pesar de no ser una enfermedad directamente relacionada con la fertilidad.

OBJETIVOS

El objetivo principal de este estudio es caracterizar el mantenimiento de los telómeros asociado al envejecimiento en el ovario humano, y estudiar el impacto de determinados factores, como el embarazo o patologías no reproductivas como la COVID-19, en la biología de los telómeros del ovario.

Para alcanzar este objetivo principal, se establecen diferentes objetivos secundarios divididos en función del proyecto de investigación a partir del cual se obtendrán. Los objetivos secundarios de este trabajo son:

Específicos del proyecto 1 titulado: *"Comprender la implicación de la vía de los telómeros en el envejecimiento ovárico y la disfunción/infertilidad"*

I. Determinar el perfil hormonal en mujeres de diferentes edades.
II. Evaluar la vía telomérica en diferentes poblaciones celulares del ovario durante la foliculogénesis.

III. Analizar los cambios a nivel de los telómeros en ovocitos, células de la granulosa, células de la teca y estroma ovárico en diferentes grupos de edad.
IV. Estudiar la presencia de actividad telomerasa en el ovario humano.
V. Evaluar las alteraciones teloméricas a nivel sistémico y su potencial uso como biomarcador telomérico ovárico.
VI. Estudiar el deterioro ovárico utilizando otros marcadores de envejecimiento como la fibrosis y un enfoque proteómico.
VII. Evaluar el impacto de la reserva ovárica (basada en los niveles de AMH), en los parámetros teloméricos independientemente de la edad a nivel ovárico y sistémico.
VIII. Analizar los parámetros teloméricos en la última fase del embarazo.

Específicos del proyecto 2 titulado: *"Efectos de la COVID-19 en la biología de los telómeros de las células de la granulosa y en la fertilidad, así como en los resultados de FIV."*

IX. Estudio de la longitud de los telómeros en las células de la granulosa y a nivel sistémico en mujeres no vacunadas que padecieron COVID-19 con diferentes grados de severidad y controles.
X. Analizar el impacto de la COVID-19, como enfermedad no reproductiva, sobre parámetros de fertilidad tras la estimulación ovárica como el número de ovocitos recuperados, el número de ovocitos maduros y la tasa de fecundación.
XI. Estudio de la correlación entre los telómeros y los parámetros de fertilidad.

MATERIALES Y MÉTODOS

1. Diseño del estudio, y recolección de muestras

Esta tesis es el resultado de dos proyectos de investigación desarrollados en humanos, donde todas las participantes fueron mujeres. Ambos proyectos contaron con la aprobación de los respectivos comités éticos para su realización.

A) PROYECTO 1: *"Comprender la implicación de la vía de los telómeros en el envejecimiento ovárico y la disfunción/infertilidad"*

En este primer proyecto analítico, prospectivo, observacional y multicéntrico, se reclutaron 65 mujeres con edades comprendidas entre 18 y 50 años en diferentes hospitales de Madrid y Valencia. Las mujeres reclutadas iban a someterse a una intervención quirúrgica ginecológica u obstétrica por motivos no relacionados con el estudio, incluida la cesárea. Se excluyeron como posibles candidatas aquellas mujeres donde el motivo de la cirugía estuviera

relacionado con el diagnóstico de cáncer. Se obtuvieron muestras de sangre y una biopsia ovárica de todas las mujeres que aceptaron participar en el estudio durante la intervención.

Parte de las muestras sanguíneas se destinaron a la obtención de suero para medir los valores hormonales de FSH, LH, AMH, estradiol y progesterona. El resto de la sangre se utilizó en el aislamiento de las células mononucleares de la sangre periférica, en los que se evaluó el mantenimiento telomérico sistémico. La biopsia de ovario se utilizó tanto para medir la longitud telomérica en los diferentes tipos celulares del ovario, como en el ensayo de actividad telomerasa, la valoración de fibrosis, y el estudio del perfil proteómico.

Las mujeres reclutadas se dividieron en tres grupos en base a la edad, los cuales a su vez se subdividieron en función del valor de AMH (reflejo de la reserva ovárica), y la concomitancia con el embarazo. Es importante especificar que los valores de corte de AMH se fundamentaron en los criterios de POSEIDON clínicamente utilizados en los tratamientos de reproducción asistida, o en los valores relativos de esta hormona en poblaciones de mujeres perimenopáusicas. Los grupos de estudio fueron:

- **Mujeres jóvenes (Y)** (n = 17): mujeres de 18 a 34 años, independientemente del valor de AMH o de la presencia o ausencia de embarazo.
    - **Y+** (n = 11): mujeres no embarazadas con un valor de AMH igual o superior a 1.2 ng/mL.
    - **Y-** (n = 2): mujeres no embarazadas con un valor de AMH inferior a 1.2 ng/mL.
    - **YPreg** (n = 4): mujeres embarazadas independientemente del valor de AMH.
- **Mujeres de mediana edad (M)** (n = 31): mujeres de 35 a 45 años, independientemente del valor de AMH o de la presencia/ausencia de embarazo.
    - **M+** (n = 6): mujeres no embarazadas con un valor de AMH igual o superior a 1.2 ng/mL.
    - **M-** (n = 16): mujeres no embarazadas con un valor de AMH inferior a 1.2 ng/mL.
    - **MPreg** (n = 9): mujeres embarazadas independientemente del valor de AMH.
- **Mujeres perimenopáusicas (P)** (n = 17): mujeres de 46 a 50 años, independientemente del valor de AMH. En este grupo no se reclutaron mujeres embarazadas.
    - **P+** (n = 8): mujeres no embarazadas de 46 a 50 años cuyo valor de AMH era igual o superior a 0.1 ng/mL.
    - **P-** (n = 9): mujeres no embarazadas de 46 a 50 años cuyo valor de AMH era inferior a 0.1 ng/mL.

B) PROYECTO 2: *"Efectos de la COVID-19 en la biología de los telómeros de las células de la granulosa y en la fertilidad, así como en los resultados de FIV."*

En este proyecto se reclutaron también un total de 65 mujeres de edades comprendidas entre 18 y 50 años, en la clínica de reproducción IVI Madrid. Se reclutaron mujeres no vacunadas frente al coronavirus que acudieron a la clínica a realizarse un tratamiento de reproducción asistida o como donantes de ovocitos. A todas ellas se les extrajeron muestras sanguíneas, y se recolectaron las células de la granulosa obtenidas durante la punción folicular.

Parte de las muestras sanguíneas se destinaron a la obtención de suero para medir la AMH y valorar la presencia de anticuerpos frente al SARS-CoV-2. La otra parte de las muestras de sangre se utilizó para el aislamiento de células mononucleares de sangre periférica en las que valorar el acortamiento telomérico sistémico. Las células de la granulosa también fueron utilizadas para la valoración telomérica. Los datos sobre fertilidad relativos al número de ovocitos obtenidos tras la estimulación ovárica, el número de ovocitos maduros, la tasa de maduración ovocitaria, y la tasa de fecundación se recogieron de la base de datos de la clínica.

En estas pacientes se anotaron datos relativos a si el sujeto sufrió la COVID-19, y en caso positivo la severidad de sus síntomas. En base a estos datos las mujeres reclutadas se agruparon de la siguiente manera:

- **Grupo de control** (n = 29): mujeres no expuestas al SARS-CoV-2.
- **Grupo COVID** (n = 36): mujeres infectadas por el SARS-CoV-2. Simultáneamente, se clasificó a las pacientes COVID según la intensidad de sus síntomas en grupos COVID leve y grave para comprender mejor el impacto de la enfermedad en las distintas variables estudiadas. El grupo de COVID leve reunió a más individuos (52,7%) que el grupo de COVID grave (47,2%). Ninguno de los pacientes incluidos requirió hospitalización debido a la COVID-19.
    - **COVID leve** (n = 19): pacientes categorizados con puntuaciones sintomáticas de 1 y 2.
        - Puntuación 1: COVID-19 asintomática (n = 7). Sujetos con presencia de anticuerpos séricos que no presentaron síntomas durante la enfermedad.
        - Puntuación 2: COVID-19 leve (n = 12). Sujetos con fiebre leve, tos y pérdida del olfato y el gusto durante un corto periodo de tiempo (aproximadamente 2 semanas).
    - **COVID grave** (n = 17): pacientes categorizados con una puntuación sintomática 3. Esta puntuación se refería a síntomas graves de COVID-19 como fiebre de alto grado, disnea, fatiga, cefalea, síntomas gastrointestinales, anosmia y disgeusia.

Las alteraciones del olfato y el gusto persistieron durante al menos un mes. Un paciente de este grupo presentó problemas de coagulación sanguínea.

2. Valoración de niveles hormonales

Las hormonas AMH, FSH, LH, E2 y P4 se evaluaron mediante ensayos de quimioluminiscencia.

3. Parámetros teloméricos

Entre los parámetros teloméricos se evaluó la **actividad telomerasa** a partir de secciones de tejido ovárico congeladas con el ensayo TRAP. Esta técnica se basa en la obtención de un extracto proteico a partir de las muestras de tejido que contienen telomerasa. A continuación, se realizan dos reacciones en cadena de la polimerasa o PCR. En la primera, conocida como elongación, al extracto proteico se le añade un cebador, en el caso de existir telomerasa, esta añadirá repeticiones teloméricas a este cebador. En la segunda PCR, se realiza un protocolo de PCR normal donde los productos elongados son amplificados. Su detección se visualiza en un gel, donde las muestras positivas para actividad telomerasa muestran un patrón en escalera característico, que representa el cebador y la adición de secuencias teloméricas en mayor o menor número.

La **longitud telomérica** se evaluó mediante la técnica de hibridación fluorescente in situ cuantitativa o qFISH. Esta técnica se realizó sobre las secciones ováricas, las células de la granulosa obtenidas en la punción folicular, y las células mononucleares de sangre periférica. Para obtener las secciones ováricas, las biopsias fueron previamente fijadas e incluidas en parafina para su sección en el microtomo. Posteriormente, fueron desparafinizadas previo al inicio del qFISH. Mediante esta técnica se permeabiliza la membrana celular y nuclear, se desnaturaliza el ADN, y se añade una sonda telomérica marcada con la partícula fluorescente Cy3 (visualizada en color rojo) que hibrida específicamente con los telómeros. Los núcleos celulares se tiñen con DAPI. Su visualización se realiza en un microscopio confocal, donde se adquieren múltiples imágenes en las que los puntos rojos teloméricos se observan en el interior del área nuclear marcado con azul. Una vez se han adquirido las imágenes, están se procesan para obtener las intensidades de los puntos teloméricos que se relacionan directamente con la longitud telomérica.

En ambas técnicas destinadas a valorar parámetros teloméricos, se incluyen células tumorales como controles positivos.

4. Fibrosis ovárica

La fibrosis se evaluó en las secciones de ovario previamente desparafinadas. Esta se analizó mediante la tinción tricrómica de Masson que tiñe las fibras de colágeno en color azul, mientras que los núcleos celulares y el citoplasma en tonos rojos o rosas. Se cuantificó el área fibrótica en diferentes secciones y se calculó el porcentaje con respecto al área total de la sección.

Los niveles de expresión de los genes TGF-β1, COL1A1, y COL3A1 se evaluaron mediante PCR en tiempo real. Estos genes están directamente relacionados con procesos fibróticos. Para la realización de esta técnica, en primer lugar, se extrajo el ARN de muestras de tejido ovárico mediante el método TRIzol, a continuación, se sintetizó el ADN complementario, y se realizó la técnica de PCR en tiempo real con el compuesto orgánico SYBR Green.

5. Análisis proteómico

El análisis proteómico se realizó mediante la técnica de espectrometría de masas (conocida como SWATH) que permitió la cuantificación y caracterización simultánea de proteínas en las muestras de tejido ovárico. Para ello, en primer lugar, se extrajeron las proteínas de la muestra biológica y se digirieron para obtener péptidos que fueron purificados. A continuación, los péptidos se introdujeron en el espectrómetro de masas, donde se ionizaron para su análisis. El espectrómetro realizó un barrido secuencial generando fragmentos de los péptidos. Con el uso de bases de datos de secuencias de proteínas, los fragmentos obtenidos se compararon con las secuencias teóricas de los péptidos para identificar las proteínas presentes en la muestra. Las intensidades de los fragmentos generados se utilizaron en la cuantificación de las proteínas basándose en la abundancia de los péptidos. Finalmente, los datos obtenidos fueron procesados mediante un software especializado.

6. Análisis estadístico

Se realizó la estadística descriptiva de todas las variables, seguida de un análisis de la normalidad de las distribuciones. En base a estos resultados, los diferentes grupos se analizaron mediante las pruebas de ANOVA o Kruskal-Wallis cuando se comparaban varios grupos, o t de Student y U de Mann-Whitney en las comparaciones entre dos grupos. A su vez, se evaluaron también las correlaciones existentes entre diferentes parámetros de interés utilizando los coeficientes de correlación de Spearman, Pearson, o Tau de Kendall.

RESULTADOS

En el apartado de resultados se diferenciaron cuatro secciones principales. Las tres primeras fueron resultado del Proyecto 1, mientras que la última se obtuvo a partir del Proyecto 2.

1. Caracterización del declive reproductivo femenino dependiente de la edad.

En este resultado se analizó detalladamente el envejecimiento ovárico desde el punto de vista hormonal, telomérico, el nivel de fibrosis, y el perfil proteómico. Para ello se compararon los grupos Y, M, y P, en los que la población del Proyecto 1 estaba exclusivamente dividida en base a la edad.

A) DATOS HORMONALES

Se observaron diferencias estadísticamente significativas en el valor de AMH entre los diferentes grupos de edad, registrando el valor más bajo el grupo P. Se observó una correlación negativa significativa entre el valor de AMH y la edad. Por el contrario, la FSH evidenció una correlación significativa positiva con la edad, al igual que la LH. En el caso de los niveles de estradiol, estos fueron menores en el grupo P, y esta hormona evidenció una correlación significativa negativa con la edad. No se observaron diferencias significativas ni correlación con la edad en el valor de progesterona.

B) PARÁMETROS TELOMÉRICOS

Longitudes teloméricas durante la foliculogénesis en poblaciones celulares ováricas:

En el análisis telomérico se evaluaron siempre tres parámetros: la longitud telomérica media, el porcentaje de telómeros cortos, y el porcentaje de telómeros largos.

En primer lugar, se evaluó la evolución de los parámetros teloméricos en ovocitos, células de la granulosa, y células de la teca durante el proceso de foliculogénesis. Concretamente, sólo pudieron analizarse los estadios foliculares primordial, primario y secundario. En los ovocitos y las células de la teca no se observaron diferencias estadísticamente significativas en ninguno de los parámetros teloméricos a lo largo de la foliculogénesis. Sin embargo, en las células de la granulosa se detectó un incremento tanto de la longitud telomérica como del porcentaje de telómeros cortos a medida que avanzaba la foliculogénesis.

Longitud telomérica en poblaciones celulares ováricas y envejecimiento:

Una vez evaluada la dinámica telomérica en los diferentes tipos celulares durante la foliculogénesis, se determinó estudiar conjuntamente o de forma separada los distintos estadios foliculares en los tipos celulares específicos. De manera que en ovocitos y células de la teca no se estudiaron de forma individual cada estadio folicular, mientras que sí se hizo de esta manera en las células de la granulosa. El estroma ovárico quedó excluido del estudio de la foliculogénesis, por tanto, no se diferenció en estadios foliculares.

- **Estroma**

No se evidenciaron diferencias estadísticamente significativas en ninguno de los parámetros teloméricos del estroma ovárico al comparar los grupos de edad Y, M y P.

- **Ovocitos**

Solo se identificaron ovocitos en los grupos de edad Y y M, por lo que no se pudieron comparar con el grupo P. Se detectó una menor longitud telomérica, un mayor porcentaje de telómeros cortos y un menor porcentaje de telómeros largos en los ovocitos de las mujeres del grupo M con respecto a Y. Concretamente, existió una correlación positiva significativa entre el porcentaje de telómeros cortos en los ovocitos y la edad.

- **Células de la granulosa de folículos primordiales**

Similar a los resultados obtenidos en los ovocitos, el grupo M registró una menor longitud telomérica, y un mayor porcentaje de telómeros cortos en las células de la granulosa que formaban los folículos primordiales. Existió una correlación significativa negativa de la edad con la longitud telomérica de estas células, y con el porcentaje de telómeros largos, mientras que entre la edad y el porcentaje de telómeros cortos esa correlación significativa fue positiva.

- **Células de la granulosa de folículos primarios**

En las células de la granulosa del estadio folicular primario, se detectó una menor longitud telomérica, un mayor porcentaje de telómeros cortos, y un menor porcentaje de telómeros largos en el grupo M al compararlo con el grupo Y. Sin embargo, se perdió la significancia en las correlaciones de estos parámetros teloméricos y la edad.

- **Células de la granulosa de folículos secundarios**

En el caso de las células de la granulosa de los folículos secundarios, no se detectaron cambios en ninguno de los parámetros teloméricos al comparar los grupos Y y M. Tampoco fueron significativas las correlaciones entre estos parámetros teloméricos y la edad.

- **Células de la teca**

La longitud telomérica de las células de la teca del grupo M fue menor en comparación con el grupo Y. Además, este grupo de mediana edad evidenció un mayor porcentaje de telómeros cortos y un menor porcentaje de telómeros largos. No existieron correlaciones significativas entre los parámetros teloméricos de este tipo celular ovárico y la edad.

Longitud telomérica sistémica en PBMCs y su evaluación como biomarcadores de envejecimiento:

A nivel sistémico, se compararon los parámetros teloméricos de los tres grupos de edad Y, M y P. No se detectaron diferencias significativas en la longitud telomérica media. Sin embargo, sí se observó un porcentaje mayor de telómeros cortos en el grupo P en comparación con los grupos Y y M. Además, la longitud telomérica evidenció una correlación significativa negativa con la edad, y el porcentaje de telómeros cortos una correlación significativa positiva con esta misma variable.

Las intensidades teloméricas en las células mononucleares de la sangre, ovocitos, células de la granulosa primordiales, células de la granulosa primarias, células de la granulosa secundarias, células de la teca y estroma ovárico se convirtieron a kilobases, y se estudiaron las correlaciones entre los diferentes parámetros teloméricos entre los distintos tipos celulares. Los tipos celulares ordenados de menor a mayor longitud telomérica fueron: células mononucleares de la sangre, células de la granulosa primordiales, células de la teca, estroma ovárico, células de la granulosa primarias, ovocitos, y células de la granulosa secundarias. No existieron correlaciones significativas en la longitud telomérica media entre ninguno de los tipos celulares del ovario y las células mononucleares de sangre periférica. En el caso del porcentaje de telómeros cortos, se evidenció una correlación significativa negativa entre esta variable a nivel sistémico y el estroma ovárico. Respecto al porcentaje de telómeros largos, la única correlación significativa, fue aquella entre células mononucleares de la sangre y células de la granulosa primordiales.

Actividad telomerasa en el ovario en los diferentes grupos de edad:

Se detectó actividad telomerasa en el ovario de todos los grupos de edad, es decir, en Y, M y P. Sin embargo, no pudo establecerse una tendencia a menor o mayor actividad telomerasa con la edad.

C) FIBROSIS OVÁRICA

El porcentaje de área fibrótica en el ovario fue significativamente mayor en el grupo P en comparación con el grupo más joven. Esta variable mostró una correlación positiva significativa con la edad. Cuando se evaluó la expresión de los genes relacionados con la fibrosis (TGF-β1, COL1A1, y COL3A1), no se observaron cambios significativos en ninguno de los grupos estudiados.

D) ANÁLISIS PROTEÓMICO

El análisis proteómico evidenció una mayor heterogeneidad y variabilidad en el grupo P en comparación con los grupos Y y M. A continuación, se realizaron análisis comparativos de los

grupos dos a dos. El análisis menos restrictivo sin ajustar el p-valor, evidenció múltiples proteínas diferencialmente expresadas. Las proteínas GGT5 y RSMN estaban diferencialmente expresadas en todas las comparaciones analizadas. La primera proteína, GGT5, que registró la expresión más baja en el grupo Y estaba directamente relacionada con el metabolismo del glutatión, un conocido antioxidante. Por el contrario, la proteína RSMN, que participa en procesos de regulación y procesamiento de la expresión génica, registró sus niveles más bajos en el grupo más joven.

2. Estudio de los parámetros teloméricos en los casos de baja reserva ovárica

Este bloque de resultados, tomando como premisa que una menor AMH se asocia a una edad avanzada, comparó los diferentes parámetros teloméricos entre los grupos de mujeres con la misma edad, pero niveles altos y bajos de AMH, y, por ende, de reserva ovárica. Las comparaciones de interés en esta sección fueron: Y+ vs. Y-; M+ vs- M-; y P+ vs. P-.

A) ANÁLISIS TELOMÉRICO SISTÉMICO

No se detectaron diferencias en ninguno de los intervalos de edad cuando se compararon mujeres con alta y baja reserva ovárica para ninguno de los parámetros teloméricos en células mononucleares de la sangre.

B) ANÁLISIS TELOMÉRICO OVÁRICO

El estroma ovárico se estudió para las tres comparaciones especificadas al inicio de este resultado. Sin embargo, en ovocitos, células de la granulosa y de la teca, únicamente se pudieron comparar los grupos M+ y M-, debido al bajo tamaño muestral del grupo Y- en el que se identificaron folículos ováricos, y la ausencia de folículos en las secciones ováricas de las mujeres que formaban los grupos P+ y P-.

Al comparar los parámetros teloméricos ováricos de los grupos M+ y M-, no se identificaron alteraciones ni en el estroma ovárico, ni en las células de la granulosa primarias. Sin embargo, sí se detectaron cambios a nivel telomérico en ovocitos, concretamente un mayor porcentaje de telómeros cortos en el grupo M-, en células de la granulosa primordiales y secundarias, y en células de la teca. Concretamente, tanto en las células de la granulosa primordiales y secundarias donde todo apuntaba a un mayor deterioro telomérico en el grupo M-, estos datos no fueron concluyentes ya que existían diferencias estadísticamente significativas en la media de edad de los grupos M+ y M- donde se identificaron y cuantificaron folículos primordiales y secundarios. Únicamente en las células de la teca, el grupo M- evidenció una menor longitud telomérica media de estas células.

El análisis de la actividad telomerasa demostró que independientemente del valor de AMH y de la edad, se detecta actividad telomerasa en todas las muestras ováricas.

3. Impacto del embarazo en la dinámica telomérica ovárica

Este bloque de resultados nació tras la detección de un menor valor de AMH en las mujeres embarazadas con respecto al resto de mujeres del mismo intervalo de edad analizado. Aclarar que las mujeres embarazadas reclutadas se encontraban durante la intervención de la cesárea en el momento de obtención de las muestras. Solo pudieron analizarse los grupos de edad Y y M, puesto que no hubo mujeres embarazadas en el grupo P. Por tanto, a lo largo de esta sección se compararon los parámetros teloméricos de los grupos Y+ vs. Ypreg, y M+ vs. Mpreg.

A) ANÁLISIS TELOMÉRICO SISTÉMICO

En los parámetros teloméricos a nivel sistémico solo se identificó un cambio estadísticamente significativo cuando se comparó el porcentaje de telómeros largos en células mononucleares de sangre periférica en los grupos M+ y Mpreg, registrando un menor porcentaje el grupo Mpreg. Sin embargo, como ocurrió en resultados anteriores, también existía una diferencia estadísticamente significativa en la edad media de los grupos M+ y Mpreg, por lo que este resultado no puede atribuirse directamente al embarazo, pudiendo influir la edad.

B) ANÁLISIS TELOMÉRICO OVÁRICO

Por un lado, se compararon los parámetros teloméricos de los diferentes tipos celulares del ovario en los grupos más jóvenes, Y+ y Ypreg. No se detectaron diferencias a nivel telomérico entre estos grupos en el estroma ni en las células de la granulosa secundarias. Sin embargo, tanto en ovocitos, como en células de la granulosa primordiales, primarias y células de la teca los resultados apuntaron a un peor mantenimiento telomérico en el grupo Ypreg.

En las comparativas de los grupos M+ y Mpreg, únicamente se observó un mantenimiento telomérico alterado en el grupo de mujeres embarazadas en los ovocitos. Tanto el estroma ovárico, como las células de la granulosa de los diferentes estadios foliculares, y las células de la teca no mostraron cambios estadísticamente significativos asociados al embarazo en sus telómeros.

De nuevo, los ovarios de todos los grupos estudiados en este epígrafe mostraron actividad telomerasa. Sin embargo, no se detectaron variaciones en estos niveles entre las mujeres embarazadas y las no embarazadas.

4. Impacto del COVID-19 en la reproducción y la ruta telomérica

Esta última sección de resultados se extrajo a partir del Proyecto 2. Se evaluó la longitud telomérica tanto en las células de la granulosa obtenidas en la punción folicular como en las

células mononucleares de sangre periférica. Además, se analizaron diferentes variables reproductivas.

Se evidenció un impacto a nivel telomérico de la COVID-19 en las células de la granulosa de los casos más severos de la enfermedad, con un mayor acortamiento de los telómeros y una correlación negativa significativa entre la longitud de los telómeros y la gravedad de la enfermedad. Esto también se observó en el porcentaje de telómeros largos, que se redujo en los casos graves y se correlacionó negativamente con la gravedad de la enfermedad. En la población sana o control, una menor longitud telomérica de las células de la granulosa se correlacionó con una menor tasa de maduración ovocitaria. Sin embargo, las mujeres que padecieron COVID-19 con mayor severidad mostraron una tasa de maduración de ovocitos reducida, aunque no un descenso del número de ovocitos recolectados.

DISCUSIÓN

1. Caracterización del declive reproductivo femenino dependiente de la edad

El ciclo menstrual determina la vida reproductiva de la mujer y responde al eje endocrino hipotálamo-hipófisis-ovario. A medida que la edad avanza, los niveles de FSH y LH aumentan, mientras que los de estrógenos y AMH disminuyen, debido a la reducción de la reserva ovárica. Sin embargo, algunos resultados del estudio no coincidieron con estas expectativas, ya que las mediciones hormonales no se hicieron en la misma fase del ciclo menstrual, y algunas de las participantes estaban embarazadas. Aunque la disminución de AMH con la edad se confirma como un indicador fiable de la reserva ovárica, los demás resultados no son concluyentes debido a las limitaciones del diseño del estudio.

En el análisis telomérico del envejecimiento sistémico, se midió la longitud de los telómeros y el porcentaje de telómeros cortos y largos en células mononucleares de sangre periférica. Estas células se seleccionaron debido a su accesibilidad y porque está demostrado que su longitud telomérica disminuye con la edad. Los resultados mostraron que no hubo cambios significativos en la longitud telomérica media entre los grupos de estudio, pero sí un aumento en el porcentaje de telómeros cortos en los grupos más mayores, lo que refleja la pérdida de longitud de los telómeros con la edad. Esta acumulación de células con telómeros más cortos indica un deterioro en su capacidad para dividirse y una mayor proximidad a la senescencia. Además, se encontró que la longitud de los telómeros de las células mononucleares de sangre periférica y el porcentaje de telómeros cortos correlacionaban significativamente con la edad, lo que confirma que el acortamiento de los telómeros es un marcador del envejecimiento. En resumen, el envejecimiento sistémico se asocia con un deterioro progresivo de la calidad de los telómeros, especialmente después de los 46 años.

El análisis telomérico de las diferentes etapas de la foliculogénesis se pudo realizar en ovocitos, células de la granulosa y de la teca. Los resultados mostraron que la longitud de los telómeros de los ovocitos y de las células de la teca, no cambió durante las primeras etapas de la foliculogénesis, lo que podría estar explicado por la ausencia o baja tasa de división celular. Por el contrario, en las células de la granulosa se observó un aumento en la longitud telomérica durante el proceso, probablemente debido a la actividad telomerasa que actuaría durante las divisiones celulares, compensando el acortamiento telomérico asociado a las mismas. También se detectó un aumento en el porcentaje de telómeros cortos en células de la granulosa de folículos secundarios, que podría venir dado por estrés oxidativo, un conocido factor exógeno que causa acortamiento telomérico, y que no podría ser totalmente compensado por la actividad telomerasa. Este incremento en el porcentaje de telómeros cortos, podría inducir la senescencia y/o apoptosis celular en las células de la granulosa, procesos directamente relacionados con la atresia folicular.

Con respecto al envejecimiento ovárico con la edad, se observó que en el estroma ovárico no hubo alteraciones en la longitud telomérica ni correlaciones con la edad, lo que podría deberse a una baja tasa de replicación celular en las células que lo componen. En ovocitos, se encontró un acortamiento de los telómeros en mujeres de mediana edad, lo que sugiere una menor calidad, hecho que podría estar relacionado con un aumento de las aneuploidías y fallos de fecundación que presentan las mujeres de mayor edad. Las células de la granulosa de los folículos primordiales y primarios evidenciaron un mayor acortamiento telomérico con la edad. Considerando que estas células constituyen el soporte directo de los ovocitos, y que están expuestas a los mismos factores exógenos y endógenos, la alteración de sus telómeros podría repercutir directamente en el desarrollo ovocitario. En las células de la teca, se observó un acortamiento similar al de las células de la granulosa primarias, pero sin correlación significativa con la edad, lo que podría explicarse por la baja tasa de división de estas células. En resumen, el envejecimiento ovárico relacionado con el acortamiento de los telómeros fue detectable en los ovocitos, células de la granulosa primordiales y primarias, y células de la teca, pero no en las células de la granulosa secundarias, posiblemente debido a la elevada actividad de la telomerasa en este estadio folicular.

Por tanto, los telómeros a nivel ovárico se acortan prematuramente con respecto a nivel sistémico. La comparativa de las longitudes de los telómeros en diferentes tipos celulares, demostraron que las células ováricas tenían longitudes teloméricas significativamente mayores que las células mononucleares de la sangre. Sin embargo, no se observó correlación significativa entre los telómeros de estas células y ninguno de los tipos celulares del ovario, lo que sugiere que la dinámica de los telómeros a nivel sistémico y ovárico es diferente. Estos hallazgos refuerzan la idea de que las células mononucleares de la sangre no son un

biomarcador telomérico adecuado del envejecimiento ovárico, como se ha descrito en estudios previos.

Con respecto a la telomerasa, enzima que se encuentra en células madre, células tumorales y células germinales, también es detectada en los ovarios humanos. Algunas células somáticas ováricas, como las células de la granulosa, también tienen actividad telomerasa, lo que permite mantener la longitud de los telómeros y la división celular continua durante la foliculogénesis. En el estudio, se detectó actividad telomerasa a todas las edades, pero sin diferencias significativas en la cuantificación. Aunque estudios previos indican que la actividad telomerasa disminuye con la edad, esto no pudo comprobarse en nuestro estudio. Esto puede deberse a que trabajamos con fragmentos ováricos, donde no se pudieron separar e identificar células específicas para determinar la actividad de esta enzima en cada población específica.

La presencia de fibrosis en el ovario afecta directamente a la función reproductiva y se asocia con menor fertilidad y menopausia prematura. Los resultados de este estudio mostraron un aumento de la fibrosis en mujeres perimenopáusicas en comparación con mujeres jóvenes, y una correlación positiva entre el área fibrótica y la edad. Aunque se observó fibrosis en el estroma ovárico relacionada con el envejecimiento, no se detectaron efectos a nivel de los telómeros en esta región. Además, la expresión de genes relacionados con la fibrosis (TGF-β1, COL1A1 y COL3A1) no evidenciaron cambios significativos con la edad. Dos hipótesis posibles para este hallazgo son la inflamación crónica asociada a la ovulación repetida y la distribución diferencial de los colágenos I y III en el ovario.

Por último, el envejecimiento ovárico fue estudiado desde una perspectiva proteómica para entender las modificaciones en el proteoma ovárico inducidas por la edad. El análisis funcional reveló que, en general, un mayor número de procesos biológicos se vieron alterados en las mujeres perimenopáusicas, en comparación con las jóvenes y las de mediana edad. Estos procesos incluían la respuesta al estrés celular, la regulación del metabolismo y la producción de energía, la regulación del ciclo celular y la homeostasis, el mantenimiento de la estructura celular e integridad, y la señalización celular. Se destacaron varias proteínas cuya expresión disminuyó en las mujeres perimenopáusicas. Entre estas proteínas, algunas estaban directamente relacionadas con la regulación de la señalización celular y su mediación por calcio, pudiendo verse alterados procesos claves para la fertilidad como la maduración de los ovocitos. También se identificaron proteínas como LDHB, que está involucrada en la conversión de lactato a piruvato, cuya expresión baja está asociada con disfunción mitocondrial y envejecimiento ovárico.

A pesar de los cambios en la expresión proteica relacionados con la edad, no se encontraron alteraciones en los telómeros de todas las células ováricas, aunque sí en las células de la

granulosa primordiales y primarias, y en los ovocitos. En resumen, el envejecimiento ovárico está vinculado a alteraciones hormonales, acortamiento de telómeros y fibrosis, y el estudio subraya la importancia del mantenimiento de los telómeros para preservar la función ovárica. Los resultados destacan la necesidad de investigar terapias antioxidantes para mitigar el daño en los telómeros y mejorar los tratamientos de fertilidad relacionados con la edad.

2. Estudio de los parámetros teloméricos en los casos de baja reserva ovárica

En esta sección se analizó si una baja reserva ovárica, reflejada en bajos niveles de AMH, se asociaba con un mantenimiento deficiente de los telómeros en las diferentes poblaciones celulares ováricas independientemente de la edad. Se observó que no había alteraciones significativas en los telómeros de las células del estroma ovárico, ni a nivel sistémico en mujeres con AMH baja. En las células de la granulosa primarias no se encontraron cambios, mientras que en los ovocitos y células de la teca sí se registró una mayor proporción de telómeros cortos en mujeres con AMH baja del grupo de mediana edad, lo que sugiere un daño acumulado posiblemente debido al estrés oxidativo. Este hallazgo resalta que los telómeros de los ovocitos y las células de la teca en mujeres con baja reserva ovárica muestran un acortamiento, lo cual podría estar relacionado con el estrés oxidativo y la baja actividad telomerasa en estas células. Sin embargo, en las células de la granulosa de folículos primordiales y secundarios, no pudieron extraerse conclusiones sólidas. El motivo residió en que al compararse las medias de edad de las mujeres del grupo de mediana edad con alto y bajo valor de AMH en las que se identificaron folículos en este estadio, las diferencias en esta variable fueron estadísticamente significativas. Por este motivo, los resultados teloméricos podrían estar influenciados por una diferencia en la edad, y no en el valor de AMH.

En resumen, aunque no se encontró una relación clara entre baja reserva ovárica y alteración de los telómeros en todos los tipos celulares, el acortamiento de los telómeros en ovocitos y células de la teca podría reflejar un daño celular más pronunciado en mujeres con baja reserva ovárica.

3. Impacto del embarazo en la dinámica telomérica ovárica

En esta sección, se investigó si el embarazo afectaba a la dinámica de los telómeros en mujeres, dada la variación hormonal y fisiológica que ocurre durante este proceso. Aunque el embarazo provoca una disminución de la AMH debido a la supresión temporal de la función ovárica, no se observaron cambios significativos en los parámetros de telómeros a nivel sistémico. Sin embargo, en los ovarios, se detectó un acortamiento de los telómeros en ovocitos y células de la teca, especialmente en mujeres jóvenes embarazadas. Este acortamiento podría ser causado por factores relacionados con el embarazo, como el estrés

oxidativo y metabólico. Es por este motivo que el embarazo se ha establecido como un modelo de envejecimiento en publicaciones científicas previas.

Se concluye que, aunque el acortamiento de los telómeros durante el embarazo es detectable, su reversibilidad postparto aún necesita ser investigada más a fondo.

4. Impacto del COVID-19 en la reproducción y la ruta telomérica

Por último, se investigó el impacto potencial de la COVID-19 en la biología de los telómeros en células somáticas ováricas, asociadas con el envejecimiento y la insuficiencia ovárica. Se encontró que, en mujeres que sufrieron COVID-19 leve, la longitud telomérica de las células de la granulosa y mononucleares de sangre periférica no se vio alterada, lo que sugiere que la enfermedad no afecta significativamente a la biología de los telómeros en estos casos. Sin embargo, en mujeres con COVID-19 grave, se observó un acortamiento de los telómeros en las células de la granulosa. En términos de fertilidad, los resultados reproductivos fueron similares entre los grupos control y COVID-19 leve, pero la tasa de maduración de ovocitos fue más baja en el grupo COVID-19 grave, lo que podría reflejar un impacto en etapas tempranas del desarrollo folicular. Estos hallazgos sugieren que la COVID-19 grave puede afectar la maduración folicular, pero la vacunación no tiene efectos adversos sobre los resultados reproductivos como han demostrado estudios posteriores en población con este perfil. También se destacó el posible papel de los telómeros largos en la maduración folicular, ya que la longitud telomérica de las células de la granulosa se correlacionó positivamente con la tasa de maduración de ovocitos.

En resumen, el estudio sugiere que la COVID-19 no afecta significativamente a la biología de los telómeros ni a los resultados reproductivos, excepto en casos graves.

CONCLUSIONES

Las conclusiones extraídas de los resultados del Proyecto 1 fueron:

1) Entre las hormonas estudiadas en las mujeres reclutadas para el Proyecto 1, los niveles de AMH y estradiol disminuyeron a medida que la edad aumentaba, mientras que en la FSH y la LH se produjo un descenso de sus niveles ligado al envejecimiento.
2) Nuestros resultados mostraron que la longitud de los telómeros de los ovocitos durante las fases de foliculogénesis estudiadas no cambió. La longitud telomérica media de las células de la granulosa aumentó en los primeros estadios de la foliculogénesis. En las células de la teca este parámetro permaneció estable en los estadios foliculares primario y secundario analizados.
3) La longitud telomérica media de los ovocitos fue menor en las mujeres de mediana edad en comparación con el grupo más joven. La longitud telomérica media de las

células de la granulosa disminuyó con la edad en los folículos primordiales y primarios, y se mantuvo sin cambios en los folículos secundarios. Los telómeros de las células de la teca fueron más cortos en el grupo de mujeres de mayor edad analizado en este trabajo. La longitud telomérica media del estroma ovárico se mantuvo constante en los distintos grupos de edad.

4) Se detectó actividad telomerasa en los fragmentos ováricos de mujeres pertenecientes a todos los grupos de edad, siendo similares en todos los grupos de edad.
5) Las mediciones de la longitud de los telómeros en muestras de células mononucleares de la sangre periférica de mujeres incluidas en el estudio 1 mostraron un desgaste de los telómeros relacionado con la edad, notable en el grupo de mayor edad, y una acumulación de telómeros cortos asociada a la edad, reforzando que el desgaste de los telómeros es un marcador fidedigno del envejecimiento. Sin embargo, nuestros resultados sugirieron que los parámetros teloméricos de estas células no pueden ser utilizados como biomarcador del envejecimiento ovárico.
6) Los porcentajes del área fibrótica mostraron un incremento significativo en el ovario de mujeres perimenopáusicas, y una correlación positiva estadísticamente significativa con la edad. Sin embargo, la expresión de los genes TGF-β1, COL1A1 y COL3A1 no varió con la edad en las muestras de ovario analizadas. El análisis proteómico evidenció un mayor número de procesos biológicos alterados en el grupo de mayor edad. Estos procesos estaban relacionados con el estrés y el daño biológico, el metabolismo y la producción de energía, el ciclo celular y la homeostasis tisular, la estructura e integridad celular, y el proceso de señalización celular.
7) La longitud telomérica media sistémica no varió en función de los valores de AMH en ninguno de los grupos de edad estudiados. La longitud telomérica media no mostró diferencias en los distintos tipos celulares ováricos según el nivel de AMH en ninguno de los grupos estudiados, excepto en el porcentaje de telómeros cortos en ovocitos de mujeres de mediana edad, con un incremento de este parámetro en el grupo de menor AMH. Las células de la teca mostraron una menor longitud telomérica en las mujeres de mediana edad con un nivel bajo de AMH.
8) El embarazo no afectó a la longitud media de los telómeros en las células mononucleares de sangre periférica y en las células ováricas estromales. Sin embargo, el mantenimiento de los telómeros se vio afectado en los ovocitos de mujeres jóvenes y de mediana edad embarazadas. En concreto, la longitud media de los telómeros de las células de la granulosa procedentes de folículos primordiales y primarios, y de las células de la teca fue menor en las mujeres jóvenes embarazadas

que en las mujeres no embarazadas de la misma edad en el momento del embarazo analizado.

Las conclusiones extraídas de los resultados del Proyecto 2 fueron:

9) La longitud de los telómeros fue similar en las células de la granulosa y en las células mononucleares de sangre periférica de los casos leves de COVID-19 y los controles. Sin embargo, en los casos graves de COVID-19, la longitud media de los telómeros fue inferior en comparación con los controles.
10) El número total de ovocitos recuperados tras la estimulación ovárica y la tasa de maduración de los ovocitos en los casos de COVID-19 y grupo control fueron similares. Sin embargo, los casos graves de COVID-19 mostraron una tasa de maduración ovocitaria inferior a la de los controles.
11) Existió una correlación positiva estadísticamente significativa entre la longitud media de los telómeros de las células de la granulosa y la tasa de maduración de los ovocitos en los individuos del grupo control. Esta correlación no se observó en los casos de COVID-19.

INTRODUCTION

1 INTRODUCTION

1.1 Reproductive senescence in women

Reproductive senescence refers to the biological process that marks the end of a woman's reproductive capacity. It is mainly associated with menopause, which typically occurs at the mean age of 50 years (Broekmans et al., 2004, Faddy et al., 1992, Faddy and Gosden, 1996). This process involves a progressive decrease in ovarian reserve and hormonal function of the ovaries, leading to the disappearance of menstruation and the inability to conceive naturally.

1.1.1 The ovary

The ovaries are the central organs of the female reproductive system. Two primary functions are attributed to these organs: the production of sex hormones and the development of oocytes. Firstly, the ovaries produce essential hormones that are crucial for the establishment and maintenance of the female phenotype, as well as hormonal support for the progression of pregnancy (Adashi, 1994). Secondly, they are the source of mature and competent oocytes for fertilization and subsequent embryo development. This occurs due to the sequential processes of oogenesis and folliculogenesis (Rimon-Dahari et al., 2016).

Anatomically, the ovaries are two oval-shaped organs, approximately the size of an almond, located in the pelvic cavity on either side of the uterus, in the lower abdomen. They are connected to the uterus by the mesovarium, the broad and ovarian ligament, and to the lateral abdominal wall by the suspensory ligament (Rendi et al., 2012). Histologically, the ovary is a highly heterogeneous organ in which different cell types with essential roles in female reproductive function coexist (Richards and Pangas, 2010). The primary cell is the oocyte, which is directly surrounded by granulosa cells. All these cells constitute the functional unit of the ovary, known as the ovarian follicle. The ovarian follicles are located in the organ's periphery, in one of the principal compartments, the ovarian cortex region, which is covered with a superficial single layer of cells known as the epithelium and the tunica albuginea (Wagner et al., 2020). The other primary compartment is the central region of the ovary, known as the medulla. This area consists mainly of blood vessels and nerves (Blaustein, 1982). However, considering the ovary as a whole, we can refer to ovarian stroma as all the components of the ovary, excluding the ovarian follicles. Thus, the ovarian stroma includes the vessels and nerves of the medulla, immune cells, lymphatic vessels, the ovarian surface epithelium, the tunica albuginea, stromal cells, and the extracellular matrix (Kinnear et al.,

2020). This heterogeneous stromal compartment is described under terms such as “ovarian interstitial stroma” (Hummitzsch et al., 2019).

1.1.1.1 Endocrinology

The ovary is indispensable for maintaining endocrine homeostasis in females, thanks to the hypothalamic-pituitary-ovarian axis (HPOA). The interaction between these structures generates a hormonal pattern that orchestrates the processes of oogenesis and folliculogenesis, as explained in detail later, throughout the menstrual cycle. Among the hormones and peptides involved are gonadotropin-releasing hormone (GnRH), follicle-stimulating hormone (FSH), luteinizing hormone (LH), estradiol (E2), a type of estrogen, progesterone (P4), and inhibin. From a reproductive perspective, the function of this axis becomes more prominent with the onset of puberty. However, two periods of axis activity preceding puberty are documented: during fetal life and the first postnatal months. FSH and LH are detected in the blood of female fetuses, exhibiting their maximum during mid-gestation and decreasing towards the end of pregnancy (Clements et al., 1976, Kaplan and Grumbach, 1976, Reyes et al., 1973). After birth, there is again an increase in FSH and LH, reaching a maximum at 3 months of age. Subsequently, in females, LH levels decrease, while FSH levels remain elevated for a more extended period. During the reactivation of the HPOA, a period known as mini-puberty, estradiol levels also increase in girls. However, these levels fluctuate until the second year of life. Although the specific functions of these early periods of axis activation are not yet defined, it is established that they play a key role in the reproductive physiology of the individual (Kuiri-Hänninen et al., 2014).

With the onset of puberty, typically at around 12.25 years of age, females experience their first menstruation, known as menarche (Biro et al., 2018). This fact is a sign of sexual maturation in females. It implies the reactivation of the HPOA, resumption of folliculogenesis and oogenesis processes, and the establishment of menstrual cycles. From this moment on, the arcuate nucleus of the hypothalamus synthesizes and produces the decapeptide GnRH (Figure 1), which is secreted into the portal circulation of the pituitary gland (Guillemin, 1967, Schally et al., 1971). In humans, three types of GnRH have been described, GnRH-I, being responsible for the secretion of the pituitary gonadotropins FSH and LH (Yao et al., 2011), GnRH-II, with a role in peripheral tissues such as the endometrium, breast, and ovaries (Cheon et al., 2001, Leung et al., 2003), and finally GnRH-III, whose role is not yet well defined (Yahalom et al., 1999). GnRH-I is released into the portal circulation in a pulsatile manner, characterized by a lifespan of only a few minutes. The frequency of the GnRH release pulse varies, and continuous secretion will suppress subsequent FSH and LH release (Yao et al., 2011, Belchetz et al., 1978, Haisenleder et al., 1991).

It is necessary to examine the menstrual cycle to study hormonal patterns and their effects at the ovarian and uterine levels. This can be divided into three phases (Figure 1): proliferative or follicular phase, ovulation, and secretory or luteal phase, depending on whether we refer to changes in the uterus or the ovaries. Its duration, from the onset of menstrual bleeding to the onset of the next menstruation, is 25-30 days (Bull et al., 2019).

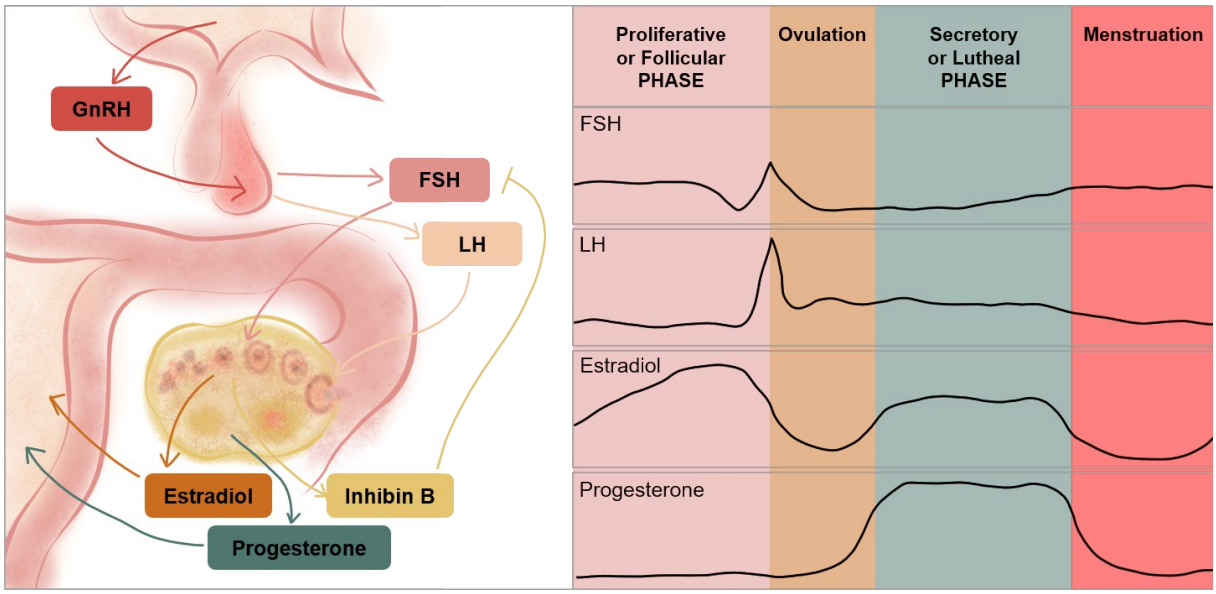


Figure 1. Hypothalamic-pituitary-ovarian axis and hormone levels during menstrual cycles.

During the menstrual cycle, GnRH from the hypothalamus stimulates the release of FSH and LH from the pituitary gland. FSH promotes follicular growth and estradiol production, which peaks just before ovulation. LH surge triggers ovulation, and after ovulation, the corpus luteum secretes progesterone, which prepares the uterus for pregnancy. Inhibin inhibits FSH release, preventing the maturation of additional follicles during the luteal phase. Self-created image.

During the first proliferative phase, a cohort of ovarian follicles is recruited for growth, and a dominant follicle is selected from among them. This follicular growth occurs due to a gradual increase in FSH production, which is caused by the adenohypophysis. FSH is a glycoprotein characterized by a half-life of several hours (Besecke et al., 1996, Weiss et al., 1995). In turn, the granulosa cells of these growing follicles increase their production of estrogen and inhibin B. Estrogens will promote uterine proliferation of the endometrial lining (Yu et al., 2022). Inhibin, specifically inhibin B, inhibits FSH secretion in the anterior pituitary (Bicsak et al., 1986). In response to this prolonged exposure of the adenohypophysis to estrogens, the adenohypophysis releases LH (Young and Jaffe, 1976). This hormone is a glycoprotein that is released gradually, and just before ovulation, its levels increase sharply, triggering ovulation during the menstrual cycle. Ovulation, understood as the release of mature oocytes from a Graafian follicle, occurs after this LH peak (Pauerstein et al., 1978). Thanks to currents of attraction, the oocyte enters the fallopian tubes, where it awaits fertilization by the sperm. After

ovulation, the secretory phase begins. This phase at the ovarian level is characterized by the fact that the granulosa cells of the follicle that has released the oocyte start the process of luteinization to form the corpus luteum. The corpus luteum is responsible for secreting progesterone, a steroid hormone required for implantation, endometrium preparation, and maintaining early pregnancy (Duncan, 2017). The endometrial lining of the uterus undergoes a transformation from proliferative to secretory in response to the increase in progesterone levels. The endometrium undergoes a morphological transformation known as decidualization, a necessary process for establishing a pregnancy (Brar et al., 1997). From this moment on, depending on whether pregnancy occurs, the corpus luteum will maintain its function as a source of progesterone until it is replaced by the placenta (Tuckey, 2005), or luteolysis will occur. This process involves the degeneration of the corpus luteum, which then becomes known as the corpus albicans. As a result, progesterone production ceases, the endometrium detaches, and menstrual bleeding occurs (Morales et al., 2000). Menstrual cycles follow one another throughout a woman's reproductive life, from menarche to menopause.

1.1.1.2 Oogenesis and folliculogenesis

The processes of oogenesis and folliculogenesis, both essential in the formation and production of the female germline, were extensively studied in animals such as mice (Ginsburg et al., 1990, Pepling and Spradling, 2001), primates (Butler and Juma, 1970), cattle (Erickson, 1966, Silva-Santos et al., 2011), or pigs (Bielanska-Osuchowska, 2006). The study of these processes in humans has many limitations because: (1) part of the processes occurs during embryo development, and (2) their culmination is in the adult ovary. In other words, collecting human ovarian samples to study the molecular mechanisms involved would be necessary. Because this organ is so valuable to women, obtaining these samples is exceedingly challenging for ethical reasons as well; even a small biopsy may be problematic. Motivated by these reasons, many studies attempted to replicate the process of gametogenesis in vitro (Yamashiro et al., 2018, Sasaki et al., 2015, Eguizabal et al., 2009).

1.1.1.2.1 Oogenesis

In early embryonic development, a cell population known as primordial germ cells (PGCs) emerges. These cells initiate migration from the yolk sac to the genital or gonadal ridges (Kanamori et al., 2019, Richardson and Lehmann, 2010). The PGCs migration is possible thanks to their active locomotion, chemoattractant interactions, and associations with surrounding somatic cells (Pereda et al., 2006). During this migratory process, many PGCs remain arrested at the cell cycle's growth 2 (G2) phase (Seki et al., 2007). However, when these cells reach the gonadal ridges, they proliferate through successive mitosis (De Felici, 2013). Part of these PGCs differentiate into oogonias, a transition mediated by signaling with

different cytokines and proteins (De Felici, 2013, Overeem et al., 2021). The oogonia continue to divide mitotically (Figure 2), forming aggregates of cells, also known as germinal cysts or nests, until they reach approximately 7 million cells during the 5th month *post-conception* (*p.c.*) (Baker, 1963). In Baker's (1963) study, using fetal ovarian samples, the concomitant presence of oogonia and primary oocytes was observed from the 2nd month post-conception (p.c.) until the 7th month *p.c.* The oogonia enters meiosis without following a synchronous pattern, and primary oocytes are obtained after the first part of this meiotic division. They will be arrested in the diplotene stage (prophase stage of meiosis I) until puberty (DiVall and Radovick, 2008). The diplotene stage is characterized by the dissolution of the synaptonemal complex, which is crucial for the cross-linking between non-sister chromatids of homologous chromosomes and the formation of chiasmata, indicating the beginning of homologous chromosome separation (Garcia et al., 1987). From adolescence onwards, the primary oocytes resume meiosis. Therefore, the primary oocyte is characterized by profound transformations, including the appearance of the zona pellucida, an increase in diameter, and the presence of the germinal vesicle (GV). GV refers to the oocyte's nucleus at prophase I, which plays an essential role in early embryonic development (Lefèvre, 2008). During the resumption of meiosis, the germinal vesicle breaks down (GVBD), the nuclear envelope dissolves, and the chromosomes become condensed (Calarco et al., 1972). Then, these homologous chromosomes are paired up at the metaphase plate. The primary oocyte at the metaphase I (MI) stage is observed to be larger and uniform, with a homogeneous granular ooplasm. In anaphase I, the homologous chromosomes are pulled toward the opposite poles of the cell, and telophase I occurs, completing the first part of meiosis in the primary oocyte (Trounson et al., 2001). In telophase I, there is no equal distribution of cytoplasm. Consequently, the first polar body (1PB) is released with minimal cytoplasm, and the main part of the cytoplasm remains in a larger secondary oocyte. During the second meiotic division, the secondary oocyte proceeds until it reaches metaphase II (MII), a stationary stage. The chromosomes are aligned along the cell's equator, and the oocyte exhibits a rounded shape, homogeneous and clear cytoplasm, the absence of the GV, and the presence of the 1PB. The oocyte in MII is mature and ready for fertilization. It remains meiotically sequestered in MII until fertilization occurs, at which time it again undergoes unequal cytokinesis, leading to the haploid second polar body (2PB) (Payne et al., 1997). When the oocyte is fertilized, the haploid maternal genome, known as the female pronucleus, fuses with the haploid male pronucleus of the sperm. A single diploid cell, known as a zygote, is formed. The zygote begins to divide by mitosis, giving rise to the stages of embryonic development.

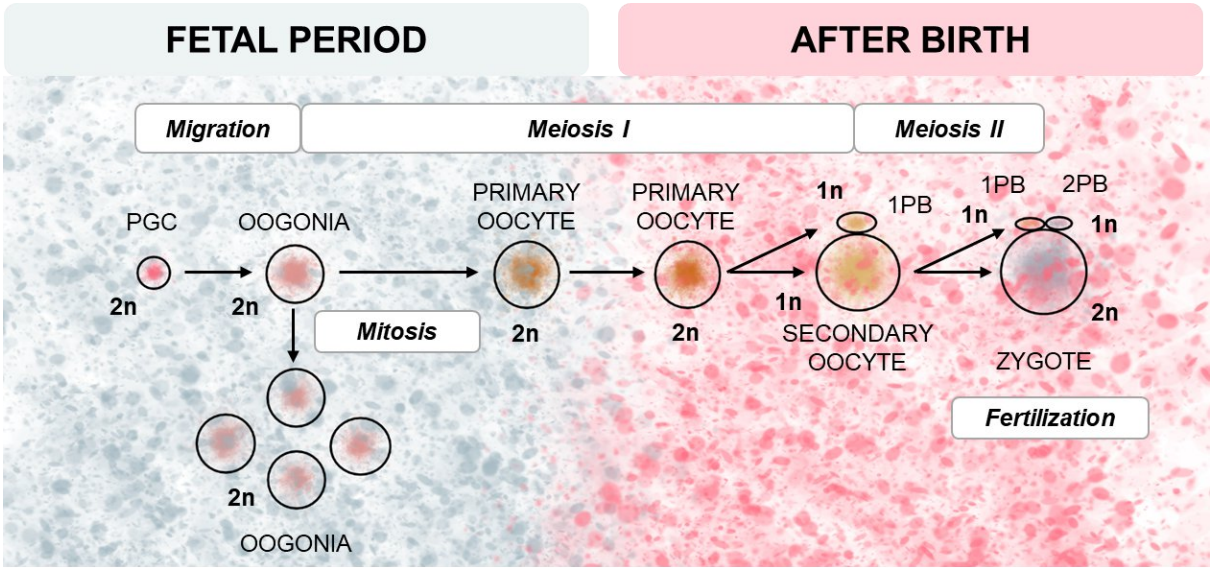


Figure 2. Oogenesis process.

During fetal development, primordial germ cells differentiate into oogonia, which undergo mitosis to increase in number. Oogonia then enter meiosis, becoming primary oocytes, which are arrested in prophase I. After birth, primary oocytes remain dormant until puberty. During ovulation, one oocyte completes meiosis I, forming a secondary oocyte (haploid, 1n) and the first polar body (also haploid). If fertilization occurs, the secondary oocyte completes meiosis II, extruding a second polar body (which is haploid) and forming a zygote (which is diploid, 2n). Self-created image.

1.1.1.2.2 Folliculogenesis

The culmination of oogenesis is not possible without the process of folliculogenesis, because both processes temporally overlap. Folliculogenesis (Figure 3) begins once the PGCs have migrated, established themselves in the ovarian cortex, and initiated mitotic divisions, resulting in the oogonia being grouped together to form a kind of nest. Somatic cells surround these structures, and they start to individualize when oogonia enter meiosis. The rupture of the germ cell nests involves the formation of primordial follicles (Wang et al., 2020). These follicles consist of a primary oocyte arrested at the diplotene stage of meiotic prophase I, enclosed by a layer of flattened somatic cells called pre-granulosa cells. In the primordial follicle stage, oocytes remain until they are recruited to resume meiosis, forming part of the quiescent follicular reserve of the ovary (Hansen et al., 2011). From the onset of puberty to menopause, various follicular recruitment processes occur, during which the follicles progress to more advanced stages (McGee and Hsueh, 2000). These recruitments can be divided into initial recruitment, cyclic recruitment, and final follicle selection. In the literature review published by McGee and Hsueh (2000), they propose a succession of two major recruitments in folliculogenesis, aiming to unify the published discrepancies about this process. They also compare folliculogenesis in humans and rats, providing an approximation of the duration of each step. However, there is not only controversy regarding the duration of each recruitment

but also which follicular stages are included within each recruitment. In general terms, initial gonadotropin-independent recruitment spans the activation of primordial follicles to their evolution into primary follicles, whereas cyclic gonadotropin-dependent recruitment encompasses the progression from secondary follicles to ovulation. In this cyclic recruitment process, the final step involves the selection of the dominant follicle that will ultimately ovulate (McGee and Hsueh, 2000).

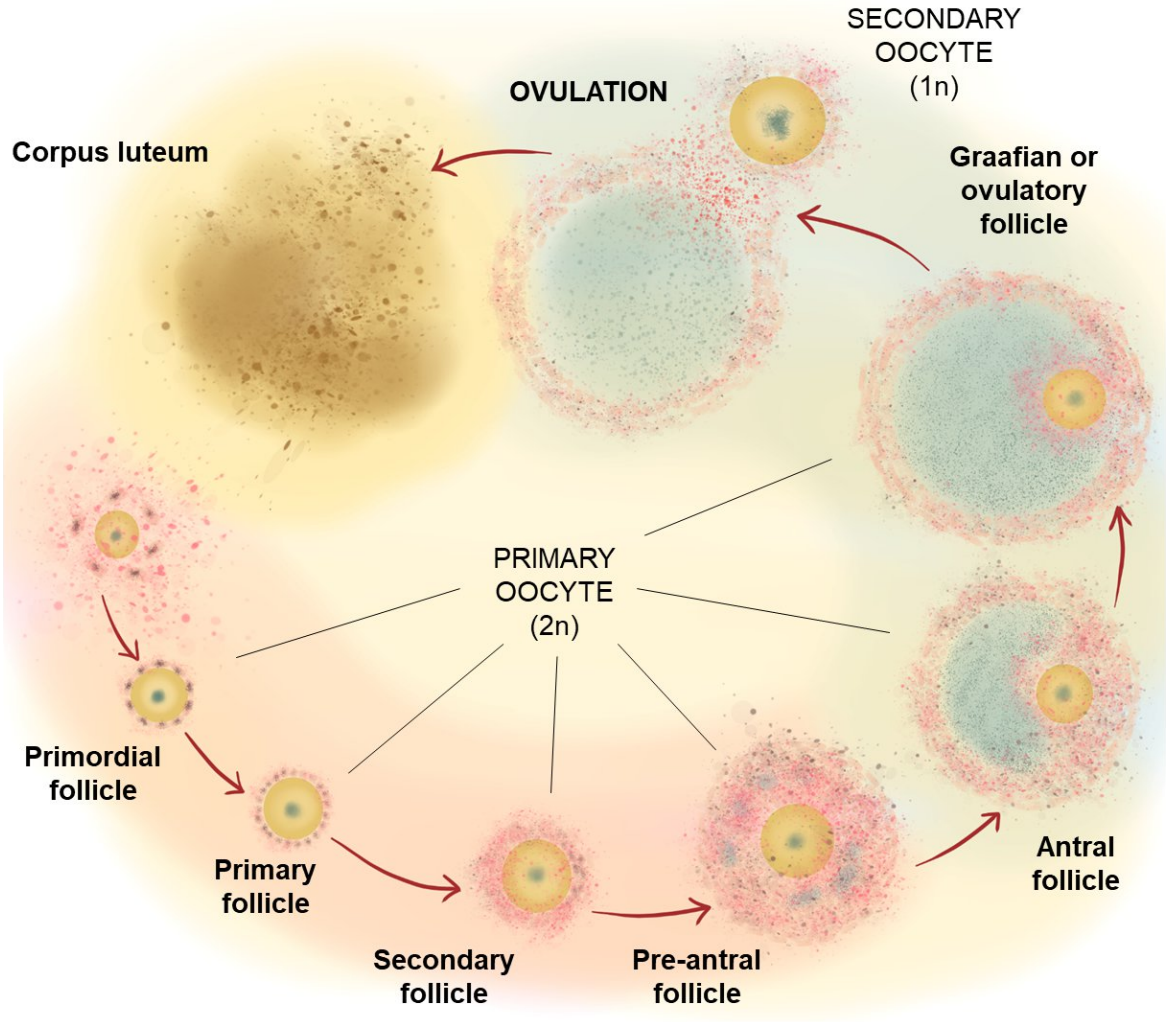


Figure 3. Folliculogenesis process.

Folliculogenesis begins with primordial follicles, consisting of an oocyte surrounded by a single layer of granulosa cells. These follicles mature into primary follicles, then secondary follicles as granulosa cells multiply. As development continues, preantral follicles form, followed by antral follicles, which develop fluid-filled cavities. The largest, the Graafian follicle, is ready for ovulation, where the oocyte is released. After ovulation, the remaining follicle cells form the corpus luteum, which secretes progesterone to support early pregnancy. Self-created image.

The pre-granulosa cells from primordial follicles undergo a morphological change from flattened to cuboidal, becoming known as granulosa cells (GCs) (Dompe et al., 2021). The zona pellucida then appears (Törmälä et al., 2008), which covers the oocyte for the remainder

of folliculogenesis. The oocyte surrounded exclusively by a layer of cuboidal granulosa cells is known as the primary follicle. Because it is a follicular transition process between the primordial and primary stages, many published works refer to the pre-granulosa cells as granulosa cells directly. In response to the FSH increase, the GCs proliferate mitotically to form multiple layers around the oocyte and recruit an additional layer of theca cells (TCs) that initially belonged to the surrounding stroma (Honda et al., 2007, Liu et al., 2020b). This stage is known as the secondary follicle. It is essential to note that throughout the entire process, bidirectional communication occurs between the oocyte and the GCs via the local production of growth factors (Monniaux, 2016) and direct contact facilitated by transzonal projections and gap junctions (Motta et al., 1994). Up to this point, these follicular stages are encompassed in the preantral phase of folliculogenesis. In the next phase, the antral phase, fluid-filled cavities begin to form between the GCs. All these cavities coalesce into a larger cavity called the follicular antrum (Gutierrez et al., 2000), which endows the follicle with the category antral follicle (AF). The GCs closest to the oocyte are called cumulus cells (CCs), which are noted for their ability to secrete hyaluronic acid (HA) (Salustri et al., 1990, Salustri et al., 1992, Suchanek et al., 1994). HA is a non-sulfated glycosaminoglycan whose accumulation in the oocyte-cumulus complex (COC) matrix induces its expulsion or mucification, which is crucial for the capture of the oocyte by the fimbriae of the oviduct. The follicular antrum gradually enlarges until the follicle develops into a Graafian or ovulatory follicle stage. However, it is essential to note that in the human case, many of the follicles degenerate into atretic follicles, and only one culminates in folliculogenesis (Rimon-Dahari et al., 2016). With ovulation, the COC, formed by the fertilizable oocyte and the cumulus cells surrounding it, is released, leaving the rest of the cells that were part of the follicle in the ovary. These cells then differentiate into a structure known as the corpus luteum. As described in the previous section on ovarian endocrinology, this structure has an endocrine function in producing progesterone, a role that is replaced by the placenta during pregnancy (Stocco et al., 2007).

1.1.1.3 Ovarian reserve

Reproductive senescence in women, marked by menopause, leads to depletion of ovarian oocytes and degenerative changes at the endocrine level. In the middle of the 20th century, the predominant principle in reproductive biology was established, which determines that female reproductive capacity is defined by the number of primordial follicles developed in the ovary during the fetal period. In other words, the follicular cohort in the ovary is finite and cannot be recovered if it is depleted (Zuckerman, 1951).

The follicular cohort is synonymous with an ovarian reserve. It is a concept that refers to the number of primordial follicles in a woman's ovary and, thus, the number of oocytes. As these follicles are recruited, activated, and developed, this reserve is depleted (Wallace and Kelsey,

2010). The hypothesis that women are born with a finite reserve of oocytes was first put forward during the 1920s. Based on oocyte counts from the ovaries of birds of reproductive age, Pearl and Schoppe (1921) stated that the number of oocytes remained constant throughout an individual's lifetime (Pearl and Schoppe, 1921). However, it was not until the publication of Zuckerman's article in 1951, which reviewed the number of oocytes in different species of mammals (including humans) at various ages, that it was concluded the number of oocytes decreased with increasing age (Zuckerman, 1951). Subsequent studies reached the same conclusion in other species as mice (Peters et al., 1962).

In quantitative terms, several episodes of follicular loss occur in women (Figure 4). In a study carried out by Baker (1963) on fetal, neonatal, and postnatal ovaries, three major waves of germ cell degeneration were established, affecting oogonia undergoing mitosis, oocytes at the pachytene stage, and oocytes at the diplotene stage (Baker, 1963). They concluded that at 2 months *p.c.* the number of germ cells is 600,000, which increases to a maximum at 5 months *p.c.* with approximately 7 million. Until birth, there is degeneration of many germ cells so that at birth, it is estimated that there are approximately 800,000 - 1,000,000 primordial follicles in the quiescent stage (Baker, 1963, Block, 1953, Forabosco and Sforza, 2007). However, this number decreases, with a total of about 300,000 recorded at 7 years of age (Baker, 1963). With the onset of puberty, when there are an average of 200,000 follicles in the ovary, the recruitment of follicles destined for ovulation begins (Block, 1952). The decline in the number of follicles is constant, but it accelerates after the age of 38 years when there are approximately 25,000 remaining follicles. When the number of primordial follicles in the ovary reaches approximately 1,000 at the age of 50, menopause is established (Faddy et al., 1992, Faddy and Gosden, 1996).

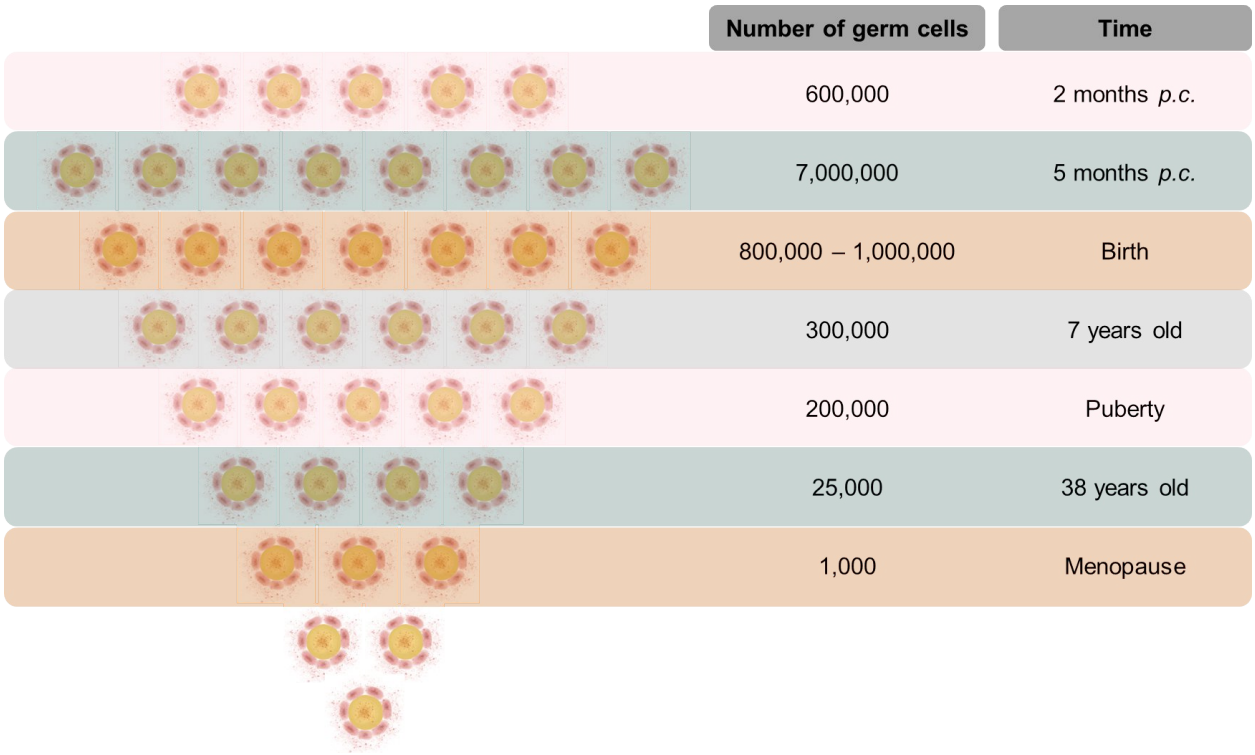


Figure 4. Ovarian reserve declines during a woman's life.

The ovarian reserve begins to form approximately 2 months after conception, with the development of primordial follicles in the ovaries. By 5 months post-conception, the number of follicles reaches its peak, typically numbering several million. At birth, the ovarian reserve is estimated to be around 1 million follicles, and by age 7, it further declines to approximately 300,000. During puberty, this reserve continues to diminish, with approximately 200,000 follicles remaining by the onset of menstruation. By age 38, the rate of decline accelerates, leading to menopause, when ovarian reserve is exhausted, and menstruation ceases. Self-created image.

Currently, in clinical evaluations, it is not possible to determine the exact number of primordial follicles present in the ovaries, nor their rate of loss and/or activation. Knowing this data would be of great help in both the clinical and personal context of the patient. Firstly, it would enable medical staff to offer more personalized treatment and advice to patients. On the other hand, women would be able to make earlier decisions about fertility preservation with a view to their reproductive future. However, an indirect approximation of ovarian reserve can be obtained through different clinically accepted methods, including basal FSH levels, antral follicle count (AFC), and measurement of serum anti-Müllerian hormones (AMH).

1.1.1.3.1 FSH

In 1988, it was first suggested that the FSH value could be a predictive parameter of ovarian reserve (Muasher et al., 1988). The adenohypophysis produces FSH, and its secretion stimulates the production of estradiol and inhibin B in the ovaries. When estradiol and inhibin levels are very high, FSH secretion in the pituitary is inhibited (Speroff and Fritz, 2012). Therefore, since this test is based on the inhibition of FSH secretion in the adenohypophysis

by ovarian factors, if FSH levels are measured on day 3 of the menstrual cycle (during the proliferative phase), this negative feedback has not yet occurred. However, if FSH levels are elevated, this implies that ovarian hormone production is very low, and negative feedback from the axis does not occur. Therefore, the number of ovarian follicles is reduced (Scott Jr et al., 1990, Toner et al., 1991). For this reason, simultaneous measurement of both FSH and estradiol is recommended, as high FSH levels, combined with low estrogen production, would be indicative of low ovarian reserve (Grisendi et al., 2014). Elevated values of this hormone have also been associated with a deficient ovarian response after stimulation in in vitro fertilization (IVF) treatments (Esposito et al., 2002, Roberts et al., 2005).

The measurement of FSH is performed by enzyme-linked immunosorbent assay (ELISA), and results are obtained quickly. However, limitations include dependence on HPOA regulation and significant variability of FSH levels throughout the menstrual cycle and even between cycles (Kwee et al., 2004, Scott Jr et al., 1990).

1.1.1.3.2 AFC

The AFC refers to the sum of follicles measuring between 2-10 mm in diameter in both ovaries, whose potential as a parameter for estimating ovarian reserve was evidenced in 1996 (Reuss et al., 1996). Therefore, this technique is based on the direct counting of the number of developing antral follicles, i.e., those in the early stages of maturation but which have not yet become dominant follicles that will ovulate. As with FSH, this variable is also used in predicting poor ovarian response to ovarian stimulation during IVF cycles (Broer et al., 2013, Reuss et al., 1996).

This counting is performed by transvaginal ultrasound during the early follicular phase (days 2-4) of the menstrual cycle by a gynecological expert. It is a straightforward technique to perform, yielding immediate results. However, it has several limitations (Broekmans et al., 2010, Fleming et al., 2015). The main limitation is its great variability at different levels. This may be due to the technology used for the ultrasound, the professional performing it, or the fact that it depends on the menstrual cycle. Furthermore, its accuracy is also compromised in overweight or obese women, where the image obtained is less clear and precise (Paladini, 2009). Currently, the AFC is a technique routinely used in clinical practice to assess ovarian reserve along with the AMH value (Fleming et al., 2015, Tal and Seifer, 2017). It is essential to note that none of these parameters provides information about oocyte quality.

1.1.1.3.3 AMH

AMH was first suggested as a marker of ovarian reserve in 2002, as a decrease in its levels was detected when other markers of ovarian aging, such as AFC or FSH, were not altered (de Vet et al., 2002). Additionally, earlier studies in mice deficient in the AMH gene demonstrated

accelerated follicular atresia (Durlinger et al., 1999). Its main function during fetal development is the induction of Müllerian duct regression in male sexual differentiation (Behringer et al., 1994, Münsterberg and Lovell-Badge, 1991). However, in the adult ovary, where it is produced by GCs of pre-antral follicles and small antral follicles, it plays two main roles (Van Houten et al., 2010). First, it inhibits the initial recruitment of primordial follicles. Second, it decreases the responsiveness of follicles to FSH. Both of these complementary functions lead to slowing follicle maturation, maintaining a follicular reserve. For this reason, in mice deficient in the AMH gene, an early depletion of primordial follicles in their ovaries was evidenced. With age, the number of follicles decreases, and consequently, the production of AMH also decreases (Durlinger et al., 1999). For this reason, this hormone serves as a reliable marker of ovarian reserve. Furthermore, unlike other female hormones, its levels remain stable throughout the menstrual cycle (Hehenkamp et al., 2006, La Marca et al., 2006, Tsepelidis et al., 2007), and the values are not altered by taking contraceptives (Streuli et al., 2008). It has also been used as a predictor of ovarian response after stimulation in IVF cycles (Broer et al., 2013), or as an additional indicator of polycystic ovary syndrome (Tal et al., 2014). Some studies attempt to directly associate the AMH value with the pregnancy rate (Iliodromiti et al., 2014, Tal et al., 2015). However, a lower AMH is associated with a reduced chance of conceiving, likely due to lower ovarian reserve (Nelson et al., 2024).

It is measured by ELISA assay. However, great variability is detected between assays and even between laboratories for the values of this hormone (Broer et al., 2014, Nelson et al., 2015, van Helden and Weiskirchen, 2015). Still, several studies have analyzed the ranges of AMH values at different age intervals. These studies are summarized in the literature review by Tal & Seifer (2017). The values expressed in ng/mL for age at five-year intervals are: 3.0 for 25 years, 2.5 for 30 years, 1.5 for 35 years, 1 for 40 years, and 0.5 for 45 years (Tal and Seifer, 2017). There is a positive correlation between AMH and AFC (Nardo et al., 2007), and a negative correlation of this hormone with age (Hansen et al., 2011).

1.1.2 Current landscape: female infertility and assisted reproduction technologies

Infertility is a condition that affects many couples who wish to conceive and is defined as the inability to achieve pregnancy after one year of unprotected intercourse (Cox et al., 2022). Infertility can have a variety of causes, including problems in both men and women (Agarwal et al., 2021). Specifically, female infertility refers to those factors that affect a woman's reproductive capacity. One of the factors contributing to the increase of female infertility in recent decades is the delay in childbearing, which is becoming increasingly frequent due to work, educational, and social demands, as well as the desire of many women to achieve

personal and professional stability before having children (Mathews and Hamilton, 2016, No, 2014, Osterman et al., 2022). This delay has significant biological implications, as ovarian aging directly affects egg quality and quantity, decreasing the likelihood of conception as women age, particularly after the age of 35 (Garcia et al., 2018, Schmidt et al., 2012).

Infertility related to ovarian aging is one of the main reasons why many women turn to assisted reproductive technologies (ART), such as artificial insemination or IVF (Chiware et al., 2021, Choi et al., 2022). These treatments aim to overcome the biological barriers that naturally prevent conception. Gynecology professionals encounter a wide range of situations and patient profiles in those who visit the assisted reproduction clinic. In some cases, these are described and diagnosed pathologies that explain infertility problems such as endometriosis (Saunders and Horne, 2021, Shan et al., 2023), polycystic ovarian syndrome (Escobar-Morreale, 2018), fallopian tube abnormalities (Pabuccu et al., 2011), among others. However, in other cases, the etiology is unclear or simply due to age-related deterioration of ovarian function.

One of the significant impacts of increasing age in women is the drop in ovarian reserve, which implies a poor ovarian response (POR) to ovarian stimulation treatments in IVF cycles. The European Society of Human Reproduction and Embryology (ESHRE) published the Bologna criteria in 2011. This classification aims to standardize the definition of poor ovarian responder (POR) and thereby homogenize the populations of patients with poor ovarian response (Ferraretti et al., 2011). A woman is classified as POR if she meets two of the following criteria: (1) advanced maternal age greater than or equal to 40 years, (2) fewer than 3 oocytes collected after a previous conventional ovarian stimulation protocol, and/or (3) abnormal ovarian reserve assessed by an AFC of less than 5-7 follicles or an AMH value below 0.5-1.1 ng/mL. However, these criteria are widely discussed, and one of the main reasons is that the woman's age is not explicitly considered a relevant factor (Younis et al., 2015, Reig et al., 2023). For this reason, and to obtain a more detailed and personalized classification that identifies patients with a worse reproductive prognosis and guides treatments more precisely, the POSEIDON (Patient-Oriented Strategies Encompassing Individualized Oocyte Number) criteria were published in 2016 (Alviggi et al., 2016). Using this new system, women predicted poor responders are classified into four groups: group I (younger, unexpected POR): <35 years old, AMH ≥1.2 ng/mL or AFC of ≥5, prior cycle with <10 MII retrieved; group II (older, unexpected POR): ≥35 years old, AMH ≥1. 2 ng/mL or AFC of ≥5, prior cycle with <10 MII retrieved; group III (younger, expected POR): <35 years old, AMH <1.2 ng/mL or AFC of <5; and group IV (older, expected POR): ≥35 years old, AMH <1.2 ng/mL or AFC of <5. This system, therefore, allows women with reproductive difficulties to be classified based on age, ovarian response, and number of eggs previously retrieved. The POSEIDON criteria emphasize the importance

of tailoring ART to the individual characteristics of each woman, enabling more effective and personalized strategies in the pursuit of pregnancy.

1.2 Biological aging: telomeres

1.2.1 Hallmarks of aging

In the last century, thanks to advances in public health and medicine, life expectancy has increased dramatically (Mathers et al., 2015). According to the Spanish National Institute of Statistics, the life expectancy in 2022 was approximately 80 years. However, aging is associated with an increase in the appearance of age-related diseases (Melzer et al., 2020), such as Alzheimer's (Liu et al., 2024), cardiovascular diseases (Qu et al., 2023), or cancer (Pilleron et al., 2022). Aging understood as a progressive degenerative process, is related to both cellular and molecular changes that lead to the functional deterioration of tissues and organs. López-Otin et al. (2013) described nine hallmarks of aging in mammals under the term “hallmarks of aging”: genomic instability, telomere attrition, epigenetic alterations, loss of proteostasis, deregulated nutrient-sensing, mitochondrial dysfunction, cellular senescence, stem cell exhaustion, and altered intercellular communication (López-Otín et al., 2013). In 2023, the same authors expanded the previously defined hallmarks to include disabled macroautophagy, chronic inflammation, and dysbiosis (Figure 5) (Lopez-Otin et al., 2023). All of them are interconnected and contribute to the aging process.

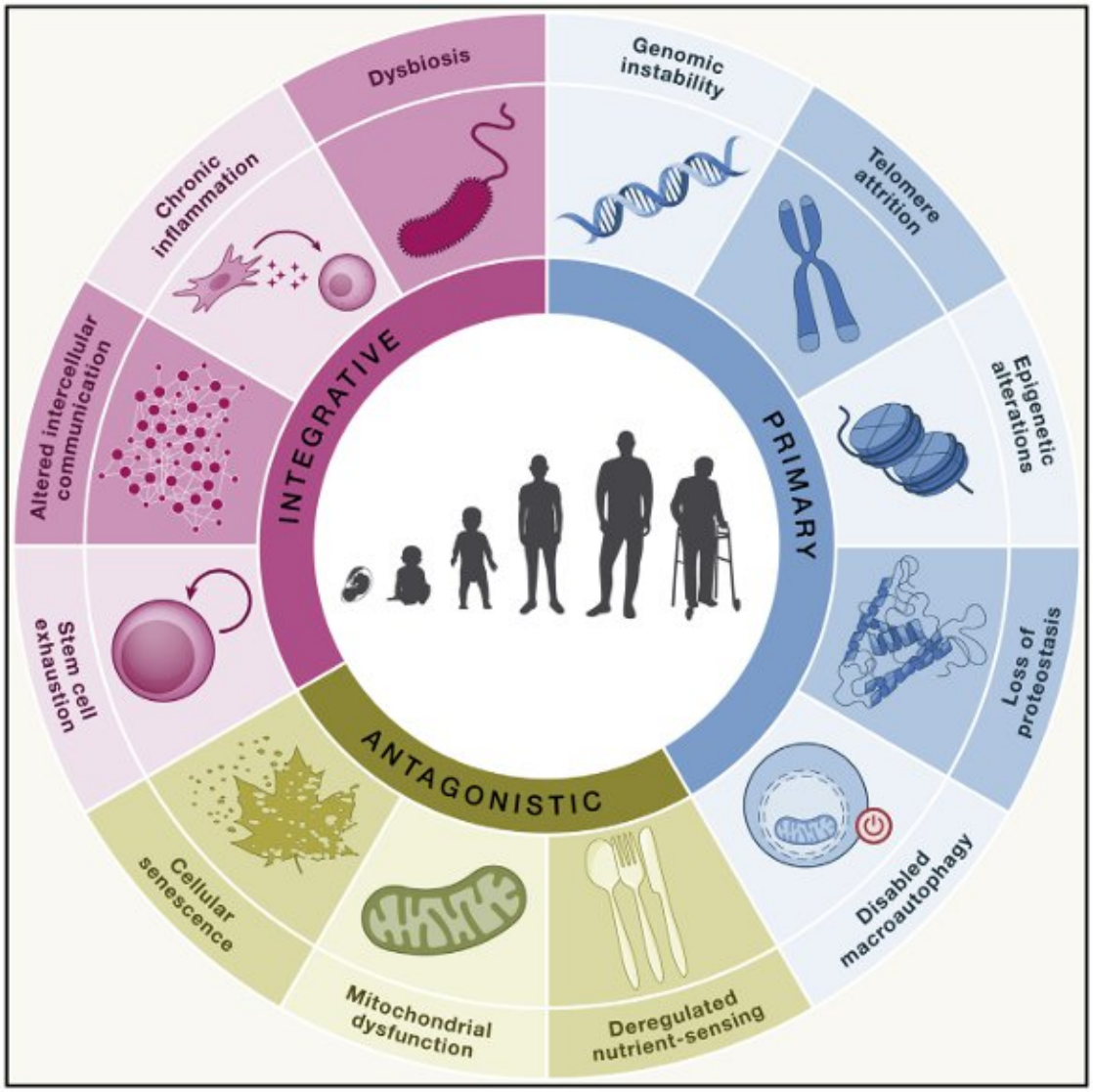


Figure 5. Hallmarks of aging.

This diagram showcases the 12 hallmarks of aging, a fascinating collection of biological changes that drive the aging process. These include genomic instability, telomere attrition, epigenetic alterations, loss of proteostasis, impaired autophagy, and mitochondrial dysfunction, among others. These hallmarks are categorized into three key groups: integrative, antagonistic, and primary, each reflecting distinct aspects of how our cells and systems deteriorate over time. The interplay between these factors—such as chronic inflammation and dysbiosis—paints a complex picture of aging at the molecular level. Figure from (Lopez-Otin et al., 2023).

Genomic instability increases with aging due to the accumulation of deoxyribonucleic acid (DNA) damage, which can be caused by internal factors such as errors in DNA replication or external factors such as radiation, toxins, or pathogens (Khazaei Monfared et al., 2023, Matsuda et al., 2024, Saini et al., 2016). This genetic damage can originate from mutations and failures in DNA repair (Blokzijl et al., 2016). Epigenetic alterations, such as histone modification (Rong et al., 2025), DNA methylation (Xiao et al., 2025), or post-transcriptional regulation (Jeon et al., 2024) can alter gene expression without modifying the DNA sequence.

These epigenetic modifications contribute to dysregulation of cellular processes and loss of repair capacity**.** Proteostasis, or the ability to maintain correct protein conformation and function, is impaired with age. Accumulation of misfolded or damaged proteins is more frequent due to a decrease in the efficiency of quality control mechanisms (Dalla Bella et al., 2021), such as the ubiquitin-proteasome system (Hoshino et al., 2024, Bernardo et al., 2024) and autophagy (Endicott, 2024, Bondy and Wu, 2024). In addition, mitochondrial dysfunction is a characteristic marker of aging, as mitochondria, which are responsible for generating energy in cells, lose efficiency, leading to an increase in the production of reactive oxygen species (ROS). These ROS contribute to cell damage and promote chronic inflammation, exacerbating oxidative stress, facilitating tissue fibrosis, and directly damaging DNA (Park et al., 2021a, Yang et al., 2021). Cellular senescence is a process in which cells stop dividing but remain metabolically active, secreting inflammatory factors, proteases, and profibrotic factors, contributing to the deterioration of surrounding tissues and fibrosis (Wang et al., 2025b). This problem is compounded by stem cell exhaustion, which limits tissue regeneration. This depletion is exacerbated by the accumulation of genetic and epigenetic damage, as well as chronic inflammation, which hinders tissue regeneration and favors the replacement of functional cells with fibrous tissue. As we age, alterations also occur in intracellular communications, such as signaling between cells through hormones, growth factors, and cytokines. Dysregulation of these signals can interfere with the ability of tissues to respond appropriately to damage. On the other hand, macroautophagy, a key cellular clearance process that eliminates waste, also declines with age. Lack of efficient autophagy contributes to the accumulation of waste products, misfolded proteins, and cellular damage, which intensifies oxidative stress and facilitates tissue fibrosis (Brakedal et al., 2022, Chen et al., 2015, Singh et al., 2022). Chronic inflammation is a prominent feature of aging, caused by the accumulation of senescent cells, cellular damage, and immune system dysfunction. Chronic inflammation perpetuates a cycle of damage and inappropriate repair. In addition, dysbiosis, characterized by an imbalance in the intestinal microbiota that leads to dysregulation in nutrient sensing, impairs the immune response and promotes systemic inflammation (Ghosh et al., 2022).

All these alterations linked to aging are considered hallmarks because they meet three main criteria: they appear over time, their accentuation accelerates the aging process, and therapeutic interventions could slow down, stop, or reverse aging (Lopez-Otin et al., 2023, López-Otín et al., 2013).

1.2.2 Telomere biology

As mentioned previously, one of the primary hallmarks of aging is telomere attrition (Lopez-Otin et al., 2023, López-Otín et al., 2013). The concept of telomere originated in the 1930s, when McClintock and Muller identified a structure at the ends of the chromosomes of maize (*Zea mays*) and *Drosophila melanogaster* that was crucial for preventing their fusion (Creighton and McClintock, 1931, Muller, 1938). Muller defined the term "telomere", which means "end part" in Greek (*telos* and *meros*). Subsequently, various studies and findings have clarified the function of these structures and the processes that maintain their dynamics. In 1961, it was discovered that human fetal cells had a limited replicative potential, known as the "Hayflick limit" (Hayflick and Moorhead, 1961, Hayflick, 1965). In the 1970s, the "end replication problem" was formulated, which explained how cell division leads to the loss of DNA at chromosomal ends (Olovnikov, 1973, Watson, 1972). This problem (Figure 6) refers to the fact that when a cell divides, the DNA does not completely replicate due to the double helix structure. During replication, both strands separate. One strand, known as the leading-strand, replicates continuously. In contrast, the other (lagging-strand) replicates in short fragments called Okazaki fragments that must subsequently be linked by a DNA ligase (Okazaki et al., 1968). At the end of the lagging-strand, there is not enough space to add an extra primer to initiate the replication of the last fragment. Consequently, in each replication cycle, a small part of the DNA at the chromosome end is lost. Therefore, considering that telomeres form the ends of chromosomes, they gradually shorten with each round of cell division.

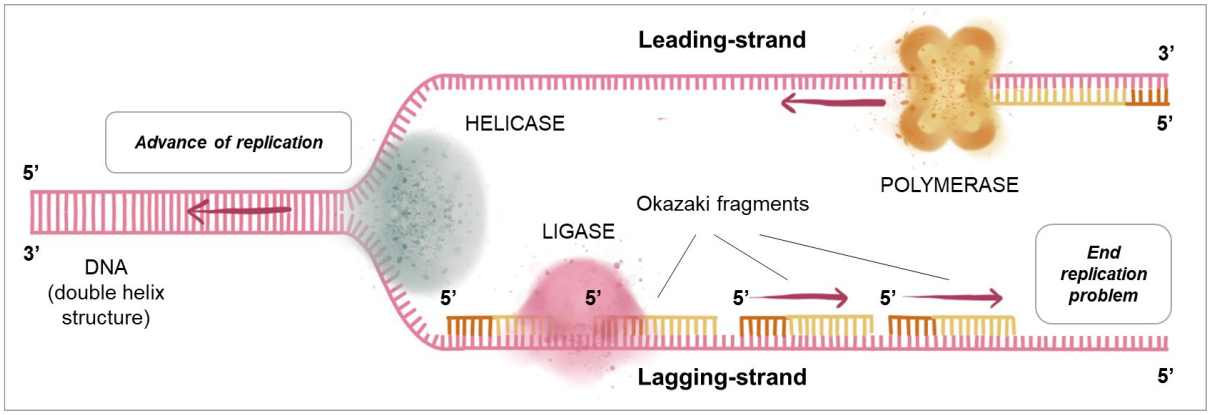


Figure 6. End replication problem.

The DNA end replication problem arises during DNA replication when the lagging-strand cannot be fully replicated at its ends. As helicase unwinds the DNA, polymerase synthesizes the leading-strand continuously, but the lagging-strand is made in short Okazaki fragments. Due to the directionality of DNA polymerase, the final RNA primer on the lagging strand cannot be replaced with DNA, leaving an unreplicated region. Ligase helps join Okazaki fragments, but the missing section at the end of the chromosome leads to telomere shortening with each replication. This shortening contributes to cellular aging and limits the number of times a cell can divide. Self-created image.

It was in 1978 when Blackburn and Gall sequenced the ribosomal DNA of *Tetrahymena thermophila*, discovering six nucleotide tandem repeats at the chromosomal ends (Blackburn and Gall, 1978). Specifically, in humans, telomeres consist of non-coding 5'-TTAGGG-3' repetitive sequences located at chromosomal ends. They are highly conserved sequences (Moyzis et al., 1988). These repetitive sequences form a loop at the end of each chromosome, known as a T-loop, where the 3' overhang end of one strand folds and hybridizes with the opposite strand. This structure is crucial in chromosome protection (Figure 7). Years later, telomere shortening was shown to be linked to cellular senescence, thus connecting telomeres to the aforementioned “Hayflick limit” (Harley et al., 1990).

1.2.3 Shelterin complex and telomerase

Telomeres are not only protected by this looped arrangement, but they are also protected by binding to the shelterin complex (Figure 7) (De Lange, 2005a, Maciejowski and de Lange, 2017). This complex consists of six specialized protein subunits: TRF1 (Telomeric Repeat-binding factor 1), TRF2 (Telomeric Repeat-binding factor 2), TIN2 (TRF1 and TRF2-Interacting Nuclear Factor 2), RAP1 (Repressor Activator Protein 1), POT1 (Protection of Telomeres 1), y TPP1 (TINT1/PTOP1/PIP1; encoded by the gene ACD). While POT1 uses its N-terminal oligosaccharide/oligonucleotide-binding fold domain to identify single-stranded telomere overhangs and its C-terminal binding protein domain to create a heterodimer with TPP1, shelterin complex attaches to the double-stranded TTAGGG repeats using TRF1 and TRF2 (Loayza and De Lange, 2003, Ye et al., 2004b). Through TIN2, which establishes a bridge between TTP1/POT1 and the double-stranded DNA-binding TRF1/TRF2 components of shelterin, the POT1/TPP1 heterodimer is linked to TRF1 and TRF2 (Takai et al., 2011, Ye et al., 2004a). By attaching itself to TRF2, RAP1 is drawn to telomeres (Li et al., 2000a). The main function of the shelterin complex is to prevent telomere fusion and inappropriate activation of DNA repair programs. Mutations in these components can cause problems such as telomere fusion and premature senescence (De Lange, 2005a, Ancelin et al., 2002, Celli and de Lange, 2005, He et al., 2009, Sfeir et al., 2010, Martinez et al., 2010, Martínez et al., 2009, Tejera et al., 2010).

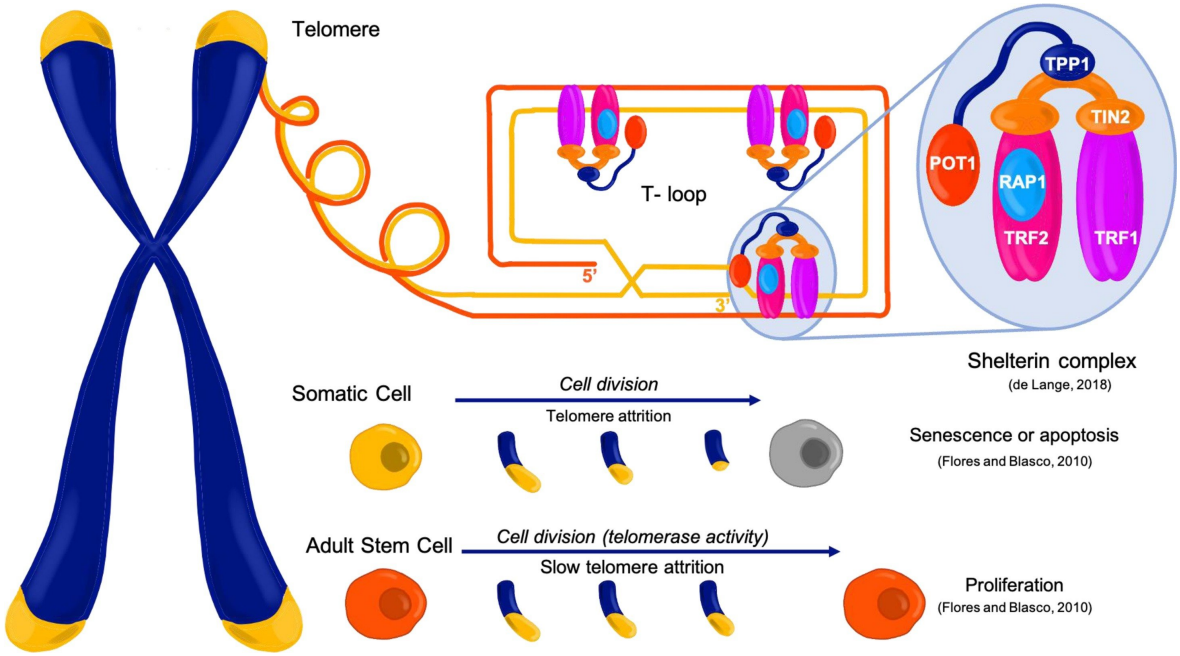


Figure 7. Telomeres and the shelterin complex.

The top panel illustrates the structure of the telomere, where the 3' overhang of the telomere invades the double helix to form the T-loop. The shelterin complex binds to telomere repeats, stabilizing the T-loop and protecting the telomere. On the right, a diagram of the shelterin complex is shown. The lower panel depicts telomere shortening during cell division. In somatic cells, telomeres shorten with each cell division, and when they become critically short, the cells enter a state of senescence or apoptosis. In adult stem cells, endogenous telomerase can maintain telomere length, resulting in telomere shortening occurring more slowly compared to somatic cells with age. Figure from (Chico-Sordo et al., 2021).

Eventually, a lack of DNA protection and the activation of DNA-damage response pathways lead to apoptosis or cell senescence due to critically short telomere accumulation (De Lange, 2005a, Martínez and Blasco, 2017, Hemann et al., 2001). However, in the face of the inevitable telomere shortening that cells undergo, they have mechanisms to lengthen telomeres. The best-known is telomerase, a ribonucleic enzyme capable of adding telomere repeats to the 3' ends de novo (Lingner et al., 1997). In 1985, Greider and Blackburn identified this enzyme (Greider and Blackburn, 1985). Telomerase activity (TA) is present in germ cells and stem cells and is highly abundant in tumor cells but has low levels in differentiated cells (Greider and Blackburn, 1985). Two main components formed this enzyme; one is the telomerase ribonucleic acid (RNA) component (TERC), and the other is the telomerase reverse transcriptase (TERT). TERC acts as a template sequence for the addition of the telomere sequence (Feng et al., 1995), while TERT acts as a reverse transcriptase adding DNA from an RNA template strand (Harrington et al., 1997). This enzyme binds to the overhanging strand and adds telomere sequences in the 5'-3' direction, thereby lengthening that strand and allowing the polymerase to continue replication by adding a new primer. Specifically, TERT expression is directly linked to telomerase activity levels (Cristofari and Lingner, 2006).

Subsequent advances, using mouse models deficient in the telomerase gene, confirmed that telomerase is crucial for maintaining telomere length (TL), and its dysfunction can cause premature aging and degenerative diseases (Blasco et al., 1997).

In the absence of telomerase activity, there is an alternative telomere lengthening (ATL) mechanism that allows telomere lengthening in specific cases, mainly in tumor cells (Liu et al., 2007, Reddel et al., 1997, Neumann et al., 2013). This mechanism is based on homologous recombination. Intact telomere sequences from other chromosomes serve as templates to lengthen short telomeres (Cesare and Reddel, 2010, Dunham et al., 2000). Regardless of whether the mechanism used to lengthen telomeres is telomerase or ATL, the ultimate goal is to avoid reaching the Hayflick limit, which regulates the number of possible cell divisions.

1.2.4 Telomere dysfunction and diseases

Telomere shortening is strongly associated with other hallmarks of aging, specifically genomic instability, cellular senescence, stem cell depletion, mitochondrial dysfunction, and altered intracellular communication (Lopez-Otin et al., 2023, López-Otín et al., 2013). Briefly explaining the integration between the mentioned hallmarks, telomere shortening contributes to genomic instability because it decreases chromosome protection, allowing shortened telomeres to cause DNA damage, which in turn leads to mutations, chromosome fragmentation, and loss of genetic material (De Lange, 2005b). Telomere shortening is a significant cause of senescence, a process triggered by accumulating a certain number of critically short telomeres (De Lange, 2005a, Martínez and Blasco, 2017, Hemann et al., 2001). Stem cells, critical for tissue regeneration and repair, have longer telomeres in the early stages of life. However, over time, telomere shortening reduces their capacity for self-renewal and differentiation, leading to tissue depletion and a decrease in regenerative capacity (Fathi et al., 2019). Additionally, as telomeres shorten and cells age, increased mitochondrial dysfunction is observed, characterized by an increased production of ROS. Mitochondrial damage and increased oxidative stress can shorten telomeres, promoting cellular senescence (Passos et al., 2007).

Throughout history, several scientific publications have linked the onset of certain diseases to the shortening of telomeres. Among the most frequently associated diseases are cancer (Artandi et al., 2000, Chin et al., 1999, Colla et al., 2015, Rudolph et al., 1999), pulmonary fibrosis (Zhang et al., 2021a), Alzheimer's disease (Fu et al., 2022), and diseases such as Werner's (Chang et al., 2004) or Hutchinson-Gilford syndrome (Decker et al., 2009). The relationship between telomere shortening and COVID-19 has also been analyzed in the last five years. Although the severity of COVID-19 is higher in the elderly, this disease affects not only older people but the entire population regardless of age (Liu et al., 2020a). In the elderly,

telomere shortening is increased, in addition to co-existing immune system dysfunction, chronic inflammation, cellular senescence, and comorbidities. COVID-19 infection and the generated hypoxia situation (Rahman et al., 2021) induce oxidative stress, leading to increased ROS production (Veenith et al., 2022). Therefore, alteration of the telomere pathway contributes to both the infection and its consequences. First, age-linked telomere shortening makes the individual more susceptible to serious infections and complications due to an impaired immune system (Dos Santos et al., 2021, Sanchez-Vazquez et al., 2021, Benetos et al., 2021, Wang et al., 2021c). Second, SARS-CoV-2 infection may accelerate the telomere shortening process and aging (Mongelli et al., 2021).

1.3 Telomere dynamics and female infertility

Telomere alterations are directly associated with aging and age-related diseases. A link between telomere impairment and infertility is also demonstrated. This condition is intrinsic to the aging process. However, aging aside, telomere shortening is defined as a key factor in ovarian dysfunction associated with infertility, early menopause, or even complications during pregnancy. Throughout this section, the biological processes related to female reproduction that may be altered by alterations in telomere maintenance in women will be explored.

1.3.1 Ovarian telomere parameters

There is TA in the ovary, as evidenced both in humans (Kinugawa et al., 2000, Uysal et al., 2021) and in other animal models (Betts and King, 1999, Eisenhauer et al., 1997, Jaskelioff et al., 2011, Lavranos et al., 1999, Russo et al., 2006, Yamagata et al., 2002, Polonio et al., 2023). This implies a special telomere dynamic in this organ. Primarily, as discussed above, germ cells possess TA (Wright et al., 2001, Wright et al., 1996). Mature oocytes are characterized by both lower TL and lower TA compared to immature oocytes (Betts and King, 1999, Eisenhauer et al., 1997, Turner and Hartshorne, 2013, Wright et al., 2001). However, oocytes are not the only cell type in the ovary where TA is present.

GCs, which record a high rate of cell division during the process of folliculogenesis, possess TA (Butts et al., 2009, Lavranos et al., 1999, Russo et al., 2006, Xu et al., 2017, Yamagata et al., 2002). Despite being somatic cells, they present higher telomerase levels than the rest of the somatic cells in the ovary (Lavranos et al., 1999, Yamagata et al., 2002). In bovine, a low TA is observed at the primordial follicle stage, which increases markedly in the remaining preantral follicles and decreases again at the antral follicle stage (Lavranos et al., 1999). Studies in pigs support these findings (Russo et al., 2006). Telomerase can be activated in response to estrogen (Bayne et al., 2007, Yamagata et al., 2002, Calado et al., 2009).

Regarding the TL of these cells, in the porcine model, it is observed that TL increases progressively from the preantral to the antral follicle stages (Russo et al., 2006). However, the CCs register a higher TL compared with GCs (Russo et al., 2006).

1.3.2 Telomeres and fertility-related cellular mechanisms

Although endocrine and uterine alterations may be the origin in some cases of female infertility, the main cause typically lies in the female germ cells (Chico-Sordo et al., 2021). For this reason, the use of donated oocytes can lead to a successful pregnancy even in women of advanced maternal age (Balmaceda et al., 1994).

Keefe et al. (2006) described the theory of reproductive aging based on oocyte telomere shortening. For this purpose, they described a model of telomere shortening based on two crucial moments, before birth and during reproductive life in women. The first principle refers to the multiple divisions that female germ cells undergo in the prenatal period. It suggests that oocytes obtained from the last divisions in the prenatal period will accumulate significant telomere shortening and will be ovulated at a later age during a woman's reproductive life. The second principle is based on the fact that in these late-ovulated oocytes, telomere deterioration is greater due to prolonged meiotic arrest. During this period an increase of ROS or mitochondrial alterations can damage oocyte telomeres (Keefe et al., 2006). Therefore, the age-related decline in oocyte quality can be largely attributed to telomere deterioration. Studies on polar bodies obtained during oogenesis have shown that a lower amount of telomere DNA is associated with a higher number of aneuploidies in human oocytes (Treff et al., 2011).

Aneuploidies are alterations in the number of chromosomes in a cell. In humans, somatic cells have 46 chromosomes, specifically 23 pairs, with one chromosome of each pair coming from each parent. In the case of germ cells, both oocytes and sperm, they have only 23 chromosomes. With increasing age, there is a significant risk of aneuploidy in offspring (Capalbo et al., 2017). The origin of these aneuploidies could be due to an inefficiency of the recombination process. In older females, a greater distance between sister chromatid kinetochores and a higher incidence of premature separation of bivalents is evidenced (Duncan et al., 2012, Lagirand-Cantaloube et al., 2017, Zielinska et al., 2015), where decreased levels of cohesins that hold chromosomes together can be crucial (Tsutsumi et al., 2014). Aneuploidies may also originate from alterations such as the presence of abnormal spindles (Liu et al., 2002a), defective microtubules (Shomper et al., 2014), and transiently multipolar spindles predisposing to defects in microtubule binding to chromosome kinetochores (Nakagawa and FitzHarris, 2017). These alterations may be directly related to telomere shortening, as telomeres play a key role in the formation of the classical bouquet structure during recombination. Chromosome telomeres are anchored to the nuclear envelope

facilitating the pairing of homologous chromosomes (Chikashige et al., 2007). The presence of shorter telomeres could affect this anchoring, resulting in reduced recombination efficiency, which could increase the risk of chromosome segregation errors and aneuploidy.

Defects in the cytoplasmic compartment of the oocyte may lead to a decrease in quality and could also be associated with telomere shortening. Specifically, alterations in the mitochondria present in the ooplasm may have an impact on the level of the telomeres. Oxidative stress is associated with impaired fertilization and oocyte developmental potential (Tarin, 1996). In older women, an increased number of mitochondrial mutations in oocytes and embryos is observed (Barritt et al., 2000, Chan et al., 2005, Keefe et al., 1995, Zhang et al., 2019b, Zhang et al., 2019a), as well as changes in membrane potential or ATP production (Ben-Meir et al., 2015, Selesniemi et al., 2011, Wilding et al., 2001).

Finally, considering that oocyte homeostasis is sustained by follicular development and that there is bidirectional communication between ovarian somatic cells and oocytes (Monniaux, 2016), telomere impairment of these cells could have a direct impact on oocytes. In these cells, increased DNA damage, defects in repair processes (Zhang et al., 2015), or an increased expression of oxidative stress response genes with aging have been reported (Brzezinski et al., 2018, Iwata, 2017). In older women, shorter TL is evidenced in GCs (Hao et al., 2023, Xu et al., 2017), although this decrease is not observed in CCs (Hanson et al., 2021, Goto et al., 2013). Both cell types exhibit TA, although there is a decrease in TA with aging (Kinugawa et al., 2000, Polonio et al., 2023). However, not only ovarian follicles are altered with age, but also the ovarian niche. Aging is associated with increased inflammatory and fibrotic processes in the ovary (Briley et al., 2016, Lliberos et al., 2021).

1.3.3 Telomere-related reproductive disorders

A relationship exists between telomere parameters, such as TL or TA, and infertility. For this reason, several studies focused on telomere analysis in women diagnosed with reproductive disorders. Among them, premature ovarian insufficiency (POI), or premature ovarian failure (POF), and polycystic ovary syndrome (PCOS) stood out. These types of studies not only analyzed telomere dynamics in ovarian cells but also in peripheral blood mononuclear cells (PBMCs) or leukocytes to test their role as ovarian telomere biomarkers.

POI or POF affects 1-4% of women before the age of 40 (Blumenfeld, 2011). This disorder is characterized by low estrogen levels, elevated FSH levels, irregular periods, and reduced reproductive potential (Hoek et al., 1997, Lakhal et al., 2010). Hanna et al. (2009) reported higher telomere length (TL) in women with premature ovarian failure (POF), attributing this to the reduced number of follicular divisions in these women (Hanna et al., 2009). Similar results were also reported by the Sayban group (Sayban et al., 2018). In contrast, Butts et al. (2009)

detected shorter telomeres in GCs from women with occult ovarian insufficiency (Butts et al., 2009). Additionally, in GCs of women with POI, lower TL and TA were also evidenced (Kinugawa et al., 2000, Xu et al., 2017). In studies conducted using blood samples, Xu et al. (2017) demonstrated that leukocytes from women with POI exhibited significantly shorter telomeres. Other studies reached the same conclusion, although they also associated this disorder with a skewed inactivation of the X chromosome (Miranda-Furtado et al., 2018).

PCOS is a multifactorial disorder characterized by hyperandrogenism, polycystic ovaries, and/or ovarian dysfunction. This syndrome affects 4-20% of premenopausal women, who usually develop associated endocrine and metabolic alterations (Azziz, 2018, Escobar-Morreale, 2018). These include acne, obesity, or insulin resistance (Witchel et al., 2019). Many studies on telomeres in women with this diagnosis have focused on the potential relationship with metabolic alterations. In women with PCOS, longer telomeres were observed in leukocytes (Pölönen et al., 2022) and GCs (Wei et al., 2017). However, when groups of women with PCOS and different weights were compared, a relationship between obesity and telomere shortening was found (Kogure et al., 2024). This result aligns with the study by Feijing et al. (2024), which found a correlation between a high concentration of leptin in follicular fluid (FF) and a higher TL (Feijing et al., 2024). However, multiple studies do not detect telomere alterations in leukocytes from women with PCOS (Tajada et al., 2022, Pedroso et al., 2015, Wang et al., 2025a). Other studies evidenced telomere shortening in women with PCOS both in leukocytes (Li et al., 2014, Pedroso et al., 2020), GCs (Li et al., 2017), CCs (Yu et al., 2023), and even alterations in TA (Li et al., 2017, Unlu et al., 2023). The use of drugs such as metformin, common in the treatment of metabolic disorders, did not show a significant increase of TL in leukocytes of women with PCOS (Kayacık Günday et al., 2022).

HYPOTHESIS

2 HYPOTHESIS

Considering that telomere shortening is a hallmark of aging and that the ovary is one of the first organs to undergo early senescence, the hypothesis of this work is that defective telomere maintenance in the ovary could lead to ovarian dysfunction, including the decline in ovarian reserve. Besides ovarian dysfunction, the telomere biology of the ovary may also be altered during transient conditions, such as pregnancy or COVID-19, despite these conditions not having a deleterious effect on fertility.

OBJECTIVES

3 OBJECTIVES

3.1 Main objective

The primary objective of this study is to characterize telomere maintenance associated with aging in the human ovary and to investigate the impact of specific factors, such as pregnancy or non-reproductive pathologies like COVID-19, on ovarian telomere biology.

3.2 Secondary objectives

To achieve the main objective, the work brings together two main projects with the following secondary objectives:

Project 1: "Understanding the implication of the telomere pathway in ovarian aging and dysfunction/infertility"

I. Determine the hormonal profile in women of different ages.
II. Evaluate the telomere pathway in different cell populations of the ovary during folliculogenesis.
III. Analyze the changes at the telomere level in oocytes, granulosa cells, theca cells, and ovarian stroma in different age groups.
IV. Study the presence of telomerase activity in the human ovary.
V. Evaluate telomere alterations at the systemic level and their potential use as an ovarian telomere biomarker.
VI. Study of ovarian decay using other markers of aging such as fibrosis and a proteomic approach.
VII. Impact of ovarian reserve (based on AMH levels) on age-independent aging at the ovarian and systemic levels.
VIII. Analyze telomere parameters in the last phase of pregnancy.

Project 2: "Effects of COVID-19 in the telomere biology of granulosa cells and in fertility as well as in IVF outcomes"

IX. Study of telomere length in ovarian granulosa cells and at the systemic level in unvaccinated women who had COVID-19 with different degrees of severity and controls.
X. Analyze the impact of COVID-19, as a non-reproductive disease, on fertility parameters such as the number of oocytes retrieved, the number of mature oocytes, and the fertilization rate after ovarian stimulation.

XI. Study of the correlation between telomere and fertility parameters.

MATERIALS & METHODS

4 MATERIALS & METHODS

4.1 Study design

The present doctoral thesis involves two main studies, both carried out in humans, where all the participants were women (Figure 8).

The first project, **"Understanding the implication of the telomere pathway in ovarian aging and dysfunction/infertility"** was designed to characterize ovarian aging in women of different ages. Moreover, we wanted to study whether ovarian aging was more critical in women with lower ovarian reserve, measured by AMH levels, independently of their age (meaning that lower ovarian reserve may involve impairing telomere maintenance in the ovary). Ultimately, we aimed to analyze the impact of pregnancy on ovarian telomere parameters. The second study, **"Effects of COVID-19 in the telomere biology of granulosa cells and in fertility as well as in IVF outcomes"**, was developed to analyze if the telomere shortening of ovarian cells, specifically GCs, can be accelerated by external factors such as COVID-19 infection, whose symptoms were not supposed to affect the ovary, and the consequences in oocyte maturation rates.

4.1.1 Project 1: "Understanding the implication of the telomere pathway in ovarian aging and dysfunction/infertility"

4.1.1.1 Project design

The proposal was classified as an analytical, cross-sectional, prospective, observational, multicenter cohort study. Recruitment took place between September 2021 and May 2023, and 65 women aged 18 - 50 years were recruited in three hospitals located in Spain: Hospital Universitario y Politécnico La Fe (Valencia), Hospital Clínico San Carlos (Madrid), and Hospital General Universitario de Valencia (Valencia). The main eligibility criterion for recruiting patients was the need for a gynecological and/or obstetric surgical intervention unrelated to the study. Before the intervention, the medical staff informed the patients of the study and provided them with the previously approved Project Information Sheet. All women whose intervention was related to a cancer diagnosis were excluded from the study. Samples were collected from those women who agreed to participate after signing the Informed Consent Form (ICF). Blood samples and an ovarian biopsy were obtained from each patient during the surgical intervention, and medical record-related data relevant to the study were also recorded before the intervention using a questionnaire.

Patients were divided according to age criteria, ovarian reserve measured by AMH levels, and pregnancy status. For both age and AMH threshold value criteria, the widely used POSEIDON clinical criteria were implemented. The age and AMH cut-off values for the oldest age group (46 - 50 years old) were established based on previous publications (Schoenaker et al., 2014, Seifer et al., 2011). The manifestation of perimenopausal symptoms in our oldest cohort (such as hot flashes, depressed mood, sleep disturbances, or vaginal dryness) was also used for group classification (Woods and Mitchell, 2005). Consequently, the following were the primary study groups (Figure 8):

- **Young women (Y)** (n = 17): women aged 18-34 years, regardless of AMH value or presence/absence of pregnancy.
    - **Y+** (n = 11): non-pregnant women with an AMH value equal to or greater than 1.2 ng/mL.
    - **Y-** (n = 2): non-pregnant women with an AMH level lower than 1.2 ng/mL.
    - **YPreg** (n = 4): pregnant women aged 18-34, regardless of AMH value.
- **Middle-aged women (M)** (n = 31): women aged 35-45 years, regardless of AMH value or presence/absence of pregnancy.
    - **M+** (n = 6): non-pregnant women with an AMH value equal to or greater than 1.2 ng/mL.
    - **M-** (n = 16): non-pregnant women with an AMH level lower than 1.2 ng/mL.
    - **MPreg** (n = 9): pregnant women aged 35-45, regardless of AMH value.
- **Perimenopausal women (P)** (n = 17): women aged 46-50, regardless of AMH value. Pregnant women were not recruited in this group.
    - **P+** (n = 8): non-pregnant women with an AMH value equal to or greater than 0.1 ng/mL.
    - **P-** (n = 9): non-pregnant women with an AMH level lower than 0.1 ng/mL.

4.1.1.2 Summary of techniques and objectives to be achieved

Blood samples were collected from recruited women for serum and PBMCs isolation, along with an ovarian cortex biopsy. Blood serum was tested for AMH, FSH, LH, E2, and P4 using ELISA assays. Systematic aging was assessed using PBMCs to measure the TL by quantitative fluorescence in situ hybridization (qFISH). The ovarian biopsy (which was a valuable sample) was optimized as much as possible to use it for multiple molecular techniques. Firstly, specific telomere techniques were carried out to analyze the presence of TA (Telomerase Repeated Amplification Protocol or TRAP assay), and to measure the TL by differentiating each cell type present in the ovary (qFISH). Secondly, to obtain a broad and more generalized view of ovarian function decay, fibrosis was assessed both by Masson's trichrome staining and by measuring the relative expression of genes directly related to

fibrosis. In addition, Liquid Chromatography – Tandem Mass Spectrometry (LC-MS/MS) and Sequential Window Acquisition of All Theoretical Mass Spectra (SWATH) were used to assess the proteomic profile.

4.1.1.3 Approval of the Ethics Committee

All study procedures were performed following the protocol approved by the Ethics Committee for Research with Medicines of the "Hospital Universitario y Politécnico La Fe" (Valencia, Spain) (Ref. HUPLF: FPNT-CEIB-04 (B), Appendix A), whose favorable report was issued on February 24, 2021. The protocol was also approved by the Institutional Review Board (IRB) of the Hospital Clínico San Carlos (Madrid, Spain) (Ref. HCSC: 21/295-E, Appendix A) and Hospital General Universitario de Valencia (Valencia, Spain) (Ref. HGUV: 105/2022, Appendix A) on April 15, 2021, and December 16, 2022, respectively. These reports concluded that the project adhered to the ethical regulations governing biomedical research involving human subjects and that it was feasible in terms of its scientific approach, objectives, materials, and methods employed. In turn, the project, registered with code 1711-FIVI-112-MV, was approved, along with a Patient Information Sheet and ICF, thereby ensuring that the project complied with the standards of Good Clinical Practice (GCP) guidelines (CPMP/ICH/135/95) and with the applicable legislation governing its operation. All the subjects who participated in the study signed the ICF.

4.1.2 Project 2: "Effects of COVID-19 in the telomere biology of granulosa cells and in fertility as well as in IVF outcomes"

4.1.2.1 Project design

Between October 2020 and May 2021, 65 women (aged 18-50) undergoing ART at IVI-RMA Madrid, Spain, were included in this analytical, cross-sectional, prospective, observational, and single-center dataset. Participants in this study were in good general health, as shown by their medical history. Women with previous illnesses, such as polycystic ovarian syndrome (PCOS) or endometriosis, were omitted. The medical professionals asked patients about the intensity of their COVID-19 symptoms after they had read the approved Project Information Sheet and signed the ICF for the project. Blood samples and GCs during oocyte retrieval were collected from patients who agreed to participate.

Participants were divided into two groups based on women's accounts of their COVID-19 illness status and subsequent serum testing. Therefore, women were classified into the following experimental groups (Figure 8):

- **Control group** (n = 29): women not exposed to SARS-CoV-2.

- **COVID group** (n = 36): women infected with SARS-CoV-2. Simultaneously, COVID patients were classified according to the intensity of their symptoms in mild and severe COVID groups to understand better the impact of the disease on the different variables studied. The mild COVID group gathered more individuals (52.7%) than the severe COVID group (47.2%). None of the included patients required hospitalization due to COVID-19.
    - **Mild COVID** (n = 19): patients categorized with symptomatic scores of 1 and 2.
        - Score 1: asymptomatic COVID-19 (n = 7). Subjects with the presence of serum antibodies who had no symptoms during the disease.
        - Score 2: mild COVID-19 (n = 12). Subjects with low-grade fever, cough, and loss of smell and taste for a short time (approximately 2 weeks).
    - **Severe COVID** (n = 17): patients categorized with a symptomatic score of 3. This score referred to severe COVID-19 symptoms such as high-grade fever, dyspnea, fatigue, headache, gastrointestinal symptoms, anosmia, and dysgeusia. Alterations in smell and taste persisted for at least one month. One patient in this group experienced issues with blood coagulation.

4.1.2.2 Summary of techniques and objectives to be achieved

Blood samples and GCs contained in the follicular fluid (FF) were collected during oocyte retrieval. Serum and PBMCs were isolated from blood samples. AMH levels were measured in serum using ELISA assays. Telomere shortening was evaluated in PBMCs and GCs by qFISH, and fertility outcomes of IVF treatments were recorded. Specifically, the fertility parameters evaluated were the number of retrieved oocytes and MII oocytes, which were used to calculate the oocyte maturation rate. The fertilization rate was also analyzed.

4.1.2.3 Approval of the Ethics Committee

The procedures carried out in this study were approved by the IRB of the Hospital Universitario Puerta de Hierro Majadahonda (Madrid, Spain). The Drug Research Ethics Committee issued a favorable opinion for the conduction of the study on June 15, 2020 (Ref. HUPHM: 11/2020, Appendix A), after evaluating the methodological and technical requirements, the competence of the researchers, the available facilities, the risks and inconveniences concerning the expected benefits, the criteria for inclusion/exclusion of patients, and the compliance with the GCP guidelines (CPMP/ICH/135/95). The Patient Information Sheet and the ICF were also approved by the IRB and signed by all the subjects who participated in the study.

Figure 8. General projects outline.

4.2 Sample collection and processing

4.2.1 Blood samples

4.2.1.1 Collection

After cleaning the skin and disinfecting the area with ethanol, blood samples were collected by venipuncture in the antecubital fossa. A total of 15 mL of blood was extracted and divided equally into tubes destined for serum or plasma. All blood samples were obtained in the operating room during the corresponding intervention, surgery (Project 1), or oocyte retrieval (Project 2). Blood samples were kept at a stable room temperature (RT) until processing.

4.2.1.2 Serum sample processing

Blood was collected in VACUETTE® 5 mL CAT Serum Separator Clot Activator tubes (Greiner Bio-One, Germany). These tubes contained a separating gel that migrated to the interface between serum and clot during centrifugation, forming a stable barrier and separating serum from fibrin and cells. After centrifugation at 1500 x g for 10 min at RT, the serum obtained at the top was transferred to sterile tubes and frozen at -80 °C until further use. The serum samples were used to measure the different hormone levels and to determine the presence of antibodies against SARS-CoV-2 (IgM and IgG).

4.2.1.3 Peripheral blood mononuclear cells isolation

Blood collected in VACUETTE® 4 mL K2E K2EDTA tubes (Greiner Bio-One, Germany) was used to isolate PBMCs. The coagulation cascade was blocked with the potassium EDTA (ethylenediaminetetraacetic acid) additive, a calcium chelating agent. For this purpose, blood was stored in the tube and inverted to facilitate mixing it with the anticoagulant. Next, a density gradient was performed with Ficoll Histopaque® (Sigma-Aldrich, United States or USA) in a 15 mL centrifuge tube. Blood was gently layered on top of Ficoll to ensure that the blood and Ficoll stayed as two different layers. A volume of 2 mL of Ficoll was used for every 5 mL of blood. The tubes were centrifuged for 30 min at 400 x g at 4 °C in a swing-out bucket without braking, thus achieving a progressive deceleration of the centrifuge to avoid mixing the phases created in the gradient. The upper phase corresponded to blood plasma, followed by a ring-shaped interphase containing PBMCs, then the Ficoll phase, and finally, at the bottom of the tube, the granulocytes and erythrocytes precipitated. The interphase containing PBMCs was carefully collected, and 500 µL of 1X Phosphate Buffered Saline or PBS (Fisher BioReagents, USA) was added for washing, followed by centrifugation. Once centrifuged at 300 x g for 5 min, the supernatant was removed, and the pellet was resuspended in 1X PBS to proceed with cell number counting. The PBS 1X volume used for the cell counting depended on the

pellet size, but this volume was considered for future calculations. Cell counting was performed from 10 µL of the cell suspension using the Neubauer Chamber (Preciss Europe, United Kingdom or UK) (Figure 9A) under a light microscope (Motic™ AE31 Microscope, China) with 10X magnification. The number of cells within the surface of the four big squares at the corners was counted (Figure 9B), including cells touching the upper and left limits and excluding those touching the lower and proper limits. The mean value was obtained after counting the number of cells in each of these squares. Taking into account that each of these big squares has an area of 1 mm^2, and the depth of the chamber with the glass cover is 0.1 mm (1 mm^2 area x 0.1 mm depth = 0.1 mm^3 = 10^{-4} mL), to calculate the cell concentration (cells/mL), the mean value obtained was multiplied by 10^4 (Figure 9C). In cases where the sample was highly concentrated, and a dilution was applied, it was subsequently multiplied by that dilution factor.

Finally, the cell suspension was centrifuged at 4 °C for 7 min at a speed of 300 x g, the supernatant removed, and the cell pellet resuspended in 1 mL of methanol (PanReac AppliChem, Spain and Germany) and glacial acetic acid (PanReac AppliChem, Spain and Germany) in a 3:1 ratio, and stored at 4 °C until use.

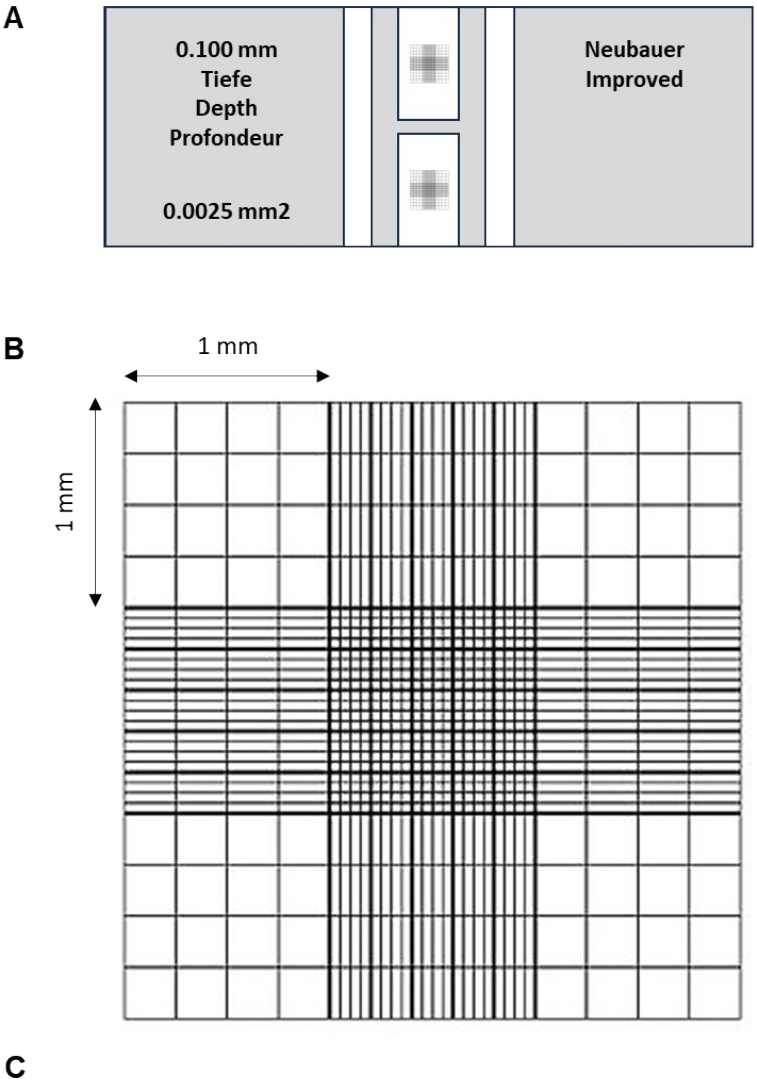


Figure 9. Cell number counting using the Neubauer chamber.

(A) Image of the Neubauer chamber where the depth (0.100 mm) and the minimum counting area (0.0025 mm^2) are specified. (B) The square pattern used in cell counting where four large squares at the corners with an area of 1 mm^2 are observed. (C) Formula to calculate the volume corresponding to each of the large squares, and the formula used to find the number of cells after counting two large squares in the grid shown in B.

4.2.2 Ovarian samples

4.2.2.1 Collection

The ovarian fragments were obtained by surgery depending on the intervention initially indicated by the medical specialists. The tissue was removed using cold scissors to minimize trauma to the surgical specimen and ovary. The biopsy was kept in sterile 1X PBS with 1% of

penicillin-streptomycin (Lonza™ BioWhittaker™, Belgium) and maintained cold during transport. Once the sample was received in the laboratory, it was washed with 1X PBS. With the help of an Nº20 steel scalpel blade (Paramount Surgimed Limited, India), the fragment was divided for future use in different techniques. It is important to note that the sizes of the ovarian fragments differed between patients, so it limited the number of techniques that could be performed in each fragment to assess the different variables. Priority was given to techniques focused on TL measurement. Further processing of each ovarian fragment depended on the techniques to be applied in the future. Those destined for histological examination (Hematoxylin & Eosin, and Masson's trichrome staining) and TL measurement (qFISH) were immediately fixed in 4% paraformaldehyde (Thermo Fisher Scientific, Germany) or formaldehyde (Sigma-Aldrich, USA) prepared in 1X PBS. The tissue was maintained for 24 h until subsequent embedding in paraffin or freezing with a cryostat medium. However, fragments intended for RNA or protein extraction were directly frozen at -80 °C until use. A summary of the ovarian sample processing and the techniques for which they were used can be seen in Figure 10.

4.2.2.2 Paraffin-embedded tissue, histological sections, and deparaffinization

Ovarian tissue, previously fixed in 4% paraformaldehyde with 1X PBS (Thermo Fisher Scientific, Germany), was dehydrated by successive 30 min immersions in increasing concentrations of ethanol (Sigma-Aldrich, USA): 1 x 70%, 1 x 80%, 1 x 96%, 3 x 100%. Then, three passes of 15 min each in xylene (Sigma-Aldrich, USA) were performed as a preliminary step to embedding the samples in paraffin. Once the xylene passages were completed, the samples were kept in liquid paraffin (PanReac, Spain) for 1 h at a stable temperature of 60 °C. This last step was repeated, thus ensuring the replacement of xylene by paraffin until the block was made (Table 1). Once the paraffin solidified, the block was carved into a pyramid to facilitate microtome sections (Shandon Finesse® 325 Manual Microtome, Thermo Fisher Scientific, Germany). Sections of 5 µm thickness were made, which, after being placed in a water bath preheated at 35 - 40 °C for the sections to stretch, were adhered to slides (Superfrost™ Plus Adhesion Microscope Slides, Epredia, Netherlands). Afterwards, sections were kept for 2 h at 37 °C for drying. The slides with the samples were stored at RT until deparaffinization to perform the successive techniques.

Table 1. Paraffin-embedded protocol.

Step	Time and temperature conditions
70% ethanol	30 min at RT
80% ethanol	30 min at RT
96% ethanol	30 min at RT
Absolute ethanol	30 min at RT
Absolute ethanol	30 min at RT
Absolute ethanol	30 min at RT
Xylene	15 min at RT
Xylene	15 min at RT
Xylene	15 min at RT
Paraffin	1 h at 60 ºC
Paraffin	1 h at 60 ºC

min: minutes, RT: room temperature, h: hours, ºC: Celsius degrees, %: percent.

The deparaffinization process (Table 2) was carried out on ovarian sections from paraffin-embedded samples intended for anatomopathological analysis by hematoxylin & eosin (H&E), fibrosis analysis using Masson's trichrome staining, or TL measurement by qFISH. For this protocol, the slides with the ovarian sections were kept at 70 °C for 30 min. Subsequently, these were immersed in xylene (Sigma-Aldrich, USA) for 15 min on three occasions. Then, the samples were hydrated by successive passes with decreasing ethanol (Sigma-Aldrich, USA) concentrations (2 x 100%, 1 x 96%, and 1 x 70%) for 5 min each. Finally, they were transferred to distilled water to hydrate the tissues before continuing the techniques.

Table 2. Deparaffinization protocol.

Step	Time and temperature conditions
Xylene	15 min at RT
Xylene	15 min at RT
Xylene	15 min at RT
Absolute ethanol	5 min at RT
Absolute ethanol	5 min at RT
96% ethanol	5 min at RT
70% ethanol	5 min at RT
Distilled water	5 min at RT

min: minutes, RT: room temperature, %: percent.

4.2.2.3 Ovarian freezing, histological sections, and washing

The ovarian fragments intended for RNA extraction or TRAP assay were frozen and stored at -80 °C until use. Other fragments were frozen with a cryostat mounting medium called OCT (Optimal Cutting Temperature, CellPath, Netherlands). In these cases, tissues previously fixed in 4% formaldehyde (Sigma-Aldrich, USA) in 1X PBS for 24 h were transferred to a 30%

sucrose solution in 0.2 M phosphate buffer (monobasic - NaH_2PO_4, and dibasic - Na_2HPO_4) and H_2O. The tissue remained in this solution for approximately 7 days at 4 °C. When the ovarian fragment reached the bottom of the conical tube, indicating that the tissue was equilibrated, the fragments were enclosed in OCT and stored at -20 °C. Histological sections of OCT blocks were made 10 µm thick in the cryostat (Leica CM 1520, Germany), adhered to slides with special treatment (Superfrost™ Plus Adhesion Microscope Slides, Epredia, Netherlands), and allowed to dry for approximately 2 h at RT.

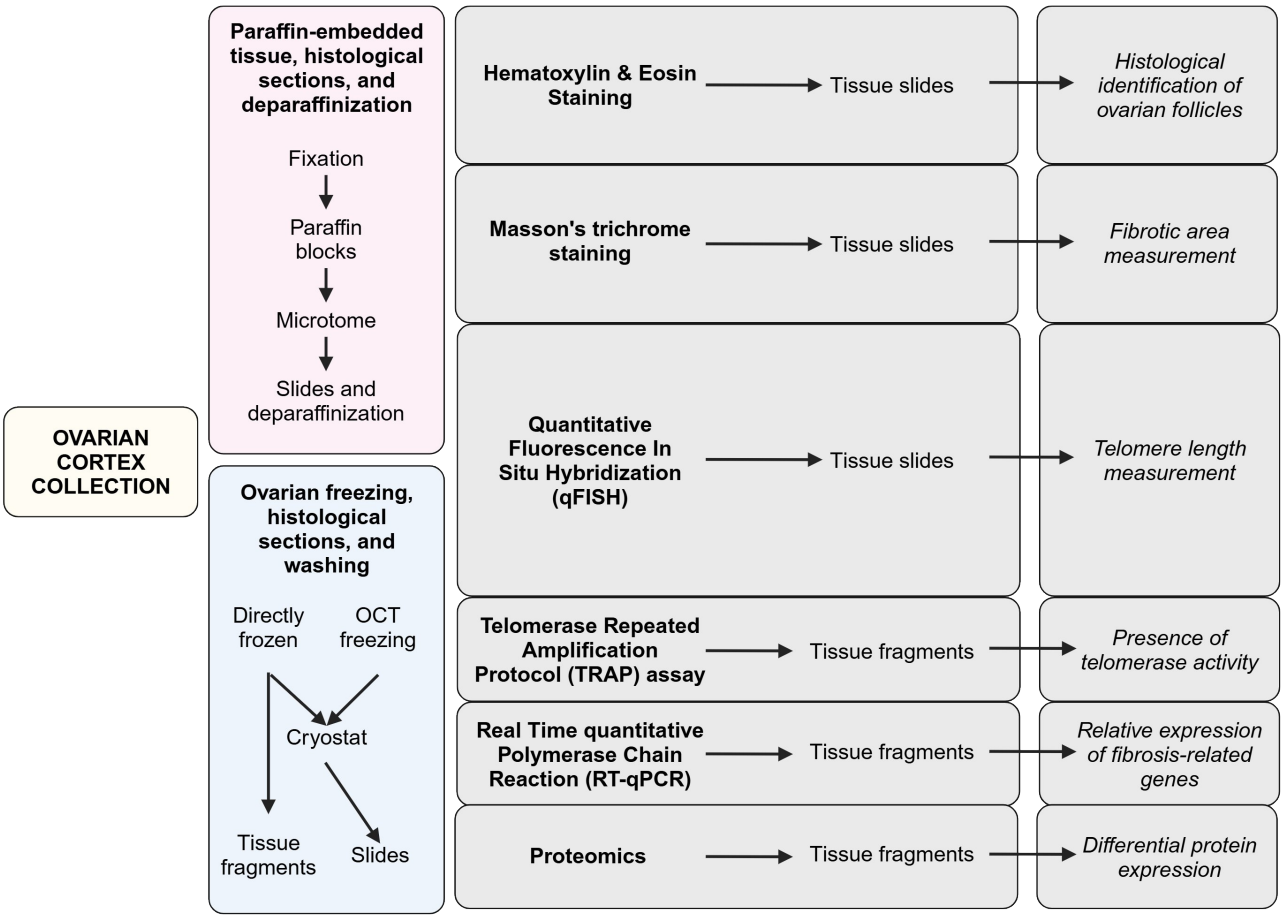


Figure 10. Ovarian cortex processing.

Outline of the techniques used for the processing of ovarian cortex biopsies, and the final purpose for which these samples were used. OCT: Optimal Cutting Temperature.

4.2.3 Granulosa cell samples

4.2.3.1 Ovarian stimulation and oocyte retrieval

GCs were collected during oocyte retrieval. All patients underwent a standard ovarian stimulation protocol with GnRH antagonists (Orgalutran, MSD, USA), together with doses (100-300 IU/day) of human menopausal gonadotropin (hMG; Menopur, Ferring Pharmaceuticals, Switzerland) and/or recombinant follicle-stimulating hormone (rFSH; Gonal-

F, Merck, Germany). When three follicles reached a size of 17 - 18 mm, and the gynecologist considered the follicular cohort to be mature, a single dose of recombinant human chorionic gonadotropin (hCG; Ovitrelle 250 µg, Merck, Germany) was administered. Follicular aspiration was performed 36 h after hCG injection. From the FF obtained during oocyte retrieval, GCs were isolated.

4.2.3.2 Isolation of granulosa cells

The FF was centrifuged in a conical tube at 300 x g for 5 min at RT. The supernatant was then carefully removed, and the pellet containing the GCs was resuspended in Dulbecco's Modified Eagle's Medium (DMEM) culture medium (Lonza™ BioWhittaker™, USA), slowly deposited through the wall of the tube over 3 mL of Ficoll Histopaque® (Sigma-Aldrich, USA). After centrifugation at 400 x g for 20 min at RT, the interphase containing the GCs was collected, and it was washed with DMEM to remove the Ficoll Histopaque® debris by centrifugation at 600 x g for 5 min. The precipitate was resuspended in 300 µL of 1X PBS, and the number of cells was counted in the Neubauer chamber (explained above in Figure 9). GCs were centrifuged at 4 °C for 7 min at 300 x g, the supernatant was removed, and the cell pellet was resuspended in 500 µL of methanol (PanReac AppliChem, Spain and Germany) and glacial acetic acid (PanReac AppliChem, Spain and Germany) in a 3:1 ratio, and stored at 4 °C until use.

4.3 Hormone levels measurements

Serum samples were analyzed by chemiluminescence on the Cobas e411 analyzer (Roche, Switzerland) to measure the levels of the different hormones of reproductive interest. Among the proteins of interest, the following stand out: AMH, FSH, LH, estradiol (E2), and progesterone (P4). Table 3 specifies the commercial kits (Roche Diagnostics, Germany) used to detect each hormone.

Table 3. Hormone commercial kits.

Hormone	Material description	Limit of detection	Analytical measuring interval
AMH	Elecsys AMH Plus	< 0.01 ng/mL	0.01 – 23 ng/mL
FSH	Elecsys FSH	< 0.3 mIU/mL	0.3 – 200 mIU/mL
LH	Elecsys LH	< 0.100 mIU/mL	0.100 – 200 mIU/mL
E2	Elecsys Estradiol III	< 5 pg/mL	5-3000 pg/mL
P4	Elecsys Progesterone III	< 0.05 ng/mL	0.05 – 60 ng/mL

AMH: anti-müllerian hormone, FSH: follicle-stimulating hormone, LH: luteinizing hormone, E2: estradiol, P4: progesterone, ng: nanogram, mL: milliliter, mIU: milli-International Unit, pg: picogram.

4.4 Reproductive and medical parameters

4.4.1 Medical history and lifestyle habits

To characterize the cohort from Project 1, data were recorded regarding menstrual and reproductive history, comorbidities, medications and supplements, and lifestyle habits. Age, weight, and height were obtained from the patients to calculate the Body Mass Index (BMI). Among the data considered relevant for the study were those parameters related to their menstrual and reproductive histories, such as the age at menarche, cycle length, bleeding duration, presence of dysmenorrhea, the use of contraceptive hormones, whether they had been pregnant previously or had suffered a miscarriage/abortion, and the previous obstetric or gynecologic surgeries. Information was also collected on the presence of any other pathologies, the use of medication for their treatment, and habits related to smoking, special diets, physical activity, or caffeine consumption.

4.4.2 Fertility outcomes

Considering that the women recruited in Project 2 were undergoing ART, data from the IVF laboratory and clinical variables were obtained from the database of the IVIRMA Madrid clinic. The number of retrieved oocytes, MII oocytes, and oocytes with two pronuclei and two polar bodies (2PN, 2PB) considered fertilized oocytes was collected. The oocyte maturation rate was calculated by dividing the number of oocytes in metaphase II by the total number of oocytes recovered. The normal fertilization rate was defined as the number of fertilized oocytes divided by the number of oocytes in metaphase II.

4.4.3 Serum SARS-CoV-2 antibody test and COVID-19 symptoms score

Participants from Project 2 were asked about symptoms associated with COVID-19, including fever, cough, dyspnea, fatigue, headache, gastrointestinal symptoms, alterations in smell, and changes in taste. Antibodies against SARS-CoV-2 (IgM and IgG) were assessed in serum samples by electrochemiluminescence immunoassay of the Elecsys® Anti-SARS-CoV-2 kit (Roche Diagnostics, Germany) on the Cobas e411. According to these results and the intensity of the symptoms, a COVID-19 score from 1 to 3 was attributed (previously explained in section 4.1.2.1.).

4.5 Telomere parameters

4.5.1 Telomerase activity

The TRAP assay is a method to determine TA in cells or tissue (Herbert et al., 2006, Kim et al., 1994, Mender and Shay, 2015). This technique involves four steps: (1) lysis and obtention of the protein extract containing telomerase, (2) extension where telomerase adds telomere repeats to a substrate, (3) classical PCR where the elongated telomerase products are amplified, and (4) detection of the presence or absence of TA by electrophoresis.

4.5.1.1 Cell lysate preparation

First, the samples were treated with a lysis buffer (Table 4). Depending on the number of cells or tissue weight, 100 - 500 µL of this buffer was added. The samples were resuspended and kept on ice for 30 min at 4 °C. Then, samples were centrifuged for 20 min at 16000 x g, and the supernatant (sample lysate) containing protein and RNA extract was collected after cell/tissue lysis. The amount of protein was quantified on the NanoPhotometer™ N60 (Implen, Germany). Sample lysates were stored at -80 °C until use, or the technique was continued.

Table 4. Lysis buffer recipe.

Reagent	Reagent Manufacturer	Final concentration
Tris-Hydrochloride pH 7.5	VWR Chemicals, USA PanReac, Spain	10 mM
Magnesium Chloride ($MgCl_2$)	Thermo Fisher Scientific, Germany	1 mM
Ethylene glycol- bis(2-aminoethylether)-N,N,N',N'-tetraacetic acid (EGTA)	Sigma-Aldrich, USA	1 mM
Glycerol	PanReac, Spain	10%
3-((3-cholamidopropyl) dimethylammonio)-1-propanesulfonate (CHAPS)	Thermo Fisher Scientific, Germany	5%
Phenylmethylsulfonyl fluoride (PMSF)	Sigma-Aldrich, USA	0.1 mM
2- mercaptoethanol	Sigma-Aldrich, USA	5 mM
Protease inhibitor	Sigma-Aldrich, USA	0.1 mM
The lysis buffer was prepared with diethylpyrocarbonate (DEPC)-treated water. Molecular-grade H_2O was used to prepare this water, and 0.1% DEPC was added. mM: millimolar, %: percentage.		

4.5.1.2 PCR

4.5.1.2.1 Elongation

In the elongation step, a primer labeled at the 5' end with Cy5, called the TS primer, was used as a substrate for telomerase. The sequence of this primer, along with the rest of the primers used in this technique, is specified in Table 5.

Table 5. Primer sequences used in the TRAP assay.

Name	Sequence (5' > 3')
TS primer	Cy5 - AATCCGTCGAGCAGAGTT
Anchor primer	GCGCGGCTAACCCTAACCCTAACC
TSNT primer	AATCCGTCGAGCAGAGTTAAAAGGCCGAGAAGCGAT
NT primer	ATCGCTTCTCGGCCTTTT
A: adenosine, C: cytidine, G: guanosine, T: thymidine.	

For each patient, two different amounts of the protein extract contained in the lysate were used: (a) 0.3 μg/μL of protein extract, and (b) 0.06 μg/μLl of protein extract. Specifically, three types of samples were prepared per patient:

I. Amount (a) of protein extract, RNase-treated as the negative control. For this purpose, 1 μg of RNase was added to the telomerase protein extract and heated at 65 °C for 10 min. During this step, the telomerase RNA component was degraded.
II. Amount (b) of protein extract.
III. Amount (a) of protein extract.

Each of the three conditions (I, II, and III) per patient was run in a total volume of 10 μL, of which 5 μL corresponded to the protein extract (regardless of concentration), and the other 5 μL to the master mix specified in Table 6.

Table 6. Elongation master mix recipe.

Reagent	Reagent Manufacturer	Final concentration
10X Stock elongation buffer (Table 7)	NA	1X
dATP, dTTP, dGTP mix	Thermo Fisher Scientific, Germany	0.6 mM each one
TS primer	Sigma-Aldrich, USA	1 μM
DEPC-treated water	Sigma-Aldrich, USA	The remaining volume to 5 μL per sample
DEPC-treated water was prepared with molecular-grade H_2O and 0.1% diethylpyrocarbonate. NA: not applicable, dATP: deoxyadenosine triphosphate, dTTP: deoxythymidine triphosphate, dGTP: deoxyguanosine triphosphate, mM: millimolar, μM: micromolar, μL: microliter, USA: United States of America.		

Table 7. 10X Stock elongation buffer recipe.

Reagent	Reagent Manufacturer	Final concentration
Tris-Acetate pH 8.5	VWR Chemicals, USA PanReac AppliChem, Spain and Germany	500 mM
Potassium Acetate	Sigma-Aldrich, USA	500 mM
$MgCl_2$	Thermo Fisher Scientific, Germany	30 mM

Spermidine	Sigma-Aldrich, USA	10 mM
EGTA	Sigma-Aldrich, USA	10 mM
2- mercaptoethanol	Sigma-Aldrich, USA	50 mM

The stock elongation buffer was prepared with DEPC-treated water. This water was prepared with molecular-grade H_2O and 0.1% diethylpyrocarbonate.
mM: millimolar, $MgCl_2$: magnesium chloride, EGTA: ethylene glycol- bis(2-aminoethylether)-N,N,N',N'-tetraacetic acid, USA: United States of America.

Once the master mix was added to the RNase-treated and untreated protein extracts, elongation was carried out for 1 h at 30 ºC in the MasterCycler® X50a thermal cycler (Eppendorf, Germany).

4.5.1.2.2 Amplification

The amplification reactions were run in a total volume of 50 µL. A volume of 40 µL of the amplification master mix specified in Table 8 was added to the 10 µL of the elongation product.

Table 8. Amplification master mix recipe.

Reagent	**Reagent Manufacturer**	**Final concentration**
10X Stock TRAP buffer (Table 9)	NA	1X
dCTP mix	Thermo Fisher Scientific, Germany	0.3 mM
TS primer	Sigma-Aldrich, USA	2.25×10^{-4} µM
Anchor primer	Sigma-Aldrich, USA	0.2 µg/µL
TSNT primer	Sigma-Aldrich, USA	0.01 ag/µL
NT primer	Sigma-Aldrich, USA	0.1 µg/µL
Taq DNA polymerase	AppiedBiosystem, USA	2 U
DEPC-treated water	Sigma-Aldrich, China	The remaining volume to 40 µL per sample

DEPC-treated water was prepared with molecular-grade H_2O and 0.1% diethylpyrocarbonate. Primer sequences were specified in the previous Table 5.
dCTP: deoxycytidine triphosphate, DNA: deoxyribonucleic acid, DEPC: diethylpyrocarbonate, NA: not applicable, mM: millimolar, µM: micromolar, µg: microgram, µL: microliter, ag: attogram, U: unit, USA: United States of America.

Table 9. 10X Stock TRAP buffer.

Reagent	Reagent Manufacturer	Final concentration
Tris-Hydrochloride pH 8.3	VWR Chemicals, USA PanReac, Spain	200 mM
Potassium Chloride (KCl)	Sigma-Aldrich, USA	680 mM
$MgCl_2$	Thermo Fisher Scientific, Germany	15 mM
EGTA	Sigma-Aldrich, USA	10 mM
Tween™ 20	Sigma-Aldrich, USA	0.5% mM

The stock TRAP buffer was prepared with DEPC-treated water. This water was prepared with molecular-grade H_2O and 0.1% diethylpyrocarbonate. $MgCl_2$: magnesium chloride, EGTA: ethylene glycol- bis(2-aminoethylether)-N,N,N',N'-tetraacetic acid, USA: United States of America, mM: millimolar, %: percent.

The master mix included the primers TS (previously included in the elongation step), Anchor, TSNT, and NT. The TSNT primer consists of 36 bp and is the internal control (IC) whose detection guarantees a successful amplification PCR. This IC has a reverse primer in the NT primer. Subsequently, this 36 bp substrate will be amplified by the Cy5-labeled TS primer. The Anchor primer constitutes the reverse primer for the telomerase-elongated products.

Once the 40 µL of the amplification master mix was added to the elongation product, the following program was run on the MasterCycler® X50a thermal cycler (Eppendorf, Germany): (1) 95 ºC for 5 min to deactivate telomerase; (2) 30 cycles at 95 ºC for 30 sec (DNA denaturation), 50 ºC for 30 sec (primers annealing), and 72 ºC for 1 min (extension); and (3) 72 ºC for 10 min to final amplification.

4.5.1.3 Running acrylamide gel

Amplification products were separated on acrylamide gels, which were prepared with 40% 19:1 acrylamide-bisacrylamide (Sigma-Aldrich, USA), ultraPure™ urea (Thermo Fisher Scientific, Germany), and Tris-Borate-EDTA buffer (TBE) (PanReac AppliChem, Spain and Germany), polymerized with 1% ammonium persulfate prepared earlier at 10% (APS, Sigma-Aldrich, USA), and 0.1% N,N,N',N'-Tetramethyl ethylenediamine (TEMED, Thermo Fisher Scientific, Germany). Electrophoresis was performed with 0.5X TBE in PROTEAN II xi Cell (Bio-Rad). 5 µL of sample and 5 µL of loading dye (1:1 ratio) prepared with deionized formamide, EDTA (Sigma-Aldrich, USA), and bromophenol blue (Sigma-Aldrich, USA) were loaded. The gels were run at 300 V until the loading dye front reached the bottom of the gel. The Cy5 signal was visualized under humid conditions in the ChemiDoc MP Basic Imaging System (Bio-Rad).

4.5.1.3.1 Intensity quantification

A positive result for telomerase was visualized by a ladder pattern, corresponding to the elongation products with a 6 bp difference and a 36 bp band corresponding to the IC. A negative result for TA or the RNase-treated sample was determined exclusively by the appearance of the IC band. The same negative result was observed in the lane where a lysis buffer replaced the sample. Signal quantification was performed using ImageLab software (version 5.0, Bio-Rad). First, the intensity of each lane was normalized after dividing by the IC intensity (TA normalized intensity = 6 bp ladder intensity/IC intensity). Next, taking as reference the intensity of Jurkat cells included as TA positive controls (100% intensity), the percentage of TA concerning these tumor cells was calculated [Relative telomerase activity (% of positive control) = (sample TA normalized intensity x 100)/Jurkat TA normalized intensity]. This was done for each of the concentrations of the protein extract used, expressed concerning Jurkat cells of the same concentration. Finally, the mean value between the two lanes not treated with RNase was calculated for each patient.

4.5.2 Telomere length

QFISH assessed TL. This technique was performed in two ways. First, in Project 1, the classical method was used for both ovarian tissue sections and fixed PBMCs. The samples were adhered to slides, the FISH technique was performed as described in section 4.5.2.1, and images were acquired on a high-resolution confocal microscope. In the second case, in Project 2, the high-throughput technique (HT-qFISH) was used, where GCs and PBMCs adhered to 96-well plates with an optical transparent bottom (Greiner, Bio-One, Germany). The FISH technique was performed as described in section 4.5.2.1., but using 96-well plates, where the reagent volumes were added and removed with the help of multichannel pipettes. The images of these plates were acquired automatically using a fluorescence microscope.

4.5.2.1 qFISH

With respect to the samples from Project 1, the ovarian sections already adhered to slides either after the deparaffinization process or after thawing for 1 h, were washed for 10 min with 1X PBS. Regarding PBMCs from this same project, cells fixed in methanol:acetic acid were adhered to slides in a hydrophobic circle delimited with PAP PEN (ENZO, USA), covered with 20 µL of poly-L-lysine (Sigma-Aldrich, USA) dissolved in distilled water at a concentration of 0.001%. The slides were kept at 37 °C for 30 min to dry the poly-L-lysine, subsequently, two 5 min washes were performed with 1X PBS to remove the excess. Fixed PBMCs, approximately 300,000 - 500,000 cells, were added and left for 20 min at 37 °C for adherence,

followed by a 10 min wash with 1X PBS. From this point on, slides containing both ovarian sections and PBMCs similarly continued the FISH process.

Regarding Project 2, both GCs and PBMCs were adhered and processed in 96-well plates. To this end, 20 µL of 0.001% poly-L-lysine (Sigma-Aldrich, USA) was added to each well, the plate was incubated for 30 min at 37 °C, the excess of poly-L-lysine was removed, and two 5-min washes in 1X PBS were performed. The 1X PBS was removed, and the cells were added, a maximum of 200,000 cells per well. Furthermore, 200 µL of 1X PBS was added, and the plate was kept overnight at 4 ºC. The following day, a 10 min wash was performed with 1X PBS, and the FISH technique was continued in the same way as with the samples of Project 1. It is important to note that in this type of plate, we always worked adding volumes of 200 µL per well. The main steps of qFISH will be detailed below, and those steps modified for any of the projects will be mentioned.

Once the samples adhered to the slides or plate wells, they were fixed with 4% formaldehyde in 1X PBS for 2 min at RT and permeabilized. In the case of Project 1, permeabilization of samples was performed with 0.5% Triton X-100 (Sigma-Aldrich, USA) in 1X PBS for 3 h at RT. In Project 2, cells were permeabilized with pepsin (Sigma-Aldrich, USA) dissolved at a final concentration of 0.1 mg/mL in H_2O with HCl (PanReac AppliChem, Spain and Germany) at 10 mM previously pre-warmed, and incubated for 10 min at 37 °C. After permeabilization, two 5 min washes were performed with 1X PBS under agitation, and samples were re-fixed for 2 min with 4% formaldehyde. Formaldehyde was removed and two 5 min washes with 1X PBS were performed again before dehydration. Samples were dehydrated with increasing concentrations of ethanol (Sigma-Aldrich, USA) (70%, 90%, and 100% for 5 min each) at RT and allowed to dry until complete evaporation of the ethanol (Sigma-Aldrich, USA). Once the samples were dehydrated, the hybridization solution, specified in Table 10, containing the telomere probe was added. This probe consists of a telomere peptidonucleic acid (PNA) sequence with three repeats of the CCCTAA sequence (complementary to the telomere sequence GGGATT) end-labeled with the fluorescent molecule Cy3 (Tel-Cy3: Cy3-(CCCTAA)3, Panagene, South Korea).

Table 10. Telomere FISH hybridization solution recipe.

Reagent	Reagent Manufacturer	Final concentration
Tris-HCl pH 7.2	PanReac AppliChem, Spain and Germany	10 mM
$MgCl_2$	Thermo Fisher Scientific, Germany	25 mM
Citric acid	Fisher Bioreagents, USA	9 mM
Na_2HPO_4	Sigma-Aldrich, USA	82 mM
Deionized formamide	Sigma-Aldrich, USA	70%
Blocking Reagent	Roche, Germany	0.5%
Telomere PNA probe	Panagene, South Korea	0.5 µg/mL
Molecular biology grade water	Corning, USA	Remaining volume

HCl: chloride acid, $MgCl_2$: magnesium chloride, Na_2HPO_4: sodium dihydrogen phosphate, PNA: peptide nucleic acid, USA: United States of America, mM: millimolar, %: percent, µg: microgram, mL: milliliter.

When the probe was added (30 µL per well and approximately 20 to 40 µL per slide, depending on the tissue section area), the plates were sealed with plastic wrap, and a coverslip was placed on the slides. The samples were then heated for 5 min (plates) or 3 min 30 sec (slides) at 85 °C for DNA denaturation to take place, and incubated for 2 h at RT in a humid and dark chamber to promote hybridization of the probe to telomeres. The hybridization solution without the probe was used as a negative control.

After the 2 h hybridization, two intense 15-min washes were performed to remove the non-specifically bound probe. The wash solution used contained 10 mM Tris-HCl (pH 7.5) and 0.1% bovine serum albumin (BSA) (Sigma-Aldrich, USA) in 70% formamide (Sigma-Aldrich, USA). Subsequently, this wash solution was replaced with 0.08% Tween 20 (Sigma-Aldrich, USA) in Tris Buffer Saline (TBS, Alaos, Spain), and three washes of 5 min each were performed. After the washes, cell nuclei were stained with 4',6-diamidino-2-phenylindole (DAPI, Thermo Fisher Scientific, Germany) (4 µg/mL for slides, and 1 µg/mL for plates). The excess was removed by washing with 1X PBS, and an antifading agent was added to prevent fluorescent signal dropout. No telomere signals were detected in samples where the hybridization solution was added without the telomere probe.

4.5.2.2 Image acquisition and analysis

4.5.2.2.1 Project 1: qFISH

Images were acquired using a TCS SP5 Leica high-resolution confocal microscope equipped with a resonant scanner and a 63x oil immersion objective with a 1.4 numerical aperture (NA) at the Microscopy and Image Analysis Service (SMAI) of the Hospital Nacional de Parapléjicos

de Toledo (HNP, Toledo, Spain). The Cy3 signal from telomeres and the DAPI signal marking cell nuclei were acquired in separate channels. The same settings were applied to acquire all images, regardless of the sample type, and acquisition was always performed under non-saturating signal conditions. This acquisition was performed manually by the user, and specifically in the case of ovarian samples, ovarian follicles were searched and identified individually before acquisition (Figure 11). The number of images acquired per individual was highly variable in the case of ovarian samples, depending on the number of follicles identified. However, in PBMCs, the analysis of a minimum of 300 cells was guaranteed. For signal quantification, the Fiji software (ImageJ 1.53f51) was used, applying two macros created in the SMAI of the HNP (Appendix B).

To detect telomere signals (Cy3), a threshold value of 70 and a rolling ball of 5 pixels were used in the maximum projections to subtract background (SBKG) noise from the acquired images. These same values were used for both ovarian slices and PBMCs. Regarding the DAPI signal, used for identifying and localizing the nuclear area (inside of which telomere signals were located), the threshold varied depending on the image to avoid saturation. This threshold did not interfere with detecting the telomere signal, which was analyzed on the Cy3 channel. In each of the images acquired, the cell types within the ovary (oocyte, GCs, TCs and stroma) were manually and restrictively selected and registered in the region of interest (ROI) Manager. Finally, telomere intensity, expressed as arbitrary units (a.u.), was extracted and quantified from the raw images based on the regions identified and registered in ROI Manager. Specifically, in the human ovarian samples, follicles in the primordial, primary, secondary, and larger preantral stages were identified (Figure 11). The telomere parameters analyzed using this technique included the mean TL, expressed in a.u. of intensity or kilobases, and the percentage of short (%short) and long telomeres (%long). Specifically, in Project 1, the 10th and 90th percentiles were used, respectively. In calculating these percents, the mean of the percentiles obtained in the control group for each cell type was used as the threshold value.

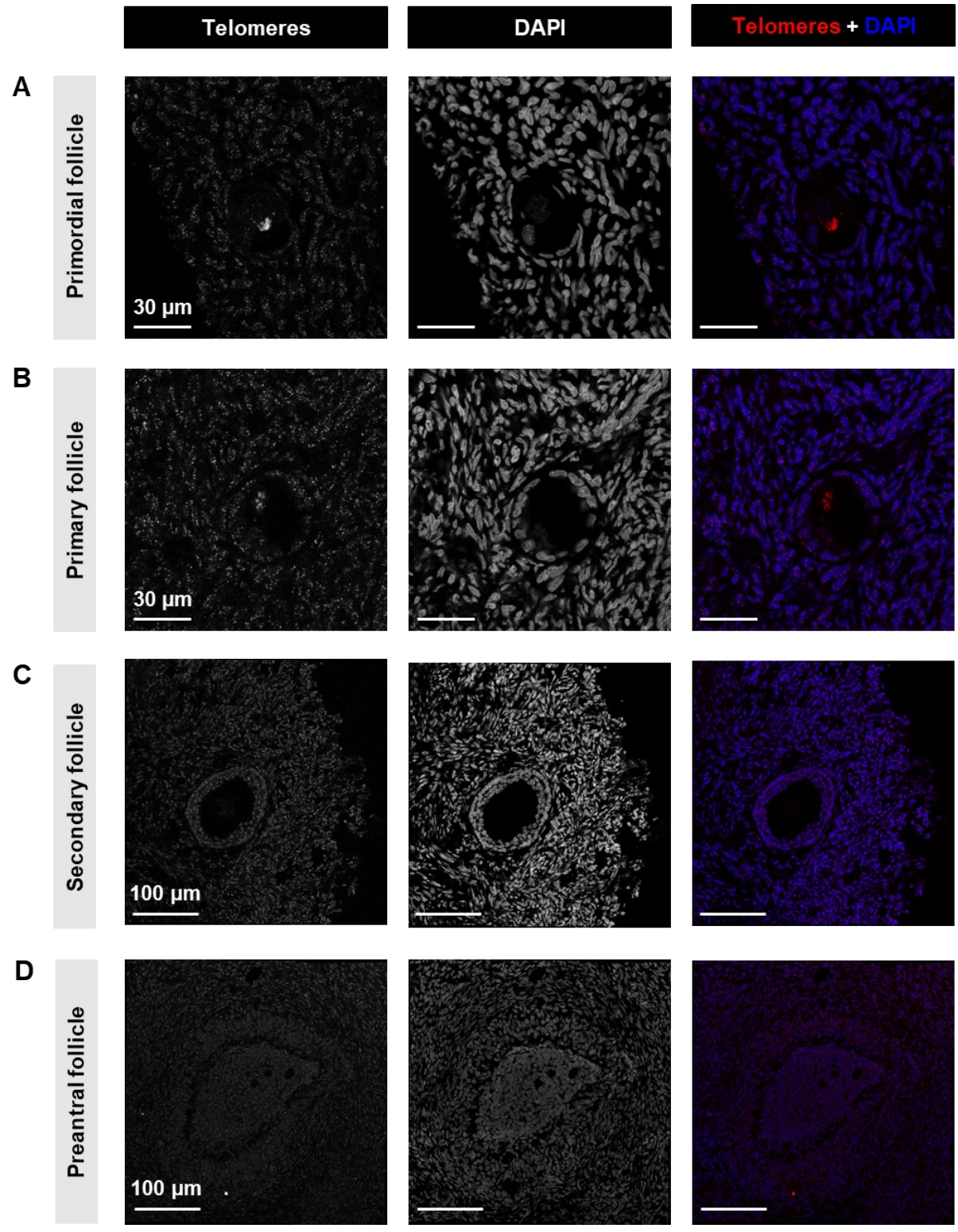


Figure 11. Representative images of ovarian follicles by FISH.

The micrographs are representative qFISH images of primordial, primary, secondary and preantral ovarian follicles. They show telomeres (left images), nuclei stained with DAPI (middle images), and the merged images (right images) of telomeres (red) and cell nuclei (blue). Scale bars represent 30 or 100 µm. DAPI: 4',6-diamidino-2-phenylindole.

4.5.2.2.2 Project 2: High-Throughput Quantitative Fluorescence In Situ Hybridization (HT-qFISH)

Images were acquired using an automated fluorescence microscope, the Opera High Content Screening System (PerkinElmer), with a 40x, 0.9 NA water immersion objective at the Confocal Microscopy Unit of the Spanish National Cancer Research Center (CNIO, Madrid, Spain). At least 300 cells were analyzed per individual, and 40 images were acquired in each well. To enable quantification, image acquisition was carried out under non-saturated signal conditions, and all images were captured with identical microscope settings. Images were analyzed with Acapella software (PerkinElmer). In quantifying the Cy3 signal, first, the mean signal intensity per telomere spot was corrected by subtracting the background intensity. This corrected mean Cy3 intensity per telomere spot was exported to Excel documents to quantify each individual's telomere length and expressed as arbitrary intensity units. As in the previous project, the telomere parameters evaluated were mean telomere length and the percentages of short and long telomeres. In this case, the percentiles evaluated were 15th and 85th, respectively.

4.5.3 Culture conditions for Jurkat cells

Jurkat E6-1 cells were a kind gift of Dr. Sara Rodriguez-Mora (National Center of Microbiology, ISCIII, Madrid, Spain). These cells were cultured at 37 °C and 5% CO_2 with humidity in Roswell Park Memorial Institute (RPMI) 1640 medium (Lonza™ BioWhittaker™, Belgium) supplemented with 10% (*v*/*v*) fetal bovine serum (FBS) (Corning, USA), 2 mM L-glutamine (Lonza™ BioWhittaker™, Belgium), and 1% of penicillin-streptomycin (Lonza™ BioWhittaker™, Belgium). This cell line was used as a positive control in the TRAP assay, for which cells were centrifuged for 1 min at 9300 x g, the supernatant was discarded, and the cell pellet was stored at -80 ºC until lysis. They were also used as a calibration standard to convert telomere fluorescence intensities from the qFISH technique into TL expressed in kilobases (section 4.5.2.1.), as their TL is stable and known (11.5 kb) (Treff et al., 2011, Sanchez-Vazquez et al., 2021). This conversion was carried out to perform correlations between the TL of different ovarian cell types and PBMCs, to explore the use of PBMCs as telomere biomarkers of ovarian aging. In this case, Jurkat cells were centrifuged at 4 °C for 7 min at a speed of 300 x g, the supernatant was removed, and the cell pellet was resuspended in methanol (PanReac AppliChem, Spain and Germany) and glacial acetic acid (PanReac AppliChem, Spain and Germany) in a 3:1 ratio, and stored at 4 °C until use.

4.6 Hematoxylin & Eosin Staining

After the deparaffinization or washing step to remove OCT, the ovarian sections were passed under running water and stained with hematoxylin for 15 min. Slides were then washed again with water for 15 min under agitation, placed four times in a mixture of ethanol and HCl (1 L of 70% ethanol and 10 mL of HCl) (Sigma-Aldrich, USA). Next, the samples were washed again with water and passed four times through a mixture of H_2O and ammonia (1 L of H_2O and 1 mL of 30% ammonia). The next step was staining with eosin for just 1 minute. The sections were dehydrated by immersing them four times in 99% ethanol. Finally, they were passed through xylene and mounted with Eukitt mounting medium (Germany) for subsequent observation under the Leica DM2000 LED brightfield microscope. In general terms, in this staining, the cell nuclei are violet because hematoxylin binds to the chromatin, and the cytoplasm is pink because of eosin. This technique was instrumental for the identification and histological examination of the structure of primordial, primary, secondary, preantral follicles, and corpus luteum in the ovarian tissue (Figure 12).

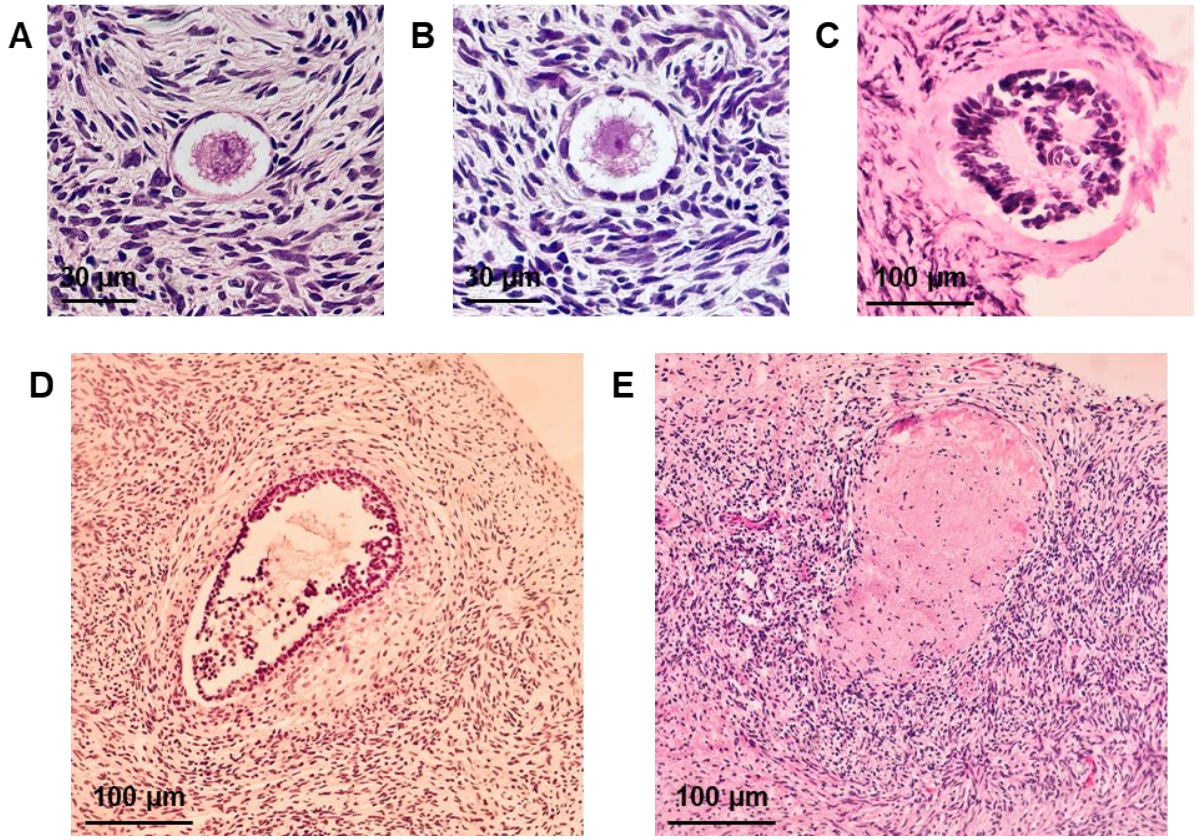


Figure 12. Representative images of ovarian follicles by H&E.

Hematoxylin stains cell nuclei dark blue to purple, while eosin stains the cytoplasm and extracellular matrix pink. (A) Primordial follicle; (B) Primary follicle; (C) Secondary follicle; (D) Preantral follicle; (E) Corpus luteum. Scale bars: 30 µm (A, B); 100 µm (C–E).

4.7 Ovarian fibrosis

Initially, fibrosis assessment was performed by the classical Masson's trichrome staining method in a small number of patients (n = 19), with representation from each age group (Y n = 6, M n = 6, P n = 7), because the ovarian sample was limited. However, quantitative PCR was performed to overcome this limitation to evaluate the expression levels of fibrosis-related genes (n = 62).

4.7.1 Masson's trichrome staining

This histological technique is commonly used to differentiate connective tissue components from other tissues, such as muscle and epithelial cells. This staining method utilizes a combination of three dyes: Weigert's iron hematoxylin (for nuclear staining in dark blue or black), Ponceau acid fuchsin (to stain cytoplasm and muscle fibers in red or pink), and aniline blue (to stain collagen fibers in blue).

Briefly explained, Masson's trichrome staining was performed on ovarian tissue samples after deparaffinization and rehydration, following the instructions of the manufacturer, LABKEM (Spain). First, the tissue was stained with Weigert's ferric hematoxylin, combining solutions A and B of this dye, for a brief period, usually 10 min, followed by 4 min with a picric acid solution to remove excess dye. The samples were then washed with a water rinse to remove excess dye. After rinsing, the tissue was stained with Ponceau acid fuchsin for 4 min and washed with distilled water. The phosphomolybdic acid solution was placed on the sections and allowed to act for 10 min to remove excess stain. Aniline blue was added directly to the sections and held for 5 min. Finally, the slides were washed in distilled water, rapidly dehydrated by ascending alcohol, stopped for 1 min in the last 100% ethanol, rinsed in xylene, and mounted with Eukitt mounting medium for subsequent observation on the Leica DM2000 LED brightfield microscope.

4.7.2 Expression of TGF-β1, COL1A1 and, COL3A1 genes

The expression analysis of TGF-β1, COL1A1, and COL3A1 genes was performed to evaluate ovarian fibrosis in RNA samples. Among fibrosis-related genes, TGF-β1 is widely recognized as a key profibrotic cytokine involved in the pathogenesis of fibrosis. Continued activation of TGF-β1 signaling drives excessive production of both COL1A1 and COL3A1, the most abundant collagen types in fibrotic tissues.

4.7.2.1 RNA isolation

For RNA extraction from the ovarian samples, the tissue was fragmented using a cryostat to obtain small sections. All the material used, including the cryostat, was previously treated with ethanol and cooled to prevent tissue thawing. Ovarian RNA isolation was then performed using the TRIzol™ (Thermo Fisher Scientific, Germany) method following the manufacturer's instructions. First, 1 mL of TRIzol was added to each sample, homogenized by vortexing, and incubated for 5 min at RT for complete dissociation of the nucleoprotein complexes. Then, 200 µL of 1-bromo-3-chloropropane (BCP, Sigma-Aldrich, USA) was added and mixed well, making about 15 inversions, and incubated at RT for 10 min. The samples were centrifuged for 10 min at 12000 x g at 4 °C to obtain three phases: the uncolored upper aqueous phase contained RNA, the interphase contained DNA, and the lower red-colored organic phase corresponded to proteins and lipids. For RNA precipitation, the upper aqueous phase was transferred to a new tube containing 500 µL isopropanol (Sigma-Aldrich, USA). The aqueous phase and isopropanol were gently mixed, incubated for 10 min at RT, and centrifuged for 10 min at 4 °C and 12000 x g. The supernatant was then discarded. The supernatant was then discarded, and the pellet was resuspended in 1 mL of 75% ethanol (Sigma-Aldrich, USA). The sample was vortexed briefly, then centrifuged for 5 min at 7500 x g at 4 ºC. This last wash with 75% ethanol was repeated again. The supernatant was discarded, and the pellet was allowed to dry at RT for 10 min. Finally, the RNA pellet was resuspended in 20 µL of RNase-free water (Qiagen, Germany). The RNA concentration was quantified on the NanoPhotometer™ N60 (Implen, Germany). The samples were stored at -80 ºC until their use.

4.7.2.2 cDNA synthesis

RNA retrotranscription to complementary DNA (cDNA) was performed according to the instructions of the iScript™ cDNA Synthesis kit (Bio-Rad). Briefly, 1 µg of ovarian template RNA was mixed with 4 µL of 5X iScript Reaction Mix, 1 µL of Reverse Transcriptase enzyme, and the remaining volume of Nuclease-free water to reach the final volume of 20 µL for the reaction. The complete reaction mixture was incubated in the MasterCycler® X50a thermal cycler (Eppendorf, Germany) using the protocol specified in Table 11. cDNA samples were stored at -20 ºC until use.

Table 11. cDNA synthesis thermal cycler protocol.

Phase	Time and temperature conditions
Priming	5 min at 25 ºC
Reverse transcription	20 min at 46 ºC
RT inactivation	1 min at 95 ºC
RT: reverse transcription, min: minutes, ºC: degrees celsius	

4.7.2.3 RT-qPCR

Real-time quantitative PCR was performed on the QuantStudio 12K Flex (Applied Biosystems – Thermo Fisher Scientific, Germany and USA) of the Genomics and Flow Cytometry Unit of the URJC, in 384-well plates using Power Track SYBR Green Master Mix (Applied Biosystems – Thermo Fisher Scientific, Germany and USA). The reactions were performed in triplicate with a ¼ dilution of the cDNA. The final reaction volume was 12 µL, where 5 µL corresponded to the cDNA, and the remaining 7 µL was a SYBR Green Master Mix (5.8 µL), the forward and reverse primers (sequences specified in Table 12) of the gene in question at a concentration of 3 µM each (1 µL), and nuclease-free H_2O until 7 µL were reached. In each well, 5 µL of the diluted cDNA and 7 µL of the master mix were deposited. After a short centrifugation of the plate, the program detailed in Table 13 was started.

Table 12. Primer sequences.

Name	Sequence (5' > 3')
TGF-β1 forward	TGGAAACCCACAACGAAATC
TGF-β1 reverse	GGGTTCAGGTACCGCTTCTC
CO1LA1 forward	GAGAGCATGACCGATGGATT
COL1A1 reverse	CCTTCTTGAGGTTGCCAGTC
COL3A1 forward	CGGCAATCCTGAACTTCCTG
COL3A1 reverse	ATCAGCTTCAGGGCCTTCTT

A: adenosine, C: cytidine, G: guanosine, T: thymidine, TGF-β1: transforming growth factor beta 1, COL1A1: collagen type I alpha 1, COL3A1: collagen type III alpha 1.

Table 13. RT-qPCR thermal cycler protocol.

Step	Time and temperature conditions	Cycles
Enzyme activation	20 sec at 95 ºC	1
Denaturation	5 sec at 95 ºC	40
Annealing/extension	30 sec at 60 ºC	
Melt Curve Stage	**Time and temperature conditions**	**Ramp rate**
1	15 sec at 95 ºC	1.99 ºC/sec
2	1 min at 60 ºC	1.6 ºC/sec
3 (Dissociation)	15 sec at 95 ºC	0.05 ºC/sec

sec: seconds, min: minutes, ºC: degrees Celsius.

To quantify the relative expression of each gene, we employed the DCq method, which uses a reference gene, a variation of the Livak method (Livak and Schmittgen, 2001). The baseline and threshold cycles (Cq) for the amplification curves were determined using the instrument software (Table 14). Non-specific amplification was checked and excluded. First, the mean of the three measurements [$Cq_{mean} = (Cq_1+Cq_2+Cq_3)/3$] per sample was calculated. Next, the

expression of TGF-β1, COL1A1, and COL3A1 (DCq) was normalized for the endogenous GAPDH gene ($DCq = Cq_{mean\ GAPDH} - Cq_{mean\ gene}$). Finally, the relative expression of the gene in question was shown as 2^{DCq}.

Table 14. RT-qPCR quantification parameters detailed.

Gene	Baseline start	Baseline end	Cq threshold	Y-Intercept	R^2	Slope	Eff %	Error
TGF-β1	3	20	0.200	33.814	0.847	-2.528	148.603	0.34
COL1A1	3	16	0.200	28.852	0.958	-2.964	117.456	0.179
COL3A1	2	11	0.200	26.777	0.883	-2.658	137.798	0.279

TGF-β1: transforming growth factor beta 1, COL1A1: collagen type I alpha 1, COL3A1: collagen type III alpha 1, Cq: quantification cycle, R^2: coefficient of determination, Eff: amplification efficiency.

4.8 Proteomic assessment of ovary samples

The proteomic analysis was conducted in the Proteomics Facility of HNP (Toledo, Spain).

4.8.1 Sample preparation

The extraction procedure was adapted from the Folch method with slight modifications (Folch et al., 1951, Folch et al., 1957). NaCl (0.88%, 90 µl) and MS-QReSS label internal standard (10 µl) were added to the sample pellets, followed by the addition of chloroform/methanol (2:1, 500 µl). The sample suspensions were incubated at –40 ºC for 15 minutes, then sonicated for 30 seconds at 80% power using a UP50H homogenizer (5 cycles) at –40 ºC. These steps were repeated three times. The samples were centrifuged at 14,000 rpm for 15 minutes at 4 ºC. The aqueous phase was transferred to a clean vial and stored at –40 ºC until injection. The organic phase was transferred to another vial and evaporated under nitrogen flow. This phase was also stored at –40 ºC until further use. The protein fraction was resuspended in lysis buffer (Table 15), and the protein concentration was determined using the Bradford-Lowry method (Bio-Rad protein assay).

Table 15. Recipe for lysis buffer used in proteomic analysis.

Reagent	Reagent Manufacturer	Final concentration
Urea	Thermo Fisher Scientific, Germany	7 M
Thiourea	Thermo Fisher Scientific, Germany	2 M
Sodium orthovanadate phosphatase inhibitor	Sigma-Aldrich, USA	1X
Protease Inhibitor Cocktail	Sigma-Aldrich, USA	1X

M: molar, USA: United States of America.

4.8.2 Sample preparation for library generation

Electrophoresis separated proteins using a 4-20% MiniPROTEAN TGX gel (Bio-Rad). The gel was visualized using Coomassie staining, and the entire lane was manually cut into 8 sections, which were then subjected to in-gel tryptic digestion (Shevchenko et al., 1996). The gel slices were incubated with 10 mM dithiothreitol or DTT (Sigma-Aldrich, USA) in 50 mM ammonium bicarbonate for 60 minutes at 37 ºC for reduction. After reduction, the slices were alkylated with 55 mM iodoacetamide (Sigma-Aldrich, USA) in 50 mM ammonium bicarbonate for 20 minutes at RT. Gel plugs were washed with 50 mM ammonium bicarbonate in 50% methanol, rinsed with acetonitrile, and dried using a Speedvac. Dry gel pieces were embedded in sequencing-grade modified porcine trypsin (Promega, USA) at 12.5 ng/µL in 20 mM ammonium bicarbonate and digested overnight at 37 ºC. After digestion, peptides were extracted using 60% acetonitrile (ACN) in 0.5% formic acid. The samples were then resuspended in 10 µL of a solution containing 98% water, 2% formic acid, and 2% acetonitrile.

4.8.3 SP3 sample preparation

Sample lysates were processed using Single-pot solid-phase-enhanced sample preparation (SP3) according to the protocol described by Hughes (Hughes et al., 2014). The lysates were reduced with DTT and alkylated with iodoacetamide (IAA). A prepared bead mix (6 µL) was added to the lysate, and the volume was adjusted to 30 µL with water. Ethanol (70% v/v) was added to the samples, and the mixture was stirred at 1000 rpm at RT for 20 minutes. The beads were immobilized using a magnetic rack for 2 minutes, and the supernatant was transferred to a new vial. This procedure was repeated to ensure complete washing of the beads with 80% ethanol in water. The beads were resuspended in 300 µL of 100 mM ammonium bicarbonate, supplemented with trypsin at a 1:25 enzyme-to-protein ratio (w/w). After overnight digestion at 37 ºC with shaking at 1000 rpm, the samples were centrifuged at 20,000 g. The supernatant was collected and acidified with 2% formic acid.

4.8.4 LC-MS/MS analysis for library construction, DDA, and SWATH

4.8.4.1 Spectral Library Generation

The peptide extracts were analyzed using a shotgun approach with nanoLC-MS/MS. Samples were pooled, and 1 µg of the peptide sample was separated using an Ekspert™ nanoLC425 system (Eksigent, USA) equipped with a C18 column (Luna Omega, 3 µm Polar C18, 100 Å, 0.3 x 150 mm, Phenomenex) at a flow rate of 5 µL/min. A precolumn (Micro Trap Luna 5 µm C18, 100 Å, 20 x 0.3 mm, Phenomenex) was used with the same 5 µL/min flow rate. Peptides were desalted for 3 minutes with Buffer A (0.1% formic acid, 2% ACN) on the precolumn,

followed by a 30-minute gradient separation using the following conditions: 6% to 30% solvent B over 30 minutes, 30% to 95% solvent B for 0.1 minutes, and 95% solvent B for 5 minutes. The buffer or solvent B composition was 98% ACN in water with 0.1% formic acid. The column was regenerated with 6% solvent B for 10 minutes.

4.8.4.2 Mass Spectrometry

Peptides were directly injected into a TripleTOF® 6600+ mass spectrometer (Sciex, USA) and ionized using an Optiflow MicroProbe source (1-50 µL/min, 4.5 kV at 75 ºC). Data were acquired in data-dependent acquisition (DDA) positive ion mode. Survey scans (MS1) were performed in the range of 350–1400 m/z for 250 ms. Ion fragmentation was performed at a "LOW" resolution for MS2 scans in the range of 240–1300 m/z for 25 ms in high sensitivity mode. Ions with charges of 2+ to 4+ and a minimum intensity of 250 counts per second were selected for fragmentation. A maximum of 100 ions per survey scan were selected for fragmentation, with dynamic exclusion set to 15 seconds.

4.8.4.3 SWATH Mode

The TripleTOF was operated in SWATH mode, acquiring a 50 ms TOF MS scan from 350–1400 m/z and 92.4 ms product ion scans from 240–1300 m/z across 40 variable windows (3.79 sec/cycle). SWATH injections were randomized.

4.8.5 Data analysis

4.8.5.1 Peptide and protein identification

Peptide and protein identifications were performed using ProteinPilot™ Software v5.0 (Sciex) and the Paragon algorithm. Each MS/MS spectrum was searched against the SProt-H.Sapiens2024_08 database, with carbamidomethyl-labeled cysteine as a fixed modification. The ProteinPilot software calculated an "unused score" to determine identification confidence, with a 99% confidence threshold corresponding to a false positive rate of approximately 1%. Only proteins with at least one peptide identified with a confidence level greater than 99% were recorded. The false discovery rate (FDR) was controlled below 1% by using a concatenated database with both forward and reverse sequences.

4.8.5.2 Spectral library construction and SWATH data processing

The SWATH Acquisition MicroApp v.2.0 was used to construct the peptide spectral library from peptides identified with a confidence score greater than 99%. This software was also used for extracting ion chromatogram traces from the SWATH raw files and for applying the previously generated spectral library. Key parameters included: 20 peptides per protein; 6

fragment ions per peptide; extraction windows of 5 minutes and 25 ppm; and peptide FDR of 1% and a confidence score threshold of 99%.

4.8.5.3 Normalization

Protein abundance measurements obtained from SWATH were normalized using MarkerView (v1.2.1, Sciex).

4.9 Statistical analysis

4.9.1 General statistical analysis

Statistical analyses and tests were performed with GraphPad, SPSS v.21.0 software (IBM), and RStudio 4.4.1. Descriptive statistics provided information on the central tendency, variability, and dispersion of the data. The parameters evaluated in the descriptive analysis were: mean, standard deviation, standard error of the mean, median, and interquartile range. The normality of the data was then assessed using the Shapiro-Wilk test ($n < 30$) and the Kolmogorov-Smirnov test (for $n > 30$). Normality tests detected data that followed a normal distribution, an essential prerequisite for further statistical analysis. The data that were normally distributed and passed the normality test were analyzed using parametric tests such as ANOVA (with Tukey's multiple comparison test) to compare the means of several groups and Student's t-test to compare two independent groups. When the data did not evidence a normal distribution, nonparametric tests such as the Kruskal-Wallis test (with Dunn's multiple comparisons test) and the Mann-Whitney U test were used to compare medians between groups. Correlation analyses were performed using the following tests: Pearson's correlation (for normally distributed numerical data), Spearman's rank correlation (for non-normally distributed or ordinal data), and Kendall's tau-b (for ordinal data with tied ranks), to assess the strength and direction of relationships between variables.

RESULTS

5 RESULTS

Results were divided into four main sections, where data for the first (5.1), second (5.2), and third (5.3) sections were obtained from Project 1, and the fourth (5.4), from Project 2.

PROJECT 1:

The first section focused on the characterization of ovarian aging from several points of view, but centered mainly in the telomere pathway. Assuming the decrease in ovarian reserve with increasing age, the second section analyzed the variations in TL in women with high and low ovarian reserve within each age group. The third section was focused on the impact of pregnancy (a period marked by low levels of AMH) on ovarian telomere maintenance.

Each section of this project was based on the study of a specific number of individuals, detailed at the beginning of the section. Age played a major role in the detailed variables, given that it influenced telomere dynamics. However, in certain results, the cohort differed from the initial cohort, with the mean value of the variable age. Some techniques could not be performed on the entire study group cohort due to the unavailability of the sample. In other techniques, as occurred in the assessment of ovarian telomere parameters, not all ovarian cell types were identified in the entire study cohort. Consequently, the initial value for the mean age of each group specified in the baseline characteristics at the beginning of the results was not valid for the new cohorts in which ovarian populations were identified. In these cases, the variable age was re-specified to check whether statistically significant differences in the mean age of the groups remained. The recalculated age values were collected in tables within the body of the text and in the appendices. Only those cases in which the age difference differed from the initial result were mentioned in the text.

PROJECT 2:

The fourth and last section studied how pathologies not directly related to the reproductive system could impact it. Specifically, cases of COVID-19 were analyzed in which the severe symptoms may have favored telomere shortening and may have had consequences on specific reproductive outcomes.

5.1 Characterization of age-dependent female reproductive decay

Ovarian decline was analyzed and characterized in women of different age groups: young (Y, 18-34 years), middle-aged (M, 35-45 years), and perimenopausal women (P, 46-50 years). All

the data collected in this section result from the work carried out with the samples from Project 1.

5.1.1 Baseline characteristics of the study population and hormonal levels

A total of 65 women who required surgery for reasons unrelated to this study (see Materials and Methods) were included in this first study section. After classification based on age at recruitment, the Y group consisted of 17 women, the M group comprised 31 patients, and the P group included 17 women. Statistically significant differences were found in the mean age of the groups (globally $p<0.0001$, Y vs. M $p<0.0001$, Y vs. P $p<0.0001$, and M vs. P $p<0.0001$). No differences were evidenced in BMI ($p = 0.2858$) or any other parameter related to the menstrual cycle, such as age at menarche ($p = 0.2478$), cycle length ($p = 0.0645$), or bleeding duration ($p = 0.2831$). Table 16 presents the baseline characteristics of patients across the different age subgroups.

Table 16. Characteristics of the study population classified by age.

	Y n = 17	**M** n = 31	**P** n = 17	**p-value**
Demographic characteristics				
Age (years)				<0.0001
Mean ± SD	30.7 ± 4.2	40.3 ± 3.0*	47.5 ± 1.1	
Median (Q1–Q3)	32.0 (29.5-34.0)	40.0 (38.0-43.0)	47.0 (47.0-48.5)	
BMI (kg/m^2)				0.2858
Mean ± SD	24.8 ± 4.2*	26.9 ± 5.0*	27.0 ± 4.5*	
Median (Q1–Q3)	23.8 (22.6-25.8)	25.3 (23.3-31.7)	26.8 (22.9-29.6)	
Menstrual-related parameters				
Age at menarche (years)				0.2478
Mean ± SD	11.8 ± 1.6*	12.5 ± 1.4	12.4 ± 1.5*	
Median (Q1–Q3)	12.0 (10.5-13.0)	12.5 (11.0-14.0)	13.0 (11.5-13.0)	
Cycle length (days)				0.0645
Mean ± SD	29.8 ± 3.5	28.3 ± 6.8	28.2 ± 1.9	
Median (Q1–Q3)	30.0 (28.0-30.0)	28.0 (26.5-28.0)	28.0 (28.0-30.0)	
Bleeding duration (days)				0.2831
Mean ± SD	5.1 ± 1.4*	5.0 ± 2.2	5.4 ± 1.3	
Median (Q1–Q3)	5.0 (4.0-6.0)	4.0 (4.0-6.0)	5.0 (5.0-6.5)	
Dysmenorrhea, n (%)	12 (70.6)	16 (51.6)	11 (64.7)	NA
Hormonal contraception, n (%)	4 (23.5)	7 (21.7)	9 (52.9)	NA
Reproductive history, n (%)				
Parity	12 (70.6)	23 (74.2)	15 (88.2)	NA
Miscarriage/abortion	6 (35.3)	16 (51.6)	6 (35.3)	NA
Obstetrics/gynecology surgery				NA
Diagnostic hysteroscopy	0 (0.0)	4 (12.9)	4 (23.5)	NA
Tubal ligation	0 (0.0)	1 (3.2)	1 (5.9)	NA
Dilation and curettage	1 (5.9)	11 (35.5)	4 (23.5)	NA
Cesarean section	4 (23.5)	6 (19.4)	4 (23.5)	NA
Myomectomy	0 (0.0)	2 (6.5)	0 (0.0)	NA
Hysterectomy	0 (0.0)	0 (0.0)	1 (5.9)	NA
Salpingectomy	0 (0.0)	1 (3.2)	0 (0.0)	NA
Ovarian cystectomy	3 (17.7)	1 (3.2)	1 (5.9)	NA
Oophorectomy	0 (0.0)	2 (6.5)	1 (5.9)	NA
Laparotomy	0 (0.0)	2 (6.5)	0 (0.0)	NA
Comorbidities, n (%)				
Hypothyroidism	3 (17.7)	5 (16.1)	4 (23.5)	NA
Diabetes	0 (0.0)	1 (3.2)	1 (5.9)	NA
Hypertension	0 (0.0)	0 (0.0)	1 (5.9)	NA
Migraine	1 (5.9)	0 (0.0)	1 (5.9)	NA
Asthma	2 (11.8)	0 (0.0)	0 (0.0)	NA
Others	1 (5.9)	3 (9.7)	2 (11.8)	NA
Medications and supplements, n (%)				
Thyroid hormone replacement	3 (17.7)	4 (12.9)	4 (23.5)	NA
Insulin	0 (0.0)	1 (3.23)	0 (0.0)	NA
Pain reliever	1 (5.9)	2 (6.5)	1 (5.9)	NA
Inhaler	0 (0.0)	3 (9.7)	0 (0.0)	NA
Omeprazole	0 (0.0)	1 (3.2)	3 (17.7)	NA
Vitamin B12	1 (5.9)	0 (0.0)	1 (5.9)	NA
Vitamin B9	0 (0.0)	2 (6.5)	0 (0.0)	NA
Iron	1 (5.9)	8 (25.8)	2 (11.8)	NA
Antidepressant	1 (5.9)	0 (0.0)	0 (0.0)	NA
Others	2 (11.8)	5 (16.1)	1 (5.9)	NA
Lifestyle and habits, n (%)				
Present smoker	3 (17.7)	5 (16.1)	1 (5.9)	NA
Caffeine	14 (82.4)	23 (74.2)	15 (88.2)	NA
Exercise	9 (52.9)	11 (35.5)	5 (29.4)	NA

Special diet	3 (17.7)	4 (12.9)	1 (5.9)	NA

Data are presented as mean ± standard deviation, median (interquartile range), or number of subjects and the percentage of their group in brackets. The mean and median are only specified for variables where statistical analysis is performed. Statistical analysis was performed on the following variables: age, BMI, age at menarche, cycle length, and bleeding duration. *Denoted the variables that passed the Shapiro-Wilk normality test. Those variables with normal distribution (BMI) were compared by one-way ANOVA (p-value specified in the table) and Tukey's multiple comparisons test (p-values not shown). The rest of the variables, which did not pass the normality test, were analyzed by Kruskal-Wallis (p-value specified in the table) and Dunn's multiple comparisons tests (p-values not shown). A p-value < 0.05 was considered statistically significant. “n” refers to the number of subjects. Y: young, M: middle-aged, P: perimenopausal, SD: standard deviation, Q1: quartile 1 (25% percentile), Q3: quartile 3 (75% percentile), BMI: body mass index, NA: not applicable.

Regarding hormonal levels (values and statistical analysis listed in Appendix C, Table C1), AMH, FSH, LH, E2, and P4 were measured by electrochemiluminescence immunoassays. The first hormone evaluated was AMH. The differences in the mean value of AMH between age groups were statistically significant (Figure 13A, globally p<0.0001); the highest value was recorded in the Y group (2.6 ± 2.5 ng/mL), followed by M (1.0 ± 1.2 ng/mL), and finally, P with the lowest levels of this hormone (0.2 ± 0.4 ng/mL). Additionally, AMH correlated negatively with age (p < 0.0001). The FSH value (Figure 13B) only showed statistical differences when comparing the Y and M groups with respect to P (p = 0.0058 and p = 0.0177, respectively). Specifically, group M (21.0 ± 51.0 mIU/mL) presented higher levels for this hormone, followed by P (14.1 ± 11.2 mIU/mL) and Y (3.7 ± 2.5 mIU/mL). FSH was also correlated with age, although, opposite to AMH, this correlation was positive (p = 0.0004). LH (Figure 13C) showed no differences when comparing age groups (Y: 5.2 ± 4.6, M: 9.8 ± 16.2, P: 9.8 ± 7.6 mIU/mL, p = 0.0903) despite correlating positively with age (p = 0.0093). The lowest levels of E2 (Figure 13D) were observed in the P (66.09 ± 58.41 pg/mL) group compared to Y (806.9 ± 1257 pg/mL, p = 0.0416) and M (992.7 ± 1341 pg/mL, p = 0.0258), and a negative correlation was also found with age (p = 0.0374). Finally, no differences were observed in P4 (Figure 13E) when comparing age groups (Y: 15.2 ± 25.8, M: 19.0 ± 27.4, P: 1.9 ± 4.0 ng/mL, p = 0.3578), nor did it correlate with the women’s age (p = 0.2454).

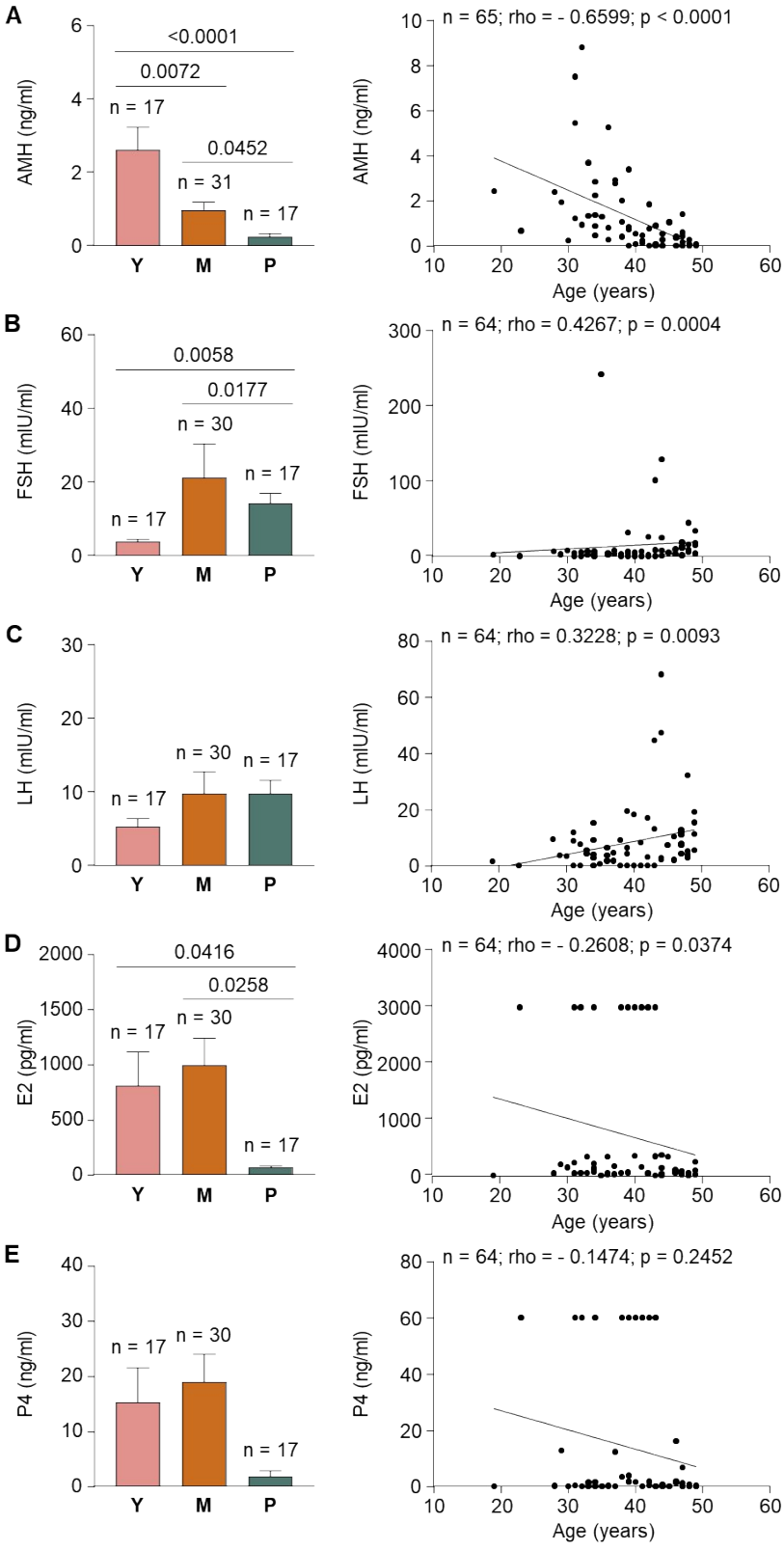


Figure 13. Analysis of the levels of AMH, FSH, LH, E2, and P4 with age.

The figure shows the comparisons of AMH (A), FSH (B), LH (C), E2 (D), and P4 (E) levels between the Y, M, and P age groups (left) and the correlation of those hormonal serum levels with age (right). The graphs (left) represent the mean value of the hormone for each group, and their error bars refer to the standard error of the mean (SEM). For comparing hormone values between the three groups, the Kruskal-Wallis and Dunn's multiple comparison tests were used because the distribution of the

variables did not follow a normal distribution (verified by the Shapiro-Wilk test). Spearman's correlation was performed for the hormonal values because none of them passed the Kolmogorov-Smirnov test for normality. A p-value < 0.05 was considered statistically significant. Only significant p-values are shown in the bar graphs. The sample size of each group is represented as n. Note that FSH, LH, E2, and P4 levels could not be measured in one subject of group M; even so, the mean age between groups in these hormones remained statistically significant. For more information, see Appendix C, Table C1. Y: young, M: middle-aged, P: perimenopause, AMH: anti-müllerian hormone, FSH: follicle-stimulating hormone, LH: luteinizing hormone, E2: estradiol, P4: progesterone, rho: Spearman correlation coefficient, ng: nanogram, mL: milliliter, mIU: milli-International Units, pg: picogram.

5.1.2 Telomere analysis

5.1.2.1 Analysis of systemic telomere status

TL in PBMCs was evaluated by qFISH to obtain a general aging condition of the organism (Figure 14).

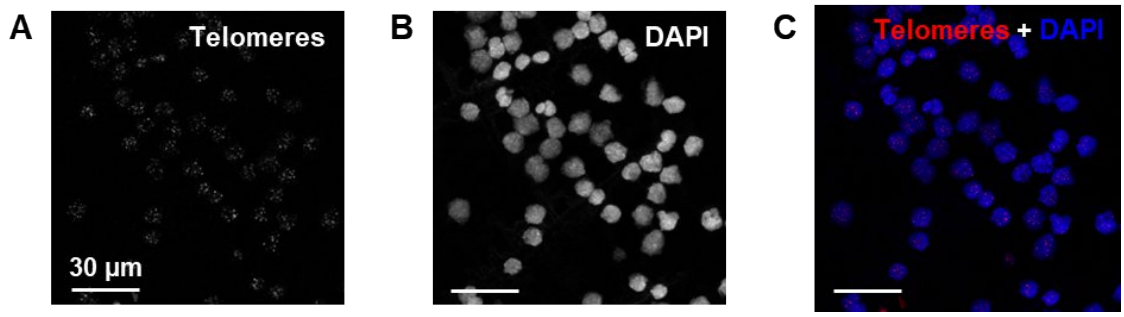


Figure 14. Telomere qFISH in PBMCs.

The micrographs are representative qFISH images showing telomeres (white dots, A), nuclei stained with DAPI (B), and the merged image (C) of telomeres (red) and cell nuclei (blue). Scale bars represent 30 µm. DAPI: 4',6-diamidino-2-phenylindole, µm: micrometer.

When the mean TL between the different age groups was compared (Figure 15A), the values obtained for Y (129.7 ± 7.3 a.u.) and M (130.7 ± 15.4 a.u.) were similar, but the mean TL in the P group (123.3 ± 7.5 a.u.) tended to be lower. However, the differences were not statistically significant ($p = 0.0735$). The percentage of short telomeres (Figure 15B) was significantly higher in the older P group (17.6 ± 8.7%) compared to Y (11.0 ± 5.9%, $p = 0.0436$) and M (11.8 ± 8.4%, $p = 0.0436$) groups. No differences were found in the percentage of long telomeres in any group (Figure 15C, $p = 0.2728$). Only the variables TL and percentage of short telomeres showed significant correlations with age (Figure 15D and E, $p = 0.0206$ and $p = 0.0092$, respectively). TL negatively correlated, while the percentage of short telomeres positively correlated with age. However, the percentage of long telomeres did not correlate with age (Figure 15F, $p = 0.0931$).

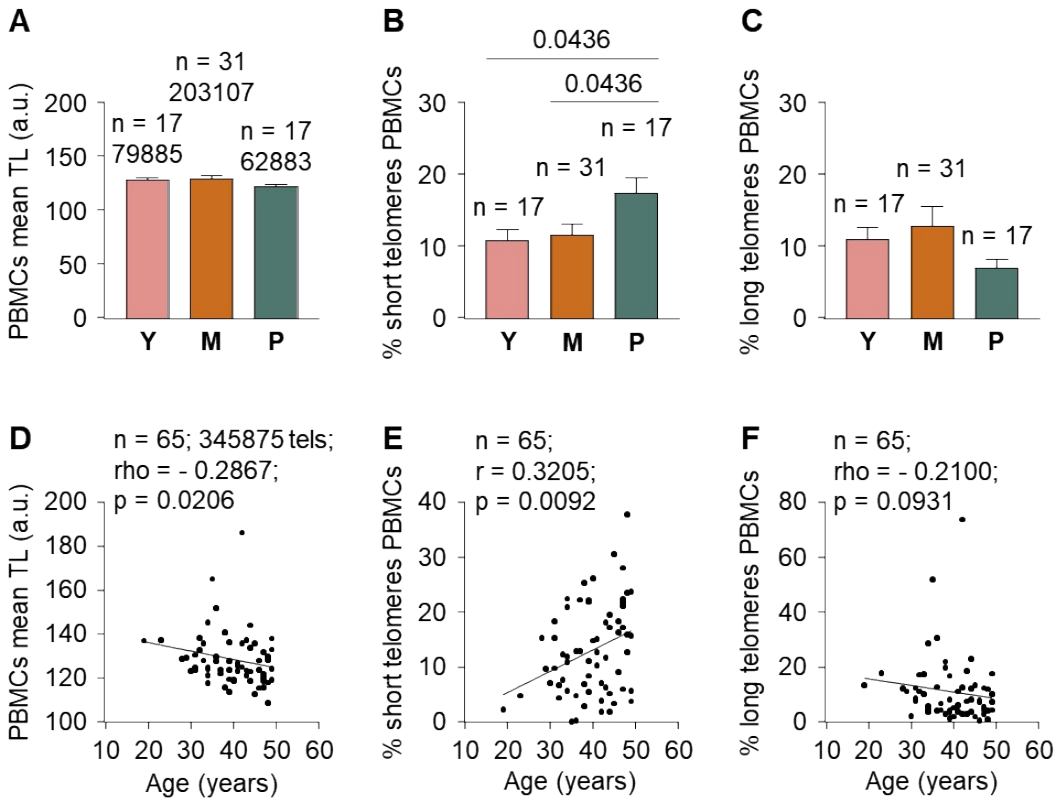


Figure 15. Analysis of telomere parameters in PBMCs in Y, M, and P women.

(A) Mean TL analyzed by qFISH in the indicated age groups. The number below n refers to the number of telomere dots analyzed. (B) Percentage of short telomeres in PBMCs. (C) Percentage of long telomeres in PBMCs. (D) Spearman correlation between mean TL and age of the recruited women. The number of telomeres analyzed is specified. (E) Positive Pearson correlation between age and percentage of short telomeres. (F) Non-significant Spearman correlation of the percentage of long telomeres and age. The bar diagrams (A, B, C) represent the mean value, and the error bars represent the SEM. Comparison between the three groups (upper panels) was performed by Kruskal-Wallis with Dunn's multiple comparison tests for the variables TL and percentage of long telomeres. The percentage of short telomeres was compared using the ANOVA corrected by Tukey's multiple comparison test. In the correlations (lower panels) Spearman was applied (TL and percentage of long telomeres) when the variables did not pass the Kolmogorov-Smirnov normality test. At the same time, Pearson was used only in those that showed normality (percentage of short telomeres). A p-value < 0.05 was considered statistically significant. Only significant p-values are shown in the bar graphs. The number of individuals analyzed in each group is represented as n. For more information, see Appendix C, Table C2. PBMCs: peripheral blood mononuclear cells, Y: young, M: middle-aged, P: perimenopausal, TL: telomere length, a.u.: arbitrary units (intensity), %: percent, tels: telomere dots, r: Pearson correlation coefficient, rho: Spearman correlation coefficient.

5.1.2.2 Analysis of reproductive telomere status

At the systemic level, telomere changes were manifested by an increase in the percentage of short telomeres when comparing the groups of women of reproductive age (Y and M) with the perimenopausal women. This data suggested the age interval of 46 to 50 years as a crucial moment in global aging. For this reason, the telomere pathway was also studied in the ovary by qFISH. Because in the ovary there are different cell types coexisting, telomere parameters

were assessed independently performing manual selection of these cells in the images. In particular ovarian stroma, oocytes, GCs, and TCs were analyzed.

5.1.2.2.1 Ovarian stroma

Firstly, the region known as the ovarian stroma, which surrounds and supports the ovarian follicles, was studied within the ovary (Figure 16).

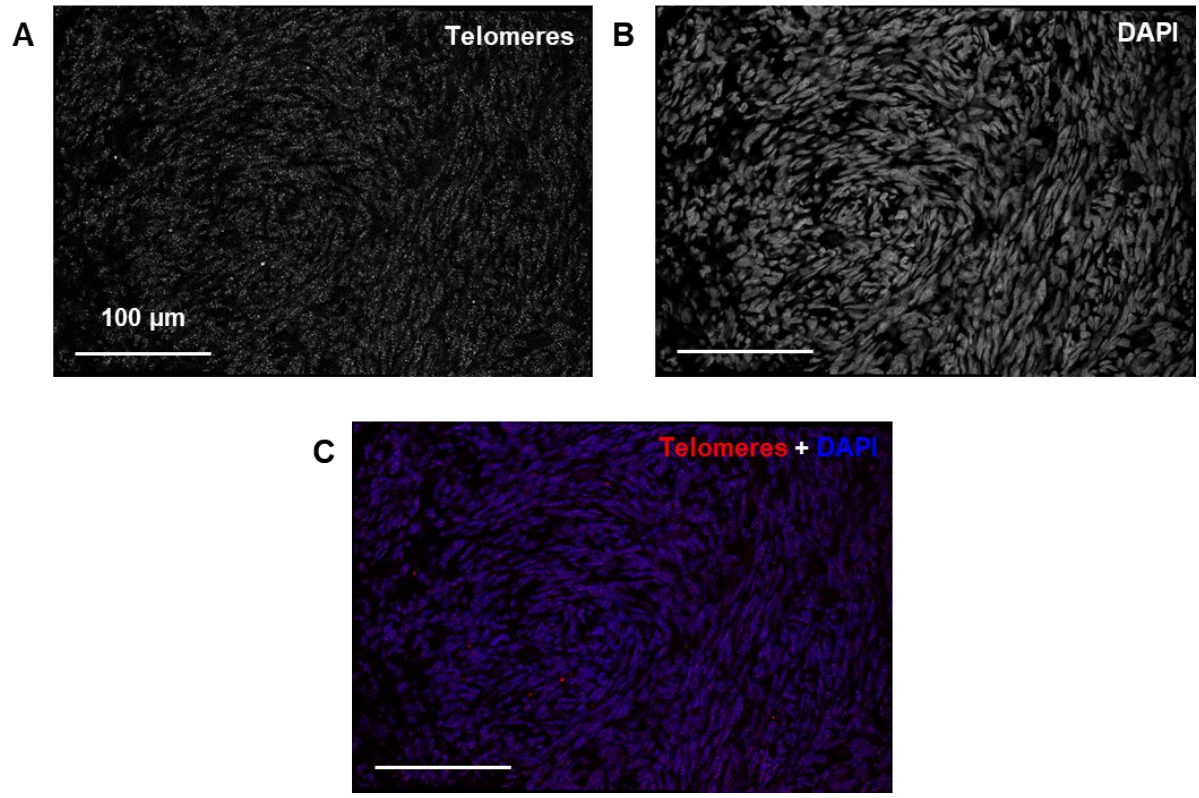


Figure 16. Telomere qFISH in ovarian stroma.

The micrographs are representative qFISH images showing telomeres (white dots, A), nuclei stained with DAPI (B), and the merged image (C) of telomeres (red) and cell nuclei (blue). Scale bars represent 100 µm. DAPI: 4',6-diamidino-2-phenylindole, µm: micrometer.

No statistically significant differences were observed when comparing the mean stromal TL (Table 17) in all subjects grouped based on age (p = 0.2729). There was no correlation between age and ovarian stroma TL (n = 65; 6332420 tels; r=-0.0072; p = 0.9544). Regarding the percentage of short and long telomeres (Table 17), no statistically significant differences were detected (p = 0.1990 and p = 0.4017, respectively) when comparing the Y, M, and P groups. Neither the percentage of short (n = 65; rho =-0.0416; p = 0.7422) or long telomeres (n = 65; rho=0.0545; p = 0.6666) correlated significantly with age.

Table 17. Ovarian stroma telomere parameters in groups based on age.

	Y n = 17	**M** n = 31	**P** n = 17	**p-value**	
TL (a.u.)					0.2729
Telomeres	1874238	3478785	979397	**Y vs. M**	0.6415
Mean ± SD	143.2 ± 11.6*	139.9 ± 12.0*	145.7 ± 13.5*	**Y vs. P**	0.8185
Median (Q1–Q3)	143.8 (134.6-152.4)	139.3 (130.2-147.3)	144.4 (133.6-156.9)	**M vs. P**	0.2585
Short telomeres (%)					0.1990
Mean ± SD	12.9 ± 12.2	17.2 ± 11.3*	12.32 ± 13.0	**Y vs. M**	0.6427
Median (Q1–Q3)	7.7 (6.4-15.9)	16.3 (6.8-27.2)	8.4 (3.0-20.6)	**Y vs. P**	>0.9999
				M vs. P	0.2942
Long telomeres (%)					0.4017
Mean ± SD	12.9 ± 10.8	10.9 ± 10.8	15.6 ± 12.7	**Y vs. M**	>0.9999
Median (Q1–Q3)	9.8 (3.3-22.5)	8.8 (3.0-13.9)	9.5 (4.5-24.0)	**Y vs. P**	>0.9999
				M vs. P	0.5600

Data are presented as mean ± standard deviation and median (interquartile range). *Denoted the variables that passed the Shapiro-Wilk normality test. The variables were analyzed by ordinary one-way ANOVA and Tukey's multiple comparisons test (TL), or Kruskal-Wallis and Dunn's multiple comparisons tests (short and long telomeres). A p-value < 0.05 was considered statistically significant. "n" refers to the number of subjects. The number of telomere dots analyzed is specified in the TL section under the heading "Telomeres". Y: young, M: middle-aged, P: perimenopausal, TL: telomere length, SD: standard deviation, Q1: quartile 1 (25% percentile), Q3: quartile 3 (75% percentile), a.u.: arbitrary units of intensity, %: percent, vs.: versus.

5.1.2.2.2 Germ cells: oocytes

Although no telomere shortening with aging was evidenced in ovarian stroma, it was expected that aging would not follow the same pattern in germ cells since cellular functions and behaviors are different. For the oocyte study, these cells were identified as forming part of follicle structures at different stages of folliculogenesis in the ovarian sections. In addition, it was impossible to find oocytes in all ovarian sections of all women who participated in the study, specifically, in group P. Thus, this older group was excluded in the telomere analysis of oocytes.

5.1.2.2.2.1 Telomere length in oocytes during folliculogenesis

Since follicles contain different cell types, we first analyzed oocyte telomere dynamics during folliculogenesis. As not all follicular stages were found in the ovarian sections, we focused on oocytes from primordial, primary, and secondary follicles despite being immature and arrested in prophase I of meiosis.

This analysis was performed jointly in all women (n = 33), where oocytes were identified at different stages and separately in the Y (n = 15) and M (n = 18) populations. In the first analysis, where both Y and M women were pooled, the mean age of subjects with oocytes analyzed at each follicular stage was similar (p = 0.5444) and, therefore, comparable. The age variable remained similar when only the Y (p = 0.5487) or M (p = 0.9585) populations were studied. A consistent average age across the different follicular stages ensured that, if there were differences in telomere parameters intrinsic to aging, the analysis of folliculogenesis would not

be affected. Focusing on the telomere pathway during folliculogenesis, no statistically significant differences were found in any comparison in TL or the percentage of short and long telomeres. The telomere parameters for each comparison are detailed in Table 18. Special attention was paid when oocytes at different stages were identified in the same woman.

Table 18. Oocyte telomere parameters during folliculogenesis.

All subjects n = 33	**Primordial (0)** n = 24	**Primary (1)** n = 29	**Secondary (2)** n = 10	**p-value**	
Age (years)					0.5444
Mean ± SD	36.6 ± 6.5	35.7 ± 5.7*	37.7 ± 4.6*	**0 vs. 1**	>0.9999
Median (Q1–Q3)	38.5 (33.0-40.8)	35.0 (32.0-39.5)	38.0 (33.8-41.0)	**0 vs. 2**	>0.9999
				1 vs. 2	>0.9999
TL (a.u.)					0.6460
Oocytes	114	212	12	**0 vs. 1**	>0.9999
Telomeres	23978	63585	5427	**0 vs. 2**	>0.9999
Mean ± SD	153.4 ± 20.2*	152.0 ± 22.8	148.5 ± 26.9*		
Median (Q1–Q3)	151.3 (140.5-166.8)	148.7 (133.9-169.4)	148.1 (134.6-166.3)	**1 vs. 2**	>0.9999
Short telomeres (%)					0.3231
Mean ± SD	18.5 ± 20.5	22.8 ± 22.4	24.1 ± 33.2	**0 vs. 1**	0.4141
Median (Q1–Q3)	9.6 (2.5-28.6)	14.4 (3.0-39.8)	13.3 (1.3-29.0)	**0 vs. 2**	>0.9999
				1 vs. 2	>0.9999
Long telomeres (%)					0.4971
Mean ± SD	16.1 ± 19.1	17.3 ± 22.1	15.6 ± 25.9	**0 vs. 1**	>0.9999
Median (Q1–Q3)	9.5 (2.3-24.6)	7.9 (1.4-25.2)	3.4 (0.0-18.1)	**0 vs. 2**	0.7322
				1 vs. 2	0.9502
Y group n = 15	**Primordial (0)** n = 8	**Primary (1)** n = 14	**Secondary (2)** n = 3	**p-value**	
Age (years)					0.5487
Mean ± SD	29.3 ± 5.4	31.0 ± 4.0	32.7 ± 1.5*	**0 vs. 1**	>0.9999
Median (Q1–Q3)	31.5 (24.5-33.0)	32.0 (29.8-34.0)	33.0 (31.0-34.0)	**0 vs. 2**	0.8676
				1 vs. 2	>0.9999
TL (a.u.)					0.2019
Oocytes	68	120	4	**0 vs. 1**	0.4302
Telomeres	18967	41692	4761	**0 vs. 2**	>0.9999
Mean ± SD	155.8 ± 18.7	154.3 ± 22.3*	160.5 ± 25.0*		
Median (Q1–Q3)	152.4 (143.5-167.7)	151.8 (134.0-170.3)	154.9 (140.2-186.3)	**1 vs. 2**	0.7127
Short telomeres (%)					0.9771
Mean ± SD	12.5 ± 13.6	20.0 ± 22.2	7.8 ± 9.0	**0 vs. 1**	>0.9999
Median (Q1–Q3)	8.4 (2.4-19.6)	9.4 (1.9-36.6)	7.6 (0.0-15.8)	**0 vs. 2**	>0.9999
				1 vs. 2	>0.9999
Long telomeres (%)					0.3029
Mean ± SD	16.7 ± 19.5	18.1 ± 20.7	25.9 ± 38.1*	**0 vs. 1**	0.6499
Median (Q1–Q3)	9.5 (4.4-25.3)	11.0 (1.9-30.0)	10.8 (0.9-66.1)	**0 vs. 2**	>0.9999
				1 vs. 2	0.8723

M group n = 18	**Primordial (0)** n = 16	**Primary (1)** n = 15	**Secondary (2)** n = 7	**p-value**	
Age (years)					0.9585
Mean ± SD	40.3 ± 2.9*	40.1 ± 3.0*	39.9 ± 3.6*	**0 vs. 1**	0.9847
Median (Q1–Q3)	39.5 (38.3-42.8)	39.0 (38.0-42.0)	39.0 (37.0-44.0)	**0 vs. 2** **1 vs. 2**	0.9564 0.9876
TL (a.u.)					0.8450
Oocytes	46	92	8	**0 vs. 1**	>0.9999
Telomeres	5011	17434	666	**0 vs. 2**	>0.9999
Mean ± SD	149.7 ± 21.8	149.1 ± 23.2	142.5 ± 27.3*		
Median (Q1–Q3)	147.1 (131.9-166.8)	144.2 (133.7-160.8)	148.1 (117.3-156.1)	**1 vs. 2**	>0.9999
Short telomeres (%)					0.9997
Mean ± SD	27.4 ± 25.3	26.5 ± 22.3	32.3 ± 38.3	**0 vs. 1**	>0.9999
Median (Q1–Q3)	26.1 (2.7-50.0)	23.1 (7.0-42.3)	13.7 (6.1-71.2)	**0 vs. 2** **1 vs. 2**	>0.9999 >0.9999
Long telomeres (%)					0.3713
Mean ± SD	15.2 ± 18.7	16.3 ± 23.9	10.4 ± 18.4	**0 vs. 1**	>0.9999
Median (Q1–Q3)	9.5 (1.6-23.9)	5.2 (0.1-23.3)	2.6 (0.0-12.2)	**0 vs. 2** **1 vs. 2**	0.5624 >0.9999

Data are presented as mean ± standard deviation and median (interquartile range). *Denoted the variables that passed the Shapiro-Wilk or Kolmogorov-Smirnov normality test. The variables were analyzed using Kruskal-Wallis and Dunn's multiple comparisons tests (non-normally distributed data) or ordinary one-way ANOVA and Tukey's multiple comparisons test (normally distributed data). A p-value < 0.05 was considered statistically significant. The n refers to the number of subjects. The number of oocytes and telomere dots analyzed is specified in the TL section. 0: primordial follicles, 1: primary follicles, 2: secondary follicles, SD: standard deviation, Q1: quartile 1 (25% percentile), Q3: quartile 3 (75% percentile), Y: young, M: middle-aged, a.u.: arbitrary units of intensity, %: percent, vs.: versus.

5.1.2.2.2.2 Telomere length in oocytes and aging

The telomeres from oocytes did not show any changes during folliculogenesis. For this reason, the study of aging in oocytes was performed with all oocytes, regardless of the follicular stage from which they originated. When comparing the Y and M groups (Figure 17A and B), a higher TL was evidenced in the oocytes of the Y group (155.0 ± 21.1 a.u.) compared to the M group (148.9 ± 22.9 a.u., p = 0.0039). Likewise, Y group oocytes had a lower percentage of short telomeres (17.1 ± 19.7% in Y compared to 27.1 ± 24.1% in M, p = 0.0002, Figure 17C) and a higher percentage of long telomeres (17.8 ± 20.7% in Y compared to 15.1 ± 21.1% in M, p = 0.0137, Figure 17D). The correlation between TL of oocytes and age was not found (p = 0.1748, Figure 17E). A similar result was observed for the percentage of long telomeres (n = 33; rho = - 0.1010; p = 0.5759). However, there was a positive correlation between the percentage of short telomeres and age (p = 0.0443, Figure 17F).

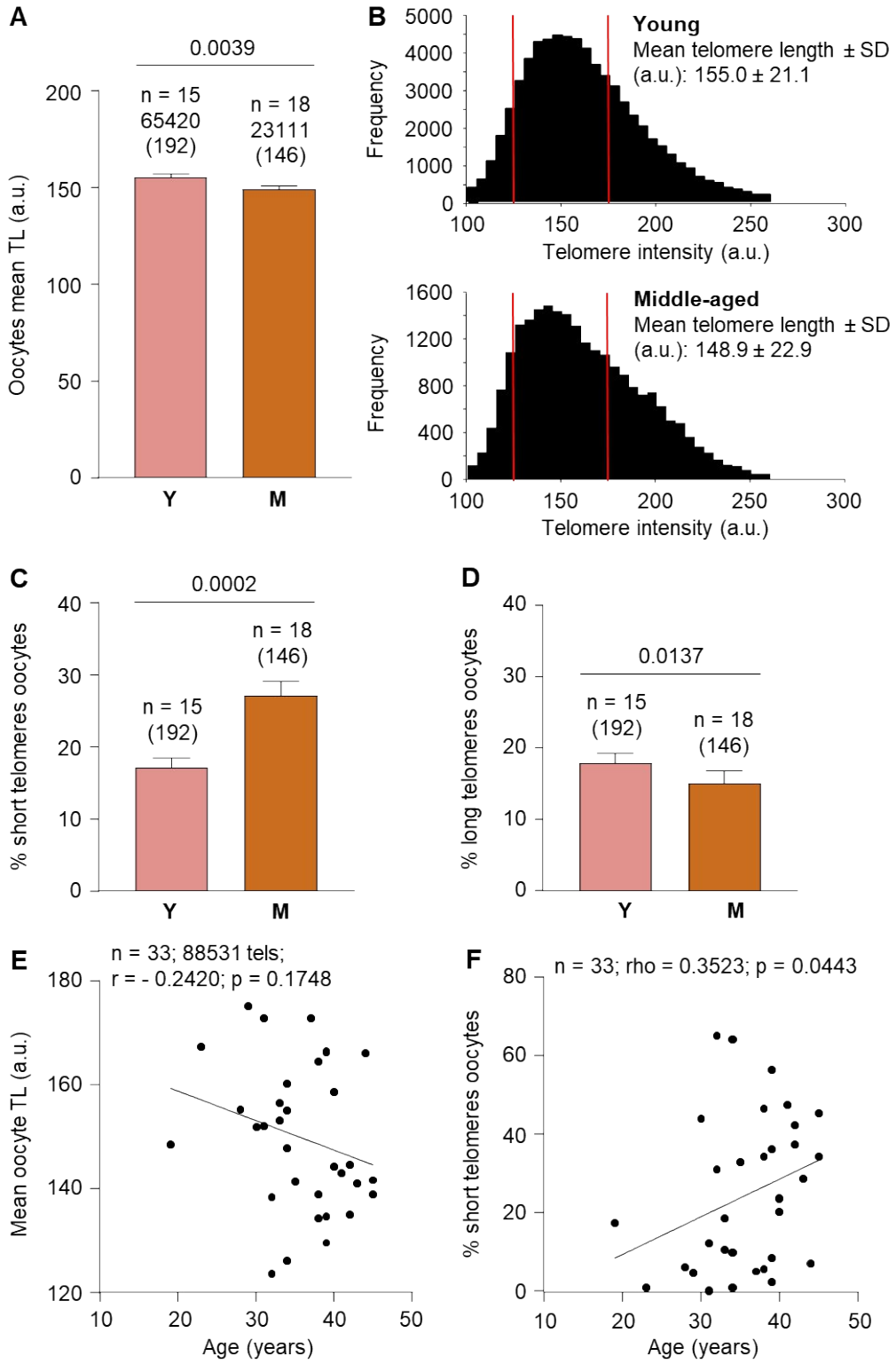


Figure 17. Analysis of telomere parameters in oocytes of Y and M women.

(A) TL in the indicated age groups. The number of individuals, the telomere dots (below), and the number of oocytes (below the number of dots) are specified. (B) Frequency histograms of telomere intensity in oocytes of the indicated groups. (C) Percentage of short telomeres in the indicated groups. (D) Percentage of long telomeres in the indicated groups. (E) Pearson correlation between the mean TL of oocytes and age. (F) Spearman correlation between the percentage of short telomeres and age. The groups were compared using the Mann-Whitney U test. The bar diagrams represent the mean

value, and the SEM is represented in the error bars. N refers to the number of subjects. A p-value < 0.05 was considered statistically significant. Only significant p-values are shown in the bar graphs. For more information, see Appendix C, Table C3. Y: young, M: middle-aged, SD: standard deviation, a.u.: arbitrary units (intensity), TL: telomere length, %: percent.

5.1.2.2.3 Follicular cells: granulosa cells

As in the previously analyzed oocytes, the GCs identified in the ovarian images were part of different follicular stages. Although the oocyte remains quiescent during the primordial, primary, and secondary follicular stages, this does not occur with GCs. They have a crucial role in the advancement of folliculogenesis. Thus, telomere parameters of GCs during folliculogenesis were analyzed, followed by the study of aging between age groups. Similarly to what happened in the oocyte analysis, the P group was excluded due to the identification of a minimal number of follicles.

5.1.2.2.3.1 Telomere length in granulosa cells during folliculogenesis

Folliculogenesis was studied in all subjects simultaneously and then, separated by age in groups Y and M. None of these analyses showed differences in the mean age of the women in which the different follicular stages were allocated (All subjects p = 0.8375, Y p = 0.7751, M p = 0.7015).

When comparing telomere parameters in the GCs of primordial, primary, and secondary follicles of all subjects included in the study (n = 39, Figure 18A), regardless of age, statistically significant differences were detected in TL (p<0.0001) and the percentage of short telomeres (p = 0.0149). Both parameters tended to increase as folliculogenesis progressed. Primordial GCs recorded the lowest TL (147.6 ± 17.0 a.u.) and the lowest percentage of short telomeres (15.8 ± 16.9%). Next, primary GCs evidenced higher TL (151.4 ± 20.9 a.u.) and percentage of short telomeres (20.0 ± 20.4%) than the previous stage (primordial stage), although the differences were not statistically significantly different (p = 0.6669 and p = 0.6887, respectively). Secondary GCs recorded the highest TL (168.4 ± 24.9 a.u.) and percentage of short telomeres (30.9 ± 27.9%). Statistically significant differences were found when comparing the TL of the secondary stage with the primordial (p<0.0001) and primary (p = 0.0004) stages. However, the percentage of short telomeres of GCs from primary follicles was only significantly different from secondary ones (p = 0.0112). Regarding the percentage of long telomeres, there was no statistically significant difference between any stages (16.8 ± 18.7% in primordial, 18.2 ± 23.0% in primary, and 18.7 ± 22.6% in secondary follicles, p = 0.4989).

When a similar analysis of follicle stages was performed separately in the Y (n = 16, Figure 18B) and M (n = 23, Figure 18C) groups, there were differences in the TL parameter (p =

0.0012 and p = 0.0063, respectively). However, statistical significance was not observed in the accumulation of short telomeres (Y p = 0.5605 and M p = 0.0561). Also, no differences were found in the percentage of long telomeres, neither in the Y group (p = 0.9860) nor the M group (p = 0.5920). Still, as occurred in the analysis with all women without age division, TL during folliculogenesis increased in both Y (151.1 ± 15.7 in primordial, 155.5 ± 19.5 in primary, and 176.3 ± 24.5 a.u. in secondary, p = 0.0012) and M groups (143.6 ± 17.8 in primordial, 147.4 ± 21.4 in primary, and 162.8 ± 24.2 a.u. in secondary, p = 0.0063). Concerning the percentage of short and long telomeres, although no statistically significant differences were detected, both means tended to increase during advancing folliculogenesis in Y (%short p = 0.5605, %long p = 0.9860) and M (%short p = 0.0561, %long p = 0.5920). Note that sometimes follicles at different stages were identified in the same woman.

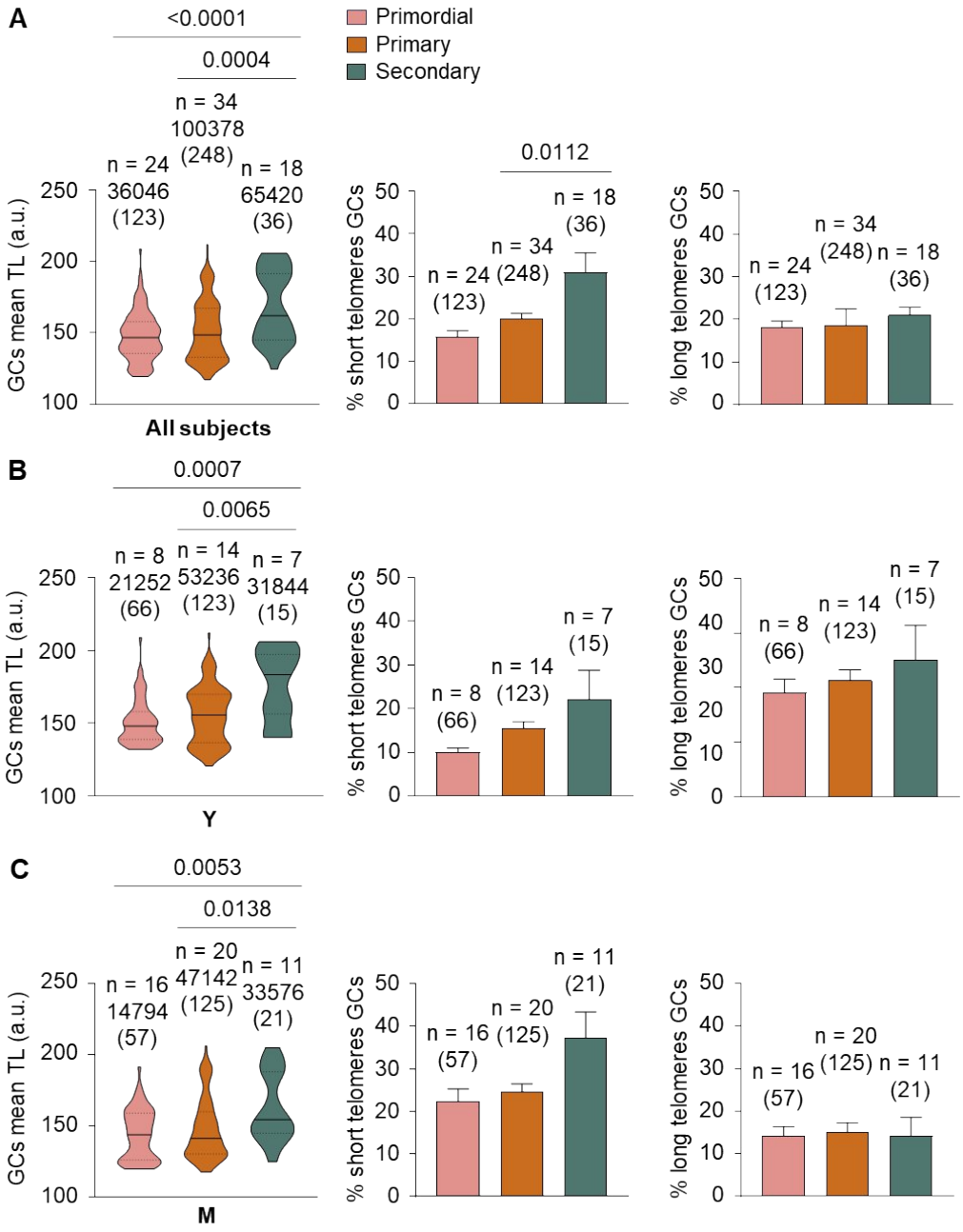


Figure 18. Analysis of telomere parameters in GCs during folliculogenesis.

(A) TL, percentage of short and long telomeres of GCs in primordial, primary, and secondary follicular stages, including all the subjects. (B) TL, percentage of short and long telomeres of GCs in primordial, primary, and secondary follicular stages identified in young women. (C) TL, percentage of short and long telomeres of GCs in primordial, primary, and secondary follicle stages identified in middle-aged women. The number of individuals, the telomere dots analyzed, and the number of follicles are specified at the top of the bar diagrams. The telomere parameters were compared using the Kruskal-Wallis test and Dunn's multiple comparisons test. The violin plots show the median and the interquartile range. The bar diagrams represent the mean value, and the error bars represent the standard error of the mean (SEM). The n refers to the number of subjects. A p-value < 0.05 was considered statistically significant. Only significant p-values are shown in the graphs. For more information, see Appendix C, Table C4. Y: young, M: middle-aged, GCs: granulosa cells, a.u.: arbitrary units (intensity), TL: telomere length, %: percent.

Therefore, since there were statistically significant differences in the TL of GCs between the follicular stages, these cells were studied individually in each follicular stage.

5.1.2.2.3.2 Telomere length in primordial granulosa cells and aging

As observed in the previous result, the primordial follicles' GCs had the lowest TL compared to other follicular stages during folliculogenesis. Thus, we set out to look for differences in TL with aging. When the TL of primordial GCs was compared between Y (151.1 ± 15.7 a.u., Figure 19A) and M (143.6 ± 17.8 a.u., Figure 19B) groups, the M group registered the lowest TL (Figure 19C, p = 0.0282). The older group also evidenced a higher percentage of short telomeres (22.4 ± 21.6%) than the Y group (10.0 ± 8.1%, p = 0.0395), as shown in Figure 19D. No statistically significant differences were found in the percentage of long telomeres (19.1 ± 20.3% in Y compared to 14.2 ± 16.5% in M, p = 0.0720, Figure 19E). Therefore, the GCs of primordial follicles of the M group accumulated significantly more short telomeres. When the correlation between age and these telomere parameters was studied, a significant negative correlation was observed between age and TL (Figure 19F, p = 0.0005), and between age and the percentage of long telomeres (Figure 19H, p = 0.0009). In addition, a positive correlation was evidenced between the percentage of short telomeres and the variable age (Figure 19G, p = 0.0017).

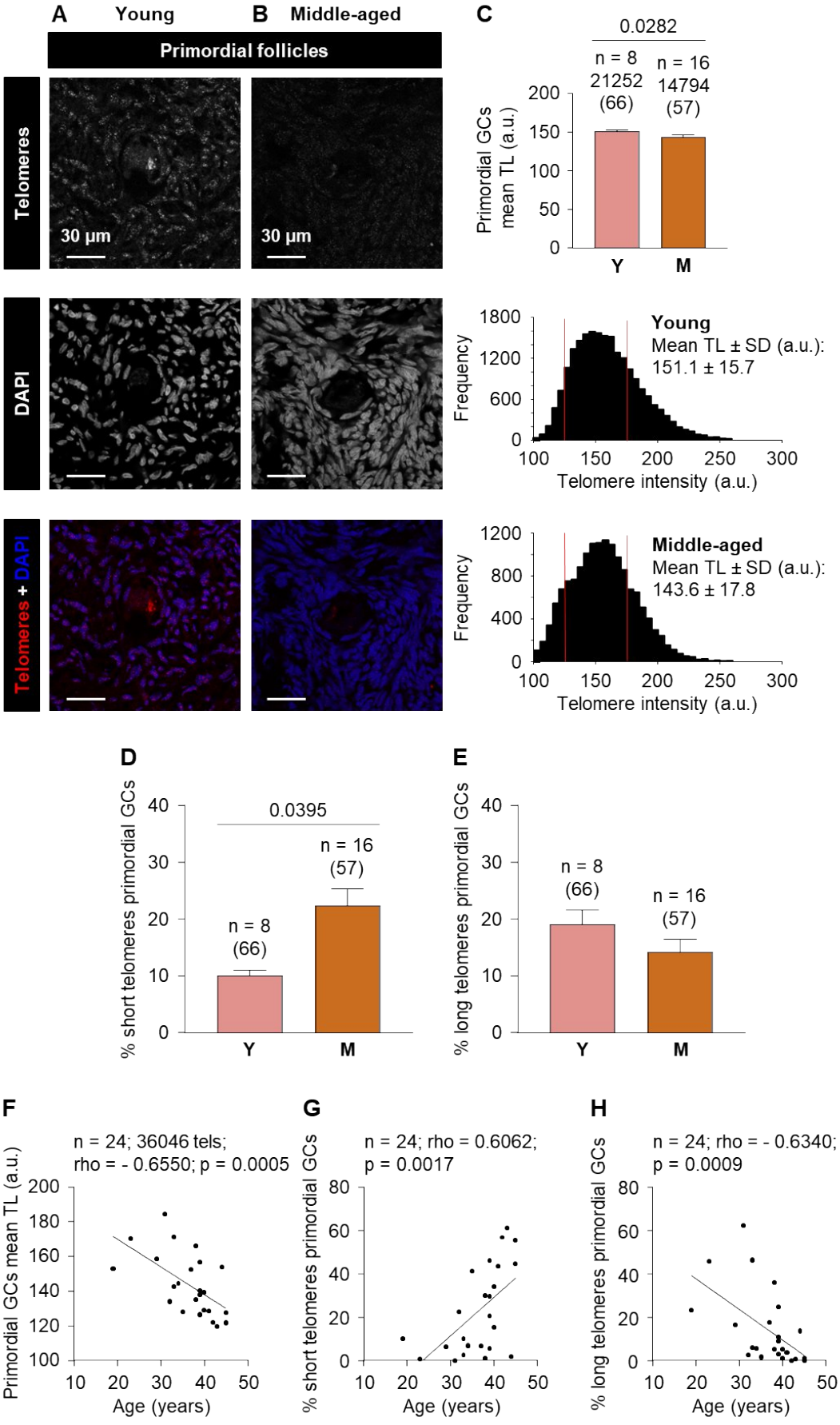


Figure 19. Analysis of telomere parameters in primordial GCs in Y and M groups.

(A) The micrograph shows representative images of a primordial follicle qFISH on women's ovaries from the Y group. (B) A representative image of a primordial follicle qFISH of women's ovaries from the M group. In A and B, the top images show telomeres (white dots), the middle images represent the nuclei stained with DAPI, and the bottom images show the merged images of telomeres (red) and cell nuclei (blue). Scale bars represent 30 µm. (C) GCs TL in Y (upper panel) and M (bottom panel) groups. The number of individuals, the telomere dots analyzed, and the number of follicles are specified. Frequency histograms of telomere intensity in primordial GCs in the young and middle-aged group. (D) Percentage of short telomeres in Y and M. (E) Percentage of long telomeres in Y and M. (F, G, H) Spearman correlations between TL, percentage of short and long telomeres with age. The groups were compared using the Mann-Whitney U test. The bar diagrams represent the mean value, and the error bars the SEM. The n refers to the number of subjects. A p-value < 0.05 was considered statistically significant. Only significant p-values are shown in the bar graphs. For more information, see Appendix C, Table C5. Y: young, M: middle-aged, GCs: granulosa cells, SD: standard deviation, a.u.: arbitrary units (intensity), TL: telomere length, %: percent, rho: Spearman correlation coefficient, DAPI: 4',6-diamidino-2-phenylindole, µm: micrometer.

5.1.2.2.3.3 Telomere length in primary granulosa cells and aging

Although the TL of primary GCs tended to be higher than in primordial follicles, this difference was not statistically significant. However, when primary GCs were compared with secondary GCs, there was a statistically significant lower TL in primary GCs. The next step was to study TL during aging in primary GCs. Comparison of TL between the Y (155.5 ± 19.5 a.u., Figure 20A) and the M (147.4 ± 21.4 a.u., Figure 20B) group evidenced a higher TL in the younger group (Figure 20C, p = 0.0003). In addition, the younger group recorded a lower percentage of short telomeres (15.4 ± 17.4%, Figure 20D) and a higher percentage of long telomeres (21.3 ± 21.8%, Figure 20E) compared to the M group (%short 24.5 ± 22.2%, p = 0.0036; %long 15.2 ± 23.7%, p = 0.0001). However, correlations between these telomere parameters and age were not detected (TL p = 0.8991; %short p = 0.7425; %long p = 0.6707; Figure 20F, G, and H).

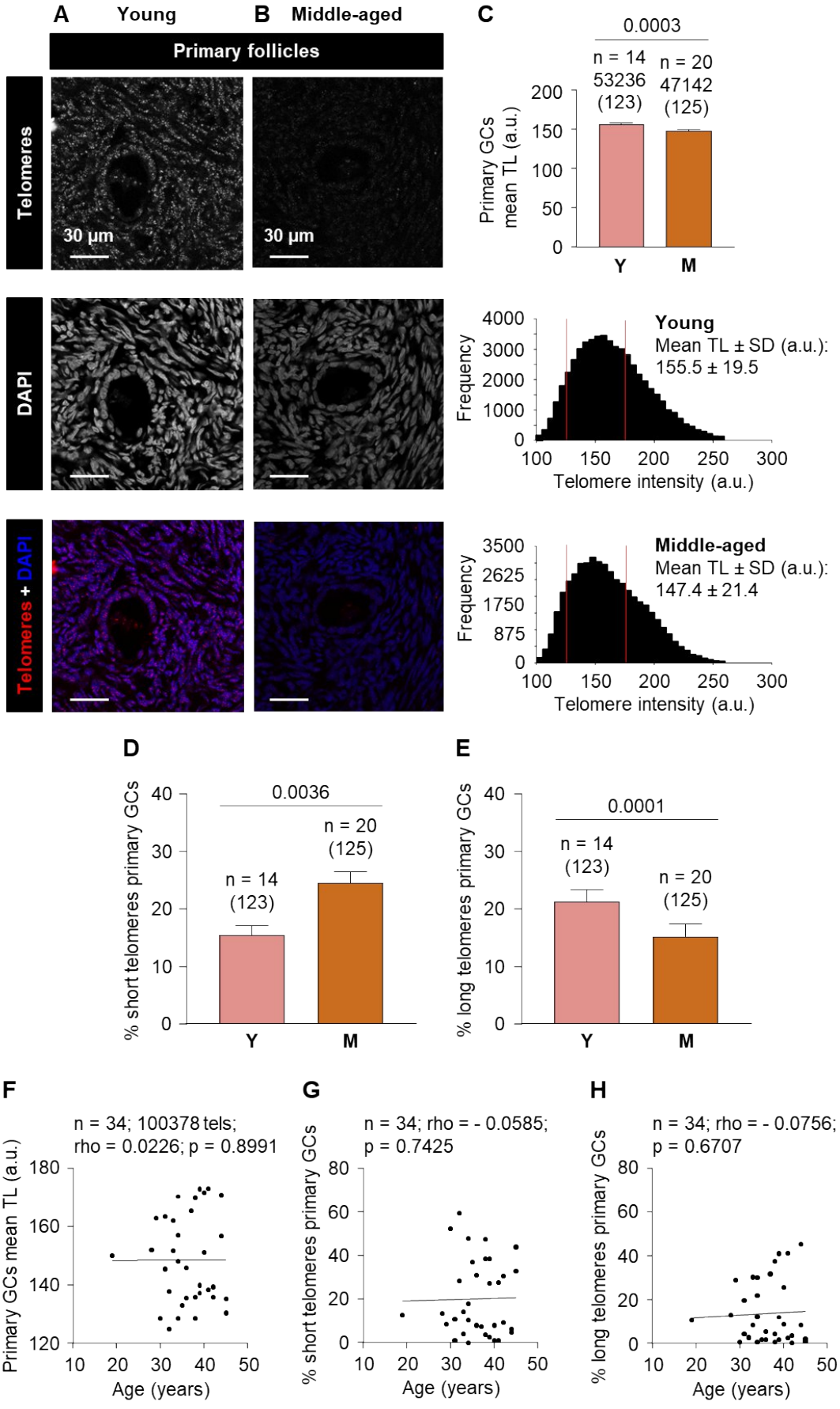


Figure 20. Analysis of telomere parameters in primary GCs in Y and M groups.

(A) Primary follicle qFISH image of women from the Y group. (B) Primary follicle qFISH image of women from the M group. In A and B, the top images show telomeres (white dots), the middle images represent the nuclear areas stained with DAPI, and the bottom images show the merged images of telomeres (red) and cell nuclei (blue). Scale bars represent 30 µm. (C) GCs TL in Y (upper panel) and M (bottom panel) groups. The number of individuals, the telomere dots analyzed, and the number of follicles are specified. Frequency histograms of telomere intensity in primary GCs in the young and middle-aged group. (D) Percentage of short telomeres in Y and M. (E) Percentage of long telomeres in Y and M. (F, G, H) Spearman correlations between TL, percentage of short and long telomeres with age. The groups were compared using the Mann-Whitney U test. The bar diagrams represent the mean value, and the error bars represent the standard error of the mean (SEM). N refers to the number of subjects. A p-value < 0.05 was considered statistically significant. Only significant p-values are shown in the bar graphs. For more information, see Appendix C, Table C6. Y: young, M: middle-aged, GCs: granulosa cells, SD: standard deviation, a.u.: arbitrary units (intensity), TL: telomere length, %: percent, rho: Spearman correlation coefficient, DAPI: 4',6-diamidino-2-phenylindole, µm: micrometer.

5.1.2.2.3.4 Telomere length in secondary granulosa cells and aging

The secondary follicle stage recorded the highest TL in their GCs during folliculogenesis. When comparing the telomere parameters of the secondary GCs in the Y and M age groups, no statistically significant differences were observed for either TL (p = 0.1103) or for the percentage of short (p = 0.1022) or long telomeres (p = 0.1264). The data obtained for the different telomere parameters are specified in Table 19. Furthermore, no correlation was observed between TL (n = 36; 65420 tels; r = - 0.1340; p = 0.5959), the percentage of short (n = 36; r = 0.1335; p = 0.5975) or long telomeres (n = 36; rho = - 0.2765; p = 0.2666) and age, despite the age difference (p<0.0001).

Table 19. Secondary GCs telomere parameters in groups based on age.

	Y n = 7	**M** n = 11	**p-value**
Age (years)			<0.0001
Mean ± SD	31.7 ± 3.9*	40.9 ± 3.2*	
Median (Q1–Q3)	31.0 (29.0-34.0)	41.0 (39.0-44.0)	
TL (a.u.)			0.1103
Follicles	15	21	
Telomeres	31844	33576	
Mean ± SD	176.0 ± 24.5*	162.8 ± 24.2*	
Median (Q1–Q3)	183.3 (156.5-197.3)	154.3 (144.7-187.9)	
Short telomeres (%)			0.1022
Mean ± SD	22.1 ± 25.9	37.2 ± 28.2*	
Median (Q1–Q3)	10.0 (2.1-35.5)	34.4 (5.9-59.9)	
Long telomeres (%)			0.1264
Mean ± SD	25.0 ± 24.7	14.2 ± 20.3	
Median (Q1–Q3)	23.9 (1.2-46.5)	1.7 (0.5-25.6)	

Data are presented as mean ± standard deviation and median (interquartile range). *Denoted the variables that passed the Shapiro-Wilk or Kolmogorov-Smirnov normality test. The Mann-Whitney U test analyzed the variables. A p-value < 0.05 was considered statistically significant. The n refers to the number of subjects. The number of follicles and telomere dots analyzed is specified in the TL section of the table. Y: young, M: middle-aged, TL: telomere length, SD: standard deviation, Q1: quartile 1 (25% percentile), Q3: quartile 3 (75% percentile), a.u.: arbitrary units of intensity, %: percent.

5.1.2.2.4 Follicular cells: theca cells

In folliculogenesis, the TCs produce hormones and promote and facilitate ovulation. These cells differentiate, forming a layer around the GCs visible at the primary follicle stage. Regarding our study, these cells were only identified in the ovarian samples analyzed as forming part of primary and secondary follicles. The P group was also excluded from this analysis for the above mentioned reasons.

5.1.2.2.4.1 Telomere length in theca cells during folliculogenesis

Considering all women where primary and secondary follicles were identified (n = 33), with similar ages, the comparison of the telomere parameters of TCs between both stages did not show any change during this follicular transition (Table 20). The results obtained were similar when the TL of TCs in these follicular stages was studied separately in the Y (n = 13) and M (n = 20) populations (Table 20). Note that sometimes follicles at different stages were identified in the same woman.

Table 20. TCs telomere parameters during folliculogenesis.

All subjects n = 33	**Primary (1)** n = 30	**Secondary (2)** n = 17	**p-value**
Age (years)			0.8936
Mean ± SD	37.2 ± 4.7*	37.4 ± 6.0*	
Median (Q1–Q3)	38.0 (33.0-41.0)	39.0 (33.5-43.0)	
TL (a.u.)			0.3541
Follicles	138	32	
Telomeres	33536	13679	
Mean ± SD	150.0 ± 20.0	145.9 ± 18.2	
Median (Q1–Q3)	149.0 (133.0-164.2)	141.6 (135.2-154.3)	
Short telomeres (%)			0.2165
Mean ± SD	21.7 ± 23.4	25.8 ± 24.2	
Median (Q1–Q3)	11.8 (3.2-35.8)	18.8 (6.9-32.7)	
Long telomeres (%)			0.6895
Mean ± SD	15.6 ± 20.4	13.5 ± 15.6	
Median (Q1–Q3)	5.4 (0.4-24.6)	7.3 (1.5-18.9)	
Y group n = 13	**Primary (1)** n = 11	**Secondary (2)** n = 6	**p-value**
Age (years)			0.9394
Mean ± SD	32.1 ± 1.7*	31.0 ± 4.1	
Median (Q1–Q3)	32.0 (31.0-34.0)	32.0 (29.0-34.0)	
TL (a.u.)			0.4426
Follicles	68	13	
Telomeres	19949	9803	
Mean ± SD	153.6 ± 19.8*	149.6 ± 15.6	
Median (Q1–Q3)	157.5 (138.7-168.1)	142.6 (140.9-157.0)	
Short telomeres (%)			0.2309
Mean ± SD	18.4 ± 23.7	16.0 ± 9.0*	
Median (Q1–Q3)	7.0 (2.9-20.0)	17.0 (7.2-21.4)	
Long telomeres (%)			0.8150
Mean ± SD	18.9 ± 19.5	16.0 ± 9.0*	
Median (Q1–Q3)	13.4 (1.4-33.0)	17.0 (7.2-21.4)	

M group n = 20	**Primary (1)** n = 19	**Secondary (2)** n = 11	**p-value**
Age (years)			0.5217
Mean ± SD	40.2 ± 2.9*	40.9 ± 3.2*	
Median (Q1–Q3)	40.0 (38.0-42.0)	41.0 (39.0-44.0)	
TL (a.u.)			0.5038
Follicles	70	19	
Telomeres	13587	3876	
Mean ± SD	146.4 ± 19.7	143.4 ± 19.8*	
Median (Q1–Q3)	140.9 (131.6-156.9)	136.8 (129.2-154.5)	
Short telomeres (%)			0.4304
Mean ± SD	24.9 ± 22.9	32.4 ± 29.0	
Median (Q1–Q3)	18.8 (3.7-44.3)	30.9 (6.7-44.9)	
Long telomeres (%)			0.8630
Mean ± SD	12.3 ± 20.9	11.8 ± 18.8	
Median (Q1–Q3)	3.0 (0.0-14.2)	2.2 (0.9-12.7)	

Data are presented as mean ± standard deviation and median (interquartile range). *Denoted the variables that passed the Shapiro-Wilk or Kolmogorov-Smirnov normality test. The Mann-Whitney U test (non-normally distributed data) or Student's t-test (normally distributed data) analyzed the variables. A p-value < 0.05 was considered statistically significant. The n refers to the number of subjects. The number of follicles and telomere dots analyzed is specified in the TL section. 1: primary follicles, 2: secondary follicles, SD: standard deviation, Q1: quartile 1 (25% percentile), Q3: quartile 3 (75% percentile), Y: young, M: middle-aged, a.u.: arbitrary units of intensity, %: percent, vs.: versus.

Considering that there were no significant differences in mean TL, in the percentage of short and long telomeres in the TCs during the transition from primary to secondary follicles, telomere maintenance through age in these cells was studied independently of the follicular stage.

5.1.2.2.4.2 Telomere length in theca cells and aging

The analysis of the TL of TCs in the different populations showed that the Y group (153.0 ± 19.1 a.u.) recorded higher TL in TCs than the M group (145.8 ± 19.7 a.u., p = 0.0041, Figure 21A). Consequently, the percentage of short telomeres in the M (26.5 ± 24.3%) group was higher than in the Y group (18.0 ± 22.0%, p = 0.0304, Figure 21B), and the percentage of long telomeres was lower in the older M group (17.8 ± 19.5% in Y compared to 12.2 ± 20.3% in M, Figure 21C). However, neither TL (n = 36; 65420 tels; r = - 0.1340; p = 0.5959), nor the percentage of short (n = 36; r = 0.1335; p = 0.5975) or long telomeres (n = 36; rho = - 0.2765; p = 0.2666) showed a significant correlation with age.

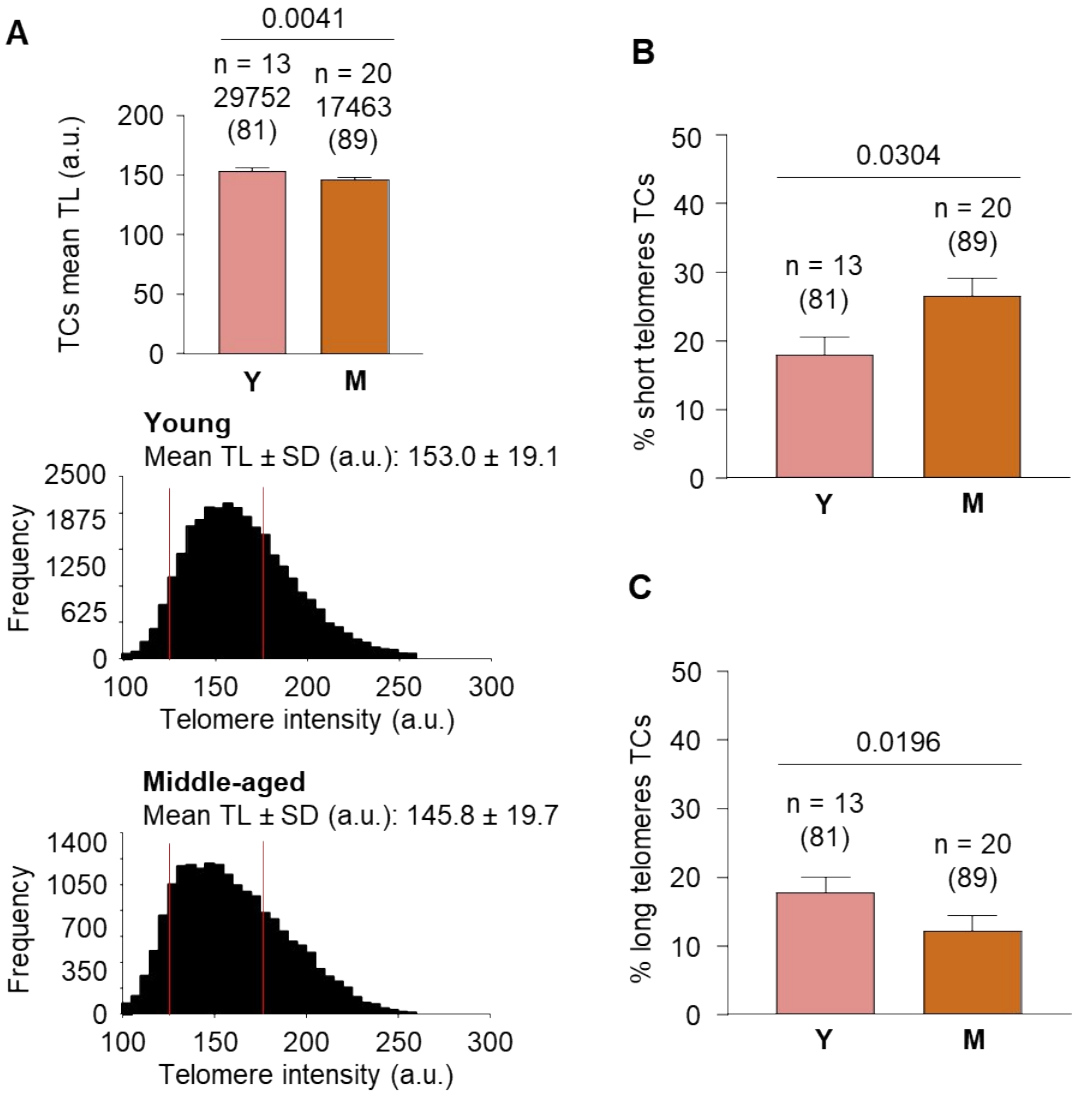


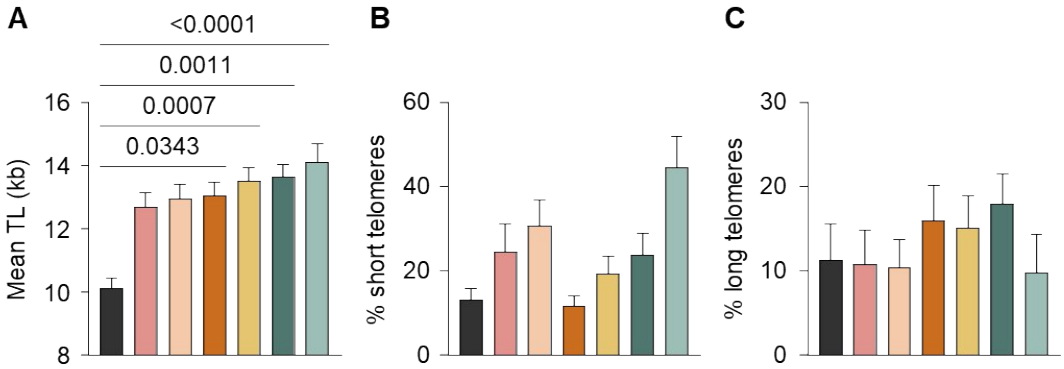
Figure 21. Analysis of telomere parameters in TCs in Y and M groups.

(A) TL in each age group. The number of individuals, the telomere dots analyzed, and the number of oocytes are specified. Frequency histograms of telomere intensity in TCs in the young (upper panel) and middle-aged (bottom panel) groups. (B) Percentage of short telomeres in Y and M. (C) Percentage of long telomeres in Y and M. The groups were compared using the Mann-Whitney U test. The bar diagrams represent the mean value, and the error bars the SEM. The n refers to the number of subjects. A p-value < 0.05 was considered statistically significant. Only significant p-values are shown in the bar graphs. For more information, see Appendix C, Table C7. Y: young, M: middle-aged, SD: standard deviation, a.u.: arbitrary units (intensity), TL: telomere length, %: percent.

5.1.2.3 Systemic telomere length as a biomarker of ovarian aging

In the previous sections, we studied systemic aging in PBMCs and reproductive aging in the different regions and populations in which the ovary comprises cells (stroma, oocytes, primordial, primary, secondary GCs, and TCs). The next goal was to determine whether ovarian cells and PBMCs had similar telomere characteristics. Thus, the validity of PBMCs as ovarian aging biomarkers could be ascertained. For this purpose, first, all telomere intensities

were converted to kilobases (kb). Second, the mean TL of each cell type from 11 women was compared. Only these 11 women were considered because all cell types (ovarian and PBMCs) were identified and measured. Following an increasing order, the mean TL of different cell populations were organized as follows: PBMCs (10.1 ± 1.1 kb), primordial GCs (12.7 ± 1.5 kb), TCs (13.0 ± 1.4 kb), stroma (13.1 ± 1.4 kb), primary GCs (13.5 ± 1.4 kb), oocytes (13.6 ± 1.4 kb) and secondary GCs (14.1 ± 2.0 kb). Since the TL of PBMCs was used as the aging marker for the organism, the rest of the population types were compared with PBMCs (Figure 22A). Statistically significant differences were found in the TL of stroma ($p = 0.0343$), primary GCs ($p = 0.0007$), oocytes ($p = 0.0011$), and secondary GCs ($p<0.0001$) compared to PBMCs. However, no differences were observed in the percentage of short telomeres (Figure 22B) or long telomeres (Figure 22C) of the different cell types compared to the same variables in PBMCs. The mean age of the 11 women in whom these analyses were performed was 37.9 ± 4.9 years.



Colour label	Cells	Telomeres	Number of follicles
■	PBMCs	57333	NA
■	Primordial GCs	15670	51
■	TCs	33821	101
■	Stroma	1804225	NA
■	Primary GCs	57784	134
■	Oocytes	56316	181
■	Secondary GCs	47279	26

Figure 22. Telomere length of PBMCs and ovarian cell populations.

(A) Mean TL expressed in kb of each cell type, indicated by color in the table below. (B) The percentage of short telomeres of all cell populations is indicated by color. (C) The percentage of long telomeres of cell populations is indicated by color. The bar diagrams represent the mean value, and the error bars represent the standard error of the mean (SEM). A p-value < 0.05 was considered statistically significant. Only significant p-values are shown in the bar graphs. The color code used for each cell population, the number of telomere points quantified and analyzed, and the number of follicles identified are detailed in the table below. TL: telomere length, kb: kilobases, PBMCs: peripheral mononuclear cells, GCs: granulosa cells, TCs: theca cells.

Finally, correlations between telomere parameters were performed using all available samples from the subjects. The sample size varied because only women were considered for whom telomere data were available in PBMCs, and in the other cell population chosen to study the possible biomarker correlation. Data resulting from the correlation analyses are detailed in Table 21. No significant correlation was detected between PBMCs TL and ovarian populations. A negative correlation was observed in the percentage of short telomeres in PBMCs and ovarian stroma (Figure 23A, p = 0.0022). However, a positive correlation (Figure 23B, p = 0.0453) was evident in the percentage of long telomeres in PBMCs and primordial GCs.

Table 21. Parameters of correlations between TL in kb of PBMCs and different ovarian cell populations.

Cell type	n	Correlation	R square	Coefficient	p-value
TL (kb)					
Stroma	65	Spearman	0.0410	- 0.1143	0.3645
Oocytes	33	Spearman	0.0020	0.1516	0.3997
Primordial GCs	24	Spearman	0.0199	0.2643	0.2119
Primary GCs	34	Spearman	0.0069	- 0.0462	0.7955
Secondary GCs	18	Spearman	0.0216	- 0.1827	0.4682
TCs	33	Spearman	0.0031	0.0421	0.8160
Short telomeres (%)					
Stroma	65	Spearman	0.1299	- 0.3736	0.0022
Oocytes	33	Spearman	0.0031	- 0.0007	0.9971
Primordial GCs	24	Spearman	0.0042	0.0661	0.7590
Primary GCs	34	Spearman	0.0062	- 0.1847	0.2956
Secondary GCs	18	Pearson	0.1665	- 0.4080	0.0928
TCs	33	Pearson	0.0371	- 0.1927	0.2827
Long telomeres (%)					
Stroma	65	Spearman	0.0082	- 0.0517	0.6828
Oocytes	33	Spearman	0.0082	0.0602	0.7295
Primordial GCs	24	Spearman	0.0348	0.4123	0.0453
Primary GCs	34	Spearman	0.0007	0.1646	0.3524
Secondary GCs	18	Spearman	0.0127	0.2590	0.2993
TCs	33	Spearman	0.0283	0.1733	0.3348

Spearman or Pearson analyzed the correlations. A p-value < 0.05 was considered statistically significant. The n refers to the number of subjects. PBMCs: peripheral blood mononuclear cells, GCs: granulosa cells, TCs: theca cells.

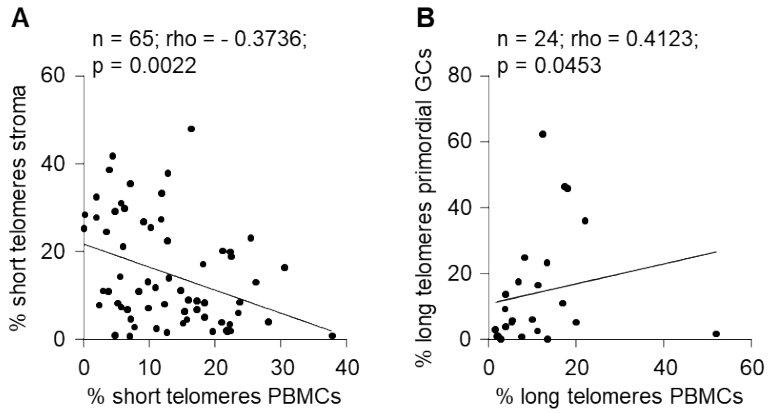
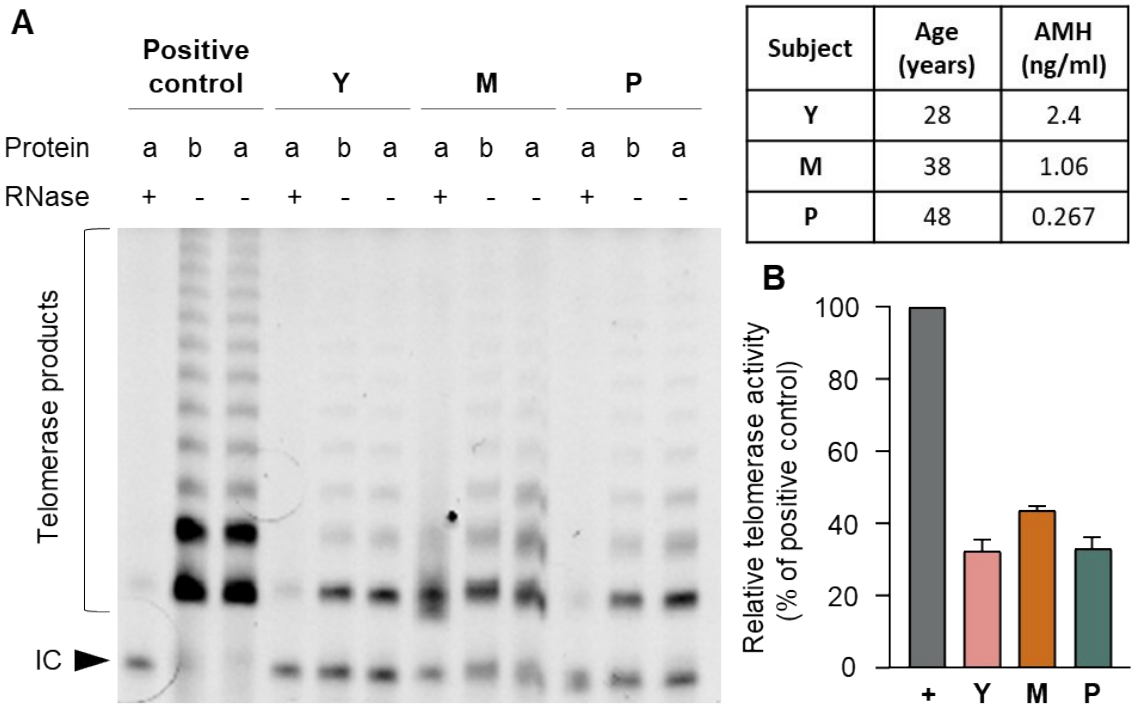


Figure 23. Telomere parameters with significant correlation in PBMCs and the ovary.

(A) Spearman correlation of the percentage of short telomeres in PBMCs and ovarian stroma. (B) Spearman correlation of the percentage of long telomeres in PBMCs and primordial GCs. Sample size (n), Spearman correlation coefficient (rho), and p-value are specified. PBMC: peripheral blood mononuclear cells, GC: granulosa cells, %: percentage.

5.1.2.4 Analysis of telomerase activity in the ovary

The TRAP assay tested the presence of telomerase in the human ovary in a small ovarian fragment. This technique verified that TA is detectable in the human ovary at different ages (Figure 24A). No characteristic pattern in TA quantification associated with age groups was observed (Figure 24B).



Subject	Age (years)	AMH (ng/ml)
Y	28	2.4
M	38	1.06
P	48	0.267

Figure 24. Analysis of telomerase activity in ovarian samples from women of Y, M, and P groups.

(A) Gel obtained from the TRAP assay from a small ovarian fragment. Two protein concentrations (a = 0.3 µg/µL, b = 0.06 µg/µL) of the same ovarian extract from each woman, and a negative control treated with RNase (+ treated, - untreated) are shown for each sample. The positive control is Jurkat tumor cells. The staircase pattern corresponds to telomerase products. The arrowhead indicates the internal control (IC) of the PCR reaction. (B) Relative TA quantification of the gel shown in A, where the first bar corresponds to the positive control. Quantification was performed referring to the positive control, being this 100% TA (see Materials and Methods, section 4.5.1.3.1.). The bar diagrams represent the mean value, and the error bars the SEM. The upper right table shows the age and AMH value of each subject. Y: young, M: middle-aged, P: perimenopause, IC: internal control, AMH: anti-müllerian hormone, ng: nanogram, mL: milliliter, %: percent.

5.1.3 Ovarian fibrosis

The analysis of the percentage of fibrotic area in ovarian histological sections by Masson's trichrome staining allowed the assessment of the fibrosis level in a representative sample from each age group. Statistically significant differences were observed in the mean age of the women from the Y (n = 6, 31.7 ± 2.1 years), M (n = 6, 40.7 ± 3.6 years), and P (n = 7, 47.0 ± 0.8 years) groups in which ovarian fibrosis was evaluated ($p<0.0001$). The percentage of fibrotic area was lower in Y (13.9 ± 8.6%) than in P (40.4 ± 9.4%, $p = 0.0007$, Figure 25A and B). However, no differences were observed when the M group (28.4 ± 12.2%) was compared with Y ($p = 0.0616$) or P ($p = 0.1125$), besides the higher percentage of fibrotic area in P. A significant positive correlation was found between the percentage of fibrotic area and the patient's age ($p<0.0001$) (Figure 25C).

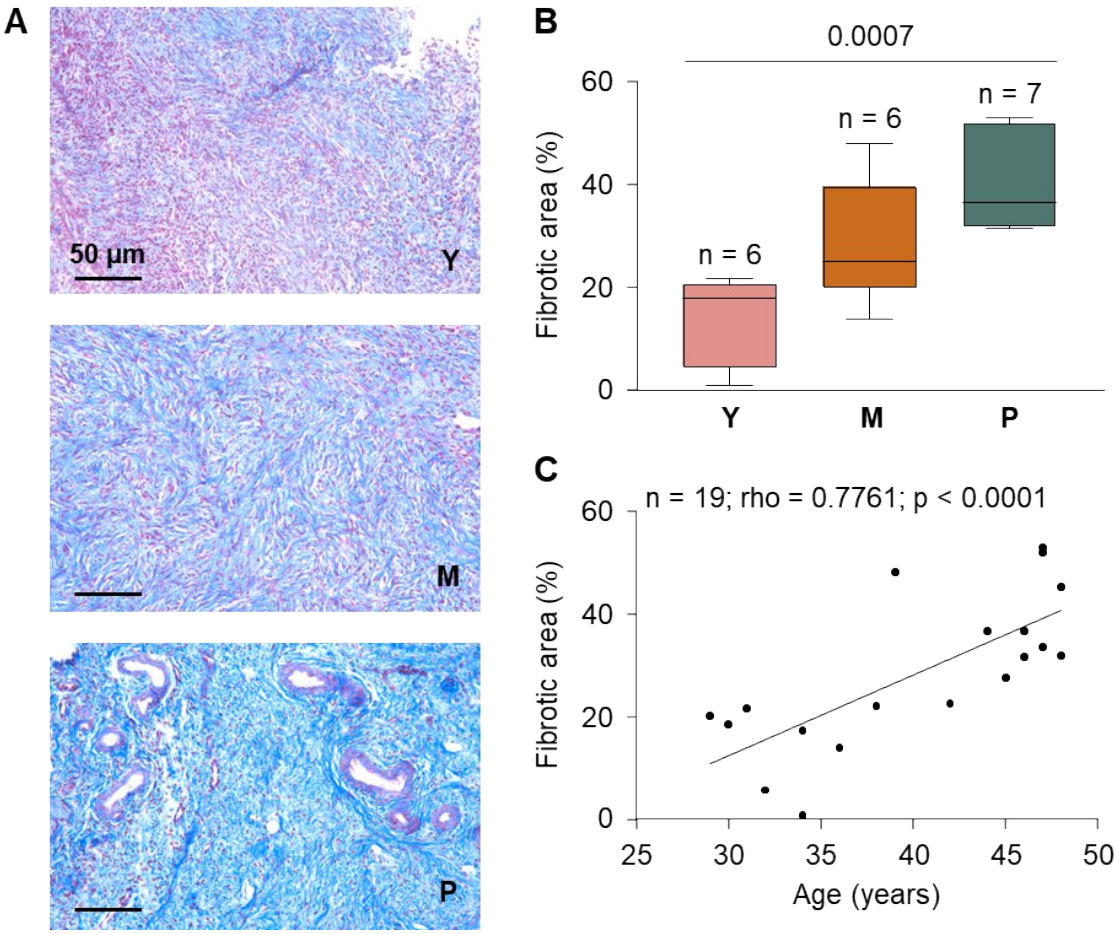


Figure 25. Fibrotic area in the ovary of Y, M, and P groups.

(A) Images from the Masson trichrome staining showing collagen-positive fibrotic area in blue. Scale bars represent 50 µm. (B) Quantification of the percentage of fibrotic area in each group. The groups were compared using ordinary one-way ANOVA and Tukey's multiple comparisons test. The graph shows the median value and the quartile 1 and 3. (C) Significant Spearman correlation between age and fibrotic area. N refers to the number of subjects included per group. A p-value < 0.05 was considered statistically significant. Only significant p-values are shown in the bar graphs. For more information, see Appendix C, Table C8. Y: young, M: middle-aged, P: perimenopausal, %: percent, rho: Spearman correlation coefficient, µm: micrometer.

The relative expression of the fibrosis-related genes TGF-β1 (transforming growth factor beta 1), COL1A1 (collagen type I alpha 1 chain), and COL3A1 (collagen type III alpha 1 chain) was assessed in a larger sample size compared to the ovarian fibrotic area evaluation. In this comparison, a statistically significant difference in mean age (p<0.0001) between the groups remained (Table 22). The analysis of TGF-β1 expression showed no statistically significant differences between any groups compared (p = 0.2144), nor correlation with age (n = 62; rho = - 0.06246; p = 0.6296). Next, the expression of COL1A1 and COL3A1 was evaluated because they showed a significant positive correlation with TGF-β1 expression levels (COL1A1 n = 62; rho = 0.5913; p < 0.0001; and COL3A1 n = 62; rho = 0.6565; p < 0.0001). When the difference in COL1A1 and COL3A1 expression between age groups was evaluated,

no statistically significant differences were observed in either age group (p = 0.3084 and p = 0.6389, respectively). The expression of each gene obtained in the different age groups is detailed in Table 22.

Table 22. Fibrosis-related gene expression (DCq) in groups based on age.

	Y	M	P	p-value	
TGF-β1					0.2144
n	15	31	16	**Y vs. M**	>0.9999
Mean ± SD	0.0035 ± 0.0043	0.0048 ± 0.0053	0.0023 ± 0.0025	**Y vs. P**	>0.9999
Median (Q1–Q3)	0.0019 (0.0007-0.0053)	0.0025 (0.0011-0.0077)	0.0015 (0.0005-0.0030)	**M vs. P**	0.2518
Age, mean ± SD (years)	30.7 ± 4.3	40.3 ± 2.9*	47.6 ± 1.1		<0.0001
COL1A1					0.3084
n	15	31	17	**Y vs. M**	>0.9999
Mean ± SD	0.1533 ± 0.2154	0.1246 ± 0.1511	0.1893 ± 0.4102	**Y vs. P**	>0.9999
Median (Q1–Q3)	0.0403 (0.0092-0.2669)	0.0812 (0.0249-0.1595)	0.0376 (0.0082-0.0860)	**M vs. P**	0.3792
Age, mean ± SD (years)	30.7 ± 4.3	40.3 ± 2.9*	47.5 ± 1.1		<0.0001
COL3A1					0.6389
n	15	31	17	**Y vs. M**	>0.9999
Mean ± SD	1.4 ± 1.9	2.0 ± 3.8	1.8 ± 3.3	**Y vs. P**	>0.9999
Median (Q1–Q3)	0.5 (0.1-1.8)	0.7 (0.2-1.7)	0.3 (0.2-1.6)	**M vs. P**	>0.9999
Age, mean ± SD (years)	30.7 ± 4.3	40.3 ± 2.9*	47.5 ± 1.1		<0.0001

Data are presented as mean ± standard deviation and median (interquartile range). *Denoted the variables that passed the Shapiro-Wilk normality test. The variables were analyzed by Kruskal-Wallis and Dunn's multiple comparisons tests. A p-value < 0.05 was considered statistically significant. The n refers to the number of subjects. Considering that the expression of these genes could not be measured in all subjects, the recalculated age value and statistical analyses are specified for each gene. Y: young, M: middle-aged, P: perimenopausal, SD: standard deviation, Q1: quartile 1 (25% percentile), Q3: quartile 3 (75% percentile), TGF-β1: transforming growth factor beta 1, COL1A1: collagen type I alpha 1 chain, COL3A1: collagen type III alpha 1 chain.

5.1.4 Proteomic analysis

The proteomic profile of the ovary from Y (n = 11, 30.1 ± 4.9 years), M (n = 12, 39.3 ± 1.8 years), and P (n = 13, 47.5 ± 1.1 years) women was assessed. The difference in the mean age of each group was statistically significant (p<0.0001, Y vs. M p = 0.0262, Y vs. P p<0.0001, M vs. P p = 0.0089). A total of 2517 proteins were identified, and 1925 proteins were quantified. The dimensionality reduction technique (principal component analysis, PCA) showed no clear separation between the groups (Figure 26). Therefore, our cohort showed no substantial differences in the proteins expressed between the groups (PC1: 10.7%, PC2: 6.9%), However, unlike the Y and M groups, whose subjects were more grouped, the P group showed more dispersion, indicating an increased variability and heterogeneity between the subjects included in this group. Next, we analyzed the differentially expressed proteins (DEPs) between the Y, M, and P conditions.

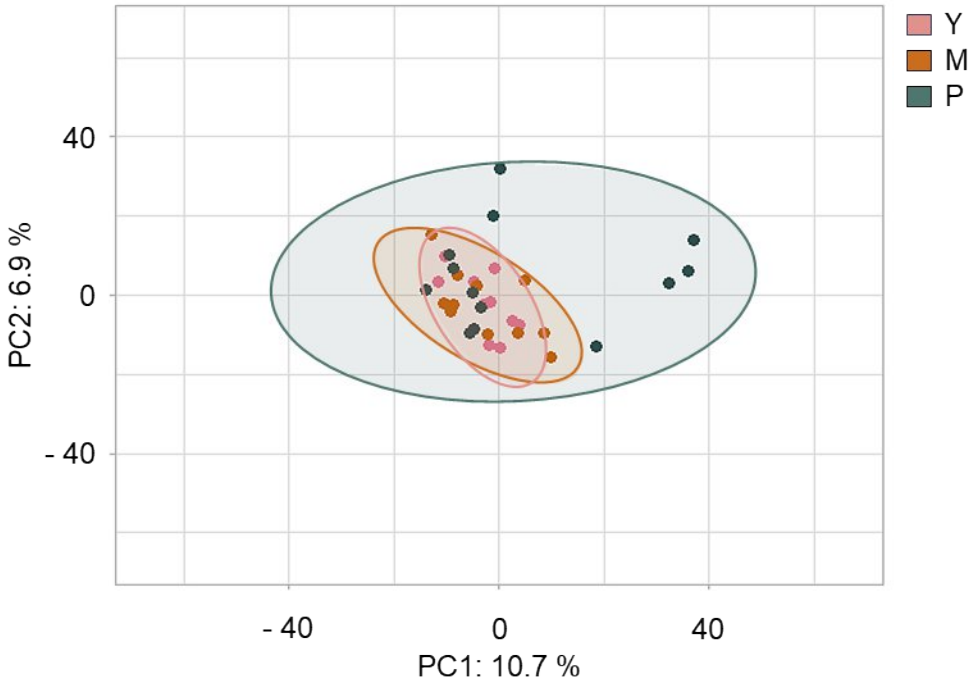


Figure 26. Proteomic profiling of the ovary in Y, M, and P groups.

Principal component analysis distinguished three major clusters with an overlap between age groups. Y: young, M: middle-aged, P: perimenopausal, PC1: principal component 1, PC2:principal component 2.

Considering the unadjusted p-value analysis, statistical analysis revealed 92 (4.8%) DEPs between Y and M, 138 (7.2%) DEPs between Y and P, and 159 (8.3%) DEPs between M and P. The identified DEPs are specified in Appendix C, Table C9. Only two DEPs were shared between the different paired comparisons (Figure 27A). Among them, the glutathione hydrolase 5 proenzyme (GGT5), related to glutathione metabolism, showed the highest level in M (Figure 27B). However, small nuclear ribonucleoprotein-associated protein (RSMN), essential in gene expression processing and regulation, was upregulated in Y and M (Figure 27C).

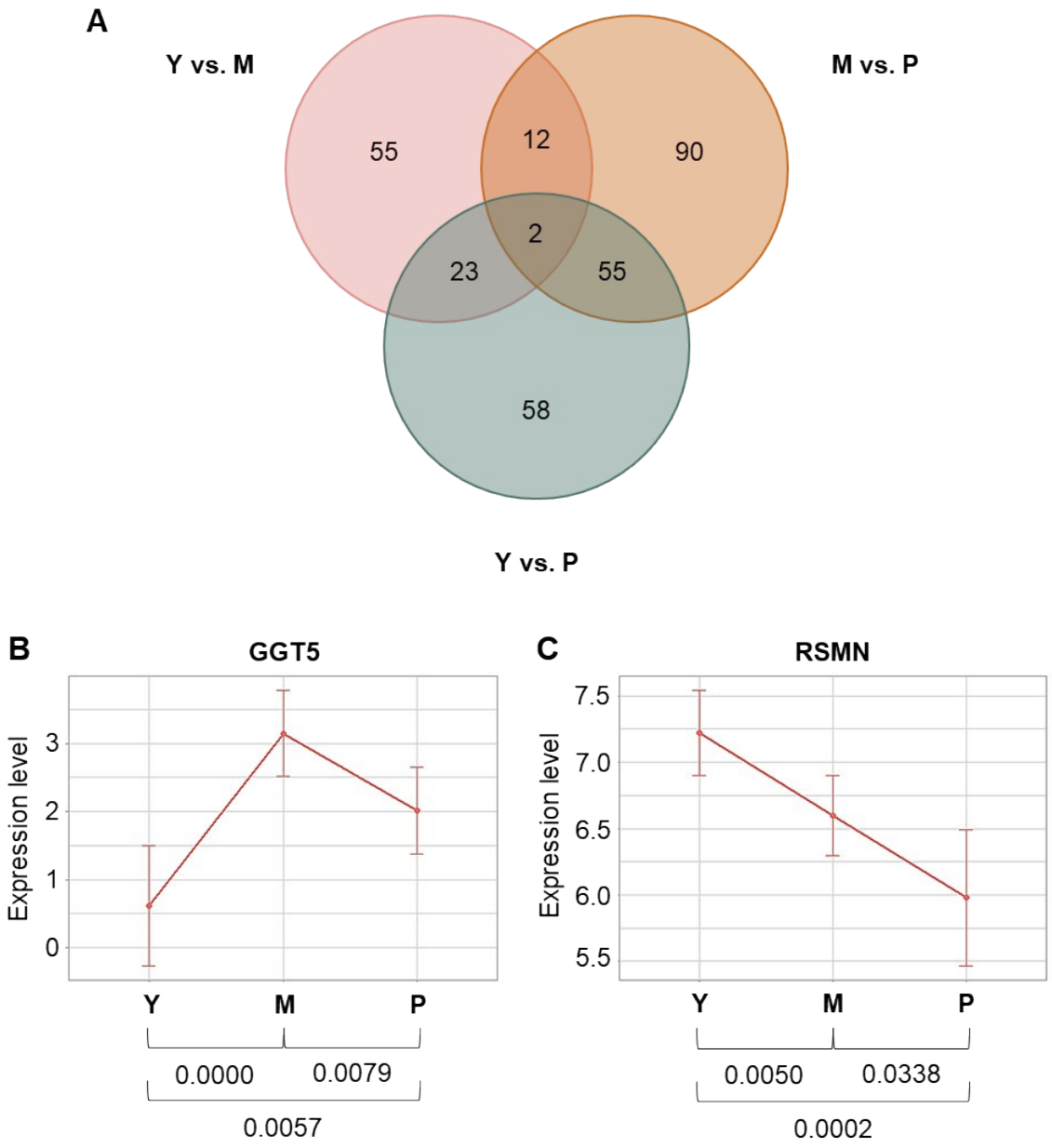


Figure 27. Ovarian proteomic changes in age groups.

(A) Venn diagram representing the shared DEPs between the different comparisons. (B) GGT5 parallel plot highlighting the protein expression tendency throughout age groups. (C) RSMN parallel plot highlighting the protein expression tendency throughout age groups. Only significant p-values are specified in B and C. Y: young, M: middle-aged, P: perimenopausal, GGT5: glutathione hydrolase 5 proenzyme, RSMN: small nuclear ribonucleoprotein-associated protein.

Focusing on the two-by-two comparisons, 48 (52.2%) proteins were upregulated and 44 (47.8%) downregulated when the Y group was compared with M (Figure 28A). In contrast, in the Y vs. P comparison (Figure 28B), 87 (63%) proteins were increased in Y, whereas 51 (37%) had lower expression. Finally, 95 (59.7%) proteins were found to be upregulated and 64 (40.3%) downregulated in the M group when compared with P (Figure 28C).

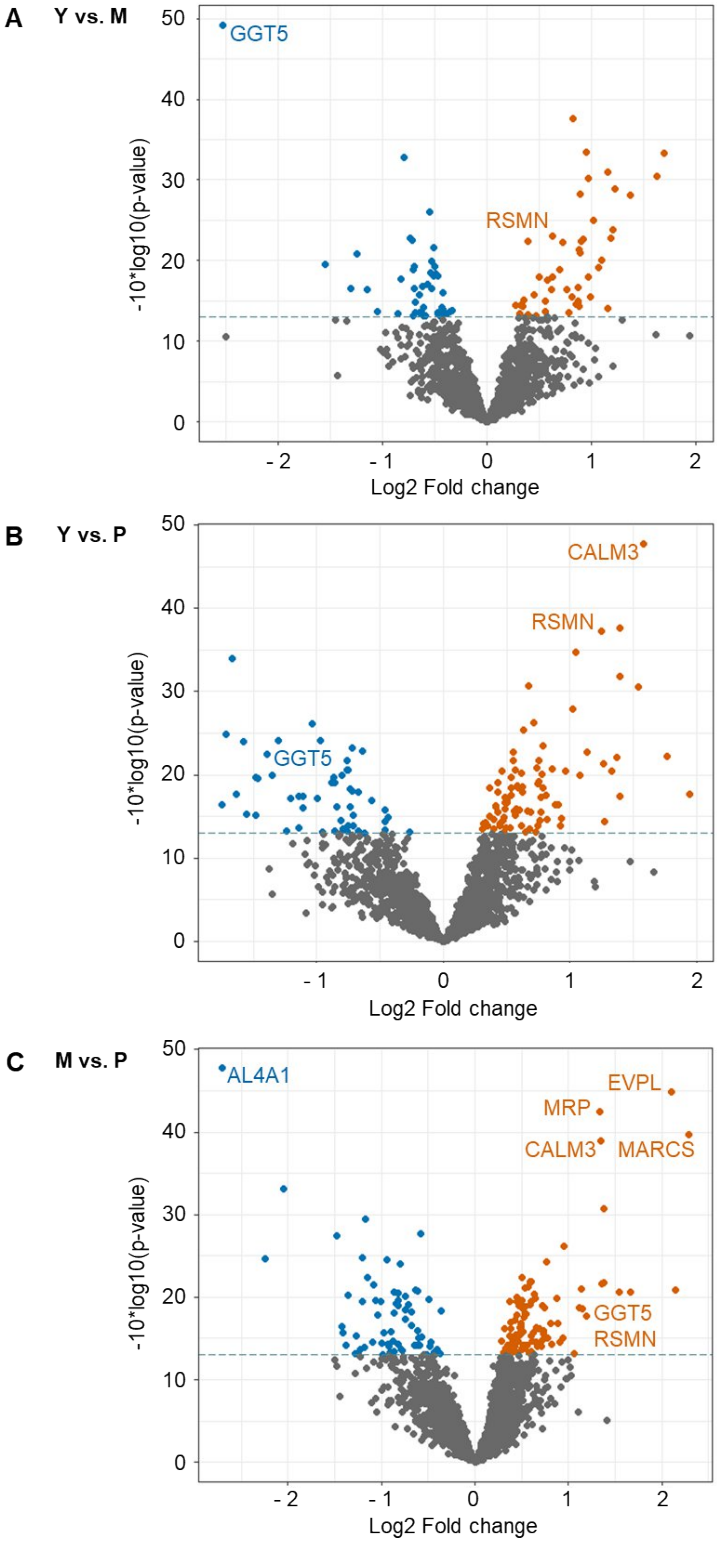


Figure 28. Volcano plot showing pairwise comparisons of protein expression levels between age groups.

(A) Volcano plot Y vs. M comparison. (B) Volcano plot Y vs. P comparison. (C) Volcano plot M vs. P comparison. Dots above dashed horizontal lines (blue and orange) represent DEPs. Y: young, M: middle-aged, P: perimenopausal, GGT5: glutathione hydrolase 5 proenzyme, RSMN: small nuclear ribonucleoprotein-associated protein, CALM3: calmodulin 3, AL4A1: delta-1-pyrroline-5-carboxylate dehydrogenase, EVPL: envoplakin, MARCS: myristoylated alanine rich C kinase substrate, MRP: MARCKS-related protein.

Among the proteins differentially expressed in the previous analyses, those shared in the [(Y vs. P) + (M vs. P)] comparisons were analyzed in detail. Four proteins, two with high expression and two with lower expression in group P, stood out compared to Y and M. The upregulated proteins were serine-protein kinase ATM (ATM) and cullin-1 (CUL1). The first one, ATM (Figure 29A), is central to maintaining genome stability, while CUL1 (Figure 29B) regulates the cell cycle, DNA damage response, and protein homeostasis. The proteins with lower expression were calmodulin-3 (CALM3, Figure 29C), a key player in mediating calcium signaling, and L-lactate dehydrogenase B chain (LDHB, Figure 29D), with a critical role in the conversion of lactate to pyruvate, which impacts a variety of metabolic processes.

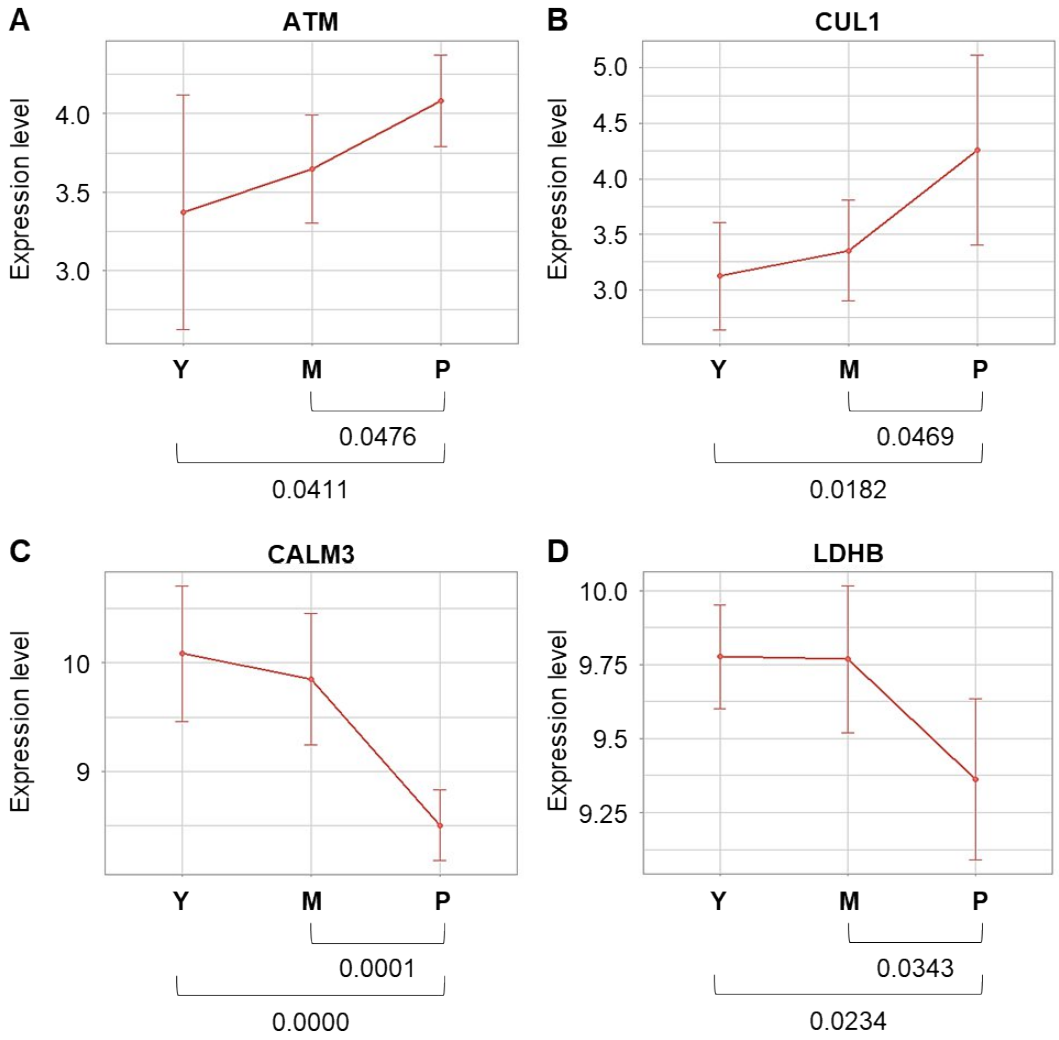


Figure 29. Parallel plots highlight ATM, CUL1, CALM3, and LDHB protein expression tendency throughout age groups.

(A) ATM parallel plot highlighting the protein expression tendency throughout age groups. (B) CUL1 parallel plot highlighting the protein expression tendency throughout age groups. (C) CALM3 parallel plot highlighting the protein expression tendency throughout age groups. (D) LDHB parallel plot highlighting the protein expression tendency throughout age groups. Only significant p-values are specified. Y: young, M: middle-aged, P: perimenopausal, ATM: serine-protein kinase, CUL1: cullin-1, CALM3: calmodulin 3, LDHB: lactate dehydrogenase B.

When the above-mentioned statistical analysis was performed restrictively, with the adjusted p-value as reference, the GGT5 protein was differentially downregulated in the younger group compared to the M group. In the Y vs. P comparison, elevated CALM3 levels were statistically significant. However, it was the M vs. P comparison the one that evidenced a greater number of differentially expressed proteins, among which the previously mentioned CALM3, with myristoylated alanine rich C kinase substrate (MARCS), MARCKS-related protein (MRP), and envoplakin (EVPL) showed higher levels in M. MRP shares many functional similarities with MARCKS, as both have a role in regulating cell migration, actin cytoskeleton remodeling, membrane trafficking, and calcium signaling. The EVPL protein participates in the integrity and function of epithelial tissues.

Finally, the mitochondrial delta-1-pyrroline-5-carboxylate dehydrogenase (AL4A1) was found to be downregulated. This protein involves essential biological processes such as stress response and mitochondrial function. The specific details of the expression of all the above-mentioned proteins are shown in Table 23.

Table 23. DEPs from p-value adjusted statistical analysis.

Protein abbreviation name	Comparison	Log Fold Change	p-value	Adjusted p-value
GGT5	**Y vs. M**	-2.53	0.0000*	0.0233*
	Y vs. P	-1.39	0.0057*	0.4727
	M vs. P	1.14	0.0079*	0.4488
CALM3	**Y vs. M**	0.23	0.5400	0.9999
	Y vs. P	1.58	0.0000*	0.0326*
	M vs. P	1.35	0.0001*	0.0492*
MARCS	**Y vs. M**	-0.53	0.2308	0.9999
	Y vs. P	1.74	0.0057*	0.4727
	M vs. P	2.29	0.0001*	0.0492*
MRP	**Y vs. M**	0.06	0.8853	0.9999
	Y vs. P	1.39	0.0007*	0.2108
	M vs. P	1.33	0.0001*	0.0363*
EVPL	**Y vs. M**	-1.14	0.0230*	0.8536
	Y vs. P	0.96	0.0758	0.6632
	M vs. P	2.10	0.0000*	0.0317*
AL4A1	**Y vs. M**	1.04	0.1239	0.9999
	Y vs. P	-1.67	0.0004*	0.1550
	M vs. P	-2.71	0.0000*	0.0317*

*Denoted the comparison with significant differential expression.
Y: young, M: middle-aged, P: perimenopausal, GGT5: glutathione hydrolase 5 proenzyme, CALM3: calmodulin 3, AL4A1: delta-1-pyrroline-5-carboxylate dehydrogenase, EVPL: envoplakin, MARCS: myristoylated alanine rich C kinase substrate, MRP: MARCKS-related protein.

5.1.5 Summary of findings in this section

Women undergo reproductive decline, evidenced by alterations in ovarian TL, even before the onset of systemic aging. This reproductive aging was reflected in ovarian reserve decline, telomere shortening, increased fibrotic area in ovarian tissue, and hormonal variations. Alterations in telomere maintenance of oocyte telomeres, primordial GCs, primary GCs, and TCs were detected in the ovaries of middle-aged women. No significant correlations were found between telomere parameters of PBMCs and ovarian cell populations, excluding PBMCs as putative telomere biomarkers of ovarian aging. Telomere characterization of folliculogenesis showed that only GCs modify their telomeres during this process, not oocytes or TCs.

5.2 Study of telomere parameters in lower ovarian reserve cases

The previous results showed that one of the main characteristics of female reproductive aging was the drop in ovarian reserve, indirectly evaluated by measuring AMH. This hormone decreases with increasing age. Considering that some women of reproductive age record low levels of this hormone, we asked whether the telomere pathway could be altered in subjects with this hormonal profile. For this purpose, women with low levels of AMH were compared with control women of the same age (who had higher levels of this hormone). As a result of this comparison, it was possible to clarify whether a lower ovarian reserve could lead to ovarian aging regardless of age. Women whose ovarian fragment was obtained during the cesarean surgery were excluded from this analysis due to the variations of AMH levels described for pregnant women.

5.2.1 Baseline characteristics of the study population and hormonal levels

The sample size was reduced to 52 women after excluding pregnant women (Table 24). These women were divided based on age and AMH value. The number of young women (n = 13) recruited with elevated AMH (Y+, n = 11) was higher than those with reduced levels of this hormone (Y-, n = 2). No statistically significant differences in age were found between Y+ and Y- ($p = 0.8462$). In the case of the middle-aged group (n = 22), the sample size was larger in the low-ovarian reserve group (M-, n = 16) compared to the group with high AMH (M+, n = 6). In this case, the mean age of M- was significantly lower than M+ ($p = 0.0145$). Both perimenopausal (n = 17) groups were balanced in sample size (P+, n = 8; P-, n = 9), and no

mean age differences were detected (p = 0.0501). No differences in BMI were observed in any of the above comparisons. All subgroups within each age range showed statistically significant differences in AMH. Regarding the remaining hormones, only when comparing M+ and M-, the LH value was statistically significantly higher in M- (p = 0.0143). The baseline characteristics of patients in each age group, categorized by AMH, and comparisons of hormone levels are summarized in Table 24.

Table 24. Baseline characteristics and hormonal parameters of the study population classified by age and AMH levels.

	Y+ n = 11	**Y-** n = 2	**M+** n = 6	**M-** n = 16	**P+** n = 8	**P-** n = 9
Demographic characteristics						
Age (years)	0.8462		0.0145		0.0501	
Mean ± SD	30.7 ± 4.4	32.0 ± 2.8	37.7 ± 2.5*	41.4 ± 3.1*	47.0 ± 0.8*	48.0 ± 1.1*
Median (Q1–Q3)	32.0 (29.0-34.0)	32.0 (30.0-34.0)	37.0 (35.8-39.8)	42.5 (39.0-44.0)	47.0 (46.3-47.8)	48.0 (47.0-49.0)
BMI (kg/m^2)	0.6061		0.3416		0.6749	
Mean ± SD	23.5 ± 3.1*	22.1 ± 1.5	24.2 ± 4.3*	26.5 ± 5.2*	27.6 ± 5.6*	26.5 ± 3.8*
Median (Q1–Q3)	23.5 (3.1-1.0)	22.1 (1.5-1.0)	23.9 (21.0-26.8)	25.0 (23.1-31.1)	26.2 (22.5-32.0)	27.2 (23.1-29.3)
Endocrine parameters						
AMH (ng/mL)	0.0256		<0.0001		<0.0001	
Mean ± SD	3.6 ± 2.5	0.6 ± 0.5	2.9 ± 1.4*	0.4 ± 0.4	0.5 ± 0.4*	0.03 ± 0.03
Median (Q1–Q3)	2.4 (1.9-5.5)	0.6 (0.3-0.9)	2.8 (1.7-3.9)	0.2 (0.01-0.8)	0.4 (0.2-0.6)	0.01 (0.01-0.05)
FSH (mIU/mL)	0.4103		0.7333		0.1139	
Mean ± SD	4.5 ± 1.7*	6.1 ± 2.2	44.6 ± 97.2	24.0 ± 38.6	9.3 ± 5.8*	18.3 ± 13.4
Median (Q1–Q3)	4.7 (2.6-6.3)	6.1 (4.5-7.6)	5.8 (2.8-66.7)	6.2 (3.5-25.7)	9.5 (4.0-13.0)	16.1 (7.7-25.9)
LH (mIU/mL)	0.3077		0.0143		0.0796	
Mean ± SD	7.3 ± 4.2*	3.8 ± 0.5	3.5 ± 2.0*	18.1 ± 19.7	6.4 ± 3.6*	12.8 ± 9.0*
Median (Q1–Q3)	7.6 (3.7-9.4)	3.8 (3.4-4.1)	3.4 (1.6-5.2)	9.2 (4.5-19.5)	5.9 (3.3-9.8)	11.2 (5.4-17.4)
E2 (pg/mL)	0.9231		0.5075		0.1388	
Mean ± SD	135.3 ± 106.2*	114.2 ± 55.6	68.5 ± 60.8*	157.9 ± 149.8	70.7 ± 26.2*	62.0 ± 78.6
Median (Q1–Q3)	119.0 (48.7-219.8)	114.2 (74.9-153.5)	56.4 (26.2-102.9)	65.5 (34.3-347.4)	72.9 (52.2-90.0)	27.7 (16.6-86.7)
P4 (ng/mL)	0.7692		0.3319		0.3213	
Mean ± SD	1.6 ± 3.8	0.7 ± 0.8	3.1 ± 4.8*	0.7 ± 1.0	3.3 ± 5.7	0.6 ± 0.6*
Median (Q1–Q3)	0.2 (0.2-1.4)	0.7 (0.1-1.3)	1.0 (0.2-6.0)	0.3 (0.1-1.5)	0.7 (0.2-5.5)	0.3 (0.1-1.0)

Data are presented as mean ± standard deviation and median (interquartile range). *Denoted the variables that passed the Shapiro-Wilk normality test. Statistical analysis of comparisons between groups with different AMH levels and similar age was performed using the Student t-test (for normally distributed data) or the Mann-Whitney U test (for non-normally distributed data). A p-value < 0.05 was considered statistically significant. The n refers to the number of subjects. There was an exception in the sample size of the M- group (n = 15) for FSH, LH, E2, and P4 hormones. Consequently, the mean age in this group was 41.2 ± 3.0*, statistically significant differences in age with M+ remained (p = 0.0207). Y: young; M: middle-aged; P: perimenopausal; SD: standard deviation; Q1: quartile 1 (25% percentile); Q3: quartile 3 (75% percentile).

5.2.2 Telomere analysis

5.2.2.1 Analysis of systemic telomere status

The analysis of telomere parameters in PBMCs from subgroups with different AMH values but similar ages did not reveal statistically significant differences in mean TL or the percentage of short and long telomeres in any age group (Table 25). No differences were seen in the telomere parameters of PBMCs even in the group of middle-aged women, whose age was significantly different (p = 0.0145).

Table 25. PBMCs telomere parameters in groups based on age and AMH levels.

	Y+ n = 11	**Y-** n = 2	**M+** n = 6	**M-** n = 16	**P+** n = 8	**P-** n = 9
TL (a.u.)	0.3077		0.3855		0.3487	
Telomeres	43187	11623	43721	80896	30072	32811
Mean ± SD	128.8 ± 6.5*	124.1 ± 1.1	137.8 ± 17.3*	130.4 ± 17.5	121.4 ± 6.4*	124.9 ± 8.3*
Median (Q1–Q3)	128.7 (124.2-135.9)	124.1 (123.3-124.9)	131.8 (123.5-155.3)	127.5 (119.0-136.3)	121.0 (119.2-127.0)	124.3 (117.0-132.5)
Short telomeres (%)	0.6410		0.2642		0.2893	
Mean ± SD	12.2 ± 6.5*	9.5 ± 3.4	8.4 ± 8.6*	13.6 ± 9.6*	20.1 ± 8.5*	15.5 ± 8.8*
Median (Q1–Q3)	10.9 (7.8-18.4)	9.5 (7.1-11.9)	7.5 (0.2-15.2)	14.1 (4.9-21.6)	19.8 (13.8-22.2)	15.9 (5.9-23.7)
Long telomeres (%)	0.1538		0.4494		0.3903	
Mean ± SD	10.6 ± 4.7*	4.1 ± 2.5	19.2 ± 18.6*	13.7 ± 17.2	6.1 ± 3.1*	8.1 ± 5.5*
Median (Q1–Q3)	11.3 (5.5-13.4)	4.1 (2.3-5.9)	10.4 (6.3-36.1)	9.7 (4.0-16.1)	5.5 (4.6-7.7)	7.6 (3.7-12.3)

Data are presented as mean ± standard deviation and median (interquartile range). *Denoted the variables that passed the Shapiro-Wilk normality test. Statistical analysis of comparisons between groups with different AMH and similar age was performed using Student t-test (normally distributed data) or the Mann-Whitney U test (non-normally distributed data). A p-value < 0.05 was considered statistically significant. The n refers to the number of subjects. The number of telomere dots analyzed is specified in the TL section under “Telomeres”. PBMCs: peripheral blood mononuclear cells; TL: telomere length; Y: young; M: middle-aged; P: perimenopausal; SD: standard deviation; Q1: quartile 1 (25% percentile); Q3: quartile 3 (75% percentile); a.u.: arbitrary units of intensity; %: percent.

5.2.2.2 Analysis of ovarian telomere status

No differences were observed in TL or associated parameters at the systemic level when the low ovarian reserve groups were compared with their age-matched control groups. This analysis was then tested at the ovarian level in the various regions and cell populations that comprise this organ.

Firstly, the ovarian stroma was analyzed. When aging was studied in this region of the ovary, although a significant increase in the percentage of fibrotic area with age was observed, no changes were noted in terms of telomeres. No changes in TL were seen in any age interval when this ovarian region was examined independently in the different age groups, comparing the high and low AMH groups. There were no differences in the comparison of middle-aged women, even though the mean age of M+ and M- differed statistically. Although there was a

relatively large difference in TL between the younger Y+ and Y- groups, this was not significant (p = 0.1026) given that the Y- group only consisted of two subjects. The same occurred for the percentage of short (p = 0.1026) and long telomeres (p = 0.0513) for this age group. In the case of the M+ and M- groups, there were no differences in the telomere measurements (TL p = 0.4070, %short p = 0.3722, %long p = 0.4494). In the comparison between the P+ and P- groups, where the number of subjects composing it was more balanced, no significant differences were detected (TL p = 0.2283, %short p = 0.1139, %long p = 0.1996). Table 26 summarizes the stroma telomere parameters and p-values after comparing age groups divided by AMH.

Table 26. Stroma telomere parameters in groups based on age and AMH divisions.

	Y+ n = 11	**Y-** n = 2	**M+** n = 6	**M-** n = 16	**P+** n = 8	**P-** n = 9
TL (a.u.)	0.1026		0.4070		0.2283	
Telomeres	1664964	13211	325509	1295540	259350	720047
Mean ± SD	143.2 ± 9.9*	126.1 ± 0.4	138.6 ± 19.8	137.9 ± 8.2*	150.0 ± 12.5*	141.9 ± 13.8*
Median (Q1–Q3)	143.8 (136.3-152.1)	126.1 (125.8-126.4)	128.1 (124.9-161.0)	138.8 (131.4-144.7)	154.9 (136.8-157.8)	142.9 (130.1-150.9)
Short telomeres (%)	0.1026		0.3722		0.1139	
Mean ± SD	11.8 ± 10.9	34.3 ± 1.5	22.6 ± 16.1*	17.6 ± 9.6*	8.4 ± 9.8	15.8 ± 14.9
Median (Q1–Q3)	7.9 (6.3-13.1)	34.3 (33.3-35.3)	26.8 (3.2-38.0)	16.7 (9.3-26.9)	3.5 (1.7-17.3)	8.9 (5.3-26.0)
Long telomeres (%)	0.0513		0.4494		0.1996	
Mean ± SD	12.3 ± 9.8*	1.7 ± 0.4	13.0 ± 18.8	8.4 ± 5.8*	18.9 ± 12.4*	12.5 ± 12.9
Median (Q1–Q3)	9.8 (4.1-21.5)	1.7 (1.4-2.0)	2.0 (1.1-31.7)	9.0 (3.0-13.2)	21.4 (6.2-26.0)	8.4 (2.7-18.8)

Data are presented as mean ± standard deviation and median (interquartile range). *Denoted the variables that passed the Shapiro-Wilk normality test. Statistical analysis of comparisons between groups with different AMH and similar age was performed using Student t-test (normally distributed data) or the Mann-Whitney U test (non-normally distributed data). A p-value < 0.05 was considered statistically significant. The n refers to the number of subjects. The number of telomere dots analyzed is specified in the TL section under the heading “Telomeres”. TL: telomere length; Y: young; M: middle-aged; P: perimenopausal; SD: standard deviation; Q1: quartile 1 (25% percentile); Q3: quartile 3 (75% percentile); a.u.: arbitrary units of intensity; %: percent.

Focusing on ovarian cells directly involved in fertility, cells that form ovarian follicles such as oocytes, GCs, and TCs, the study of telomere shortening could only be performed in the middle-aged group, comparing M+ and M-. It was impossible to study the younger group because of the difficulty in finding young women with low ovarian reserve. As observed in the study of ovarian stroma, when excluding pregnant women and dividing based on AMH, only two women were classified within the Y- group, and not enough ovarian follicles were identified in them to perform the statistical analysis. In the perimenopausal, P+, and P- groups of women, no follicles were identified in the ovarian sections of these women.

Among the subjects in the middle-aged groups in which oocytes were detected, there were no statistically significant differences in the age parameter (p = 0.0906), with M+ and M- being comparable. Concerning the AMH parameter, values were statistically different from each other (p = 0.0040). No differences in the mean TL (Figure 30A, p = 0.1095) or the percentage

of long telomeres (Figure 30C, p = 0.2584) of the oocytes between the M+ (TL: 156.4 ± 24.0 a.u., %long: 20.9 ± 35.5%) and M- (TL: 147.2 ± 23.3 a.u., %long: 14.1 ± 19.9%) groups were detected. However, there was a higher percentage of short telomeres (Figure 30B, p = 0.0416) in the M- group (29.3 ± 26.0%) compared to M+ (18.7 ± 19.5%).

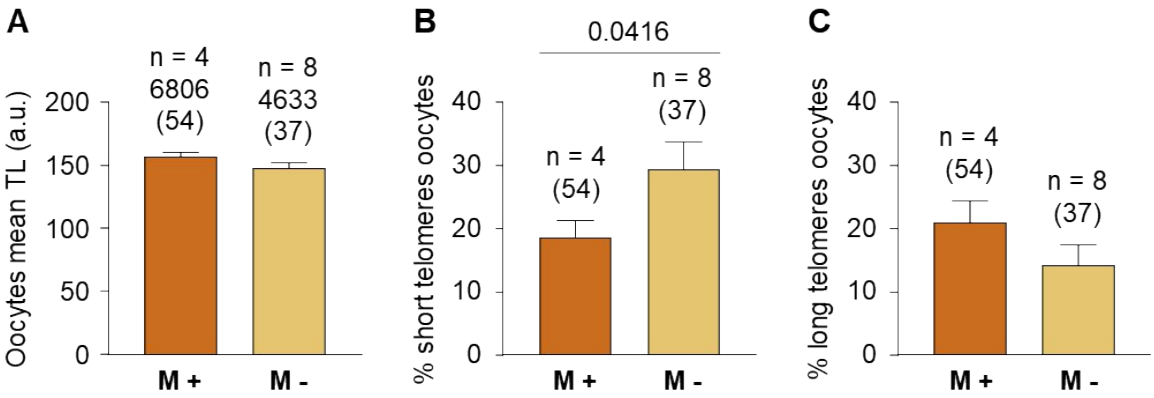


Figure 30. Analysis of telomere parameters in oocytes from M+ and M- women.

(A) TL in each AMH group. The number of individuals, the telomere dots analyzed, and the number of oocytes are specified. (B) Percentage of short telomeres in M+ and M-. (C) Percentage of long telomeres in M+ and M-. The groups were compared using the Mann-Whitney U test. The bar diagrams represent the mean value, and the error bars the SEM. A p-value < 0.05 was considered statistically significant. Only significant p-values are shown in the bar graphs. For more information, see Appendix D, Table D1. M: middle-aged, SD: standard deviation, a.u.: arbitrary units (intensity), TL: telomere length, %: percent.

Comparison of telomere parameters in GCs of different follicular stages in M- women and their M+ control group showed statistically significant differences only in primordial and secondary follicles. Telomere parameters of GCs and p-values obtained in statistical analyses are specified in Table 27.

Table 27. GCs telomere parameters in middle-aged women classified by AMH.

GCs primordial follicles	**M+** n = 3		**M-** n = 7
Age (years)		0.0199	
Mean ± SD	37.0 ± 2.0*		42.1 ± 2.7*
Median (Q1–Q3)	37.0 (35.0-39.0)		43.0 (39.0-45.0)
AMH (ng/mL)		0.0028	
Mean ± SD	2.5 ± 1.0*		0.5 ± 0.5*
Median (Q1–Q3)	2.9 (1.3-3.4)		0.3 (0.01-1.1)
TL (a.u.)		0.0169	
Follicles	20		10
Telomeres	4661		1843
Mean ± SD	149.4 ± 15.3*		134.9 ± 13.4*
Median (Q1–Q3)	151.7 (139.1-161.8)		134.1 (121.3-144.4)
Short telomeres (%)		0.0311	
Mean ± SD	14.7 ± 17.4		31.6 ± 22.6*
Median (Q1–Q3)	8.1 (1.3-21.4)		28.8 (9.1-56.5)
Long telomeres (%)		0.0213	
Mean ± SD	18.7 ± 14.3*		6.2 ± 7.5
Median (Q1–Q3)	18.5 (7.7-29.9)		4.6 (0.6-8.6)

GCs primary follicles	**M+** n = 5		**M-** n = 9
Age (years)		0.0671	
Mean ± SD	37.8 ± 2.8*		41.3 ± 3.3*
Median (Q1–Q3)	37.0 (35.5-40.5)		41.0 (38.5-44.5)
AMH (ng/mL)		0.0010	
Mean ± SD	2.9 ± 1.5*		0.6 ± 0.5
Median (Q1–Q3)	2.9 (1.6-4.3)		0.8 (0.1-1.1)
TL (a.u.)		0.3020	
Follicles	43		36
Telomeres	13192		13276
Mean ± SD	149.7 ± 22.5		145.6 ± 22.1
Median (Q1–Q3)	140.8 (132.2-169.4)		137.3 (129.1-157.4)
Short telomeres (%)		0.1698	
Mean ± SD	21.3 ± 20.8		28.1 ± 22.5
Median (Q1–Q3)	15.7 (2.3-36.4)		31.2 (6.6-46.2)
Long telomeres (%)		0.7737	
Mean ± SD	17.3 ± 25.1		15.2 ± 24.8
Median (Q1–Q3)	3.1 (0.0-28.9)		1.7 (0.7-14.3)
GCs secondary follicles	**M+** n = 2		**M-** n = 7
Age (years)		0.0278	
Mean ± SD	36.0 ± 1.4		42.4 ± 2.4*
Median (Q1–Q3)	36.0 (35.0-37.0)		44.0 (40.0-44.0)
AMH (ng/mL)		0.0556	
Mean ± SD	2.1 ± 1.2*		0.3 ± 0.4
Median (Q1–Q3)	2.1 (1.3-2.9)		0.1 (0.02-0.9)
TL (a.u.)		0.0948	
Follicles	6		13
Telomeres	9242		20531
Mean ± SD	178.9 ± 26.3*		159.0 ± 21.1*
Median (Q1–Q3)	188.0 (146.9-201.2)		154.3 (143.5-176.9)
Short telomeres (%)		0.2100	
Mean ± SD	22.1 ± 28.0		38.9 ± 25.9*
Median (Q1–Q3)	5.9 (2.6-57.4)		34.4 (18.5-58.9)
Long telomeres (%)		0.0282	
Mean ± SD	29.1 ± 25.8		9.4 ± 15.5
Median (Q1–Q3)	27.5 (2.3-56.9)		1.4 (0.2-16.1)

Data are presented as mean ± standard deviation and median (interquartile range). *Denoted the variables that passed the Shapiro-Wilk normality test. Statistical analysis of comparisons between M+ and M- was performed using Student t-test (normally distributed data) or the Mann-Whitney U test (non-normally distributed data). A p-value < 0.05 was considered statistically significant. The n refers to the number of subjects. The number of follicles and telomere dots analyzed is specified in the TL section. AMH: anti-müllerian hormone, TL: telomere length, M: middle-aged, SD: standard deviation, Q1: quartile 1 (25% percentile), Q3: quartile 3 (75% percentile), ng: nanogram, mL: milliliter, a.u.: arbitrary units of intensity; %: percent.

The M- group had a lower mean TL in primordial GCs than the M+ group (Figure 31A, p = 0.0169). However, this comparison had a major limitation, as the mean age difference between individuals where primordial follicles were detected in M+ and M- groups was statistically significantly different (p = 0.0199). There was also a higher percentage of short telomeres in M- (Figure 31B, p = 0.0311) and a lower percentage of long telomeres (Figure 31C, p = 0.0213) compared to M+. In primary GCs, both TL (Figure 31D), percentage of short (Figure 31E) and

long telomeres (Figure 31F) in the M+ and M- groups were similar. In these comparisons of primary GCs, the mean age of the groups was comparable (p = 0.0671). Special emphasis should be placed on the case of secondary GCs (Figure 31G, H, and I), since, similar to primordial follicles, the mean age was significantly different (p = 0.0278). However, the mean AMH values between M+ and M- were similar (p = 0.0556). Therefore, statistically significant differences were found in the percentage of long telomeres in M+ and M- from GCs of secondary follicles (p = 0.0282), but that age was also different.

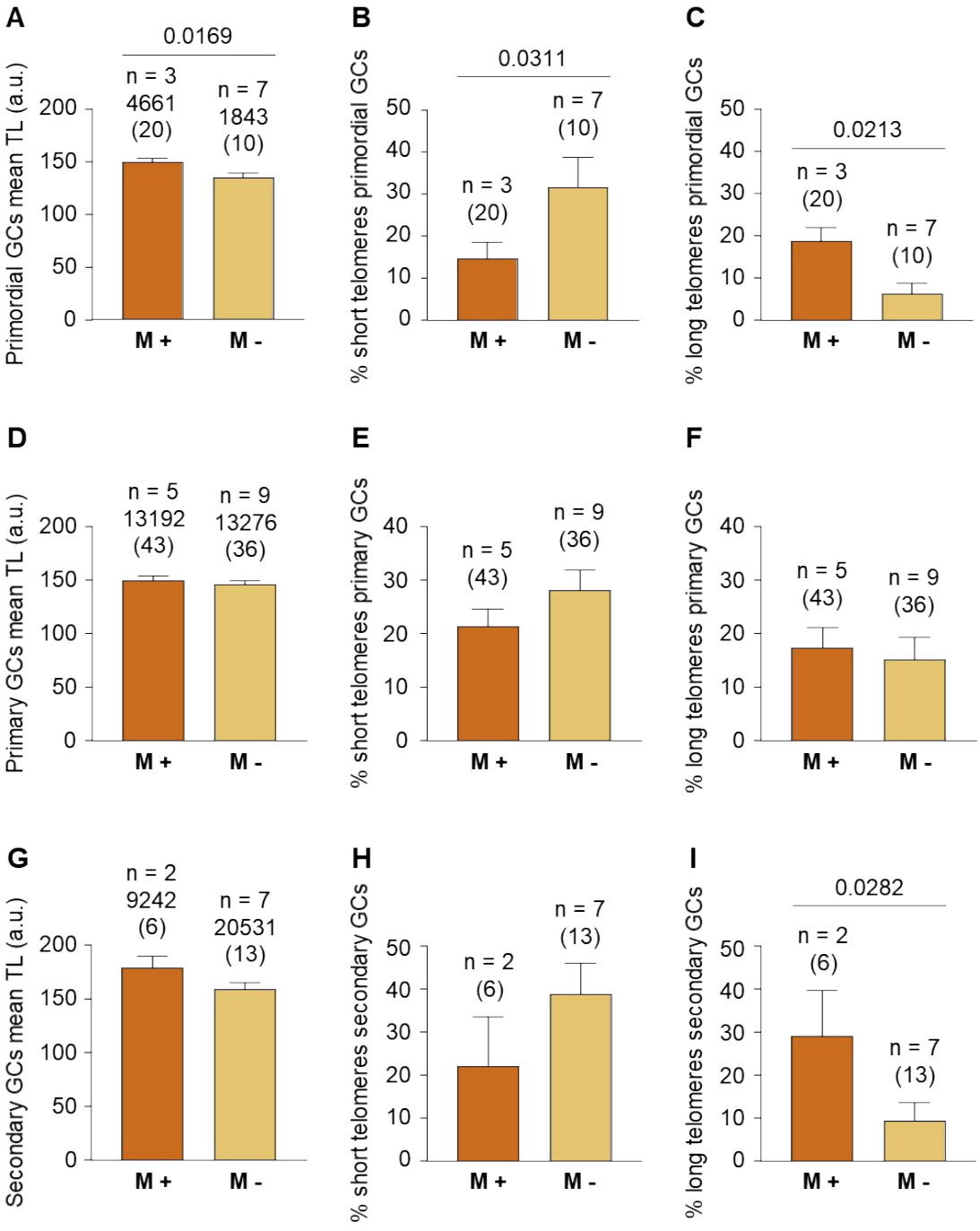


Figure 31. Analysis of telomere parameters in M+ and M- groups.

(A) Mean TL in each AMH group in GCs of primordial follicles. The number of individuals, the telomere dots analyzed, and the number of follicles are specified at the top of the bar diagrams. (B) Percentage of short telomeres in primordial follicles. (C) Percentage of long telomeres in primordial follicles. (D) Mean TL in GC of primary follicles in each AMH group. The number of individuals, the telomere dots analyzed, and the number of follicles are specified on the top bar diagrams. (E) Percentage of short telomeres in GCs of primordial follicles. (F) Percentage of long telomeres in GCs of primary follicles. (G) Mean TL in GCs of secondary follicles of each AMH group. The number of individuals, the telomere dots analyzed, and the number of follicles are specified on the top bar diagrams. (H) Percentage of short telomeres in GCs of secondary follicles. (I) Percentage of long telomeres in the groups described in G. Statistical analysis of comparisons between groups with different AMH and similar age was performed using Student t-test (normally distributed data) or the Mann-Whitney U test (non-normally distributed data). The bar diagrams represent the mean value, and the error bars the SEM. A p-value < 0.05 was considered statistically significant. Only significant p-values are shown in the bar graphs. M: middle-aged, GCs: granulosa cells, SD: standard deviation, a.u.: arbitrary units (intensity), TL: telomere length, %: percent.

The TL of TCs forming part of primary and secondary follicles in the M+ (n = 4) and M- (n = 10) groups, with similar ages (M+: 38.3 ± 3.0, M-: 41.6 ± 3.2 years, p = 0.1000), were compared. The mean TL of these cells in both groups was different (Figure 32A, p = 0.0229), with a higher TL in the M+ control group (150.8 ± 22.6 a.u.) compared to M- (147.2 ± 23.3 a.u.). However, despite a higher percentage of short telomeres in the M- group (Figure 32B), no statistically significant differences were observed (26.3 ± 31.7% in M+ compared to 30.8 ± 20.9%, p = 0.1386). In the case of the percentage of long telomeres found in each of the groups (Figure 32C), the same occurred; there were no statistically significant differences despite a lower mean percentage in the M- group (18.6 ± 23.3% in M+ compared to 5.8 ± 9.3% in M-, p = 0.1567).

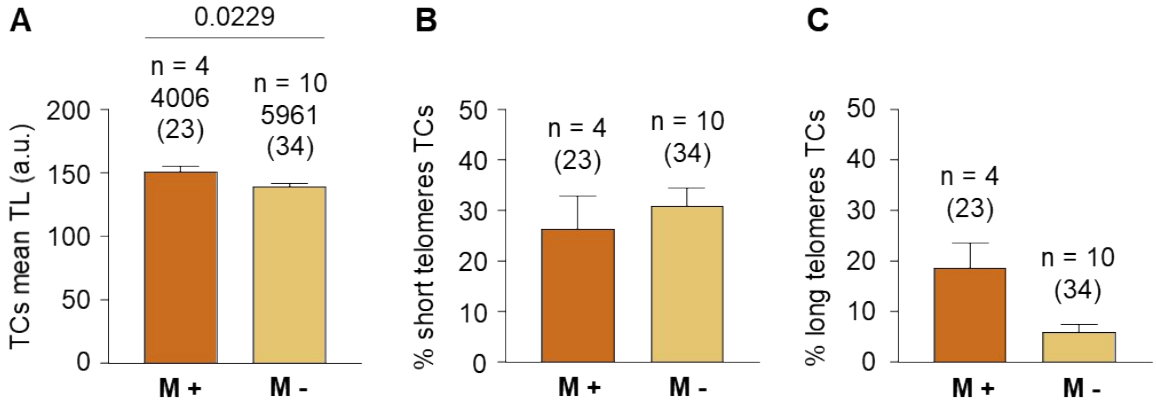
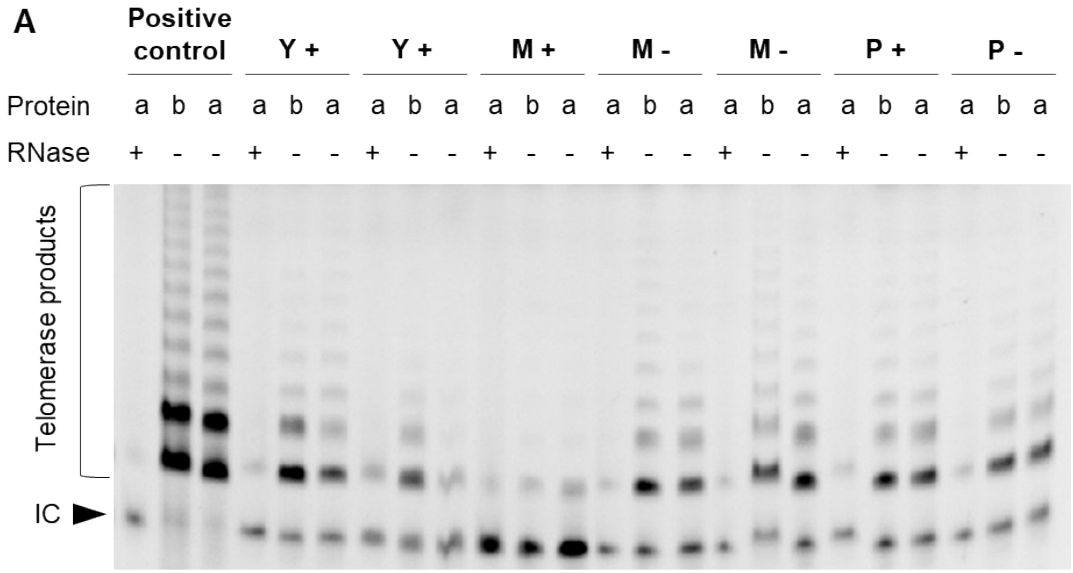


Figure 32. Analysis of telomere parameters in TCs from M+ and M- women.

(A) Mean TL in AMH groups. The number of individuals, the telomere dots analyzed, and the number of follicles are specified. (B) Percentage of short telomeres in M+ and M-. (C) Percentage of long telomeres in M+ and M-. Statistical analysis of comparisons between M+ and M- was performed using Student t-test (normally distributed data distribution) or the Mann-Whitney U test (non-normally distributed data distribution). The bar diagrams represent the mean value, and the error bars the SEM. A p-value < 0.05 was considered statistically significant. Only significant p-values are shown in the bar graphs. For more information, see Appendix D, Table D2. TCs: theca cells, M: middle-aged, SD: standard deviation, a.u.: arbitrary units (intensity), TL: telomere length, %: percent.

5.2.2.3 Analysis of telomerase activity in the ovary

The TRAP assay was performed to determine whether lower ovarian reserve may affect TA. Our results (Figure 33A) showed that TA was detectable in women with low ovarian reserve, even in those where the AMH level was undetectable (AMH = 0.01 ng/mL). No characteristic pattern of TA associated with high or low AMH levels was observed in any age group studied (Figure 33B). The Y- group is not represented in the TRAP assay gel because no tissue from this group was available.



Subject	Age (years)	AMH (ng/ml)
Y +	31	7.52
Y +	29	1.93
M +	42	1.84
M -	44	0.551
M -	44	0.01
P +	47	0.171
P +	49	0.079

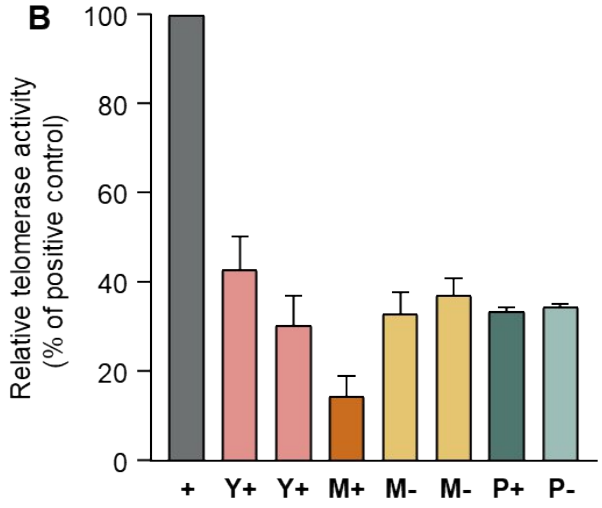


Figure 33. Analysis of telomerase activity in ovarian samples from women classified by age and AMH.

(A) Representative micrograph of the TRAP assay from small ovarian fragments. Two protein concentrations (a = 0.3 µg/µL, b = 0.06 µg/µL) of the same ovarian extract from each woman, and a negative control treated with RNase (+ treated, - untreated) are shown for each sample. The positive control is Jurkat tumor cells. The ladder pattern corresponds to telomerase products. The arrowhead indicates the internal control (IC) of the PCR reaction. Underneath the gel, a table shows the age and AMH values of the samples tested by TRAP. (B) Relative TA quantification of the gel shown in A, where the first bar corresponds to the positive control. Quantification was performed referring to the

positive control, which was 100% TA. The bar diagrams represent the mean value, and the error bars the SEM. Y: young, M: middle-aged, P: perimenopause, IC: internal control, AMH: anti-mullerian hormone, ng: nanogram, mL: milliliter, %: percent.

5.2.3 Summary of findings in this section

Although the age ranges described above were analyzed separately, and depending on the AMH values in some cell types, the mean ages were statistically different. This could have affected the results in a way that may not be independent of the age. Considering exclusively those where the age variable could be controlled, a lower AMH was associated with a higher percentage of short telomeres in oocytes, and a lower TL in TCs in middle-aged women.

5.3 Impact of pregnancy on ovarian telomere dynamics

In the population of pregnant women, it was determined that telomere dynamics should be investigated separately. This unique analysis arose for two reasons. The first reason was derived from the previous result, in which women within each age group were divided according to AMH value and, consequently, according to ovarian reserve. The blood and ovarian samples of the pregnant women were collected during a cesarean section, so they were all in a late pregnancy state. As explained later, these women registered very low levels of AMH, so their classification according to this hormone value would be inadequate. The second reason was that multiple studies linked infertility to telomere attrition. Pregnancy, in its final stage, would be considered a positive control of fertility.

5.3.1 Baseline characteristics of the study population and hormonal levels

This analysis of pregnancy effects on telomere parameters could only be carried out in the Y and M groups, since no women in the P group had undergone pregnancy. Specifically, the pregnant groups (Ypreg and Mpreg) were compared with the control groups of the previous section. These women were classified in the same age interval with high AMH value (Y+ and M+, respectively). Pregnant or parturient women were compared with women of the same age who had high AMH levels for several reasons. Firstly, the comparison with women with low AMH would introduce more confounding variables, as was shown in the previous result, and in the case of young women, statistical analysis would not be possible due to the reduced sample size of the Y- group. Lastly, whether pregnancy status has a positive or negative telomere impact on the ovary is unknown.

No statistically significant differences were observed in the age of the young groups ($p = 0.8388$), but there was a difference in middle-aged groups ($p = 0.0440$) when comparing

controls and pregnant women. Statistically significant differences were also observed in BMI (Y+ vs Ypreg p = 0.0360; M+ vs Mpreg p = 0.0150), although we must consider that weight gain is inherent to pregnancy. When AMH, FSH, LH, E2, and P4 levels were compared, statistically significant differences were found in all hormones between pregnant and control groups in young and middle-aged women. Specifically, the pregnant groups registered the lower detectable levels of AMH, FSH, and LH and the higher detectable levels of E2 and P4. The p-values for each comparison are listed in Table 28.

Table 28. Baseline characteristics and hormonal parameters of the study population classified by age and pregnancy.

	Y+ n = 11	**Ypreg** n = 4	**M+** n = 6	**Mpreg** n = 9
Demographic characteristics				
Age (years)		0.8388		0.0440
Mean ± SD	30.7 ± 4.4	30.0 ± 4.8*	37.7 ± 2.5*	40.1 ± 1.8*
Median (Q1–Q3)	32.0 (29.0-34.0)	31.5 (25.0-33.5)	37.0 (35.8-39.8)	40.0 (38.5-41.5)
BMI (kg/m^2)		0.0360		0.0267
Mean ± SD	23.5 ± 3.1*	29.2 ± 4.8*	24.2 ± 4.3*	29.9 ± 4.1*
Median (Q1–Q3)	23.5 (3.1-1.0)	29.3 (24.9-33.4)	23.9 (21.0-26.8)	29.1 (26.6-34.4)
Endocrine parameters				
AMH (ng/mL)		0.0015		0.0007
Mean ± SD	3.6 ± 2.5	0.8 ± 0.3*	2.9 ± 1.4*	0.7 ± 0.6*
Median (Q1–Q3)	2.4 (1.9-5.5)	0.8 (0.5-1.1)	2.8 (1.7-3.9)	0.6 (0.3-0.8)
FSH (mIU/mL)		0.0015		0.0001
Mean ± SD	4.5 ± 1.7*	0.3 ± 0.0	44.6 ± 97.2	0.3 ± 0.0
Median (Q1–Q3)	4.7 (2.6-6.3)	0.3 (0.3-0.3)	5.8 (2.8-66.7)	0.3 (0.3-0.3)
LH (mIU/mL)		0.0015		0.0001
Mean ± SD	7.3 ± 4.2*	0.1 ± 0.0	3.5 ± 2.0*	0.1 ± 0.0
Median (Q1–Q3)	7.6 (3.7-9.4)	0.1 (0.1-0.1)	3.4 (1.6-5.2)	0.1 (0.1-0.1)
E2 (pg/mL)		0.0015		0.0001
Mean ± SD	135.3 ± 106.2*	3000 ± 0.0	68.5 ± 60.8*	3000 ± 0.0
Median (Q1–Q3)	119.0 (48.7-219.8)	3000 (3000-3000)	56.4 (26.2-102.9)	3000 (3000-3000)
P4 (ng/mL)		0.0015		0.0001
Mean ± SD	1.6 ± 3.8	60.0 ± 0.0	3.1 ± 4.8*	60.0 ± 0.0
Median (Q1–Q3)	0.2 (0.2-1.4)	60.0 (60.0-60.0)	1.0 (0.2-6.0)	60.0 (60.0-60.0)

Data are presented as mean ± standard deviation and median (interquartile range). *Denoted the variables that passed the Shapiro-Wilk normality test. Statistical analysis of comparisons between groups was performed using Student's t-test (normally distributed data) or the Mann-Whitney U test (non-normally distributed data). A p-value < 0.05 was considered statistically significant. The n refers to the number of subjects. Y: young; M: middle-aged; SD: standard deviation; Q1: quartile 1 (25% percentile); Q3: quartile 3 (75% percentile); %: percent.

5.3.2 Telomere analysis

Although pregnant women are considered a positive fertility control group, it is unknown whether this transient reproductive situation impacts the telomere dynamics of these patients. In this section, we studied telomere maintenance at the systemic and ovarian levels and the presence of TA in the ovary of pregnant women.

5.3.2.1 Analysis of systemic telomere status

At the systemic level, evaluated in PBMCs, pregnancy-derived changes were observed neither in TL nor in the percentage of short and long telomeres, except in the middle-aged comparison. However, the difference in age between the middle-aged groups was statistically significantly different. Specifically, depending on the age group, the means were opposite. In the younger group (Figure 34A), pregnant women (Ypreg) tended to have better telomere maintenance in terms of TL (128.8 ± 6.5 a.u. in Y+ compared to 134.9 ± 8.9 a.u. in Ypreg, p = 0.1647), with a slightly lower percentage of short telomeres (12.2 ± 6.5% in Y+ compared to 8.2 ± 4.9% in Ypreg, p = 0.2773) and higher percentage of long telomeres (10.6 ± 4.7% in Y+ compared to 16.4 ± 9.2% in Ypreg, p = 0.1216). In the case of the middle-aged groups (Figure 34B), the pregnant group registered a lower mean TL (137.8 ± 17.3 a.u. in M+ compared to 126.7 ± 8.2 a.u. in Mpreg, p = 0.1810), a higher percentage of short telomeres (8.4 ± 8.6% in M+ compared to 10.8 ± 5.5% in Mpreg, p = 0.5228), and a statistically significantly lower percentage of long telomeres (19.2 ± 18.6% in M+ compared to 7.6 ± 7.7% in Mpreg, p = 0.0360).

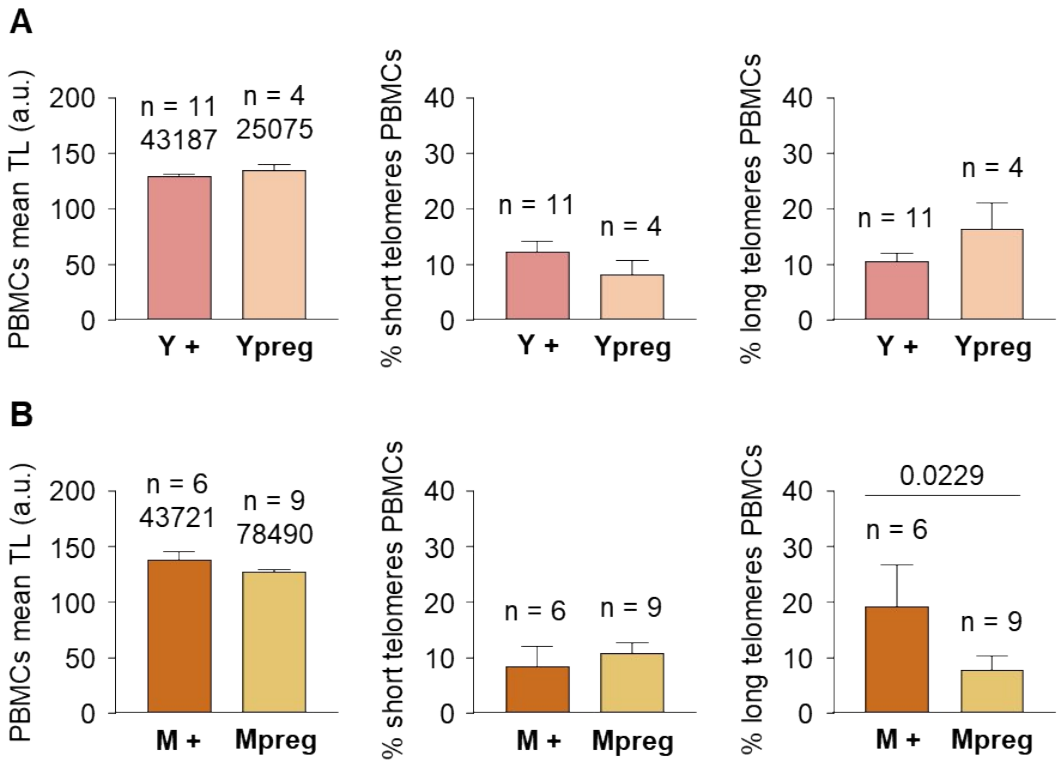


Figure 34. Analysis of telomere parameters in PBMCs from pregnant and non-pregnant women.

(A) Telomere parameters of PBMCs in the different young groups. The number below n refers to the number of telomere dots analyzed. (B) Telomere parameters of PBMCs in the different middle-aged groups. The number below n refers to the number of telomere dots analyzed. The bar diagrams represent the mean value, and the error bars the SEM. Statistical analysis of comparisons between groups was performed using Student's t-test (normally distributed data) or the Mann-Whitney U test (non-normally distributed data). A p-value < 0.05 was considered statistically significant. Only significant p-values are shown in the bar graphs. The sample size of each group is represented as n.

For more information, see Appendix E, Table E1. PBMCs: peripheral blood mononuclear cells, Y: young, M: middle-aged, TL: telomere length, a.u.: arbitrary units (intensity), %: percent.

5.3.2.2 Analysis of ovarian telomere status

The impact of pregnancy on different ovarian cell populations was also studied. In line with previous results, no changes were detected in any telomere parameters in the ovarian stroma (Table 29). In the younger and middle-aged groups (M+ and Mpreg with statistically significant differences in mean age, $p = 0.0440$), there were no significant changes in mean TL, the percentage of short telomeres, or the percentage of long telomeres.

Table 29. Stroma telomere parameters in pregnant and non-pregnant women.

	Y+ n = 11	**Ypreg** n = 4	**M+** n = 6	**Mpreg** n = 9
TL (a.u.)	0.1671		0.2238	
Telomeres	1664964	196063	325509	1857736
Mean ± SD	143.2 ± 9.9*	151.7 ± 9.8*	138.6 ± 19.8	144.2 ± 11.6*
Median (Q1–Q3)	143.8 (136.3-152.1)	151.9 (142.1-161.1)	128.1 (124.9-161.0)	142.3 (133.6-153.8)
Short telomeres (%)	0.1377		0.1644	
Mean ± SD	11.8 ± 10.9	5.3 ± 2.9	22.6 ± 16.1*	12.8 ± 10.0*
Median (Q1–Q3)	7.9 (6.3-13.1)	6.6 (2.3-7.1)	26.8 (3.2-38.0)	11.0 (3.2-23.9)
Long telomeres (%)	0.2125		0.2238	
Mean ± SD	12.3 ± 9.8*	20.2 ± 11.8*	13.0 ± 18.8	13.9 ± 11.2
Median (Q1–Q3)	9.8 (4.1-21.5)	21.3 (8.5-30.9)	2.0 (1.0-31.7)	9.4 (6.6-23.5)

Data are presented as mean ± standard deviation and median (interquartile range). *Denoted the variables that passed the Shapiro-Wilk normality test. Statistical analysis of comparisons between groups was performed using Student's t-test (normally distributed data) or the Mann-Whitney U test (non-normally distributed data). A p-value < 0.05 was considered statistically significant. The n refers to the number of subjects. The number of telomere dots analyzed is specified in the TL section under “Telomeres”. TL: telomere length; Y: young; M: middle-aged; SD: standard deviation; Q1: quartile 1 (25% percentile); Q3: quartile 3 (75% percentile); a.u.: arbitrary units of intensity; %: percent.

In the oocytes, altered TL was observed in the pregnant groups in both age intervals. However, this impairment was more drastic in the young group. In this group (Figure 35A), pregnant women had a lower mean TL (157.3 ± 21.3 a.u. in Y+ compared to 141.9 ± 14.0 a.u. in Ypreg, p = 0.0001), a higher percentage of short telomeres (15.1 ± 19.4% in Y+ compared to 26.6 ± 17.8% in Ypreg, p = 0.0004), and a lower percentage of long telomeres (19.6 ± 21.5% in Y+ compared to 6.6 ± 9.6% in Ypreg, p = 0.0002). The same results were observed in the middle-aged groups: lower mean TL (156.4 ± 34.0 a.u. in M+ compared to 142.8± 19.6 a.u. in Mpreg, p = 0.0033), the higher percentage of short telomeres (18.7 ± 19.5% in M+ compared to 33.8 ± 24.9% in Mpreg, p = 0.0008), and the lower percentage of long telomeres (20.9 ± 25.5% in M+ compared to 11.5 ± 18.8% in Mpreg, p = 0.0141) (Figure 35B). The mean ages of the women in whom oocytes were identified were comparable (young p = 0.9780, middle-aged p = 0.3556), and significant differences in AMH values remained (young p = 0.0055, middle-aged p = 0.0381).

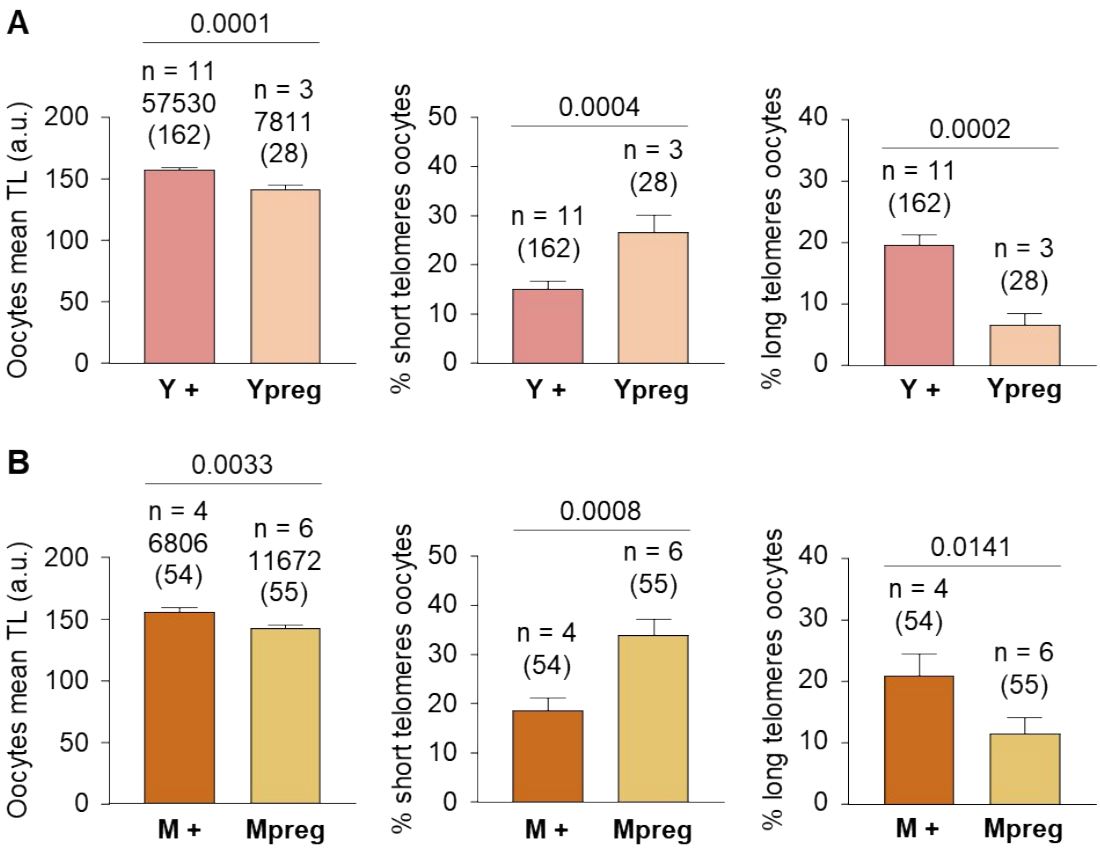


Figure 35. Analysis of telomere parameters in oocytes from pregnant and non-pregnant women.

(A) Telomere parameters of oocytes in the different young groups. The numbers below n refer to the number of telomere dots analyzed and oocytes identified. (B) Telomere parameters of oocytes in the different middle-aged groups. The numbers below n refer to the number of telomere dots analyzed and oocytes identified. The bar diagrams represent the mean value, and the error bars the SEM. Statistical analysis of comparisons between groups was performed using the Mann-Whitney U test. A p-value < 0.05 was considered statistically significant. Only significant p-values are shown in the bar graphs. The sample size of each group is represented as n. For more information, see Appendix E, Table E2. Y: young, M: middle-aged, TL: telomere length, a.u.: arbitrary units (intensity), %: percent.

The analysis of the GCs in the different follicular stages (primordial, primary, and secondary) showed different results between the young and the middle-aged population. Specifically, in the young population, pregnancy was marked by a lower TL (152.2 ± 15.3 a.u. in Y+ compared to 143.0 ± 17.1 a.u. in Ypreg, p = 0.0156) and a higher percentage of short telomeres (9.0 ± 7.0% in Y+ compared to 17.3 ± 11.5% in Ypreg, p = 0.0425) in the primordial stage (Figure 36A). No changes in the percentage of long telomeres were detected in these cells in the Y+ and Ypreg groups (19.8 ± 20.4% in Y+ compared to 13.7 ± 20.6% in Ypreg, p = 0.1104). However, at the primary stage, everything pointed to a deleterious telomere effect of this stage in the Ypreg group (Figure 36B). Young pregnant women recorded a lower TL (158.6 ± 19.3 a.u. in Y+ compared to 141.0 ± 12.6 a.u. in Ypreg, p<0.0001), a higher percentage of short telomeres (13.2 ± 16.7% in Y+ compared to 25.3 ± 16.3% in Ypreg, p = 0.0101), and a lower

percentage of long telomeres (24.7 ± 22.2% in Y+ compared to 5.2 ± 9.1% in Ypreg, p<0.0001) in the GCs of primary follicles. GCs from secondary follicles (Figure 36C) of the Y+ (TL: 176.7 ± 23.6 a.u., %short: 21.2 ± 25.2%, %long: 24.8 ± 24.3%) and Ypreg (TL: 175.0 ± 30.6 a.u., %short: 24.6 ± 31.6%, %long: 25.7 ± 29.8%) groups showed no differences (TL p = 0.9117, %short p = 0.8513, %long p = 0.9485).

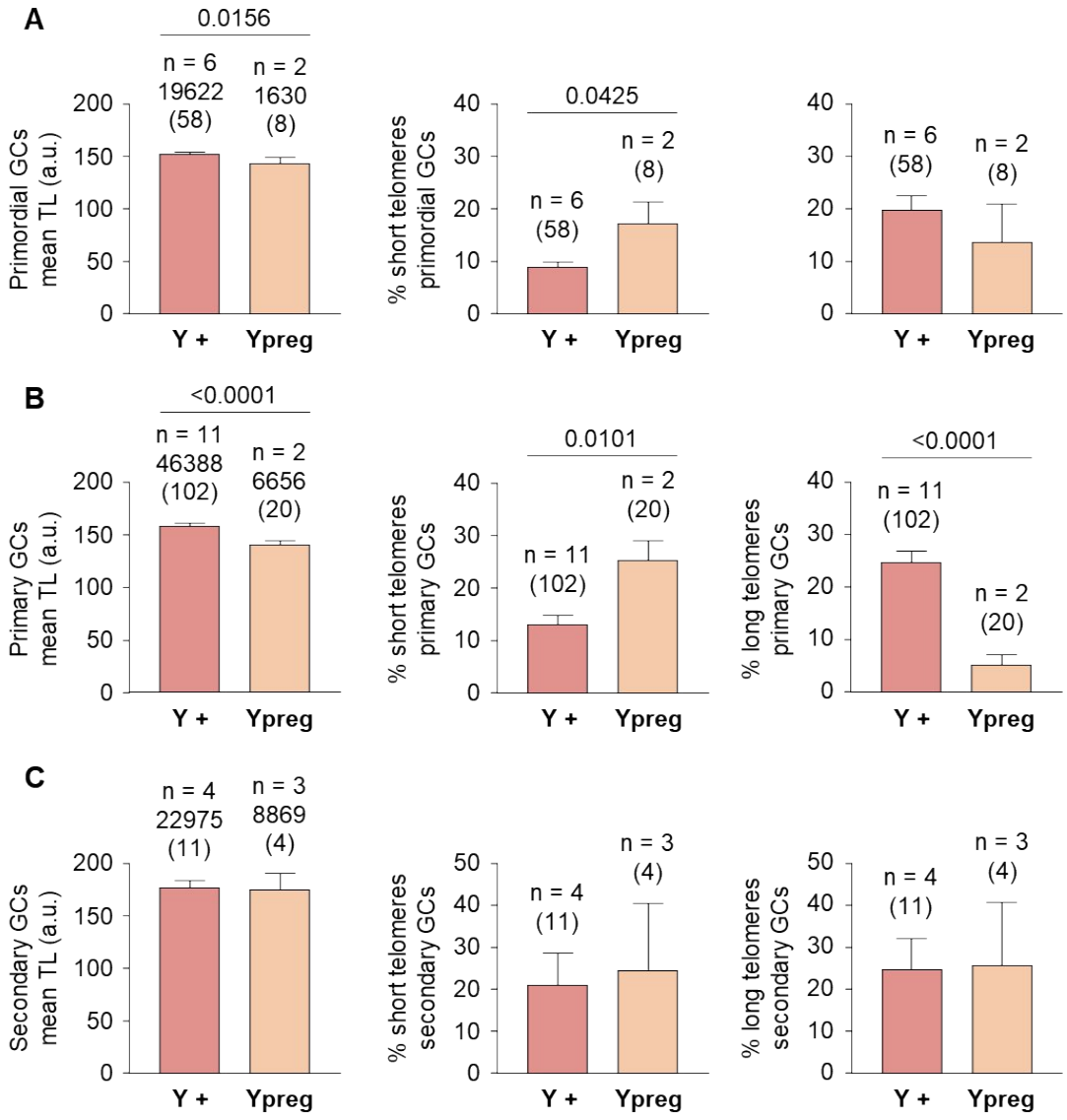


Figure 36. Analysis of telomere parameters in GCs from pregnant and non-pregnant women.

(A) Telomere parameters from primordial follicles (mean TL, left graph; percentage of short telomeres in the middle graph; and percentage of long telomeres in the right graph) in the indicated group. (B) telomere parameters, as described in A, from primordial follicles in the indicated group. (C) Telomere parameters, as indicated in A, secondary follicles in each indicated group. The number of individuals, the telomere dots analyzed, and the number of follicles are specified. Statistical analysis of comparisons between groups was performed using the Student t-test (normally distributed data) or the Mann-Whitney U test (non-normally distributed data). The bar diagrams represent the mean value, and the error bars, the SEM. A p-value < 0.05 was considered statistically significant. Only significant p-values are shown in the bar graphs. For more information, see Appendix E, Table E3. Y: young,

GCs: granulosa cells, SD: standard deviation, a.u.: arbitrary units (intensity), TL: telomere length, %: percent.

In the middle-aged population, telomere parameters did not differ significantly across any follicular stages (Table 30).

Table 30. GCs telomere parameters in middle-aged pregnant and non-pregnant women.

GCs primordial follicles	**M+** n = 3		**Mpreg** n = 6
Age (years)		0.0676	
Mean ± SD	37.0 ± 2.0*		39.7 ± 1.6*
Median (Q1–Q3)	37.0 (35.0-39.0)		39.5 (38.0-41.3)
AMH (ng/mL)		0.0476	
Mean ± SD	2.5 ± 1.0*		0.8 ± 0.6
Median (Q1–Q3)	2.9 (1.3-3.4)		0.6 (0.5-1.1)
TL (a.u.)		0.1144	
Follicles	20		27
Telomeres	4661		8290
Mean ± SD	149.4 ± 15.3*		142.6 ± 19.9
Median (Q1–Q3)	151.7 (139.1-161.8)		137.6 (123.5-159.7)
Short telomeres (%)		0.2285	
Mean ± SD	14.7 ± 17.4		24.7 ± 22.8
Median (Q1–Q3)	8.1 (1.3-21.4)		21.8 (1.6-47.2)
Long telomeres (%)		0.1234	
Mean ± SD	18.7 ± 14.3*		13.9 ± 19.5
Median (Q1–Q3)	18.5 (7.7-29.9)		5.7 (0.8-20.5)
GCs primary follicles	**M+** n = 5		**Mpreg** n = 6
Age (years)		0.1973	
Mean ± SD	37.8 ± 2.8*		29.7 ± 1.6*
Median (Q1–Q3)	37.0 (35.5-40.5)		39.5 (38.0-41.3)
AMH (ng/mL)		0.0173	
Mean ± SD	2.9 ± 1.5*		0.8 ± 0.6
Median (Q1–Q3)	2.9 (1.6-4.3)		0.6 (0.5-1.1)
TL (a.u.)		0.6167	
Follicles	43		46
Telomeres	13192		20674
Mean ± SD	149.7 ± 22.5		146.6 ± 20.1
Median (Q1–Q3)	140.8 (132.2-169.4)		143.3 (129.6-158.2)
Short telomeres (%)		0.5589	
Mean ± SD	21.3 ± 20.8		24.6 ± 23.2
Median (Q1–Q3)	15.7 (2.3-36.4)		16.9 (4.4-46.5)
Long telomeres (%)		0.7169	
Mean ± SD	17.3 ± 25.1		13.2 ± 21.8
Median (Q1–Q3)	3.1 (0.0-28.9)		4.0 (1.1-12.9)

GCs secondary follicles	M+ n = 2		Mpreg n = 2
Age (years)		0.3333	
Mean ± SD	36.0 ± 1.4		40.5 ± 2.1
Median (Q1–Q3)	36.0 (35.0-37.0)		40.5 (39.0-42.0)
AMH (ng/mL)		0.3333	
Mean ± SD	2.1 ± 1.2*		0.7 ± 0.03
Median (Q1–Q3)	2.1 (1.3-2.9)		0.7 (0.7-0.8)
TL (a.u.)		0.0714	
Follicles	6		2
Telomeres	9242		3803
Mean ± SD	178.9 ± 26.3*		139.3 ± 7.6
Median (Q1–Q3)	188.0 (146.9-201.2)		139.3 (133.9-144.6)
Short telomeres (%)		0.0714	
Mean ± SD	22.1 ± 28.0		71.0 ± 15.7
Median (Q1–Q3)	5.9 (2.6-57.4)		71.0 (60.0-82.1)
Long telomeres (%)		0.0714	
Mean ± SD	29.1 ± 25.8		0.5 ± 0.7
Median (Q1–Q3)	27.5 (2.3-56.9)		0.5 (0.03-1.0)

Data are presented as mean ± standard deviation and median (interquartile range). *Denoted the variables that passed the Shapiro-Wilk normality test. Statistical analysis of comparisons was performed using Student's t-test (normally distributed data) or the Mann-Whitney U test (non-normally distributed data). A p-value < 0.05 was considered statistically significant. The n refers to the number of subjects. The number of follicles and telomere dots analyzed is specified in the TL section. AMH: antimullerian, M: middle-aged, TL: telomere length, SD: standard deviation, Q1: quartile 1 (25% percentile), Q3: quartile 3 (75% percentile), a.u.: arbitrary units of intensity, %: percent, ng: nanogram, mL: milliliter.

In the TCs something similar occurred, the comparison between the young control group and the group of pregnant women of the same age showed that the pregnant women had a lower TL (154.8 ± 19.2 a.u. in Y+ compared to 143.1 ± 14.0 a.u. in Ypreg, p = 0.0379, Figure 37A), no changes were observed in the percentage of short telomeres (16.5 ± 22.1% in Y+ compared to 24.6 ± 16.5% in Ypreg, p = 0.1060, Figure 37B). Still, there were statistically significant changes in the percentage of long telomeres (19.7 ± 20.0% in Y+ compared to 6.2 ± 10.2% in Ypreg, p = 0.0226, Figure 37C). It is important to note that the individuals were comparable in age (p = 0.2793). However, there were no statistically significant differences in the AMH value between the control group and the pregnant women (p = 0.0603).

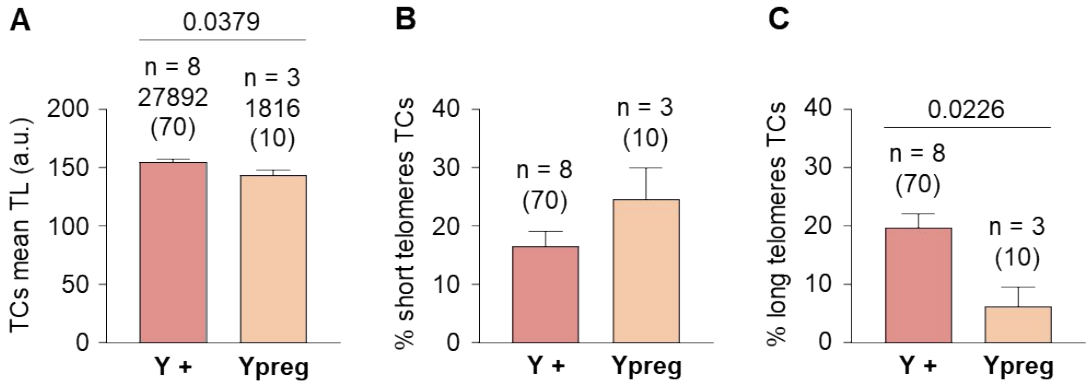


Figure 37. Analysis of telomere parameters in TCs from pregnant and non-pregnant women.

(A) Mean TL in the indicated group. The number of individuals, the telomere dots analyzed, and the number of follicles are specified. (B) Percentage of short telomeres in Y+ and Ypreg. (C) Percentage of long telomeres in Y+ and Ypreg. Statistical analysis of comparisons between Y+ and Ypreg was performed using the Mann-Whitney U test. The bar diagrams represent the mean value, and the error bars the SEM. A p-value < 0.05 was considered statistically significant. Only significant p-values are shown in the bar graphs. For more information, see Appendix E, Table E4. TCs: theca cells, Y: young, SD: standard deviation, a.u.: arbitrary units (intensity), TL: telomere length, %: percent.

In the comparison between M+ and Mpreg (Table 31), whose ages were similar and there were statistically significant differences in mean AMH (p = 0.0381), there were no differences in any of the telomere parameters analyzed (TL p = 0.7768, % short p = 0.8689, % long p = 0.5357).

Table 31. TCs telomere parameters in young pregnant and non-pregnant women.

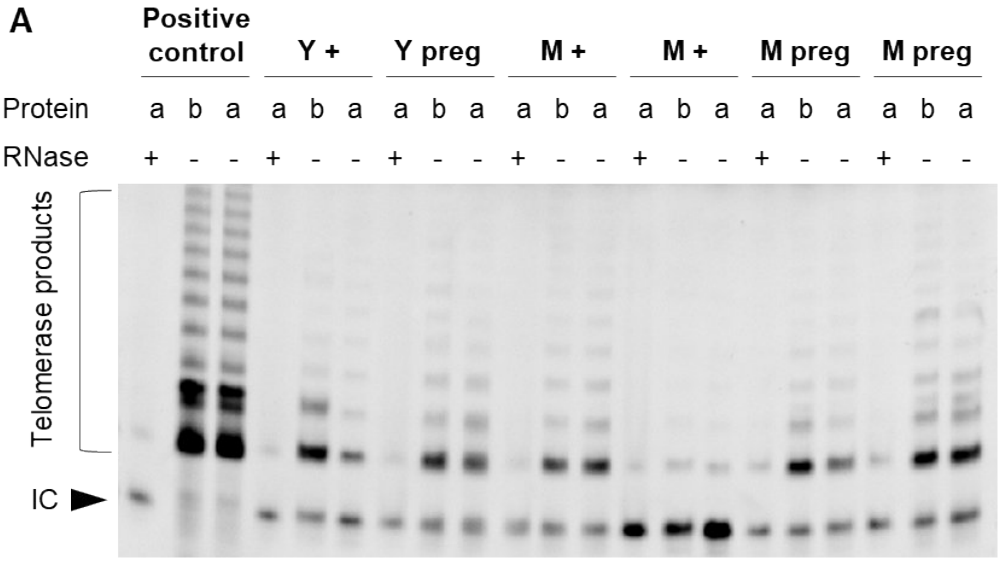
	M+ n = 4		**Mpreg** n = 6
Age (years)		0.3556	
Mean ± SD	38.3 ± 3.0*		39.7 ± 1.6*
Median (Q1–Q3)	38.0 (35.5-41.3)		39.5 (38.0-41.3)
AMH (ng/mL)		0.0381	
Mean ± SD	2.4 ± 1.0*		0.8 ± 0.6
Median (Q1–Q3)	2.4 (1.4-3.3)		0.6 (0.5-1.1)
TL (a.u.)		0.7768	
Follicles	23		32
Telomeres	4006		7496
Mean ± SD	150.8 ± 22.6*		148.8 ± 21.5
Median (Q1–Q3)	144.6 (131.5-170.0)		143.4 (132.6-158.8)
Short telomeres (%)		0.8689	
Mean ± SD	26.3 ± 31.7		22.1 ± 21.5
Median (Q1–Q3)	15.4 (1.3-47.1)		16.8 (1.4-38.9)
Long telomeres (%)		0.5357	
Mean ± SD	18.6 ± 23.3		14.4 ± 24.9
Median (Q1–Q3)	4.8 (0.0-38.4)		3.0 (0.5-14.1)

Data are presented as mean ± standard deviation and median (interquartile range). *Denoted the variables that passed the Shapiro-Wilk normality test. Statistical analysis of comparisons between M+ and Mpreg was performed using Student's t-test (normally distributed data) or the Mann-Whitney U test (non-normally distributed data). A p-value < 0.05 was considered statistically significant. The n refers to the number of subjects. The number of follicles and telomere dots analyzed is specified in the TL section. TCs: theca cells, AMH: anti-müllerian hormone, TL: telomere length, M: middle-aged, SD: standard deviation, Q1: quartile 1 (25% percentile), Q3: quartile 3 (75% percentile), ng: nanogram, mL: milliliter, a.u.: arbitrary units of intensity; %: percent.

5.3.2.3 Analysis of telomerase activity in the ovary

To test the impact of pregnancy on the enzyme telomerase in the ovary, TA was evaluated by TRAP assay in non-pregnant and pregnant women in the young and middle-aged groups (Figure 38A). TA was detected in the ovaries of women of all groups and ages. However, neither a significant decrease nor a significant increase in TA with pregnancy was observed (Figure 38B). The middle-aged group showed the most tremendous variation, as the TA in one of the non-pregnant women in this group was very low, probably reflecting interindividual

variations. Since another of the women in the same condition did not show this decrease, this result can be attributed to the nature of the tissue rather than to a pregnancy-derived effect.



Subject	Age (years)	AMH (ng/ml)
Y +	34	2.84
Y preg	34	0.46
M +	37	2.77
M +	42	1.84
M preg	38	0.41
M preg	42	0.77

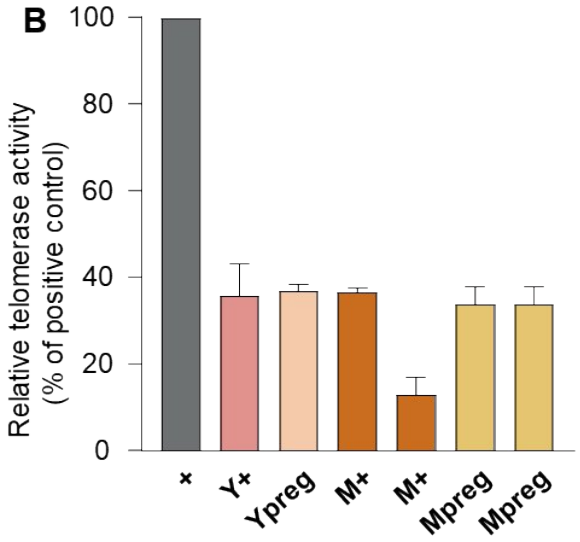


Figure 38. Analysis of telomerase activity in ovarian samples from pregnant and non-pregnant women.

(A) Representative image showing the results of the TRAP assay from a small ovarian fragment. Two protein concentrations (a = 0.3 µg/µL, b = 0.06 µg/µL) of the same ovarian extract from each woman, and a negative control treated with RNase (+ treated, - untreated) are shown for each sample. The positive control is Jurkat tumor cells. The ladder pattern corresponds to telomerase products. The arrowhead indicates the internal control (IC) of the PCR reaction. Underneath the TRAP micrograph table shows each subject's age and AMH value. (B) Relative TA quantification on the gel shown in A, where the first bar corresponds to the positive control. Quantification referred to the positive control, which was 100% TA. The bar diagrams represent the mean value, and the error bars, the SEM. The bottom left Y: young, M: middle-aged, IC: internal control, AMH: anti-mullerian hormone, ng: nanogram, mL: milliliter, %: percent.

5.3.3 Summary of findings in this section

Unexpectedly, pregnancy not only impacted hormone levels but also ovarian telomere parameters. Considering only those results where the mean age of the groups was

comparable, pregnancy was associated with lower mean TL in the oocytes of young and middle-aged pregnant women. Oocytes from pregnant women recorded lower TL, a higher percentage of short telomeres, and a lower percentage of long telomeres. In GCs, the results were different depending on the age group analyzed. Only young pregnant women showed lower mean TL in primordial and primary GCs. In the TCs, the same occurred, exclusively in the young pregnant women, where a lower TL and a lower percentage of long telomeres were detected.

5.4 Impact of COVID-19 disease on reproduction and the telomere pathway

This last result, extracted from Project 2, focused on the study of how a non-fertility-related pathology, such as COVID-19, can impact fertility and reproductive telomere dynamics. This virus could induce a significant inflammatory response in the body by increasing oxidative stress levels, which could cause the telomeres to shorten prematurely.

5.4.1 Baseline characteristics of the study population and hormonal levels

The study involved 65 women between the ages of 18 and 50, categorized as either controls (n = 29) or COVID cases (n = 36) based on their serum SARS-CoV-2 antibody test results. The antibody test detected COVID-19 antibodies in four women initially placed in the control group; these individuals were subsequently reclassified as asymptomatic cases. The COVID-19 group exhibited varying levels of symptom severity (specified in section 4.1.2.1). Overall, there were no statistically significant differences in age, AMH levels, or BMI between the control and case groups, including those with severe COVID-19 (Table 32).

Table 32. Baseline characteristics of the COVID-19 study population.

	Control	COVID	Mild COVID	Severe COVID
Age (years)		0.731	0.533	0.936
n	29	36	19	17
Mean ± SD	35.3 ± 5.8	35.8 ± 5.9	35.8 ± 6.7	35.6 ± 5.2
Median (Q1-Q3)	37 (34-39)	37 (33-39)	38 (33-40)	36 (33-39)
BMI (kg/m^2)		0.511	[0.884]	0.243
n	22	30	17	13
Mean ± SD	22.3 ± 2.7	23.4 ± 4.2	22.4 ± 3.2	24.6 ± 5.1
Median (Q1-Q3)	21.9 (20.4-23.6)	22.3 (20.6-24.7)	21.9 (20.4-23.8)	24.4 (20.7-27.3)
AMH (ng/mL)		0.457	0.175	0.861
n	28	36	19	17
Mean ± SD	0.9 ± 0.9	0.8 ± 0.6	1 ± 0.6	0.7 ± 0.5
Median (Q1-Q3)	0.5 (0.2-1.3)	0.7 (0.3-1.3)	1.1 (0.6-1.4)	0.7 (0.2-0.9)

n indicates the number of individuals analyzed. *p-value was calculated between control and each group (COVID, mild COVID, and severe COVID) separately. Brackets indicate p-value calculated using Student t-test (normal distribution of data). The rest of the p-values were calculated using the Mann-Whitney U test.

5.4.2 Telomere length in GCs obtained during oocyte retrieval

In this study, we aimed to determine whether TL in GCs might also be affected in COVID-19 cases. The average TL of GCs was similar between the control group (141.4 ± 67.5 a.u.) and the COVID group (143.2 ± 72.9 a.u.) (Figure 39A), and it remained consistent across the age range of the study participants (Figures 39B and C).

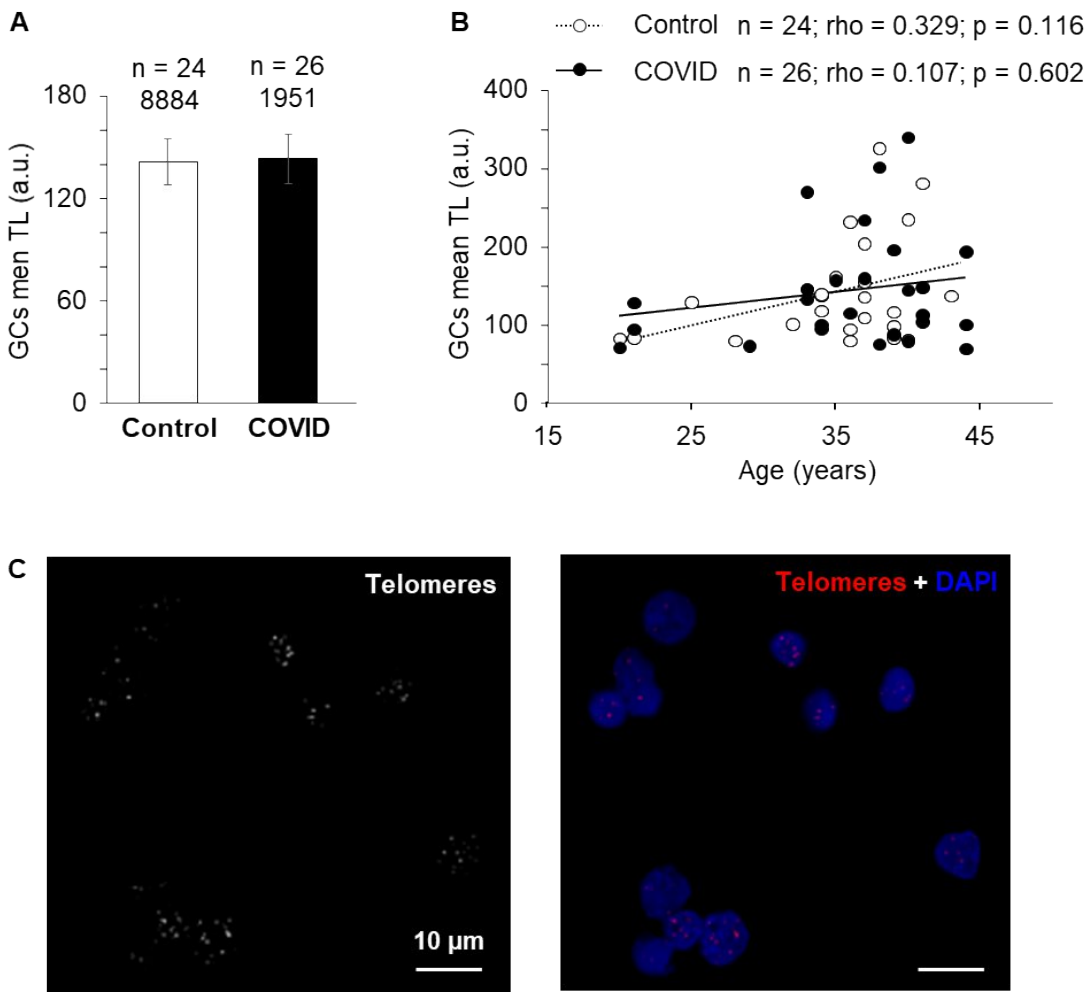


Figure 39. Analysis of telomere length by HT-qFISH in GCs in control and COVID-19 patients.

(A) Mean TL of GCs in control and COVID groups. The number of subjects and telomeres analyzed is detailed. Statistical analysis was determined by the U Mann-Whitney test. (B) Spearman correlations between TL of GCs and age in control (white, dashed line) and case (black line) groups. (C) The micrographs show representative images of telomere FISH (white dots, left panel) and the merged (right panel) of nuclei (blue) and telomeres (red), in GCs. Images were acquired with 60x magnification. n indicates the number of individuals analyzed in each experiment. The error bars show the standard. Scale bar = 10 µm. GCs: granulosa cells, TL: telomere length, a.u.: arbitrary units of intensity, rho: Spearman's correlation coefficient, DAPI: 4',6-diamidino-2-phenylindole, µm: micrometer.

The average TL of GCs in severe COVID-19 cases was significantly lower (96.1 ± 21.9 a.u., p = 0.017) compared to the control group (141.4 ± 67.5 a.u., Figure 40A), and TL declined progressively with increasing symptom severity (p = 0.012, Figure 40B). The proportion of critically short telomeres in GCs was similar across the control (33.8 ± 17.5%), COVID (36.4 ± 15%), and severe COVID (39.5 ± 15.2%) groups (Figures 40C and D). In contrast, the percentage of long telomeres (85th percentile) was higher in the control group (8.4 ± 10.2%) compared to the severe COVID group (1.1 ± 1.9%, p = 0.003, Figure 40E). Among COVID-19 cases, the proportion of long telomeres decreased significantly (p = 0.004) with increasing symptom severity scores (Figure 40F).

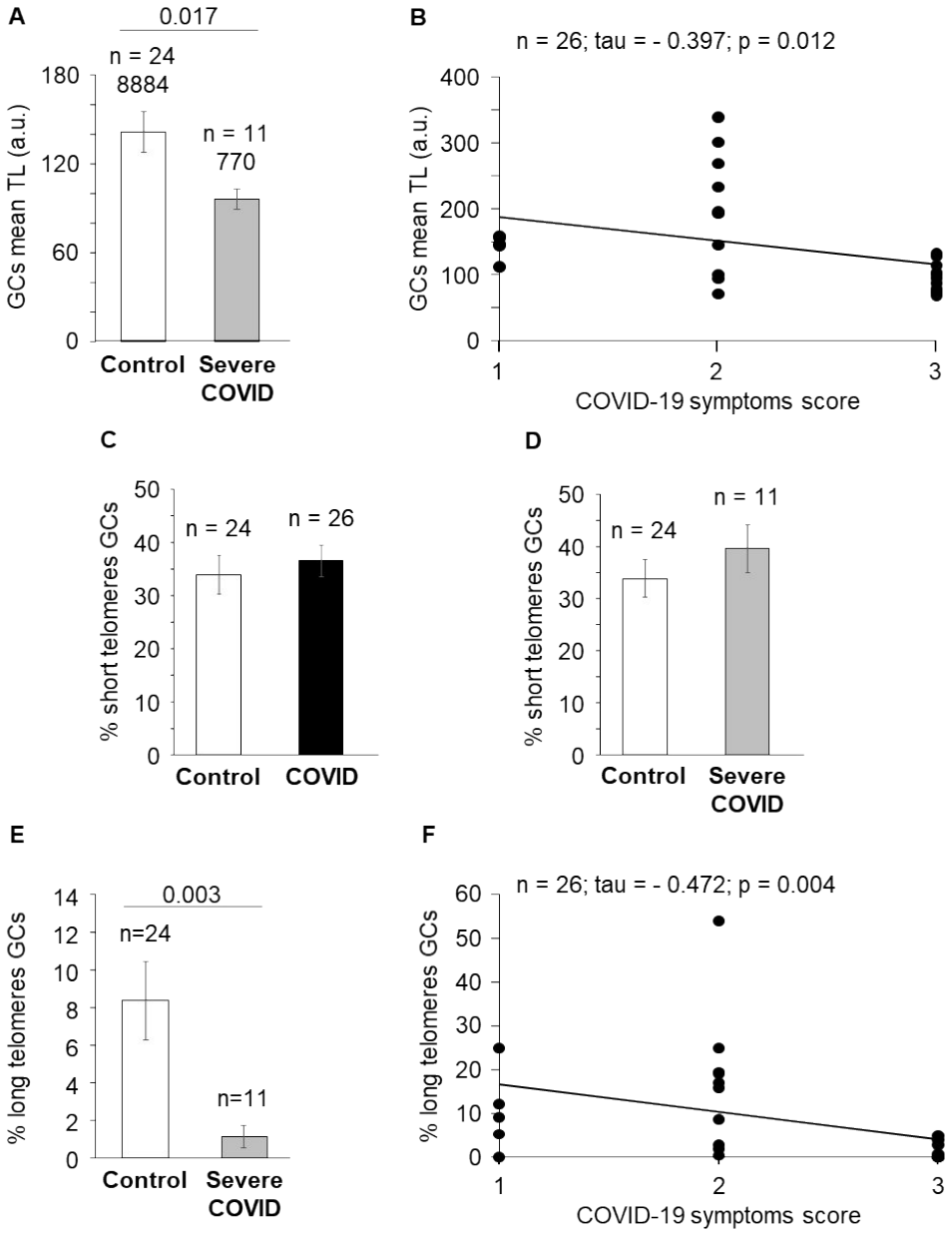


Figure 40. Analysis of telomere parameters in GCs.

(A) Mean TL of GCs in control and severe COVID groups. (B) Correlation between COVID-19 symptom score and TL in GCs. (C) Percentage of short telomeres of GCs in the control and COVID groups. (D) Percentage of short telomeres of GCs in the control and severe COVID groups. (E) Percentage of long telomeres of GCs in the control and severe COVID groups. (F) Correlation between COVID-19 symptom score and the percentage of long telomeres in GCs. n indicates the number of individuals analyzed in each experiment. The error bars show the standard error. Statistical significance was determined by a two-tailed Mann-Whitney U test or an unpaired t-test according to data distribution type. Rho is Spearman's correlation coefficient, and Kendall's tau-b was computed to measure the correlation between telomere parameters and the symptom score in COVID patients. A p-value < 0.05 was considered statistically significant. Only significant p-values are shown in the bar graphs. For more information, see Appendix F, Table F1.

In contrast to the severe cases, women with mild COVID-19 showed TL comparable to those of the control group, both in GCs (Figure 41A) and PBMCs (Figure 41B). In PBMCs, the control group registered 74.3 ± 12.0 a.u. and mild COVID 76.2 ± 12.2 a.u. However, in GCs the

difference was greater as the control group evidenced 141.4 ± 67.5 a.u., and mild COVID 177.6 ± 78.4 a.u., but still the difference did not become statistically significant.

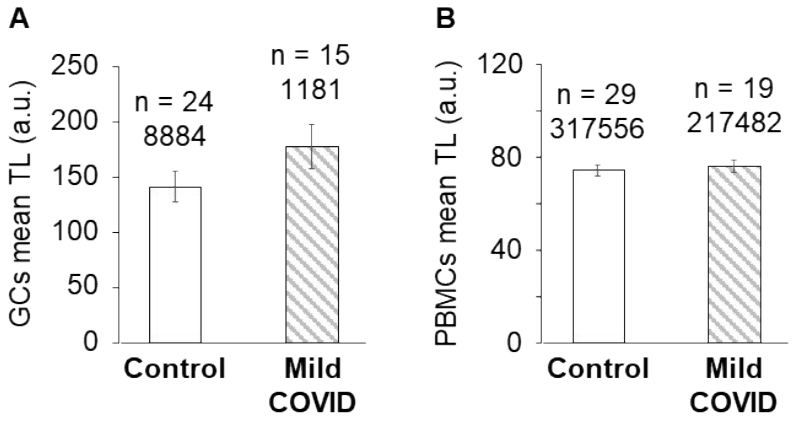


Figure 41. Analysis of telomere parameters in GCs and PBMCs from control and mild COVID groups.

(A) Mean TL of GCs in control and mild COVID groups. (B) Mean TL of PBMCs in control and mild COVID groups. n indicates the number of individuals analyzed in each experiment. The error bars show the standard error. Statistical significance was determined by a two-tailed Mann-Whitney U test or an unpaired t-test according to data distribution type. A p-value < 0.05 was considered statistically significant. Only significant p-values are shown in the bar graphs.

5.4.3 Fertility outcomes: oocyte retrieval and maturation rate

We evaluated reproductive outcomes following controlled ovarian stimulation to assess whether COVID-19 could impact ovarian function. The total number of oocytes retrieved was similar between the control (10.4 ± 9.3) and COVID groups (11.9 ± 7.6, p = 0.171, Figure 42A) and showed an age-related decline in both groups (Figure 42B; p = 0.011 for controls and p = 0.023 for COVID cases). Additionally, no significant differences were observed in the number of oocytes retrieved between controls (10.4 ± 9.3) and severe COVID cases (11.5 ± 7.4, p = 0.294, Figure 42C).

We then examined the oocyte maturation rate and found no differences between the control (86.7 ± 12.3%) and COVID and mild COVID groups (COVID: 80.1 ± 15.9% and p = 0.171; mild COVID: 85.6 ± 11.5% and p = 0.620; Figure 42D). However, women with severe COVID-19 had a significantly lower oocyte maturation rate (73.9 ± 18%) compared to controls (p = 0.018, Figure 42E), and the maturation rate declined with increasing symptom severity (Figure 42F; p = 0.005).

A positive correlation was observed between oocyte maturation rate and TL in the control group (p = 0.024), a relationship that was not present in the COVID group (p = 0.600, Figure 42G)

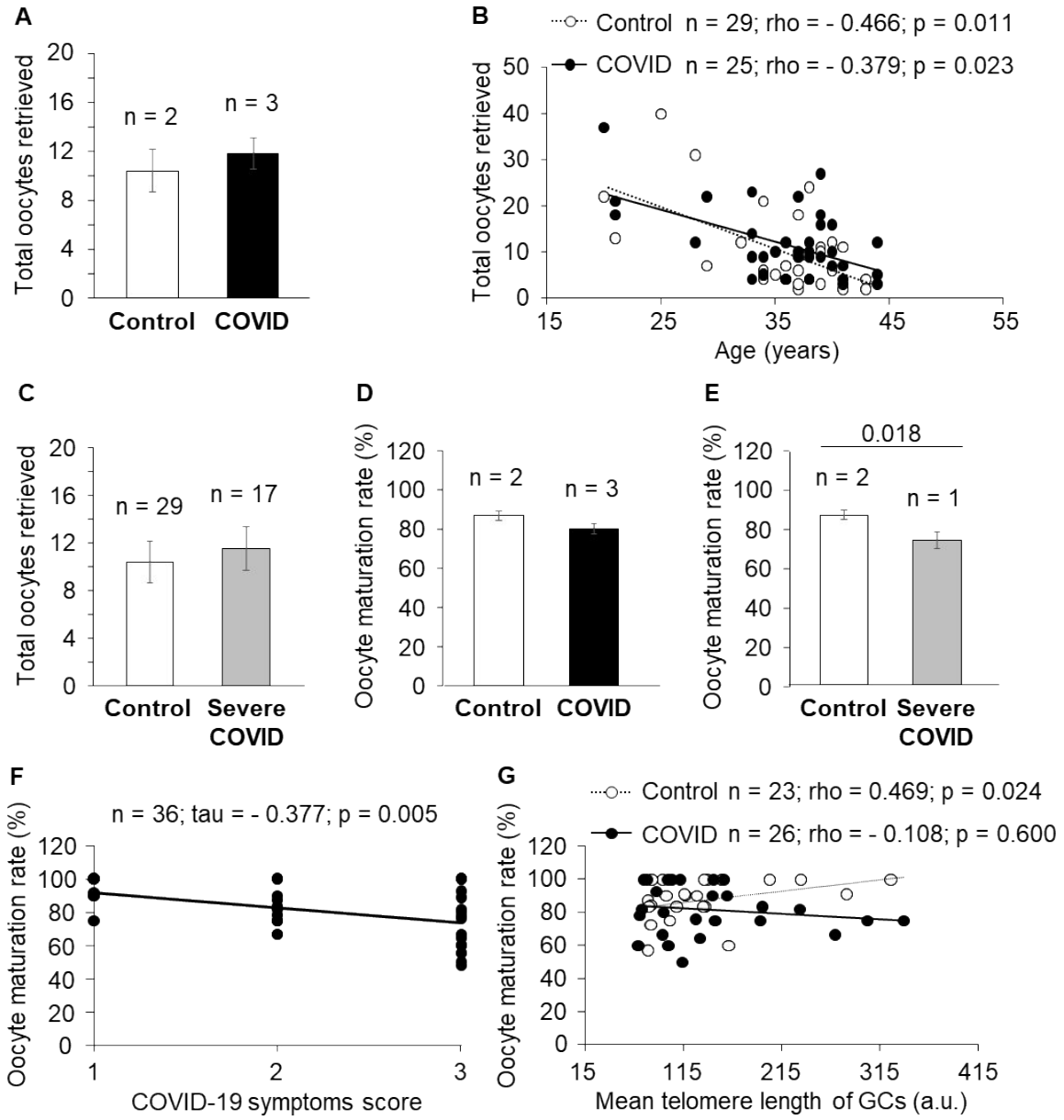


Figure 42. Analysis of fertility outcomes in controls and COVI groups.

*(A) Mean number of total oocytes retrieved in the control and COVID groups. (B) Correlation between the age of the subjects and the number of oocytes retrieved after follicular puncture. (C) Mean number of total oocytes retrieved in the control and severe COVID groups. (D) The oocyte maturation rate in the control and COVID groups. (E) The oocyte maturation rate in the control and severe COVID groups. (F) Correlation between the COVID-19 symptoms score and the oocyte maturation rate in patients. (G) Correlation between the TL of GCs and the oocyte maturation rate in control (white, dashed line) and case (black line) groups. n indicates the number of individuals analyzed in each experiment. The error bars show the standard error (A, C, D, and E). Statistical significance was determined by a two-tailed Mann-Whitney U test (A, C, D, and E). Rho is Spearman's correlation coefficient (B and G), and Kendall's tau-b was computed as a measurement of correlation between oocyte maturation rate and symptom score in COVID patients (F). *p-values < 0.05 were considered statistically significant. For more information, see Appendix F, Table F2.*

5.4.4 Summary of findings in this section

COVID-19 impacted the telomeres of GCs in more severe cases, with higher telomere shortening, and a significant negative correlation between GCs TL and disease severity. This was also observed in the percentage of long telomeres, which was reduced in severe cases and correlated negatively with disease severity. A lower TL of GCs correlated with a lower oocyte maturation rate in the healthy population. However, those women who suffered COVID-19 with a higher severity reduced oocyte maturation rate, although not the number of oocytes collected.

DISCUSSION

6 DISCUSSION

Telomeres play a fundamental role in the aging process due to their progressive shortening with each cell division (Blackburn, 1991, Olovnikov, 1973). At the reproductive level, telomeres are essential in germ cells to maintain their ability to divide and give rise to healthy offspring (Kalmbach et al., 2013, Keefe et al., 2006). Specifically, in humans, women are born with a finite ovarian reserve and a fixed number of oocytes (Chico-Sordo et al., 2021). Moreover, these oocytes remain long and are detained in meiotic prophase I, forming part of the ovarian follicles, until their release during ovulation (Baker, 1963). As women age, their fertility decreases, and the difficulties in achieving pregnancy increase (Polonio et al., 2020). Nowadays, this problem affects many women due to the tendency to delay childbearing for various reasons (Chico-Sordo et al., 2021). Therefore, deepening the study of reproductive aging and dysfunction not only allows its understanding but also offers potential tools to develop strategies aimed at delaying or mitigating the effects of aging on female fertility.

6.1 Characterization of age-dependent female reproductive aging

Women's reproductive life ceases with the onset of menopause (Broekmans et al., 2004, Faddy et al., 1992, Faddy and Gosden, 1996). However, as women age, different body changes occur, gradually reducing their ability to conceive. These changes become especially noticeable after age 35 when reproductive decline accelerates (Garcia et al., 2018, Schmidt et al., 2012). For this reason, the women who participated in Project 1, from which this result is also concluded, were divided based on this age threshold, which is also included in the POSEIDON criteria (Reig et al., 2023, Chinta et al., 2021, Haahr et al., 2019). In addition, another age group was created from 46 to 50, an age range in which the perimenopausal period was identified (Hale et al., 2014). Thus, having the age ranges 18-34 (Y), 35-45 (M), and 46-50 years (P) as study groups, reproductive aging in women was approached from different points of view.

6.1.1 Endocrine parameters

The reproductive life of a woman is determined by the menstrual cycle. This cycle responds to the hypothalamus-pituitary-ovary endocrine axis, where the pituitary gland releases the hormones FSH and LH, and the ovary, in response, synthesizes estrogen and progesterone, among others (Speroff and Fritz, 2012). Focusing on these four main hormones, when the

correlation of each of these hormones with age was analyzed, FSH and LH correlated positively with this variable, while estrogens correlated negatively. FSH and LH levels increased with age, while estrogen levels decreased. These results are consistent with multiple previously published studies (Besong et al., 2024, Freeman et al., 2008, Park et al., 2021b, Wiacek et al., 2011, Vaninetti et al., 2000, van Rooij et al., 2005). The main reason for the increase in FSH and LH is that as age advances, the quantity of oocytes decreases, the ovaries respond less efficiently to these hormones, and there is a decrease in their production of estrogen, which leads to a reduction in negative feedback to the hypothalamus and pituitary gland. As a result, the pituitary gland produces more FSH to stimulate ovarian function and compensate for the oocyte deterioration. The decrease in estrogen levels is because estrogens are synthesized mainly by the GCs of the ovarian follicles, and as age increases, the ovarian reserve decreases (Evans et al., 1981, Park et al., 2021b). However, the results did not support these observations when comparing the Y, M, and P groups. According to these correlations, one would expect to find the lowest FSH and LH levels in the Y group, followed by M and P with the highest levels. However, in FSH, the M group registered higher levels of this hormone than P, and no statistically significant differences were directly observed in LH. Something similar occurred with estrogens, where a higher amount in the Y group and lower levels in the P group were expected. In our results, group M recorded higher estrogen levels. Several reasons may explain these discrepancies, but the main one lies in a limitation of this study that should be considered. The hormone levels of the recruited patients were not assessed at the same phase of the menstrual cycle, and some of them were pregnant when the serum sample was collected. Female hormone levels fluctuate throughout the menstrual cycle (Hehenkamp et al., 2006, Tsepelidis et al., 2007, La Marca et al., 2006). For this reason, for the data to be comparable, it is essential to assess their levels at the same phase of the cycle, which was a limitation in this study design and the general clinical practice. Another hormone measured was AMH. This hormone does not show significant alterations in its levels throughout the menstrual cycle (Hehenkamp et al., 2006, La Marca et al., 2006, Tsepelidis et al., 2007), and its levels are not affected by taking hormonal contraceptives (Streuli et al., 2008). Increasing age was associated with a decrease in AMH levels, both when comparing the age groups and in the correlation of this hormone with age. This hormone is synthesized and released by GCs of developing ovarian follicles, preantral and small antral follicles mainly, so it is a reliable biomarker of ovarian reserve along with other parameters such as AFC (Nardo et al., 2007).

Therefore, the results showed that aging implies an increase in FSH and LH and a decrease in estrogen and AMH. However, due to the study design, only the AMH result can be firmly accepted.

6.1.2 Telomere parameters

6.1.2.1 Systemic aging

Aging was studied at the systemic and reproductive levels. For analysis of systemic aging, TL and the associated percentage of short and long telomeres were measured in PBMCs (Demanelis et al., 2020). These cells, including lymphocytes, monocytes, and macrophages, were chosen for several reasons. Firstly, their collection is accessible and minimally invasive. Secondly, it is widely documented that TL decreases in PBMCs with aging (Zglinicki and Martin-Ruiz, 2005, Sanchez-Vazquez et al., 2021, Müezzinler et al., 2013, Canela et al., 2007).

Additionally, PBMCs reflect various aspects of the organism's overall health state, as they respond to infections or other stimuli. Consequently, they will reflect the impact of different factors throughout the individual's life (Kundu et al., 2020, Li et al., 2019, Pinna et al., 2017, Zhu et al., 2021). Our results showed that no significant changes in mean TL were detected when the study age-groups were compared. This may be due to a balance between telomere shortening and regeneration. The telomerase can promote this balance, which preferentially elongates short telomeres (Bianchi and Shore, 2007). Another possible reason could be the presence of cells with longer telomeres that compensate for the short telomeres or other cells, keeping the average TL stable. Individual variation and multiple influencing factors also contribute to TL heterogeneity (Canela et al., 2007). However, an increase in the percentage of short telomeres was observed in group P compared to groups Y and M, but not between Y and M themselves. This fact indicates systemic telomere shortening associated with aging. Such telomere shortening, reflected in the accumulation of short telomeres, becomes more detectable with broader age comparisons. This observation aligns with Iwama et al. (1998), who reported faster telomere shortening in individuals aged 4–39 compared to those over 40, alongside higher telomerase activity in the younger group (Iwama et al., 1998). These findings support that PBMC TL reflects a balance between telomere loss and telomerase action. The increased percentage of short telomeres in the older group implies an accumulation of cells with reduced proliferative capacity, approaching senescence (Kaul et al., 2012, Hemann et al., 2001). Senescent cell accumulation contributes to tissue function deterioration (Donate and Blasco, 2011) during aging, whereas their removal rejuvenates tissues (Serrano, 2017). Finally, correlation analyses confirmed these trends. The negative correlation of PBMCs TL with age and the positive correlation of the percentage of short telomeres with age in these same cells, both significant, reinforce the idea that, indeed, systemic aging implies telomere shortening and thus, telomere shortening is a bona fide marker of aging (Lopez-Otin et al., 2023).

In summary, there is a progressive deterioration of telomere status in PBMCs with age, and this systemic aging is particularly noticeable after the age of 46 years.

6.1.2.2 Ovarian aging

Once telomere dynamics were characterized at the systemic level, reproductive aging was investigated further. Although aging as such is a biological process in which an organism undergoes progressive changes leading to dysfunction and deterioration of the organism (Lopez-Otin et al., 2023, López-Otín et al., 2013), systemic and reproductive aging do not progress at the same rate. A clear example of this can be seen when comparing the lifespan of women and their reproductive lifespan. In Spain, for instance, according to the Spanish National Institute of Statistics, the female life expectancy was 83.6 years in 2005 (and has remained unchanged since then). A comparative study published in the same year, comparing the mean age of natural menopause in women in Spain and the United States, found that the mean age in Spain was 51.7 years (Reynolds and Obermeyer, 2005). However, although menopause marks the end of reproductive life, women experience a drastic and accelerated decline in fertility after the age of 35 (Schmidt et al., 2012). Thus, the two types of aging do not overlap in women, and reproductive aging progresses more rapidly. Reproductive aging status was analyzed directly in the ovarian tissue of young, middle-aged, and perimenopausal women, all representing crucial moments with hormonal and functional changes in women's reproductive lives. When studying this tissue, several challenges and/or limitations were considered: (1) different cell types coexist in the ovary, (2) not all cell types were identified in the analyzed ovarian fragment of each woman, and (3) when they were identified, mainly in ovarian follicles, they were at different stages of the folliculogenesis process. The approach was to investigate whether the telomeres remained unchanged during folliculogenesis in the cell types that formed part of ovarian follicles (oocytes, GCs, and TCs). Once this point was clarified, the aging status of each cell type was analyzed individually.

6.1.2.2.1 Study of folliculogenesis

Folliculogenesis is the process by which ovarian follicles containing oocytes develop and mature to release the oocyte at ovulation (Gougeon, 2010, Rimon-Dahari et al., 2016). This process begins with the primordial follicle stage, followed by the primary, secondary, antral, and Graafian follicle stages. The first three stages (primordial, primary, and secondary) were mainly identified in the ovarian fragments of women analyzed in this study. Some early antral follicles were also identified but were not included in the statistical analysis since there were not enough to perform the analysis and draw conclusions.

To date, telomere dynamics during the process of folliculogenesis in humans have not been described in ovarian tissue, although they have been described in other animal models

(Polonio et al., 2023, Russo et al., 2006). Due to the difficulty in obtaining this type of sample, studies in humans have been carried out in oocytes and GCs collected during oocyte retrieval in IVF treatments (Butts et al., 2009, Lara-Molina et al., 2020, Xu et al., 2017). However, in this work, we directly studied the ovarian cortex, where ovarian follicles were identified, and oocytes, GCs, and TCs were analyzed independently. The analysis of the telomere parameters in oocytes showed no changes in TL or percentage of short and long telomeres throughout the primordial, primary, and secondary follicular stages. This is consistent with oocytes originating during fetal development and remaining arrested in the prophase of the first meiotic division until ovulation (Baker, 1963). Therefore, telomere shortening due to replication is not expected since they do not divide between the primordial and secondary follicle transition studied. Studies in pigs showed that oocytes from later stages (preantral and antral follicles) had significantly lower telomere intensity values by FISH than primary follicles (Russo et al., 2006). In humans, the TL of GV oocytes was longer than that of 2-cell stage embryos (Turner et al., 2010). In addition, TA was lower in mature oocytes than in immature oocytes (Wright et al., 2001). These findings suggest that the telomere maintenance in oocytes may be compromised during advanced folliculogenesis, especially if oocytes experience oxidative stress. Supporting this idea, TL analyses in human oocytes, usually in ART donors, showed that immature oocytes tended to have longer telomeres than mature ones (Turner and Hartshorne, 2013).

However, from our study, we cannot confirm or deny what happens at the telomere level in the oocyte beyond the secondary follicle stage. Based on previously published reports, in the successive follicular stages after the secondary follicle, it would be expected that telomere shortening would not occur until the oocyte is released and meiosis culminates. Based on our results, the TL of oocytes remains unaltered during the first stages of folliculogenesis. This analysis of folliculogenesis was possible because the ages of the women in whom oocytes were identified at the different stages were similar. Had this not been the case, as discussed in the next section, the oocytes could have undergone telomere shortening intrinsic to aging and not to the folliculogenesis process.

In the telomere analysis of GCs during folliculogenesis, an increase in TL was observed in these cells during this process. This was observed when all subjects were studied together and separated into young and middle-aged groups. In all these comparisons, the mean age of the subjects between the different follicular stages was comparable. Considering that GCs undergo intensive and repetitive proliferation during folliculogenesis (Gaytan et al., 1996, Wang et al., 2021a, Gougeon, 2010), it would be expected that telomere shortening in these cells will be detected as folliculogenesis progresses. However, these cells possess TA that could compensate for the telomere shortening undergone by multiple divisions (Butts et al.,

2009, Russo et al., 2006, Lavranos et al., 1999, Xu et al., 2017, Turner and Hartshorne, 2013, Yamagata et al., 2002). A study of folliculogenesis in the porcine ovary showed that GCs of preantral and antral follicles had longer telomeres than those of earlier stages (Russo et al., 2006). These results agree with the results of our study, where the TL of GCs increases with folliculogenesis. However, our results stopped the telomere analysis in the secondary follicles, and the latter follicular stages could not be tested. Differences were found when comparing GCs from the most advanced stage studied, the secondary follicle, to GCs from primordial and primary follicles. No differences were observed between the TL of primordial GCs and primary GCs. This may be due to limited cell proliferation at these early stages of follicular development, which does not cause noticeable telomere lengthening by telomerase (Gougeon, 2010). Another telomere parameter of GCs that showed significant changes during folliculogenesis was the percentage of short telomeres, which increased at the secondary follicle stage compared to the primary stage. This is striking, considering that TL was higher in secondary GCs. Although this result was only observed when all women were analyzed together, this may be due to a trade-off between short and long telomeres that maintains the mean TL value stable. Another explanation could be that the percentage of short telomeres is higher because of the large number of cell divisions and the increased oxidative stress due to the metabolic activation of these cells (Liu et al., 2023). A high percentage of short telomeres indicates cellular senescence (Hemann et al., 2001, Kaul et al., 2012), a reason consistent with the fact that many secondary follicles fail to reach the antral follicle stage and undergo a process of follicular atresia (Chico-Sordo et al., 2021).

The last cells that were studied during the folliculogenesis process were the TCs. These cells were only identified in the primary and secondary follicles. The TCs divide at the secondary follicle stage, forming two layers: inner theca, responsible for androgen production, and outer theca, with a structural support function (Guahmich et al., 2023). Because only cell nuclei and telomere dots are visualized with the qFISH technique, it was impossible to differentiate between the inner and outer theca. The comparison of telomere parameters between primary TCs and secondary TCs revealed that TL remains stable during this transition. This may be mainly because, in these early stages, the TCs hardly undergo cell division. In addition, TCs exhibit low TA in rats, relative to GCs, despite their comparatively lower proliferation rates (Yamagata et al., 2002). This observation suggests the possibility of minimal telomere shortening during advanced stages of folliculogenesis, as cells hardly divide, a phenomenon that could potentially compensate for the lower levels of the telomerase enzyme. In the published literature, these cells have not been studied as much as oocytes and GCs, so it is as far as we known the first study analyzing telomere status in TCs in humans.

6.1.2.2.2 Aging in ovarian populations

Once each cell type was analyzed during the folliculogenesis process, aging was studied using telomeres as a biomarker of aging. For this purpose, young, middle-aged, and perimenopausal groups were compared in each region or cell type. In addition, the existence of significant correlations between telomere parameters and age was evaluated.

First, the ovarian region known as the stroma was studied. This region was not previously analyzed during the folliculogenesis process since it is constituted by connective tissue that is not involved in folliculogenesis (Kinnear et al., 2020). This was the only area of the ovary that could be analyzed in the 65 women recruited. No alterations in TL or the distribution of intensities were detected in any age group compared. There were also no correlations between telomere parameters and age. No telomere shortening was evident in the ovarian stroma in the 18 to 50-year-olds. The non-detection of telomere shortening in the stroma does not imply that there is no aging in the ovary at these ages. Rather, such aging is not detectable in the cells' telomeres, constituting the stroma. The maintenance of a relatively stable TL over time could be due to a low rate of cell replication, as occurs in other somatic tissues such as skeletal muscle (Tarry-Adkins et al., 2021) or endothelial cells (Chang and Harley, 1995).

Next, aging was analyzed in the different populations that constitute ovarian follicles and whose telomere dynamics during folliculogenesis were previously studied. In the case of oocytes and TCs, the different follicular stages were studied together since no telomere alterations were inherent to folliculogenesis. At the same time, GCs were evaluated independently in each follicular stage. In this way, some of the limitations of the study design were solved, but another one remained pending. This limitation is based on the fact that ovarian follicles were not identified, nor were all the stages, in all the women recruited. Consequently, only women in the young and middle-aged groups could be compared, excluding the group of perimenopausal women. In addition, it was necessary to recalculate the mean age of each of the groups to ensure the existence of statistically significant differences in the age of the groups and thus be able to study aging. Indeed, the mean age was different in the new Y and M cohorts, where aging was studied in oocytes, primordial GCs, primary GCs, secondary GCs, and TCs.

In oocytes, in contrast to the ovarian stroma, our results evidenced a lower TL, a higher percentage of short telomeres, and a lower percentage of long telomeres in the middle-aged group compared to the young group. Although oocytes remain arrested in prophase I of meiosis during folliculogenesis until the time of ovulation, and thus do not actively shorten telomeres by cellular divisions, telomere damage may still occur (Barnes et al., 2022, Singh et al., 2019). This is possible due to environmental factors such as oxidative stress or chronic

inflammation (Martín-Romero et al., 2008, Miyamoto et al., 2010). Specifically, oxidative stress is strongly related to the percentage of short telomeres, whose percentage was higher in older women (Richter and von Zglinicki, 2007, Von Zglinicki, 2002) as the redox potential of the telomere repeats is high because it is rich in guanine. Thus, ROS can easily oxidize guanines and cause DNA ruptures (Lin and Epel, 2022). However, this telomere shortening could be compensated for the telomerase enzyme. Some studies observed that oocytes from preantral and preovulatory follicles have high TA, whereas this activity is low in ovulated oocytes (Betts and King, 1999, Eisenhauer et al., 1997). Considering that TA decreases with age (Kinugawa et al., 2000), the compensation in the oocytes from middle-aged group could not be efficient.

Telomere shortening in the oocytes of older women implies a decrease in oocyte quality and oocyte quantity. The lower oocyte quality would explain a lower capacity for division during meiosis, which, together with chromosomal instability during this process, may result in a higher rate of aneuploidy and chromosome segregation errors (Capalbo et al., 2017, Meena et al., 2015, Treff et al., 2011). This telomere shortening could also explain the increased risk of fertilization failure and miscarriages from oocytes of older women due to poor chromosomal quality (Cheng et al., 2013, Ozturk et al., 2014). In addition, the increase in the percentage of short telomeres in older women and the positive correlation with age, as evidenced, would partly explain the decrease in ovarian reserve, also demonstrated by a low AMH value. This may be because the accumulation of critically short telomeres leads to cellular senescence and apoptosis (Hemann et al., 2001, Kaul et al., 2012). Therefore, telomere shortening in oocytes was detected in the middle-aged group, whose mean age was 40.2 years. Although unable to compare telomeres in oocytes from perimenopausal women, where ovarian reserve is diminished and the probability of finding follicles in an ovarian fragment is lower, one would expect an elevated telomere shortening in this age group. There is a significant lack of human studies analyzing telomere parameters in oocytes from older women or women with infertility-related pathologies such as diminished ovarian reserve or POF. Given that this study is challenging to carry out in humans, since women with these profiles resort to ART and all the oocytes are used for this purpose, the study has been carried out in animal models. These models include the murine model deficient in the telomerase gene (Liu et al., 2002a, Liu et al., 2002b), or mice with germline deletions (Cozzolino et al., 2024, Cozzolino and Seli, 2022). In these models, germline decline is sought to mimic the effects of aging. In the telomerase-deficient mouse model, where oocyte telomeres were dysfunctional, fertility-reducing phenomena such as chromosome misalignments during meiotic division of oocytes, aberrant fertilization, and abnormal cleavage of embryos were observed (Liu et al., 2002a, Liu et al., 2002b). Models with germline deletions of genes such as Clpp (caseinolytic peptidase P) or Mfn1 (mitofusin-1), both genes with function at the mitochondrial level, evidenced greater

telomere shortening in oocytes with mutated Clpp (Cozzolino et al., 2024), whereas no differences in TL were observed in oocytes with deletion in Mfn1 (Cozzolino and Seli, 2022). Another of the murine models studied is the phenotypic model of accelerated senescence, which is independent of gene mutations, and allows the study of reproductive aging in young mice with signs of older age. However, no alterations in oocyte TL were observed in these mice at 7 months of age (Polonio et al., 2023). Therefore, if we take into account that in the process of oogenesis, in the transition from immature oocyte to mature oocyte, there is a telomere shortening, in older women whose immature oocytes already have short telomeres, the culmination of oogenesis would further reduce this TL.

GCs were the only cell type where aging was studied independently at each follicular stage because they showed increased TL as folliculogenesis progressed. In primordial GCs, the results obtained after comparing the telomere intensities of young and middle-aged women were similar to those observed in oocytes. This makes sense given that the primordial follicle structure is formed before birth (Gougeon, 2010). The middle-aged group evidenced lower TL and a higher percentage of short telomeres. No significant decrease in the percentage of long telomeres was observed. However, all three telomere parameters correlated significantly with age. Both TL and the percentage of long telomeres decreased with age, whereas the percentage of short telomeres increased. Thus, it was observed that GCs of primordial follicles, which have not yet begun to proliferate actively, experienced telomere shortening. This phenomenon may be due to the accumulation of oxidative stress damage in the ovary during the quiescent period (Von Zglinicki, 2002), the undetectable or low TA of GCs at this follicular stage (Lavranos et al., 1999), or even being in a transitional phase to the primary follicular stage that may make them vulnerable to telomere damage (Maidarti et al., 2019). Telomere shortening of GCs at this stage could contribute not only to the reduction of oocyte quality, since there is a bi-directional communication of factors, hormones, and nutrients between these cells and the oocyte. Still, it could also be key in the decrease of ovarian reserve. As explained above in oocytes, an accumulation of short telomeres induces cellular senescence and apoptosis (Hemann et al., 2001, Kaul et al., 2012), and the oocyte would not be able to maintain or continue its development if the surrounding GCs are dysfunctional. Indirectly, telomere shortening in these cells could also contribute to the decline in ovarian reserve with age because if the primordial follicles are dysfunctional, this causes an increase in the number of follicles recruited to increase pregnancy options.

At the next follicular stage, the primary GCs also evidenced telomere shortening in the middle-aged group of women compared to the young women. That is, middle-aged women recorded shorter TL, greater accumulation of short telomeres, and less accumulation of long telomeres. However, it was curious that in primary GCs, none of the telomere parameters correlated with

age, as opposed to primordial GCs, where all showed this correlation. Therefore, we can find an explanation if we analyze the differences between primordial GCs and primary GCs. Apart from the flattened morphology of primordial GCs versus the more cuboidal shape of primary GCs, primordial GCs are at rest, supporting the oocyte. In contrast, primary GCs begin to divide, forming a thicker and more organized cell layer (Rimon-Dahari et al., 2016, Sanchez and Smitz, 2012). The primordial GCs play a more passive role, interacting with the oocyte through paracrine signals and regulating its metabolic activity. Still, the primary GCs actively protect the oocyte and produce key hormones for follicular development and oocyte maturation (Canipari, 2000). And finally, TA is increased at a higher rate of cell replication of primary GCs compared to primordial GCs (Russo et al., 2006). This increase in TA implies better telomere maintenance that may trigger a positive selection of those primary follicles with better telomere parameters after activation of primordial follicles. Therefore, although there is telomere shortening in the GCs of primary follicles in middle-aged women, this may be the direct consequence of the shortening previously produced in the primordial follicles. Proof of this would be that the percentage of long telomeres is statistically reduced in older women at this stage. However, TA increases and does not allow the exclusive effect of aging to be detected. This is why the correlations of telomere parameters with age previously observed in the primordial stage disappear in this more advanced stage.

Following this reasoning, in the GCs of secondary follicles where the division rate increases (Gougeon, 2010), and with it the TA (Lavranos et al., 1999), in these follicles, one would expect to find that the effect of aging on telomere shortening disappears. The result showed lower mean TL, a greater accumulation of short telomeres, and a lesser accumulation of long telomeres in the GCs of secondary follicles in older women. However, the differences were not statistically significant. Similarly, correlations of telomere parameters with age were not significant. Therefore, the question arises of whether the effects of aging will be compensated by the action of telomerase in future stages of folliculogenesis. In bovine and rats, high TA was observed in small pre-antral follicles, gradually decreasing in the transition from small to medium follicles (Eisenhauer et al., 1997, Lavranos et al., 1999). In summary, the pattern of TA during folliculogenesis would start with undetectable levels of this enzyme in the primordial stage, a gradual increase in the primary and secondary stages, and a final drop in the larger diameter follicles. Taking as a premise this profile of TA in the GCs of the Graafian follicle, the effect of aging in older women would be significant and would evidence a greater telomere shortening, or a direct impact of aging in the TA. This would coincide with the results of works that analyzed TL in GCs obtained during oocyte retrieval in women who underwent IVF, where TL decreased with increasing age (Hao et al., 2023, Lara-Molina et al., 2020). Therefore, this added to the fact that the oocytes that are ovulated in older women also have a shorter TL, the

reproductive capacity in these women may be diminished. However, one of the unanswered questions is whether the impaired telomere maintenance in oocytes is caused by an aging ovarian environment where GCs have altered telomere pathways, or whether telomere shortening in both cell populations co-occurs.

Finally, ovarian aging was also studied in TCs. As in oocytes, no telomere impact of folliculogenesis was observed, so all follicular stages were examined together, primary and secondary, in this case. A comparison between young and middle-aged women showed a shorter TL, a higher percentage of short telomeres, and a lower percentage of long telomeres in the group of middle-aged women. However, no correlation between telomere parameters and age was observed. This profile of telomere shortening with aging is quite similar to that obtained in primary GCs. The most feasible explanation in these cells was attributed to the TA that characterizes them. In the case of TCs, these have lower telomerase levels than GCs and would not be sufficient to compensate for the telomere shortening derived from cell divisions (Yamagata et al., 2002) or other cellular insults such as ROS. However, in primary GCs, the correlation between telomere parameters and age was lost, and a possible explanation was the high TA. In TCs, these correlations would not exist due to the low cell division rate of these cells compared to GCs. In other words, the low TA of these cells is sufficient to manage with telomere shortening resulting from aging, for example, due to oxidative stress.

Ovarian aging, understood as telomere shortening, was detectable in oocytes, primordial GCs, primary GCs, and TCs. However, it was not observed in secondary GCs. A possible explanation could be TA, which is very low in oocytes, TCs, and primordial follicles, but gradually increases in primary and secondary follicles. Another cell type that would have been interesting to analyze is cumulus cells. However, considering that the number of antral follicles detected in our ovarian sections was very small and that the oocyte did not appear in the same section on many occasions, it was impossible to study cell types.

6.1.2.2.3 PBMCs as telomere biomarkers of the ovary

Middle-aged women exhibited significant telomere shortening in their ovaries, whereas in PBMCs, this phenomenon was observed in the group of perimenopausal women. Therefore, shorter TL in ovaries was observed in women of reproductive age, earlier than at the systemic level. Considering that our study collected both PBMCs and ovarian samples from the same women during surgery, and that the age range of the studied women mostly spans reproductive life, we explored the potential of telomere parameters in PBMCs as biomarkers of reproductive aging.

First, TL expressed as intensities were transformed to kilobases for appropriate correlations (Canela et al., 2007). To avoid telomere bias due to age, and assuming that telomeres shorten

with increasing age, only those women with all ovarian cell types and PBMCs were considered. The mean age of this new cohort was approximately 38 years. The TL of the different cell types was compared. Specifically, and ordered from shortest to longest, the TL of the cell types studied were: PBMCs (10.1 kb), primordial GCs (12.7 kb), TCs (13.0 kb), ovarian stroma (13.1 kb), primary GCs (13.5 kb), oocytes (13.6 kb), and secondary GCs (14.1 kb). All ovarian cell types showed significantly higher TL compared to PBMCs. According to human studies, the TL in somatic cells ranges from 4 to 12 kb (Factor-Litvak et al., 2016), whereas in germ cells, the range is 10 to 20 kb (Samassekou et al., 2010). Indeed, the TL of PBMCs as somatic cells, and the TL of oocytes, as germ cells, are within the published range. However, the same is not true for some studied somatic cells such as stroma cells, GCs and TCs. In humans, the TL of all somatic tissues is synchronized According to human studies, the TL in somatic cells ranges from 4 to 12 kb (Factor-Litvak et al., 2016), whereas in germ cells, the range is 10 to 20 kb (Samassekou et al., 2010). Indeed, the TL of PBMCs as somatic cells, and the TL of oocytes, as germ cells, are within the published range. However, the same is not true for some somatic cells studied, such as stroma cells, GCs, and TCs. In humans, the TL of all somatic tissues is synchronized at birth (Youngren et al., 1998). Nevertheless, telomere dynamics evolve at a different rate, the correlations in TL are maintained (Daniali et al., 2013). Therefore, if all these somatic cell types start from the same TL, at the blastocyst stage, differences in this parameter may be due to a different rate of cell division, telomere maintenance, or a different rhythm of cell differentiation during development, which also promotes telomere shortening (Varela et al., 2011). As mentioned above, GCs, despite having a high replication rate, have TA that would compensate for telomere shortening (Toupance et al., 2021). Although TCs have lower TA, their division rate is also lower. The most striking case is the ovarian stroma, which maintains a high TL for PBMCs despite not having TA. This may be mainly due to the difference in cell replication rate, where PBMCs divide actively while the stroma hardly undergoes any division (Demanelis et al., 2020).

Since PBMCs exhibit different telomere dynamics with both germ cells and ovarian somatic cells, the next step was to study the correlation between the telomere parameters of PBMCs and ovarian cells. Gray et al. (2014) compared the TL of leukocytes in postmenopausal women and age-matched women who were still menstruating. The results showed a relationship between leukocyte TL and reproductive life span, with women with longer telomeres entering menopause later than those with shorter telomeres (Gray et al., 2014). Our results showed no correlation between the TL of PBMCs and the TL of any ovarian cell type. Only a significant correlation was detected between PBMCs and ovarian stroma regarding the percentage of short telomeres. However, this correlation was negative, i.e., a higher percentage of short telomeres in PBMCs was associated with a lower accumulation of short telomeres in the

stroma. This reinforces the idea that telomere dynamics at the systemic and ovarian levels are entirely different in our cohort, as other studies have shown in other cohorts (Lara-Molina et al., 2020, Demanelis et al., 2020). Furthermore, a positive correlation was observed between the percentage of long telomeres in PBMCs and primordial GCs. However, considering that recurring correlations were not demonstrated in ovarian cells, these two significant correlations should be interpreted cautiously. Besides, the threshold used to determine short and long telomeres was specific and different for each cell type. In the published scientific literature in humans analyzing this role of PBMCs as ovarian aging biomarkers, the vast majority analyze this relationship with GCs obtained during oocyte collection in IVF treatments, not in women undergoing surgery, as in our case. These studies rejected using PBMCs as biomarkers of ovarian aging (Demanelis et al., 2020, Lara-Molina et al., 2020).

6.1.2.3 Telomerase activity in the ovary

Telomerase is the enzyme responsible for telomere synthesis at the ends of chromosomes and is found in stem cells, tumor cells, and germ cells (Greider and Blackburn, 1985). However, some somatic ovarian cells also have detectable TA. Among these are GCs, in which telomeres maintain their length due to the action of this enzyme, allowing cells to divide continuously according to the demands of folliculogenesis. The presence of TA in the ovary and in the cells that comprise this structure was detected in humans (Kinugawa et al., 2000, Wright et al., 2001, Wright et al., 1996), and animals (Eisenhauer et al., 1997, Goto et al., 2013, Lavranos et al., 1999, Russo et al., 2006, Yamagata et al., 2002). In our study, we evaluated the presence of TA in ovarian fragments from women across all age groups. The TRAP assay demonstrated the presence of TA in the ovaries of young, middle-aged, and perimenopausal women, indicating that TA in this organ is maintained throughout reproductive life. Moreover, considering that the cell type least represented in quantitative terms in an ovarian fragment is the oocyte, the detection of TA reinforces the fact that there are more cells in the ovary that possess TA, such as GCs or TCs. However, no differences were observed after quantification. Published studies indicate that TA in the ovary decreases with age (Kinugawa et al., 2000, Polonio et al., 2023). Therefore, the non-detection of this lower TA in the samples of this study could be due to one of the following reasons. Since this assay is not performed on the whole ovary, but on a small fragment, it is impossible to guarantee the presence of oocytes, GCs, or TCs in the fragment processed and analyzed. Although the TRAP assay has the advantage of directly measuring the functional activity of telomerase (Burger, 2002, Herbert et al., 2006, Kim and Wu, 1997, Wright et al., 1995) compared to the quantification of TERT levels by RT-qPCR, which only reflect gene expression and not necessarily its functional activity, its quantification should be taken with caution. The study by Ludlow et al. (2014) evidenced that although the traditional TRAP assay readily detects TA, there is a significant variability in gel-

based quantification that does not allow its use to quantify differences of 20-30% (Ludlow et al., 2014). Therefore, it was impossible to attribute ovarian TA to any particular cell type, nor was it possible to determine its higher or lower expression in follicular stages.

6.1.3 Ovarian fibrosis

Fibrosis is a pathological process characterized by an excessive deposition of extracellular matrix, particularly collagen (Ricard-Blum et al., 2018). It is known that increased tissue fibrosis, highly documented in different organs such as the liver, lungs, or heart (Denic et al., 2016, Kapetanaki et al., 2013, Sangaralingham et al., 2016, Horn and Trafford, 2016), is linked to the aging process. This link between aging and fibrosis mainly relies on the decline in regenerative capacity and altered extracellular matrix homeostasis. Its presence in the ovary has a direct impact on reproductive function and is associated with decreased fertility and premature menopause (Briley et al., 2016, Meirow et al., 2007, Secomandi et al., 2021). Our results showed an increased percentage of ovarian fibrosis, as area analyzed by Masson's trichrome staining, in perimenopausal women compared to young women. Additionally, a significant positive correlation was found between the ovarian fibrotic area and age. These results agreed with previous studies claiming an increase in fibrosis with aging in the ovary (Winkler et al., 2024, Landry et al., 2020, Briley et al., 2016). This extended collagen deposition in the ovarian stroma is associated with a decrease in ovarian reserve and an impaired ability to support follicular maturation (Landry et al., 2022, Umehara et al., 2022). Oxidative stress accumulated with age plays a key role in ovarian fibrogenesis, as reactive oxygen species damage ovarian cells, promoting collagen production by fibroblasts (Liu et al., 2016). Although the ovarian stroma exhibited some aging-related signs, such as fibrosis, no effects were detected at the telomere level in this ovarian region. This finding may be partially because fibroblasts do not proliferate as intensely as to generate significant telomere shortening with age (Allsopp et al., 1992). Still, they increase the production and accumulation of collagens and other extracellular components.

The analysis of the ovarian fibrotic area supported an increase in fibrosis in this organ linked to aging. However, due to the limited availability of ovarian samples, it could only be evaluated in 19 of the recruited women. To enhance the relevance of our results with a higher sample size, we also decided to assess the expression of those genes directly related to fibrosis, such as TGF-β1, COL1A1, and COL3A1 since ovarian RNA of a larger sample size was available (Bhogal et al., 2005, Miao et al., 2008).

TGF-β1 is a cytokine released in response to injury, cellular stress, or chronic inflammation. Acting primarily through the Smad signaling pathway, this cytokine binds to its receptor on the cell surface and triggers an intracellular signaling cascade that terminates in the activation of

Smad2 and Smad3 (Wrana et al., 1994, Yan et al., 2018). These transcription factors promote the expression of genes such as COL1A1 and COL3A1 that code for type I and type II collagen, major components of the ovarian extracellular matrix (Lind et al., 2006). A significant positive correlation was observed in the expression of both genes coding for collagen and TGF-β1 in the analyzed ovarian samples. However, no changes in the expression of either of these genes were detected with aging, nor was there a significant correlation with age.

Altogether, the results of this study suggest that the increased levels of fibrosis and collagen deposition associated with aging are not directly linked to the expression of TGF-β1, COL1A1, and COL3A1 genes. However, two possible hypotheses could explain this fact. The first would be related to the repetitive ovulation process, characterized by inflammation (Duffy et al., 2018, Ny et al., 2002, Büscher et al., 1999), and extracellular matrix remodeling (Woessner et al., 1989). The second one, closely related to collagens I and III, is based on their differential distribution in the ovary (Lind et al., 2006, Grosbois et al., 2023). Specifically, both collagens are distributed in distinct concentric layers in the external ovarian stroma, between the tunica albuginea and the stromal layer containing the primordial follicles. Considering that ovarian fragments of different sizes were used for RNA extraction and not the whole ovary, the level of expression of these genes could be biased according to the size and localization of the fragment or even the ovarian section.

6.1.4 Proteomic analysis of the ovary

Ovarian aging was also studied from a proteomic point of view to understand those modifications of the ovarian proteome induced by aging. Functional analysis suggested that, in general, a greater number of biological processes were altered in the population of perimenopausal women compared to the young and middle-aged group. Biological processes included response to cellular stress and damage, regulation of metabolism and energy production, regulation of cell cycle and homeostasis, maintenance of cell structure and integrity, and cell signaling.

In the perimenopausal women, the majority of DEPs detected were compared to the middle-aged group, suggesting that as menopause approaches, the ovary undergoes multiple alterations. As previously mentioned, during this time in a woman's reproductive life, the female body undergoes several modifications (Besong et al., 2024, Freeman et al., 2008, Park et al., 2021b, Samami et al., 2022, Woods and Mitchell, 2005, Zhu et al., 2020). Among the DEPs found in perimenopausal women, both the RSMN and CALM3 stood out and are related to the regulation of cell signaling. Their expression decreased in the group of perimenopausal women. RSMN plays a crucial role in regulating gene expression and RNA processing (Zhang et al., 2021b), and lower expression in the P group may trigger the generation of misfolded or

defective proteins in aged cells. CALM3 is a protein involved in calcium signaling (Alphonse et al., 2022, Tsang et al., 2006); its decrease with age could affect different cellular signaling processes in aged ovaries and have direct consequences in infertility-related processes such as impaired oocyte maturation (Tosti, 2006) or failed fertilization (Homa et al., 1993).

LDHB is another protein with a lower expression in perimenopausal women than young or middle-aged women. This is a key protein in converting lactate to pyruvate that localizes to the mitochondria (Chen et al., 2016). Low levels of LDHB would be associated with a decreased capacity for energy generation and mitochondrial dysfunction in cells, directly contributing to ovarian aging (Kasapoğlu and Seli, 2020). Among the proteins regulating cellular metabolism and energy production, AL4A1 was highly expressed in the perimenopausal group. This nuclear-encoded mitochondrial matrix protein participates in proline amino acid catabolism (Srivastava et al., 2012). Therefore, an increased expression could be part of the adaptive response to metabolic stress, since it promotes cellular energy and maintenance of mitochondrial function.

Proteins involved in cell cycle regulation and homeostasis were also identified within the DEPs in the perimenopausal group. CUL1, whose levels were increased with aging, participates in protein degradation through the ubiquitin-ligase E3 complex (Liwocha et al., 2024, Scott et al., 2016). This increase could be part of the response to maintain cellular homeostasis against accumulating defective or damaged proteins. Other DEPs involved in the regulation of cycling and homeostasis were MRP and MARCS, both of which are closely related and whose expression was decreased in the perimenopausal ovary. This decrease could reflect a decline in cellular dynamics (Björkblom et al., 2012, Issara-Amphorn et al., 2023, Rodriguez Peña et al., 2013), and in the capacity for cellular adaptation. However, the last-mentioned protein, MARCS, also has an essential role as a regulator of ROS production, evidenced in monocytic cells (Huber); ROS can directly damage telomeres and cause telomere shortening. Other DEPs directly related to oxidative stress are GGT5 and ATM proteins; they increased with age. GGT5 is involved in the metabolism of glutathione, a key antioxidant that helps maintain redox homeostasis (Wickham et al., 2011). Its increase with aging may be due to increased peroxide detoxification demands involved in aging. The second protein mentioned, ATM, regulates the response to DNA damage and maintains genomic stability (Cortez et al., 1999, Li et al., 2000b, Wu et al., 2000). Therefore, its expression could be increased with age in response to accumulated DNA damage during cellular aging, to facilitate DNA repair. Finally, low levels of EVPL protein were detected in the ovary of perimenopausal women compared to middle-aged women. At the same time, there was no difference between the young and middle-aged groups. Its decrease could reflect a decline in tissue repair and be related to increased fibrosis since it connects intermediate filaments to cellular junctions (Fogl et al., 2016).

In summary, the results of this work allow us to characterize and understand human ovarian aging from different points of view. From the hormonal point of view, aging is associated with high levels of FSH and LH, as well as low levels of estrogen and AMH. Since AMH indicates the ovarian reserve, increasing age implies a reduction in ovarian reserve. However, with age, the number of oocytes decreases, and so does their telomere maintenance and, therefore, their quality. Indeed, a greater telomere shortening was detected in oocytes, primordial and primary GCs, and ovarian TCs. However, no changes were detected in the telomeres of GCs from secondary follicles or ovarian stroma. This could be explained by the fact that GCs exhibit TA, and the ovarian stroma has a low cell division rate (Kinugawa et al., 2000, Liu and Zhu, 2003, Uysal et al., 2021). Although telomere alterations were observed at the systemic level, demonstrated by telomere shortening in PBMCs, these cells cannot be telomere biomarkers of ovarian aging since they present a completely different dynamic. Other non-telomere alterations also showed evidence of ovarian aging progression, including an increase in the ovary's fibrotic area and alteration of this organ's proteomic profile. Specifically, proteins differentially expressed with age are involved in multiple biological processes, some specifically related to the response to oxidative stress.

The characterization of human ovarian aging performed in this thesis project will be very relevant to improve prevention, early diagnosis, and treatments for various age-related fertility disorders. Specifically, this work studied the age range of women currently resorting to ART to achieve pregnancy with their oocytes, and in many cases, the cause of infertility is unknown. Our results highlight the importance of telomere maintenance for preserving ovarian function, suggesting that further research on using antioxidants and other therapies to reduce or recover telomere damage should be performed. However, it is also important to highlight one of the main limitations of this study: the use of a small fragment of ovarian cortex. Although this limitation is challenging to overcome in human studies, as the use of a complete healthy ovary would be unethical, parallel human and animal studies could be conducted to complement the results obtained.

6.2 Study of telomere parameters in lower ovarian reserve cases

This section, also obtained from Project 1, was born as a consequence of one of the results obtained in the previous section. The drop in the value of AMH associated with age and aging led us to consider the profile of women who, being young, already have a low level of this hormone. The question to be resolved centers on whether the lower ovarian reserve in these women also implies a lower quality, in terms of telomeres, in the different ovarian populations.

Although the conclusions drawn in this section could partially apply to women diagnosed with DOR or POI, these populations have not been specifically and concretely studied in this work. Therefore, in this section, the previously analyzed population was classified according to the AMH value, and the telomere dynamics among them were investigated. The division into age groups was maintained because age was linked to telomere alterations.

6.2.1 Endocrine parameters

As for the rest of the hormones, a significant difference was only recorded for LH hormone when comparing the M+ and M- groups. However, the comparison between these middle-aged groups also showed statistically significant differences in mean age, with the M+ group recording a higher mean age. This suggests that, even though the 1.2 ng/mL AMH threshold value has significant clinical relevance, perhaps another threshold value would have been more appropriate for this age group. However, it was not recalculated since the number of individuals, and thus the mean age value, varied in the telomere analyses of the different ovarian cell populations. Therefore, taking into account the age difference between the M+ and M- groups and the fact that the menstrual cycle phase variable was not standardized in the sample collection, no results were extracted from the hormonal analyses, being only a characterization of the cohort for future telomere analysis.

6.2.2 Telomere parameters

6.2.2.1 Systemic analysis

At the systemic level, no telomere alteration was detected in PBMCs when groups with the same age but different AMH value were compared. The explanation for this result implies that telomere shortening in PBMCs and AMH value are not directly linked. Both parameters are linked to aging as evidenced in the previous result, but there is no relationship between them. This reinforces the results obtained when evaluating the possible role of PBMCs as telomere biomarkers of ovarian aging, evidencing that telomere dynamics at the systemic and ovarian levels were different. However, published studies regarding the TL of leukocytes and women with POI who have diminished ovarian reserve as assessed by AFC are in some cases contradictory. At this point it is important to note that the AMH value is not a classic criterion in the diagnosis of POI, but the AFC is. The studies published by Xu and coworkers (2017), and Miranda and coworkers (2018) demonstrated telomere shortening in the leukocytes of women with POI (Miranda-Furtado et al., 2018, Xu et al., 2017), while the study by Hanna et al. (2009) evidenced the opposite (Hanna et al., 2009). For instance, in Xu et al. study, POI and control showed statistical differences in the AMH value and in the mean age between the groups. The studies from Miranda et al. and Hanna et al. evidenced different mean age between their study

population also. This raises the question whether the differences in leukocyte TL are really directly associated with POI status or whether the effect of age interferes with this relationship. For this type of study, it would be necessary to work with age-matched groups as had been done in the present work. Therefore, prior to this study, a strong and verified association between leukocyte TL and established markers of ovarian reserve such as AMH level had not been evidenced, with no differences in the mean age of their groups. In this work, with the exception of the group of middle-aged women, no changes in systemic telomere dynamics associated with lower AMH were detected.

6.2.2.2 Ovarian analysis

The observation at the systemic level makes sense from the perspective that it is challenging to establish a direct relationship between PBMCs and ovarian reserve. However, a reduction in ovarian reserve at an early age could be associated with defective telomere maintenance in the ovary. Previous studies that have attempted to relate these two phenomena were based on TL of GCs obtained during oocyte collection (Butts et al., 2009, Xu et al., 2017). In this work, the study was performed on ovarian tissue directly. Telomere parameters were compared between the high and low AMH groups. In young women, there was not a large enough sample to carry out additional procedures like the TRAP assay, nor did we find enough follicles in this group to do statistical analysis. This is consistent with the fact that in young women, the probability of a low ovarian reserve is minimal, and that in this profile of women, it will be more challenging to find ovarian follicles. No ovarian follicles were seen in any of the perimenopausal women in the cohort, all of whom were characterized by low ovarian reserve (Nelson et al., 2023).

The results in the ovarian stroma evidenced that there were no significant changes in either TL or in the percentage of short and long telomeres when comparing the groups with different AMH values in any of the age intervals studied. This result aligns with the previous finding, where these changes were also not observed during the aging process in this ovarian tissue. Although the main function of the ovarian stroma is to support and sustain the ovarian follicles, this region also participates in the reparative response, as it can produce growth factors and cytokines that can influence the regeneration of the ovarian microenvironment, thereby promoting follicular development (Kinnear et al., 2020). However, it was observed that a greater or lesser ovarian reserve is not linked to the telomere dynamics of the stromal tissue.

Oocytes, GCs at different follicular stages and TCs could only be studied in the group of middle-aged women. As all cell types were not identified in the ovarian fragments of the entire cohort, the mean age for each group varied. In the comparisons of oocytes, primary GCs and TCs, the ages were comparable, whereas in the GCs of primordial and secondary follicles the

mean age was significantly different. In oocytes, with no difference in mean age, a higher percentage of short telomeres was recorded in women with low AMH. This accumulation of short telomeres could reflect significant cumulative damage due to oxidative stress (Ahmed and Lingner, 2018, Martín-Romero et al., 2008, Von Zglinicki, 2002), accelerated cellular aging, and germ cell senescence (Hemann et al., 2001, Kaul et al., 2012). The decrease in ovarian reserve in these women may be associated with increased exposure to these damaging factors, leading to more pronounced telomere shortening in oocytes. It would expect to find results with the same trend in primordial GCs. However, in this comparison the mean age was different, so despite observing a lower TL, a higher percentage of short telomeres and a lower percentage of long telomeres in the M- group, these changes may be due to the older age of these women. In primary GCs, no changes were detected in any of the telomere parameters when comparing the M+ and M- groups, nor in the age variable. In secondary GCs, significant changes were only observed in the percentage of long telomeres, specifically a lower percentage in the group of women with low AMH. Again, this comparison was made in groups with different ages, so this result could be attributed to an age effect rather than being associated with a low AMH value. Finally, the TCs recorded a lower TL in the group of women with low AMH, and the ages were comparable.

From our findings, considering that in some comparisons the result obtained could be due more to an age effect, we could only conclude that middle-aged women with low ovarian reserve are characterized by a higher percentage of short telomeres in their oocytes, no telomere change in primary GCs, and a lower TL in TCs. The results obtained in oocytes are of great relevance, as there are no previously published studies. The relationship between low ovarian reserve and an increase in short telomeres could be explained by an accumulation of damage caused, for example, by increased oxidative stress. Consequently, the accumulation of critically short telomeres in oocytes could trigger cellular senescence and follicle loss (Hemann et al., 2001, Kaul et al., 2012). Regarding GCs, no changes were detected in the primary stage, but no conclusive data were obtained in the other follicular stages analyzed. However, the study by Butts et al. (2009) evidenced a greater telomere shortening in GCs obtained from oocyte collection in women with occult ovarian failure (Butts et al., 2009). In this study, there was no difference in the mean age of the problem and control cohorts, but they did not rely on the criterion of low AMH to define the population of women with occult ovarian failure. Therefore, it is tough to conclude whether lower AMH is linked to defective telomere maintenance in GCs. Although based on the fact that it is the GCs of early and mid-developing preantral and antral follicles that produce AMH (Jeppesen et al., 2013), and we did not observe differences in primary GCs (early preantral follicle stage), we would not expect to find telomere differences in GCs. In addition, GCs have high TA responsible for telomere maintenance

(Betts and King, 1999, Eisenhauer et al., 1997, Goto et al., 2013, Kalmbach et al., 2013, Lavranos et al., 1999, Russo et al., 2006). The last of the cell types that evidenced telomere differences in women with low AMH were the TCs. Low AMH was associated with shorter TL in these cells; this could be explained if the ovarian follicles in women with lower AMH are subjected to and exposed to greater oxidative stress (Ahmed and Lingner, 2018, Von Zglinicki, 2002). This telomere shortening in TCs in the low AMH group, similar to that obtained in oocytes in the same group, could be visible in these two cell types and not in GCs due to the lower TA in meiosis detained oocytes (Eisenhauer et al., 1997) and TCs (Yamagata et al., 2002).

Considering that the telomere alteration detected in oocytes and TCs in women with low AMH could be attributed to the synergy of the telomere damage caused by oxidative stress and the low level of TA in these cells, the next technique performed was the TRAP assay. The study by Kinugawa et al. (2000) analyzed TA in normal ovaries and ovaries from women with POF (Kinugawa et al., 2000). From the women with POF, they were unable to draw any conclusions since out of 5 women tested, two had high TA, and three had low TA in the ovary. They concluded that the lack of TA in POF patients was related to the lack of follicles in the ovary of these patients. Based on this, we could conclude that the quantity of TA in our work could be related to the quantity of follicles in the ovarian fragment, which could not represent the ovarian reserve or AMH. Therefore, their results are in agreement with those obtained in this work, where despite comparing women with high and low AMH in the different age groups, with the exception of the young group, no clear evidence of higher or lower TA was observed in the profile of women with low AMH. As occurred in the analysis of the effect of aging on TA, the results show no differences because we worked with an ovarian fragment and not with the whole organ.

In summary, the study of whether a lower ovarian reserve is linked to defective telomere maintenance at the systemic and ovarian level should be evaluated with caution. At the systemic level there were no differences, nor at the ovarian stromal level. However, although differences in ovarian telomere parameters were detected, specifically a higher percentage of short telomeres in oocytes and a lower TL in TCs. In the telomere parameters of GCs, of great importance in follicular structures, it can only be corroborated that in middle-aged women no changes in primary GCs associated with low AMH were observed.

6.3 Impact of pregnancy on ovarian telomere dynamics

Pregnant women were included in the recruitment of Project 1, taking advantage of the moment of cesarean section to obtain a small ovarian fragment. After the telomere study of

aging, a different analysis was carried out to find out whether the telomere pathway could be altered during pregnancy, a process in which the hormone profile and physiology of women change.

In previous analyses, pregnant women could not be included since their AMH levels were very low. The population of perimenopausal women could not be used in this section since none of them were pregnant at the time of recruitment.

6.3.1 Endocrine parameters

The reproductive life of women involves multiple variations in hormonal patterns, as can be observed during the menstrual cycle or with the arrival of menopause. However, another period that involves many hormonal changes is pregnancy. During this time, it is widely known that both FSH and LH decrease due to a temporary cessation of the ovarian cycle, thus stopping follicular recruitment and, with it, ovulation (La Marca et al., 2005). In contrast, progesterone and estrogen increase in pregnancy (Dukic et al., 2024). The corpus luteum initially produces progesterone until the placenta is formed, which becomes the primary source of this hormone during pregnancy (Tuckey, 2005). The elevated level of P4 keeps the uterus in a quiescent state by inhibiting uterine contractions, thus preventing premature labor (Ruddock et al., 2008). Estrogens, which are mainly produced in the ovarian follicles, are also synthesized by the placenta during pregnancy (Loriaux et al., 1972, Levitz and Young, 1978). Their primary function is the growth and development of the fetus and its organs (Ritzén et al., 2000). Together, both P4 and estrogens prepare the mammary glands for lactation (Ladyman et al., 2010, Pang and Hartmann, 2007). This decrease in FSH and LH and an increase in E2 and P4 were detected in our cohort of pregnant women in both the Y and M groups. In the case of AMH, the scenario is more complicated. As mentioned above, this hormone is stable and independent of fluctuations derived from the menstrual cycle (Hehenkamp et al., 2006, Tsepelidis et al., 2007, La Marca et al., 2006). Thanks to its stability and decline linked to increasing age, it is a good approximation of ovarian reserve. However, during pregnancy, the levels of this hormone drastically decrease (Köninger et al., 2013, McCredie et al., 2023), as was observed in our Y and M pregnant populations. This drop in AMH is a reflection of the ovarian suppression that takes place during pregnancy. Since preantral and small antral follicles produce AMH, if there is a temporary suppression of the menstrual cycle and, thus, folliculogenesis, its production will not occur (Iwase et al., 2023). Once delivery has occurred, the levels of this hormone are restored (Köninger et al., 2013). The reason for the decrease in AMH during pregnancy is the same as in the case of FSH and LH. However, many studies affirm that a lower AMH implies lower fecundability, significantly reducing the chances of conceiving given that the ovarian reserve is lower (Nelson et al., 2024, Steiner et al., 2011,

Yarde et al., 2013). It is essential to clarify that the decrease in AMH values during pregnancy does not imply a diminished ovarian reserve but reflects ovarian suppression in this period.

6.3.2 Telomere parameters

In a vast majority of studies TL is analyzed as a marker for pregnancy achievement (Purdue-Smithe et al., 2021, Thilagavathi et al., 2013). Consequently, and focusing on pregnancy as a positive fertility control, an optimal telomere profile is expected to be obtained in pregnant women. However, pregnancy was proposed as a model of aging (Giller et al., 2020, Jasienska, 2009), and was linked to an increased risk of developing chronic diseases (Atsma et al., 2008, Lawlor et al., 2003).

6.3.2.1 Systemic analysis

When telomere parameters were compared in PBMCs from pregnant women and the age-matched control group, no significant changes were observed except a drop in the percentage of long telomeres in the middle-pregnant women. This fact can be explained by considering that the mean age was statistically significantly different in the comparison of middle-aged pregnant and non-pregnant women. According to the published results that evaluated the leukocytes TL at different times during pregnancy, it has no impact on the TL of these cells (Mitchell et al., 2018, Panelli et al., 2022, Zota et al., 2018). The other studies about telomeres and pregnancy analyzed the association between parity and TL, getting contradictory results. Michaeli et al. (2022) and Lane-Cordova et al. (2017) did not find a correlation between parity and leukocytes TL (Lane-Cordova et al., 2017, Michaeli et al., 2022). One of the studies that analyzed TL from genomic DNA extracted from saliva and buccal samples showed a positive association between these variables (Barha et al., 2016). However, other studies in blood cells described that increasing parity was associated with shorter TL (Kresovich et al., 2018, Pollack et al., 2018, Ryan et al., 2018). These last studies attributed the telomere shortening to the changes related to oxidative stress and inflammation that occur during pregnancy (Hung et al., 2010, Mor and Cardenas, 2010, Toboła-Wróbel et al., 2020, Ziomkiewicz et al., 2016).

6.3.2.2 Ovarian analysis

Although no changes were detected in the telomere parameters of PBMCs linked to pregnancy, ovarian telomere dynamics never was studied in pregnant women. During pregnancy, ovarian functions are “temporarily” suspended, resulting in low AMH values (Iwase et al., 2023, Köninger et al., 2013). However, two of the hormones with high levels during pregnancy, estrogens and progesterone, may have an impact on telomeres because they regulate TA. This enzyme is activated by estrogens (Bayne et al., 2007, Lin et al., 2011). Some studies in endometrial or breast cancer suggested an inhibition of telomerase by progesterone

(Wang et al., 2000). Although our comparison of TA in the ovary of pregnant and non-pregnant women did not show any substantial change, telomere parameters were studied in each ovarian cell type to obtain more information.

In the ovarian stroma, no changes with pregnancy were detected following the previous results. Special attention was paid to the group of middle-aged women since there were significant age differences. In oocytes, changes in TL were observed in both the young and middle-aged groups. In both comparisons, the group of pregnant women recorded a shorter TL, a higher percentage of short telomeres, and a lower percentage of long telomeres. These results were not previously established in the scientific literature, but there is a possible biological reasoning behind them. Oocyte telomeres could be affected by certain pregnancy-related factors such as increased oxidative stress and metabolic stress, which could cause TL shortening (Hung et al., 2010, Toboła-Wróbel et al., 2020). In other words, although pregnancy itself would not be the direct cause of this shortening, it could be the trigger for all the processes that occur during pregnancy. In any case, it is important to keep in mind that pregnancy can be associated with specific disorders or health conditions, such as gestational diabetes (Zhu and Zhang, 2016) or hypertension (Regitz-Zagrosek et al., 2018), that could generate or enhance cellular stress. Another study by Martens et al. (2021) linked a higher TL in the mother with a lower telomere attrition in their offspring. Thus, another interesting question is whether the TL shortening observed in oocytes (this study) will have repercussions on the offspring's TL (Martens et al., 2021). Although, according to the literature, telomeres lengthen during the early stages of embryonic development, particularly at the blastocyst stage, and not during the early stages of embryonic development (Liu et al., 2007) this would ensure the TL of the species (Martínez and Blasco, 2017).

The study of telomere shortening in these groups in GCs evidenced changes in the primordial and primary follicular stages. Interestingly, these changes were only observed in the young group, but not in the middle-aged group. Worse telomere maintenance or more drastic telomere impairment was detected in the GCs of young pregnant women compared to their control group of non-pregnant women. This result was unexpected and could be due to the low number of pregnant women in this group (4 women). It is essential to say that telomere shortening happens more rapidly in the early stages of life (Zeichner et al., 1999) compared to older ages (Canela et al., 2007). However, whether telomere shortening in GCs of pregnant young women may occur faster than that of pregnant middle-aged women is a question that we cannot certainly answer from the results of this study. A larger number of samples should be analyzed to properly address this point. Other possible explanations could be cumulative telomere damage from previous pregnancies or a high variability in this older population. Although published studies point to a restoring effect and damage reversal during postpartum

(Michaeli et al., 2015, Ross et al., 2020), as occurs with AMH levels (Köninger et al., 2013). In the secondary stage, the GCs show no changes in the young or the middle-aged group. One of the reasons could be that in this follicular stage, TA was higher, and could compensate for the telomere shortening caused by pregnancy. Finally, the TCs were studied, which despite being part of the ovarian follicles, their division rate is lower than in GCs. In the group of young pregnant women, a lower mean TL and a lower percentage of long telomeres were detected in these cells. Although they have low TA, telomerase could be responsible for the lengthening of critically short telomeres to prevent cellular senescence (Hemann et al., 2001), and for that reason, this parameter would not be affected. In these cells, there were no differences in the middle-aged pregnant population.

Therefore, although telomere shortening during pregnancy was detected in oocytes, primordial and primary GCs, and TCs, it is unknown whether this shortening is temporary and reversible. Ideally, one should look at these parameters in the same women in pregnancy and after some time postpartum. In the same way that AMH is restored after delivery, something similar could occur at the telomere level or at least a partial recovery of TL associated with hormonal changes. Still, it is important to note that the control group used consisted of women of the same age with optimal ovarian function, since they all had high levels of AMH, and based on the above result.

6.4 Impact of COVID-19 disease on reproduction and the telomere pathway

This analysis, extracted from Project 2, examined the potential impact of COVID-19 on the telomere pathway in ovarian somatic cells, which have been associated with ovarian failure (Butts et al., 2009, Xu et al., 2017) and aging (Kohlrausch et al., 2021), as well as the subsequent effects on reproductive outcomes prior to the administration of vaccination.

TL was found to be similar in women with mild COVID-19 and the control group, suggesting that the disease did not significantly alter telomere biology in these individuals, as evidenced in both GCs and PBMCs. This finding aligns with previous reports indicating that telomere maintenance remains unchanged in PBMCs of individuals with mild COVID-19 (Dos Santos et al., 2021, Sanchez-Vazquez et al., 2021). The TL of GCs was preserved within our cohort of women of reproductive age, likely due to the TA present in these cells (Liu and Zhu, 2003, Wang et al., 2014, Xu et al., 2017), which may delay telomere attrition (Flores et al., 2008, Tümpel and Rudolph, 2012). These cells also exhibit a unique telomere and epigenetic profile, distinct from that of other somatic cells (Lara-Molina et al., 2020, Olsen et al., 2020). Consistent with these findings, the percentage of short telomeres was comparable between the control

and mild COVID groups, potentially reflecting the elongating effects of telomerase on shorter telomeres (Prescott and Blackburn, 2000). However, differences in telomere biology were observed between the control and severe COVID-19 groups, with the latter exhibiting a reduced average TL in GCs. This result is consistent with studies reporting telomere shortening in PBMCs of COVID-19 survivors (Mongelli et al., 2021). The observed reduction in mean TL in the severe COVID group was attributed to a decrease in the percentage of long telomeres, a phenomenon also observed in PBMCs of individuals with severe COVID-19 (Sanchez-Vazquez et al., 2021). Longer telomeres are beneficial for the organism, contributing to increased lifespan, improved metabolic aging (Muñoz-Lorente et al., 2019) and enhanced tissue regeneration (Varela et al., 2016). Moreover, cumulus cells, which surround the oocyte in mature follicles, are derived from GCs and possess very long telomeres, even longer than those found in PBMCs (Lara-Molina et al., 2020).

In terms of fertility, reproductive outcomes were similar between the control and mild COVID groups, consistent with previous studies suggesting that asymptomatic or mildly symptomatic COVID-19 patients do not experience ovarian dysfunction (Bentov et al., 2021, Wang et al., 2021b, Hu et al., 2024). In contrast, the oocyte maturation rate was lower in the severe COVID group, despite comparable ovarian reserve to the control group. These results corroborate the findings of Castiglioni et al. (2024), who reported a reduced number of mature oocytes in COVID-19 patients compared to non-infected or vaccinated women (Castiglione Morelli et al., 2024). Given that human cumulus cells express low levels of TMPRSS2, it is less likely for the virus to infect these cells at later stages of folliculogenesis (Stanley et al., 2020). Therefore, if the reduced oocyte maturation rate observed in the severe COVID group was directly related to viral infection, it would likely have occurred during earlier stages of follicular development in GCs.

A lower number of mature oocytes can reduce the potential for successful embryo generation. This may not significantly affect fertility outcomes in younger individuals, as hormone stimulation typically yields a strong response (Polonio et al., 2020). Additionally, higher estrogen levels in younger women may exert a protective effect against COVID-19 (Stelzig et al., 2020). However, in older women, a lower number of mature oocytes could present a challenge, as fewer oocytes are retrieved after stimulation, and the rate of aneuploidy increases (Franasiak et al., 2014), making it more challenging to generate healthy embryos for transfer. Notably, except the study by Eckstein et al. (2024), which identified an increased risk of miscarriage in women infected with SARS-CoV-2 (Eckstein et al., 2024), no significant impact of COVID-19 infection on ART outcomes has been reported (Ovalı, 2020, Kyle et al., 2020, Hu et al., 2024, Huang et al., 2023, Rageh et al., 2023). Recent studies suggest that

vaccination does not adversely affect reproductive outcomes following ART (Chamani et al., 2024, Eckstein et al., 2024).

Our findings suggest a potential role for long telomeres in follicular maturation. Supporting this hypothesis, the oocyte maturation rate was positively correlated with the TL of GCs in the control group. Longer telomeres in GCs may enhance follicular maturation by providing greater division potential to these cells, as demonstrated in porcine follicles (Russo et al., 2006). Additionally, as previously discussed, shorter telomeres in GCs are observed in women with ovarian insufficiency (Butts et al., 2009, Xu et al., 2017). However, further investigation is requested to explore this observation in greater detail.

Taken together, our findings suggest that SARS-CoV-2 does not significantly affect the telomere pathway or fertility outcomes in COVID-19 patients, except in severe cases, in agreement with previous research. Considering the emergence of two SARS-CoV viruses within a relatively short timeframe (2003 and 2019) (Peiris et al., 2004), and recognizing that the ovary may be susceptible to alterations in severe cases, it may be prudent to reconsider ART protocols for patients in the event of a new viral outbreak. Some studies have proposed a dual trigger strategy (hCG and GnRH agonist) to enhance oocyte maturation in patients with previously low maturation rates (Fabris et al., 2017, Griffin et al., 2014). Another potential strategy for these patients is in vitro oocyte maturation (Chang et al., 2014), though this approach is not routinely employed.

Regarding limitations, this work was an observational pilot study with a limited number of women, recruited before and during the early establishment of the COVID-19 vaccination protocols in Spain.

CONCLUSIONS

7 CONCLUSIONS

The conclusions drawn from the results of Project 1 were:

1) Among the hormones studied in the women recruited for Project 1, AMH and estradiol levels decreased as age increased, while FSH and LH levels decreased age-relatedly.
2) Our results showed that the telomere length of oocytes during the studied folliculogenesis stages did not change. The mean telomere length of granulosa cells increased during the first stages of folliculogenesis. In contrast, the mean telomere length of theca cells remained stable during the stages of folliculogenesis analyzed in this work.
3) The mean telomere length of oocytes was lower in the middle-aged group compared with the younger group. The mean telomere length of granulosa cells decreased with age in primordial and primary follicles and was maintained in secondary follicles. The mean telomere length of theca cells was shorter in the older group of women analyzed in this work. The mean telomere length of the stroma remained constant during aging.
4) Telomerase activity was detected in the ovarian fragments of women of all age groups, and the levels were similar in all age groups.
5) The measurements of telomere length in peripheral blood mononuclear cells from women included in Project 1 showed telomere attrition related to age, noticeable in the oldest group, and an accumulation of short telomeres with age, reinforcing that telomere attrition is a bona fide marker of aging. However, our results suggested that the telomere parameters of these cells cannot be used as biomarkers of ovarian aging.
6) The percents of fibrotic area showed a statistically significant increase in the ovary from older women and a statistically significant positive correlation with age. However, the expression of the genes TGF-β1, COL1A1, and COL3A1 did not vary with age in the ovarian samples analyzed. Proteomic analysis showed that more biological processes were altered in the older group. These processes were related to biological stress and damage, metabolism and energy production, cell cycle and tissue homeostasis, cell structure and integrity, and cell signalling process.
7) The mean systemic telomere length did not differ according to the AMH values in any age group studied. Mean telomere length did not show differences in the different ovarian cell types according to the AMH level in any groups studied, except for the percentage of short telomeres in oocytes in middle-aged women, with an increase of this parameter in the lower AMH group. Theca cells showed lower telomere length in middle-aged women with low AMH.

8) Pregnancy did not affect the mean telomere length in peripheral blood mononuclear cells and stromal ovarian cells. However, telomere maintenance was impaired in oocytes from pregnant young and middle-aged women. Specifically, the mean telomere length of the primordial and primary granulosa and theca cells was shorter in young pregnant women than in non-pregnant women of the same age at the time of the pregnancy analyzed.

The conclusions drawn from the results of Project 2 were:

9) Telomere length was similar in granulosa cells and peripheral blood mononuclear cells of control and mild cases of COVID-19 cases. However, in severe COVID-19 cases, the mean telomere length was lower compared to controls.
10) The total number of oocytes retrieved after ovarian stimulation and the oocyte maturation rate in control and COVID-19 cases were similar. However, the severe COVID-19 cases showed a lower oocyte maturation rate than controls.
11) There was a positive statistically significant correlation between the mean telomere length of granulosa cells and the maturation rate of oocytes in control individuals. This correlation was not observed in the COVID-19 cases.

8 REFERENCES

ADASHI, E. Y. 1994. Endocrinology of the ovary. *Human Reproduction,* 9**,** 815-27.

AGARWAL, A., BASKARAN, S., PAREKH, N., CHO, C.-L., HENKEL, R., VIJ, S., ARAFA, M., SELVAM, M. K. P. & SHAH, R. 2021. Male infertility. *The Lancet,* 397**,** 319-333.

AHMED, W. & LINGNER, J. 2018. Impact of oxidative stress on telomere biology. *Differentiation,* 99**,** 21-27.

ALLSOPP, R. C., VAZIRI, H., PATTERSON, C., GOLDSTEIN, S., YOUNGLAI, E. V., FUTCHER, A. B., GREIDER, C. W. & HARLEY, C. B. 1992. Telomere length predicts replicative capacity of human fibroblasts. *Proceedings of the National Academy of Sciences of the United States of America,* 89**,** 10114-8.

ALPHONSE, N., WANFORD, J. J., VOAK, A. A., GAY, J., VENKHAYA, S., BURROUGHS, O., MATHEW, S., LEE, T., EVANS, S. L. & ZHAO, W. 2022. A family of conserved bacterial virulence factors dampens interferon responses by blocking calcium signaling. *Cell,* 185**,** 2354-2369. e17.

ALVIGGI, C., ANDERSEN, C. Y., BUEHLER, K., CONFORTI, A., DE PLACIDO, G., ESTEVES, S. C., FISCHER, R., GALLIANO, D., POLYZOS, N. P. & SUNKARA, S. K. 2016. A new more detailed stratification of low responders to ovarian stimulation: from a poor ovarian response to a low prognosis concept. *Fertility and Sterility,* 105**,** 1452-1453.

ANCELIN, K., BRUNORI, M., BAUWENS, S., KOERING, C.-E., BRUN, C., RICOUL, M., POMMIER, J.-P., SABATIER, L. & GILSON, E. 2002. Targeting assay to study the cis functions of human telomeric proteins: evidence for inhibition of telomerase by TRF1 and for activation of telomere degradation by TRF2. *Molecular Cellular Biology,* 22**,** 3474-3487.

ARTANDI, S. E., CHANG, S., LEE, S.-L., ALSON, S., GOTTLIEB, G. J., CHIN, L. & DEPINHO, R. A. 2000. Telomere dysfunction promotes non-reciprocal translocations and epithelial cancers in mice. *Nature,* 406**,** 641-645.

ATSMA, F., BARTELINK, M.-L. E., GROBBEE, D. E., RUTTEN, A., BOTS, M. L., PROKOP, M. & VAN DER SCHOUW, Y. T. 2008. Reproductive factors, metabolic factors, and coronary artery calcification in older women. *Menopause,* 15**,** 899-904.

AZZIZ, R. 2018. Polycystic ovary syndrome. *Obstetrics & Gynecology,* 132**,** 321-336.

BAKER, T. G. 1963. A Quantitative and Cytological Study of Germ Cells in Human Ovaries. *Proceedings of the Royal Society of London. Biological Sciences,* 158**,** 417-33.

BALMACEDA, J. P., BERNARDINI, L., CIUFFARDI, I., FELIX, C., ORD, T., SUELDO, C. E. & ASCH, R. H. 1994. Implantation: Oocyte donation in humans: a model to study the effect of age on embryo implantation rate. *Human Reproduction,* 9**,** 2160-2163.

BARHA, C. K., HANNA, C. W., SALVANTE, K. G., WILSON, S. L., ROBINSON, W. P., ALTMAN, R. M. & NEPOMNASCHY, P. A. 2016. Number of children and telomere length in women: a prospective, longitudinal evaluation. *PLOS ONE,* 11**,** e0146424.

BARNES, R. P., DE ROSA, M., THOSAR, S. A., DETWILER, A. C., ROGINSKAYA, V., VAN HOUTEN, B., BRUCHEZ, M. P., STEWART-ORNSTEIN, J. & OPRESKO, P. L. 2022. Telomeric 8-oxo-guanine drives rapid premature senescence in the absence of telomere shortening. *Nature Strcutural & Molecular Biology,* 29**,** 639-652.

BARRITT, J. A., COHEN, J. & BRENNER, C. A. 2000. Mitochondrial DNA point mutation in human oocytes is associated with maternal age. *Reproductive BioMedicine Online,* 1**,** 96-100.

BAYNE, S., JONES, M. E., LI, H. & LIU, J. P. 2007. Potential roles for estrogen regulation of telomerase activity in aging. *Annals of the New York Academy of Sciences,* 1114**,** 48-55.

BEHRINGER, R. R., FINEGOLD, M. J. & CATE, R. L. 1994. Müllerian-inhibiting substance function during mammalian sexual development. *Cell,* 79**,** 415-425.

BELCHETZ, P., PLANT, T., NAKAI, Y., KEOGH, E. & KNOBIL, E. 1978. Hypophysial responses to continuous and intermittent delivery of hypothalamic gonadotropin-releasing hormone. *Science,* 202**,** 631-633.

BEN-MEIR, A., BURSTEIN, E., BORREGO-ALVAREZ, A., CHONG, J., WONG, E., YAVORS KA, T., NARANIAN, T., CHI, M., WANG, Y. & BENTOV, Y. 2015. Coenzyme Q10 restores oocyte mitochondrial function and fertility during reproductive aging. *Aging Cell,* 14**,** 887-895.

BENETOS, A., LAI, T.-P., TOUPANCE, S., LABAT, C., VERHULST, S., GAUTIER, S., UNGEHEUER, M.-N., PERRET-GUILLAUME, C., LEVY, D. & SUSSER, E. 2021. The nexus between telomere length and lymphocyte count in seniors hospitalized with COVID-19. *The Journals of Gerontology: Series A,* 76**,** e97-e101.

BENTOV, Y., BEHARIER, O., MOAV-ZAFRIR, A., KABESSA, M., GODIN, M., GREENFIELD, C. S., KETZINEL-GILAD, M., ASH BRODER, E., HOLZER, H. E. & WOLF, D. 2021. Ovarian follicular function is not altered by SARS–CoV-2 infection or BNT162b2 mRNA COVID-19 vaccination. *Human Reproduction,* 36**,** 2506-2513.

BERNARDO, G., PRADO, M. A., DASHTMIAN, A. R., FAVARO, M., MAURI, S., BORSETTO, A., MARCHESAN, E., PAULO, J. A., GYGI, S. P., FINLEY, D. J. & ZIVIANI, E. 2024. USP14 inhibition enhances Parkin-independent mitophagy in iNeurons. *Pharmacological Research,* 210**,** 107484.

BESECKE, L. M., GUENDNER, M. J., SCHNEYER, A. L., BAUER-DANTOIN, A. C., JAMESON, J. L. & WEISS, J. 1996. Gonadotropin-releasing hormone regulates follicle-stimulating hormone-beta gene expression through an activin/follistatin autocrine or paracrine loop. *Endocrinology,* 137**,** 3667-3673.

BESONG, C., PHILIPPEAUX, S., BHAM, A., GUSTINVIL, N., CASTINE, A., VARRASSI, G., SUTKER, P., MILLER, B. C., BURROUGHS, C. R., GENNUSO, S., SHEKOOHI, S. & KAYE, A. D. 2024. Managing Menopause: The Evolving Role of Estrogens, Selective Serotonin Reuptake Inhibitors, and Phytoestrogens in Balancing Hormonal Fluctuations. *Cureus,* 16**,** e70440.

BETTS, D. H. & KING, W. A. 1999. Telomerase activity and telomere detection during early bovine development. *Developmental Genetics,* 25**,** 397-403.

BHOGAL, R. K., STOICA, C. M., MCGAHA, T. L. & BONA, C. A. 2005. Molecular Aspects of Regulation of Collagen Gene Expression in Fibrosis. *Journal of Clinical Immunology,* 25**,** 592-603.

BIANCHI, A. & SHORE, D. 2007. Increased association of telomerase with short telomeres in yeast. *Genes & Development,* 21**,** 1726-1730.

BICSAK, T. A., TUCKER, E. M., CAPPEL, S., VAUGHAN, J., RIVIER, J., VALE, W. & HSUEH, A. J. 1986. Hormonal regulation of granulosa cell inhibin biosynthesis. *Endocrinology,* 119**,** 2711-2719.

BIELANSKA-OSUCHOWSKA, Z. 2006. Oogenesis in pig ovaries during the prenatal period: ultrastructure and morphometry. *Reproductive Biology,* 6**,** 161-193.

BIRO, F. M., PAJAK, A., WOLFF, M. S., PINNEY, S. M., WINDHAM, G. C., GALVEZ, M. P., GREENSPAN, L. C., KUSHI, L. H. & TEITELBAUM, S. L. 2018. Age of Menarche in a Longitudinal US Cohort. *Journal of Pediatric and Adolescent Gynecology,* 31**,** 339-345.

BJÖRKBLOM, B., PADZIK, A., MOHAMMAD, H., WESTERLUND, N., KOMULAINEN, E., HOLLOS, P., PARVIAINEN, L., PAPAGEORGIOU, A. C., ILJIN, K. & KALLIONIEMI, O. 2012. c-Jun N-terminal kinase phosphorylation of MARCKSL1 determines actin stability and migration in neurons and in cancer cells. *Molecular Cellular Biology,* 32**,** 3513-3526.

BLACKBURN, E. H. 1991. Structure and function of telomeres. *Nature,* 350**,** 569-573.

BLACKBURN, E. H. & GALL, J. G. 1978. A tandemly repeated sequence at the termini of the extrachromosomal ribosomal RNA genes in Tetrahymena. *Journal of Molecular Biology,* 120**,** 33-53.

BLASCO, M. A., LEE, H.-W., HANDE, M. P., SAMPER, E., LANSDORP, P. M., DEPINHO, R. A. & GREIDER, C. W. 1997. Telomere shortening and tumor formation by mouse cells lacking telomerase RNA. *Cell,* 91**,** 25-34.

BLAUSTEIN, A. 1982. Anatomy and Histology of the Human Ovary. *In:* BLAUSTEIN, A. (ed.) *Pathology of the Female Genital Tract.* New York, NY: Springer New York.

BLOCK, E. 1952. Quantitative morphological investigations of the follicular system in women. *Acta Anatomica,* 14**,** 108-123.

BLOCK, E. 1953. A quantitative morphological investigation of the follicular system in newborn female infants. *Acta Anatomica,* 17**,** 201-206.

BLOKZIJL, F., DE LIGT, J., JAGER, M., SASSELLI, V., ROERINK, S., SASAKI, N., HUCH, M., BOYMANS, S., KUIJK, E. & PRINS, P. 2016. Tissue-specific mutation accumulation in human adult stem cells during life. *Nature,* 538**,** 260-264.

BLUMENFELD, Z. 2011. Fertility treatment in women with premature ovarian failure. *Expert Review of Obstetrics Gynecology,* 6**,** 321-330.

BONDY, S. C. & WU, M. 2024. The Critical Role of Autophagy and Phagocytosis in the Aging Brain. *International Journal of Molecular Sciences,* 26.

BRAKEDAL, B., DÖLLE, C., RIEMER, F., MA, Y., NIDO, G. S., SKEIE, G. O., CRAVEN, A. R., SCHWARZLMÜLLER, T., BREKKE, N. & DIAB, J. 2022. The NADPARK study: A randomized phase I trial of nicotinamide riboside supplementation in Parkinson's disease. *Cell Metabolism,* 34**,** 396-407. e6.

BRAR, A. K., FRANK, G. R., KESSLER, C. A., CEDARS, M. I. & HANDWERGER, S. 1997. Progesterone-dependent decidualization of the human endometrium is mediated by cAMP. *Endocrine,* 6**,** 301-307.

BRILEY, S. M., JASTI, S., MCCRACKEN, J. M., HORNICK, J. E., FEGLEY, B., PRITCHARD, M. T. & DUNCAN, F. E. 2016. Reproductive age-associated fibrosis in the stroma of the mammalian ovary. *Reproduction,* 152**,** 245-260.

BROEKMANS, F. J., DE ZIEGLER, D., HOWLES, C. M., GOUGEON, A., TREW, G. & OLIVENNES, F. 2010. The antral follicle count: practical recommendations for better standardization. *Fertility and Sterility,* 94**,** 1044-1051.

BROEKMANS, F. J., FADDY, M. J., SCHEFFER, G. & TE VELDE, E. R. 2004. Antral follicle counts are related to age at natural fertility loss and age at menopause. *Menopause,* 11**,** 607-614.

BROER, S. L., BROEKMANS, F. J., LAVEN, J. S. & FAUSER, B. C. 2014. Anti-Müllerian hormone: ovarian reserve testing and its potential clinical implications. *Human Reproduction Update,* 20**,** 688-701.

BROER, S. L., VAN DISSELDORP, J., BROEZE, K. A., DOLLEMAN, M., OPMEER, B. C., BOSSUYT, P., EIJKEMANS, M. J., MOL, B.-W. J. & BROEKMANS, F. J. 2013. Added value of ovarian reserve testing on patient characteristics in the prediction of ovarian response and ongoing pregnancy: an individual patient data approach. *Human Reproduction Update,* 19**,** 26-36.

BRZEZINSKI, A., SAADA, A., MILLER, H., BRZEZINSKI-SINAI, N. & BEN-MEIR, A. 2018. Is the aging human ovary still ticking?: Expression of clock-genes in luteinized granulosa cells of young and older women. *Journal of Ovarian Research,* 11**,** 1-4.

BULL, J. R., ROWLAND, S. P., SCHERWITZL, E. B., SCHERWITZL, R., DANIELSSON, K. G. & HARPER, J. 2019. Real-world menstrual cycle characteristics of more than 600,000 menstrual cycles. *NPJ Digital Medicine,* 2**,** 83.

BURGER, A. M. 2002. Standard TRAP assay. *Telomeres and Telomerase: Methods and Protocols***,** 109-124.

BÜSCHER, U., CHEN, F. C. K., KENTENICH, H. & SCHMIADY, H. 1999. Cytokines in the follicular fluid of stimulated and non-stimulated human ovaries; is ovulation a suppressed inflammatory reaction? *Human Reproduction,* 14**,** 162-166.

BUTLER, H. & JUMA, M. 1970. Oogenesis in an adult prosimian. *Nature,* 226**,** 552-553.

BUTTS, S., RIETHMAN, H., RATCLIFFE, S., SHAUNIK, A., COUTIFARIS, C. & BARNHART, K. 2009. Correlation of telomere length and telomerase activity with occult ovarian insufficiency. *The Journal of Clinical Endocrinology & Metabolism,* 94**,** 4835-43.

CALADO, R. T., YEWDELL, W. T., WILKERSON, K. L., REGAL, J. A., KAJIGAYA, S., STRATAKIS, C. A. & YOUNG, N. S. 2009. Sex hormones, acting on the TERT gene, increase telomerase activity in human primary hematopoietic cells. *The Journal of the American Society of Hematology,* 114**,** 2236-2243.

CALARCO, P. G., DONAHUE, R. & SZOLLOSI, D. 1972. Germinal vesicle breakdown in the mouse oocyte. *Journal of Cell Science,* 10**,** 369-385.

CANELA, A., VERA, E., KLATT, P. & BLASCO, M. A. 2007. High-throughput telomere length quantification by FISH and its application to human population studies. *Proceedings of the National Academy of Sciences of the United States of America,* 104**,** 5300-5305.

CANIPARI, R. 2000. Oocyte–granulosa cell interactions. *Human Reproduction Update,* 6**,** 279-289.

CAPALBO, A., HOFFMANN, E. R., CIMADOMO, D., MARIA UBALDI, F. & RIENZI, L. 2017. Human female meiosis revised: new insights into the mechanisms of chromosome segregation and aneuploidies from advanced genomics and time-lapse imaging. *Human Reproduction Update,* 23**,** 706-722.

CASTIGLIONE MORELLI, M. A., IULIANO, A., VIGGIANI, L., MATERA, I., PISTONE, A., SCHETTINI, S. C. A., COLUCCI, P. & OSTUNI, A. 2024. Redox Balance and Inflammatory Response in Follicular Fluids of Women Recovered by SARS-CoV-2 Infection or Anti-COVID-19 Vaccinated: A Combined Metabolomics and Biochemical Study. *International Journal of Molecular Sciences,* 25.

CELLI, G. B. & DE LANGE, T. 2005. DNA processing is not required for ATM-mediated telomere damage response after TRF2 deletion. *Nature Cell Biology,* 7**,** 712-718.

CESARE, A. J. & REDDEL, R. R. 2010. Alternative lengthening of telomeres: models, mechanisms and implications. *Nature Reviews Genetics,* 11**,** 319-330.

CHAMANI, I. J., TAYLOR, L. L., DADOUN, S. E., MCKENZIE, L. J., DETTI, L., OUELLETTE, L., MCCULLOH, D. H. & LICCIARDI, F. L. 2024. Coronavirus Disease 2019 (COVID-19) Vaccination and Assisted Reproduction Outcomes: A Systematic Review and Meta-analysis. *Obstetrics & Gynecology,* 143**,** 210-218.

CHAN, C., LIU, V., LAU, E., YEUNG, W., NG, E. & HO, P. 2005. Mitochondrial DNA content and 4977 bp deletion in unfertilized oocytes. *Molecular Human Reproduction,* 11**,** 843-846.

CHANG, E. & HARLEY, C. B. 1995. Telomere length and replicative aging in human vascular tissues. *Proceedings of the National Academy of Sciences of the United States of America,* 92**,** 11190-11194.

CHANG, E. M., SONG, H. S., LEE, D. R., LEE, W. S. & YOON, T. K. 2014. In vitro maturation of human oocytes: Its role in infertility treatment and new possibilities. *Clinical Experimental Reproductive Medicine,* 41**,** 41.

CHANG, S., MULTANI, A. S., CABRERA, N. G., NAYLOR, M. L., LAUD, P., LOMBARD, D., PATHAK, S., GUARENTE, L. & DEPINHO, R. A. 2004. Essential role of limiting telomeres in the pathogenesis of Werner syndrome. *Nature Genetics,* 36**,** 877-882.

CHEN, A. C., MARTIN, A. J., CHOY, B., FERNÁNDEZ-PEÑAS, P., DALZIELL, R. A., MCKENZIE, C. A., SCOLYER, R. A., DHILLON, H. M., VARDY, J. L. & KRICKER, A. 2015. A phase 3 randomized trial of nicotinamide for skin-cancer chemoprevention. *New England Journal of Medicine,* 373**,** 1618-1626.

CHEN, Y.-J., MAHIEU, N. G., HUANG, X., SINGH, M., CRAWFORD, P. A., JOHNSON, S. L., GROSS, R. W., SCHAEFER, J. & PATTI, G. J. 2016. Lactate metabolism is associated with mammalian mitochondria. *Nature Chemical Biology,* 12**,** 937-943.

CHENG, E.-H., CHEN, S.-U., LEE, T.-H., PAI, Y.-P., HUANG, L.-S., HUANG, C.-C. & LEE, M.-S. 2013. Evaluation of telomere length in cumulus cells as a potential biomarker of oocyte and embryo quality†. *Human Reproduction,* 28.

CHEON, K. W., LEE, H.-S., PARHAR, I. S. & KANG, I. S. 2001. Expression of the second isoform of gonadotrophin-releasing hormone (GnRH-II) in human endometrium throughout the menstrual cycle. *Molecular Human Reproduction,* 7**,** 447-452.

CHICO-SORDO, L., CORDOVA-ORIZ, I., POLONIO, A. M., LS, S. M., MEDRANO, M., GARCIA-VELASCO, J. A. & VARELA, E. 2021. Reproductive aging and telomeres: Are women and men equally affected? *Mechanisms of Ageing and Development,* 198**,** 111541.

CHIKASHIGE, Y., HARAGUCHI, T. & HIRAOKA, Y. 2007. Another way to move chromosomes. *Chromosoma,* 116**,** 497-505.

CHIN, L., ARTANDI, S. E., SHEN, Q., TAM, A., LEE, S.-L., GOTTLIEB, G. J., GREIDER, C. W. & DEPINHO, R. A. 1999. p53 deficiency rescues the adverse effects of telomere loss and cooperates with telomere dysfunction to accelerate carcinogenesis. *Cell,* 97**,** 527-538.

CHINTA, P., ANTONISAMY, B., MANGALARAJ, A. M., KUNJUMMEN, A. T. & KAMATH, M. S. 2021. POSEIDON classification and the proposed treatment options for groups 1 and 2: time to revisit? A retrospective analysis of 1425 ART cycles. *Human Reproduction,* 2021**,** hoaa070.

CHIWARE, T. M., VERMEULEN, N., BLONDEEL, K., FARQUHARSON, R., KIARIE, J., LUNDIN, K., MATSASENG, T. C., OMBELET, W. & TOSKIN, I. J. H. R. U. 2021. IVF and other ART in low-and middle-income countries: a systematic landscape analysis. 27**,** 213-228.

CHOI, S. K., VENETIS, C., LEDGER, W., HAVARD, A., HARRIS, K., NORMAN, R. J., JORM, L. R. & CHAMBERS, G. M. 2022. Population-wide contribution of medically assisted reproductive technologies to overall births in Australia: temporal trends and parental characteristics. *Human Reproduction,* 37**,** 1047-1058.

CLEMENTS, J., REYES, F., WINTER, J. & FAIMAN, C. 1976. Studies on human sexual development. III. Fetal pituitary and serum, and amniotic fluid concentrations of LH, CG, and FSH. *The Journal of Clinical Endocrinology & Metabolism,* 42**,** 9-19.

COLLA, S., ONG, D. S. T., OGOTI, Y., MARCHESINI, M., MISTRY, N. A., CLISE-DWYER, K., ANG, S. A., STORTI, P., VIALE, A. & GIULIANI, N. 2015. Telomere dysfunction drives aberrant hematopoietic differentiation and myelodysplastic syndrome. *Cancer Cell,* 27**,** 644-657.

CORTEZ, D., WANG, Y., QIN, J. & ELLEDGE, S. J. 1999. Requirement of ATM-dependent phosphorylation of brca1 in the DNA damage response to double-strand breaks. *Science,* 286**,** 1162-1166.

COX, C., THOMA, M., TCHANGALOVA, N., MBURU, G., BORNSTEIN, M., JOHNSON, C. & KIARIE, J. 2022. Infertility prevalence and the methods of estimation from 1990 to 2021: a systematic review and meta-analysis. *Human Reproduction,* 2022**,** hoac051.

COZZOLINO, M., ERGUN, Y., RISTORI, E., GARG, A., IMAMOGLU, G. & SELI, E. 2024. Disruption of mitochondrial unfolded protein response results in telomere shortening in mouse oocytes and somatic cells. *Aging (Albany NY),* 16**,** 2047-2060.

COZZOLINO, M. & SELI, E. 2022. Mitochondrial dysfunction caused by targeted deletion of Mfn1 does not result in telomere shortening in oocytes. *Zygote,* 30**,** 735-737.

CREIGHTON, H. B. & MCCLINTOCK, B. 1931. A correlation of cytological and genetical crossing-over in Zea mays. *Proceedings of the National Academy of Sciences of the United States of America,* 17**,** 492-497.

CRISTOFARI, G. & LINGNER, J. 2006. Telomere length homeostasis requires that telomerase levels are limiting. *The EMBO journal,* 25**,** 565-574.

DALLA BELLA, E., BERSANO, E., ANTONINI, G., BORGHERO, G., CAPASSO, M., CAPONNETTO, C., CHIÒ, A., CORBO, M., FILOSTO, M. & GIANNINI, F. 2021. The unfolded protein response in amyotrophic later sclerosis: results of a phase 2 trial. *Brain,* 144**,** 2635-2647.

DANIALI, L., BENETOS, A., SUSSER, E., KARK, J. D., LABAT, C., KIMURA, M., DESAI, K. K., GRANICK, M. & AVIV, A. 2013. Telomeres shorten at equivalent rates in somatic tissues of adults. *Nature Communications,* 4**,** 1597.

DE FELICI, M. 2013. Origin, migration, and proliferation of human primordial germ cells. *Oogenesis***,** 19-37.

DE LANGE, T. 2005a. Shelterin: the protein complex that shapes and safeguards human telomeres. *Genes & Development,* 19**,** 2100-2110.

DE LANGE, T. Telomere-related genome instability in cancer. Cold Spring Harbor symposia on quantitative biology, 2005b. Cold Spring Harbor Laboratory Press, 197-204.

DE VET, A., LAVEN, J. S., DE JONG, F. H., THEMMEN, A. P. & FAUSER, B. C. 2002. Antimüllerian hormone serum levels: a putative marker for ovarian aging. *Fertility and Sterility,* 77**,** 357-362.

DECKER, M. L., CHAVEZ, E., VULTO, I. & LANSDORP, P. M. 2009. Telomere length in Hutchinson-Gilford progeria syndrome. *Mechanisms of Ageing and Development,* 130**,** 377-383.

DEMANELIS, K., JASMINE, F., CHEN, L. S., CHERNOFF, M., TONG, L., DELGADO, D., ZHANG, C., SHINKLE, J., SABARINATHAN, M. & LIN, H. 2020. Determinants of telomere length across human tissues. *Science,* 369**,** eaaz6876.

DENIC, A., GLASSOCK, R. J. & RULE, A. D. 2016. Structural and functional changes with the aging kidney. *Advances in Chronic Kidney Disease,* 23**,** 19-28.

DIVALL, S. A. & RADOVICK, S. 2008. Pubertal development and menarche. *Annals of the New York Academy of Sciences,* 1135**,** 19-28.

DONATE, L. E. & BLASCO, M. A. 2011. Telomeres in cancer and ageing. *Philosophical Transactions of the Royal Society B: Biological Sciences,* 366**,** 76-84.

DOS SANTOS, G. A., PIMENTA, R., VIANA, N. I., GUIMARÃES, V. R., ROMÃO, P., CANDIDO, P., DE CAMARGO, J. A., HATANAKA, D. M., QUEIROZ, P. G. & TERUYA, A. 2021. Shorter leukocyte telomere length is associated with severity of COVID-19 infection. *Biochemistry Biophysics Reports,* 27**,** 101056.

DUFFY, D. M., KO, C., JO, M., BRANNSTROM, M. & CURRY, T. E., JR. 2018. Ovulation: Parallels With Inflammatory Processes. *Endocrine Reviews,* 40**,** 369-416.

DUKIC, J., JOHANN, A., HENNINGER, M. & EHLERT, U. 2024. Estradiol and progesterone from pregnancy to postpartum: a longitudinal latent class analysis. *Frontiers in Global Women's Health,* 5**,** 1428494.

DUNCAN, F. E., HORNICK, J. E., LAMPSON, M. A., SCHULTZ, R. M., SHEA, L. D. & WOODRUFF, T. K. 2012. Chromosome cohesion decreases in human eggs with advanced maternal age. *Aging Cell,* 11**,** 1121-1124.

DUNCAN, W. C. 2017. The corpus luteum and women's health. *The Life Cycle of the Corpus Luteum***,** 249-275.

DUNHAM, M. A., NEUMANN, A. A., FASCHING, C. L. & REDDEL, R. R. 2000. Telomere maintenance by recombination in human cells. *Nature Genetics,* 26**,** 447-450.

DURLINGER, A. L., KRAMER, P., KARELS, B., DE JONG, F. H., UILENBROEK, J. T. J., GROOTEGOED, J. A. & THEMMEN, A. P. 1999. Control of primordial follicle recruitment by anti-Mullerian hormone in the mouse ovary. *Endocrinology,* 140**,** 5789-5796.

ECKSTEIN, V., GLAß, K., LEßMANN, M. E., SCHAAR, J., KLIMOVA, A., WIMBERGER, P. & GOECKENJAN, M. 2024. Assisted reproduction after SARS-CoV-2-infection: results of a single-center cohort-study. *Archives of Gynecology and Obstetrics,* 309**,** 305-313.

EGUIZABAL, C., SHOVLIN, T. C., DURCOVA-HILLS, G., SURANI, A. & MCLAREN, A. 2009. Generation of primordial germ cells from pluripotent stem cells. *Differentiation,* 78**,** 116-123.

EISENHAUER, K. M., GERSTEIN, R. M., CHIU, C. P., CONTI, M. & HSUEH, A. J. 1997. Telomerase activity in female and male rat germ cells undergoing meiosis and in early embryos. *Biology of Reproduction,* 56**,** 1120-5.

ENDICOTT, S. J. 2024. Chaperone-mediated autophagy as a modulator of aging and longevity. *Frontiers in Aging,* 5**,** 1509400.

ERICKSON, B. 1966. Development and senescence of the postnatal bovine ovary. *Journal of Animal Science,* 25**,** 800-805.

ESCOBAR-MORREALE, H. F. 2018. Polycystic ovary syndrome: definition, aetiology, diagnosis and treatment. *Nature Reviews Endocrinology,* 14**,** 270-284.

ESPOSITO, M., COUTIFARIS, C. & BARNHART, K. 2002. A moderately elevated day 3 FSH concentration has limited predictive value, especially in younger women. *Human Reproduction,* 17**,** 118-123.

EVANS, G., DOBIAS, M., KING, G. & ARMSTRONG, D. 1981. Estrogen, androgen, and progesterone biosynthesis by theca and granulosa of preovulatory follicles in the pig. *Biology of Reproduction,* 25**,** 673-682.

FABRIS, A. M., CRUZ, M., LEGIDOS, V., IGLESIAS, C., MUÑOZ, M. & GARCÍA-VELASCO, J. 2017. Dual triggering with gonadotropin-releasing hormone agonist and standard dose human chorionic gonadotropin in patients with a high immature oocyte rate. *Reproductive Sciences,* 24**,** 1221-1225.

FADDY, M. & GOSDEN, R. 1996. Ovary and ovulation: a model conforming the decline in follicle numbers to the age of menopause in women. *Human Reproduction,* 11**,** 1484-1486.

FADDY, M., GOSDEN, R., GOUGEON, A., RICHARDSON, S. J. & NELSON, J. 1992. Accelerated disappearance of ovarian follicles in mid-life: implications for forecasting menopause. *Human Reproduction,* 7**,** 1342-1346.

FATHI, E., CHAROUDEH, H. N., SANAAT, Z. & FARAHZADI, R. 2019. Telomere shortening as a hallmark of stem cell senescence. *Stem Cell Investigation,* 6.

FEIJING, Z., SUN, Z., CHENG, L. & DONG, Y. 2024. Leptin Modulates Ovarian Granulosa Cell Apoptosis by Regulating Telomerase Activity and Telomere Length in Polycystic Ovary Syndrome. *Laboratory Investigation,* 105**,** 102169.

FENG, J., FUNK, W. D., WANG, S.-S., WEINRICH, S. L., AVILION, A. A., CHIU, C.-P., ADAMS, R. R., CHANG, E., ALLSOPP, R. C. & YU, J. 1995. The RNA component of human telomerase. *Science,* 269**,** 1236-1241.

FERRARETTI, A., LA MARCA, A., FAUSER, B., TARLATZIS, B., NARGUND, G. & GIANAROLI, L. 2011. ESHRE consensus on the definition of 'poor response'to ovarian stimulation for in vitro fertilization: the Bologna criteria. *Human Reproduction,* 26**,** 1616-1624.

FLEMING, R., SEIFER, D. B., FRATTARELLI, J. L. & RUMAN, J. 2015. Assessing ovarian response: antral follicle count versus anti-Müllerian hormone. *Reproductive BioMedicine Online,* 31**,** 486-496.

FLORES, I., CANELA, A., VERA, E., TEJERA, A., COTSARELIS, G. & BLASCO, M. A. 2008. The longest telomeres: a general signature of adult stem cell compartments. *Genes & Development,* 22**,** 654-667.

FOGL, C., MOHAMMED, F., AL-JASSAR, C., JEEVES, M., KNOWLES, T. J., RODRIGUEZ-ZAMORA, P., WHITE, S. A., ODINTSOVA, E., OVERDUIN, M. & CHIDGEY, M. 2016. Mechanism of intermediate filament recognition by plakin repeat domains revealed by envoplakin targeting of vimentin. *Nature Communications,* 7**,** 10827.

FOLCH, J., ASCOLI, I., LEES, M., MEATH, J. & LEBARON, F. 1951. Preparation of lipide extracts from brain tissue. *Journal of Biological Chemistry,* 191**,** 833-841.

FOLCH, J., LEES, M. & STANLEY, G. S. 1957. A simple method for the isolation and purification of total lipides from animal tissues. *Journal of Biological Chemistry,* 226**,** 497-509.

FORABOSCO, A. & SFORZA, C. 2007. Establishment of ovarian reserve: a quantitative morphometric study of the developing human ovary. *Fertility and Sterility,* 88**,** 675-683.

FRANASIAK, J. M., FORMAN, E. J., HONG, K. H., WERNER, M. D., UPHAM, K. M., TREFF, N. R. & SCOTT JR, R. T. 2014. The nature of aneuploidy with increasing age of the female partner: a review of 15,169 consecutive trophectoderm biopsies evaluated with comprehensive chromosomal screening. *Fertility and Sterility,* 101**,** 656-663. e1.

FREEMAN, E. W., SAMMEL, M. D., LIN, H., GRACIA, C. R. & KAPOOR, S. 2008. Symptoms in the menopausal transition: hormone and behavioral correlates. *Obstetrics & Gynecology,* 111**,** 127-36.

FU, J., JI, X., LIU, J., CHEN, X. & SHANG, H. 2022. Meta-analysis of the connection between Alzheimer disease and telomeres. *Alzheimer Disease & Associated Disorders* 36**,** 73-79.

GARCIA, D., BRAZAL, S., RODRIGUEZ, A., PRAT, A. & VASSENA, R. 2018. Knowledge of age-related fertility decline in women: A systematic review. *European Journal of Obstetrics, Gynecology and Reproductive Biology,* 230**,** 109-118.

GARCIA, M., DIETRICH, A., FREIXA, L., VINK, A., PONSA, M. & EGOZCUE, J. 1987. Development of the first meiotic prophase stages in human fetal oocytes observed by light and electron microscopy. *Human Genetics,* 77**,** 223-232.

GAYTAN, F., MORALES, C., BELLIDO, C., AGUILAR, E. & SANCHEZ-CRIADO, J. 1996. Proliferative activity in the different ovarian compartments in cycling rats estimated by the 5-bromodeoxyuridine technique. *Biology of Reproduction,* 54**,** 1356-1365.

GHOSH, T. S., SHANAHAN, F. & O'TOOLE, P. W. 2022. The gut microbiome as a modulator of healthy ageing. *Nature Reviews Gastroenterology & Hepatology,* 19**,** 565-584.

GILLER, A., ANDRAWUS, M., GUTMAN, D. & ATZMON, G. 2020. Pregnancy as a model for aging. *Ageing Research Reviews,* 62**,** 101093.

GINSBURG, M., SNOW, M. H. & MCLAREN, A. 1990. Primordial germ cells in the mouse embryo during gastrulation. *Development,* 110**,** 521-528.

GOTO, H., IWATA, H., TAKEO, S., NISINOSONO, K., MURAKAMI, S., MONJI, Y. & KUWAYAMA, T. 2013. Effect of bovine age on the proliferative activity, global DNA methylation, relative telomere length and telomerase activity of granulosa cells. *Zygote,* 21**,** 256-64.

GOUGEON, A. Human ovarian follicular development: from activation of resting follicles to preovulatory maturation. Annales d'endocrinologie, 2010. Elsevier, 132-143.

GRAY, K. E., SCHIFF, M. A., FITZPATRICK, A. L., KIMURA, M., AVIV, A. & STARR, J. R. 2014. Leukocyte telomere length and age at menopause. *Epidemiology,* 25**,** 139-146.

GREIDER, C. W. & BLACKBURN, E. H. 1985. Identification of a specific telomere terminal transferase activity in Tetrahymena extracts. *Cell,* 43**,** 405-413.

GRIFFIN, D., FEINN, R., ENGMANN, L., NULSEN, J., BUDINETZ, T. & BENADIVA, C. 2014. Dual trigger with gonadotropin-releasing hormone agonist and standard dose human chorionic gonadotropin to improve oocyte maturity rates. *Fertility and Sterility,* 102**,** 405-409.

GRISENDI, V., SPADA, E., ARGENTO, C., PLEBANI, M., MILANI, S., SERACCHIOLI, R., VOLPE, A. & LA MARCA, A. 2014. Age-specific reference values for serum FSH and estradiol levels throughout the reproductive period. *Gynecological Endocrinology,* 30**,** 451-455.

GROSBOIS, J., BAILIE, E. C., KELSEY, T. W., ANDERSON, R. A. & TELFER, E. E. 2023. Spatio-temporal remodelling of the composition and architecture of the human ovarian cortical extracellular matrix during in vitro culture. *Human Reproduction,* 38**,** 444-458.

GUAHMICH, N. L., MAN, L., WANG, J., ARAZI, L., KALLINOS, E., TOPPER-KROOG, A., GRULLON, G., ZHANG, K., STEWART, J. & SCHATZ-SIEMERS, N. 2023. Human theca arises from ovarian stroma and is comprised of three discrete subtypes. *Communications Biology,* 6**,** 7.

GUILLEMIN, R. 1967. Chemistry and physiology of hypothalamic releasing factors for gonadotrophins. *International Journal of Fertility,* 12**,** 359-367.

GUTIERREZ, C. G., RALPH, J. H., TELFER, E. E., WILMUT, I. & WEBB, R. 2000. Growth and antrum formation of bovine preantral follicles in long-term culture in vitro. *Biology of Reproduction,* 62**,** 1322-1328.

HAAHR, T., DOSOUTO, C., ALVIGGI, C., ESTEVES, S. C. & HUMAIDAN, P. 2019. Management strategies for POSEIDON groups 3 and 4. *Frontiers in Endocrinology,* 10**,** 614.

HAISENLEDER, D. J., DALKIN, A. C., ORTOLANO, G. A., MARSHALL, J. C. & SHUPNIK, M. A. 1991. A pulsatile gonadotropin-releasing hormone stimulus is required to increase transcription of the gonadotropin subunit genes: evidence for differential regulation of transcription by pulse frequency in vivo. *Endocrinology,* 128**,** 509-517.

HALE, G. E., ROBERTSON, D. M. & BURGER, H. G. 2014. The perimenopausal woman: endocrinology and management. *The Journal of Steroid Biochemistry Molecular Biology,* 142**,** 121-131.

HANNA, C. W., BRETHERICK, K. L., GAIR, J. L., FLUKER, M. R., STEPHENSON, M. D. & ROBINSON, W. P. 2009. Telomere length and reproductive aging. *Human Reproduction,* 24**,** 1206-1211.

HANSEN, K. R., HODNETT, G. M., KNOWLTON, N. & CRAIG, L. B. 2011. Correlation of ovarian reserve tests with histologically determined primordial follicle number. *Fertility and Sterility,* 95**,** 170-175.

HANSON, B. M., TAO, X., ZHAN, Y., KIM, J. G., KLIMCZAK, A. M., HERLIHY, N. S., SCOTT JR, R. T. & SELI, E. 2021. Shorter telomere length of white blood cells is associated with higher rates of aneuploidy among infertile women undergoing in vitro fertilization. *Fertility and Sterility,* 115**,** 957-965.

HAO, Y., LV, M., PENG, J., KUANG, D., ZHANG, Z., ZHANG, Z., WANG, T., YANG, B., WEI, Z., ZHOU, P., ZHANG, Z. & CAO, Y. 2023. Alteration of relative telomere length and telomerase reverse transcriptase expression in the granulosa cells of women during aging and assessment of in vitro fertilization outcomes. *Molecular Medicine Reports,* 28**,** 206.

HARLEY, C. B., FUTCHER, A. B. & GREIDER, C. W. 1990. Telomeres shorten during ageing of human fibroblasts. *Nature,* 345**,** 458-460.

HARRINGTON, L., MCPHAIL, T., MAR, V., ZHOU, W., OULTON, R., PROGRAM, A. E., BASS, M. B., ARRUDA, I. & ROBINSON, M. O. 1997. A mammalian telomerase-associated protein. *Science,* 275**,** 973-977.

HAYFLICK, L. 1965. The limited in vitro lifetime of human diploid cell strains. *Experimental Cell Research,* 37**,** 614-636.

HAYFLICK, L. & MOORHEAD, P. S. 1961. The serial cultivation of human diploid cell strains. *Experimental Cell Research,* 25**,** 585-621.

HE, H., WANG, Y., GUO, X., RAMCHANDANI, S., MA, J., SHEN, M.-F., GARCIA, D. A., DENG, Y., MULTANI, A. S. & YOU, M. J. 2009. Pot1b deletion and telomerase haploinsufficiency in mice initiate an ATR-dependent DNA damage response and elicit phenotypes resembling dyskeratosis congenita. *Molecular Cellular Biology,* 29**,** 229-240.

HEHENKAMP, W. J., LOOMAN, C. W., THEMMEN, A. P., DE JONG, F. H., TE VELDE, E. R. & BROEKMANS, F. J. 2006. Anti-Müllerian hormone levels in the spontaneous menstrual cycle do not show substantial fluctuation. *The Journal of Clinical Endocrinology & Metabolism,* 91**,** 4057-63.

HEMANN, M. T., STRONG, M. A., HAO, L.-Y. & GREIDER, C. W. 2001. The shortest telomere, not average telomere length, is critical for cell viability and chromosome stability. *Cell,* 107**,** 67-77.

HERBERT, B.-S., HOCHREITER, A. E., WRIGHT, W. E. & SHAY, J. W. 2006. Nonradioactive detection of telomerase activity using the telomeric repeat amplification protocol. *Nature Protocols,* 1**,** 1583-1590.

HOEK, A., SCHOEMAKER, J. & DREXHAGE, H. 1997. Premature ovarian failure and ovarian autoimmunity. *Endocrine Reviews,* 18**,** 107-134.

HOMA, S., CARROLL, J. & SWANN, K. 1993. Fertilization and early embryology: The role of calcium in mammalian oocyte maturation and egg activation. *Human Reproduction,* 8**,** 1274-1281.

HONDA, A., HIROSE, M., HARA, K., MATOBA, S., INOUE, K., MIKI, H., HIURA, H., KANATSU-SHINOHARA, M., KANAI, Y. & KONO, T. 2007. Isolation, characterization, and in vitro and in vivo differentiation of putative thecal stem cells. *Proceedings of the National Academy of Sciences of the United States of America,* 104**,** 12389-12394.

HORN, M. A. & TRAFFORD, A. W. 2016. Aging and the cardiac collagen matrix: Novel mediators of fibrotic remodelling. *Journal of Molecular and Cellular Cardiology,* 93**,** 175-185.

HOSHINO, T., MUKAI, A., YAMASHITA, H., MISAWA, H., URUSHITANI, M., TASHIRO, Y., MATSUZAWA, S. I. & TAKAHASHI, R. 2024. NDRG1 upregulation by ubiquitin proteasome system dysfunction aggravates neurodegeneration. *Molecular Brain,* 17**,** 77.

HU, X., FENG, G., CHEN, Q., SANG, Y., CHEN, Q., WANG, S., LIU, S., BAI, L. & ZHU, Y. 2024. The impact and inflammatory characteristics of SARS-CoV-2 infection during ovarian stimulation on the outcomes of assisted reproductive treatment. *Frontiers in Endocrinology,* 15**,** 1353068.

HUANG, J., LIU, Y., XIA, L., ZHAO, Y., TIAN, L., XU, D., SU, Q., HU, Y., XIE, Q., CHEN, J., LI, Y., AI, X., WANG, J. & WU, Q. 2023. Effect of prior female SARS-CoV-2 infection on IVF outcomes: a prospective cohort study. *Frontiers in Endocrinology,* 14**,** 1239903.

HUGHES, C. S., FOEHR, S., GARFIELD, D. A., FURLONG, E. E., STEINMETZ, L. M. & KRIJGSVELD, J. 2014. Ultrasensitive proteome analysis using paramagnetic bead technology. *Molecular Systems Biology,* 10**,** 757.

HUMMITZSCH, K., HATZIRODOS, N., MACPHERSON, A. M., SCHWARTZ, J., RODGERS, R. J. & IRVING-RODGERS, H. F. 2019. Transcriptome analyses of ovarian stroma: tunica albuginea, interstitium and theca interna. *Reproduction,* 157**,** 545-565.

HUNG, T.-H., LO, L.-M., CHIU, T.-H., LI, M.-J., YEH, Y.-L., CHEN, S.-F. & HSIEH, T. S.-T. A. 2010. A longitudinal study of oxidative stress and antioxidant status in women with uncomplicated pregnancies throughout gestation. *Reproductive Sciences,* 17**,** 401-409.

ILIODROMITI, S., KELSEY, T. W., WU, O., ANDERSON, R. A. & NELSON, S. M. 2014. The predictive accuracy of anti-Müllerian hormone for live birth after assisted conception: a systematic review and meta-analysis of the literature. *Human Reproduction Update,* 20**,** 560-570.

ISSARA-AMPHORN, J., SJOELUND, V. H., SMELKINSON, M., MONTALVO, S., YOON, S. H., MANES, N. P. & NITA-LAZAR, A. 2023. Myristoylated, alanine-rich C-kinase substrate (MARCKS) regulates toll-like receptor 4 signaling in macrophages. *Scientific Reports,* 13**,** 19562.

IWAMA, H., OHYASHIKI, K., OHYASHIKI, J. H., HAYASHI, S., YAHATA, N., ANDO, K., TOYAMA, K., HOSHIKA, A., TAKASAKI, M. & MORI, M. J. H. G. 1998. Telomeric length and telomerase activity vary with age in peripheral blood cells obtained from normal individuals. 102**,** 397-402.

IWASE, A., HASEGAWA, Y., TSUKUI, Y., KOBAYASHI, M., HIRAISHI, H., NAKAZATO, T. & KITAHARA, Y. 2023. Anti-Müllerian hormone beyond an ovarian reserve marker: the relationship with the physiology and pathology in the life-long follicle development. *Frontiers in Endocrinology,* 14**,** 1273966.

IWATA, H. 2017. Age-associated changes in granulosa cells and follicular fluid in cows. *Journal of Reproduction Development,* 63**,** 339-345.

JASIENSKA, G. 2009. Reproduction and lifespan: Trade-offs, overall energy budgets, interge nerational costs, and costs neglected by research. *American Journal of Human Biology: The Official Journal of the Human Biology Association,* 21**,** 524-532.

JASKELIOFF, M., MULLER, F. L., PAIK, J.-H., THOMAS, E., JIANG, S., ADAMS, A. C., SAHIN, E., KOST-ALIMOVA, M., PROTOPOPOV, A. & CADINANOS, J. 2011. Telomerase reactivation reverses tissue degeneration in aged telomerase-deficient mice. *Nature,* 469**,** 102-106.

JEON, J., JANG, S., PARK, K. S., KIM, H. G., LEE, J., HWANG, T. S., KOH, J. S. & KIM, J. 2024. Identification of differentially expressed miRNAs involved in vascular aging reveals pathways associated with the endocrine hormone regulation. *Biogerontology,* 26**,** 23.

JEPPESEN, J., ANDERSON, R., KELSEY, T., CHRISTIANSEN, S. L., KRISTENSEN, S., JAYAPRAKASAN, K., RAINE-FENNING, N., CAMPBELL, B. & YDING ANDERSEN, C. 2013. Which follicles make the most anti-Müllerian hormone in humans? Evidence for an abrupt decline in AMH production at the time of follicle selection. *Molecular Human Reproduction,* 19**,** 519-527.

KALMBACH, K. H., FONTES ANTUNES, D. M., DRACXLER, R. C., KNIER, T. W., SETH-SMITH, M. L., WANG, F., LIU, L. & KEEFE, D. L. 2013. Telomeres and human reproduction. *Fertility and Sterility,* 99**,** 23-29.

KANAMORI, M., OIKAWA, K., TANEMURA, K. & HARA, K. 2019. Mammalian germ cell migration during development, growth, and homeostasis. *Reproductive Medicine and Biology,* 18**,** 247-255.

KAPETANAKI, M. G., MORA, A. L. & ROJAS, M. 2013. Influence of age on wound healing and fibrosis. *The Journal of Pathology,* 229**,** 310-322.

KAPLAN, S. L. & GRUMBACH, M. M. 1976. The ontogenesis of human foetal hormones. II. Luteinizing hormone (LH) and follicle stimulating hormone (FSH). *European Journal of Endocrinology,* 81**,** 808-829.

KASAPOĞLU, I. & SELI, E. 2020. Mitochondrial dysfunction and ovarian aging. *Endocrinology,* 161**,** bqaa001.

KAUL, Z., CESARE, A. J., HUSCHTSCHA, L. I., NEUMANN, A. A. & REDDEL, R. R. 2012. Five dysfunctional telomeres predict onset of senescence in human cells. *EMBO Reports,* 13**,** 52-59.

KAYACıK GÜNDAY, Ö., ÖZDEMIR ERDOĞAN, M., PEHLIVAN, A. & YıLMAZER, M. 2022. The effect of metformin treatment on leukocyte telomere length in patients with polycystic ovary syndrome: a prospective case-control study. *Journal of Assisted Reproduction and Genetics,* 39**,** 2153-2161.

KEEFE, D. L., MARQUARD, K. & LIU, L. 2006. The telomere theory of reproductive senescence in women. *Current Opinion in Obstetrics and Gynecology,* 18**,** 280-5.

KEEFE, D. L., NIVEN-FAIRCHILD, T., POWELL, S. & BURADAGUNTA, S. 1995. Mitochondrial deoxyribonucleic acid deletions in oocytes and reproductive aging in women. *Fertility and Sterility,* 64**,** 577-583.

KHAZAEI MONFARED, Y., HEIDARI, P., KLEMPNER, S. J., MAHMOOD, U., PARIKH, A. R., HONG, T. S., STRICKLAND, M. R. & ESFAHANI, S. A. 2023. DNA Damage by Radiopharmaceuticals and Mechanisms of Cellular Repair. *Pharmaceutics,* 15.

KIM, N. W., PIATYSZEK, M. A., PROWSE, K. R., HARLEY, C. B., WEST, M. D., HO, P. L., COVIELLO, G. M., WRIGHT, W. E., WEINRICH, S. L. & SHAY, J. W. 1994. Specific association of human telomerase activity with immortal cells and cancer. *Science,* 266**,** 2011-2015.

KIM, N. W. & WU, F. 1997. Advances in quantification and characterization of telomerase activity by the telomeric repeat amplification protocol (TRAP). *Nucleic Acids Research,* 25**,** 2595-2597.

KINNEAR, H. M., TOMASZEWSKI, C. E., CHANG, F. L., MORAVEK, M. B., XU, M., PADMANABHAN, V. & SHIKANOV, A. 2020. The ovarian stroma as a new frontier. *Reproduction,* 160**,** R25-R39.

KINUGAWA, C., MURAKAMI, T., OKAMURA, K. & YAJIMA, A. 2000. Telomerase activity in normal ovaries and premature ovarian failure. *The Tohoku Journal of Experimental Medicine,* 190**,** 231-238.

KOGURE, G. S., VERRUMA, C. G., SANTANA, B. A., CALADO, R. T., FERRIANI, R. A., FURTADO, C. L. M. & DOS REIS, R. M. 2024. Obesity contributes to telomere shortening in polycystic ovary syndrome. *Reproductive Sciences,* 31**,** 1601-1609.

KOHLRAUSCH, F. B., WANG, F., CHAMANI, I. & KEEFE, D. L. 2021. Telomere shortening and fusions: A link to aneuploidy in early human embryo development. *Obstetrical & Gynecological Survey,* 76**,** 429-436.

KÖNINGER, A., KAUTH, A., SCHMIDT, B., SCHMIDT, M., YERLIKAYA, G., KASIMIR-BAUER, S., KIMMIG, R. & BIRDIR, C. 2013. Anti-Mullerian-hormone levels during pregnancy and postpartum. *Reproductive Biology and Endocrinology,* 11**,** 60.

KRESOVICH, J. K., PARKS, C. G., SANDLER, D. P. & TAYLOR, J. A. 2018. Reproductive history and blood cell telomere length. *Aging (Albany NY),* 10**,** 2383.

KUIRI-HÄNNINEN, T., SANKILAMPI, U. & DUNKEL, L. 2014. Activation of the hypothalamic-pituitary-gonadal axis in infancy: minipuberty. *Hormone Research in Paediatrics,* 82**,** 73-80.

KUNDU, J., BAKSHI, S., JOSHI, H., BHADADA, S. K., VERMA, I. & SHARMA, S. 2020. Proteomic profiling of peripheral blood mononuclear cells isolated from patients with tuberculosis and diabetes copathogenesis-A pilot study. *PLOS ONE,* 15**,** e0233326.

KWEE, J., SCHATS, R., MCDONNELL, J., LAMBALK, C. & SCHOEMAKER, J. 2004. Intercycle variability of ovarian reserve tests: results of a prospective randomized study. *Human Reproduction,* 19**,** 590-595.

KYLE, M. H., GLASSMAN, M. E., KHAN, A., FERNANDEZ, C. R., HANFT, E., EMERUWA, U. N., SCRIPPS, T., WALZER, L., LIAO, G. V. & SASLAW, M. A review of newborn outcomes during the COVID-19 pandemic. Seminars in perinatology, 2020. Elsevier, 151286.

LA MARCA, A., GIULINI, S., ORVIETO, R., DE LEO, V. & VOLPE, A. 2005. Anti-Müllerian hormone concentrations in maternal serum during pregnancy. *Human Reproduction,* 20**,** 1569-72.

LA MARCA, A., STABILE, G., ARTENISIO, A. C. & VOLPE, A. 2006. Serum anti-Mullerian hormone throughout the human menstrual cycle. *Human Reproduction,* 21**,** 3103-7.

LADYMAN, S., AUGUSTINE, R. & GRATTAN, D. 2010. Hormone interactions regulating energy balance during pregnancy. *Journal of Neuroendocrinology,* 22**,** 805-817.

LAGIRAND-CANTALOUBE, J., CIABRINI, C., CHARRASSE, S., FERRIERES, A., CASTRO, A., ANAHORY, T. & LORCA, T. 2017. Loss of centromere cohesion in aneuploid human oocytes correlates with decreased kinetochore localization of the sac proteins Bub1 and Bubr1. *Scientific Reports,* 7**,** 44001.

LAKHAL, B., BRAHAM, R., BERGUIGUA, R., BOUALI, N., ZAOUALI, M., CHAIEB, M., VEITIA, R., SAAD, A. & ELGHEZAL, H. 2010. Cytogenetic analyses of premature ovarian failure using karyotyping and interphase fluorescence in situ hybridization (FISH) in a group of 1000 patients. *Clinical Genetics,* 78**,** 181-185.

LANDRY, D. A., VAISHNAV, H. T. & VANDERHYDEN, B. C. 2020. The significance of ovarian fibrosis. *Oncotarget,* 11**,** 4366-4370.

LANDRY, D. A., YAKUBOVICH, E., COOK, D. P., FASIH, S., UPHAM, J. & VANDERHYDEN, B. C. 2022. Metformin prevents age-associated ovarian fibrosis by modulating the immune landscape in female mice. *Science Advances,* 8**,** eabq1475.

LANE-CORDOVA, A. D., PUTERMAN, E., GUNDERSON, E. P., CHAN, C., HOU, L. & CARNETHON, M. 2017. Gravidity is not associated with telomere length in a biracial cohort of middle-aged women: The Coronary Artery Risk Development in Young Adults (CARDIA) study. *PLOS ONE,* 12**,** e0186495.

LARA-MOLINA, E. E., FRANASIAK, J. M., MARIN, D., TAO, X., DIAZ-GIMENO, P., FLORENSA, M., MARTIN, M., SELI, E. & PELLICER, A. 2020. Cumulus cells have longer telomeres than leukocytes in reproductive-age women. *Fertility and Sterility,* 113**,** 217-223.

LAVRANOS, T. C., MATHIS, J. M., LATHAM, S. E., KALIONIS, B., SHAY, J. W. & RODGERS, R. J. 1999. Evidence for ovarian granulosa stem cells: telomerase activity and localization of the telomerase ribonucleic acid component in bovine ovarian follicles. *Biology of Reproduction,* 61**,** 358-66.

LAWLOR, D. A., EMBERSON, J. R., EBRAHIM, S., WHINCUP, P. H., WANNAMETHEE, S. G., WALKER, M. & SMITH, G. D. 2003. Is the association between parity and coronary heart disease due to biological effects of pregnancy or adverse lifestyle risk factors associated with child-rearing? Findings from the British Women's Heart and Health Study and the British Regional Heart Study. *Circulation,* 107**,** 1260-1264.

LEFÈVRE, B. 2008. The nucleolus of the maternal gamete is essential for life. *BioEssays,* 30**,** 613-616.

LEUNG, P. C., CHENG, C. K. & ZHU, X.-M. 2003. Multi-factorial role of GnRH-I and GnRH-II in the human ovary. *Molecular and Cellular Endocrinology,* 202**,** 145-153.

LEVITZ, M. & YOUNG, B. K. 1978. Estrogens in pregnancy. *Vitamins and Hormones,* 35**,** 109-147.

LI, B., OESTREICH, S. & DE LANGE, T. 2000a. Identification of human Rap1: implications for telomere evolution. *Cell,* 101**,** 471-483.

LI, H., MAO, Y., XIONG, Y., ZHAO, H. H., SHEN, F., GAO, X., YANG, P., LIU, X. & FU, D. 2019. A comprehensive proteome analysis of peripheral blood mononuclear cells (PBMCs) to identify candidate biomarkers of pancreatic cancer. *Cancer Genomics and Proteomics,* 16**,** 81-89.

LI, Q., DU, J., FENG, R., XU, Y., WANG, H., SANG, Q., XING, Q., ZHAO, X., JIN, L., HE, L. & WANG, L. 2014. A possible new mechanism in the pathophysiology of polycystic ovary syndrome (PCOS): the discovery that leukocyte telomere length is strongly

associated with PCOS. *The Journal of Clinical Endocrinology & Metabolism,* 99**,** E234-40.

LI, S., TING, N. S., ZHENG, L., CHEN, P.-L., ZIV, Y., SHILOH, Y., LEE, E. Y.-H. & LEE, W.-H. 2000b. Functional link of BRCA1 and ataxia telangiectasia gene product in DNA damage response. *Nature,* 406**,** 210-215.

LI, Y., DENG, B., OUYANG, N., YUAN, P., ZHENG, L. & WANG, W. 2017. Telomere length is short in PCOS and oral contraceptive does not affect the telomerase activity in granulosa cells of patients with PCOS. *Journal of Assisted Reproduction and Genetics,* 34**,** 849-859.

LIN, J. & EPEL, E. 2022. Stress and telomere shortening: Insights from cellular mechanisms. *Ageing Research Reviews,* 73**,** 101507.

LIN, J., KROENKE, C. H., EPEL, E., KENNA, H. A., WOLKOWITZ, O. M., BLACKBURN, E. & RASGON, N. L. 2011. Greater endogenous estrogen exposure is associated with longer telomeres in postmenopausal women at risk for cognitive decline. *Brain Research,* 1379**,** 224-231.

LIND, A. K., WEIJDEGÅRD, B., DAHM-KÄHLER, P., MÖLNE, J., SUNDFELDT, K. & BRÄNNSTRÖM, M. 2006. Collagens in the human ovary and their changes in the perifollicular stroma during ovulation. *Acta Obstetricia et Gynecologica Scandinavica,* 85**,** 1476-1484.

LINGNER, J., HUGHES, T. R., SHEVCHENKO, A., MANN, M., LUNDBLAD, V. & CECH, T. R. 1997. Reverse transcriptase motifs in the catalytic subunit of telomerase. *Science,* 276**,** 561-567.

LIU, C., YANG, Q., FANG, G., LI, B. S., WU, D. B., GUO, W. J., HONG, S. S. & HONG, L. 2016. Collagen metabolic disorder induced by oxidative stress in human uterosacral ligament-derived fibroblasts: A possible pathophysiological mechanism in pelvic organ prolapse. *Molecular Medicine Reports,* 13**,** 2999-3008.

LIU, K., CHEN, Y., LIN, R. & HAN, K. 2020a. Clinical features of COVID-19 in elderly patients: A comparison with young and middle-aged patients. *Journal of Infection,* 80**,** e14-e18.

LIU, L., BAILEY, S. M., OKUKA, M., MUÑOZ, P., LI, C., ZHOU, L., WU, C., CZERWIEC, E., SANDLER, L. & SEYFANG, A. 2007. Telomere lengthening early in development. *Nature Cell Biology,* 9**,** 1436-1441.

LIU, L., BLASCO, M. A. & KEEFE, D. L. 2002a. Requirement of functional telomeres for metaphase chromosome alignments and integrity of meiotic spindles. *EMBO Reports*.

LIU, L., BLASCO, M. A., TRIMARCHI, J. R. & KEEFE, D. L. 2002b. An essential role for functional telomeres in mouse germ cells during fertilization and early development. *Developmental Biology,* 249**,** 74-84.

LIU, S., JIA, Y., MENG, S., LUO, Y., YANG, Q. & PAN, Z. 2023. Mechanisms of and potential medications for oxidative stress in ovarian granulosa cells: a review. *International Journal of Molecular Sciences,* 24**,** 9205.

LIU, T., HOU, K., LI, J., HAN, T., LIU, S. & WEI, J. 2024. Alzheimer's Disease and Aging Association: Identification and Validation of Related Genes. *The Journal of Prevention of Alzheimer's Disease,* 11**,** 196-213.

LIU, T., QIN, Q.-Y., QU, J.-X., WANG, H.-Y. & YAN, J. 2020b. Where are the theca cells from: the mechanism of theca cells derivation and differentiation. *Chinese Medical Journal,* 133**,** 1711-1718.

LIU, W. & ZHU, G. 2003. Expression of telomerase in human ovarian luteinized granulosa cells and its relationship to ovarian function. *Zhonghua Fu Chan Ke Za Zhi,* 38**,** 402-404.

LIVAK, K. J. & SCHMITTGEN, T. D. 2001. Analysis of relative gene expression data using real-time quantitative PCR and the 2(-Delta Delta C(T)) Method. *Methods,* 25**,** 402-8.

LIWOCHA, J., LI, J., PURSER, N., RATTANASOPA, C., MAIWALD, S., KRIST, D. T., SCOTT, D. C., STEIGENBERGER, B., PRABU, J. R. & SCHULMAN, B. A. 2024. Mechanism of millisecond Lys48-linked poly-ubiquitin chain formation by cullin-RING ligases. *Nature Structural and Molecular Biology,* 31**,** 378-389.

LLIBEROS, C., LIEW, S. H., ZAREIE, P., LA GRUTA, N. L., MANSELL, A. & HUTT, K. 2021. Evaluation of inflammation and follicle depletion during ovarian ageing in mice. *Scientific Reports,* 11**,** 278.

LOAYZA, D. & DE LANGE, T. 2003. POT1 as a terminal transducer of TRF1 telomere length control. *Nature,* 423**,** 1013-1018.

LOPEZ-OTIN, C., BLASCO, M. A., PARTRIDGE, L., SERRANO, M. & KROEMER, G. 2023. Hallmarks of aging: An expanding universe. *Cell,* 186**,** 243-278.

LÓPEZ-OTÍN, C., BLASCO, M. A., PARTRIDGE, L., SERRANO, M. & KROEMER, G. 2013. The hallmarks of aging. *Cell,* 153**,** 1194-1217.

LORIAUX, D., RUDER, H., KNAB, D. & LIPSETT, M. 1972. Estrone sulfate, estrone, estradiol and estriol plasma levels in human pregnancy. *The Journal of Clinical Endocrinology and Metabolism,* 35**,** 887-891.

LUDLOW, A. T., ROBIN, J. D., SAYED, M., LITTERST, C. M., SHELTON, D. N., SHAY, J. W. & WRIGHT, W. E. 2014. Quantitative telomerase enzyme activity determination using droplet digital PCR with single cell resolution. *Nucleic Acids Research,* 42**,** e104-e104.

MACIEJOWSKI, J. & DE LANGE, T. 2017. Telomeres in cancer: tumour suppression and genome instability. *Nature Reviews Molecular Cell Biology,* 18**,** 175-186.

MAIDARTI, M., CLARKSON, Y. L., MCLAUGHLIN, M., ANDERSON, R. A. & TELFER, E. E. 2019. Inhibition of PTEN activates bovine non-growing follicles in vitro but increases DNA damage and reduces DNA repair response. *Human Reproduction,* 34**,** 297-307.

MARTENS, D. S., VAN DER STUKKEN, C., DEROM, C., THIERY, E., BIJNENS, E. M. & NAWROT, T. S. 2021. Newborn telomere length predicts later life telomere length: Tracking telomere length from birth to child-and adulthood. *EBioMedicine,* 63.

MARTÍN-ROMERO, F. J., MIGUEL-LASOBRAS, E. M., DOMÍNGUEZ-ARROYO, J. A., GONZÁLEZ-CARRERA, E. & ÁLVAREZ, I. S. 2008. Contribution of culture media to oxidative stress and its effect on human oocytes. *Reproductive BioMedicine Online,* 17**,** 652-661.

MARTÍNEZ, P. & BLASCO, M. A. 2017. Telomere-driven diseases and telomere-targeting therapies. *Journal of Cell Biology,* 216**,** 875-887.

MARTINEZ, P., THANASOULA, M., CARLOS, A. R., GÓMEZ-LÓPEZ, G., TEJERA, A. M., SCHOEFTNER, S., DOMINGUEZ, O., PISANO, D. G., TARSOUNAS, M. & BLASCO, M. A. 2010. Mammalian Rap1 controls telomere function and gene expression through binding to telomeric and extratelomeric sites. *Nature Cell Biology,* 12**,** 768-780.

MARTÍNEZ, P., THANASOULA, M., MUÑOZ, P., LIAO, C., TEJERA, A., MCNEES, C., FLORES, J. M., FERNÁNDEZ-CAPETILLO, O., TARSOUNAS, M. & BLASCO, M. A. 2009. Increased telomere fragility and fusions resulting from TRF1 deficiency lead to degenerative pathologies and increased cancer in mice. *Genes and Development,* 23**,** 2060-2075.

MATHERS, C. D., STEVENS, G. A., BOERMA, T., WHITE, R. A. & TOBIAS, M. I. 2015. Causes of international increases in older age life expectancy. *The Lancet,* 385**,** 540-548.

MATHEWS, T. J. & HAMILTON, B. E. 2016. Mean age of mothers is on the rise: United States, 2000-2014. *NCHS Data Brief*, 1-8.

MATSUDA, K., KUROHAMA, H., KUWATSUKA, Y., IWANAGA, A., MUROTA, H. & NAKASHIMA, M. 2024. Detection of genome instability by 53BP1 expression as a long-lasting health effect in human epidermis surrounding radiation-induced skin cancers. *Journal of Radiation Rsearch,* 65**,** i57-i66.

MCCREDIE, S., AN, B., MCSHANE, M., LEDGER, W. & VENETIS, C. A. 2023. Serum anti-Müllerian hormone (AMH) concentration during pregnancy: a longitudinal study. *Reproduction and Fertility,* 4**,** e220128.

MCGEE, E. A. & HSUEH, A. J. 2000. Initial and cyclic recruitment of ovarian follicles. *Endocrine Reviews,* 21**,** 200-214.

MEENA, J. K., CERUTTI, A., BEICHLER, C., MORITA, Y., BRUHN, C., KUMAR, M., KRAU S, J. M., SPEICHER, M. R., WANG, Z. Q. & KESTLER, H. A. 2015. Telomerase abro gates aneuploidy-induced telomere replication stress, senescence and cell depletion. *The EMBO journal,* 34**,** 1371-1384.

MEIROW, D., DOR, J., KAUFMAN, B., SHRIM, A., RABINOVICI, J., SCHIFF, E., RAANANI, H., LEVRON, J. & FRIDMAN, E. 2007. Cortical fibrosis and blood-vessels damage in human ovaries exposed to chemotherapy. Potential mechanisms of ovarian injury. *Human Reproduction,* 22**,** 1626-1633.

MELZER, D., PILLING, L. C. & FERRUCCI, L. 2020. The genetics of human ageing. *Nature Reviews Genetics,* 21**,** 88-101.

MENDER, I. & SHAY, J. W. 2015. Telomerase repeated amplification protocol (TRAP). *Bio-Protocol,* 5**,** e1657-e1657.

MIAO, Z.-L., WANG, Z.-N., YANG, Y.-D., CHEN, L.-Q., CUI, R., WANG, X.-L. & OU, R.-Q. 2008. Role of TGF-β1 in the Formation of Ovarian Interstitial Fibrosis in PCOS Rat. *Journal of Reproduction and Contraception,* 19**,** 83-92.

MICHAELI, J., SMOOM, R., SERRUYA, N., EL AYOUBI, H., ROTSHENKER-OLSHINKA, K., SREBNIK, N., MICHAELI, O., ELDAR-GEVA, T. & TZFATI, Y. 2022. Leukocyte telomere length correlates with extended female fertility. *Cells,* 11**,** 513.

MICHAELI, T. F., BERGMAN, Y. & GIELCHINSKY, Y. 2015. Rejuvenating effect of pregnancy on the mother. *Fertility and Sterility,* 103**,** 1125-1128.

MIRANDA-FURTADO, C. L., LUCHIARI, H. R., PEDROSO, D. C. C., KOGURE, G. S., CAETANO, L. C., SANTANA, B. A., SANTANA, V. P., BENETTI-PINTO, C. L., REIS, F. M. & MACIEL, M. A. 2018. Skewed X-chromosome inactivation and shorter telomeres associate with idiopathic premature ovarian insufficiency. *Fertility and Sterility,* 110**,** 476-485. e1.

MITCHELL, A. M., KOWALSKY, J. M., EPEL, E. S., LIN, J. & CHRISTIAN, L. M. 2018. Childhood adversity, social support, and telomere length among perinatal women. *Psychoneuroendocrinology,* 87**,** 43-52.

MIYAMOTO, K., SATO, E. F., KASAHARA, E., JIKUMARU, M., HIRAMOTO, K., TABATA, H., KATSURAGI, M., ODO, S., UTSUMI, K. & INOUE, M. 2010. Effect of oxidative stress during repeated ovulation on the structure and functions of the ovary, oocytes, and their mitochondria. *Free Radical Biology and Medicine,* 49**,** 674-681.

MONGELLI, A., BARBI, V., GOTTARDI ZAMPERLA, M., ATLANTE, S., FORLEO, L., NESTA, M., MASSETTI, M., PONTECORVI, A., NANNI, S. & FARSETTI, A. 2021. Evidence for biological age acceleration and telomere shortening in COVID-19 survivors. *International Journal of Molecular Sciences,* 22**,** 6151.

MONNIAUX, D. 2016. Driving folliculogenesis by the oocyte-somatic cell dialog: Lessons from genetic models. *Theriogenology,* 86**,** 41-53.

MOR, G. & CARDENAS, I. 2010. The immune system in pregnancy: a unique complexity. *American Journal of Reproductive Immunology,* 63**,** 425-433.

MORALES, C., GARCÍA-PARDO, L., REYMUNDO, C., BELLIDO, C., SÁNCHEZ-CRIADO, J. E. & GAYTÁN, F. 2000. Different patterns of structural luteolysis in the human corpus luteum of menstruation. *Human Reproduction,* 15**,** 2119-2128.

MOTTA, P. M., MAKABE, S., NAGURO, T. & CORRER, S. 1994. Oocyte follicle cells association during development of human ovarian follicle. A study by high resolution scanning and transmission electron microscopy. *Archives of Histology and Cytology,* 57**,** 369-394.

MOYZIS, R. K., BUCKINGHAM, J. M., CRAM, L. S., DANI, M., DEAVEN, L. L., JONES, M. D., MEYNE, J., RATLIFF, R. L. & WU, J.-R. 1988. A highly conserved repetitive DNA sequence,(TTAGGG) n, present at the telomeres of human chromosomes. *Proceedings of the National Academy of Sciences of the United States of America,* 85**,** 6622-6626.

MUASHER, S. J., OEHNINGER, S., SIMONETTI, S., MATTA, J., ELLIS, L. M., LIU, H.-C., JONES, G. S. & ROSENWAKS, Z. 1988. The value of basal and/or stimulated serum gonadotropin levels in prediction of stimulation response and in vitro fertilization outcome. *Fertility and Sterility,* 50**,** 298-307.

MÜEZZINLER, A., ZAINEDDIN, A. K. & BRENNER, H. 2013. A systematic review of leukocyte telomere length and age in adults. *Ageing Research Reviews,* 12**,** 509-519.

MULLER, H. J. 1938. The remaking of chromosomes. *The Collecting Net,* 8**,** 198.

MÜNSTERBERG, A. & LOVELL-BADGE, R. 1991. Expression of the mouse anti-Müllerian hormone gene suggests a role in both male and female sexual differentiation. *Development,* 113**,** 613-624.

MUÑOZ-LORENTE, M. A., CANO-MARTIN, A. C. & BLASCO, M. A. 2019. Mice with hyper-long telomeres show less metabolic aging and longer lifespans. *Nature Communications,* 10**,** 4723.

NAKAGAWA, S. & FITZHARRIS, G. 2017. Intrinsically Defective Microtubule Dynamics Contribute to Age-Related Chromosome Segregation Errors in Mouse Oocyte Meiosis-I. *Current Biology,* 27**,** 1040-1047.

NARDO, L. G., CHRISTODOULOU, D., GOULD, D., ROBERTS, S. A., FITZGERALD, C. T. & LAING, I. 2007. Anti-Müllerian hormone levels and antral follicle count in women enrolled in in vitro fertilization cycles: relationship to lifestyle factors, chronological age and reproductive history. *Gynecological Endocrinology,* 23**,** 486-93.

NELSON, S. M., DAVIS, S. R., KALANTARIDOU, S., LUMSDEN, M. A., PANAY, N. & ANDERSON, R. A. 2023. Anti-Müllerian hormone for the diagnosis and prediction of menopause: a systematic review. *Human Reproduction Update,* 29**,** 327-346.

NELSON, S. M., PASTUSZEK, E., KLOSS, G., MALINOWSKA, I., LISS, J., LUKASZUK, A., PLOCIENNIK, L. & LUKASZUK, K. 2015. Two new automated, compared with two enzyme-linked immunosorbent, antimüllerian hormone assays. *Fertility and Sterility,* 104**,** 1016-1021. e6.

NELSON, S. M., SHAW, M., EWING, B. J., MCLEAN, K., VECHERY, A. & BRIGGS, S. F. 2024. Antimüllerian hormone levels are associated with time to pregnancy in a cohort study of 3,150 women. *Fertility and Sterility*.

NEUMANN, A. A., WATSON, C. M., NOBLE, J. R., PICKETT, H. A., TAM, P. P. & REDDEL, R. R. 2013. Alternative lengthening of telomeres in normal mammalian somatic cells. *Genes and Development,* 27**,** 18-23.

NO, C. O. 2014. Female age-related fertility decline. *Fertility and Sterility,* 101**,** 633-634.

NY, T., WAHLBERG, P. & BRÄNDSTRÖM, I. J. M. 2002. Matrix remodeling in the ovary: regulation and functional role of the plasminogen activator and matrix metalloproteinase systems. *Molecular and Cellular Endocrinology,* 187**,** 29-38.

OKAZAKI, R., OKAZAKI, T., SAKABE, K., SUGIMOTO, K., KAINUMA, R., SUGINO, A. & IWATSUKI, N. In vivo mechanism of DNA chain growth. Cold Spring Harbor Symposia on Quantitative Biology, 1968. Cold Spring Harbor Laboratory Press, 129-143.

OLOVNIKOV, A. M. 1973. A theory of marginotomy: the incomplete copying of template margin in enzymic synthesis of polynucleotides and biological significance of the phenomenon. *Journal of Theoretical Biology,* 41**,** 181-190.

OLSEN, K., CASTILLO-FERNANDEZ, J., ZEDELER, A., FREIESLEBEN, N. L. C., BUNGUM, M., CHAN, A., CARDONA, A., PERRY, J., SKOUBY, S. & BORUP, R. 2020. A distinctive epigenetic ageing profile in human granulosa cells. *Human Reproduction,* 35**,** 1332-1345.

OSTERMAN, M. J., HAMILTON, B. E., MARTIN, J. A., DRISCOLL, A. K. & VALENZUELA, C. P. 2022. Births: final data for 2020. *NCHS National Vital Statistics Reports*.

OVALı, F. 2020. SARS-CoV-2 infection and the newborn. *Frontiers in Pediatrics,* 8**,** 294.

OVEREEM, A. W., CHANG, Y. W., SPRUIT, J., ROELSE, C. M. & CHUVA DE SOUSA LOPES, S. M. 2021. Ligand–receptor interactions elucidate sex-specific pathways in the trajectory from primordial germ cells to gonia during human development. *Frontiers in Cell and Developmental Biology,* 9**,** 661243.

OZTURK, S., SOZEN, B. & DEMIR, N. 2014. Telomere length and telomerase activity during oocyte maturation and early embryo development in mammalian species. *Molecular Human Reproduction,* 20**,** 15-30.

PABUCCU, E., KAHRAMAN, K., TASKıN, S. & ATABEKOGLU, C. 2011. Unilateral absence of fallopian tube and ovary in an infertile patient. *Fertility and Sterility,* 96**,** e55-e57.

PALADINI, D. 2009. Sonography in obese and overweight pregnant women: clinical, medicolegal and technical issues. *Ultrasound in Obstetrics Gynecology: The Official Journal of the International Society of Ultrasound in Obstetrics and Gynecology,* 33**,** 720-729.

PANELLI, D. M., LEONARD, S. A., WONG, R. J., BECKER, M., MAYO, J. A., WU, E., GIRSEN, A. I., GOTLIB, I. H., AGHAEEPOUR, N. & DRUZIN, M. L. 2022. Leukocyte telomere dynamics across gestation in uncomplicated pregnancies and associations with stress. *BMC Pregnancy and Childbirth,* 22**,** 381.

PANG, W. W. & HARTMANN, P. E. 2007. Initiation of human lactation: secretory differentiation and secretory activation. *Journal of Mammary Gland Biology and Neoplasia,* 12**,** 211-221.

PARK, S. U., WALSH, L. & BERKOWITZ, K. M. 2021a. Mechanisms of ovarian aging. *Reproduction,* 162**,** R19-R33.

PARK, Y. M., JANKOWSKI, C. M., SWANSON, C. M., HILDRETH, K. L., KOHRT, W. M. & MOREAU, K. L. 2021b. Bone Mineral Density in Different Menopause Stages is Associated with Follicle Stimulating Hormone Levels in Healthy Women. *International Journal of Environmental Research and Public Health,* 18.

PASSOS, J. F., SARETZKI, G. & VON ZGLINICKI, T. 2007. DNA damage in telomeres and mitochondria during cellular senescence: is there a connection? *Nucleic Acids Research,* 35**,** 7505-7513.

PAUERSTEIN, C., EDDY, C., CROXATTO, H., HESS, R., SILER-KHODR, T. & CROXATTO, H. 1978. Temporal relationships of estrogen, progesterone, and luteinizing hormone levels to ovulation in women and infrahuman primates. *American Journal of Obstetrics and Gynecology,* 130**,** 876-886.

PAYNE, D., FLAHERTY, S. P., BARRY, M. F. & MATTHEWS, C. D. 1997. Preliminary observations on polar body extrusion and pronuclear formation in human oocytes using time-lapse video cinematography. *Human Reproduction,* 12**,** 532-541.

PEARL, R. & SCHOPPE, W. 1921. Studies on the physiology of reproduction in the domestic fowl. *Journal of Experimental Zoology,* 34**,** 101-118.

PEDROSO, D. C., MIRANDA-FURTADO, C. L., KOGURE, G. S., MEOLA, J., OKUKA, M., SILVA, C., CALADO, R. T., FERRIANI, R. A., KEEFE, D. L. & DOS REIS, R. M. 2015. Inflammatory biomarkers and telomere length in women with polycystic ovary syndrome. *Fertility and Sterility,* 103**,** 542-7.e2.

PEDROSO, D. C. C., SANTANA, V. P., DONAIRES, F. S., PICINATO, M. C., GIORGENON, R. C., SANTANA, B. A., PIMENTEL, R. N., KEEFE, D. L., CALADO, R. T., FERRIANI, R. A., FURTADO, C. L. M. & REIS, R. M. 2020. Telomere Length and Telomerase Activity in Immature Oocytes and Cumulus Cells of Women with Polycystic Ovary Syndrome. *Reproductive Sciences,* 27**,** 1293-1303.

PEIRIS, J. S. M., GUAN, Y. & YUEN, K. Y. 2004. Severe acute respiratory syndrome. *Nature Medicine,* 10**,** S88-S97.

PEPLING, M. E. & SPRADLING, A. C. 2001. Mouse ovarian germ cell cysts undergo programmed breakdown to form primordial follicles. *Developmental Biology,* 234**,** 339-351.

PEREDA, J., ZORN, T. & SOTO-SUAZO, M. 2006. Migration of human and mouse primordial germ cells and colonization of the developing ovary: an ultrastructural and cytochemical study. *Microscopy Research and Technique,* 69**,** 386-395.

PETERS, H., LEVY, E. & CRONE, M. 1962. Deoxyribonucleic acid synthesis in oocytes of mouse embryos. *Nature,* 195**,** 915-916.

PILLERON, S., ALQURINI, N., FERLAY, J., HAASE, K. R., HANNAN, M., JANSSEN-HEIJNEN, M., KANTILAL, K., KATANODA, K., KENIS, C. & LU-YAO, G. 2022. International trends in cancer incidence in middle-aged and older adults in 44 countries. *Journal of Geriatric Oncology,* 13**,** 346-355.

PINNA, S., PASELLA, S., DEIANA, M., BARALLA, A., MANNU, A., MASALA, A. G. E., PILERI, P. V., DEIANA, N., SCOGNAMILLO, F. & PALA, C. 2017. Proteomic analysis of human plasma and peripheral blood mononuclear cells in systemic lupus erythematosus patients. *Journal of Immunological Methods,* 446**,** 37-46.

POLLACK, A., RIVERS, K. & AHRENS, K. 2018. Parity associated with telomere length among US reproductive age women. *Human Reproduction,* 33**,** 736-744.

PÖLÖNEN, J., PINOLA, P., RONKAINEN, J., BLAKEMORE, A. I., BUXTON, J. L., TAPANAINEN, J. S., FRANKS, S., PILTONEN, T. T., SEBERT, S. & MORIN-PAPUNEN, L. 2022. Polycystic ovary syndrome and leukocyte telomere length: cross-sectional and longitudinal changes. *European Journal of Endocrinology,* 187**,** 651-661.

POLONIO, A. M., CHICO-SORDO, L., CORDOVA-ORIZ, I., MEDRANO, M., GARCIA-VELASCO, J. A. & VARELA, E. 2020. Impact of Ovarian Aging in Reproduction: From

Telomeres and Mice Models to Ovarian Rejuvenation. *Yale Journal of Biology and Medicine,* 93**,** 561-569.

POLONIO, A. M., MEDRANO, M., CHICO-SORDO, L., CÓRDOVA-ORIZ, I., COZZOLINO, M., MONTANS, J., HERRAIZ, S., SELI, E., PELLICER, A. & GARCÍA-VELASCO, J. A. 2023. Impaired telomere pathway and fertility in Senescence-Accelerated Mice Prone 8 females with reproductive senescence. *Aging (Albany NY),* 15**,** 4600.

PRESCOTT, J. C. & BLACKBURN, E. H. 2000. Telomerase RNA template mutations reveal sequence-specific requirements for the activation and repression of telomerase action at telomeres. *Molecular and Cellular Biology*.

PURDUE-SMITHE, A. C., KIM, K., ANDRIESSEN, V. C., POLLACK, A. Z., SJAARDA, L. A., SILVER, R. M., SCHISTERMAN, E. F. & MUMFORD, S. L. 2021. Preconception leukocyte telomere length and pregnancy outcomes among women with demonstrated fecundity. *Human Reproduction,* 36**,** 3122-3130.

QU, C., LIAO, S., ZHANG, J., CAO, H., ZHANG, H., ZHANG, N., YAN, L., CUI, G., LUO, P., ZHANG, Q. & CHENG, Q. 2023. Burden of cardiovascular disease among elderly: based on the Global Burden of Disease Study 2019. *European Heart Journal - Quality of Care and Clinical Outcomes,* 10**,** 143-153.

RAGEH, K. E. A., FARAG, E. A., BEHERY, M. A., BADRELDIN, M. A. & ALI, E. A. 2023. The Impact of Previous Exposure to COVID-19 on the Outcome of ICSI Cycles. *JBRA Assisted Reproduction,* 27**,** 367-372.

REDDEL, R., BRYAN, T. & MURNANE, J. 1997. Immortalized cells with no detectable telomerase activity. A review. *Biochemistry-New York-English Translation of Biokhimiya,* 62**,** 1254-1262.

REGITZ-ZAGROSEK, V., ROOS-HESSELINK, J. W., BAUERSACHS, J., BLOMSTRÖM-LUNDQVIST, C., CIFKOVA, R., DE BONIS, M., IUNG, B., JOHNSON, M. R., KINTSCHER, U. & KRANKE, P. 2018. 2018 ESC guidelines for the management of cardiovascular diseases during pregnancy: the task force for the management of cardiovascular diseases during pregnancy of the European Society of Cardiology (ESC). *European Heart Journal,* 39**,** 3165-3241.

REIG, A., GARCIA-VELASCO, J. A. & SELI, E. 2023. Bologna vs. POSEIDON criteria as predictors of the likelihood of obtaining at least one euploid embryo in poor ovarian response: an analysis of 6,889 cycles. *Fertility and Sterility,* 120**,** 605-614.

RENDI, M. H., MUEHLENBACHS, A., GARCIA, R. L. & BOYD, K. L. 2012. Female Reproductive System. *Comparative anatomy and histology.* Elsevier.

REUSS, M. L., KLINE, J., SANTOS, R., LEVIN, B. & TIMOR-TRITSCH, I. 1996. Age and the ovarian follicle pool assessed with transvaginal ultrasonography. *American Journal of Obstetrics and Gynecology,* 174**,** 624-627.

REYES, F., WINTER, J. & FAIMAN, C. 1973. Studies on human sexual development. I. Fetal gonadal and adrenal sex steroids. *The Journal of Clinical Endocrinology and Metabolism,* 37**,** 74-78.

REYNOLDS, R. F. & OBERMEYER, C. M. 2005. Age at natural menopause in Spain and the United States: results from the DAMES project. *American Journal of Human Biology,* 17**,** 331-40.

RICARD-BLUM, S., BAFFET, G. & THÉRET, N. 2018. Molecular and tissue alterations of collagens in fibrosis. *Matrix Biology,* 68**,** 122-149.

RICHARDS, J. S. & PANGAS, S. A. 2010. The ovary: basic biology and clinical implications. *The Journal of Clinical Investigation,* 120**,** 963-72.

RICHARDSON, B. E. & LEHMANN, R. 2010. Mechanisms guiding primordial germ cell migration: strategies from different organisms. *Nature Reviews Molecular Cell Biology,* 11**,** 37-49.

RICHTER, T. & VON ZGLINICKI, T. 2007. A continuous correlation between oxidative stress and telomere shortening in fibroblasts. *Experimental Gerontology,* 42**,** 1039-1042.

RIMON-DAHARI, N., YERUSHALMI-HEINEMANN, L., ALYAGOR, L. & DEKEL, N. 2016. Ovarian folliculogenesis. *Molecular Mechanisms of Cell Differentiation in Gonad Development***,** 167-190.

RITZÉN, E. M., NILSSON, O., GRIGELIONIENE, G., HOLST, M., SÄVENDAHL, L. & WROBLEWSKI, J. 2000. Estrogens and human growth. *The Journal of Steroid Biochemistry and Molecular Biology,* 74**,** 383-386.

ROBERTS, J. E., SPANDORFER, S., FASOULIOTIS, S. J., KASHYAP, S. & ROSENWAKS, Z. 2005. Taking a basal follicle-stimulating hormone history is essential before initiating in vitro fertilization. *Fertility and Sterility,* 83**,** 37-41.

RODRIGUEZ PEÑA, M. J., CASTILLO BENNETT, J. V., SOLER, O. M., MAYORGA, L. S. & MICHAUT, M. A. 2013. MARCKS protein is phosphorylated and regulates calcium mobilization during human acrosomal exocytosis. *PLOS ONE,* 8**,** e64551.

RONG, Y., WU, Y. K., CHEN, Y., LIU, Q., AI, L., WU, Y. W., ZHU, Y., ZHANG, Y. L., LIU, C., MA, Y., TONG, X., JIN, J., LI, X., ZHOU, Y., JI, S. Y., ZHANG, S. & FAN, H. Y. 2025. ZAR1/2-Regulated Epigenetic Modifications are Essential for Age-Associated Oocyte Quality Maintenance and Zygotic Activation. *Advanced Science***,** e2410305.

ROSS, K. M., CARROLL, J., HORVATH, S., HOBEL, C. J., COUSSONS-READ, M. E. & DU NKEL SCHETTER, C. 2020. Immune epigenetic age in pregnancy and 1 year after bi rth: associations with weight change. *American Journal of Reproductive Immunology,* 83**,** e13229.

RUDDOCK, N. K., SHI, S.-Q., JAIN, S., MOORE, G., HANKINS, G. D., ROMERO, R. & GARFIELD, R. E. 2008. Progesterone, but not 17-alpha-hydroxyprogesterone caproate, inhibits human myometrial contractions. *American Journal of Obstetrics and Gynecology,* 199**,** 391. e1-391. e7.

RUDOLPH, K. L., CHANG, S., LEE, H.-W., BLASCO, M., GOTTLIEB, G. J., GREIDER, C. & DEPINHO, R. A. 1999. Longevity, stress response, and cancer in aging telomerase-deficient mice. *Cell,* 96**,** 701-712.

RUSSO, V., BERARDINELLI, P., MARTELLI, A., DI GIACINTO, O., NARDINOCCHI, D., FANTASIA, D. & BARBONI, B. 2006. Expression of telomerase reverse transcriptase subunit (TERT) and telomere sizing in pig ovarian follicles. *Journal of Histochemistry & Cytochemistry,* 54**,** 443-55.

RYAN, C. P., HAYES, M. G., LEE, N. R., MCDADE, T. W., JONES, M. J., KOBOR, M. S., KUZAWA, C. W. & EISENBERG, D. T. 2018. Reproduction predicts shorter telomeres and epigenetic age acceleration among young adult women. *Scientific Reports,* 8**,** 11100.

SAINI, N., ROBERTS, S. A., KLIMCZAK, L. J., CHAN, K., GRIMM, S. A., DAI, S., FARGO, D. C., BOYER, J. C., KAUFMANN, W. K. & TAYLOR, J. A. 2016. The impact of environmental and endogenous damage on somatic mutation load in human skin fibroblasts. *PLOS Genetics,* 12**,** e1006385.

SALUSTRI, A., ULISSE, S., YANAGISHITA, M. & HASCALL, V. C. 1990. Hyaluronic acid synthesis by mural granulosa cells and cumulus cells in vitro is selectively stimulated by a factor produced by oocytes and by transforming growth factor-beta. *Journal of Biological Chemistry,* 265**,** 19517-19523.

SALUSTRI, A., YANAGISHITA, M., UNDERHILL, C. B., LAURENT, T. C. & HASCALL, V. C. 1992. Localization and synthesis of hyaluronic acid in the cumulus cells and mural granulosa cells of the preovulatory follicle. *Developmental Biology,* 151**,** 541-551.

SAMAMI, E., SHAHHOSSEINI, Z. & ELYASI, F. 2022. The effects of psychological interventions on menopausal hot flashes: A systematic review. *International Journal of Reproductive Biomedicine,* 20**,** 255-272.

SAMASSEKOU, O., GADJI, M., DROUIN, R. & YAN, J. 2010. Sizing the ends: normal length of human telomeres. *Annals of Anatomy-Anatomischer Anzeiger,* 192**,** 284-291.

SANCHEZ-VAZQUEZ, R., GUÍO-CARRIÓN, A., ZAPATERO-GAVIRIA, A., MARTÍNEZ, P. & BLASCO, M. A. 2021. Shorter telomere lengths in patients with severe COVID-19 disease. *Aging (Albany NY),* 13**,** 1.

SANCHEZ, F. & SMITZ, J. 2012. Molecular control of oogenesis. *Biochimica et Biophysica Acta,* 1822**,** 1896-912.

SANGARALINGHAM, S. J., WANG, B. H., HUANG, L., KUMFU, S., ICHIKI, T., KRUM, H. & BURNETT JR, J. C. 2016. Cardiorenal fibrosis and dysfunction in aging: imbalance in mediators and regulators of collagen. *Peptides,* 76**,** 108-114.

SASAKI, K., YOKOBAYASHI, S., NAKAMURA, T., OKAMOTO, I., YABUTA, Y., KURIMOTO, K., OHTA, H., MORITOKI, Y., IWATANI, C. & TSUCHIYA, H. 2015. Robust in vitro induction of human germ cell fate from pluripotent stem cells. *Cell Stem Cell,* 17**,** 178-194.

SAUNDERS, P. T. K. & HORNE, A. W. 2021. Endometriosis: Etiology, pathobiology, and therapeutic prospects. *Cell,* 184**,** 2807-2824.

SAYBAN, S., MIRFAKHRAIE, R., OMRANI, M. D., GHAEDI, H., HEIDARY, H., YAGHOOBI, H., AZIZI, F. & POURESMAEILI, F. 2018. Idiopathic Premature Ovarian Failure and its association to the abnormal longitudinal changes of telomere length in a population of Iranian Infertile Women: A pilot study. *Meta Gene,* 18**,** 58-61.

SCHALLY, A. V., ARIMURA, A., KASTIN, A., MATSUO, H., BABA, Y., REDDING, T., NAIR, R., DEBELJUK, L. & WHITE, W. 1971. Gonadotropin-releasing hormone: one polypeptide regulates secretion of luteinizing and follicle-stimulating hormones. *Science,* 173**,** 1036-1038.

SCHMIDT, L., SOBOTKA, T., BENTZEN, J. G., NYBOE ANDERSEN, A., REPRODUCTION, E. & FORCE, S. T. 2012. Demographic and medical consequences of the postponement of parenthood. *Human Reproduction Update,* 18**,** 29-43.

SCHOENAKER, D. A., JACKSON, C. A., ROWLANDS, J. V. & MISHRA, G. D. 2014. Socioeconomic position, lifestyle factors and age at natural menopause: a systematic review and meta-analyses of studies across six continents. *International Journal of Epidemiology,* 43**,** 1542-1562.

SCOTT, D. C., RHEE, D. Y., DUDA, D. M., KELSALL, I. R., OLSZEWSKI, J. L., PAULO, J. A., DE JONG, A., OVAA, H., ALPI, A. F. & HARPER, J. W. 2016. Two distinct types of E3 ligases work in unison to regulate substrate ubiquitylation. *Cell,* 166**,** 1198-1214. e24.

SCOTT JR, R. T., HOFMANN, G. E., OEHNINGER, S. & MUASHER, S. J. 1990. Intercycle variability of day 3 follicle-stimulating hormone levels and its effect on stimulation quality in in vitro fertilization. *Fertility and Sterility,* 54**,** 297-302.

SECOMANDI, L., BORGHESAN, M., VELARDE, M. & DEMARIA, M. 2021. The role of cellular senescence in female reproductive aging and the potential for senotherapeutic interventions. *Human Reproduction Update,* 28**,** 172-189.

SEIFER, D. B., BAKER, V. L. & LEADER, B. 2011. Age-specific serum anti-Müllerian hormone values for 17,120 women presenting to fertility centers within the United States. *Fertility and Sterility,* 95**,** 747-750.

SEKI, Y., YAMAJI, M., YABUTA, Y., SANO, M., SHIGETA, M., MATSUI, Y., SAGA, Y., TACHIBANA, M., SHINKAI, Y. & SAITOU, M. 2007. Cellular dynamics associated with the genome-wide epigenetic reprogramming in migrating primordial germ cells in mice. *Development*.

SELESNIEMI, K., LEE, H.-J., MUHLHAUSER, A. & TILLY, J. L. 2011. Prevention of maternal aging-associated oocyte aneuploidy and meiotic spindle defects in mice by dietary and genetic strategies. *Proceedings of the National Academy of Sciences of the United States of America,* 108**,** 12319-12324.

SERRANO, M. 2017. Tools to eliminate senescent cells. *Nature,* 545**,** 294-295.

SFEIR, A., KABIR, S., VAN OVERBEEK, M., CELLI, G. B. & DE LANGE, T. 2010. Loss of Rap1 induces telomere recombination in the absence of NHEJ or a DNA damage signal. *Science,* 327**,** 1657-1661.

SHAN, J., LI, D. J. & WANG, X. Q. 2023. Towards a Better Understanding of Endometriosis-Related Infertility: A Review on How Endometriosis Affects Endometrial Receptivity. *Biomolecules,* 13.

SHEVCHENKO, A., WILM, M., VORM, O. & MANN, M. 1996. Mass spectrometric sequencing of proteins from silver-stained polyacrylamide gels. *Analytical Chemistry,* 68**,** 850-858.

SHOMPER, M., LAPPA, C. & FITZHARRIS, G. 2014. Kinetochore microtubule establishment is defective in oocytes from aged mice. *Cell Cycle,* 13**,** 1171-1179.

SILVA-SANTOS, K., SANTOS, G., SILOTO, L., HERTEL, M., ANDRADE, E., RUBIN, M., STURION, L., MELO-STERZA, F. & SENEDA, M. 2011. Estimate of the population of preantral follicles in the ovaries of Bos taurus indicus and Bos taurus taurus cattle. *Theriogenology,* 76**,** 1051-1057.

SINGH, A., D'AMICO, D., ANDREUX, P. A., FOUASSIER, A. M., BLANCO-BOSE, W., EVANS, M., AEBISCHER, P., AUWERX, J. & RINSCH, C. 2022. Urolithin A improves muscle strength, exercise performance, and biomarkers of mitochondrial health in a randomized trial in middle-aged adults. *Cell Reports Medicine,* 3.

SINGH, A., KUKRETI, R., SASO, L. & KUKRETI, S. 2019. Oxidative stress: role and response of short guanine tracts at genomic locations. *International Journal of Molecular Sciences,* 20**,** 4258.

SPEROFF, L. & FRITZ, M. 2012. Endocrinología Ginecológica Clínica y Esterilidad, VIII Edición, Filadelfia: WoltersKluwer. Lippincott Williams &Wilkins.

SRIVASTAVA, D., SINGH, R. K., MOXLEY, M. A., HENZL, M. T., BECKER, D. F. & TANNER, J. J. 2012. The three-dimensional structural basis of type II hyperprolinemia. *Journal of Molecular Biology,* 420**,** 176-189.

STANLEY, K. E., THOMAS, E., LEAVER, M. & WELLS, D. 2020. Coronavirus disease-19 and fertility: viral host entry protein expression in male and female reproductive tissues. *Fertility and Sterility,* 114**,** 33-43.

STEINER, A. Z., HERRING, A. H., KESNER, J. S., MEADOWS, J. W., STANCZYK, F. Z., HOBERMAN, S. & BAIRD, D. D. 2011. Antimüllerian hormone as a predictor of natural fecundability in women aged 30-42 years. *Obstetrics & Gynecology,* 117**,** 798-804.

STELZIG, K. E., CANEPA-ESCARO, F., SCHILIRO, M., BERDNIKOVS, S., PRAKASH, Y. & CHIARELLA, S. E. 2020. Estrogen regulates the expression of SARS-CoV-2 receptor ACE2 in differentiated airway epithelial cells. *American Journal of Physiology-Lung Cellular and Molecular Physiology,* 318**,** L1280-L1281.

STOCCO, C., TELLERIA, C. & GIBORI, G. 2007. The molecular control of corpus luteum formation, function, and regression. *Endocrine Reviews,* 28**,** 117-149.

STREULI, I., FRAISSE, T., PILLET, C., IBECHEOLE, V., BISCHOF, P. & DE ZIEGLER, D. 2008. Serum antimüllerian hormone levels remain stable throughout the menstrual cycle and after oral or vaginal administration of synthetic sex steroids. *Fertility and Sterility,* 90**,** 395-400.

SUCHANEK, E., SIMUNIC, V., JURETIC, D. & GRIZELJ, V. 1994. Follicular fluid contents of hyaluronic acid, follicle-stimulating hormone and steroids relative to the success of in vitro fertilization of human oocytes. *Fertility and Sterility,* 62**,** 347-352.

TAJADA, M., DIESTE-PÉREZ, P., SANZ-ARENAL, A., PÉREZ-RONCERO, G., LÓPEZ-BAENA, M. T. & PÉREZ-LÓPEZ, F. R. 2022. Leukocyte telomere length in women with and without polycystic ovary syndrome: a systematic review and meta-analysis. *Gynecological Endocrinology,* 38**,** 391-397.

TAKAI, K. K., KIBE, T., DONIGIAN, J. R., FRESCAS, D. & DE LANGE, T. 2011. Telomere protection by TPP1/POT1 requires tethering to TIN2. *Molecular Cell,* 44**,** 647-659.

TAL, R. & SEIFER, D. B. 2017. Ovarian reserve testing: a user's guide. *American Journal of Obstetrics and Gynecology,* 217**,** 129-140.

TAL, R., SEIFER, D. B., KHANIMOV, M., MALTER, H. E., GRAZI, R. V. & LEADER, B. 2014. Characterization of women with elevated antimüllerian hormone levels (AMH): correlation of AMH with polycystic ovarian syndrome phenotypes and assisted reproductive technology outcomes. *American Journal of Obstetrics and Gynecology,* 211**,** 59. e1-59. e8.

TAL, R., TAL, O., SEIFER, B. J. & SEIFER, D. B. 2015. Antimüllerian hormone as predictor of implantation and clinical pregnancy after assisted conception: a systematic review and meta-analysis. *Fertility and Sterility,* 103**,** 119-130. e3.

TARIN, J. 1996. Potential effects of age-associated oxidative stress on mammalian oocytes/embryos. *J MHR: Basic science of reproductive medicine,* 2**,** 717-724.

TEJERA, A. M., D'ALCONTRES, M. S., THANASOULA, M., MARION, R. M., MARTINEZ, P., LIAO, C., FLORES, J. M., TARSOUNAS, M. & BLASCO, M. A. 2010. TPP1 is required for TERT recruitment, telomere elongation during nuclear reprogramming, and normal skin development in mice. *Developmental Cell,* 18**,** 775-789.

THILAGAVATHI, J., MISHRA, S., KUMAR, M., VEMPRALA, K., DEKA, D., DHADWAL, V. & DADA, R. 2013. Analysis of telomere length in couples experiencing idiopathic recurrent pregnancy loss. *Journal of Assisted Reproduction and Genetics,* 30**,** 793-798.

TOBOŁA-WRÓBEL, K., PIETRYGA, M., DYDOWICZ, P., NAPIERAŁA, M., BRĄZERT, J. & FLOREK, E. 2020. Association of oxidative stress on pregnancy. *Oxidative Medicine and Cellular Longevity,* 2020**,** 6398520.

TONER, J. P., PHILPUT, C. B., JONES, G. S. & MUASHER, S. J. 1991. Basal follicle-stimulating hormone level is a better predictor of in vitro fertilization performance than age. *Fertility and Sterility,* 55**,** 784-791.

TOSTI, E. 2006. Calcium ion currents mediating oocyte maturation events. *Journal Reproductive Biology Endocrinology,* 4**,** 1-9.

TOUPANCE, S., FATTET, A.-J., THORNTON, S. N., BENETOS, A., GUÉANT, J.-L. & KOSCINSKI, I. 2021. Ovarian Telomerase and Female Fertility. *Biomedicines,* 9**,** 842.

TREFF, N. R., SU, J., TAYLOR, D. & SCOTT JR, R. T. 2011. Telomere DNA deficiency is associated with development of human embryonic aneuploidy. *PLOS Genetics,* 7**,** e1002161.

TROUNSON, A., ANDERIESZ, C. & JONES, G. 2001. Maturation of human oocytes in vitro and their developmental competence. *Reproduction,* 121**,** 51-75.

TSANG, W. Y., SPEKTOR, A., LUCIANO, D. J., INDJEIAN, V. B., CHEN, Z., SALISBURY, J. L., SÁNCHEZ, I. & DYNLACHT, B. D. 2006. CP110 cooperates with two calcium-binding proteins to regulate cytokinesis and genome stability. *Molecular Biology of the Cell,* 17**,** 3423-3434.

TSEPELIDIS, S., DEVREKER, F., DEMEESTERE, I., FLAHAUT, A., GERVY, C. & ENGLERT, Y. 2007. Stable serum levels of anti-Müllerian hormone during the menstrual cycle: a prospective study in normo-ovulatory women. *Human Reproduction,* 22**,** 1837-40.

TSUTSUMI, M., FUJIWARA, R., NISHIZAWA, H., ITO, M., KOGO, H., INAGAKI, H., OHYE, T., KATO, T., FUJII, T. & KURAHASHI, H. 2014. Age-related decrease of meiotic cohesins in human oocytes. *PLOS ONE,* 9**,** e96710.

TUCKEY, R. C. 2005. Progesterone synthesis by the human placenta. *Placenta,* 26**,** 273-281.

TÜMPEL, S. & RUDOLPH, K. L. 2012. The role of telomere shortening in somatic stem cells and tissue aging: lessons from telomerase model systems. *Annals of the New York Academy of Sciences,* 1266**,** 28-39.

TURNER, S. & HARTSHORNE, G. M. 2013. Telomere lengths in human pronuclei, oocytes and spermatozoa. *Molecular Human Reproduction,* 19**,** 510-8.

TURNER, S., WONG, H. P., RAI, J. & HARTSHORNE, G. M. 2010. Telomere lengths in human oocytes, cleavage stage embryos and blastocysts. *Molecular Human Reproduction,* 16**,** 685-94.

UMEHARA, T., WINSTANLEY, Y. E., ANDREAS, E., MORIMOTO, A., WILLIAMS, E. J., SMITH, K. M., CARROLL, J., FEBBRAIO, M. A., SHIMADA, M., RUSSELL, D. L. & ROBKER, R. L. 2022. Female reproductive life span is extended by targeted removal of fibrotic collagen from the mouse ovary. *Science Advances,* 8**,** eabn4564.

UNLU, C., GUNEY, G., TUGRUL ERSAK, D., KOSEM, A., TARLAN, N. & TOKMAK, A. 2023. Evaluation of serum telomerase activity in normal-weight young girls with polycystic ovary syndrome and its relation to metabolic parameters. *Journal of Pediatric Endocrinology and Metabolism,* 36**,** 283-289.

UYSAL, F., KOSEBENT, E. G., TORU, H. S. & OZTURK, S. 2021. Decreased expression of TERT and telomeric proteins as human ovaries age may cause telomere shortening. *Journal of Assisted Reproduction and Genetics,* 38**,** 429-441.

VAN HELDEN, J. & WEISKIRCHEN, R. 2015. Performance of the two new fully automated anti-Müllerian hormone immunoassays compared with the clinical standard assay. *Human Reproduction,* 30**,** 1918-1926.

VAN HOUTEN, E., THEMMEN, A. & VISSER, J. Anti-Müllerian hormone (AMH): regulator and marker of ovarian function. Annales d'endocrinologie, 2010. Elsevier, 191-197.

VAN ROOIJ, I. A. J., BROEKMANS, F. J. M., SCHEFFER, G. J., LOOMAN, C. W. N., HABBEMA, J. D. F., DE JONG, F. H., FAUSER, B. J. C. M., THEMMEN, A. P. N. & TE VELDE, E. R. 2005. Serum antimüllerian hormone levels best reflect the reproductive decline with age in normal women with proven fertility: A longitudinal study. *Fertility and Sterility,* 83**,** 979-987.

VANINETTI, S., BACCARELLI, A., ROMOLI, R., FANELLI, M., FAGLIA, G. & SPADA, A. 2000. Effect of aging on serum gonadotropin levels in healthy subjects and patients with nonfunctioning pituitary adenomas. *European Journal of Endocrinology,* 142**,** 144-149.

VARELA, E., MUNOZ-LORENTE, M. A., TEJERA, A. M., ORTEGA, S. & BLASCO, M. A. 2016. Generation of mice with longer and better preserved telomeres in the absence of genetic manipulations. *Nature Communications,* 7**,** 11739.

VARELA, E., SCHNEIDER, R. P., ORTEGA, S. & BLASCO, M. A. 2011. Different telomere-length dynamics at the inner cell mass versus established embryonic stem (ES) cells. *Proceedings of the National Academy of Sciences of the United States of America,* 108**,** 15207-15212.

VEENITH, T., MARTIN, H., LE BREUILLY, M., WHITEHOUSE, T., GAO-SMITH, F., DUGGAL, N., LORD, J. M., MIAN, R., SARPHIE, D. & MOSS, P. 2022. High generation of reactive oxygen species from neutrophils in patients with severe COVID-19. *Scientific Reports,* 12**,** 10484.

VON ZGLINICKI, T. 2002. Oxidative stress shortens telomeres. *Trends in Biochemical Sciences,* 27**,** 339-344.

WAGNER, M., YOSHIHARA, M., DOUAGI, I., DAMDIMOPOULOS, A., PANULA, S., PETROPOULOS, S., LU, H., PETTERSSON, K., PALM, K., KATAYAMA, S., HOVATTA, O., KERE, J., LANNER, F. & DAMDIMOPOULOU, P. 2020. Single-cell analysis of human ovarian cortex identifies distinct cell populations but no oogonial stem cells. *Nature Communications,* 11**,** 1147.

WALLACE, W. H. B. & KELSEY, T. W. 2010. Human ovarian reserve from conception to the menopause. *PLOS ONE,* 5**,** e8772.

WANG, A., CORLEY, J., JASWA, E. G., LIN, J., SMITH, D. L., MCCULLOCH, C. E., HUDDLESTON, H. & CEDARS, M. I. 2025a. Association of Polycystic Ovarian Syndrome with Endothelial Health, Cardiovascular Risk, and Cellular Aging. *Fertility and Sterility*.

WANG, J., CHU, K., WANG, Y., LI, J., FU, J., ZENG, Y. A. & LI, W. 2021a. Procr-expressing granulosa cells are highly proliferative and are important for follicle development. *Iscience,* 24.

WANG, M., YANG, Q., REN, X., HU, J., LI, Z., LONG, R., XI, Q., ZHU, L. & JIN, L. 2021b. Investigating the impact of asymptomatic or mild SARS-CoV-2 infection on female fertility and in vitro fertilization outcomes: a retrospective cohort study. *EClinicalMedicine,* 38.

WANG, Q., CODD, V., RAISI-ESTABRAGH, Z., MUSICHA, C., BOUNTZIOUKA, V., KAPTOGE, S., ALLARA, E., DI ANGELANTONIO, E., BUTTERWORTH, A. S. & WOOD, A. M. 2021c. Shorter leukocyte telomere length is associated with adverse COVID-19 outcomes: a cohort study in UK Biobank. *EBioMedicine,* 70.

WANG, W., CHEN, H., LI, R., OUYANG, N., CHEN, J., HUANG, L., MAI, M., ZHANG, N., ZHANG, Q. & YANG, D. 2014. Telomerase activity is more significant for predicting the outcome of IVF treatment than telomere length in granulosa cells. *Reproduction,* 147**,** 649-657.

WANG, X., ZHU, Y., LIU, H., WANG, X., ZHANG, H. & CHEN, X. 2025b. Nitazoxanide alleviates experimental pulmonary fibrosis by inhibiting the development of cellular senescence. *Life Sciences,* 361**,** 123302.

WANG, Z., KYO, S., TAKAKURA, M., TANAKA, M., YATABE, N., MAIDA, Y., FUJIWARA, M., HAYAKAWA, J., OHMICHI, M. & KOIKE, K. 2000. Progesterone regulates human telomerase reverse transcriptase gene expression via activation of mitogen-activated protein kinase signaling pathway. *Cancer Research,* 60**,** 5376-5381.

WANG, Z., LIU, C.-Y., ZHAO, Y. & DEAN, J. 2020. FIGLA, LHX8 and SOHLH1 transcription factor networks regulate mouse oocyte growth and differentiation. *Nucleic Acids Research,* 48**,** 3525-3541.

WATSON, J. 1972. Nature (London) New Biol. 239, 197-201.

WEI, D., XIE, J., YIN, B., HAO, H., SONG, X., LIU, Q., ZHANG, C. & SUN, Y. 2017. Significantly lengthened telomere in granulosa cells from women with polycystic ovarian syndrome (PCOS). *Journal of Assisted Reproduction and Genetics,* 34**,** 861-866.

WEISS, J., GUENDNER, M. J., HALVORSON, L. M. & JAMESON, J. L. 1995. Transcriptional activation of the follicle-stimulating hormone beta-subunit gene by activin. *Endocrinology,* 136**,** 1885-1891.

WIACEK, M., HAGNER, W. & ZUBRZYCKI, I. Z. 2011. Measures of menopause driven differences in levels of blood lipids, follicle-stimulating hormone, and luteinizing hormone in women aged 35 to 60 years: National Health and Nutrition Examination Survey III and National Health and Nutrition Examination Survey 1999-2002 study. *Menopause,* 18.

WICKHAM, S., WEST, M. B., COOK, P. F. & HANIGAN, M. H. 2011. Gamma-glutamyl compounds: substrate specificity of gamma-glutamyl transpeptidase enzymes. *Analytical Biochemistry,* 414**,** 208-214.

WILDING, M., DALE, B., MARINO, M., DI MATTEO, L., ALVIGGI, C., PISATURO, M. L., LOMBARDI, L. & DE PLACIDO, G. 2001. Mitochondrial aggregation patterns and activity in human oocytes and preimplantation embryos. *Human Reproduction,* 16**,** 909-917.

WINKLER, I., TOLKACHOV, A., LAMMERS, F., LACOUR, P., DAUGELAITE, K., SCHNEIDER, N., KOCH, M.-L., PANTEN, J., GRÜNSCHLÄGER, F., POTH, T., ÁVILA, B. M. D., SCHNEIDER, A., HAAS, S., ODOM, D. T. & GONÇALVES, Â. 2024. The cycling and aging mouse female reproductive tract at single-cell resolution. *Cell,* 187**,** 981-998.e25.

WITCHEL, S. F., OBERFIELD, S. E. & PEÑA, A. S. 2019. Polycystic ovary syndrome: pathophysiology, presentation, and treatment with emphasis on adolescent girls. *Journal of the Endocrine Society,* 3**,** 1545-1573.

WOESSNER, J. F., MORIOKA, N., ZHU, C., MUKAIDA, T., BUTLER, T. & LEMAIRE, W. J. 1989. Connective tissue breakdown in ovulation. *Steroids,* 54**,** 491-499.

WOODS, N. F. & MITCHELL, E. S. 2005. Symptoms during the perimenopause: prevalence, severity, trajectory, and significance in women's lives. *The American Journal of Medicine,* 118**,** 14-24.

WRANA, J. L., ATTISANO, L., WIESER, R., VENTURA, F. & MASSAGUÉ, J. 1994. Mechanism of activation of the TGF-β receptor. *Nature,* 370**,** 341-347.

WRIGHT, D. L., JONES, E. L., MAYER, J. F., OEHNINGER, S., GIBBONS, W. E. & LANZENDORF, S. E. 2001. Characterization of telomerase activity in the human oocyte and preimplantation embryo. *Molecular Human Reproduction,* 7**,** 947-55.

WRIGHT, W. E., PIATYSZEK, M. A., RAINEY, W. E., BYRD, W. & SHAY, J. W. 1996. Telomerase activity in human germline and embryonic tissues and cells. *Developmental Genetics,* 18**,** 173-179.

WRIGHT, W. E., SHAY, J. W. & PIATYSZEK, M. A. 1995. Modifications of a telomeric repeat amplification protocol (TRAP) result in increased reliability, linearity and sensitivity. *Nucleic Acids Research,* 23**,** 3794.

WU, X., RANGANATHAN, V., WEISMAN, D. S., HEINE, W. F., CICCONE, D. N., O'NEILL, T. B., CRICK, K. E., PIERCE, K. A., LANE, W. S. & RATHBUN, G. 2000. ATM phosphorylation of Nijmegen breakage syndrome protein is required in a DNA damage response. *Nature,* 405**,** 477-482.

XIAO, F. H., WANG, H. T., ZHAO, L., XIA, T. R., YANG, L. Q., MA, S. Y. & KONG, Q. P. 2025. Methylome analysis in long-lived men deciphers DNA methylation modifications associated with male longevity in humans. *Cell Reports,* 44**,** 115158.

XU, X., CHEN, X., ZHANG, X., LIU, Y., WANG, Z., WANG, P., DU, Y., QIN, Y. & CHEN, Z. J. 2017. Impaired telomere length and telomerase activity in peripheral blood leukocytes and granulosa cells in patients with biochemical primary ovarian insufficiency. *Human Reproduction,* 32**,** 201-207.

YAHALOM, D., CHEN, A., BEN-AROYA, N., RAHIMIPOUR, S., KAGANOVSKY, E., OKON, E., FRIDKIN, M. & KOCH, Y. 1999. The gonadotropin-releasing hormone family of ne uropeptides in the brain of human, bovine and rat: identification of a third isoform. *FE BS Letters, Experimental & Molecular Biology Journal,* 463**,** 289-294.

YAMAGATA, Y., NAKAMURA, Y., UMAYAHARA, K., HARADA, A., TAKAYAMA, H., SUGINO, N. & KATO, H. 2002. Changes in telomerase activity in experimentally induced atretic follicles of immature rats. *Endocrine Journal,* 49**,** 589-595.

YAMASHIRO, C., SASAKI, K., YABUTA, Y., KOJIMA, Y., NAKAMURA, T., OKAMOTO, I., YOKOBAYASHI, S., MURASE, Y., ISHIKURA, Y. & SHIRANE, K. 2018. Generation of human oogonia from induced pluripotent stem cells in vitro. *Science,* 362**,** 356-360.

YAN, Z., SHEN, D., LIAO, J., ZHANG, Y., CHEN, Y., SHI, G. & GAO, F. 2018. Hypoxia Suppresses TGF-B1-Induced Cardiac Myocyte Myofibroblast Transformation by Inhibiting Smad2/3 and Rhoa Signaling Pathways. *Cellular Physiology and Biochemistry,* 45**,** 250-257.

YANG, L., CHEN, Y., LIU, Y., XING, Y., MIAO, C., ZHAO, Y., CHANG, X. & ZHANG, Q. 2021. The role of oxidative stress and natural antioxidants in ovarian aging. *Frontiers in Pharmacology,* 11**,** 617843.

YAO, B., LIU, H.-Y., GU, Y.-C., SHI, S.-S., TAO, X.-Q., LI, X.-J., GE, Y.-F., CUI, Y.-X. & YANG, G.-B. 2011. Gonadotropin-releasing hormone positively regulates steroidogenesis via extracellular signal-regulated kinase in rat Leydig cells. *Asian Journal of Andrology,* 13**,** 438.

YARDE, F., VOORHUIS, M., DÓLLEMAN, M., KNAUFF, E. A., EIJKEMANS, M. J. & BROEKMANS, F. J. 2013. Antimüllerian hormone as predictor of reproductive outcome in subfertile women with elevated basal follicle-stimulating hormone levels: a follow-up study. *Fertility and Sterility,* 100**,** 831-8.

YE, J. Z.-S., DONIGIAN, J. R., VAN OVERBEEK, M., LOAYZA, D., LUO, Y., KRUTCHINSKY, A. N., CHAIT, B. T. & DE LANGE, T. 2004a. TIN2 binds TRF1 and TRF2 simultaneously and stabilizes the TRF2 complex on telomeres. *Journal of Biological Chemistry,* 279**,** 47264-47271.

YE, J. Z.-S., HOCKEMEYER, D., KRUTCHINSKY, A. N., LOAYZA, D., HOOPER, S. M., CHAIT, B. T. & DE LANGE, T. 2004b. POT1-interacting protein PIP1: a telomere length regulator that recruits POT1 to the TIN2/TRF1 complex. *Genes and Development,* 18**,** 1649-1654.

YOUNG, J. R. & JAFFE, R. B. 1976. Strength-duration characteristics of estrogen effects on gonadotropin response to gonadotropin-releasing hormone in women. II. Effects of varying concentrations of estradiol. *The Journal of Clinical Endocrinology and Metabolism,* 42**,** 432-442.

YOUNGREN, K., JEANCLOS, E., AVIV, H., KIMURA, M., STOCK, J., HANNA, M., SKURNICK, J., BARDEGUEZ, A. & AVIV, A. 1998. Synchrony in telomere length of the human fetus. *Human Genetics,* 102**,** 640-643.

YOUNIS, J. S., BEN-AMI, M. & BEN-SHLOMO, I. 2015. The Bologna criteria for poor ovarian response: a contemporary critical appraisal. *Journal of Ovarian Research,* 8**,** 76.

YU, K., HUANG, Z.-Y., XU, X.-L., LI, J., FU, X.-W. & DENG, S.-L. 2022. Estrogen receptor function: impact on the human endometrium. *Frontiers in Endocrinology,* 13**,** 827724.

YU, T. N., CHENG, E. H., LIN, Y. P., CHEN, Y. C., HUANG, C. C., LEE, T. H. & LEE, M. S. 2023. Significantly shortened telomere length and altered androgen receptor level in cumulus cells from women with polycystic ovary syndrome. *Taiwanese Journal od Obstetrics and Gynecology,* 62**,** 845-851.

ZEICHNER, S. L., PALUMBO, P., FENG, Y., XIAO, X., GEE, D., SLEASMAN, J., GOODENOW, M., BIGGAR, R. & DIMITROV, D. 1999. Rapid telomere shortening in children. *The Journal of the American Society of Hematology,* 93**,** 2824-2830.

ZGLINICKI, T. V. & MARTIN-RUIZ, C. 2005. Telomeres as biomarkers for ageing and age-related diseases. *Current Molecular Medicine,* 5**,** 197-203.

ZHANG, D., ZHANG, X., ZENG, M., YUAN, J., LIU, M., YIN, Y., WU, X., KEEFE, D. L. & LIU, L. 2015. Increased DNA damage and repair deficiency in granulosa cells are associated with ovarian aging in rhesus monkey. *Journal of Assisted Reproduction and Genetics,* 32**,** 1069-1078.

ZHANG, K., XU, L. & CONG, Y.-S. 2021a. Telomere dysfunction in idiopathic pulmonary fibrosis. *Frontiers in Medicine,* 8**,** 739810.

ZHANG, M., BENER, M. B., JIANG, Z., WANG, T., ESENCAN, E., SCOTT III, R., HORVATH, T. & SELI, E. 2019a. Mitofusin 1 is required for female fertility and to maintain ovarian follicular reserve. *Cell Death and Disease,* 10**,** 560.

ZHANG, M., BENER, M. B., JIANG, Z., WANG, T., ESENCAN, E., SCOTT III, R., HORVATH, T. & SELI, E. 2019b. Mitofusin 2 plays a role in oocyte and follicle development, and is required to maintain ovarian follicular reserve during reproductive aging. *Aging (Albany NY),* 11**,** 3919.

ZHANG, S., AIBARA, S., VOS, S. M., AGAFONOV, D. E., LÜHRMANN, R. & CRAMER, P. 2021b. Structure of a transcribing RNA polymerase II–U1 snRNP complex. *Science,* 371**,** 305-309.

ZHU, D., CHUNG, H.-F., DOBSON, A. J., PANDEYA, N., BRUNNER, E. J., KUH, D., GREENWOOD, D. C., HARDY, R., CADE, J. E., GILES, G. G., BRUINSMA, F., DEMAKAKOS, P., SIMONSEN, M. K., SANDIN, S., WEIDERPASS, E. & MISHRA, G. D. 2020. Type of menopause, age of menopause and variations in the risk of incident cardiovascular disease: pooled analysis of individual data from 10 international studies. *Human Reproduction,* 35**,** 1933-1943.

ZHU, J., HAN, L., LIU, R., ZHANG, Z., HUANG, Q., FANG, X., YANG, K., HUANG, G., ZHENG, Z. & YAWALKAR, N. 2021. Identification of proteins associated with development of psoriatic arthritis in peripheral blood mononuclear cells: a quantitative iTRAQ-based proteomics study. *Journal of Translational Medicine,* 19**,** 331.

ZHU, Y. & ZHANG, C. 2016. Prevalence of gestational diabetes and risk of progression to type 2 diabetes: a global perspective. *Current Diabetes Reports,* 16**,** 1-11.

ZIELINSKA, A. P., HOLUBCOVA, Z., BLAYNEY, M., ELDER, K. & SCHUH, M. 2015. Sister kinetochore splitting and precocious disintegration of bivalents could explain the maternal age effect. *Elife,* 4**,** e11389.

ZIOMKIEWICZ, A., SANCILIO, A., GALBARCZYK, A., KLIMEK, M., JASIENSKA, G. & BRIBIESCAS, R. G. 2016. Evidence for the cost of reproduction in humans: high lifetime reproductive effort is associated with greater oxidative stress in post-menopausal women. *PLOS ONE,* 11**,** e0145753.

ZOTA, A. R., GELLER, R. J., ROMANO, L. E., COLEMAN-PHOX, K., ADLER, N. E., PARRY, E., WANG, M., PARK, J.-S., ELMI, A. F. & LARAIA, B. A. 2018. Association between

persistent endocrine-disrupting chemicals (PBDEs, OH-PBDEs, PCBs, and PFASs) and biomarkers of inflammation and cellular aging during pregnancy and postpartum. *Environment International,* 115**,** 9-20.

ZUCKERMAN, S. 1951. The number of oocytes in the mature ovary. *Recent Progress in Hormone Research,* 6**,** 63-109.

9 APPENDICES

9.1 Appendix A. Approval of the Ethics Committee

The project approvals by the Ethics Committees of HUPLF, HCSC, HGUV, and HUPHM are listed in this appendix.

La Fe
Departament de Salut

FPNT-CEIB-04 (B)

DICTAMEN DEL COMITÉ DE ÉTICA DE LA INVESTIGACIÓN CON MEDICAMENTOS

Dña. María Tordera Baviera, titular de la Secretaría Técnica del Comité de Ética de la Investigación con medicamentos del **Hospital Universitario y Politécnico La Fe,**

C E R T I F I C A

Que este Comité ha evaluado en su sesión de fecha **24 de febrero de 2021**, el Proyecto de Investigación:

Título: **"UNDERSTANDING THE IMPLICATION OF THE TELOMERE PATHWAY IN OVARIAN AGING AND DYSFUNCTION/INFERTILITY."**
Código de protocolo: **1711-FIVI-112-MV**
Promotor: **FUNDACIÓN IVI**
Versión/fecha del protocolo: **1.0/ 21 de septiembre de 2020**
Versión/fecha de la Hoja de Información al Paciente y Consentimiento Informado: **1.1/ 21 de septiembre de 2020**

Que dicho proyecto se ajusta a las normativas éticas sobre investigación biomédica con sujetos humanos y es viable en cuanto al planteamiento científico, objetivos, material y métodos, etc, descritos en la solicitud, así como la Hoja de Información al Paciente y el Consentimiento Informado.

En consecuencia, este Comité acuerda emitir **INFORME FAVORABLE** de dicho Proyecto de Investigación que será realizado en el Hospital Universitario y Politécnico La Fe por el/la **Dr. / Dra. Mónica Romeu Villarroya** del servicio/unidad/grupo de investigación de **REPRODUCCIÓN** como Investigador Principal.

Que el CEIm del Hospital Universitario y Politécnico La Fe, tanto en su composición como en sus procedimientos, cumple con las normas de BPC (CPMP/ICH/135/95) y con la legislación vigente que regula su funcionamiento, y que la composición del CEIm del Hospital Universitario y Politécnico La Fe es la indicada en el anexo I, teniendo en cuenta que, en el caso de que algún miembro participe en el estudio o declare algún conflicto de interés, no habrá participado en la evaluación ni en el dictamen de la solicitud de autorización del estudio clínico.

Lo que firmo en Valencia, a 24 de febrero de 2021

Fdo.: Dra. María Tordera Baviera
Secretaria Técnica del Comité de Ética de la Investigación con medicamentos

CSV:TC47RXM2-2IISCCFEN-TIIC5XQM4 **URL de validació**https://www.tramita.gva.es/csv-front/index.faces?cadena=TC47RXM2-2IISCCFEN-TIIC5XQM4

Hospital Clínico San Carlos
SaludMadrid
Comité de Ética de la Investigación con Medicamentos

Informe Favorable Protocolo
C.P. 21/295-E- C.I. 21/295-E

15 de abril de 2021

DÑA. Mª DEL MAR GARCÍA ARENILLAS, PRESIDENTA DEL COMITÉ ÉTICO DE INVESTIGACIÓN CON MEDICAMENTOS DEL HOSPITAL CLÍNICO SAN CARLOS DE MADRID.

CERTIFICA

1. Que se ha recibido el proyecto: **"ESTUDIO DE LA IMPLICACIÓN DE LOS TELÓMEROS EN EL ENVEJECIMIENTO Y LA DISFUNCIÓN/INFERTILIDAD DE LOS OVARIOS."**

"UNDERSTANDING THE IMPLICATION OF THE TELOMERE PATHWAY IN OVARIAN AGING AND DYSFUNCTION/INFERTILITY."

Código Interno: **21/295-E**
Promotor: **IVI Madrid**

Tipo documento	Versión
Protocolo	Versión 1.0 Fecha versión: 21 de septiembre del 2020
Hoja de Información al Paciente y Consentimiento Informado	Versión 1.0 Fecha versión: 21 de septiembre del 2020

2. Que la documentación requerida es la adecuada.

3. Que dentro de la documentación se incluye el informe favorable del CEIm HOSPITAL UNIVERSITARIO LA FE DE VALENCIA de fecha 24/02/2021. El CEIm HOSPITAL CLÍNICO SAN CARLOS lo considera válido para la realización del proyecto por IGNACIO CRISTÓBAL GARCÍA del Servicio de Obstetricia y Ginecología en este centro.

4. Que se procede al registro de la documentación recibida, para realizar el posterior seguimiento del mismo.

5. Que este Comité cumple con la legislación vigente, así como las normas de Buena Práctica Clínica.

Lo que firmo en Madrid, a 15 de abril de 2021

Fdo.: Dra. Mar García Arenillas
Presidenta del CEIm Hospital Clínico San Carlos

APROBACIÓN PROYECTOS DE INVESTIGACIÓN

- ANEXO 11 -

Este CEIm tras evaluar en su reunión de 16 de Diciembre de 2022 el Proyecto de Investigación:

Título:	Estudio de la implicación de los telómeros en el envejecimiento y la disfunción/infertilidad de los ovarios.		
I.P.:	Mónica Romeu Villarroya	Servicio/Unidad	Ginecología

Acuerda respecto a esta documentación:

REGISTRO:105/2022
Protocolo: Versión 1.0; 21/09/2020
HIP- HIP/CI versión 1 del 31/10/2022
Que se cumplen los requisitos éticos y metodológicos y la Hoja de Información al Paciente y Consentimiento Informado presentado reúnen las condiciones exigidas por este CEIm, por tanto se decide su APROBACIÓN.

COMPOSICIÓN DEL CEIm

Presidente: Dr. LOPEZ ALCINA, EMILIO (Especialista en Urología)
Vicepresidente: Dr. GARCIA DEL TORO, MIGUEL (Especialista en Enf.Infecciosas)
Vocales:
Dr., ALVAREZ PITI, JULIO (Especialista en Pediatría)
Dr. ANTON GARCIA, FRANCISCO (Especialista en M.Familia Atención Primaria)
Dra. LOPEZ ALARCON, DOLORES (Especialista Anestesia y Reanimación)
Dra. MARCAIDA BENITO, GOITZANE (Especialista en Análisis Clínicos)
Dr. MARTORELL ARAGONES, ANTONIO (Especialista en Pediatría)
Dra. MIR SANCHEZ CAROLINA (Especialista en M.Familia Atención Primaria)
Dra. OCETE MOCHON DOLORES (Especialista en Microbiología)
Dr. QUESADA DORADOR, AURELIO (Especialista en Cardiología)
Dra SAFONT AGUILERA, Mª JOSE (Especialista en Oncología)
Dr. VALDERRAMA ZURIAN JUAN CARLOS (Especialista en Historia de la ciencia y documentación)
Dr. SANCHEZ CARAZO, JOSE LUIS (Especialista en Dermatología)
Dr. SANCHEZ JUAN, CARLOS (Especialista en Endocrinología)
Dr. RUIZ ROJO, ELIAS (Farmacéutico de Atención Primaria)
Dra. PEDROS CHOLVI, CONSUELO (Especialista en Farmacología clínica)
Dra. OISHI KONARI, MIRIAM NATSUKI (Especialista en Otorrinolaringología)
Dr. PEREZ SILVESTRE, JOSE (Especialista en Medicina Interna)
Don GRACIA PEREZ FRANCISCO JAVIER (Enfermero)
Dña. MARTÍ MONROS, ANNA (Enfermera)
Doña SARMIENTO CABANES, Mª DEL CARMEN (Miembro independiente del centro)
Doña DOMINGUEZ GARCIA, CONCEPCION (Licenciado en derecho)
Dr. CORTIJO GIMENO, JULIO (Especialista en Farmacia)
Don MARTINEZ GARCIA, NEMESIO (Licenciado en derecho)
Secretaria Técnica: BERNALTE SESE, ALEJANDRO (Especialista en Farmacia Hospitalaria)

Ref: 47/293174.9/20

Hospital Universitario
Puerta de Hierro Majadahonda

INFORME DEL COMITÉ ÉTICO DE INVESTIGACIÓN CON MEDICAMENTOS

Código de protocolo de promotor: 2004-FIVI-041-MV

Protocolo Version: 1.0 Version Date: 15 May 2020
Hoja de Información al Paciente Versión: Versión 1.0. Fecha versión: 05 de Junio del 2020
Cosentimiento Informado Versión: 1.0 Fecha: 5 junio 2020

Título: Efectos de la Covid-19 en la biología de los telómeros de las células de la granulosa y en la fertilidad así como en los resultados de la fecundación in vitro.

Tipo de estudio: Proyecto de Investigación

El Comité Ético de Investigación con Medicamentos del Hospital Universitario Puerta de Hierro Majadahonda en su reunión del 15/06/2020 (Acta nº 11/2020) tras la evaluación del estudio especificado, considera que:

1. El estudio evaluado cumple los requisitos metodológicos y técnicos.
2. La competencia de los investigadores y los medios disponibles son apropiados para llevar a cabo el estudio.
3. Los riesgos y molestias previsibles de la investigación son aceptables en relación con los beneficios esperados.
4. El proceso de selección de los sujetos participantes es apropiado.
5. Se considera adecuado el procedimiento previsto para información y obtención del consentimiento informado o, alternativamente, se acepta la exención de consentimiento propuesta para este estudio.
6. Las compensaciones económicas previstas son adecuadas y no interfieren con el resto de postulados éticos.
7. El CEIm del Hospital Universitario Puerta de Hierro Majadahonda, tanto en su composición como en sus PNT's, cumple con las normas de BPC (CPMP/ICH/135/95).

Emite un DICTAMEN FAVORABLE para la realización del estudio tras la respuesta a los cambios menores del 15/07/20

Majadahonda, a 15 de julio de 2020

Fdo.: Dra. Cristina Avendaño Solá
Presidenta del CEIm

La autenticidad de este documento se puede comprobar en www.madrid.org/csv
mediante el siguiente código seguro de verificación: 12765881734842252965133

ZONA NOROESTE
C/ Joaquín Rodrigo, 2
28222 Majadahonda / Madrid
Tel.: 91 191 60 00
Fax: 91 373 05 35

Red HsH Hospitales sin Humo

9.2 Appendix B. Fiji software macro for FISH quantification.

9.2.1 Macro 1

```
//Macro creada por Javier Mazarío. Servicio de Microscopía y Análisis de Imagen. Hospital Nacional de Parapléjicos.
//jmazario@sescam.jccm.es

/*Esta macro sirve para dibujar distintas ROIs en una imagen de ovario (óvulo, granulosa, teca y estroma) y detectar partículas de FISH en el canal 2 para cada una de las regiones. Guarda las ROIs de las distintas regiones dibujadas y las de las partículas detectadas en cada región con sus valores medidos en el canal 2 de la imagen procesada.

run("Set Measurements...", "area mean standard min integrated area_fraction limit display redirect=None decimal=6");
setForegroundColor(255, 255, 255);
roiManager("Associate", "false");
setTool("polygon");

umbral2 = getNumber ("Umbral de FISH", 50);
sbkg = getNumber ("Introduce el valor del Rolling Ball en píxeles", 5);

print("Imágenes analizadas en esta sesión:\n");
print("Umbral de FISH: "+umbral2);
print("Radio del Rolling Ball empleado: "+sbkg+"\n");

bucle=0;
while(bucle==0){
        //Este bucle es para seguir analizando imágenes hasta que se quiera parar

    waitForUser ("Abre la imagen a analizar y DESPUÉS pulsa OK");
    title = getTitle;
    nombre = File.nameWithoutExtension;
    path = File.directory;
    print(nombre);
    run("Duplicate...", "duplicate");
```

```
waitForUser ("Dibuja el óvulo y DESPUÉS pulsa OK \nSi no hay óvulo, dibuja una región pequeña dentro de una zona con núcleos \ny FISH en la capa granulosa");
run("Draw");
roiManager("Add");
roiManager("Select", 0);
roiManager("Rename", "Ovulo");
//  roiManager("show none");

run("Enlarge...", "enlarge=1 pixel");

//Este conjunto de instrucciones (11 líneas) ya no es necesario, pero lo mantengo para no tener que modificar el código para hacer las selecciones de la capa granulosa, teca y estroma
//waitForUser ("Dibuja el espacio vacío y DESPUÉS pulsa OK \n \nSi no hay espacio vacío, pulsa directamente OK");
run("Draw");
roiManager("Add");
roiManager("Select", newArray(0,1));
roiManager("XOR");
roiManager("Add");
roiManager("Select", 2);
roiManager("Rename", "Vacio");
roiManager("Select", 1);
roiManager("Delete");
run("Select None");

waitForUser ("Dibuja la capa granulosa y DESPUÉS pulsa OK");
run("Draw");
roiManager("Add");
roiManager("Select", newArray(0,1,2));
roiManager("XOR");
roiManager("Add");
roiManager("Select", 3);
roiManager("Rename", "Granulosa");
roiManager("Select", 2);
roiManager("Delete");
run("Select None");
```

```
waitForUser ("Dibuja la teca y DESPUÉS pulsa OK \nPara secciones discontinuas, pulsa MAYÚSCULAS antes de empezar a dibujar cada sección");
run("Draw");
roiManager("Add");
roiManager("Select", newArray(0,1,2,3));
roiManager("OR");
roiManager("Add");
roiManager("Select", newArray(0,1,2,4));
roiManager("XOR");
roiManager("Add");
roiManager("Select", 5);
roiManager("Rename", "Teca");
roiManager("Select", 3);
roiManager("Delete");
roiManager("Select", 3);
roiManager("Delete");
run("Select None");

waitForUser ("Dibuja el estroma y DESPUÉS pulsa OK");
run("Draw");
roiManager("Add");
roiManager("Select", newArray(0,1,2,3,4));
roiManager("XOR");
roiManager("Add");
roiManager("Select", 5);
roiManager("Rename", "Estroma");
roiManager("Select", 4);
roiManager("Delete");
run("Select None");

selectWindow(nombre+"-1.tif");
close();

//Detecta el área ocupada por los núcleos (canal 1) ajustando manualmente el umbral de DAPI
selectWindow(title);
Stack.setChannel(1);
run("Gaussian Blur...", "sigma=2 slice");
```

```
Stack.setDisplayMode("grayscale");
run("Threshold...");
waitForUser("Ajusta el umbral del DAPI y pulsa OK");
getThreshold(lower, upper);
run("Create Selection");
Roi.setPosition(1, 1, 1);
roiManager("Add");
roiManager("Select", 5);
roiManager("Rename", "Nucleos");
run("Select None");
print("Umbral DAPI = " + lower+"\n");

//Aplicamos al canal 2 (FISH) el SBKG definido anteriormente
Stack.setChannel(2);
run("Subtract Background...", "rolling="+sbkg+" slice");

//Creamos las ROIs de las partes que contienen núcleos de las capas dibujadas anteriormente
roiManager("Select", newArray(0,5));
roiManager("AND");
roiManager("Add");
roiManager("Select", 6);
roiManager("Rename", "Ovulo y nucleo");
roiManager("Measure");

roiManager("Select", newArray(2,5));
roiManager("AND");
roiManager("Add");
roiManager("Select", 7);
roiManager("Rename", "Granulosa y nucleos");
roiManager("Measure");

roiManager("Select", newArray(3,5));
roiManager("AND");
roiManager("Add");
roiManager("Select", 8);
roiManager("Rename", "Teca y nucleos");
roiManager("Measure");
```

```
roiManager("Select", newArray(4,5));
roiManager("AND");
roiManager("Add");
roiManager("Select", 9);
roiManager("Rename", "Estroma y nucleos");
roiManager("Measure");


roiManager("Save", path+nombre+" ROIs.zip");


//Detectamos las partículas de FISH en cada una de las regiones, las medimos y guardamos las detecciones y los resultados
roiManager("Select", 6);
Stack.setChannel(2);
setThreshold(umbral2, 65535);
run("Analyze Particles...", "display include summarize add slice");
roiManager("Select", newArray(0,1,2,3,4,5,6,7,8,9));
roiManager("Delete");
roiManager("Save", path+nombre+" FISH ovulo.zip");
roiManager("Deselect");
roiManager("Delete");


roiManager("Open", path+nombre+" ROIs.zip");
roiManager("Select", 7);
run("Analyze Particles...", "display include summarize add slice");
roiManager("Select", newArray(0,1,2,3,4,5,6,7,8,9));
roiManager("Delete");
roiManager("Save", path+nombre+" FISH granulosa.zip");
roiManager("Deselect");
roiManager("Delete");


roiManager("Open", path+nombre+" ROIs.zip");
roiManager("Select", 8);
run("Analyze Particles...", "display include summarize add slice");
roiManager("Select", newArray(0,1,2,3,4,5,6,7,8,9));
roiManager("Delete");
roiManager("Save", path+nombre+" FISH teca.zip");
roiManager("Deselect");
```

```
		roiManager("Delete");

		roiManager("Open", path+nombre+" ROIs.zip");
		roiManager("Select", 9);
		run("Analyze Particles...", "display include summarize add slice");
		roiManager("Select", newArray(0,1,2,3,4,5,6,7,8,9));
		roiManager("Delete");
		roiManager("Save", path+nombre+" FISH estroma.zip");
		roiManager("show none");
		roiManager("Deselect");
		roiManager("Delete");



		selectWindow("Summary of "+title);
		saveAs("Results", path+nombre+" RESUMEN.xls");
		run("Close");
		selectWindow("Results");
		saveAs("Results", path+nombre+" RESULTADOS SBKG"+sbkg+".xls");
		run("Close");

		run("Close All");

		//Crea un diálogo para seguir analizando más imágenes o concluir el análisis

		Dialog.create("Analizar otra imagen");
		Dialog.addMessage("Pulsa OK para analizar otra imagen");
		Dialog.addCheckbox("Selecciona para finalizar", false);
		Dialog.show();
		bucle = Dialog.getCheckbox();
}

showMessage("Finalizado \nGuarda el Log si quieres conservar el registro de esta sesión");
```

9.2.2 Macro 2

//Macro creada por Javier Mazarío. Servicio de Microscopía y Análisis de Imagen. Hospital Nacional de Parapléjicos.

//jmazario@sescam.jccm.es

/*Al ejecutar esta macro se obtienen los valores de intensidad original (sin preprocesado) en las partículas detectadas en el canal 2 (FISH) de las imágenes analizadas previamente con la macro "Análisis FISH con ROIs ovarios solapando teca.ijm" Para que funcione es IMPRESCINDIBLE haber corrido esa macro anteriormente.

```
run("Set Measurements...", "area mean standard min integrated area_fraction limit display redirect=None decimal=6");
dir1 = getDirectory("Elige la carpeta con las fotos a analizar");
list = getFileList(dir1);

setBatchMode(true);

for (i=0; i<list.length; i++)
    {
        path = dir1+list[i];

        if (endsWith(path, ".tif")){
            open(path);
                //Abre la imagen a analizar
            nombre=File.nameWithoutExtension ;
            setSlice(2);

            //Carga las partículas detectadas previamente en el óvulo, mide la intensidad y guarda los resultados
            roiManager("Open", dir1+nombre+" FISH ovulo.zip");
            roiManager("Measure");
            selectWindow("Results");
            saveAs("Results", dir1+nombre+" RESULTADOS original FISH ovulo.xls");
            run("Close");
            roiManager("Deselect");
            roiManager("Delete");
```

```
                    //Carga las partículas detectadas previamente en la granulosa, mide la intensidad y guarda los resultados
                    roiManager("Open", dir1+nombre+" FISH granulosa.zip");
                    roiManager("Measure");
                    selectWindow("Results");
                    saveAs("Results", dir1+nombre+" RESULTADOS original FISH granulosa.xls");
                    run("Close");
                    roiManager("Deselect");
                    roiManager("Delete");

                    //Carga las partículas detectadas previamente en la teca, mide la intensidad y guarda los resultados
                    roiManager("Open", dir1+nombre+" FISH teca.zip");
                    roiManager("Measure");
                    selectWindow("Results");
                    saveAs("Results", dir1+nombre+" RESULTADOS original FISH teca.xls");
                    run("Close");
                    roiManager("Deselect");
                    roiManager("Delete");

                    //Carga las partículas detectadas previamente en la granulosa, mide la intensidad y guarda los resultados
                    roiManager("Open", dir1+nombre+" FISH estroma.zip");
                    roiManager("Measure");
                    selectWindow("Results");
                    saveAs("Results", dir1+nombre+" RESULTADOS original FISH estroma.xls");
                    run("Close");
                    roiManager("Deselect");
                    roiManager("Delete");

                    close();
                    }
        }

showMessage("Análisis completo");
```

9.3 Appendix C. Supplemental material result 5.1.

Table C1. Endocrine parameters in groups based on age.

	Y	M	P	p-value	
AMH (ng/mL)					<0.0001
n	17	31	17	**Y vs. M**	0.0072
Mean ± SD	2.6 ± 2.5	1.0 ± 1.2	0.2 ± 0.4	**Y vs. P**	<0.0001
Median (Q1–Q3)	1.9 (0.9-3.3)	0.6 (0.1-1.1)	0.1 (0.0-0.4)	**M vs. P**	0.0452
Age, mean ± SD (years)	30.7 ± 4.2	40.3 ± 3.0*	47.5 ± 1.1		<0.0001
FSH (mIU/mL)					0.0039
n	17	30	17	**Y vs. M**	>0.9999
Mean ± SD	3.7 ± 2.5*	21.0 ± 51.0	14.1 ± 11.2	**Y vs. P**	0.0058
Median (Q1–Q3)	3.9 (1.2-5.9)	4.1 (0.3-8.1)	11.7 (5.0-17.8)	**M vs. P**	0.0177
Age, mean ± SD (years)	30.7 ± 4.2	40.2 ± 2.9*	47.5 ± 1.1		<0.0001
LH (mIU/mL)					0.0903
n	17	30	17	**Y vs. M**	>0.9999
Mean ± SD	5.2 ± 4.6*	9.8 ± 16.2	9.8 ± 7.6	**Y vs. P**	0.1851
Median (Q1–Q3)	4.1 (0.9-9.0)	3.4 (0.1-10.2)	7.8 (4.2-12.4)	**M vs. P**	0.1355
Age, mean ± SD (years)	30.7 ± 4.2	40.2 ± 2.9*	47.5 ± 1.1		<0.0001
E2 (pg/mL)					0.0157
n	17	30	17	**Y vs. M**	>0.9999
Mean ± SD	806.9 ± 1257	992.7 ± 1341	66.09 ± 58.41	**Y vs. P**	0.0416
Median (Q1–Q3)	153.5 (56.8-1675)	174.8 (50.5-3000)	53.6 (26.2-89.5)	**M vs. P**	0.0258
Age, mean ± SD (years)	30.7 ± 4.2	40.2 ± 2.9*	47.5 ± 1.1		<0.0001
P4 (ng/mL)					0.3578
n	17	30	17	**Y vs. M**	>0.9999
Mean ± SD	15.2 ± 25.8	19.0 ± 27.4	1.9 ± 4.0	**Y vs. P**	>0.9999
Median (Q1–Q3)	0.4 (0.2-36.5)	1.5 (0.2-60.0)	0.5 (0.2-1.3)	**M vs. P**	0.4579
Age, mean ± SD (years)	30.7 ± 4.2	40.2 ± 2.9*	47.5 ± 1.1		<0.0001

Data are presented as mean ± standard deviation and median (interquartile range). Considering that the hormones FSH, LH, E2 and P4 could not be measured in one subject of group M, it is specified for all hormones whether there are still statistically significant differences in the age variable excluding that individual. *Denoted the variables that passed the Shapiro-Wilk normality test. The variables were analyzed by Kruskal-Wallis and Dunn's multiple comparisons tests, both p-values specified in the table. A p-value < 0.05 was considered statistically significant. The n refers to the number of subjects. Y: young, M: middle-aged, P: perimenopausal, vs.: versus, SD: standard deviation, Q1: quartile 1 (25% percentile), Q3: quartile 3 (75% percentile), AMH: anti-müllerian hormone, FSH: follicle-stimulating hormone, LH: luteinizing hormone, E: estradiol, PG: progesterone, ng: nanogram, mL: milliliter, mIU: mili-International Units, pg: picogram.

Table C2. PBMCs telomere parameters in groups based on age.

	Y n = 17	M n = 31	P n = 17	p-value	
TL (a.u.)					0.0735
Telomeres	79885	203107	62883	**Y vs. M**	>0.9999
Mean ± SD	129.7 ± 7.3*	130.7 ± 15.4	123.3 ± 7.5*	**Y vs. P**	0.0816
Median (Q1–Q3)	128.7 (124.2-136.6)	125.6 (121.5-136.4)	121.8 (118.9-129.1)	**M vs. P**	0.2476
Short telomeres (%)					0.0264
Mean ± SD	11.0 ± 5.9*	11.8 ± 8.4*	17.6 ± 8.7*	**Y vs. M**	0.9398
Median (Q1–Q3)	9.8 (6.2-15.4)	11.1 (4.8-18.2)	17.2 (10.9-23.0)	**Y vs. P** **M vs. P**	0.0436 0.0436
Long telomeres (%)					0.2728
Mean ± SD	11.2 ± 6.6*	13.0 ± 15.5	7.2 ± 4.5*	**Y vs. M**	>0.9999
Median (Q1–Q3)	11.3 (5.7-15.3)	7.7 (3.9-16.9)	5.6 (4.4-11.2)	**Y vs. P** **M vs. P**	0.3252 0.9074

Data are presented as mean ± standard deviation and median (interquartile range). *Denoted the variables that passed the Shapiro-Wilk normality test. The variables were analyzed by Kruskal-Wallis and Dunn's multiple comparisons tests (TL and long telomeres), or ordinary one-way ANOVA and Tukey's multiple comparisons test (short telomeres). A p-value < 0.05 was considered statistically significant. The n refers to the number of subjects. The number of telomere dots analyzed is specified in the TL section under the heading "Telomeres". PBMCs: peripheral blood mononuclear cells, TL: telomere length, Y: young, M: middle-aged, P: perimenopausal, SD: standard deviation, Q1: quartile 1 (25% percentile), Q3: quartile 3 (75% percentile), a.u.: arbitrary units of intensity, %: percent, vs.: versus.

Table C3. Oocytes telomere parameters in groups based on age.

	Y n = 15	M n = 18	p-value
Age (years)			<0.0001
Mean ± SD	30.5 ± 4.3	40.2 ± 2.8*	
Median (Q1–Q3)	32.0 (29.0-34.0)	39.5 (38.0-42.3)	
TL (a.u.)			0.0039
Oocytes	192	146	
Telomeres	65420	23111	
Mean ± SD	155.0 ± 21.1*	148.9 ± 22.9	
Median (Q1–Q3)	152.2 (14.2-169.8)	145.5 (132.6-161.1)	
Short telomeres (%)			0.0002
Mean ± SD	17.1 ± 19.7	27.1 ± 24.1	
Median (Q1–Q3)	8.9 (2.2-26.3)	23.1 (5.0-43.4)	
Long telomeres (%)			0.0137
Mean ± SD	17.8 ± 20.7	15.1 ± 21.1	
Median (Q1–Q3)	10.1 (2.2-26.6)	6.3 (0.0-23.1)	

Data are presented as mean ± standard deviation and median (interquartile range). *Denoted the variables that passed the Kolmogorov-Smirnov normality test. The variables were analyzed by the Mann-Whitney U test. A p-value < 0.05 was considered statistically significant. The n refers to the number of subjects. The number of oocytes and telomere dots analyzed is specified in the TL section. Y: young, M: middle-aged, TL: telomere length, SD: standard deviation, Q1: quartile 1 (25% percentile), Q3: quartile 3 (75% percentile), a.u.: arbitrary units of intensity, %: percent.

Table C4. GCs telomere parameters during folliculogenesis.

All subjects n = 39	**Primordial (0)** n = 24	**Primary (1)** n = 34	**Secondary (2)** n = 18	**p-value**	
Age (years)				0.8375	
Mean ± SD	36.6 ± 6.5	36.3 ± 5.6*	36.9 ± 6.1*	**0 vs. 1**	>0.9999
Median (Q1–Q3)	38.5 (33.0-40.8)	36.5 (32.8-40.3)	38.0 (32.5-42.5)	**0 vs. 2**	>0.9999
				1 vs. 2	>0.9999
TL (a.u.)				<0.0001	
Follicles	123	248	36	**0 vs. 1**	0.6669
Telomeres	36046	100378	65420	**0 vs. 2**	<0.0001
Mean ± SD	147.6 ± 17.0*	151.4 ± 20.9	168.4 ± 24.9		
Median (Q1–Q3)	146.7 (135.7-158.0)	148.6 (133.0-167.2)	162.1 (145.0-191.6)	**1 vs. 2**	0.0004
Short telomeres (%)				0.0149	
Mean ± SD	15.8 ± 16.9	20.0 ± 20.4	30.9 ± 27.9	**0 vs. 1**	0.6887
Median (Q1–Q3)	10.2 (2.1-21.8)	11.0 (2.7-36.7)	25.0 (4.1-59.0)	**0 vs. 2**	0.0112
				1 vs. 2	0.0581
Long telomeres (%)				0.4989	
Mean ± SD	16.8 ± 18.7	18.2 ± 23.0	18.7 ± 22.6	**0 vs. 1**	0.9224
Median (Q1–Q3)	9.3 (3.3-24.9)	6.5 (1.2-30.9)	3.7 (0.5-36.8)	**0 vs. 2**	>0.9999
				1 vs. 2	>0.9999
Y group n = 16	**Primordial (0)** n = 8	**Primary (1)** n = 14	**Secondary (2)** n = 7	**p-value**	
Age (years)				0.7751	
Mean ± SD	29.3 ± 5.4	31.0 ± 4.0	30.7 ± 3.9*	**0 vs. 1**	>0.9999
Median (Q1–Q3)	31.5 (24.5-33.0)	32.0 (29.8-34.0)	31.0 (29.0-34.0)	**0 vs. 2**	>0.9999
				1 vs. 2	>0.9999
TL (a.u.)				0.0012	
Follicles	66	123	15	**0 vs. 1**	0.4951
Telomeres	21252	53236	31844	**0 vs. 2**	0.0007
Mean ± SD	151.1 ± 15.7	155.5 ± 19.5	176.3 ± 24.5*		
Median (Q1–Q3)	148.2 (139.0-158.0)	155.7 (136.9-169.9)	183.3 (156.5-197.3)	**1 vs. 2**	0.0065
Short telomeres (%)				0.5605	
Mean ± SD	10.0 ± 8.1	15.4 ± 17.4	22.1 ± 25.9	**0 vs. 1**	>0.9999
Median (Q1–Q3)	8.3 (3.3-15.5)	7.5 (2.0-24.6)	10.0 (2.1-35.5)	**0 vs. 2**	0.8617
				1 vs. 2	>0.9999
Long telomeres (%)				0.9860	
Mean ± SD	19.1 ± 20.3	21.3 ± 21.8	25.0 ± 24.7	**0 vs. 1**	>0.9999
Median (Q1–Q3)	9.9 (4.4-28.7)	12.9 (3.0-35.3)	23.9 (1.3-46.5)	**0 vs. 2**	>0.9999
				1 vs. 2	>0.9999

M group n = 23	**Primordial (0)** n = 16	**Primary (1)** n = 20	**Secondary (2)** n = 11	**p-value**	
Age (years)				0.7015	
Mean ± SD	40.3 ± 2.9*	40.0 ± 3.0*	40.9 ± 3.2*	**0 vs. 1**	0.9530
Median (Q1–Q3)	39.5 (38.3-42.8)	39.5 (38.0-42.0)	41.0 (39.0-44.0)	**0 vs. 2** **1 vs. 2**	0.8439 0.6777
TL (a.u.)				0.0063	
Follicles	57	125	21	**0 vs. 1**	>0.9999
Telomeres	14794	47142	33576	**0 vs. 2**	0.0053
Mean ± SD	143.6 ± 17.8	147.4 ± 21.4	162.8 ± 24.2*		
Median (Q1–Q3)	143.6 (125.9-158.8)	141.0 (130.1-159.9)	154.3 (144.7-187.9)	**1 vs. 2**	0.0138
Short telomeres (%)				0.0561	
Mean ± SD	22.4 ± 21.6	24.5 ± 22.2	37.2 ± 28.2*	**0 vs. 1**	>0.9999
Median (Q1–Q3)	15.7 (1.7-44.8)	19.7 (3.8-43.6)	34.4 (5.9-59.9)	**0 vs. 2** **1 vs. 2**	0.0544 0.1002
Long telomeres (%)				0.5920	
Mean ± SD	14.2 ± 16.5	15.2 ± 23.7	14.2 ± 20.3	**0 vs. 1**	>0.9999
Median (Q1–Q3)	8.7 (1.0-21.7)	3.1 (0.7-16.6)	1.7 (0.5-25.6)	**0 vs. 2** **1 vs. 2**	>0.9999 >0.9999

Data are presented as mean ± standard deviation and median (interquartile range). *Denoted the variables that passed the Shapiro-Wilk or Kolmogorov-Smirnov normality test. The variables were analyzed by Kruskal-Wallis and Dunn's multiple comparisons tests (non-normally distributed data), or ordinary one-way ANOVA and Tukey's multiple comparisons test (normally distributed data). A p-value < 0.05 was considered statistically significant. The n refers to the number of subjects. The number of follicles and telomere dots analyzed is specified in the TL section. 0: primordial follicles, 1: primary follicles, 2: secondary follicles, SD: standard deviation, Q1: quartile 1 (25% percentile), Q3: quartile 3 (75% percentile), Y: young, M: middle-aged, a.u.: arbitrary units of intensity, %: percent, vs.: versus.

Table C5. Primordial GCs telomere parameters in groups based on age.

	Y n = 8	**M** n = 16	**p-value**
Age (years)			<0.0001
Mean ± SD	29.3 ± 5.4	40.3 ± 2.9*	
Median (Q1–Q3)	31.5 (24.5-33.0)	39.5 (38.3-42.8)	
TL (a.u.)			0.0282
Follicles	66	57	
Telomeres	21252	14794	
Mean ± SD	151.1 ± 15.7	143.6 ± 17.8	
Median (Q1–Q3)	148.2 (139.0-158.0)	143.6 (125.9-158.8)	
Short telomeres (%)			0.0395
Mean ± SD	10.0 ± 8.1	22.4 ± 21.6	
Median (Q1–Q3)	8.3 (3.3-15.5)	15.7 (1.7-44.8)	
Long telomeres (%)			0.0720
Mean ± SD	19.1 ± 20.3	14.2 ± 16.5	
Median (Q1–Q3)	9.9 (4.4-28.7)	8.7 (1.0-21.7)	

Data are presented as mean ± standard deviation and median (interquartile range). *Denoted the variables that passed the Shapiro-Wilk or Kolmogorov-Smirnov normality test. The variables were analyzed by the Mann-Whitney U test. A p-value < 0.05 was considered statistically significant. The n refers to the number of subjects. The number of follicles and telomere dots analyzed is specified in the TL section. Y: young, M: middle-aged, TL: telomere length, SD: standard deviation, Q1: quartile 1 (25% percentile), Q3: quartile 3 (75% percentile), a.u.: arbitrary units of intensity, %: percent.

Table C6. Primary GCs telomere parameters in groups based on age.

	Y n = 14	M n = 20	p-value
Age (years)			<0.0001
Mean ± SD	31.0 ± 4.0	40.0 ± 3.0*	
Median (Q1–Q3)	32.0 (29.8-34.0)	39.5 (38.0-42.0)	
TL (a.u.)			0.0003
Follicles	123	125	
Telomeres	53236	47142	
Mean ± SD	155.5 ± 19.5	147.4 ± 21.4	
Median (Q1–Q3)	155.7 (136.9-169.9)	141.0 (130.1-159.9)	
Short telomeres (%)			0.0036
Mean ± SD	15.4 ± 17.4	24.5 ± 22.2	
Median (Q1–Q3)	7.5 (2.0-24.6)	19.7 (3.8-43.6)	
Long telomeres (%)			0.0001
Mean ± SD	21.3 ± 21.8	15.2 ± 23.7	
Median (Q1–Q3)	12.9 (3.0-35.3)	3.1 (0.7-16.6)	

Data are presented as mean ± standard deviation and median (interquartile range). *Denoted the variables that passed the Shapiro-Wilk or Kolmogorov-Smirnov normality test. The variables were analyzed by the Mann-Whitney U test. A p-value < 0.05 was considered statistically significant. The n refers to the number of subjects. The number of follicles and telomere dots analyzed is specified in the TL section. Y: young, M: middle-aged, TL: telomere length, SD: standard deviation, Q1: quartile 1 (25% percentile), Q3: quartile 3 (75% percentile), a.u.: arbitrary units of intensity, %: percent.

Table C7. TCs telomere parameters in groups based on age.

	Y n = 13	M n = 20	p-value
Age (years)			<0.0001
Mean ± SD	31.3 ± 3.0	40.4 ± 3.0*	
Median (Q1–Q3)	32.0 (30.5-33.5)	40.0 (38.0-43.5)	
TL (a.u.)			0.0041
Follicles	81	89	
Telomeres	29752	17463	
Mean ± SD	153.0 ± 19.1*	145.8 ± 19.7	
Median (Q1–Q3)	155.2 (139.5-167.4)	140.6 (131.6-156.3)	
Short telomeres (%)			0.0304
Mean ± SD	18.0 ± 22.0	26.5 ± 24.3	
Median (Q1–Q3)	8.3 (3.2-20.0)	21.9 (5.1-44.4)	
Long telomeres (%)			0.0196
Mean ± SD	17.8 ± 19.5	12.2 ± 20.3	
Median (Q1–Q3)	11.6 (1.4-32.6)	3.0 (0.2-13.8)	

Data are presented as mean ± standard deviation and median (interquartile range). *Denoted the variables that passed the Shapiro-Wilk or Kolmogorov-Smirnov normality test. The variables were analyzed by the Mann-Whitney U test. A p-value < 0.05 was considered statistically significant. The n refers to the number of subjects. The number of follicles and telomere dots analyzed is specified in the TL section. Y: young, M: middle-aged, TL: telomere length, SD: standard deviation, Q1: quartile 1 (25% percentile), Q3: quartile 3 (75% percentile), a.u.: arbitrary units of intensity, %: percent.

Table C8. Ovarian fibrotic area in groups based on age.

	Y n = 6	M n = 6	P n = 7	p-value	
Age (years)				<0.0001	
Mean ± SD	31.7 ± 2.1*	40.7 ± 3.6*	47.0 ± 0.8*	**Y vs. M**	<0.0001
Median (Q1–Q3)	31.5 (29.8-34.0)	40.5 (37.5-44.2)	47.0 (46.0-48.0)	**Y vs. P**	<0.0001
				M vs. P	0.0005
Fibrotic area (%)				0.0010	
Mean ± SD	13.9 ± 8.6*	28.4 ± 12.2*	40.4 ± 9.4*	**Y vs. M**	0.0616
Median (Q1–Q3)	17.8 (4.4-20.5)	25.0 (19.8-39.5)	36.5 (31.8-51.8)	**Y vs. P**	0.0007
				M vs. P	0.1125

Data are presented as mean ± standard deviation and median (interquartile range). *Denoted the variables that passed the Shapiro-Wilk normality test. The variables were analyzed by ordinary one-way ANOVA and Tukey's multiple comparisons test. A p-value < 0.05 was considered statistically significant. The n refers to the number of subjects. Y: young; M: middle-aged; P: perimenopausal; SD: standard deviation; Q1: quartile 1 (25% percentile); Q3: quartile 3 (75% percentile); %: percent.

Table C9. Differentially expressed proteins in ovarian samples of women of different ages.

	Upregulated	Downregulated
Y vs. M	TEBP, SORCN, ARL1, TIM13, ACTB, S10AB, CSN5, STX12, ATP5J, GBG12, NH2L1, RSMN, ITA6, RBPMS, RL30, PDLI1, QCR7, LEG3, LAP2A, MIF, TYB4, ITPR1, ARL3, IMDH2, APOH, ASC, S10A6, CUTA, BAF, ANTR2, GNPI2, CTL1, DP13A, DYL1, ENPP4, ENY2, ATP5I, NTF2, RS12, CALD1, STMN1, SRRM1, DOPD, HSPB6, AL1B1, TOM70, EDF1, UBQL2	GGT5, ITA3, ECH1, NFIX, ZA2G, RD23B, TBG2, SYTC, CO8A1, ERLEC, IF4A1, PSMD4, DDX5, HDGR3, RS7, PIPNA, NLGNY, PRS10, GREB1, MAOM, TCPZ, ANM5, EVPL, RS24, LAMP1, NCOA5, OPA1, COTL1, BCAT2, CAZA2, LSM5, ANK3, ATLA3, S10A9, BLVRB, RS27A, SMC1A, LRC47, AHSA1, SC24C, SNX2, SYVC, ERG1, PNCB
Y vs. P	CALM3, BASP1, RSMN, PODN, MRP, PSMD7, PTN11, RBPMS, LA, DP13A, ROA0, TYB10, MYDGF, MARCS, TCAL3, TYB4, SORCN, TMA7, S10AB, DD19A, DEST, STX12, LSM2, ARC1A, RBMX, TIM13, HAP28, PP1R7, RS14, RS10, CBPQ, RAN, EWS, TBB1, AKA12, DAG1, ROA1, LEG3, SUCB2, KTU, DHSO, PALM, DRB1, AOFB, K1C19, PRDX5, TEBP, HCDH, NH2L1, GPDM, ENY2, LDHB, ANTR2, ERP29, HSPB1, MIF, HDGF, RFA1, SRSF3, CALD1, GDIR1, K1C14, PDIA6, RS28, WASF2, KAP0, DOPD, FMOD, DHB12, RUSC2, CAND1, RLA1, ROA2, ODPB, RCC2, HEP2, ACTZ, SAE1, ARL1, APMAP, SEP10, EIF3H, KCD12, SDHA, E41L3, VP26B, ASC	AL4A1, IF4G2, CO8A1, GOSR2, PSMD2, GHITM, RL28, NU155, GGT5, LAMP1, HPF1, RS9, DDX21, RS24, RS23, ACTS, PRTN3, BLVRB, GTR1, TPM1, TIM50, SIAS, SAP, AP2A2, CUL1, TBG2, CATB, NUP98, CBPE, RPF2, PNCB, RL35, ERAP1, THOC6, MIOS, OCAD2, NUP62, SYUA, RL26, ANAG, ATM, NCLN, FRIL, RL5, AK1C2, SAMP, RL21, HBG2, GCP2, RAB10, ATX10
M vs. P	EVPL, MRP, MARCS, CALM3, BASP1, OTUB1, ROA0, DDX5, PP1R7, RBMX, PTN11, TCAL3, PSMD7, ROA2, GGT5, KTU, RUSC2, RAB21, LAMA2, PDCD4, 1433F, IF4A1, ROA1, APMAP, TBB1, MOES, ANK2, HCDH, PODN, DHB12, FBN2, COCA1, ERG1, PSB3, UCRI, CISD1, C1QBP, EIF3G, PEDF, THIO, PLEC, ELOC, CIRBP, SCAF8, ROAA, CALU, IPYR2, G3BP1, LSM8, ITIH2, TBB5, GCP60, SEP10, RUXF, DEST, ROA3, SRSF3, SUCB1, ARP2, HNRPC, PSA2, CD99, TBB3, PXDC2, RSMN, HDGF, ATPB, LDHB, LA, SAE1, AKA12, RAVR1, CBG, CBPQ, FKBP4, SRPX, MYDGF, ANT3, PGS2, PSMD4, EF1B, KCD12, RTN4, TCTP, HEP2, PDIA6, FBRL, LMA2L, KHDR1, EIF3F, EWS, RLA1, LYPL1, LSM2, SCFD1	AL4A1, SAP, IF4G2, A16A1, APOH, S10A6, CBPE, GBB2, QCR7, SPHM, CLP1L, TPP1, SIAS, TPM1, S10AA, GHITM, SPTB1, EMD, PSMD2, ITA6, IF5, DDX21, CATA, HEXA, RS9, SE1L1, KCC2D, DHPR, STMN1, CSN5, RPF2, SMCA5, MFAP2, BST1, GBG12, KAIN, CYRIB, OCAD2, UFL1, ASPN, PERE, RAB1A, EIF3B, GOSR2, KC1A, BRX1, PRTN3, RAC1, HRG, VATA, NUP98, FUCO, DQA1, FRIL, DHCR7, ERMP1, CATB, RMD1, CUL1, ATM, PLCX3, PGBM, H12, RL28

Exclusively the abbreviated protein name is shown. Y: young, M: middle-aged, P: perimenopausal.

9.4 Appendix D. Supplemental material result 5.2.

Table D1. Oocyte telomere parameters in middle-aged women classified by AMH.

	M+ n = 4		**M-** n = 8
Age (years)		0.0906	
Mean ± SD	38.3 ± 3.0*		41.6 ± 2.9*
Median (Q1–Q3)	38.0 (35.5-41.3)		41.5 (39.0-44.8)
AMH (ng/mL)		0.0040	
Mean ± SD	2.4 ± 1.0*		0.6 ± 0.5
Median (Q1–Q3)	2.4 (1.4-3.3)		0.6 (0.03-1.1)
TL (a.u.)		0.1095	
Oocytes	54		37
Telomeres	6806		4633
Mean ± SD	156.4 ± 24.0		147.2 ± 23.3*
Median (Q1–Q3)	151.2 (136.9-172.4)		145.5 (131.0-161.5)
Short telomeres (%)		0.0416	
Mean ± SD	18.7 ± 19.5		29.3 ± 26.0
Median (Q1–Q3)	11.9 (0.9-32.7)		25.5 (4.7-44.6)
Long telomeres (%)		0.2584	
Mean ± SD	20.9 ± 35.5		14.1 ± 19.9
Median (Q1–Q3)	11.2 (1.7-27.8)		6.7 (1.1-15.3)

Data are presented as mean ± standard deviation and median (interquartile range). *Denoted the variables that passed the Shapiro-Wilk or Kolmogorov-Smirnov normality test. Statistical analysis of comparisons between groups was performed using Student t-test (normally distributed data) or the Mann-Whitney U test (non-normally distributed data). A p-value < 0.05 was considered statistically significant. The n refers to the number of subjects. The number of oocytes and telomere dots analyzed is specified in the TL section. AMH: antimullerian hormone, TL: telomere length; M: middle-aged; SD: standard deviation; Q1: quartile 1 (25% percentile); Q3: quartile 3 (75% percentile); ng: nanogram, mL: milliliter, a.u.: arbitrary units of intensity; %: percent.

Table D2. TCs telomere parameters in middle-aged women classified by AMH.

	M+ n = 4		**M-** n = 10
Age (years)		0.1000	
Mean ± SD	38.3 ± 3.0*		41.6 ± 3.2*
Median (Q1–Q3)	38.0 (35.5-41.3)		42.5 (38.8-44.3)
AMH (ng/mL)		0.0020	
Mean ± SD	2.4 ± 1.0*		0.5 ± 0.5
Median (Q1–Q3)	2.4 (1.4-3.3)		0.5 (0.1-1.1)
TL (a.u.)		0.0229	
Follicles	23		34
Telomeres	4006		5961
Mean ± SD	150.8 ± 22.6*		147.2 ± 23.3*
Median (Q1–Q3)	144.6 (131.5-170.0)		137.3 (130.0-150.2)
Short telomeres (%)		0.1386	
Mean ± SD	26.3 ± 31.7		30.8 ± 20.9*
Median (Q1–Q3)	15.4 (1.3-47.1)		31.8 (11.1-45.2)
Long telomeres (%)		0.1567	
Mean ± SD	18.6 ± 23.3		5.8 ± 9.3
Median (Q1–Q3)	4.8 (0.0-38.4)		2.2 (0.3-7.1)

Data are presented as mean ± standard deviation and median (interquartile range). *Denoted the variables that passed the Shapiro-Wilk normality test. Statistical analysis of comparisons between M+ and M- was performed using Student t-test (normally distributed data) or the Mann-Whitney U test (non-normally distributed data). A p-value < 0.05 was considered statistically significant. The n refers to the number of subjects. The number of follicles and telomere dots analyzed is specified in the TL section. TCs: theca cells, AMH: antimullerian hormone, TL: telomere length, M: middle-aged, SD: standard deviation, Q1: quartile 1 (25% percentile), Q3: quartile 3 (75% percentile), ng: nanogram, mL: milliliter, a.u.: arbitrary units of intensity; %: percent.

9.5 Appendix E. Supplemental material result 5.3.

Table E1. PBMCs telomere parameters in pregnant and non-pregnant women.

	Y+ n = 11	**Ypreg** n = 4	**M+** n = 6	**Mpreg** n = 9
TL (a.u.)	0.1647		0.1810	
Telomeres	43187	25075	43721	78490
Mean ± SD	128.8 ± 6.5*	134.9 ± 8.9*	137.8 ± 17.3*	126.7 ± 8.2
Median (Q1–Q3)	128.7 (124.2-135.9)	135.2 (126.3-143.3)	131.8 (123.5-155.3)	124.0 (120.6-133.1)
Short telomeres (%)	0.2773		0.5228	
Mean ± SD	12.2 ± 6.5*	8.2 ± 4.9*	8.4 ± 8.6*	10.8 ± 5.5*
Median (Q1–Q3)	10.9 (7.8-18.4)	6.2 (5.1-13.2)	7.5 (0.2-15.2)	10.3 (7.1-13.8)
Long telomeres (%)	0.1216		0.0360	
Mean ± SD	10.6 ± 4.7*	16.4 ± 9.2*	19.2 ± 18.6*	7.6 ± 7.7
Median (Q1–Q3)	11.3 (5.5-13.4)	14.6 (8.6-26.0)	10.4 (6.3-36.1)	4.0 (3.0-13.2)

Data are presented as mean ± standard deviation and median (interquartile range). *Denoted the variables that passed the Shapiro-Wilk normality test. Statistical analysis of comparisons between groups was performed using Student t-test (normally distributed data) or the Mann-Whitney U test (non-normally distributed data). A p-value < 0.05 was considered statistically significant. The n refers to the number of subjects. The number of telomere dots analyzed is specified in the TL section under the heading “Telomeres”. PBMCs: peripheral blood mononuclear cells, TL: telomere length, Y: young, M: middle-aged, SD: standard deviation, Q1: quartile 1 (25% percentile), Q3: quartile 3 (75% percentile), a.u.: arbitrary units of intensity, %: percent, vs.: versus.

Table E2. Oocytes telomere parameters in pregnant and non-pregnant women.

	Y+ n = 11	Ypreg n = 3	M+ n = 4	Mpreg n = 6
Age (years)	0.9780		0.3556	
Mean ± SD	30.7 ± 4.4	29.7 ± 5.9*	38.3 ± 3.0*	39.7 ± 1.6*
Median (Q1–Q3)	32.0 (29.0-34.0)	2.0 (23.0-34.0)	38.0 (35.5-41.3)	39.5 (38.0-41.3)
AMH (ng/mL)	0.0055		0.0381	
Mean ± SD	3.6 ± 2.5	0.7 ± 0.2*	2.4 ± 1.0*	0.8 ± 0.6
Median (Q1–Q3)	2.4 (1.9-5.5)	0.7 (0.5-0.9)	2.4 (1.4-3.3)	0.6 (0.5-1.1)
TL (a.u.)	0.0001		0.0033	
Oocytes	162	28	54	55
Telomeres	57530	7811	6806	11672
Mean ± SD	157.3 ± 21.3*	141.9 ± 14.0	156.4 ± 34.0	142.8± 19.6*
Median (Q1–Q3)	155.4 (143.7-170.5)	135.4 (132.4-150.5)	151.2 (136.9-172.4)	143.7 (128.-151.4)
Short telomeres (%)	0.0004		0.0008	
Mean ± SD	15.1 ± 19.4	26.6 ± 17.8*	18.7 ± 19.5	33.8 ± 24.9*
Median (Q1–Q3)	7.2 (1.4-18.4)	27.0 (7.8-36.9)	11.9 (0.9-32.7)	33.3 (11.-54.2)
Long telomeres (%)	0.0002		0.0141	
Mean ± SD	19.6 ± 21.5	6.6 ± 9.6	20.9 ± 25.5	11.5 ± 18.8
Median (Q1–Q3)	11.3 (3.7-30.4)	2.6 (0.4-11.4)	11.2 (1.7-27.8)	2.7 (0.0-16.9)

Data are presented as mean ± standard deviation and median (interquartile range). *Denoted the variables that passed the Shapiro-Wilk normality test. Statistical analysis of comparisons between groups was performed using Student t-test (normally distributed data) or the Mann-Whitney U test (non-normally distributed data). A p-value < 0.05 was considered statistically significant. The n refers to the number of subjects. The number of oocytes and telomere dots analyzed is specified in the TL section. AMH: antimullerian hormone, TL: telomere length; Y: young; M: middle-aged; SD: standard deviation; Q1: quartile 1 (25% percentile); Q3: quartile 3 (75% percentile); ng: nanogram, mL: milliliter, a.u.: arbitrary units of intensity; %: percent.

Table E3. GCs telomere parameters in young pregnant and non-pregnant women.

GCs primordial follicles	Y+ n = 6	Ypreg n = 2
Age (years)	0.5714	
Mean ± SD	29.8 ± 5.6	27.5 ± 6.4
Median (Q1–Q3)	32.0 (26.5-33.3)	27.5 (23.0-32.0)
AMH (ng/mL)	0.0714	
Mean ± SD	3.2 ± 2.3	0.8 ± 0.2
Median (Q1–Q3)	2.3 (1.8-4.7)	0.8 (0.7-0.9)
TL (a.u.)	0.0156	
Follicles	58	8
Telomeres	19622	1630
Mean ± SD	152.2 ± 15.3	143.0 ± 17.1
Median (Q1–Q3)	149.1 (140.4-158.0)	134.8 (132.6-157.0)
Short telomeres (%)	0.0425	
Mean ± SD	9.0 ± 7.0	17.3 ± 11.5*
Median (Q1–Q3)	7.4 (3.3-13.4)	20.1 (5.1-23.0)
Long telomeres (%)	0.1104	
Mean ± SD	19.8 ± 20.4	13.7 ± 20.6
Median (Q1–Q3)	10.8 (4.6-28.7)	3.9 (1.7-27.9)

GCs primary follicles	Y+ n = 11		Ypreg n = 2
Age (years)		0.5128	
Mean ± SD	30.7 ± 4.4		33.0 ± 1.4
Median (Q1–Q3)	32.0 (29.0-34.0)		33.0 (32.0-34.0)
AMH (ng/mL)		0.0256	
Mean ± SD	3.6 ± 2.5		0.7 ± 0.3
Median (Q1–Q3)	2.4 (1.9-5.5)		0.7 (0.5-0.9)
TL (a.u.)		<0.0001	
Follicles	102		20
Telomeres	46388		6656
Mean ± SD	158.6 ± 19.3*		141.0 ± 12.6
Median (Q1–Q3)	160.5 (143.4-171.6)		135.1 (132.3-147.3)
Short telomeres (%)		0.0101	
Mean ± SD	13.2 ± 16.7		25.3 ± 16.3
Median (Q1–Q3)	6.3 (1.7-16.1)		29.0 (6.0-38.1)
Long telomeres (%)		<0.0001	
Mean ± SD	24.7 ± 22.2		5.2 ± 9.1
Median (Q1–Q3)	18.5 (4.2-39.7)		1.3 (0.5-6.2)
GCs secondary follicles	**Y+** n = 4		**Ypreg** n = 3
Age (years)		0.4632	
Mean ± SD	31.8 ± 2.2*		29.3 ± 5.7*
Median (Q1–Q3)	32.0 (29.5-33.8)		31.0 (23.0-34.0)
AMH (ng/mL)		0.0464	
Mean ± SD	3.3 ± 1.6*		0.8 ± 0.4*
Median (Q1–Q3)	3.0 (2.0-5.0)		0.7 (0.5-1.2)
TL (a.u.)		0.9117	
Follicles	11		4
Telomeres	22975		8869
Mean ± SD	176.7 ± 23.6*		175.0 ± 30.6*
Median (Q1–Q3)	183.3 (156.6-197.3)		177.6 (145.0-202.5)
Short telomeres (%)		0.8513	
Mean ± SD	21.2 ± 25.2		24.6 ± 31.6*
Median (Q1–Q3)	10.0 (3.0-35.5)		13.9 (1.8-58.1)
Long telomeres (%)		0.9485	
Mean ± SD	24.8 ± 24.3*		25.7 ± 29.8*
Median (Q1–Q3)	23.9 (2.4-46.5)		21.7 (0.3-55.2)

Data are presented as mean ± standard deviation and median (interquartile range). *Denoted the variables that passed the Shapiro-Wilk or Kolmogorov-Smirnov normality test. Statistical analysis of comparisons was performed using Student t-test (normally distributed data) or the Mann-Whitney U test (non-normally distributed data). A p-value < 0.05 was considered statistically significant. The n refers to the number of subjects. The number of follicles and telomere dots analyzed is specified in the TL section. AMH: antimullerian, Y: young, TL: telomere length, SD: standard deviation, Q1: quartile 1 (25% percentile), Q3: quartile 3 (75% percentile), a.u.: arbitrary units of intensity, %: percent, ng: nanogram, mL: milliliter.

Table E4. TCs telomere parameters in young pregnant and non-pregnant women.

	Y+ n = 8		Ypreg n = 3
Age (years)		0.2793	
Mean ± SD	32.1 ± 1.7*		29.7 ± 5.9*
Median (Q1–Q3)	32.5 (31.0-33.8)		32.0 (23.0-34.0)
AMH (ng/mL)		0.0603	
Mean ± SD	4.2 ± 2.8*		0.7 ± 0.2*
Median (Q1–Q3)	3.3 (2.0-7.0)		0.7 (0.5-0.9)
TL (a.u.)		0.0379	
Follicles	70		10
Telomeres	27892		1816
Mean ± SD	154.8 ± 19.2*		143.1 ± 14.0
Median (Q1–Q3)	157.5 (141.2-168.6)		137.4 (132.8-150.9)
Short telomeres (%)		0.1060	
Mean ± SD	16.5 ± 22.1		24.6 ± 16.5*
Median (Q1–Q3)	7.0 (3.1-17.5)		25.5 (12.7-41.4)
Long telomeres (%)		0.0226	
Mean ± SD	19.7 ± 20.0		6.2 ± 10.2
Median (Q1–Q3)	13.9 (1.5-35.1)		1.3 (0.0-11.7)

Data are presented as mean ± standard deviation and median (interquartile range). *Denoted the variables that passed the Shapiro-Wilk or Kolmogorov-Smirnov normality test. Statistical analysis of comparisons between Y+ and Ypreg was performed using Student t-test (normally distributed data) or the Mann-Whitney U test (non-normally distributed data). A p-value < 0.05 was considered statistically significant. The n refers to the number of subjects. The number of follicles and telomere dots analyzed is specified in the TL section. TCs: theca cells, AMH: antimullerian hormone, TL: telomere length, Y: young, SD: standard deviation, Q1: quartile 1 (25% percentile), Q3: quartile 3 (75% percentile), ng: nanogram, mL: milliliter, a.u.: arbitrary units of intensity; %: percent.

9.6 Appendix F. Supplemental material result 5.4.

Table F1. Telomere parameters of granulosa cells.

	Control	COVID	Mild COVID	Severe COVID
TL (a.u.)	-	0.877	0.089	0.017
n	24	26	15	11
Mean ± SD	141.4 ± 67.5	143.2 ± 72.9	177.6 ± 78.4	96.1 ± 21.9
Median (Q1-Q3)	123.3 (85.8-159.5)	121.3 (92.4-168.1)	156.7 (112.2-233.8)	95.3 (75.2-114.7)
Short telomeres (%)	-	[0.572]	[0.950]	0.248
n	24	26	15	11
Mean ± SD	33.8 ± 17.5	36.4 ± 15	34.2 ± 14.9	39.5 ± 15.2
Median (Q1-Q3)	39.8 (19.2-46.8)	35.5 (25-48.7)	27.9 (25-47.5)	47.5 (20-50)
Long telomeres (%)	-	0.526	0.149	0.003
n	24	26	15	11
Mean ± SD	8.4 ± 10.2	8.8 ± 12.4	14.4 ± 13.8	1.1 ± 1.9
Median (Q1-Q3)	4.7 (0.7-11)	3.4 (0-16.1)	12.1 (2.8-19.4)	0 (0-2.9)

n indicates the number of individuals analyzed. *p-value was calculated between control and each group (COVID, mild COVID and severe COVID) separately. Brackets indicate p-value calculated using Student t-test (normal distribution of data). The rest p-values were calculated with Mann-Whitney U test.

Table F2. Fertility outcomes.

	Control	COVID	Mild COVID	Severe COVID
Number of oocytes	-	0.171	0.224	0.294
n	29	36	19	17
Mean ± SD	10.4 ± 9.3	11.9 ± 7.6	12.2 ± 8.0	11.5 ± 7.4
Median (Q1-Q3)	7 (4-12.5)	10 (5.5-16)	10 (7-16)	9 (5-17.5)
Number of metaphase II	-	0.352	0.227	0.760
n	28	36	19	17
Mean ± SD	8.9 ± 8.2	9.39 ±6.2	10.1 ± 6.2	8.6 ± 6.2
Median (Q1-Q3)	5 (3.3-10.8)	9 (4.3-12)	9 (6-12)	7 (3.5-11.5)
Oocyte Maturation Rate (%)	-	0.094	0.620	0.018
n	28	36	19	17
Mean ± SD	86.7 ±12.3	80.1 ±15.9	85.6 ± 11.5	73.9 ±18
Median (Q1-Q3)	88.5 (79.4-100)	80.9 (66.7-92.4)	87.5 (75-100)	76.2 (57.8-90.7)
Normal Fertilization Rate (%)	-	[0.272]	[0.374]	[0.386]
n	14	27	13	14
Mean ± SD	64.8 ± 29.6	73.5 ± 20.2	73.9 ± 21.9	73.1 ± 19.3
Median (Q1-Q3)	66.7 (47.5-88.2)	75 (63.7-91.7)	75 (61.9-95.8)	75 (60.2-89.7)

n indicates the number of individuals analyzed. *p-value was calculated between control and each group (COVID, mild COVID and severe COVID) separately. Brackets indicate p-value calculated using Student t-test (normal distribution of data). The rest p-values were calculated with Mann-Whitney U test.

9.7 Appendix G. Scientific contributions.

A. PhD student' scientific contributions directly related to this doctoral thesis

Research articles

First author:

Chico-Sordo, L., Polonio, A. M., Córdova-Oriz, I., Medrano, M., Herraiz, S., Bronet, F., ... & Varela, E. (2022). Telomeres and oocyte maturation rate are not reduced by COVID-19 except in severe cases. Reproduction, 164(5), 259-267.

Collaborator:

Polonio, A. M., Medrano, M., Chico-Sordo, L., Córdova-Oriz, I., Cozzolino, M., Montans, J., ... & Varela, E. (2023). Impaired telomere pathway and fertility in Senescence-Accelerated Mice Prone 8 females with reproductive senescence. Aging (Albany NY), 15(11), 4600.

Córdova-Oriz, I., Kohls, G., Iglesias, C., Polonio, A. M., Chico-Sordo, L., Toribio, M., ... & García-Velasco, J. A. (2023). A randomized controlled intervention trial with danazol to improve telomeric and fertility parameters in women with diminished ovarian reserve: a pilot study. Women's Health Reports, 4(1), 305-318.

Review articles

First author:

Chico-Sordo, L., Cordova-Oriz, I., Polonio, A. M., S-Mellado, L. S., Medrano, M., García-Velasco, J. A., & Varela, E. (2021). Reproductive aging and telomeres: Are women and men equally affected?. Mechanisms of Ageing and Development, 198, 111541.

Collaborator:

Córdova-Oriz, I., Polonio, A. M., Cuadrado-Torroglosa, I., Chico-Sordo, L., Medrano, M., García-Velasco, J. A., & Varela, E. (2023). Chromosome ends and the theory of marginotomy: implications for reproduction. Biogerontology, 1-22.

Córdova-Oriz, I., Chico-Sordo, L., & Varela, E. (2022). Telomeres, aging and reproduction. Current Opinion in Obstetrics and Gynecology, 34(3), 151-158.

Polonio, A. M., Chico-Sordo, L., Córdova-Oriz, I., Medrano, M., García-Velasco, J. A., & Varela, E. (2020). Focus: Sex & reproduction: Impact of ovarian aging in reproduction: From telomeres and mice models to ovarian rejuvenation. The Yale journal of biology and medicine, 93(4), 561.

Works submitted to international conferences

First author:

Telomere length maintenance of granulosa cells during folliculogenesis in humans. Lucía Chico-Sordo; Noelia Ramirez Martín; Mónica Romeu; Sonia Herraiz; Alba Maria Polonio; Isabel Córdova Oriz; Juan A. García Velasco; Elisa Varela. Society for Reproductive Investigation (SRI Congress 2023). Brisbane, Australia. 21-25 March 2023. Poster

Assessment of telomere parameters in short-term cultures of granulosa cells. Lucía Chico-Sordo; Elena Martínez-Iglesias; Alba María Polonio; Isabel Córdova-Oriz; Marta Medrano; Juan A. García-Velasco; Elisa Varela. American Society for Reproductive Medicine (ASRM Congress 2022). Anaheim, United States. 22-26 October 2022. Poster

Telomere length in graulosa cells is affected in women who had stronger COVID-19 symptoms. Lucia Chico-Sordo; Alba María Polonio; Isabel Cordova-Oriz; Marta Medrano; Juan Antonio García-Velasco; Elisa Varela. Cold Spring Harbor Laboratory (CSHL Telomeres & Telomerase 2021). Online. 14-17 December 2021. Poster

Young women diagnosed with distal cancer show telomere alteratios in the ovary. Lucía Chico-Sordo; Inmaculada Soler; Isabel Córdova-Oriz; Alba María Polonio; Marta Medrano; César Díaz-García; Juan Antonio García-Velasco; Elisa Varela. American Society for Reproductive Medicine (ASRM Congress 2021). Baltimore, United States. 17-20 October 2021. Poster

Mild cases of COVID-19 disease show alterations in blood telomere length and oocyte maturation. Lucía Chico-Sordo; Isabel Córdova-oriz; Eva Loustau-Rodriguez; Cristina Durán de la Torre; Testillano González; Juan Antonio García-Velasco; Elisa Varela. Society for Reproductive Investigation (SRI Congress 2021). Boston, United States. 06-09 July 2021. Poster

Effect of distal cancer on the telomeric length of ovarian cortex cells. Lucía Chico-Sordo; Inmaculada Soler; Jose Manuel Mateu-Pascual; Isabel Córdova-Oriz; Alba María Polonio; Marta Medrano; María José Soriano; Juan Antonio García-Velasco; Elisa Varela. American Society for Reproductive Medicine (ASRM Congress 2020). Portland, United States. 17-21 October 2020. Poster

Collaborator:

Telomere maintenance improves in the ovary after SC-PRP treatment. Alba M. Polonio, Anna Buigues, Jessica Martínez, Isabel Córdova-Oriz, Lucía Chico-Sordo, Marta Medrano, María Madero-Molina, Paula Blázquez, Cristina RodríguezHernández, Ángela Rodríguez-García, Antonio Pellicer, Juan A. García-Velasco, Sonia Herraiz, Elisa Varela. Society for

Reproductive Investigation (SRI Congress 2024). Vancouver, Canada. 12-16 March 2024. Poster

Telomere protection is impaired in the ovary of SAMP8 mouse model with reproductive senescence. Alba M. Polonio, Marta Medrano, Lucía Chico-Sordo, Isabel Córdova-Oriz, Ángela Rodríguez-García, María Madero-Molina, Juan A. García-Velasco Elisa Varela. Society for Reproductive Investigation (SRI Congress 2024). Vancouver, Canada. 12-16 March 2024. Poster

Telomere maintenance is altered in patients diagnosed with polycystic ovary syndrome. Isabel Córdova-Oriz, Iván Delgado-Sánchez, Lucía Sánchez S-Mellado, Alba María Polonio, Lucia Chico-Sordo, Marta Medrano, Juan A García-Velasco, Elisa Varela. Society for Reproductive Investigation (SRI Congress 2024). Vancouver, Canada. 12-16 March 2024. Poster

Underlying mechanisms in clinical manifestations of polycystic ovarian morphology (PCOM) and PCOS women. Noelia Ramírez-Martín, Mónica Romeu, Jessica Martínez, Irene Peinado, Lucía Chico-Sordo, Anna Buigues, María José Soriano, Nuria Pellicer, Antonio Pellicer y Sonia Herraiz. European Society of Human Reproduction and Embryology (ESHRE Congress 2023). Copenhagen, Denmark. 25-28 June 2023. Poster

Analysis of the impact of SARS-CoV-2 (Covid-19) in ovarian stimulation. Rubio, S., Henzenn, E., Díaz, M., Chico-Sordo, L., Cruz, M., Requena, A., Pacheco, A. International IVIRMA Congress 2023. 20-22 April 2023. Poster

Differential effects of tobacco on telomeres and fertility depending on women´s age and ovarian reserve. Alba Maria Polonio; Isabel Córdova Oriz; Lucía Sánchez Sánchez-Mellado; Lucía Chico Sordo; Marta Medrano; Marta Lázaro López; María Salguero; Fernando Bronet; Juan A. García Velasco; Elisa Varela. Society for Reproductive Investigation (SRI Congress 2023). Brisbane, Australia. 21-25 March 2023. Poster

Effect of maternal age on telomere maintenance in SAMP8 (Senescence Accelerated Mouse Prone 8) females with premature reproductive senescence. Alba Maria Polonio; Marta Medrano; Isabel Córdova Oriz; Lucía Chico Sordo; Juan A. García Velasco; Elisa Varela. Society for Reproductive Investigation (SRI Congress 2023). Brisbane, Australia. 21-25 March 2023. Poster

A prospective, randomized, placebo-controlled pilot trial investigating telomere length dynamics and ovarian function in patients with diminished ovarian reserve (DOR) after danazol treatment. sabel Córdova-Oriz; Mónica Toribio; Graciela Khols; Carlos Iglesias; Lucía Chico-Sordo; Alba María Polonio; Marta Medrano; María Díaz-Gómez; Ana Molinero-Ballesteros; Marcos Meseguer; Juan A. García-Velasco; Elisa Varela. European Society of Human Reproduction and Embryology (ESHRE Congress 2022). Milan, Italy. 03-06 July 2022. Poster

Telomere maintenance is altered is SAMP8 (Senescence Accelerated Mouse Prone 8) females with premature reproductive senescence. Alba María Polonio; Marta Medrano; Lucía Chico-Sordo; Isabel Córdova-Oriz; Juan Antonio García-Velasco; Elisa Varela. Society for Reproductive Investigation (SRI Congress 2022). Denver, United States. 15-19 March 2022. Poster

Study of the premature fertility decay in senescence accelerated mouse prone 8 (SAMP8) and its relation with systemic age. Alba María Polonio; Lucía Chico-Sordo; Isabel Córdova-Oriz; Marta Medrano; Juan Antonio García-Velasco; Elisa Varela.American Society for Reproductive Medicine (ASRM 2021). Baltimore, United States. 17-20 October 2021. Poster

Mouse model has lower ovarian function compared to the control SAMR1. Isabel Córdova-Oriz; Alba María Polonio; Lucía Chico-Sordo; Marta Medrano; Juan Antonio García-Velasco; Elisa Varela. Society for Reproductive Investigation (SRI Congress 2021). Boston, United States. 06-09 July 2021. Poster

Characterization of telomere status during ovarian aging in the SAMP8 (Senescence Accelerated Mouse Prone 8). Alba María Polonio; María Tránsito Gónzalez-García; Isabel Córdova-Oriz; Marta Medrano; Lucía Chico-Sordo; Juan Antonio García-Velasco; Elisa Varela. American Society for Reproductive Medicine (ASRM Congress 2020). Portland, United States. 17-21 October 2020. Poster

B. PhD student's scientific contributions indirectly related to this doctoral thesis

<u>Research articles</u>

First author:

Chico-Sordo, L., Ruiz-Martínez, T., Toribio, M., González-Martín, R., Spagnolo, E., Domínguez, F., Hernández-Gutiérrez, A., & García-Velasco, J. A. (2024). Identification of miR-30c-5p microRNA in Serum as a Candidate Biomarker to Diagnose Endometriosis. International Journal of Molecular Sciences, 25(3), 1853.

Collaborator:

Balmori, C., Cordova-Oriz, I., De Alba, G., Medrano, M., Jiménez-Tormo, L., Polonio, A. M., Chico-Sordo, L. ... & Varela, E. (2022). Effects of age and oligoasthenozoospermia on telomeres of sperm and blood cells. Reproductive Biomedicine Online, 44(6), 1090-1100.

<u>Review articles</u>

First author:

Chico-Sordo, L., & García-Velasco, J. A. (2024). MicroRNAs as Biomarkers and Therapeutic Targets in Female Infertility. International Journal of Molecular Sciences, 25(23), 12979.

Works submitted to international conferences

First author:

Deciphering endometriosis: lower levels of miR-30c-5p in serum of women with endometriosis. Lucía Chico-Sordo, Tamara Ruiz-Martínez, Mónica Toribio, Alicia Hernández-Gutiérrez, Francisco Dominguez, and Juan A. García-Velasco. 15th World Congress on Endometriosis (WCE 2023). Edinburgh, Scotland. 3-6 May 2023. Poster

Collaborator:

Exploring the Biological Roles of miR-191-5p and miR-30c-5p in Impaired Fertility and Their Potential as Diagnostic Biomarkers in Adenomyosis. Ana Corachán, Elena Juárez-Barber, Ana Belén Albert, Lucía Chico-Sordo, Amparo Faus, Carmen Vidal, Juan Giles, Juan Antonio García-Velasco, Hortensia Ferrero. Society for Reproductive Investigation (SRI Congress 2025). Charlotte, United States. 25-29 March 2025. Poster

Evaluation of telomere maintenance in spermatozoa to find new biomarkers to assess sperm quality. Isabel Córdova Oriz; Carlos Balmori; Marta Medrano; Alba Maria Polonio; Lucía Chico Sordo; Isabel Cuadrado Torroglosa; Alberto Pacheco; Juan A. García Velasco; Elisa Varela. Society for Reproductive Investigation (SRI Congress 2023). Brisbane, Australia. 21-25 March 2023. Poster

Use of sperm telomere length as a potential biomarker of outcomes after Intracytoplasmic sperm injection (ICSI). Isabel Córdova-Oriz; Carlos Balmori; Marta Medrano; Alba María Polonio; Lucía Chico-Sordo; Soraya Rubio; Rubén Salvanés; Nuria García; Alberto Pacheco; Juan Antonio García-Velasco; Elisa Varela. Society for Reproductive Investigation (SRI Congress 2022). Denver, United States. 15-19 March 2022. Poster

Older oligoastenozoospermic men have altered telomere biology and less chances than controls for assited reproductive technology outcomes (ART). Isabel Córdova-Oriz; Raquel García-Panadero; Guillermo de Alba; Alberto Pacheco; Carlos Balmori; Lucía Chico-Sordo; Alba María Polonio; Marta Medrano; Juan Antonio García-Velasco; Elisa Varela. American Society for Reproductive Medicine (ASRM Congress 2020). Portland, United States. 17-21 October 2020. Poster

9.8 Appendix H. Complete scientific papers by the student as first author.

Below is a copy of the complete works to which the student contributed as the first author as a PhD student.

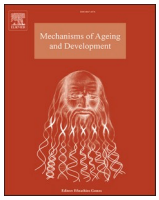
Mechanisms of Ageing and Development 198 (2021) 111541



Contents lists available at ScienceDirect

Mechanisms of Ageing and Development

journal homepage: www.elsevier.com/locate/mechagedev





Reproductive aging and telomeres: Are women and men equally affected?

Lucía Chico-Sordo [a,b], Isabel Córdova-Oriz [a,b], Alba María Polonio [a,b], Lucía Sánchez S-Mellado [a,b], Marta Medrano [a,c], Juan Antonio García-Velasco [a,b,c,d], Elisa Varela [a,b,d,*]

[a] IVI Foundation, Instituto de Investigación Sanitaria La Fe (IISLAFE), Valencia, Spain
[b] Instituto de Investigación Sanitaria La Fe, Valencia, Spain
[c] IVIRMA Madrid, Spain
[d] Rey Juan Carlos University, Madrid, Spain

ARTICLE INFO

Keywords:
Reproduction
Aging
Telomeres
Oocyte
Sperm

ABSTRACT

Successful reproduction is very important for individuals and for society. Currently, the human health span and lifespan are the object of intense and productive investigation with great achievements, compared to the last century. However, reproduction span does not progress concomitantly with lifespan. Reproductive organs age, decreasing the levels of sexual hormones, which are protectors of health through their action on several organs of the body. Thus, this is the starting point of the organismal decay and infertility. This starting point is easily detected in women. In men, it goes under the surface, undetected, but it goes, nevertheless.

Regarding fertility, aging alters the hormonal equilibrium, decreases the potential of reproductive organs, diminishes the quality of the gametes and worsen the reproductive outcomes. All these events happen at a different pace and affecting different organs in women and men. The question is what molecular pathways are involved in reproductive aging and if there is a possible halting or even reversion of the aging events. Answers to all these points will be explained in the present review.

1. Introduction

Aging decreases the reproductive capacity of women and men. Because at present there is a tendency to delay childbearing due to socioeconomic reasons, a number of couples find problems to conceive and have to use assisted reproduction techniques (ART). Considering the female and male factors, about 9% of couples worldwide face infertility problems according to the World Health Organization. However, around 40–50% of the cases are due to the male factor (Fainberg and Kashanian, 2019). Regarding women, data obtained from the National Survey of Family Growth in United States show that 12 % of them demanded fertility services in 2006–2010 (Chandra et al., 2014). Strikingly, infertility, both in men and women, may happen at very young ages. In fact, a poor response to hormone stimulation in young women is indicator of fast declining fertility (Lawson et al., 2003). Anyway, even if menopause happens at the age of 50 years, the female decline of fertility occurs early compared to men and the relationship of lifespan and fertility span in humans, is very different from other related species such as great apes. These points are of interest for geneticists and evolutionary scientists, which have proposed the grandmother hypothesis which postulates that in humans, early menopause liberates older women to support early reproduction of younger women (daughters) by taking care of their grandchildren (Hawkes et al., 2009). However, given the habit of delaying childbearing, geneticists search for the possibility

Abreviations: ALT, Alternative lengthening of telomeres; ART, Assisted reproduction techniques; ATP, Adenosine triphosphate; BPH, Bening protate hyperplasia; CCs, Cumulus cells; DFR, DNA fragmentation rates; DHEA, Dehydroepiandrosterone; DHEAS, Dehydroepiandrosterone sulfate; DZ, Dizygotic twins; FSH, Follicle-stimulating hormone; GCs, Granulosa cells; GnRH, Gonadotropin-releasing hormone; ICSI, Intracytoplasmic sperm injection; IVF, In vitro fertilization; LH, Luteinizing hormone; mtDNa, Mitochondrial DNA; PAC, Paternal age at conception; PAE, Paternal age effect; POI, Primary ovarian insufficiency; PBMCs, Peripheral blood mononuclear cells; ROS, Reactive oxygen species; SHBG, Sex hormone binding globulin; SNPs, Single nucleotide polymorphisms; SSCs, Spermatogonial stem cells; TA, Telomerase activity; TL, Telomere length; TERRAs, Telomeric long non-coding RNAs; TUNEL, Transferase dUTP nick end labeling.

* Corresponding author at: IVI Foundation, EDIFICIO BIOPOLO - LA FE, Avenida Fernando Abril Martorell, 106 - Torre A, Planta 1ª, 46026, Valencia, Spain.
E-mail addresses: Lucia.Chico@ivirma.com (L. Chico-Sordo), Isabel_cordova@iislafe.es (I. Córdova-Oriz), albam_polonio@iislafe.es (A.M. Polonio), Lucia.Sanchez@ivirma.com (L.S. S-Mellado), Marta.MedranoFer@ivirma.com (M. Medrano), Juan.Garcia.Velasco@ivirma.com (J.A. García-Velasco), MariaElisa.Varela@ivirma.com (E. Varela).

https://doi.org/10.1016/j.mad.2021.111541
Received 31 March 2021; Received in revised form 1 July 2021; Accepted 5 July 2021
Available online 7 July 2021
0047-6374/© 2021 Elsevier B.V. All rights reserved.

to enlarge reproductive lifespan. In this review, we will focus on the genetics of aging.

One of the main pathways implicated in aging is telomere attrition. Telomeres are structures localized at chromosome ends (Fig. 1) that safeguard genome integrity preventing chromosome fusions and degradation and aiding cells to distinguish chromosome breaks from chromosome ends (Martínez and Blasco, 2017). Telomeres were first described by Blackburn and Gall in the protozoan *Tetrahymena thermophila* (Blackburn and Gall, 1978). In vertebrates, telomeres consist of tandem repeats of the hexanucleotide "TTAGGG", with a normal length of 10–15 kb in humans and 40 kb in mice (Varela et al., 2016). Telomeric DNA is bound by a complex of proteins called Shelterin (Fig. 1) which protect chromosomes from unscheduled DNA repair and degradation (telomere capping) and control telomere length (TL)(Martínez and Blasco, 2017; de Lange, 2018). Telomeres end in a structure called the telomere loop, which is stabilized by the shelterin complex, further contributing to the protection of these chromosome loci (Martínez and Blasco, 2017). Telomeres are epigenetically regulated, with methylation marks generating a heterochromatic structure refractory for transcription (Martínez and Blasco, 2017). Despite telomere protection, with every round of DNA replication when cells divide, telomeres shorten due to the inability of the replication machinery to copy the very ends of linear chromosomes (Martínez and Blasco, 2017). Nature solves this problem with the enzyme telomerase, which can add the novo repeats onto the 3ends of chromosomes (Greider and Blackburn, 1985). However, telomerase is only active in embryonic and adult stem cells, the germline and cancer cells, while is silenced in most of the cells of the organism. Thus, telomere attrition happens at a faster pace in somatic cells than in adult stem cells (Flores and Blasco, 2010). Critically short telomeres impair cell division leading to senescence or apoptosis and therefore to the accumulation of senescent cells in tissues which limit their regenerative capacity causing to aging (Flores and Blasco, 2010). New evidences support the telomere pathway causing an impact in different areas of reproduction, both in women and men. This review will focus on this topic.

2. Effects of aging on the female reproductive system

Aging affects the reproductive system of women, through alterations in the endocrine system, the uterus, the ovary, and oocytes. From the clinical point of view, the effects of aging in women culminate with menopause, but the reproductive decline starts earlier in life, and the fertility outcomes are altered before menopause onset.

2.1. Endrocrine system

The most extended theory regarding female fertility, proposes that there is a fixed number of oocytes at birth, bordered by somatic cells, granulose and cumulus cells (GCs and CCs respectively) inside the primordial follicles. Oocytes are arrested in prophase I and will remain quiescent until puberty, when their periodic recruitment will start, causing a progressive reduction of oocytes until menopause (Broekmans et al., 2007).

All these events are accompanied by variations in the hormone levels to regulate women's menstrual cycle (Fig. 2, top panel), orchestrated by the hypothalamus-hypophysis-ovarian axis. The hypothalamus produces pulses of gonadotropin-releasing hormone (GnRH). This hormone acts on the anterior lobe of the pituitary gland, in response secretes follicle-stimulating hormone (FSH) and luteinizing hormone (LH) (Fig. 2, top panel). During the follicular phase of the menstrual cycle, FSH stimulates follicle growth and secretion of sex hormones. A rise of FSH and a peak of LH triggers ovulation. Indeed, follicle growth previous to ovulation, requires intensive GCs and CCs cell division, a process that would shorten telomeres. However, GCs and CCs possess active telomerase, despite being somatic cells, what probably prevents excessive telomere attrition, therefore allowing multiple divisions (Polonio et al., 2020). Sex hormones produced during follicle growth stimulate telomerase expression through the estrogen receptor (ER), which can target telomerase gene since there is an estrogen response element present in the promoter region of hTERT (Misiti et al., 2000). In fact, several steroid hormones may be able to activate telomerase expression (Aldous et al., 1999; Nakayama et al., 2000), not only in the reproductive organs,

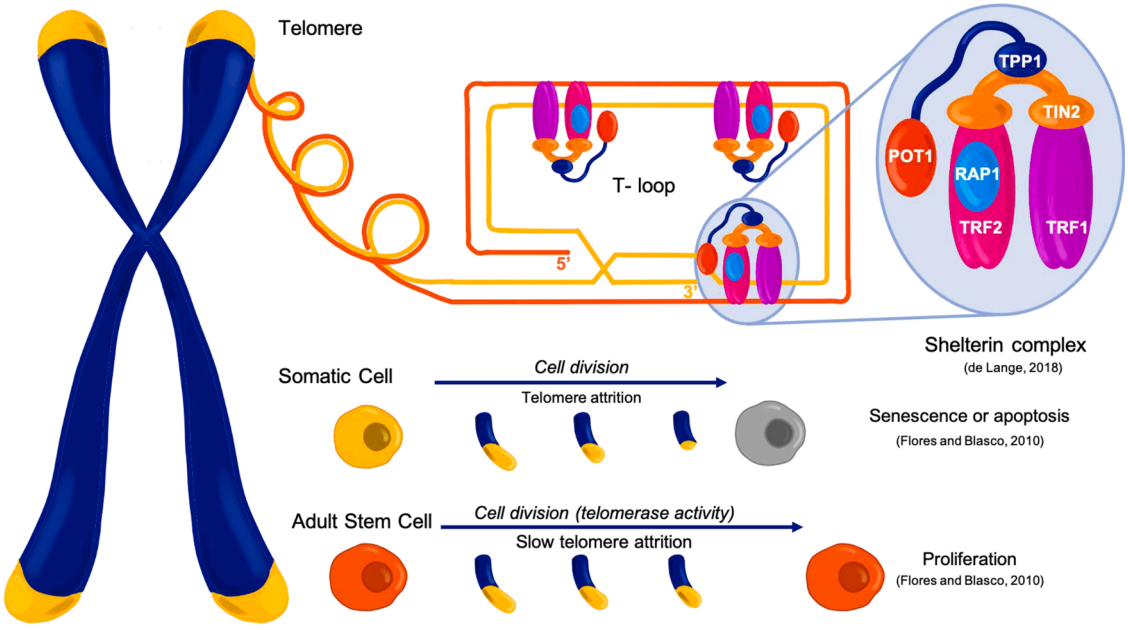


Fig. 1. Telomere structure and dynamics.
In the top panel the telomere structure is represented. The 3overhang of telomeres invade the double helix to form the telomere loop (T-loop). The sheltering complex binds telomeric repeats and stabilize the T-loop structure, ensuring telomere protection. On the right side, a scheme of the shelterin complex is shown. In the lower panel, telomere shortening trough cell division is depicted. In the case of somatic cells, telomeres shorten with every cell division. If telomeres reach a critically short length, cells will undergo senescence or apoptosis. In adult stem cells, endogenous TA can maintain telomeres. Therefore, over age telomeres will shorten, but at a slower rhythm compared to somatic cells.

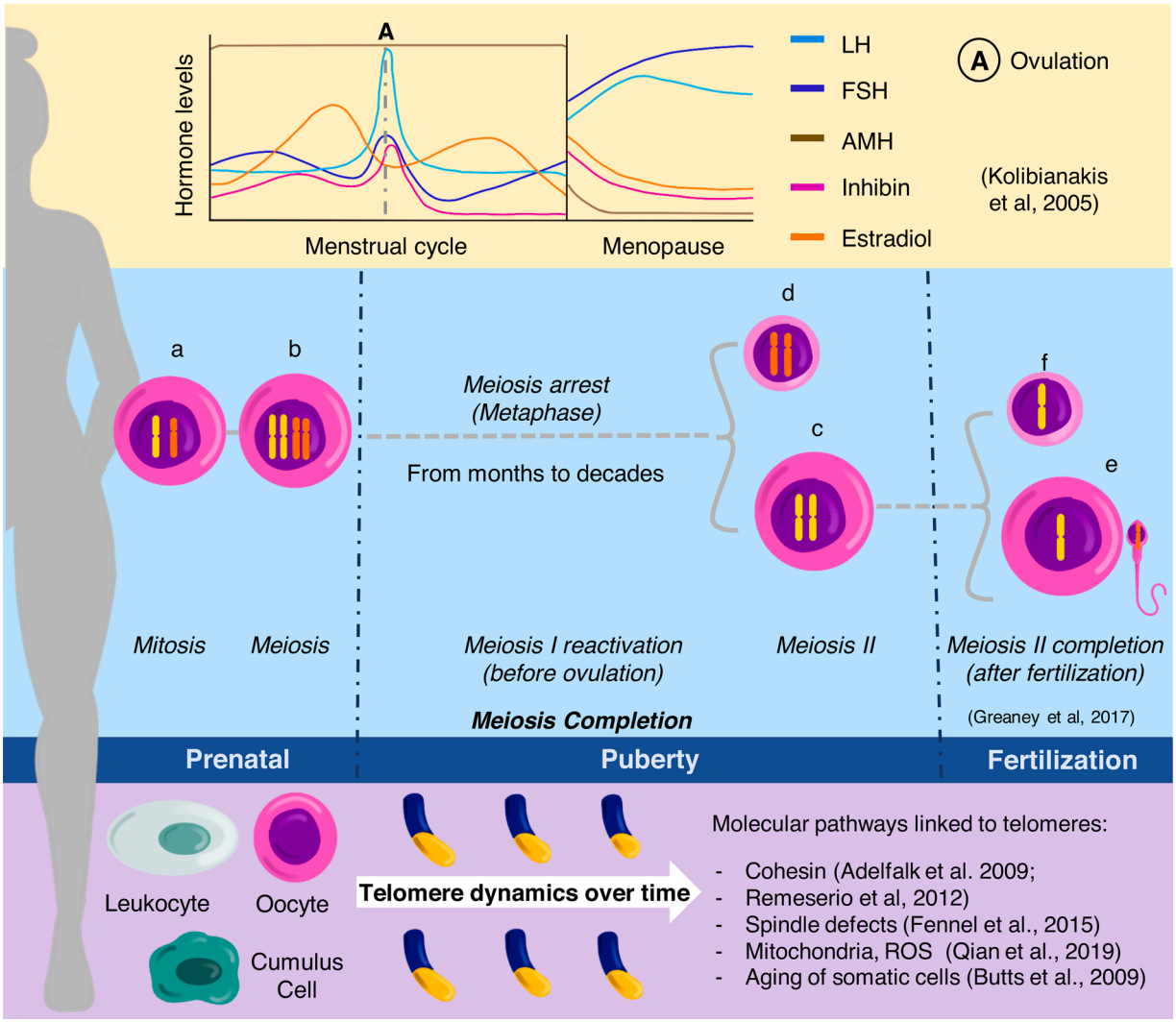


Fig. 2. Female reproductive aging.
In the top panel, hormone levels through female menstrual cycle are represented. Follicle Stimulating Hormone (FSH), Luteinizing Hormone (LH), anti-müllerian hormone (AMH), estrogens and inhibin are depicted. In menopause, FSH and LH levels are increased while estrogens and inhibin levels decay. AMH levels are decreased due to follicular reserve decay. In the middle panel, oogenesis is represented. In this panel, (a) represent oogonia, (b) primary oocyte, (c) secondary oocyte, (d) first polar body, (e) oocyte and (f) second polar body. Oogonia divide by mitosis in the ovary during fetal life and primary oocytes start meiosis. Meiosis is arrested in Metaphase I during decades. In puberty, a pool of follicles is rescued in each cycle and meiosis I completion occurs before ovulation, resulting in a mature oocyte (metaphase II) and the first polar body. Only once fertilization occurs, meiosis II is completed, and the extrusion of the second polar body from oocyte happens. In the lower panel, telomere attrition over time is shown in leukocyte and sperm. Cumulus cells show a different pattern from others somatic cells, with a lower rate of telomere shortening. Different factors are associated with oocyte aging such us cohesion impairment, spindle aberrations, recombination deficiency and mitochondrial dysfunction and ROS, etc. These factors are also linked to the telomere pathway.

but also in every tissue containing ER receptors. This is very important for cell proliferation and tissue homeostasis ((Martínez and Blasco, 2017)Martinez and Blasco 2017).

In the luteal phase, after ovulation, FSH and LH levels are relatively low and the GCs of the ovulated follicle, which remain in the ovary are luteinized by LH forming the corpus luteum (Polonio et al., 2020), which is the major producer of progesterone for the initial phase of pregnancy (Yamamoto et al., 1997). GCs also produce inhibins (A and B) that participate in the inhibition of FSH secretion by the adenohypophysis (Groome et al., 1996). The maintenance and regulation of this axis is decisive for the female reproductive capacity. Menopause occurs approximately at the age of 50 years and is characterized by the cessation of menstruation, with an altered profile of hormone secretion (Fig. 2, top panel). However, this transition is gradual and may last several years, a period known as perimenopause (Ottolenghi et al., 2004). In the early perimenopausal phase, women suffer a drop in inhibins leading to the increase of FSH (Burger et al., 1998). At this point, oestradiol and estrogen production decrease, also in the blood stream, leading to increased GnRH production in the hypothalamus and higher amounts of FSH which cannot stimulate follicles because they are absent in the ovaries. Analysis of androgen levels during menopause shows that free testosterone increases, which may reduce the expression levels of telomerase, because androgens are negative regulators of hTERT in non-cancerous tissues, as observed in rats and monkey (Meeker et al., 1996; Ravindranath et al., 2001). In addition, at the menopause stage GCs, which are almost absent, could not convert androgens to estrogens.

Menopause terminates the reproductive capacity of women, but it also has physical, emotional, and functional consequences due to the presence of estrogen receptors in different target tissues such as the brain, bones, uterus, or cardiovascular system (Dennerstein et al., 2000). Hormone replacement therapy can improve the alterations that

accompany menopause, and in turn have an effect on the telomere level. The study by Lee et al. (2005) observed increased telomere length in postmenopausal women on hormone therapy (Lee et al., 2005). However, there are different opinions on its use due to side effects (Hickey et al., 2005; Poudou et al., 2021).

2.2. Uterine aging

The uterus is the central organ for pregnancy because it is where embryo implantation and fetal development occur. Normal length telomeres and active telomerase in adult stem cells niches are required for proper organ function (Donate and Blasco, 2011). In telomerase-deficient mice of the sixth generation, which bear very short telomeres, the uterine horns are reduced in diameter due to atrophy of the smooth muscle. Endometrium histological analysis in this model was normal, but litter size was drastically reduced (Lee et al., 1998). In humans, the endometrium undergoes about 400 menstrual cycles during the reproductive lifespan, showing a high regenerative capacity. Indeed, there is evidence for the existence of endometrial progenitor cells, with stem cell characteristics (Chan et al., 2004; Cervello et al., 2011; Miyazaki et al., 2012) which express telomerase activity (TA) (Cervello et al., 2011). Endometrial TA is thought to be activated by estrogens (Tanaka et al., 1998; Vidal et al., 2002) and has been proposed to maintain and protect telomeres from the endometrium as well as to promote proliferation (Valentijn et al., 2015). Endometrial TA fluctuates with the menstrual cycle (Yokoyama et al., 1998). During the proliferative phase, TA is elevated, and is inhibited during the mid-secretion phase. The expression of endometrial TA declines after ovulation on the start of the secretory phase. Progesterone rises in the initial secretory phase, reaching its maximum value in the middle, and falls during the late secretory phase. TL of endometrial cells also fluctuates and is shorter when progesterone levels are higher (Valentijn et al., 2015). The levels of TA expression correlate negatively with serum progesterone levels (Williams et al., 2001), supporting the notion that progesterone could inhibit telomerase (Valentijn et al., 2015).

The integrity of telomerase and other telomerase-associated proteins, such as Dyskerin are important for endometrial function and to avoid endometrial pathologies (Alnafakh et al., 2020, 2021) such as cancer, which seems to happen at a higher frequency during post menopause (Paleari et al., 2021). At this point, estrogens drop and low TA could lead to telomere shortening limiting proliferation of epithelial cells during the menstrual cycle, causing pathologies (Hapangama et al., 2017). These cells could undergo genetic instability aiding their transformation into cancer cells (Artandi et al., 2000). Accordingly, TERRAS, which are telomeric long non-coding RNAs which contribute to genome stability (Schoeftner and Blasco, 2008) have been found in healthy endometrium, in contrast to the low levels found in endometrial cancer (Adishesh et al., 2020). Thus, the telomere pathway is important for endometrial function and alterations in this pathway, such as elevated telomerase levels, which are associated with uterine and endometrial dysfunction and ultimately reproductive failure (Hapangama et al., 2008; Long et al., 2016).

The question whether the uterus ages in humans is lively discussed. On one hand, some studies conclude that there is a decrease in uterine receptivity with age. On the other hand, some women accomplished their wish to became mothers at the age of 66 years (Cutas and Smajdor, 2015). In the 1990s, several studies approached this question (Table 1), using donor oocytes and ART. Lower pregnancy rates were observed in women in their 40s compared to younger women (Abdalla et al., 1990). Similar results were found in other studies that measured implantation and pregnancy rates (Chetkowski et al., 1991; Flamigni et al., 1993; Pantos et al., 1993; Yaron et al., 1993; Check et al., 1994). In addition, there was a significant increase in the number of miscarriages in older women, supporting the idea that the uterus ages (Levran et al., 1991; Cano et al., 1995; Pellicer et al., 1995). However, no differences in endometrial receptivity in women of different ages were found when

Table 1
Impact of age in the uterus, in experiments with donor oocytes.

Authors	Study design and population	Main outcomes measure	Conclusions
Abdalla et al., 1990	Prospective longitudinal study. 100 cycles, 82 recipients	Pregnancy rate	The pregnancy rate is affected by the recipient age. This rate in the group 25–29 years old was 50% and decreased by 9.7% in the 45–49 age group.
Levran et al., 1991	Retrospective study. 91 donation cycles, 169 recipients	Pregnancy and spontaneous abortion rate	Recipients who conceived were younger than those who did not. The donors age influenced the risk of abortion.
Pantos et al., 1993	Retrospective study 134 recipients (minimum age 40 years) divided into three age groups	Implantation and pregnancy rate	Only 41 clinical pregnancies were established in 134 recipient cycles. The implantation rate per embryo was constant in all age groups. 14 pregnancies ended in miscarriage.
Flamigni et al., 1993	Prospective study 141 cycles, 87 recipients	Pregnancy and implantation rate	A lower pregnancy and implantation rate in older recipient women due to increased uterine age.
Yaron et al., 1993	Retrospective. Standard IVF. IVF: 325 transfer cycles in older patients and 1103 in younger women Oocyte donation: 236 cycles in older patients and 222 in younger women	Clinical pregnancy rate	The clinical pregnancy rates were lower in older patients in standard IVF and in oocyte donation. A higher rate of implantation failure in older women.
Check et al., 1994	Prospective study 155 donor-recipient cycles. Two groups, under or over 40 years old.	Pregnancy and live birth rates	The pregnancy rate per transfer and the live birth rate were higher in younger women compared to older recipients.
Pellicer et al., 1995	Prospective study Oocytes from the same donor were divided for younger and older recipients	Abortion rate	Higher abortion rates in older patients compare to younger recipients.
Cano et al., 1995	Prospective longitudinal study 90 cycles	Pregnancy, implantation and abortion rates	Higher abortion rates in older women and similar implantation rates in younger and older recipients.
(Soares, 2005)	Retrospective study 3089 cycles	Pregnancy, implantation and miscarriage rates	Pregnancy and implantation rates were lower in women over 45 years of age. In these women the miscarriage rate was increased.
Navot et al., 1991	Prospective study Women aged 40 years or older 210 self-oocytes cycles and 50 donated oocytes cycles, 35 recipients	Pregnancy, implantation and delivery rates	The implantation rate was higher in the case of donated oocytes compared to self-oocytes. There was not differences between donors and recipients in clinical pregnancy and delivery rates.
Sauer et al., 1992	Prospective study	Embryo implantation	No age-related decline in fertility was

(continued on next page)

Table 1 (*continued*)

Authors	Study design and population	Main outcomes measure	Conclusions
	Women aged 40 years 218 recipient cycles and 157 recipients	and pregnancy rates	demonstrated in cases where donated oocytes were used. The female fertility decline can be corrected with donated oocytes.
Navot et al., 1994	Prospective study 102 recipient cycles, 38 donors	Clinical pregnancy and pregnancy loss rates	There was not significant difference in the number of oocytes received and fertilized, and in the number of embryos transferred. The pregnancy loss rates were higher in older women but not significantly different.
Balmaceda et al., 1994	Retrospective study 258 cycles and 140 recipients	Pregnancy, implantation and abortion rates	Donor's age affects implantation. Recipient women in the range of 30–50 years of age have similar chances when using donor oocytes.
Stolwijk et al., 1997	Historical cohort study 294 women with donated oocytes and standard IVF in 277 women	IVF outcomes and pregnancy loss	The age effect was only found in the cases of standard IVF but not when donated oocytes were used.

oocytes were donated (Navot et al., 1991; Sauer et al., 1992; Balmaceda et al., 1994; Navot et al., 1994; Stolwijk et al., 1997) supporting the notion that high-quality donated oocytes can compensate possible age-related changes in the uterus. To further clarify this point, histologic evaluation of the uterus and endometrium showed no significant alterations with age (Sterzik et al., 1988; Sauer et al., 1992). More recently, the evaluation of senescent cells in tissues, which accumulate with age and impair tissue renewal (Muñoz-Espín and Serrano, 2014), has evidenced an increase of β-galactosidase-positive cells (arrested in G0) in women older than 45 years, what could lead to failures in implantation (Laser et al., 2010).

Because progesterone is essential for embryo development, when it was supplied to women using donated oocytes the endometrium was better prepared for implantation, overcoming the age effect (Meldrum, 1993). In addition, when progesterone was supplied to 50-years-old women, the pregnancy rates, multiple gestation and miscarriage rates after ART were similar to those found in younger women (Paulson et al., 2002). Thus, endometrial receptivity is a key point for uterine function. While the uterus may have age signs, the use of hormones can improve uterine function beyond menopause. Therefore, the impact of aging in the uterus seems to be reversible. Future research might address whether the use of sex hormones is in fact reactivating telomerase to rejuvenate the uterus, improving its function.

2.3. Ovarian aging and fertility outcomes

The ovary is an exceptional organ in terms of aging because its senescence is established earlier compared to other organs and its function declines at a time when most other systems in the body maintain their functionality at near peak (Polonio et al., 2020). The loss of the initial pool of oocytes and the accumulation of errors in old oocytes are thought to be the primary cause of ovarian failure and aging (Te Velde and Pearson, 2002). However, defects in the telomere pathway may also cause ovarian aging. In telomerase-deficient mice of the sixth generation, the ovarian atrophy was evident, with less oocytes ovulated compared to controls and those that were fertilized hardly reached the blastocyst stage (Lee et al., 1998). The histology of the ovary showed all types of follicles, however, ovulated oocytes had misaligned chromosomes at the metaphase plate and aberrant spindles, suggesting that appropriate telomere integrity may help spindle assembly and proper chromosome segregation (Liu et al., 2002). In fact, the rate of aneuploidy in oocytes is higher when TL is shorter (Treff et al., 2011). In fact, more than 80 % of embryos are altered in women older than 40 years old (Munné et al., 2007).

In contrast to what occurs in the male reproductive system, where gametes are produced throughout the whole reproductive life and meiosis completion takes place in less than 75 days (spermatogenesis), oogenesis begins during fetal life (Fig. 2, middle panel). The pool of primordial follicles remains arrested in metaphase I from this moment until their progressive recruitment in each cycle from puberty onwards. The duration of this arrest, which can last for decades, provides wide opportunity for errors and damage to accumulate in the oocyte. In fact, an average aneuploidy rate of 10–70 % in oocytes has been observed, depending on maternal age, whereas, in sperm the average ratio is 1–4 % (Nagaoka et al., 2012; Greaney et al., 2018). This phenomenon has been the basis for multiple hypothesis attempting to explain the effect of maternal age on the oocyte.

The function of the ovary culminates with menopause and the cessation of ovulation, with less than 1000 follicles remaining in the ovary. However, a 6% of European women suffer premature ovarian failure at the age of 40 years and a 1%, at the age of 30 years. Premature ovarian aging has been related to telomeres. Short telomeres have been found in GCs of women with occult ovarian insufficiency, as well as null TA in these cells (Butts et al., 2009) and similar results have been linked to premature ovarian insufficiency (Xu et al., 2017). Numerous recent studies aim to achieve ovarian rejuvenation in women with premature aging of their gonads. Some of the studies with this objective are based on the potential of bone marrow-derived stem cells (BMDSCs) to regenerate the ovarian niche, and activate dormant follicles (Herraiz et al., 2018). However, other studies are focused on the use of different drugs to lengthen telomeres, based on previous results in the treatment of certain telomeric diseases in humans (Townsley et al., 2016), or in animal models (Jaskelioff et al., 2011).

Ultimately, ovarian aging has a strong impact on fertility outcomes, leading to an increase in miscarriages (Andersen et al., 2000; Grande et al., 2012), implantation failure and a decrease in pregnancy rates related with age, independently of the male factor (Schwartz and Mayaux, 1982; van Noord-Zaadstra et al., 1991). Advanced maternal age has also been associated with adverse perinatal outcomes such us low weight at birth, perinatal mortality, still birth or congenital malformations (Pinheiro et al., 2019; Kortekaas et al., 2020). A comparison of healthy women with those who needed IVF showed that infertile women had shorter telomere length (Czamanski-Cohen et al., 2015). Accordingly, a higher mean TL is found in oocytes from patients who achieved pregnancy (Turner and Hartshorne, 2013). Indeed, oocytes with short TL have a low probability of success in IVF (Keefe et al., 2007). Finally, TL of Peripheral Blood Mononuclear Cells (PBMCs) is shorter in older women with new-borns with Down syndrome (Ghosh et al., 2010).

2.4. Theories of oocyte aging

To explain the oocyte quality weakening with age, different mechanisms have been proposed, most of them associated with the increase in oocyte aneuploidies with age.

Due to the close association between the telomere pathway and ovarian atrophy, oocyte ovulation and aneuploidies, it not surprising that telomeres come under the spotlight when talking about ovarian aging.

TL and the accumulation of critically short telomeres have extensively

linked to reproductive age in women. In fact, there is a positive correlation between TL in blood cells and women's reproductive lifespan (Aydos et al., 2005; Fagan et al., 2017), hypothesizing that differences in TL could reflect differences in the replicative capacity of primordial germ cells and follicle numbers (Aydos et al., 2005). In line with this hypothesis, telomeres are thought to be good indicators of menopausal age (Gray et al., 2014) and TL of CCs has been proposed as a biomarker of oocyte quality for IVF (Cheng et al., 2013). Telomere shortening in oocytes (Fig. 2, lower panel) are thought to happen as the result of the many divisions of the oogonia during fetal life and also, due to the action of reactive oxygen species (ROS) on telomeres during the long period of oocyte meiotic arrest (Keefe et al., 2006). These alterations in telomere integrity may be worsened by different lifestyle factors (Keefe et al., 2006). TL maintenance depends on TA, which decreases during oocyte maturation and early embryo development and is reactivated at the blastocyst stage (Wright et al., 2001). At this point of development, the longest telomeres are found in the inner cell mass of the blastocyst (Schaetzlein et al., 2004; Varela et al., 2011, 2016). Thus, telomere shortening has been proposed as one of the possible mechanisms leading the decrease in oocyte quality through time as it affects genome stability and correct chromosome segregation (Liu et al., 2002). In that context, a lower amount of telomeric DNA in polar bodies correlates with more aneuploidies in human oocytes (Treff et al., 2011). In addition, shorter TL in oocytes has been associated with a higher rate of embryo fragmentation (Keefe et al., 2005).

Apart from telomere attrition, different theories have also been proposed to explain the decline in oocyte quality over time. However, many of them do not exclude telomeres maintenance being involved at different levels.

Recombination inefficiency has been proposed as a cause of the increase of aneuploidies with age. The hypothesis is that first-ovulated oocytes initiate meiosis sooner and have the highest number of intercrosses (Henderson and Edwards, 1968; Polani and Crolla, 1991). Telomeres of eukaryotes tether to the nuclear envelope during meiosis to form the bouquet structure, which is thought to help the pairing of homologous chromosomes, prior to recombination (Chikashige et al., 2007). Short telomeres from older mothers might impair proper telomere tethering and subsequent meiotic events. In fact, some genetic linkage studies report lower levels of recombination in pregnancies of older women, which is associated with a higher risk of chromosome miss-segregation (Hussin et al., 2011; Bleazard et al., 2013), but not all studies are consistent with these results (Kong et al., 2004; Campbell et al., 2015; Martin et al., 2015). Moreover, the moment of meiosis entering (in the mother) does not affect to the level of recombination found in fetal oocytes (Rowsey et al., 2014). Thus, this hypothesis may need to be further explored to explain the decrease in oocyte quality through maternal age.

Cohesin degradation during meiotic arrest has also been suggested as one of the main contributors to the decrease in oocyte quality with advanced maternal age including telomere shortening (Hodges et al., 2005; Chiang et al., 2010; Revenkova et al., 2010; Adelfalk et al., 2009; Chiang et al., 2011), because the loss of cohesion between homologous chromosomes leads to the generation of aneuploidies. In mice somatic cells, the lack of cohesion at telomeres leads to defects in telomere replication causing aneuploidies. A similar mechanism may be taking place in oocytes (Remeseiro et al., 2012). In this context, a major separation between kinetochores or the division of bivalents into individual chromosomes have been observed in aged oocytes in humans and murine model (Chiang et al., 2010; Duncan et al., 2012; Sakakibara et al., 2015; Zielinska et al., 2015; Patel et al., 2016). In murine oocytes, age-related deterioration of chromosome-associated cohesin has been described and in humans, the total cohesin fraction of oocytes remaining from IVF cycles is highly variable (Garcia-Cruz et al., 2010). These facts support the idea of the cohesion degradation hypothesis. In addition, a decrease of cohesin in the germinal vesicles from aged mothers has been shown (Tsutsumi et al., 2014).

Spindle defects with age have also been analysed. Classical studies show defective spindle morphology in oocytes from older women (Battaglia et al., 1996; Volarcik et al., 1998), which may lead to incorrect segregations (Shomper et al., 2014). Using confocal time-lapse technology Nagakawa and co-workers found a higher percentage of oocytes from older mice undergoing a transient multipolar spindle state, which was associated with impairment of junctions with chromosomes (Nakagawa and FitzHarris, 2017). Recent work shows that there is a connection between telomeres, spindles and meiotic prophase progression. In fission yeast, the meiosis-specific cyclin Crs1, localizes to the spindle during meiotic prophase and stabilizes the telomeres bouquet (Bustamante-Jaramillo et al., 2021).

The cytoplasmic compartment has an impact on oocyte aging. Both the ooplasmic fraction of vacuoles and the frequency of enlarged smooth endoplasmic reticulum and Golgi are increased in older oocytes (De Bruin et al., 2004). Also, the mitochondrial status is altered, probably caused by cellular stress which accelerates aging (López-Otín et al., 2013) and mitochondrial dysfunction (Sun et al., 2016). Interestingly, mitochondrial alterations have an impact on telomeres (Lopez-Otin et al., 2013), connecting the ooplasm with the nucleus and telomeres. In fact, classical studies associate oxidative stress with impaired oocyte fertilization and developmental potential (Tarin, 1996). In mice, genetic alterations of mitochondria accelerate follicle depletion, leading to subfertility (Zhang et al., 2019a, 2019b). Regarding mitochondrial mutations in oocytes and embryos, some studies show an increased number in older women (Keefe et al., 1995; Barritt et al., 2000; Chan et al., 2005), whereas other reports do not find these differences (Fragouli et al., 2015). Higher mitochondrial DNA copy number has also been detected in embryos from older mothers and in aneuploid embryos, suggesting a higher metabolic activity in embryos under stress (Leese, 2002). Finally, a higher mitochondrial DNA content in euploid embryos is associated with reduced implantation rates (Diez-Juan et al., 2015).

Somatic cells. In spite of the central role of oocytes for female reproductive aging, oocyte maturation could not happen without the bidirectional communication with the somatic cells of the ovary, both GCs and CCs (Dumesic et al., 2015). Hence, it has been proposed that age-related decline in oocyte quality could be determined by somatic cells aging. GCs suffer several changes with age such as an increased DNA damage and DNA repair impairment in mammals (Zhang et al., 2015), as well as an increase in oxidative-stress response genes in bovine and humans (Iwata, 2017; Brzezinski et al., 2018). In fact, co-incubation of follicles from older mothers with GCs from younger ones improves the developmental potential of these follicles (Iwata, 2017). Another change is the decrease in the number of somatic cells in follicles of older mothers (Itami et al., 2014), which is a key determinant of oocyte energetic status. A positive correlation has been found between the number of somatic cells of the follicles and lipid and ATP content as well as ATP acetylation levels in oocytes from porcine follicles (Munakata et al., 2016; Sugiyama et al., 2016; Itami et al., 2017). In addition, these somatic cells seem to age at a different speed compared to other somatic cells. A higher accumulation of age-associated methylation pattern changes has been described in GCs compared to leukocytes, suggesting a different aging trajectory for ovarian somatic cells (Olsen et al., 2020). In contrast, CCs derived from GCs (Goto et al., 2013), seem to remain juvenile despite women's age. The chromatin of CCs bears very long telomeres, longer than leukocyte telomeres (Lara-Molina et al., 2020), and a demethylated genome (Morin et al., 2018). Both GCs and CCs have TA (which is an exceptional characteristic for somatic cells) allowing a slow attrition of telomeres and therefore, maintaining the ability of these cells to divide and nurture the oocyte (Lavranos et al., 1999; Cheng et al., 2013; Lara-Molina et al., 2020). However, the rate of oocyte apoptosis increases around menopause, promoted by the translocation of ceramides (implicated in apoptosis) from the CCs to oocytes (Payne et al., 1997; Perez et al., 2005). Regarding fertility outcomes, women with ovarian insufficiency show decreased TA and TL in GCs and leukocytes (Butts et al., 2009; Xu et al., 2017) and shorter TL in leukocytes

has also been associated with other infertility factors such as recurrent miscarriage (Hanna et al., 2009) and aneuploidies (Hanson et al., 2021).

Taking everything into account, the impact of age on the ovary may be caused by different factors interlinked. Indeed, the telomere pathway seems to affect other pathways involved in oocyte aging such as cohesin, recombination, spindle, deterioration of follicular somatic cells or mitochondrial dysfunction (Liu et al., 2004, Alsheimer et al. 2009, Fennell et al., 2015; Qian et al., 2019).

3. Effects of aging on the male reproductive system

In men, the effects of aging over the reproductive capacity are less noticeable because spermatogenesis continues nonstop throughout mens life since puberty. In contrast to women, the etiology of mens reproductive aging is still poorly understood. However, there is growing evidence of the implication of telomere biology in male fertility. So far, meta-analysis studies have demonstrated the impact of male aging on sperm quality and on hormonal changes along the hypothalamic-pituitary-gonadal axis, concomitant with changes in TL dynamics. In addition, a high prevalence of genetic abnormalities and detrimental defects in children from older fathers have been described (Reichman and Teitler, 2006; Fang et al., 2020). Furthermore, male age and the telomere status at older ages affects the TL and health of their offspring.

3.1. The endocrine system and the sexual organs

Age-related hormonal disruptions in males begin with a decrease in steroid levels at around the age of 50 years, when andropause starts (Fig. 3, top panel). Thus, as described for women, the drop of steroids, which activate telomerase (Calado et al., 2009), may lead to a faster telomere shortening in tissues. Indeed, men have shorter telomeres compared to women (Dalgård et al., 2015) and telomere loss seems to occur faster in men with age (Dalgård et al., 2015; Huang et al., 2021), due to the loss of the protective effect of estrogens on telomere attrition

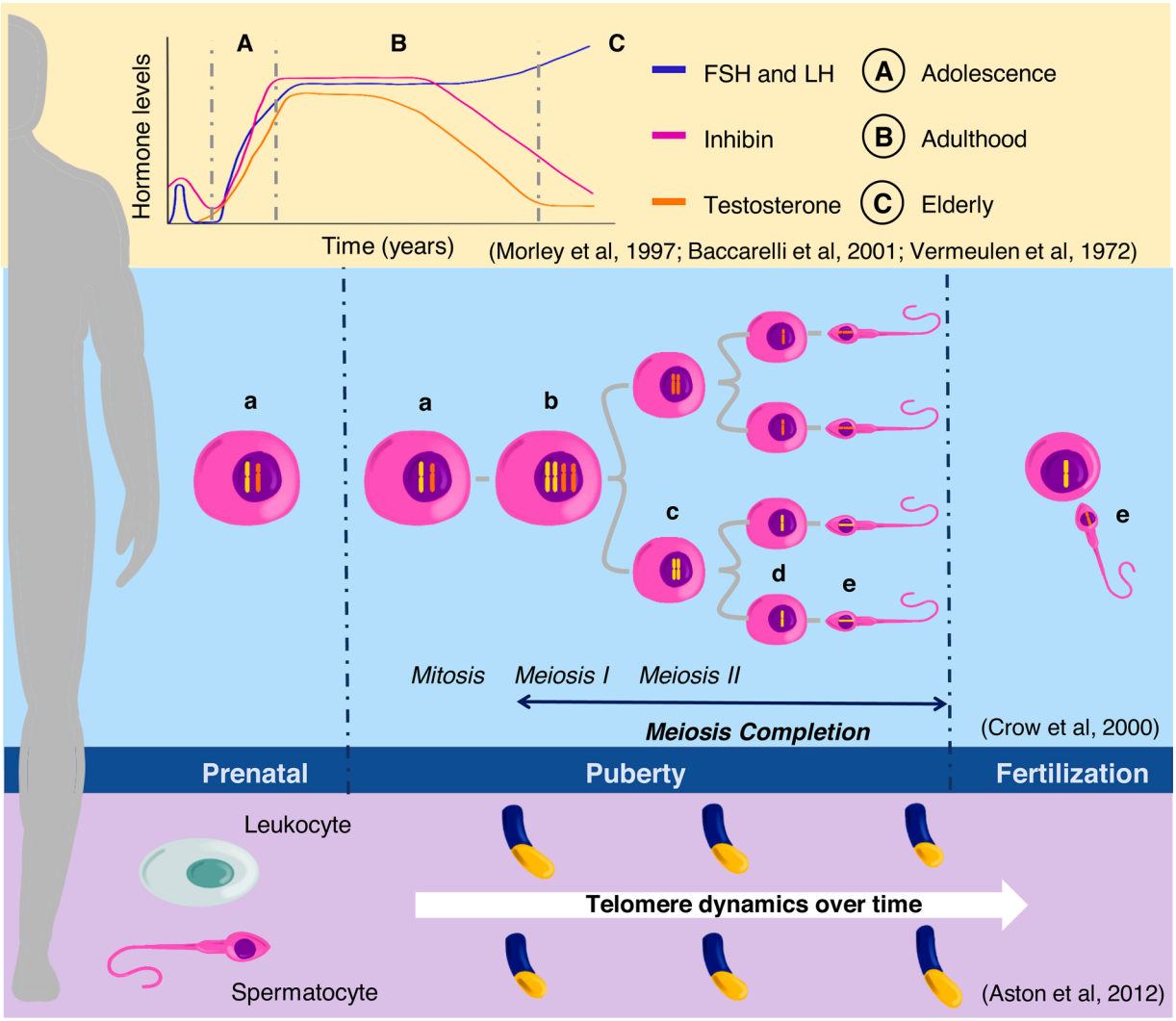


Fig. 3. Male reproductive aging.
In the top panel, hormone levels through male lifespan (adolescence, adulthood and senescence) are represented. Follicle Stimulating Hormone (FSH), Luteinizing Hormone (LH), inhibin and testosterone are depicted. In adolescence, the levels of the four hormones increase with age (A). In adulthood, the levels of these hormones are maintained, then as they approach elderly, inhibin and testosterone decline while LH and FSH increase dramatically (B). This last trend is maintained onwards (C). In the middle panel, spermatogenesis is represented. In this panel, (a) represents Spermatogonia, (b) Primary spermatocyte, (c) Secondary spermatocyte, (d) Spermatid, (e) Spermatozoa. In puberty, spermatogonia divide by mitosis in testicles leading to primary spermatocytes. Afterwards, primary spermatocytes start a process called meiosis which is divided into two sub-stages: Meiosis I and Meiosis II, the end products of which are secondary spermatocytes and spermatids respectively. Finally, through a process of spermiogenesis the maturation of spermatids to spermatozoa occurs. In the lower panel, telomere attrition over time is shown in leukocytes and sperm. Spermatozoa show a different pattern from the rest of somatic cells, with telomere elongation with age instead of attrition.

(Lin et al., 2011). Among the steroids that decrease with age, testosterone concentration changes in blood (Hollander and Hollander, 1958; Vermeulen et al., 1972; Giusti et al., 1975; Camacho et al., 2013) and serum (Morley et al., 1997; Zmuda et al., 1997; Harman et al., 2001; Feldman et al., 2002) and these changes are associated to sexual dysfunction, osteoporosis, muscle decay and other aging-associated pathologies (Huhtaniemi and Forti, 2011) as well as to leukocyte TL attrition observed with aging (Huang et al., 2019). Indeed, in men, testosterone and estradiol levels positively correlate with TL in peripheral blood cells (Yeap et al., 2016; Fang et al., 2020; Yeap et al., 2020). In older men with coronary artery disease, the levels of sex hormones are lower and correlated with lower levels of TL and telomerase in PBMCs as well as with lower expression of telomerase in older men, supporting the notion that sex hormones, telomere length and aging are linked (Huang et al., 2019).

In addition, the increase of sex hormone-binding globulin (SHBG) levels (Vermeulen et al., 1996; Ferrini and Barrett-Connor, 1998; Feldman et al., 2002) may change the availability of testosterone and may alter the function of the hypothalamic-pituitary axis . Certainly, an increase in LH, involved in testosterone generation, and FSH, which promotes spermiogenesis (Fig. 3, middle panel), is found with age (Morley et al., 1997; Baccarelli et al., 2001; Liu et al., 2021). Other hormones change with age, including inhibin (Baccarelli et al., 2001), dehydroepiandrosterone (DHEA) and dehydroepiandrosterone sulfate (DHEAS), precursors of testosterone and estradiol, which decline with age (Feldman et al., 2002). Hormonal changes are linked to lifestyle factors, such as tobacco and obesity, which can increase the age-related testicular impairment (Vermeulen et al., 1996; Wu et al., 2008; Camacho et al., 2013; Liu et al., 2021). The lifestyle factors are also associated to telomere homeostasis. Longer telomeres, higher shelterin expression and TA are found in athletes, in addition to lower inflammation and oxidative stress levels compared to age-matched non-athletes (Aguiar et al., 2021; Gavia-Garcia et al., 2021). Therefore, healthy lifestyle habits could ameliorate telomere deterioration caused by the decay of sex hormones.

Regarding sexual organs, one noticeable effect in male aging is the variation on the testicular morphology. Testicular volume and glucose metabolism decrease after the age of 60 years (Yang et al., 2011), in associated with hormonal changes during andropause (Mahmoud et al., 2003; Well et al., 2007). These findings are consistent with a decline of seminiferous tubules, determined by a reduced Sertoli cell mass and Leydig cell mass (Ayisi et al., 1982; Johnson et al., 1984) and increasing fibrosis in interstitial tissues (Kaler and Neaves, 1978), compensated by an increased gonadotropins stimulation (FSH, LH) (Neaves et al., 1984). These phenotypes are similar to what happens in mice lacking telomerase. In fact, telomerase reactivation in these mice reverses testis atrophy and infertility (Jaskelioff et al., 2011).

Finally, the prostate gland, located at the base of the urethra and responsible to produce 30 % of the seminal fluid, in some cases is enlarged with age (benign prostatic hyperplasia; BPH). This is caused by changes in basal and stromal cells (muscle cells and fibroblasts), located around the urethra (Untergasser et al., 2005). Lower TL and elevated telomere fusions, a type of telomere aberration, have been found in PBMCs of patients with BPH (Cheng et al., 2020).

Taking together all the changes both at the hormone level and in sexual organs, the fertility outcomes are affected with age (Zitzmann, 2013).

3.2. The decline of semen parameters

Numerous studies report changes in semen parameters during male aging. In fact, daily sperm production, semen volume, total sperm count, motility and vitality negatively correlate with age (Homonnai et al., 1982; Johnson et al., 1984; Neaves et al., 1984; Stone et al., 2013; Johnson et al., 2015). At the age of 34, the ejaculate parameters begin to worsen, and at the age of 45, semen volume and sperm morphology gradually decrease due to a dysfunction of the accessory glands (Stone et al., 2013). The administration of different exogenous compounds such as vitamin D (Blomberg Jensen et al., 2016), or inositol combined with other vitamins can have a beneficial effect on altered seminal parameters (Canepa et al., 2018).

Some authors suggested that telomere attrition, and consequently shorter telomeres in spermatozoa, could be a cause of reduced fertility (Antunes et al., 2015; Biron-Shental et al., 2018; Lafuente et al., 2018; Darmishonnejad et al., 2019, 2020). In normozoospermic individuals, TL in sperm increases with age (Fig. 3, lower panel), both in mice and humans (Allsopp et al., 1992; Baird et al., 2006; Kimura et al., 2008; Aston et al., 2012; Ramos-Ibeas et al., 2019). Interestingly, in infertile patients, sperm TL is lower compared with age-matched controls (Ferlin et al., 2013; Thilagavathi et al., 2013). A positive correlation between seminal parameters and sperm TL has been found as well as lower DNA fragmentation in sperm with longer telomeres (Johnson et al., 2015; Cariati et al., 2016; Rocca et al., 2016, 2019; Tahamtan et al., 2019). A recent study has found association between sperm parameters and single nucleotide polymorphisms (SNPs) in telomerase genes, which could determine TL of sperm (Gentiluomo et al., 2021).

Laurentino and coworkers (2020) found that the drastic increase in sperm DNA instability happens especially after the sixth decade (Laurentino, 2020). Moreover, genome instability can be enhanced by various genotoxic agents such as chemotherapeutics and air pollution, which reduce the TL of the male germ lines (Zhao et al., 2018; Miri et al., 2019). This testicular alterations and variations in the parameters of the seminogram, could generate problems in the offspring (Liu et al., 2015). In fact, a negative correlation has been observed between some lifestyle factors such as tobacco with TL (Holohan et al., 2015) and the seminal parameters (Verón et al., 2018).

3.3. The reproductive outcomes

Many studies support the importance of the male factor for fertility outcomes (Table 2). A large, retrospective, population-based study of 3287 couples undergoing natural fertilization demonstrated an increased delay in pregnancy onset and difficulties in having newborns in the cases where men were over 40 years (De la Rochebrochard and Thonneau, 2003). When ART are used and fertilization is performed by intracytoplasmic sperm injection (ICSI), sperm age should not make a difference. Indeed, several studies support this idea (Frattarelli et al., 2008; Begueria et al., 2014; García-Ferreyra et al., 2015). However, other studies reported a decrease in pregnancy and live-birth rates when men were around 40 years old (Klonoff-Cohen and Natarajan, 2004), with a 26% decrease in the live birth rate for every 5 years increase in paternal age (Robertshaw et al., 2014). Sperm age also lowers the rates of blastocyst formation, implantation and elevated pregnancy loss when men are older than 60 years (Luna et al., 2009). In addition, higher rates of aneuploidy is associated with men older than 50 years, together with increased DNA Fragmentation Rates (DFR) in sperm (García-Ferreyra et al., 2015).

Telomeres are important for the male factor. Indeed, sperm TL varies from 10 to 17 kb (Achi et al., 2000; Baird et al., 2006) and long telomeres are important for their tethering to the nuclear membrane during meiosis, to ensure proper recombination (Boateng et al., 2013; Link et al., 2013), pro-nucleus formation and microtubule-guided movement (Ward and Zalensky, 1996). Interestingly, in a study with sand lizards they found that males with longer telomeres had a higher probability of siring offspring (Pauliny et al., 2018). In men, less TA (Biron-Shental et al., 2018) and shorter sperm telomeres are found in subfertile patients (Darmishonnejad et al., 2019) and sperm with shorter TL is associated with abnormal cell division, lower implantation rates and idiopathic recurrent pregnancy loss (Thilagavathi et al., 2013; Rocca et al., 2016; Biron-Shental et al., 2018; Darmishonnejad et al., 2019; Berneau et al., 2020). In telomerase-null mice with short telomeres, both synapsis and recombination are altered, and male germ cells undergo apoptosis (Liu et al., 2004). In addition, short telomeres in telomerase-deficient mice

Table 2
Summary of the studies about male aging on fertility outcomes.

Study	Objective	Design	Patients	Main results
De la Rochebrochard et al., 2003	How paternal age impacts on infertility.	Retrospective, population-based study	3287 couples (natural fertilization)	Women with older partners (> 40 y.o.) have elevated risk for failure to conceive within 12 months, or pregnancy not resulting in a live birth.
Frattarelli et al., 2008	How male age impacts on semen parameters and embryo development after ART.	Retrospective cohort study	1023 couples (donor oocytes; IVF and ICSI cycles)	Older men (> 45 y. o.) have less semen volume and less motile sperm. Older men (> 50 y. o.) have decreased blastocyst formation, more pregnancy loss and decreased live birth rate.
Luna et al., 2009	How advancing paternal age impacts on ART.	Retrospective study	672 couples (donor oocytes; ICSI cycles)	A negative correlation between paternal age (> 50 y. o.) and implantation, fertilization and blastocyst formation rates.
Klonoff-Cohen et al., 2004	How paternal age impacts sperm parameters and reproductive outcomes.	Prospective study	221 couples (own oocytes; IVF and gamete intrafallopian transfer)	There is no correlation between paternal age and semen parameters, and between paternal age and fertilization rate. Each additional year of paternal age associates with 11 % increase odds of not achieving a pregnancy, and a 12 % of not having live birth delivery.
Robertshaw et al., 2014	How paternal age impacts implantation and live birth rates	Retrospective study	237 couples (donor oocytes, IVF cycles)	With increasing age, there is a decrease in pregnancy rates and an increase in spontaneous abortion. There is 26 % lower odds of a live birth with each 5-year increase in paternal age.
Begueria et al., 2014	How paternal age affects semen quality and reproductive outcomes	Retrospective cohort study	4887 couples (donor oocyes, ICSI cycles)	For every 5 years of age, sperm volume decreases, sperm concentration increases and percentage motile spermatozoa decreases. No differences are found in reproductive outcomes assessed.
García-Ferreyra et al., 2015	How paternal age impacts on aneuploidy rates	Retrospective study	286 embryos (from 32 IVF/ICSI cycles with donated oocytes)	Older men (> 50 y. o.) have low blastocyst rates and higher aneuploidy rates in embryos.
Yang et al., 2015	How sperm TL impacts on early embryonic development	Retrospective, observational study	418 couples (own oocytes, IVF cycles)	There is a positive association between TL and sperm count. No association between TL and the fertilization rate is found. However, TL is positively associated with the embryo quality rate.
Berneau et al., 2020	How TL impacts on semen parameters and clinical outcomes	Retrospective, observational study	66 normozoospermic couples (own oocytes, IVF and ICSI cycles)	No associations are observed between TL and sperm count or progressive motility. TL is positively correlated with fertilization rates but not with embryo cleavage rates and post-implantation clinical outcomes.

* The table shows studies where couples have undergone ART treatments.

lead to aberrant early embryo development (Liu et al., 2002) and a decrease in the number of pups per litter (Lee et al., 1998; Jaskelioff et al., 2011). These effects could be rescued by telomerase reactivation (Jaskelioff et al., 2011). Sperm TL and TERRAs have also been positively correlated with good quality embryos after IVF (Yang et al., 2015; Rocca et al., 2021), although a recent study did not find this correlation (Berneau et al., 2020). Conversely, short sperm TL has been found in couples who did not achieve pregnancies (Lafuente et al., 2018).

3.4. *The impact of advanced paternal age on the offspring*

Spermatogonial stem cells (SSCs) have the capacity to self-renew and produce spermatozoa. They can accumulate genetic alterations due to the continuous DNA replication and cell division during the entire reproductive male lifespan. In fact, germline mutations are generally much higher in men compared to women (Crow, 2000). In addition, some mutations may acquire a selective growth advantage and may lead to clonal expansion of mutant SSCs in older men (Maher et al., 2014). This phenomenon is called “selfish spermatogonia selection” and nucleotide substitutions are more frequent (Yoon et al., 2009; Grégoire et al., 2013). Besides advantageous growth mutations, these SSCs may have longer telomeres (Malaspina et al., 2014). These mutations, which accumulate at the pace of 2 per year, are often transmitted to the offspring (Maher et al., 2014, 2018). Longer telomeres in sperm will ensure fertilization (Darmishonnejad et al., 2019), good genome integrity and also embryo survival (Wiener-Megnazi et al., 2012; Darmishonnejad et al., 2020) better pronuclear decompaction after fertilization (Morimoto et al., 2012) and transmission of telomere epigenetic marks that may regulate gene expression in the early embryo (Hales et al., 2011; Zalenskaya et al., 2000).

The relationship between the father’s age at conception and the biological effects present on their children is termed paternal age effect (PAE). In recent years, several genetic, monogenic or multifactorial disorders have been associated with the offspring from older fathers, stating the importance of father age on the risk of schizophrenia, autism and cognitive ability (Malaspina et al., 2005; Hultman et al., 2011; Kong et al., 2012; Sørensen et al., 2014). In the case of older fathers with schizophrenia, a history of psychosis in the family is associated with long TL in leukocytes (Malaspina et al., 2014). The most common PAE disorders are due to autosomal dominant mutations in genes of the tyrosine kinase receptor/RAS/MAPK signaling pathway, which are responsible for syndromes such as achondroplasia, Aper, Costello and Noonan (Moloney et al., 1996; Blumsohn et al., 2001; Tiemann-Boege et al., 2002; Glaser et al., 2003). These syndromes are characterized by congenital skeletal deformities, growth retardation, cardiac disorder and cancer susceptibility, among other signs (Crow, 2000; Yoon et al., 2009). For this reason, the American Society for Reproductive Medicine and the British Andrology Society set up the age limit of 40 years old for sperm donors (de La Rochebrochard et al., 2006).

Paternal age positively correlates with the TL of their offspring, for two successive generations (Eisenberg et al., 2012; Factor-Litvak et al., 2016). This is detected both in leukocytes and spermatozoa (Unryn et al., 2005; Ferlin et al., 2013). The inheritance of longer telomeres from older father has been called the paternal age at conception (PAC) and is thought to be a consequence of the longer telomeres of the sperm of older men (Aston et al., 2012). The PAC effect is also observed in

chimpanzees with a more pronounced effect compared to humans (Eisenberg et al., 2017). A theory proposes the positive selection of the germ stem cells with very long telomeres in older men compared to the germ cells with short telomeres, which would not survive the aging effects (Kimura et al., 2008; Eisenberg et al., 2019). This age-dependent selection of germ stem cells with longer telomeres was studied in dizygotic twins (DZ) from older parents, where an increased similarity in the TL of their leukocytes was observed (Hjelmborg et al., 2015). Longer telomeres of sperm would promote better adaptation of the offspring for increased reproductive potential at older ages (Eisenberg, 2011).

3.5. Theories of male reproductive aging

There are several theories to explain why aging occurs and its mechanisms on the male reproductive system. Three theories will be discussed in this review: the "Telomere theory", the "Oxidative stress theory" and the "Immune theory".

Telomere attrition is one of the main causes of aging (López-Otín et al., 2013). However, in males, sperm TL increases during development from spermatogonia to spermatozoa and this is inversely correlated with the expression of TA (Ravindranath et al., 1997; Achi et al., 2000). This telomere elongation was also observed in mouse sperm during aging (Ramos-Ibeas et al., 2019) and in rat models (Fice and Robaire, 2019). Epididymal spermatozoa have longer telomeres (10−20 kb) so they don't seem to undergo the shortening that takes place in somatic cells with age (Allsopp et al., 1992; Wright et al., 1996). One hypothesis postulates that the sperm long TL is generated in the spermatogonial cells, which bear high TA and then, telomeres would not shorten during the spermatogenesis process (Jørgensen et al., 2013). However, TL heterogeneity would be reduced because telomerase preferentially elongates the shortest telomeres (Bryan et al., 1995).

Another hypothesis is that, because TA is lost gradually during spermatogenesis (Ravindranath et al., 1997; Achi et al., 2000) the alternative Telomere Lengthening mechanism (ALT) could be involved in sperm telomere elongation (Antunes et al., 2015). The ALT pathway, which depends on recombination, would explain the increased sperm TL heterogeneity found on samples from older men compared to younger ones (Cesare and Reddel, 2010). Moreover, it has been suggested that TERRAs, containing telomere repeats (Azzalin et al., 2007), might promote ALT mechanism, but this idea has not been proven (Rocca et al., 2019). Finally, Gentiluomo et al. have found associations between sperm parameters and four SNPs related to telomerase. These findings could provide evidence of the role of telomeres in the spermatogenic process (Gentiluomo et al., 2021).

The *oxidative stress theory* postulates that the progressive decline of physiological functions with aging is the result of the accumulation of damage in cells, induced by ROS. In ejaculate, ROS are physiologically produced as mediators of important processes such as sperm capacitation, acrosome reaction or the regulation of spermatozoa and oocyte fusion (Koksal et al., 2003; de Lamirande and Lamothe, 2009). External sources can increase ROS production in testes and epididymis generating an excess of ROS (Telisman et al., 2000; Esfandiari et al., 2002; Chitra et al., 2003; Hammadeh et al., 2010; Kim et al., 2012; Narayana et al., 2012) that is associated with the loss of sperm motility and vitality (Aitken et al., 1996; Nakamura et al., 2002; Koksal et al., 2003; Meseguer et al., 2008; Shi et al., 2012), and the loss of sperm function and infertility (El-Taieb et al., 2009; Shi et al., 2012). Ultimately, ROS may target the polyunsaturated fatty acids of the sperm membrane, structural proteins and the nucleic acids, accumulating cellular and DNA damage in the nucleus and causing the loss of telomere repeats (Bui et al., 2018; Rocca et al., 2019) and apoptosis (Koksal et al., 2003; de Lamirande and Lamothe, 2009), similarly to what happens in somatic cells (López-Otín et al., 2013). In support of this idea, in older men the apoptotic rate of spermatocytes, measured by TUNEL, is elevated (Chitra et al., 2003) and the balance between proliferation and apoptosis in the germ cells of older testes is disturbed in humans (Jiang et al., 2014). This is important because if DNA damage is not repaired and apoptosis does not occur, chromosomal aberrations and gene mutations can be transmitted after fertilization, increasing the risk of genetic defects in embryos. In subfertile men, oxidative stress was correlated with telomere interaction impairment and chromatin condensation defects (Berby et al., 2021). In addition, sperm is more susceptible to oxidative stress because it has a low amount of antioxidant enzymes due to their small cytoplasm (Aitken et al., 1996) generating an imbalance between ROS production and antioxidants in spermatozoa, both in men and rats, with age (Wyrobek et al., 2006; Weir and Robaire, 2007; Cohen-Bacrie et al., 2009; Belloc et al., 2014; Ozkosem et al., 2015).

The *immune theory* states that with aging there is a deterioration in the blood-testis barrier in rats due to the absence of tight junctions between Sertoli cells (Hoffer and Hinton, 1984; Levy et al., 1999). This barrier is responsible for protecting spermatozoa in the seminiferous tubules from the access of the immune system and prevents autoimmune reactions from destroying germ cells (O'Donnell et al., 2021). Thus, with aging there is an infiltration of immune cells and, therefore, a degeneration of male germ cells which can lead to reduce fertility, representing an early apoptotic marker of sperm cells (Levy et al., 1999).

4. Conclusions

Similarly to what happens in the body organs, the reproductive system of both, women and men, suffer the age effect, not only decreasing fertility but also enhancing the risk of suffering aging-associated diseases as well as making psychological impacts. Strikingly, reproductive aging occurs in an abrupt manner in women, whereas in men, it happens gradually, so that they continue to produce gametes during their entire lifespan.

Scientists is intensively working on elucidating the molecular mechanisms responsible for these reproductive differences in both sexes, so that in future the reproductive span can be extended (especially in the case of women) and the quality of gametes can be improved, avoiding other risks for the organism. This is important currently because of the tendency of the society to delay parenthood, the increased human lifespan and the low natality rate found in developed countries, particularly in Europe.

Among the pathways involved in aging, telomere biology is one of the most important and recently there is accumulating evidence of its implication in fertility. Thus, it is a potential target for medical interventions to rejuvenate reproductive organs and increase the quality of the gametes. However, more work is needed to safely and efficiently rejuvenate both reproductive organs and gametes.

Aknowledgements

The laboratory of Telomeres and Reproduction is supported by the Instituto de Salud Carlos III through PI20/00,252 to E.V. (Spanish Government); by CDTI and FEDER through IDI-20190160 and IDI-20181240 *to* J.A.G.V.; by Ferring COVID-19 grant in RM to E.V.; by FINOX through FORWARD2018_6 to E.V. and J.A.G.V. and by IVIRMA (1711-FIVI-111-MV; 1707-FIVI-084-MV; 1711-FIVI-112-MV).

References

Abdalla, H.I., Baber, R., Kirkland, A., Leonard, T., Power, M., Studd, J.W., 1990. A report on 100 cycles of oocyte donation; factors affecting the outcome. Hum. Reprod. 5 (8), 1018–1022.

Achi, M.V., Ravindranath, N., Dym, M., 2000. Telomere length in male germ cells is inversely correlated with telomerase activity. Biol. Reprod. 63 (2), 591–598.

Adelfalk, C., Janschek, J., Revenkova, E., Blei, C., Liebe, B., Göb, E., Alsheimer, M., Benavente, R., de Boer, E., Novak, I., Höög, C., Scherthan, H., Jessberger, R., 2009. Cohesin SMC1beta protects telomeres in meiocytes. J. Cell Biol. 187, 18599Alsheimer.

Adishesh, M., Alnafakh, R., Baird, D.M., Jones, R.E., Simon, S., Button, L., Kamal, A.M., Kirwan, J., DeCruze, S.B., Drury, J., Saretzki, G., Hapangama, D.K., 2020. Human endometrial carcinogenesis is associated with significant reduction in long non-coding RNA, TERRA. Int. J. Mol. Sci. 21 (22).

Aguiar, S.S., Sousa, C.V., Santos, P.A., Barbosa, L.P., Maciel, L.A., Coelho-Junior, H.J., Motta-Santos, D., Rosa, T.S., Degens, H., Simoes, H.G., 2021. Master athletes have longer telomeres than age-matched non-athletes. A systematic review, meta-analysis and discussion of possible mechanisms. Exp. Gerontol. 146, 111212.
Aitken, R.J., Buckingham, D.W., Carreras, A., Irvine, D.S., 1996. Superoxide dismutase in human sperm suspensions: relationship with cellular composition, oxidative stress, and sperm function. Free Radic. Biol. Med. 21 (4), 495–504.
Aldous, W.K., Marean, A.J., DeHart, M.J., Matej, L.A., Moore, K.H., 1999. Effects of tamoxifen on telomerase activity in breast carcinoma cell lines. Cancer 85 (7), 1523–1529.
Allsopp, R.C., Vaziri, H., Patterson, C., Goldstein, S., Younglai, E.V., Futcher, A.B., Greider, C.W., Harley, C.B., 1992. Telomere length predicts replicative capacity of human fibroblasts. Proc. Natl. Acad. Sci. 89 (21), 10114–10118.
Alnafakh, R., Choi, F., Bradfield, A., Adishesh, M., Saretzki, G., Hapangama, D.K., 2020. Endometriosis is associated with a significant increase in hTERC and altered Telomere/Telomerase associated genes in the eutopic endometrium, an ex-vivo and in silico study. Biomedicines 8 (12).
Alnafakh, R., Saretzki, G., Midgley, A., Flynn, J., Kamal, A.M., Dobson, L., Natarajan, P., Stringfellow, H., Martin-Hirsch, P., DeCruze, S.B., Coupland, S.E., Hapangama, D.K., 2021. Aberrant dyskerin expression is related to proliferation and poor survival in endometrial cancer. Cancers (Basel) 13 (2).
Andersen, A.-M.N., Wohlfahrt, J., Christens, P., Olsen, J., Melbye, M., 2000. Maternal age and fetal loss: population based register linkage study. Bmj 320 (7251), 1708–1712.
Antunes, D.M., Kalmbach, K.H., Wang, F., Dracxler, R.C., Seth-Smith, M.L., Kramer, Y., Buldo-Licciardi, J., Kohlrausch, F.B., Keefe, D.L., 2015. A single-cell assay for telomere DNA content shows increasing telomere length heterogeneity, as well as increasing mean telomere length in human spermatozoa with advancing age. J. Assist. Reprod. Genet. 32 (11), 1685–1690.
Artandi, S.E., Chang, S., Lee, S.L., Alson, S., Gottlieb, G.J., Chin, L., DePinho, R.A., 2000. Telomere dysfunction promotes non-reciprocal translocations and epithelial cancers in mice. Nature 406 (6796), 641–645.
Aston, K.I., Hunt, S.C., Susser, E., Kimura, M., Factor-Litvak, P., Carrell, D., Aviv, A., 2012. Divergence of sperm and leukocyte age-dependent telomere dynamics: implications for male-driven evolution of telomere length in humans. MHR: Basic science of reproductive medicine 18 (11), 517–522.
Aydos, S.E., Elhan, A.H., Tükün, A., 2005. Is telomere length one of the determinants of reproductive life span? Arch. Gynecol. Obstet. 272 (2), 113–116.
Ayisi, K., Schmiegelow, P., Lindner, J., Sames, K., 1982. Connective tissue ageing in the human hypophysis-gonadal system. Pathology-Research and Practice 173 (3), 294–302.
Azzalin, C.M., Reichenbach, P., Khoriauli, L., Giulotto, E., Lingner, J., 2007. Telomeric repeat–containing RNA and RNA surveillance factors at mammalian chromosome ends. Science 318 (5851), 798–801.
Baccarelli, A., Morpurgo, P., Corsi, A., Vaghi, I., Fanelli, M., Cremonesi, G., Vaninetti, S., Beck-Peccoz, P., Spada, A., 2001. Activin A serum levels and aging of the pituitary-gonadal axis: a cross-sectional study in middle-aged and elderly healthy subjects. Exp. Gerontol. 36 (8), 1403–1412.
Baird, D.M., Britt-Compton, B., Rowson, J., Amso, N.N., Gregory, L., Kipling, D., 2006. Telomere instability in the male germline. Hum. Mol. Genet. 15 (1), 45–51.
Balmaceda, J.P., Bernardini, L., Ciuffardi, I., Felix, C., Ord, T., Sueldo, C.E., Asch, R.H., 1994. Implantation: oocyte donation in humans: a model to study the effect of age on embryo implantation rate. Hum. Reprod. 9 (11), 2160–2163.
Barritt, J.A., Cohen, J., Brenner, C.A., 2000. Mitochondrial DNA point mutation in human oocytes is associated with maternal age. Reprod. Biomed. Online 1 (3), 96–100.
Battaglia, D., Goodwin, P., Klein, N., Soules, M., 1996. Fertilization and early embryology: influence of maternal age on meiotic spindle assembly oocytes from naturally cycling women. Hum. Reprod. 11 (10), 2217–2222.
Begueria, R., Garcia, D., Obradors, A., Poisot, F., Vassena, R., Vernaeve, V., 2014. Paternal age and assisted reproductive outcomes in ICSI donor oocytes: is there an effect of older fathers? Hum. Reprod. 29 (10), 2114–2122.
Belloc, S., Benkhalifa, M., Cohen-Bacrie, M., Dalleac, A., Amar, E., Zini, A., 2014. Sperm deoxyribonucleic acid damage in normozoospermic men is related to age and sperm progressive motility. Fertil. Steril. 101 (6), 1588–1593.
Berby, B., Bichara, C., Rives-Feraille, A., Jumeau, F., Pizio, P.D., Setif, V., Sibert, L., Dumont, L., Rondanino, C., Rives, N., 2021. Oxidative stress is associated with telomere interaction impairment and chromatin condensation defects in spermatozoa of infertile males. Antioxidants (Basel) 10 (4).
Berneau, S.C., Shackleton, J., Nevin, C., Altakroni, B., Papadopoulos, G., Horne, G., Brison, D.R., Murgatroyd, C., Povey, A.C., Carroll, M., 2020. Associations of sperm telomere length with semen parameters, clinical outcomes and lifestyle factors in human normozoospermic samples. Andrology 8 (3), 583–593.
Biron-Shental, T., Wiser, A., Hershko-Klement, A., Markovitch, O., Amiel, A., Berkovitch, A., 2018. Sub-fertile sperm cells exemplify telomere dysfunction. J. Assist. Reprod. Genet. 35 (1), 143–148.
Blackburn, E.H., Gall, J.G., 1978. A tandemly repeated sequence at the termini of the extrachromosomal ribosomal RNA genes in Tetrahymena. J. Mol. Biol. 120 (1), 33–53.
Bleazard, T., Ju, Y.S., Sung, J., Seo, J.-S., 2013. Fine-scale mapping of meiotic recombination in Asians. BMC Genet. 14 (1), 1–10.
Blomberg Jensen, M., Gerner Lawaetz, J., Andersson, A.-M., Petersen, J.H., Nordkap, L., Bang, A.K., Ekbom, P., Joensen, U.N., Prætorius, L., Lundstrøm, P., 2016. Vitamin D deficiency and low ionized calcium are linked with semen quality and sex steroid levels in infertile men. Hum. Reprod. 31 (8), 1875–1885.
Blumsohn, A., McAllion, S., Paterson, C., 2001. Excess paternal age in apparently sporadic osteogenesis imperfecta. Am. J. Med. Genet. 100 (4), 280–286.
Boateng, K.A., Bellani, M.A., Gregoretti, I.V., Pratto, F., Camerini-Otero, R.D., 2013. Homologous pairing preceding SPO11-mediated double-strand breaks in mice. Dev. Cell 24 (2), 196–205.
Broekmans, F.J., Knauff, E.A., te Velde, E.R., Macklon, N.S., Fauser, B.C., 2007. Female reproductive ageing: current knowledge and future trends. Trends Endocrinol. Metab. 18 (2), 58–65.
Bryan, T.M., Englezou, A., Gupta, J., Bacchetti, S., Reddel, R.R., 1995. Telomere elongation in immortal human cells without detectable telomerase activity. EMBO J. 14 (17), 4240–4248.
Brzezinski, A., Saada, A., Miller, H., Brzezinski-Sinai, N., Ben-Meir, A., 2018. Is the aging human ovary still ticking?: expression of clock-genes in luteinized granulosa cells of young and older women. J. Ovarian Res. 11 (1), 1–4.
Bui, A., Sharma, R., Henkel, R., Agarwal, A., 2018. Reactive oxygen species impact on sperm DNA and its role in male infertility. Andrologia 50 (8), e13012.
Burger, H., Cahir, N., Robertson, D., Groome, N., Dudley, E., Green, A., Dennerstein, L., 1998. Serum inhibins A and B fall differentially as FSH rises in perimenopausal women. Clin. Endocrinol. (Oxf) 48 (6), 809–813.
Bustamante-Jaramillo, L.F., Ramos, C., Martin-Castellanos, C., 2021. The meiosis-specific Crs1 cyclin is required for efficient S-Phase progression and stable nuclear architecture. Int. J. Mol. Sci. 22 (11).
Butts, S., Riethman, H., Ratcliffe, S., Shaunik, A., Coutifaris, C., Barnhart, K., 2009. Correlation of telomere length and telomerase activity with occult ovarian insufficiency. J. Clin. Endocrinol. Metab. 94 (12), 4835–4843.
Calado, R.T., Yewdell, W.T., Wilkerson, K.L., Regal, J.A., Kajigaya, S., Stratakis, C.A., Young, N.S., 2009. Sex hormones, acting on the TERT gene, increase telomerase activity in human primary hematopoietic cells. Blood 114 (11), 2236–2243.
Camacho, E., Huhtaniemi, I., O'neill, T., Finn, J., Pye, S., Lee, D., Tajar, A., Bartfai, G., Boonen, S., Casanueva, F., 2013. Age-associated changes in hypothalamic–pituitary–testicular function in middle-aged and older men are modified by weight change and lifestyle factors: longitudinal results from the European Male Ageing Study. Eur. J. Endocrinol. 168 (3), 445–455.
Campbell, C.L., Furlotte, N.A., Eriksson, N., Hinds, D., Auton, A., 2015. Escape from crossover interference increases with maternal age. Nat. Commun. 6 (1), 1–7.
Canepa, P., Dal Lago, A., De Leo, C., Gallo, M., Rizzo, C., Licata, E., Anserini, P., Rago, R., Scaruffi, P., 2018. Combined treatment with myo-inositol, alpha-lipoic acid, folic acid and vitamins significantly improves sperm parameters of sub-fertile men: a multi-centric study. Eur. Rev. Med. Pharmacol. Sci. 22 (20), 7078–7085.
Cano, F., Simón, C., Remohí, J., Pellicer, A., 1995. Effect of aging on the female reproductive system: evidence for a role of uterine senescence in the decline in female fecundity. Fertil. Steril. 64 (3), 584–589.
Cariati, F., Jaroudi, S., Alfarawati, S., Raberi, A., Alviggi, C., Pivonello, R., Wells, D., 2016. Investigation of sperm telomere length as a potential marker of paternal genome integrity and semen quality. Reprod. Biomed. Online 33 (3), 404–411.
Cervello, I., Mas, A., Gil-Sanchis, C., Peris, L., Faus, A., Saunders, P.T., Critchley, H.O., Simon, C., 2011. Reconstruction of endometrium from human endometrial side population cell lines. PLoS One 6 (6), e21221.
Cesare, A.J., Reddel, R.R., 2010. Alternative lengthening of telomeres: models, mechanisms and implications. Nat. Rev. Genet. 11 (5), 319–330.
Chan, R.W., Schwab, K.E., Gargett, C.E., 2004. Clonogenicity of human endometrial epithelial and stromal cells. Biol. Reprod. 70 (6), 1738–1750.
Chan, C., Liu, V., Lau, E., Yeung, W., Ng, E., Ho, P., 2005. Mitochondrial DNA content and 4977 bp deletion in unfertilized oocytes. Mol. Hum. Reprod. 11 (12), 843–846.
Chandra, A., Copen, C.E., Stephen, E.H., 2014. Infertility Service Use in the United States: Data From the National Survey of Family Growth, 1982-2010. US Department of Health and Human Services. Centers for Disease Control and ….
Check, J.H., Askari, H.A., Fisher, C., Vanaman, L., 1994. The use of a shared donor oocyte program to evaluate the effect of uterine senescence. Fertil. Steril. 61 (2), 252–256.
Cheng, E.-H., Chen, S.-U., Lee, T.-H., Pai, Y.-P., Huang, L.-S., Huang, C.-C., Lee, M.-S., 2013. Evaluation of telomere length in cumulus cells as a potential biomarker of oocyte and embryo quality†. Hum. Reprod. 28 (4).
Cheng, G., Dai, M., Xin, Q., Wang, L., Kong, F., Xu, D., 2020. Patients with benign prostatic hyperplasia show shorter leukocyte telomere length but no association with telomerase gene polymorphisms in Han Chinese males. Int. J. Clin. Exp. Pathol. 13 (8), 2123–2129.
Chetkowski, R.J., Rode, R.A., Burruel, V., Nass, T.E., 1991. The effect of pituitary suppression and the women's age on embryo viability and uterine receptivity. Fertil. Steril. 56 (6), 1095–1103.
Chiang, T., Duncan, F.E., Schindler, K., Schultz, R.M., Lampson, M.A., 2010. Evidence that weakened centromere cohesion is a leading cause of age-related aneuploidy in oocytes. Curr. Biol. 20 (17), 1522–1528.
Chiang, T., Schultz, R.M., Lampson, M.A., 2011. Age-dependent susceptibility of chromosome cohesion to premature separase activation in mouse oocytes. Biol. Reprod. 85 (6), 1279–1283.
Chikashige, Y., Haraguchi, T., Hiraoka, Y., 2007. Another way to move chromosomes. Chromosoma 116 (6), 497–505.
Chitra, K., Latchoumycandane, C., Mathur, P., 2003. Induction of oxidative stress by bisphenol A in the epididymal sperm of rats. Toxicology 185 (1-2), 119–127.
Cohen-Bacrie, P., Belloc, S., Ménézo, Y.J., Clement, P., Hamidi, J., Benkhalifa, M., 2009. Correlation between DNA damage and sperm parameters: a prospective study of 1,633 patients. Fertil. Steril. 91 (5), 1801–1805.
Crow, J.F., 2000. The origins, patterns and implications of human spontaneous mutation. Nat. Rev. Genet. 1 (1), 40–47.
Cutas, D., Smajdor, A., 2015. Postmenopausal motherhood reloaded: advanced age and in vitro derived gametes. Hypatia 30 (2), 386–402.

Czamanski-Cohen, J., Sarid, O., Cwikel, J., Douvdevani, A., Levitas, E., Lunenfeld, E., Har-Vardi, I., 2015. Cell-free DNA and telomere length among women undergoing in vitro fertilization treatment. J. Assist. Reprod. Genet. 32 (11), 1697–1703.
Dalgård, C., Benetos, A., Verhulst, S., Labat, C., Kark, J.D., Christensen, K., Kimura, M., Kyvik, K.O., Aviv, A., 2015. Leukocyte telomere length dynamics in women and men: menopause vs age effects. Int. J. Epidemiol. 44 (5), 1688–1695.
Darmishonnejad, Z., Tavalaee, M., Izadi, T., Tanhaei, S., Nasr-Esfahani, M.H., 2019. Evaluation of sperm telomere length in infertile men with failed/low fertilization after intracytoplasmic sperm injection. Reprod. Biomed. Online 38 (4), 579–587.
Darmishonnejad, Z., Zarei-Kheirabadi, F., Tavalaee, M., Zarei-Kheirabadi, M., Zohrabi, D., Nasr-Esfahani, M.H., 2020. Relationship between sperm telomere length and sperm quality in infertile men. Andrologia 52 (5), e13546.
De Bruin, J., Dorland, M., Spek, E., Posthuma, G., Van Haaften, M., Looman, C., Te Velde, E., 2004. Age-related changes in the ultrastructure of the resting follicle pool in human ovaries. Biol. Reprod. 70 (2), 419–424.
de La Rochebrochard, E., de Mouzon, J., Thépot, F., Thonneau, P., F. N. I. R. Association, 2006. Fathers over 40 and increased failure to conceive: the lessons of in vitro fertilization in France. Fertil. Steril. 85 (5), 1420–1424.
De la Rochebrochard, E., Thonneau, P., 2003. Paternal age≥ 40 years: an important risk factor for infertility. Am. J. Obstet. Gynecol. 189 (4), 901–905.
de Lamirande, E., Lamothe, G., 2009. Reactive oxygen-induced reactive oxygen formation during human sperm capacitation. Free Radic. Biol. Med. 46 (4), 502–510.
de Lange, T., 2018. Shelterin-mediated telomere protection. Annu. Rev. Genet. 52, 223–247.
Dennerstein, L., Dudley, E.C., Hopper, J.L., Guthrie, J.R., Burger, H.G., 2000. A prospective population-based study of menopausal symptoms. Obstet. Gynecol. 96 (3), 351–358.
Diez-Juan, A., Rubio, C., Marin, C., Martinez, S., Al-Asmar, N., Riboldi, M., Díaz-Gimeno, P., Valbuena, D., Simón, C., 2015. Mitochondrial DNA content as a viability score in human euploid embryos: less is better. Fertil. Steril. 104 (3), 534–541 e531.
Donate, L.E., Blasco, M.A., 2011. Telomeres in cancer and ageing. Philos. Trans. R. Soc. Lond., B, Biol. Sci. 366 (1561), 76–84.
Dumesic, D.A., Meldrum, D.R., Katz-Jaffe, M.G., Krisher, R.L., Schoolcraft, W.B., 2015. Oocyte environment: follicular fluid and cumulus cells are critical for oocyte health. Fertil. Steril. 103 (2), 303–316.
Duncan, F.E., Hornick, J.E., Lampson, M.A., Schultz, R.M., Shea, L.D., Woodruff, T.K., 2012. Chromosome cohesion decreases in human eggs with advanced maternal age. Aging Cell 11 (6), 1121–1124.
Eisenberg, D.T., 2011. An evolutionary review of human telomere biology: the thrifty telomere hypothesis and notes on potential adaptive paternal effects. Am. J. Hum. Biol. 23 (2), 149–167.
Eisenberg, D.T., Hayes, M.G., Kuzawa, C.W., 2012. Delayed paternal age of reproduction in humans is associated with longer telomeres across two generations of descendants. Proc. Natl. Acad. Sci. 109 (26), 10251–10256.
Eisenberg, D.T., Tackney, J., Cawthon, R.M., Cloutier, C.T., Hawkes, K., 2017. Paternal and grandpaternal ages at conception and descendant telomere lengths in chimpanzees and humans. Am. J. Phys. Anthropol. 162 (2), 201–207.
Eisenberg, D.T., Lee, N.R., Rej, P.H., Hayes, M.G., Kuzawa, C.W., 2019. Older paternal ages and grandpaternal ages at conception predict longer telomeres in human descendants. Proceedings of the Royal Society B 286 (1903), 20190800.
El-Taieb, M.A., Herwig, R., Nada, E.A., Greilberger, J., Marberger, M., 2009. Oxidative stress and epididymal sperm transport, motility and morphological defects. Eur. J. Obstet. Gynecol. Reprod. Biol. 144, S199–S203.
Esfandiari, N., Saleh, R.A., Blaut, A.P., Sharma, R.K., Nelson, D.R., Thomas, A.J., Falcone, T., Agarwal, A., 2002. Effects of temperature on sperm motion characteristics and reactive oxygen species. Int. J. Fertil. Womens Med. 47 (5), 227–235.
Factor-Litvak, P., Susser, E., Kezios, K., McKeague, I., Kark, J.D., Hoffman, M., Kimura, M., Wapner, R., Aviv, A., 2016. Leukocyte telomere length in newborns: implications for the role of telomeres in human disease. Pediatrics 137 (4).
Fagan, E., Sun, F., Bae, H., Elo, I., Andersen, S.L., Lee, J., Christensen, K., Thyagarajan, B., Sebastiani, P., Perls, T., Honig, L.S., Schupf, N., Long Life Family, S., 2017. Telomere length is longer in women with late maternal age. Menopause 24 (5), 497–501.
Fainberg, J., Kashanian, J.A., 2019. Recent advances in understanding and managing male infertility. F1000Research 8.
Fang, Y., Wang, Y., Peng, M., Xu, J., Fan, Z., Liu, C., Zhao, K., Zhang, H., 2020. Effect of paternal age on offspring birth defects: a systematic review and meta-analysis. Aging (Albany NY) 12 (24), 25373.
Feldman, H.A., Longcope, C., Derby, C.A., Johannes, C.B., Araujo, A.B., Coviello, A.D., Bremner, W.J., McKinlay, J.B., 2002. Age trends in the level of serum testosterone and other hormones in middle-aged men: longitudinal results from the Massachusetts male aging study. J. Clin. Endocrinol. Metab. 87 (2), 589–598.
Fennell, A., Fernández-Álvarez, A., Tomita, K., Cooper, J.P., 2015. Telomeres and centromeres have interchangeable roles in promoting meiotic spindle formation. J. Cell Biol. 208 (4), 415–428.
Ferlin, A., Rampazzo, E., Rocca, M.S., Keppel, S., Frigo, A.C., De Rossi, A., Foresta, C., 2013. In young men sperm telomere length is related to sperm number and parental age. Hum. Reprod. 28 (12), 3370–3376.
Ferrini, R.L., Barrett-Connor, E., 1998. Sex hormones and age: a cross-sectional study of testosterone and estradiol and their bioavailable fractions in community-dwelling men. Am. J. Epidemiol. 147 (8), 750–754.
Fice, H.E., Robaire, B., 2019. Telomere dynamics throughout spermatogenesis. Genes (Basel) 10 (7).
Flamigni, C., Borini, A., Violini, F., Bianchi, L., Serrao, L., 1993. Infertility: oocyte donation: comparison between recipients from different age groups. Hum. Reprod. 8 (12), 2088–2092.
Flores, I., Blasco, M.A., 2010. The role of telomeres and telomerase in stem cell aging. FEBS Lett. 584 (17), 3826–3830.
Fragouli, E., Spath, K., Alfarawati, S., Kaper, F., Craig, A., Michel, C.-E., Kokocinski, F., Cohen, J., Munne, S., Wells, D., 2015. Altered levels of mitochondrial DNA are associated with female age, aneuploidy, and provide an independent measure of embryonic implantation potential. PLoS Genet. 11 (6), e1005241.
Frattarelli, J.L., Miller, K.A., Miller, B.T., Elkind-Hirsch, K., Scott Jr., R.T., 2008. Male age negatively impacts embryo development and reproductive outcome in donor oocyte assisted reproductive technology cycles. Fertil. Steril. 90 (1), 97–103.
Garcia-Cruz, R., Brieno, M., Roig, I., Grossmann, M., Velilla, E., Pujol, A., Cabero, L., Pessarrodona, A., Barbero, J., Garcia Caldes, M., 2010. Dynamics of cohesin proteins REC8, STAG3, SMC1 β and SMC3 are consistent with a role in sister chromatid cohesion during meiosis in human oocytes. Hum. Reprod. 25 (9), 2316–2327.
García-Ferreyra, J., Luna, D., Villegas, L., Romero, R., Zavala, P., Hilario, R., Dueñas-Chacón, J., 2015. High aneuploidy rates observed in embryos derived from donated oocytes are related to male aging and high percentages of sperm DNA fragmentation. Clin. Med. Insights Reprod. Health 9. CMRH. S32769.
Gavia-Garcia, G., Rosado-Perez, J., Arista-Ugalde, T.L., Aguiniga-Sanchez, I., Santiago-Osorio, E., Mendoza-Nunez, V.M., 2021. Telomere length and oxidative stress and its relation with metabolic syndrome components in the aging. Biology (Basel) 10 (4).
Gentiluomo, M., Luddi, A., Cingolani, A., Fornili, M., Governini, L., Lucenteforte, E., Baglietto, L., Piomboni, P., Campa, D., 2021. Telomere length and male fertility. Int. J. Mol. Sci. 22 (8).
Ghosh, S., Feingold, E., Chakraborty, S., Dey, S.K., 2010. Telomere length is associated with types of chromosome 21 nondisjunction: a new insight into the maternal age effect on Down syndrome birth. Hum. Genet. 127 (4), 403–409.
Giusti, G., Gonnelli, P., Borrelli, D., Fiorelli, G., Forti, G., Pazzagli, M., Serio, M., 1975. Age-related secretion of androstenedione, testosterone and dihydrotestosterone by the human testis. Exp. Gerontol. 10 (5), 241–245.
Glaser, R.L., Broman, K.W., Schulman, R.L., Eskenazi, B., Wyrobek, A.J., Jabs, E.W., 2003. The paternal-age effect in Apert syndrome is due, in part, to the increased frequency of mutations in sperm. Am. J. Hum. Genet. 73 (4), 939–947.
Goto, H., Iwata, H., Takeo, S., Nisinosono, K., Murakami, S., Monji, Y., Kuwayama, T., 2013. Effect of bovine age on the proliferative activity, global DNA methylation, relative telomere length and telomerase activity of granulosa cells. Zygote 21 (3), 256–264.
Grande, M., Borrell, A., Garcia-Posada, R., Borobio, V., Muñoz, M., Creus, M., Soler, A., Sanchez, A., Balasch, J., 2012. The effect of maternal age on chromosomal anomaly rate and spectrum in recurrent miscarriage. Hum. Reprod. 27 (10), 3109–3117.
Gray, K.E., Schiff, M.A., Fitzpatrick, A.L., Kimura, M., Aviv, A., Starr, J.R., 2014. Leukocyte telomere length and age at menopause. Epidemiology 25 (1), 139.
Greaney, J., Wei, Z., Homer, H., 2018. Regulation of chromosome segregation in oocytes and the cellular basis for female meiotic errors. Hum. Reprod. Update 24 (2), 135–161.
Grégoire, M.-C., Massonneau, J., Simard, O., Gouraud, A., Brazeau, M.-A., Arguin, M., Leduc, F., Boissonneault, G., 2013. Male-driven de novo mutations in haploid germ cells. MHR: Basic Sci. Reprod. Med 19 (8), 495–499.
Greider, C.W., Blackburn, E.H., 1985. Identification of a specific telomere terminal transferase activity in Tetrahymena extracts. Cell 43 (2), 405–413.
Groome, N.P., Illingworth, P.J., O'Brien, M., Pai, R., Rodger, F., Mather, J., McNeilly, A., 1996. Measurement of dimeric inhibin B throughout the human menstrual cycle. J. Clin. Endocrinol. Metab. 81 (4), 1401–1405.
Hales, Barbara F., Grenier, Lisanne, Lalancette, Claudia, Robaire, Bernard, 2011. Epigenetic programming: from gametes to blastocyst. Birth Defects Res. Part A: Clin. Mol. Teratol. https://doi.org/10.1002/bdra.20781.
Hammadeh, M., Hamad, M., Montenarh, M., Fischer-Hammadeh, C., 2010. Protamine contents and P1/P2 ratio in human spermatozoa from smokers and non-smokers. Hum. Reprod. 25 (11), 2708–2720.
Hanna, C.W., Bretherick, K.L., Gair, J.L., Fluker, M.R., Stephenson, M.D., Robinson, W.P., 2009. Telomere length and reproductive aging. Hum. Reprod. 24 (5), 1206–1211.
Hanson, B.M., Tao, X., Zhan, Y., Kim, J.G., Klimczak, A.M., Herlihy, N.S., Scott Jr., R.T., Seli, E., 2021. Shorter telomere length of white blood cells is associated with higher rates of aneuploidy among infertile women undergoing in vitro fertilization. Fertil. Steril. 115 (4), 957–965.
Hapangama, D., Turner, M., Drury, J., Martin-Ruiz, C., Von Zglinicki, T., Farquharson, R., Quenby, S., 2008. Endometrial telomerase shows specific expression patterns in different types of reproductive failure. Reprod. Biomed. Online 17 (3), 416–424.
Hapangama, D.K., Kamal, A., Saretzki, G., 2017. Implications of telomeres and telomerase in endometrial pathology. ." Hum Reprod Update 23 (2), 166–187.
Harman, S.M., Metter, E.J., Tobin, J.D., Pearson, J., Blackman, M.R., 2001. Longitudinal effects of aging on serum total and free testosterone levels in healthy men. J. Clin. Endocrinol. Metab. 86 (2), 724–731.
Hawkes, K., Smith, K.R., Robson, S.L., 2009. Mortality and fertility rates in humans and chimpanzees: how within-species variation complicates cross-species comparisons. Am. J. Human Biol. Off. J. Human Biol. Assoc. 21 (4), 578–586.
Henderson, S., Edwards, R., 1968. Chiasma frequency and maternal age in mammals. Nature 218 (5136), 22–28.
Herraiz, S., Buigues, A., Diaz-Garcia, C., Romeu, M., Martinez, S., Gomez-Segui, I., Simon, C., Hsueh, A.J., Pellicer, A., 2018. Fertility rescue and ovarian follicle growth promotion by bone marrow stem cell infusion. Fertil. Steril. 109 (5), 908–918 e902.
Hickey, M., Davis, S.R., Sturdee, D.W., 2005. Treatment of menopausal symptoms: what shall we do now? Lancet 366 (9483), 409–421.

Hjelmborg, J.B., Dalgård, C., Mangino, M., Spector, T.D., Halekoh, U., Möller, S., Kimura, M., Horvath, K., Kark, J.D., Christensen, K., 2015. Paternal age and telomere length in twins: the germ stem cell selection paradigm. Aging Cell 14 (4), 701–703.
Hodges, C.A., Revenkova, E., Jessberger, R., Hassold, T.J., Hunt, P.A., 2005. SMC1β-deficient female mice provide evidence that cohesins are a missing link in age-related nondisjunction. Nat. Genet. 37 (12), 1351–1355.
Hoffer, A.P., Hinton, B.T., 1984. Morphological evidence for a blood-epididymis barrier and the effects of gossypol on its integrity. Biol. Reprod. 30 (4), 991–1004.
Hollander, N., Hollander, V., 1958. The microdetermination of testosterone in human spermatic vein blood. J. Clin. Endocrinol. Metab. 18 (9), 966–971.
Holohan, B., De Meyer, T., Batten, K., Mangino, M., Hunt, S.C., Bekaert, S., De Buyzere, M.L., Rietzschel, E.R., Spector, T.D., Wright, W.E., 2015. Decreasing initial telomere length in humans intergenerationally understates age-associated telomere shortening. Aging Cell 14 (4), 669–677.
Homonnai, Z., Fainman, N., David, M., Paz, G., 1982. Semen quality and sex hormone pattern of 29 middle aged men. Andrologia 14 (2), 164–170.
Huang, Y., Dai, W., Li, Y., 2019. Potential associations of testosterone/estradiol ratio, leukocyte hTERT expression and PBMC telomerase activity with aging and the presence of coronary artery disease in men. Exp. Gerontol. 117, 38–44.
Huang, Z., Liu, C., Ruan, Y., Guo, Y., Sun, S., Shi, Y., Wu, F., 2021. Dynamics of leukocyte telomere length in adults aged 50 and older: a longitudinal population-based cohort study. GeroScience 1–10.
Huhtaniemi, I., Forti, G., 2011. Male late-onset hypogonadism: pathogenesis, diagnosis and treatment. Nat. Rev. Urol. 8 (6), 335.
Hultman, C., Sandin, S., Levine, S., Lichtenstein, P., Reichenberg, A., 2011. Advancing paternal age and risk of autism: new evidence from a population-based study and a meta-analysis of epidemiological studies. Mol. Psychiatry 16 (12), 1203–1212.
Hussin, J., Roy-Gagnon, M.-H., Gendron, R., Andelfinger, G., Awadalla, P., 2011. Age-dependent recombination rates in human pedigrees. PLoS Genet. 7 (9), e1002251.
Itami, N., Kawahara-Miki, R., Kawana, H., Endo, M., Kuwayama, T., Iwata, H., 2014. Age-associated changes in bovine oocytes and granulosa cell complexes collected from early antral follicles. J. Assist. Reprod. Genet. 31 (8), 1079–1088.
Itami, N., Munakata, Y., Shirasuna, K., Kuwayama, T., Iwata, H., 2017. Promotion of glucose utilization by insulin enhances granulosa cell proliferation and developmental competence of porcine oocyte grown in vitro. Zygote 25 (1), 65.
Iwata, H., 2017. Age-associated changes in granulosa cells and follicular fluid in cows. J. Reprod. Dev. 63 (4), 339–345.
Jaskelioff, M., Muller, F.L., Paik, J.H., Thomas, E., Jiang, S., Adams, A.C., Sahin, E., Kost-Alimova, M., Protopopov, A., Cadinanos, J., Horner, J.W., Maratos-Flier, E., Depinho, R.A., 2011. Telomerase reactivation reverses tissue degeneration in aged telomerase-deficient mice. Nature 469 (7328), 102–106.
Jiang, H., Zhu, W.-J., Li, J., Chen, Q.-J., Liang, W.-B., Gu, Y.-Q., 2014. Quantitative histological analysis and ultrastructure of the aging human testis. Int. Urol. Nephrol. 46 (5), 879–885.
Jørgensen, P.B., Fedder, J., Koelvraa, S., Graakjaer, J., 2013. Age-dependence of relative telomere length profiles during spermatogenesis in man. Maturitas 75 (4), 380–385.
Johnson, L., Petty, C., Neaves, W., 1984. Influence of age on sperm production and testicular weights in men. Reproduction 70 (1), 211–218.
Johnson, S.L., Dunleavy, J., Gemmell, N.J., Nakagawa, S., 2015. Consistent age-dependent declines in human semen quality: a systematic review and meta-analysis. Ageing Res. Rev. 19, 22–33.
Kaler, L.W., Neaves, W.B., 1978. Attrition of the human Leydig cell population with advancing age. Anat. Rec. 192 (4), 513–518.
Keefe, D.L., Niven-Fairchild, T., Powell, S., Buradagunta, S., 1995. Mitochondrial deoxyribonucleic acid deletions in oocytes and reproductive aging in women. Fertil. Steril. 64 (3), 577–583.
Keefe, D.L., Franco, S., Liu, L., Trimarchi, J., Cao, B., Weitzen, S., Agarwal, S., Blasco, M. A., 2005. Telomere length predicts embryo fragmentation after in vitro fertilization in women—toward a telomere theory of reproductive aging in women. Am. J. Obstet. Gynecol. 192 (4), 1256–1260.
Keefe, D.L., Marquard, K., Liu, L., 2006. The telomere theory of reproductive senescence in women. Curr. Opin. Obstet. Gynecol. 18 (3), 280–285.
Keefe, D., Liu, L., Marquard, K., 2007. Telomeres and aging-related meiotic dysfunction in women. Cell. Mol. Life Sci. 64 (2).
Kim, J.S., Heo, K., Yi, J.M., Gong, E.J., Yang, K., Moon, C., Kim, S.H., 2012. Genistein mitigates radiation-induced testicular injury. Phytother. Res. 26 (8), 1119–1125.
Kimura, M., Cherkas, L.F., Kato, B.S., Demissie, S., Hjelmborg, J.B., Brimacombe, M., Cupples, A., Hunkin, J.L., Gardner, J.P., Lu, X., 2008. Offspring's leukocyte telomere length, paternal age, and telomere elongation in sperm. PLoS Genet. 4 (2), e37.
Klonoff-Cohen, H.S., Natarajan, L., 2004. The effect of advancing paternal age on pregnancy and live birth rates in couples undergoing in vitro fertilization or gamete intrafallopian transfer. Am. J. Obstet. Gynecol. 191 (2), 507–514.
Koksal, I., Usta, M., Orhan, I., Abbasoglu, S., Kadioglu, A., 2003. Potential role of reactive oxygen species on testicular pathology associated with infertility. Asian J. Androl. 5 (2), 95–100.
Kong, A., Barnard, J., Gudbjartsson, D.F., Thorleifsson, G., Jonsdottir, G., Sigurdardottir, S., Richardsson, B., Jonsdottir, J., Thorgeirsson, T., Frigge, M.L., 2004. Recombination rate and reproductive success in humans. Nat. Genet. 36 (11), 1203–1206.
Kong, A., Frigge, M.L., Masson, G., Besenbacher, S., Sulem, P., Magnusson, G., Gudjonsson, S.A., Sigurdsson, A., Jonasdottir, A., Jonasdottir, A., 2012. Rate of de novo mutations and the importance of father's age to disease risk. Nature 488 (7412), 471–475.
Kortekaas, J.C., Kazemier, B.M., Keulen, J.K., Bruinsma, A., Mol, B.W., Vandenbussche, F., Van Dillen, J., De Miranda, E., 2020. Risk of adverse pregnancy outcomes of late-and postterm pregnancies in advanced maternal age: a national cohort study. Acta Obstet. Gynecol. Scand. 99 (8), 1022–1030.
Lafuente, R., Bosch-Rue, E., Ribas-Maynou, J., Alvarez, J., Brassesco, C., Amengual, M., Benet, J., Garcia-Peiró, A., Brassesco, M., 2018. Sperm telomere length in motile sperm selection techniques: a qFISH approach. Andrologia 50 (2), e12840.
Lara-Molina, E.E., Franasiak, J.M., Marin, D., Tao, X., Díaz-Gimeno, P., Florensa, M., Martin, M., Seli, E., Pellicer, A., 2020. Cumulus cells have longer telomeres than leukocytes in reproductive-age women. Fertil. Steril. 113 (1), 217–223.
Laser, J., Lee, P., Wei, J.-J., 2010. Cellular senescence in usual type uterine leiomyoma. Fertil. Steril. 93 (6), 2020–2026.
Laurentino, S., Jann-Frederik, C., Horsthemke, B., 2020. A germ cell-specific ageing pattern in otherwise healthy men. Aging Cell. https://doi.org/10.1111/acel.13242.
Lavranos, T.C., Mathis, J.M., Latham, S.E., Kalionis, B., Shay, J.W., Rodgers, R.J., 1999. Evidence for ovarian granulosa stem cells: telomerase activity and localization of the telomerase ribonucleic acid component in bovine ovarian follicles. Biol. Reprod. 61 (2), 358–366.
Lawson, R., El-Toukhy, T., Kassab, A., Taylor, A., Braude, P., Parsons, J., Seed, P., 2003. Poor response to ovulation induction is a stronger predictor of early menopause than elevated basal FSH: a life table analysis. ." Human Reproduction 18 (3), 527–533.
Lee, H.W., Blasco, M.A., Gottlieb, G.J., Horner 2nd., J.W., Greider, C.W., DePinho, R.A., 1998. Essential role of mouse telomerase in highly proliferative organs. Nature 392 (6676), 569–574.
Lee, D.C., Im, J.A., Kim, J.H., Lee, H.R., Shim, J.Y., 2005. Effect of long-term hormone therapy on telomere length in postmenopausal women. Yonsei Med. J. 46 (4), 471–479.
Leese, H.J., 2002. Quiet please, do not disturb: a hypothesis of embryo metabolism and viability. Bioessays 24 (9), 845–849.
Leitao, E., Di Persio, S., Laurentino, S., Woste, M., Dugas, M., Kliesch, S., Neuhaus, N., Horsthemke, B., 2020. The sperm epigenome does not display recurrent epimutations in patients with severely impaired spermatogenesis. Clin. Epigenetics 12 (1), 61.
Levran, D., Ben-Shlomo, I., Dor, J., Ben-Rafael, Z., Nebel, L., Mashiach, S., 1991. Aging of endometrium and oocytes: observations on conception and abortion rates in an egg donation model. Fertil. Steril. 56 (6), 1091–1094.
Levy, S., Serre, V., Hermo, L., Robaire, B., 1999. The effects of aging on the seminiferous epithelium and the blood—testis barrier of the Brown Norway rat. J. Androl. 20 (3), 356–365.
Lin, J., Kroenke, C.H., Epel, E., Kenna, H.A., Wolkowitz, O.M., Blackburn, E., Rasgon, N. L., 2011. Greater endogenous estrogen exposure is associated with longer telomeres in postmenopausal women at risk for cognitive decline. Brain Res. 1379, 224–231.
Link, J., Jahn, D., Schmitt, J., Göb, E., Baar, J., Ortega, S., Benavente, R., Alsheimer, M., 2013. The meiotic nuclear lamina regulates chromosome dynamics and promotes efficient homologous recombination in the mouse. PLoS Genet. 9 (1), e1003261.
Liu, L., Blasco, M.A., Keefe, D.L., 2002. Requirement of functional telomeres for metaphase chromosome alignments and integrity of meiotic spindles. EMBO Rep. 3 (3), 230–234.
Liu, L., Franco, S., Spyropoulos, B., Moens, P.B., Blasco, M.A., Keefe, D.L., 2004. Irregular telomeres impair meiotic synapsis and recombination in mice. Proc. Natl. Acad. Sci. 101 (17), 6496–6501.
Liu, M., Maselli, J., Hales, B., Robaire, B., 2015. The effects of chemotherapy with bleomycin, etoposide, and cis-platinum on telomeres in rat male germ cells. Andrology 3 (6), 1104–1112.
Liu, Q., Peng, X., Gu, Y., Shang, X., Zhou, Y., Zhang, H., Zuo, L., Mei, G., Xiong, C., Li, H., 2021. Associations between smoking, sex hormone levels and late-onset hypogonadism in men differ depending on age. Aging (Albany NY) 13 (4), 5226.
Long, N., Liu, N., Liu, X., Li, J., Cai, B., Cai, X., 2016. Endometrial expression of telomerase, progesterone, and estrogen receptors during the implantation window in patients with recurrent implantation failure. Genet. Mol. Res. 15.
López-Otín, C., Blasco, M.A., Partridge, L., Serrano, M., Kroemer, G., 2013. The hallmarks of aging. Cell 153 (6), 1194–1217.
Luna, M., Finkler, E., Barritt, J., Bar-Chama, N., Sandler, B., Copperman, A.B., Grunfeld, L., 2009. Paternal age and assisted reproductive technology outcome in ovum recipients. Fertil. Steril. 92 (5), 1772–1775.
Maher, G., Goriely, A., Wilkie, A., 2014. Cellular evidence for selfish spermatogonial selection in aged human testes. Andrology 2 (3), 304–314.
Maher, G.J., Ralph, H.K., Ding, Z., Koelling, N., Mlcochova, H., Giannoulatou, E., Dhami, P., Paul, D.S., Stricker, S.H., Beck, S., 2018. Selfish mutations dysregulating RAS-MAPK signaling are pervasive in aged human testes. Genome Res. 28 (12), 1779–1790.
Mahmoud, A., Goemaere, S., El-Garem, Y., Van Pottelbergh, I., Comhaire, F., Kaufman, J., 2003. Testicular volume in relation to hormonal indices of gonadal function in community-dwelling elderly men. J. Clin. Endocrinol. Metab. 88 (1), 179–184.
Malaspina, D., Reichenberg, A., Weiser, M., Fennig, S., Davidson, M., Harlap, S., Wolitzky, R., Rabinowitz, J., Susser, E., Knobler, H.Y., 2005. Paternal age and intelligence: implications for age-related genomic changes in male germ cells. Psychiatr. Genet. 15 (2), 117–125.
Malaspina, D., Dracxler, R., Walsh-Messinger, J., Harlap, S., Goetz, R.R., Keefe, D., Perrin, M.C., 2014. Telomere length, family history, and paternal age in schizophrenia. Mol. Genet. Genomic Med. 2 (4), 326–331.
Martin, H.C., Christ, R., Hussin, J.G., O'Connell, J., Gordon, S., Mbarek, H., Hottenga, J.-J., McAloney, K., Willemsen, G., Gasparini, P., 2015. Multicohort analysis of the maternal age effect on recombination. Nat. Commun. 6 (1), 1–10.
Martínez, P., Blasco, M.A., 2017. Telomere-driven diseases and telomere-targeting therapies. J. Cell Biol. 216 (4), 875–887.

Meeker, A.K., Sommerfeld, H.J., Coffey, D.S., 1996. Telomerase is activated in the prostate and seminal vesicles of the castrated rat. Endocrinology 137 (12), 5743–5746.
Meldrum, D.R., 1993. Female reproductive aging—ovarian and uterine factors. Fertil. Steril. 59 (1), 1–5.
Meseguer, M., Martinez-Conejero, J., O'Connor, J.E., Pellicer, A., Remohí, J., Garrido, N., 2008. The significance of sperm DNA oxidation in embryo development and reproductive outcome in an oocyte donation program: a new model to study a male infertility prognostic factor. Fertil. Steril. 89 (5), 1191–1199.
Miri, M., Nazarzadeh, M., Alahabadi, A., Ehrampoush, M.H., Rad, A., Lotfi, M.H., Sheikhha, M.H., Sakhvidi, M.J.Z., Nawrot, T.S., Dadvand, P., 2019. Air pollution and telomere length in adults: a systematic review and meta-analysis of observational studies. Environ Pollut 244, 636–647.
Misiti, S., Nanni, S., Fontemaggi, G., Cong, Y.S., Wen, J., Hirte, H.W., Piaggio, G., Sacchi, A., Pontecorvi, A., Bacchetti, S., Farsetti, A., 2000. Induction of hTERT expression and telomerase activity by estrogens in human ovary epithelium cells. Mol. Cell. Biol. 20 (11), 3764–3771.
Miyazaki, K., Maruyama, T., Masuda, H., Yamasaki, A., Uchida, S., Oda, H., Uchida, H., Yoshimura, Y., 2012. Stem cell-like differentiation potentials of endometrial side population cells as revealed by a newly developed in vivo endometrial stem cell assay. PLoS One 7 (12), e50749.
Moloney, D.M., Slaney, S.R., Oldridge, M., Wall, S.A., Sahlin, P., Stenman, G., Wilkie, A. O., 1996. Exclusive paternal origin of new mutations in Apert syndrome. Nat. Genet. 13 (1), 48–53.
Morimoto, A., Shibuya, H., Zhu, X., Kim, J., Ishiguro, K.-i., Han, M., Watanabe, Y., 2012. A conserved KASH domain protein associates with telomeres, SUN1, and dynactin during mammalian meiosisMammalian meiotic KASH domain protein KASH5. J. Cell Biol. 198 (2), 165–172.
Morin, S.J., Tao, X., Marin, D., Zhan, Y., Landis, J., Bedard, J., Scott, R.T., Seli, E., 2018. DNA methylation-based age prediction and telomere length in white blood cells and cumulus cells of infertile women with normal or poor response to ovarian stimulation. Aging (Albany NY) 10 (12), 3761–3773.
Morley, J.E., Kaiser, F.E., Perry III., H.M., Patrick, P., Morley, P.M., Stauber, P.M., Vellas, B., Baumgartner, R.N., Garry, P.J., 1997. Longitudinal changes in testosterone, luteinizing hormone, and follicle-stimulating hormone in healthy older men. Metabolism 46 (4), 410–413.
Munakata, Y., Ichinose, T., Ogawa, K., Itami, N., Tasaki, H., Shirasuna, K., Kuwayama, T., Iwata, H., 2016. Relationship between the number of cells surrounding oocytes and energy states of oocytes. Theriogenology 86 (7), 1789–1798 e1781.
Munné, S., Chen, S., Colls, P., Garrisi, J., Zheng, X., Cekleniak, N., Lenzi, M., Hughes, P., Fischer, J., Garrisi, M., 2007. Maternal age, morphology, development and chromosome abnormalities in over 6000 cleavage-stage embryos. Reprod. Biomed. Online 14 (5), 628–634.
Muñoz-Espín, D., Serrano, M., 2014. Cellular senescence: from physiology to pathology. Nat. Rev. Mol. Cell Biol. 15 (7), 482–496.
Nagaoka, S.I., Hassold, T.J., Hunt, P.A., 2012. Human aneuploidy: mechanisms and new insights into an age-old problem. Nat. Rev. Genet. 13 (7), 493–504.
Nakagawa, S., FitzHarris, G., 2017. Intrinsically defective microtubule dynamics contribute to age-related chromosome segregation errors in mouse oocyte meiosis-I. Curr. Biol. 27 (7), 1040–1047.
Nakamura, H., Kimura, T., Nakajima, A., Shimoya, K., Takemura, M., Hashimoto, K., Isaka, S., Azuma, C., Koyama, M., Murata, Y., 2002. Detection of oxidative stress in seminal plasma and fractionated sperm from subfertile male patients. Eur. J. Obstet. Gynecol. Reprod. Biol. 105 (2), 155–160.
Nakayama, Y., Sakamoto, H., Satoh, K., Yamamoto, T., 2000. Tamoxifen and gonadal steroids inhibit colon cancer growth in association with inhibition of thymidylate synthase, survivin and telomerase expression through estrogen receptor beta mediated system. Cancer Lett. 161 (1), 63–71.
Narayana, K., Al-Bader, M., Mousa, A., Khan, K.M., 2012. Molecular effects of chemotherapeutic drugs and their modulation by antioxidants in the testis. Eur. J. Pharmacol. 674 (2–3), 207–216.
Navot, D., Bergh, R., Williams, M.A., Garrisi, G.J., Guzman, I., Sandler, B., Grunfeld, L., 1991. Poor oocyte quality rather than implantation failure as a cause of age-related decline in female fertility. Lancet 337 (8754), 1375–1377.
Navot, D., Drews, M.R., Bergh, P.A., Guzman, I., Karstaedt, A., Scott Jr., R.T., Garrisi, G. J., Hofmann, G.E., 1994. Age-related decline in female fertility is not due to diminished capacity of the uterus to sustain embryo implantation. Fertil. Steril. 61 (1), 97–101.
Neaves, W.B., Johnson, L., Porter, J.C., Parker JR., C.R., Petty, C.S., 1984. Leydig cell numbers, daily sperm production, and serum gonadotropin levels in aging men. J. Clin. Endocrinol. Metab. 59 (4), 756–763.
O'Donnell, L., Rebourcet, D., Dagley, L.F., Sgaier, R., Infusini, G., O'Shaughnessy, P.J., Chalmel, F., Fietz, D., Weidner, W., Legrand, J.M.D., Hobbs, R.M., McLachlan, R.I., Webb, A.I., Pilatz, A., Diemer, T., Smith, L.B., Stanton, P.G., 2021. Sperm proteins and cancer-testis antigens are released by the seminiferous tubules in mice and men. FASEB J. 35 (3), e21397.
Olsen, K., Castillo-Fernandez, J., Zedeler, A., Freiesleben, N., Bungum, M., Chan, A., Cardona, A., Perry, J., Skouby, S., Borup, R., 2020. A distinctive epigenetic ageing profile in human granulosa cells. Hum. Reprod. 35 (6), 1332–1345.
Ottolenghi, C., Uda, M., Hamatani, T., Crisponi, L., GARCIA, J.E., Ko, M., Pilia, G., Sforza, C., Schlessinger, D., Forabosco, A., 2004. Aging of oocyte, ovary, and human reproduction. Ann. N. Y. Acad. Sci. 1034 (1), 117–131.
Ozkosem, B., Feinstein, S.I., Fisher, A.B., O'Flaherty, C., 2015. Advancing age increases sperm chromatin damage and impairs fertility in peroxiredoxin 6 null mice. Redox Biol. 5, 15–23.
Paleari, L., Pesce, S., Rutigliani, M., Greppi, M., Obino, V., Gorlero, F., Vellone, V.G., Marcenaro, E., 2021. New insights into endometrial Cancer. Cancers (Basel) 13 (7).
Pantos, K., Meimeti-Damianaki, T., Vaxevanoglou, T., Kapetanakis, E., 1993. Oocyte donation in menopausal women aged over 40 years. Hum. Reprod. 8 (3), 488–491.
Patel, J., Tan, S.L., Hartshorne, G.M., McAinsh, A.D., 2016. Unique geometry of sister kinetochores in human oocytes during meiosis I may explain maternal age-associated increases in chromosomal abnormalities. Biol. Open 5 (2), 178–184.
Pauliny, A., Miller, E., Rollings, N., Wapstra, E., Blomqvist, D., Friesen, C.R., Olsson, M., 2018. Effects of male telomeres on probability of paternity in sand lizards. Biol. Lett. 14 (8), 20180033.
Paulson, R.J., Boostanfar, R., Saadat, P., Mor, E., Tourgeman, D.E., Slater, C.C., Francis, M.M., Jain, J.K., 2002. Pregnancy in the sixth decade of life: obstetric outcomes in women of advanced reproductive age. Jama 288 (18), 2320–2323.
Payne, D., Flaherty, S.P., Barry, M.F., Matthews, C.D., 1997. Preliminary observations on polar body extrusion and pronuclear formation in human oocytes using time-lapse video cinematography. Hum. Reprod. 12 (3), 532–541.
Pellicer, A., Simón, C., Remohí, J., 1995. Effects of aging on the female reproductive system. Hum. Reprod. 10 (suppl_2), 77–83.
Perez, G.I., Jurisicova, A., Matikainen, T., Moriyama, T., Kim, M.-R., Takai, Y., Pru, J.K., Kolesnick, R.N., Tilly, J.L., 2005. A central role for ceramide in the age-related acceleration of apoptosis in the female germline. Faseb J. 19 (7), 1–23.
Pinheiro, R.L., Areia, A.L., Mota Pinto, A., Donato, H., 2019. Advanced Maternal Age: Adverse Outcomes of Pregnancy, A Meta-Analysis. Acta Med. Port. 32 (3), 219–226.
Polani, P.E., Crolla, J.A., 1991. A test of the production line hypothesis of mammalian oogenesis. Hum. Genet. 88 (1), 64–70.
Polonio, A.M., Chico-Sordo, L., Cordova-Oriz, I., Medrano, M., Garcia-Velasco, J.A., Varela, E., 2020. Impact of ovarian aging in reproduction: from telomeres and mice models to ovarian rejuvenation. Yale J. Biol. Med. 93 (4), 561–569.
Poudou, C., Baffet, H., Nadeau, C., Rolland, A.-L., Catteau-Jonard, S., Robin, G., 2021. La balance bénéfice-risque du THM: cancers et mortalité. RPC Les femmes ménopausées CNGOF-GEMVi. Gynã©cologie Obs. Fertil. Sã©nologieâ.
Qian, W., Kumar, N., Roginskaya, V., Fouquerel, E., Opresko, P.L., Shiva, S., Watkins, S. C., Kolodieznyi, D., Bruchez, M.P., Van Houten, B., 2019. Chemoptogenetic damage to mitochondria causes rapid telomere dysfunction. Proc. Natl. Acad. Sci. 116 (37), 18435–18444.
Ramos-Ibeas, P., Pericuesta, E., Peral-Sanchez, I., Heras, S., Laguna-Barraza, R., Pérez-Cerezales, S., Gutiérrez-Adán, A., 2019. Longitudinal analysis of somatic and germ-cell telomere dynamics in outbred mice. Mol. Reprod. Dev. 86 (8), 1033–1043.
Ravindranath, N., Dalal, R., Solomon, B., Djakiew, D., Dym, M., 1997. Loss of telomerase activity during male germ cell differentiation. Endocrinology 138 (9), 4026–4029.
Ravindranath, N., Ioffe, S.L., Marshall, G.R., Ramaswamy, S., Plant, T.M., Dym, M., 2001. Androgen depletion activates telomerase in the prostate of the nonhuman primate, Macaca mulatta. Prostate 49 (1), 79–89.
Reichman, N.E., Teitler, J.O., 2006. Paternal age as a risk factor for low birthweight. Am. J. Public Health 96 (5), 862–866.
Remeseiro, S., Cuadrado, A., Carretero, M., Martinez, P., Drosopoulos, W.C., Canamero, M., Schildkraut, C.L., Blasco, M.A., Losada, A., 2012. Cohesin-SA1 deficiency drives aneuploidy and tumourigenesis in mice due to impaired replication of telomeres. EMBO J. 31 (9), 2076–2089.
Revenkova, E., Herrmann, K., Adelfalk, C., Jessberger, R., 2010. Oocyte cohesin expression restricted to predictyate stages provides full fertility and prevents aneuploidy. Curr. Biol. 20 (17), 1529–1533.
Robertshaw, I., Khoury, J., Abdallah, M.E., Warikoo, P., Hofmann, G.E., 2014. The effect of paternal age on outcome in assisted reproductive technology using the ovum donation model. Reprod. Sci. 21 (5), 590–593.
Rocca, M., Speltra, E., Menegazzo, M., Garolla, A., Foresta, C., Ferlin, A., 2016. Sperm telomere length as a parameter of sperm quality in normozoospermic men. Hum. Reprod. 31 (6), 1158–1163.
Rocca, M.S., Foresta, C., Ferlin, A., 2019. Telomere length: lights and shadows on their role in human reproduction. Biol. Reprod. 100 (2), 305–317.
Rocca, M.S., Dusi, L., Di Nisio, A., Alviggi, E., Iussig, B., Bertelle, S., De Toni, L., Garolla, A., Foresta, C., Ferlin, A., 2021. TERRA: a novel biomarker of embryo quality and art outcome. Genes (Basel) 12 (4).
Rowsey, R., Gruhn, J., Broman, K.W., Hunt, P.A., Hassold, T., 2014. Examining variation in recombination levels in the human female: a test of the production-line hypothesis. Am. J. Hum. Genet. 95 (1), 108–112.
Sakakibara, Y., Hashimoto, S., Nakaoka, Y., Kouznetsova, A., Höög, C., Kitajima, T.S., 2015. Bivalent separation into univalents precedes age-related meiosis I errors in oocytes. Nat. Commun. 6 (1), 1–8.
Sauer, M.V., Paulson, R.J., Lobo, R.A., 1992. Reversing the natural decline in human fertility: an extended clinical trial of oocyte donation to women of advanced reproductive age. Jama 268 (10), 1275–1279.
Schaetzlein, S., Lucas-Hahn, A., Lemme, E., Kues, W.A., Dorsch, M., Manns, M.P., Niemann, H., Rudolph, K.L., 2004. Telomere length is reset during early mammalian embryogenesis. Proc. Natl. Acad. Sci. 101 (21), 8034–8038.
Schoeftner, S., Blasco, M.A., 2008. Developmentally regulated transcription of mammalian telomeres by DNA-dependent RNA polymerase II. Nat. Cell Biol. 10 (2), 228–236.
Schwartz, D., Mayaux, M., 1982. Female fecundity as a function of age: results of artificial insemination in 2193 nulliparous women with azoospermic husbands. N. Engl. J. Med. 306 (7), 404–406.
Shi, T.Y., Chen, G., Huang, X., Yuan, Y., Wu, X., Wu, B., Li, Z., Shun, F., Chen, H., Shi, H., 2012. Effects of reactive oxygen species from activated leucocytes on human sperm motility, viability and morphology. Andrologia 44, 696–703.
Shomper, M., Lappa, C., FitzHarris, G., 2014. Kinetochore microtubule establishment is defective in oocytes from aged mice. Cell Cycle 13 (7), 1171–1179.

Soares, S., Bosh, E., Serra, V., 2005. Age and uterine receptiveness: predicting the outcome of oocyte donation cycles. The J. Clin. Endocrinol. Metab. https://doi.org/10.1210/jc.2004-2252.
Sørensen, H.J., Pedersen, C.B., Nordentoft, M., Mortensen, P.B., Ehrenstein, V., Petersen, L., 2014. Effects of paternal age and offspring cognitive ability in early adulthood on the risk of schizophrenia and related disorders. Schizophr. Res. 160 (1–3), 131–135.
Sterzik, K., Dallenbach, C., Schneider, V., Sasse, V., Dallenbach-Hellweg, G., 1988. In vitro fertilization: the degree of endometrial insufficiency varies with the type of ovarian stimulation. Fertil. Steril. 50 (3), 457–462.
Stolwijk, A.M., Zielhuis, G.A., Sauer, M.V., Hamilton, C.J., Paulson, R.J., 1997. The impact of the woman's age on the success of standard and donor in vitro fertilization. Fertil. Steril. 67 (4), 702–710.
Stone, B.A., Alex, A., Werlin, L.B., Marrs, R.P., 2013. Age thresholds for changes in semen parameters in men. Fertil. Steril. 100 (4), 952–958.
Sugiyama, M., Sumiya, M., Shirasuna, K., Kuwayama, T., Iwata, H., 2016. Addition of granulosa cell mass to the culture medium of oocytes derived from early antral follicles increases oocyte growth, ATP content, and acetylation of H4K12. Zygote 24 (6), 848.
Sun, N., Youle, R.J., Finkel, T., 2016. The mitochondrial basis of aging. Mol. Cell 61 (5), 654–666.
Tahamtan, S., Tavalaee, M., Izadi, T., Barikrow, N., Zakeri, Z., Lockshin, R.A., Abbasi, H., Nasr-Esfahani, M.H., 2019. Reduced sperm telomere length in individuals with varicocele is associated with reduced genomic integrity. Sci. Rep. 9 (1), 1–7.
Tanaka, M., Kyo, S., Takakura, M., Kanaya, T., Sagawa, T., Yamashita, K., Okada, Y., Hiyama, E., Inoue, M., 1998. Expression of telomerase activity in human endometrium is localized to epithelial glandular cells and regulated in a menstrual phase-dependent manner correlated with cell proliferation. Am. J. Pathol. 153 (6), 1985–1991.
Tarin, J.J., 1996. Potential effects of age-associated oxidative stress on mammalian oocytes/embryos. MHR: Basic science of reproductive medicine 2 (10), 717–724.
Telisman, S., Cvitković, P., Jurasović, J., Pizent, A., Gavella, M., Rocić, B., 2000. Semen quality and reproductive endocrine function in relation to biomarkers of lead, cadmium, zinc, and copper in men. Environ. Health Perspect. 108 (1), 45–53.
Thilagavathi, J., Kumar, M., Mishra, S., Venkatesh, S., Kumar, R., Dada, R., 2013. Analysis of sperm telomere length in men with idiopathic infertility. Arch. Gynecol. Obstet. 287 (4), 803–807.
Tiemann-Boege, I., Navidi, W., Grewal, R., Cohn, D., Eskenazi, B., Wyrobek, A.J., Arnheim, N., 2002. The observed human sperm mutation frequency cannot explain the achondroplasia paternal age effect. Proc. Natl. Acad. Sci. 99 (23), 14952–14957.
Townsley, D.M., Dumitriu, B., Young, N.S., 2016. Danazol treatment for telomere diseases. N. Engl. J. Med. 375 (11), 1095–1096.
Treff, N.R., Su, J., Taylor, D., Scott Jr., R.T., 2011. Telomere DNA deficiency is associated with development of human embryonic aneuploidy. PLoS Genet. 7 (6), e1002161.
Tsutsumi, M., Fujiwara, R., Nishizawa, H., Ito, M., Kogo, H., Inagaki, H., Ohye, T., Kato, T., Fujii, T., Kurahashi, H., 2014. Age-related decrease of meiotic cohesins in human oocytes. PLoS One 9 (5), e96710.
Turner, S., Hartshorne, G., 2013. Telomere lengths in human pronuclei, oocytes and spermatozoa. MHR: Basic Sci. Reprod. Med. 19 (8), 510–518.
Unryn, B.M., Cook, L.S., Riabowol, K.T., 2005. Paternal age is positively linked to telomere length of children. Aging Cell 4 (2), 97–101.
Untergasser, G., Gander, R., Lilg, C., Lepperdinger, G., Plas, E., Berger, P., 2005. Profiling molecular targets of TGF-β1 in prostate fibroblast-to-myofibroblast transdifferentiation. Mech. Ageing Dev. 126 (1), 59–69.
Valentijn, A., Saretzki, G., Tempest, N., Critchley, H., Hapangama, D., 2015. Human endometrial epithelial telomerase is important for epithelial proliferation and glandular formation with potential implications in endometriosis. Hum. Reprod. 30 (12), 2816–2828.
van Noord-Zaadstra, B.M., Looman, C.W., Alsbach, H., Habbema, J.D., te Velde, E.R., Karbaat, J., 1991. Delaying childbearing: effect of age on fecundity and outcome of pregnancy. Br. Med. J. 302 (6789), 1361–1365.
Varela, E., Schneider, R.P., Ortega, S., Blasco, M.A., 2011. Different telomere-length dynamics at the inner cell mass versus established embryonic stem (ES) cells. Proc. Natl. Acad. Sci. 108 (37), 15207–15212.
Varela, E., Munoz-Lorente, M.A., Tejera, A.M., Ortega, S., Blasco, M.A., 2016. Generation of mice with longer and better preserved telomeres in the absence of genetic manipulations. Nat. Commun. 7 (1), 1–16.
Te Velde, E.R., Pearson, P.L., 2002. The variability of female reproductive ageing. Hum. Reprod. Update 8 (2), 141–154.
Vermeulen, A., Rubens, R., Verdonck, L., 1972. Testosterone secretion and metabolism in male senescence. J. Clin. Endocrinol. Metab. 34 (4), 730–735.
Vermeulen, A., Kaufman, J., Giagulli, V., 1996. Influence of some biological indexes on sex hormone-binding globulin and androgen levels in aging or obese males. J. Clin. Endocrinol. Metab. 81 (5), 1821–1826.
Verón, G.L., Tissera, A.D., Bello, R., Beltramone, F., Estofan, G., Molina, R.I., Vazquez-Levin, M.H., 2018. Impact of age, clinical conditions, and lifestyle on routine semen parameters and sperm kinematics. Fertil. Steril. 110 (1), 68–75 e64.
Vidal, J.D., Register, T.C., Gupta, M., Cline, J.M., 2002. Estrogen replacement therapy induces telomerase RNA expression in the macaque endometrium. Fertil. Steril. 77 (3), 601–608.
Volarcik, K., Sheean, L., Goldfarb, J., Woods, L., Abdul-Karim, F.W., Hunt, P., 1998. The meiotic competence of in-vitro matured human oocytes is influenced by donor age: evidence that folliculogenesis is compromised in the reproductively aged ovary. Hum. Reprod. 13 (1), 154–160.
Ward, W.S., Zalensky, A.O., 1996. The unique, complex organization of the transcriptionally silent sperm chromatin. Crit. Rev. Eukaryot. Gene Expr. 6 (2–3).
Weir, C.P., Robaire, B., 2007. Spermatozoa have decreased antioxidant enzymatic capacity and increased reactive oxygen species production during aging in the Brown Norway rat. J. Androl. 28 (2), 229–240.
Well, D., Yang, H., Houseni, M., Iruvuri, S., Alzeair, S., Sansovini, M., Wintering, N., Alavi, A., Torigian, D.A., 2007. Age-related structural and metabolic changes in the pelvic reproductive end organs. Semin. Nucl. Med. Elsevier.
Wiener-Megnazi, Z., Auslender, R., Dirnfeld, M., 2012. Advanced paternal age and reproductive outcome. Asian J. Androl. 14 (1), 69.
Williams, C.D., Boggess, J.F., LaMarque, L.R., Meyer, W.R., Murray, M.J., Fritz, M.A., Lessey, B.A., 2001. A prospective, randomized study of endometrial telomerase during the menstrual cycle. J. Clin. Endocrinol. Metab. 86 (8), 3912–3917.
Wright, W.E., Piatyszek, M.A., Rainey, W.E., Byrd, W., Shay, J.W., 1996. Telomerase activity in human germline and embryonic tissues and cells. Dev. Genet. 18 (2), 173–179.
Wright, D.L., Jones, E.L., Mayer, J.F., Oehninger, S., Gibbons, W.E., Lanzendorf, S.E., 2001. Characterization of telomerase activity in the human oocyte and preimplantation embryo. Mol. Hum. Reprod. 7 (10), 947–955.
Wu, F.C., Tajar, A., Pye, S.R., Silman, A.J., Finn, J.D., O'Neill, T.W., Bartfai, G., Casanueva, F., Forti, G., Giwercman, A., 2008. Hypothalamic-pituitary-testicular axis disruptions in older men are differentially linked to age and modifiable risk factors: the European Male Aging Study. J. Clin. Endocrinol. Metab. 93 (7), 2737–2745.
Wyrobek, A.J., Eskenazi, B., Young, S., Arnheim, N., Tiemann-Boege, I., Jabs, E., Glaser, R., Pearson, F., Evenson, D., 2006. Advancing age has differential effects on DNA damage, chromatin integrity, gene mutations, and aneuploidies in sperm. Proc. Natl. Acad. Sci. 103 (25), 9601–9606.
Xu, X., Chen, X., Zhang, X., Liu, Y., Wang, Z., Wang, P., Du, Y., Qin, Y., Chen, Z.J., 2017. Impaired telomere length and telomerase activity in peripheral blood leukocytes and granulosa cells in patients with biochemical primary ovarian insufficiency. Hum. Reprod. 32 (1), 201–207.
Yamamoto, S., Konishi, I., Tsuruta, Y., Nanbu, K., Mandai, M., Kuroda, H., Matsushita, K., Hamid, A., Yura, Y., Mori, T., 1997. Expression of vascular endothelial growth factor (VEGF) during folliculogenesis and corpus luteum formation in the human ovary. Gynecol. Endocrinol. 11 (6), 371–381.
Yang, H., Chryssikos, T., Houseni, M., Alzeair, S., Sansovini, M., Iruvuri, S., Torigian, D. A., Zhuang, H., Dadparvar, S., Basu, S., 2011. The effects of aging on testicular volume and glucose metabolism: an investigation with ultrasonography and FDG-PET. Mol. Imaging Biol. 13 (2), 391–398.
Yang, Q., Zhao, F., Dai, S., Zhang, N., Zhao, W., Bai, R., Sun, Y., 2015. Sperm telomere length is positively associated with the quality of early embryonic development. Hum. Reprod. 30 (8), 1876–1881.
Yaron, Y., Botchan, A., Amit, A., Kogosowski, A., Yovel, I., Lessing, J.B., 1993. Endometrial receptivity: the age-related decline in pregnancy rates and the effect of ovarian function. Fertil. Steril. 60 (2), 314–318.
Yeap, B.B., Knuiman, M.W., Divitini, M.L., Hui, J., Arscott, G.M., Handelsman, D.J., McLennan, S.V., Twigg, S.M., McQuillan, B., Hung, J., Beilby, J.P., 2016. Epidemiological and mendelian randomization studies of dihydrotestosterone and estradiol and leukocyte telomere length in men. J. Clin. Endocrinol. Metab. 101 (3), 1299–1306.
Yeap, B.B., Hui, J., Knuiman, M.W., S. A. P. C, Ken, K.Y.H., Flicker, L., Divitini, M.L., Arscott, G.M., Twigg, S.M., Almeida, O.P., Hankey, G.J., Golledge, J., Beilby, J.P., 2020. Associations of plasma IGF1, IGFBP3 and estradiol with leucocyte telomere length, a marker of biological age, in men. Eur. J. Endocrinol. 182 (1), 23–33.
Yokoyama, Y., Takahashi, Y., Morishita, S., Hashimoto, M., Niwa, K., Tamaya, T., 1998. Telomerase activity in the human endometrium throughout the menstrual cycle. Mol. Hum. Reprod. 4 (2), 173–177.
Yoon, S.-R., Qin, J., Glaser, R.L., Jabs, E.W., Wexler, N.S., Sokol, R., Arnheim, N., Calabrese, P., 2009. The ups and downs of mutation frequencies during aging can account for the Apert syndrome paternal age effect. PLoS Genet. 5 (7), e1000558.
Zhang, D., Zhang, X., Zeng, M., Yuan, J., Liu, M., Yin, Y., Wu, X., Keefe, D.L., Liu, L., 2015. Increased DNA damage and repair deficiency in granulosa cells are associated with ovarian aging in rhesus monkey. J. Assist. Reprod. Genet. 32 (7), 1069–1078.
Zalenskaya, A., Bradbury, E.M., Zalensky, A.O., 2000. Chromatin structure of telomere domain in human sperm. Biochem. Biophys. Res. Commun. https://doi.org/10.1006/bbrc.2000.3917.
Zhang, M., Bener, M.B., Jiang, Z., Wang, T., Esencan, E., Scott III., R., Horvath, T., Seli, E., 2019a. Mitofusin 1 is required for female fertility and to maintain ovarian follicular reserve. Cell Death Dis. 10 (8), 1–15.
Zhang, M., Bener, M.B., Jiang, Z., Wang, T., Esencan, E., Scott III., R., Horvath, T., Seli, E., 2019b. Mitofusin 2 plays a role in oocyte and follicle development, and is required to maintain ovarian follicular reserve during reproductive aging. Aging (Albany NY) 11 (12), 3919.
Zhao, B., Vo, H.Q., Johnston, F.H., Negishi, K., 2018. Air pollution and telomere length: a systematic review of 12,058 subjects. Cardiovasc. Diagn. Ther. 8 (4), 480–492.
Zielinska, A.P., Holubcova, Z., Blayney, M., Elder, K., Schuh, M., 2015. Sister kinetochore splitting and precocious disintegration of bivalents could explain the maternal age effect. Elife 4, e11389.
Zitzmann, M., 2013. Effects of age on male fertility. Best Pract. Res. Clin. Endocrinol. Metab. 27 (4), 617–628.
Zmuda, J.M., Cauley, J.A., Kriska, A., Glynn, N.W., Gutai, J.P., Kuller, L.H., 1997. Longitudinal relation between endogenous testosterone and cardiovascular disease risk factors in middle-aged men: a 13-year follow-up of former multiple risk factor intervention trial participants. Am. J. Epidemiol. 146 (8), 609–617.

AUTHOR COPY ONLY

REPRODUCTION

RESEARCH

Telomeres and oocyte maturation rate are not reduced by COVID-19 except in severe cases

L Chico-Sordo[1], A M Polonio[1], I Córdova-Oriz[1], M Medrano[1], S Herraiz[1], F Bronet[2], J A García-Velasco[1,2,3] and E Varela[1,3]

[1]IVI Foundation, The Health Research Institute La Fe (IIS La Fe) – Edificio Biopolo, Valencia, Spain, [2]IVIRMA Madrid, Madrid, Spain and [3]Rey Juan Carlos University, Edificio Departamental II, Alcorcón, Madrid, Spain

Correspondence should be addressed to E Varela; Email: Mariaelisa.Varela@ivirma.com

Abstract

In brief: COVID-19 does not affect the telomeres or fertility outcomes in mild cases. However, in women with severe symptoms, telomeres of granulosa cells are shorter, and the oocyte maturation rate is decreased.

Abstract: The coronavirus SARS-CoV-2 causes COVID-19 disease and affects primarily the lungs and also other organs, causing accelerated cell aging. One of the main pathways involved in aging is telomere attrition, which ultimately leads to defective tissue regeneration and organ dysfunction. Indeed, short telomeres in aged people aggravate the COVID-19 symptoms, and COVID-19 survivors showed shorter telomeres in blood cells. The SARS-CoV-2 has been detected in testis, but the ovaries, which express the viral entry factors, have not been fully explored. Our objective was to analyze telomeres and reproductive outcomes in women who had COVID-19 and controls. In this prospective cohort study, granulosa cells (GCs) and blood were collected from 65 women. Telomere length (TL) was measured by high-throughput *in situ* hybridization. Mean TL of GCs and peripheral blood mononuclear cells (PBMCs) was alike in control and mild cases. However, mean TL of GCs was lower in severe cases compared to controls ($P=0.017$). Control and COVID groups had similar ovarian reserve and number of total oocytes after puncture. However, the oocyte maturation rate was lower in severe cases ($P=0.018$). Interestingly, a positive correlation between the oocyte maturation rate and TL of GCs was found in the control group ($P=0.024$). Our findings point to a potential impact of the coronavirus infection on telomeres and reproductive outcomes in severe cases. This might be considered upon possible new SARS-CoV threats, to favor treatments that enhance oocyte maturation in women severely affected by coronavirus undergoing ART.

Reproduction (2022) **164** 259–267

Introduction

The severe acute respiratory syndrome coronavirus 2 (SARS-CoV-2) did emerge and spread worldwide, causing the coronavirus disease 2019 (COVID-19). This disease affects mainly the lungs (Huang *et al.* 2020) and also other organs (Zaim *et al.* 2020), even the testis (Ma *et al.* 2021). It is transmitted from person to person (Phan *et al.* 2020), including asymptomatic carriers (Rothe *et al.* 2020). The most common symptoms are fever, shortness of breath, dyspnea, and hypoxia (Kashani 2020). COVID-19 long-term manifestations, such as persistent respiratory impairment, increase the risk of progression to organ failure and death (Ackermann *et al.* 2020, Wu *et al.* 2020). One molecular pathway involved in organ failure and aging is telomere attrition (Lopez-Otin *et al.* 2013). Telomeres are protective structures located at chromosome ends that safeguard genome integrity (Blackburn 1991). In mammals, telomeres consist of tandem repeats of the DNA sequence 'TTAGGG' (Varela & Blasco 2010, Polonio *et al.* 2020, Chico-Sordo *et al.* 2021) ending in a 3´ overhang of ssDNA which can make a loop structure to protect the ends of chromosomes (de Lange 2005, Varela & Blasco 2010). Telomere chromatin is bound by a protein complex called shelterin (de Lange 2005). The shelterin complex is involved in protecting telomeres (telomere capping) (Erdel *et al.* 2017), anchoring the complex to telomeric DNA (de Lange 2005), and replicating (Martinez *et al.* 2009, Sfeir *et al.* 2009). The very ends of chromosomes shorten as cells divide due to the unidirectional nature of the replication machinery (Olovnikov 1973) and the influence of other factors such as oxidative stress or lifestyle choices (Martinez & Blasco 2017). The accumulation of critically short telomeres leads to the loss of protection and ultimately to the activation of the DNA-damage response pathways (de Lange 2005, Martinez & Blasco 2017), causing cell senescence or apoptosis (Martinez & Blasco 2017). Only a few critically short telomeres can lead to the cell cycle halt, limiting the regenerative capacity of tissues (Donate & Blasco 2011) and causing organ dysfunction

© 2022 Society for Reproduction and Fertility
ISSN 1470–1626 (paper) 1741–7899 (online)

https://doi.org/10.1530/REP-22-0243
Online version via https://rep.bioscientifica.com

AUTHOR COPY ONLY

and aging-associated diseases (Martinez & Blasco 2017). Interestingly, several lines of evidence show that short telomeres are linked to reproduction disorders. A correlation between short telomeres of GCs and occult ovarian insufficiency has been shown (Butts 2009), and short telomeres in GCs have also been found in women with premature ovarian failure (Xu *et al.* 2017). With respect to COVID-19, the accumulation of short telomeres in PBMCs increases the risk of developing severe COVID-19 (Benetos *et al.* 2021, Dos Santos *et al.* 2021, Sanchez-Vazquez *et al.* 2021, Wang *et al.* 2021*b*), and in COVID-19 survivors, accelerated telomere attrition and cell aging have been observed (Mongelli *et al.* 2021). Curiously, whether COVID-19 may affect the telomeres of GCs and fertility outcomes is hardly explored despite evidence showing a possible susceptibility of the reproductive organs to the viral infection. On one hand, previous literature has shown that coronaviruses can replicate in chicken's ovaries, reducing the number of germ cells (Crinion & Hofstad 1972). On the other hand, in humans, the virus can infect cells which express the angiotensin-converting enzyme 2 (ACE 2) receptor, found in ovary, vagina, and uterus (Segars *et al.* 2020), and the transmembrane serine protease 2 (TMPRSS2), which cleaves the spike protein allowing viral infection (Hoffmann *et al.* 2020). TMPRSS2 is present in oocytes and GCs, together with ACE2, suggesting that SARS-CoV-2 may target ovarian cells (Wu *et al.* 2021). We have hypothesized that COVID-19 might affect the telomere pathway in somatic ovarian cells, altering fertility factors. Therefore, the objective of this work was to analyze TL in GCs and fertility parameters in women who had or had not COVID-19 disease with several symptomatic degrees and were undergoing controlled ovarian stimulation.

Materials and methods

Ethical approval

The study was approved by the Institutional Review Board of Hospital Universitario Puerta de Hierro (2004-FIVI-041-MV), Madrid, Spain, on July 5, 2020. All participants signed informed consents. The study followed the principles set out in the Declaration of Helsinki.

Study population

This study is a single-center prospective observational cohort study, including non-COVID-19 vaccinated women who attended the IVI-RMA Madrid clinic to undergo assisted reproductive technology. Recruitment was carried out between October 2020 and May 2021. A total of 65 women aged 20–44 years were recruited for this pilot study. Participants were classified into two groups based on women's reports about COVID-19 disease status and subsequent confirmation by serum SARS-CoV-2 antibody testing. Controls were women who had not been exposed to the SARS-CoV-2 (control; $n = 29$), while cases were infected participants (COVID; $n = 36$). Inclusion criteria involved good general health as evidenced by medical history to avoid preexisting conditions (such as endometriosis and polycystic ovarian syndrome) and other confounders that might alter the results.

Serum samples

Before oocyte retrieval, subjects underwent blood extraction (5 mL) by venipuncture (at the antecubital fossa) in serum-separator gel tubes for serum collection to measure AMH levels. The number of individuals whose samples were analyzed for AMH is specified in Table 1.

Table 1 Baseline characteristics study population.

	Control	COVID	Mild COVID	Severe COVID
Age (years)				
n	29	36	19	17
Mean ± s.d.	35.3 ± 5.8	35.8 ± 5.9	35.8 ± 6.7	35.6 ± 5.2
Median (Q1–Q3)	37 (34–39)	37 (33–39)	38 (33–40)	36 (33–39)
P-value*	–	0.731	0.533	0.936
BMI (kg/m^2)				
n	22	30	17	13
Mean ± s.d.	22.3 ± 2.7	23.4 ± 4.2	22.4 ± 3.2	24.6 ± 5.1
Median (Q1–Q3)	21.9 (20.4–23.6)	22.3 (20.6–24.7)	21.9 (20.4–23.8)	24.4 (20.7–27.3)
P-value*	–	0.511	0.884†	0.246
AMH (ng/mL)				
n	28	36	19	17
Mean ± s.d.	0.9 ± 0.9	0.8 ± 0.6	1 ± 0.6	0.7 ± 0.5
Median (Q1–Q3)	0.5 (0.2–1.3)	0.7 (0.3–1.3)	1.1 (0.6–1.4)	0.7 (0.2–0.9)
P-value*	–	0.457	0.175	0.861

n indicates the number of individuals analyzed.
**P*-value was calculated between control and each group (COVID, mild COVID, and severe COVID) separately.
†*P*-value calculated using Student's *t*-test (normal distribution of data). The rest *P*-values were calculated with Mann–Whitney *U* test.

AUTHOR COPY ONLY

Serum SARS-CoV-2 antibody test and COVID-19 symptoms score

Participants were asked about the COVID-19 symptoms. Antibodies against SARS-CoV-2 (IgM and IgG) in serum samples were measured using electrochemiluminescence immunoassay of the Elecsys® Anti-SARS-CoV-2 kit (Roche) on the Cobas e411 immunoassay. COVID patients were classified according to the intensity of their symptoms: (1) asymptomatic COVID-19, subjects with the presence of serum antibodies who had no symptoms during the disease; (2) mild COVID-19, subjects with low-grade fever, cough, and loss of smell and taste for a short period of time (approximately 2 weeks), and (3) severe COVID-19 symptoms, subjects with high-grade fever, dyspnea, fatigue, headache, gastrointestinal symptoms, anosmia and dysgeusia. Alterations in smell and taste persisted for at least 1 month. One of the patients within this score presented blood coagulation problems. All COVID-19 cases were then divided into two bigger groups to better understand the impact of the disease on different variables studied. Patients categorized with symptomatic score of 1 and 2 were grouped into mild COVID. The mild COVID group gathered more individuals (52.7%) than the severe COVID group (47.2%). None of the included patients required hospitalization due to COVID-19.

Ovarian stimulation and oocyte retrieval

All patients underwent a standard protocol of ovarian stimulation with gonadotropin-releasing hormone (GnRH) antagonist. Doses (100–300 IU/day) of human menopausal gonadotropin (Menopur, Ferring Pharmaceuticals) and/or recombinant follicle-stimulating hormone (Gonal-F, Merck Serono) were used along with a GnRH antagonist (Orgalutran, Merck Sharp & Dohme). When three follicles reached a diameter of 17–18 mm or the patient's physician considered the follicular cohort to be mature, oocyte maturation was triggered with a single dose of recombinant human chorionic gonadotropin (hCG; Ovitrelle 250 µg, Merck Serono). Follicular aspiration was performed 36 h after hCG injection.

Peripheral blood mononuclear cells isolation

PBMCs were isolated from 10 mL of blood obtained before oocyte retrieval. Samples were collected in EDTA tubes, and PBMCs were purified using a Ficoll gradient (Histopaque, Sigma–Aldrich). The interphase formed after centrifugation at 400 ***g*** for 30 min, containing these cells, was collected for the counting. PBMCs were fixed with methanol:acetic acid (3:1) and stored at 4°C until use.

Granulosa cells isolation

GCs were contained in the follicular fluid obtained during oocyte retrieval. The follicular fluid was centrifuged at 300 ***g*** for 5 min at room temperature (RT). Then, pellet was resuspended in 2 mL of DMEM (Lonza, Walkersville, MD, USA), placed in 3 mL of Ficoll (Histopaque, Sigma–Aldrich), and centrifuged at 400 ***g*** for 20 min. The interphase containing GCs was collected and washed with DMEM followed by centrifugation at 600 ***g*** for 5 min. The pellet was resuspended in 300 µL of phosphate buffer (1× PBS; Fisher), and cells were counted in a Neubauer chamber. GCs were fixed with methanol:acetic acid (3:1) and stored at 4°C until use. Due to the reduced number of recovered GCs in some patients, it was not possible to obtain TL intensity measurements, in all participants of this study. The number of individuals whose samples were analyzed for TL is specified in Table 2.

Telomere length measurement

High-throughput quantitative *in situ* hybridization (qFISH) was performed on PBMCs and GCs as previously described (Canela *et al.* 2007). Briefly, cells were fixed with methanol:acetic acid (3:1) and adhered with poly-L-Lysine (Sigma–Aldrich) on 96-well plates with a transparent bottom (Greiner Bio-One, Frickenhausen, Germany). Cells were seeded at a maximum density of 200,000 cells per well. PBMCs and GCs were fixed with 4% formaldehyde and permeabilized with pepsin (Sigma–Aldrich) for 10 min at 37°C. Cells were dehydrated

Table 2 Telomere parameters of granulosa cells.

	Control	COVID	Mild COVID	Severe COVID
Telomere length				
n	24	26	15	11
Mean ± S.D.	141.4 ± 67.5	143.2 ± 72.9	177.6 ± 78.4	96.1 ± 21.9
Median (Q1–Q3)	123.3 (85.8–159.5)	121.3 (92.4–168.1)	156.7 (112.2–233.8)	95.3 (75.2–114.7)
P-value*	–	0.877	0.089	0.017
% short telomeres				
n	24	26	15	11
Mean ± S.D.	33.8 ± 17.5	36.4 ± 15	34.2 ± 14.9	39.5 ± 15.2
Median (Q1–Q3)	39.8 (19.2–46.8)	35.5 (25–48.7)	27.9 (25–47.5)	47.5 (20–50)
P-value*	–	0.572†	0.950†	0.248
% long telomeres				
n	24	26	15	11
Mean ± S.D.	8.4 ± 10.2	8.8 ± 12.4	14.4 ± 13.8	1.1 ± 1.9
Median (Q1–Q3)	4.7 (0.7–11)	3.4 (0–16.1)	12.1 (2.8–19.4)	0 (0–2.9)
P-value*	–	0.526	0.149	0.003

n indicates the number of individuals analyzed.
**P*-value was calculated between control and each group (COVID, mild COVID, and severe COVID) separately.
†*P*-value was calculated using Student's *t*-test (normal distribution of data). The rest of *P*-values were calculated with Mann–Whitney *U* test.

AUTHOR COPY ONLY

with increasing concentrations of EtOH (70%, 90%, and 100%) for 5 min at RT. DNA was hybridized with a telomere probe labeled with CY3 (Panagene) and nuclei were stained with 4′,DAPI (Invitrogen) at 1 µg/mL. The hybridization solution without probe was added as control. Intensive washes were performed to remove the non-specific probe and then, an antifading agent was added (Vectashield, Vector Laboratories). Images were acquired with an Opera High Content Screening System (PerkinElmer) and 40 images were acquired in each well. At least 300 cells were analyzed per individual. Images were analyzed with Acapella software (PerkinElmer). The Cy3 intensity per telomere spot was exported to Excel documents. Without the telomeric probe, no telomeric signals were detected. Representative images for telomere length qFISH were acquired in a confocal microscope (Olympus IX83 FP, FV3000) with an Olympus X-Line 60X/1.42NA oil objective, using the cellSens software.

Fertility parameters

Serum AMH was detected using a sensitive Elecsys ® AMH Plus Assay (Roche), following the manufacturer's instructions (range of quantitation 0.01–23 ng/mL). Samples were analyzed by chemiluminescence on the Cobas e411 analyzer. *In vitro* fertilization laboratory data and clinical variables were obtained from the IVI-RMA Madrid clinic database (number of total and MII oocytes). The oocyte maturation rate was calculated by dividing the number of metaphase II oocytes by the total number of oocytes retrieved. Normal fertilization rate was defined as the number of oocytes with two pronuclei and two polar bodies (2PN, 2PB) divided by the number of metaphase II oocytes. The number of individuals analyzed for fertility parameters is detailed in Table 3.

Statistical analysis

All statistical analyses and tests were performed with SPSS v.21.0 software (IBM). Continuous data were presented as mean and standard deviation (mean ± S.D.) and median with interquartile range (median, Q1–Q3). The ordinal categorical variable symptomatic score is presented as a number, and the Shapiro–Wilk test was used to determine whether the data of the continuous variables followed a normal distribution. Continuous variables that followed a normal distribution were compared by applying Student's *t*-test. The two-tailed Mann–Whitney *U* test was applied as a nonparametric method to analyze continuous variables that did not follow a normal distribution. In patients infected with COVID-19, Kendall's tau-b rank correlation coefficient was used to examine the relationship between symptomatic score and continuous fertility and telomere variables. Spearman's correlation coefficient was used to examine the relationship between continuous variables. *P* values <0.05 were considered statistically significant.

Results

Patient characteristics

The study included a total of 65 women aged 20–44 years, classified as controls ($n = 29$) or COVID ($n = 36$), according to the serum SARS-CoV-2 antibody test results. Serum COVID-19 antibody test identified four women originally assigned to the control group. These women were re-classified as asymptomatic cases. COVID-19 patients had different symptomatic severity levels (Fig. 1; Materials and Methods). Overall, there were no statistically significant differences in age, AMH levels,

Table 3 Fertility outcomes.

	Control	COVID	Mild COVID	Severe COVID
Number of oocytes				
n	29	36	19	17
Mean ± S.D.	10.4 ± 9.3	11.9 ± 7.6	12.2 ± 8.0	11.5 ± 7.4
Median (Q1–Q3)	7 (4–12.5)	10 (5.5–16)	10 (7–16)	9 (5–17.5)
P-value*	–	0.171	0.224	0.294
Number of metaphase II				
n	28	36	19	17
Mean ± S.D.	8.9 ± 8.2	9.39 ±6.2	10.1 ± 6.2	8.6 ± 6.2
Median (Q1–Q3)	5 (3.3–10.8)	9 (4.3–12)	9 (6–12)	7 (3.5–11.5)
P-value*	–	0.352	0.227	0.760
Oocyte maturation rate (%)				
n	28	36	19	17
Mean ± S.D.	86.7 ±12.3	80.1 ±15.9	85.6 ± 11.5	73.9 ±18
Median (Q1–Q3)	88.5 (79.4–100)	80.9 (66.7–92.4)	87.5 (75–100)	76.2 (57.8–90.7)
P-value*	–	0.094	0.620	0.018
Normal fertilization rate (%)				
n	14	27	13	14
Mean ± S.D.	64.8 ± 29.6	73.5 ± 20.2	73.9 ± 21.9	73.1 ± 19.3
Median (Q1–Q3)	66.7 (47.5–88.2)	75 (63.7–91.7)	75 (61.9–95.8)	75 (60.2–89.7)
P-value*	–	0.272†	0.374†	0.386†

n indicates the number of individuals analyzed.
*P-value was calculated between control and each group (COVID, mild COVID, and severe COVID) separately.
†P-value was calculated using Student's *t*-test (normal distribution of data). The rest of *P*-values were calculated with Mann–Whitney *U* test.

AUTHOR COPY ONLY

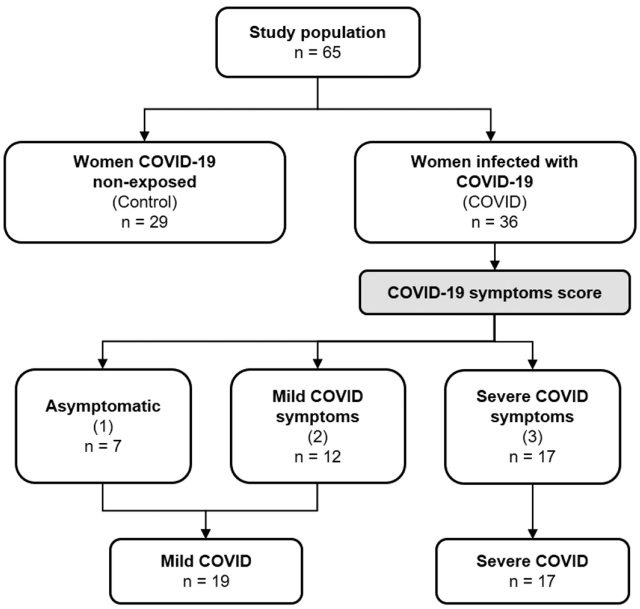


Figure 1 Flow chart showing the distribution of the study population in the different groups. COVID-19-infected women were classified into three categories, based on the disease symptoms, to analyze the correlations between telomere variables and the grading of the disease. These three arms of the study were grouped into two classes (mild and severe COVID) for a better understanding of the effects of the COVID-19 in severe cases. None of the patients were vaccinated against COVID-19. n indicates the number of individuals recruited and included in each group.

and BMI between the control and the case groups, including the severe COVID group (Table 1).

The telomere length of GCs was similar in control and COVID-19 groups but decreased in patients with severe symptoms

TL alterations and cell age acceleration have been observed in PBMCs from COVID-19 survivors (Mongelli *et al.* 2021). Here we sought to analyze whether in COVID-19 cases, TL of GCs might be altered. Mean TL of GCs was similar in the control and COVID groups (Fig. 2A) and was maintained within the age range of this study's subjects (Fig. 2B and C). Interestingly, mean TL of GCs from severe COVID-19 cases was statistically significantly lower ($P=0.017$) compared to controls (Fig. 2D) and TL decreased as the severity of the symptoms increased (Fig. 2E; $P=0.012$). The accumulation of critically short telomeres limits cell division (Allsopp *et al.* 1992, Hemann *et al.* 2001), and thus, we calculated the percentage of short telomeres (15th percentile, (Vera *et al.* 2012)) accumulated in GCs and found similar percentages for controls, COVID, and severe COVID groups (Fig. 2F and G). Long telomeres, acquired during development (Liu *et al.* 2007, Varela *et al.* 2011), are advantageous for tissue regeneration (Varela *et al.* 2016). Thus, we analyzed the percentage

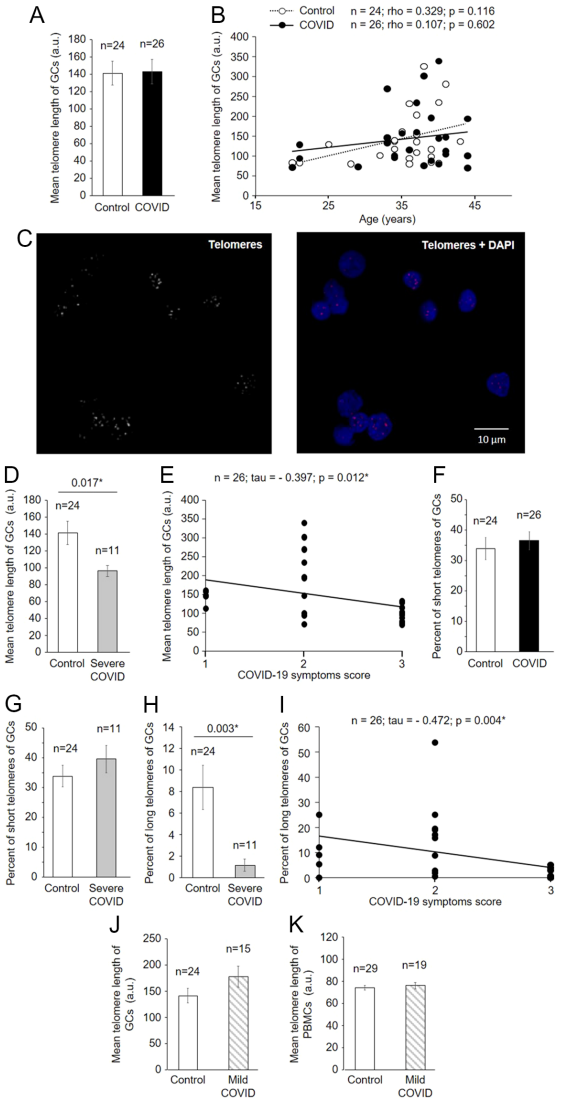


Figure 2 Analysis of telomere length in GCs. (A) Mean TL of GCs in control and COVID groups. (B) Correlation between TL of GCs and age in control (white, dashed line) and case (black line) groups. (C) The micrographs show representative images of telomere FISH (white dots, left panel) and the merge (right panel) of nuclei (blue) and telomeres (red), in GCs. Images were acquired with 60× magnification. (D) Mean TL of GCs in control and severe COVID groups. (E) Correlation between COVID-19 symptoms score and TL in GCs. (F) Percent of short telomeres of GCs in control and COVID groups. (G) Percent of short telomeres of GCs in control and severe COVID groups. (H) Percent of long telomere of GCs in control and severe COVID groups. (I) Correlation between COVID-19 symptoms score and the percent of long telomeres in GCs. (J) Mean TL of GCs in control and mild COVID groups. (K) Mean TL of PBMCs in control and mild COVID groups. *n* indicates the number of individuals analyzed in each experiment. The error bars show the S.E. (A, D, F, G, H, J and K). Scale bar = 10 µm. Statistical significance was determined by two-tailed Mann–Whitney *U* test (A, D, H, J and K) or unpaired *t*-test (F and G) according to data distribution type. Rho is the Spearman's correlation coefficient (b) and Kendall's tau-b was computed as a measurement of the correlation between telomere parameters and the symptoms score in COVID patients (E and I). *P-values <0.05 were considered statistically significant.

AUTHOR COPY ONLY

of long telomeres (85th percentile) in GCs and found that controls had a higher percentage of long telomeres ($P=0.003$) when compared to the severe COVID group (Fig. 2H). In COVID cases, the percentage of long telomeres decreased ($P=0.004$) as the severity of the symptoms score increased (Fig. 2I). In contrast to severe cases, TL of women with mild COVID was similar to controls (Fig. 2J) not only in GCs but also in PBMCs (Fig. 2K).

Total and MII oocytes were similar in controls and COVID-19 cases, but the oocyte maturation rate decreased in severe cases

To determine whether COVID-19 might affect the ovaries, we analyzed reproductive outcomes after controlled ovarian stimulation. The number of total oocytes retrieved was similar in control and COVID groups (Fig. 3A) and decayed with age in both groups (Fig. 3B, $P=0.011$ and 0.023 for control and COVID, respectively). In addition, no differences were found in total collected oocytes between controls and severe cases (Fig. 3C). Next, we analyzed the oocyte maturation rate, finding no differences between the control and COVID groups (Fig. 3D). However, statistically significantly lower oocyte maturation rate ($P=0.018$) was found in the severe COVID cases compared to controls (Fig. 3E). The oocyte maturation rate decreased as the severity symptoms score increased (Fig. 3F; $P=0.005$). Interestingly, a positive correlation was found between the oocyte maturation rate and TL in control cases ($P=0.024$), which was not found in COVID cases (Fig. 3G). Fertility outcome data analysis is shown in Table 3.

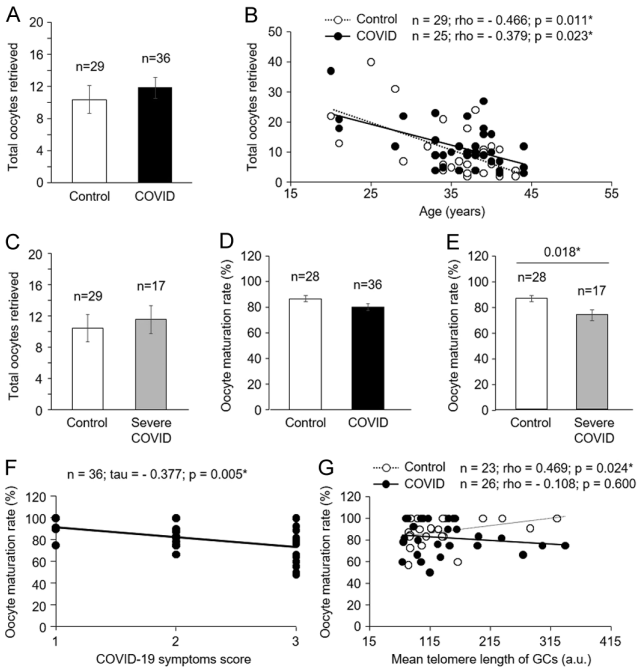


Figure 3 Analysis of fertility outcomes in controls and COVID groups. (A) Mean number of total oocytes retrieved in control and COVID groups. (B) Correlation between the age of the subjects and the number of oocytes retrieved after follicular puncture. (C) Mean number of total oocytes retrieved in control and severe COVID groups. (D) The oocyte maturation rate in control and COVID groups. (E) The oocyte maturation rate in control and severe COVID groups. (F) Correlation between the COVID-19 symptoms score and the oocyte maturation rate in patients. (G) Correlation between the TL of GCs and the oocyte maturation rate in control (white, dashed line) and case (black line) groups. *n* indicates the number of individuals analyzed in each experiment. The error bars show the S.E. (A, C, D and E). Statistical significance was determined by two-tailed Mann–Whitney *U* test (A, C, D and E). Rho is the Spearman's correlation coefficient (B and G) and Kendall's tau-b was computed as a measurement of correlation between oocyte maturation rate and symptoms score in COVID patients (F). *P-values <0.05 were considered statistically significant.

Discussion

This study investigated whether the COVID-19 disease affected the telomere pathway of ovarian somatic cells, which have been linked to ovarian failure (Butts *et al.* 2009, Xu *et al.* 2017) and aging (Kohlrausch *et al.* 2021), as well as the consequences for reproductive outcomes before women were vaccinated.

Telomere length was similar in mild COVID cases and controls, suggesting that the disease did not alter telomere biology in these women as observed in both GCs and PBMCs. This result is in agreement with reports showing that in mild COVID-19 cases, telomere maintenance is not altered in PBMCs (Dos Santos *et al.* 2021, Sanchez-Vazquez *et al.* 2021). TL of GCs was maintained in our cohort of women at reproductive age, probably because these cells have telomerase activity (Liu & Zhu 2003, Wang *et al.* 2014, Xu *et al.* 2017), which may decelerate telomere attrition (Flores *et al.* 2008, Tumpel & Rudolph 2012). Indeed, these cells have a characteristic telomere and epigenetic profile that is dissimilar from other somatic cells (Lara-Molina *et al.* 2020, Olsen *et al.* 2020). In line with these results, we found that the percentage of short telomeres was similar in controls and cases, possibly due to the elongating action of telomerase on short telomeres (Prescott & Blackburn 2000). Interestingly, the differences in telomere biology were found between control and severe COVID group, which had a lower average TL in GCs. This result is congruent with a study showing telomere shortening in PBMCs in COVID-19 survivors (Mongelli *et al.* 2021). The shorter mean TL found in the severe COVID group was due to the reduction in the percentage of long telomeres, as observed by others in PBMCs of people with severe COVID (Sanchez-Vazquez *et al.* 2021). Indeed, longer telomeres are beneficial for the organism, contributing to longer lifespan and improving metabolic aging (Munoz-Lorente *et al.* 2019) along with better support of tissue regeneration (Varela *et al.* 2016). In addition, cumulus cells, which are near the oocyte in mature

AUTHOR COPY ONLY

follicles, are derived from granulosa cells and have very long telomeres, even longer than PBMCs (Lara-Molina *et al.* 2020).

Regarding fertility, control and mild cases had similar reproductive outcomes, in agreement with previous work showing that asymptomatic COVID-19 patients do not present ovarian dysfunction (Bentov *et al.* 2021, Wang *et al.* 2021*a*). In contrast, the oocyte maturation rate was lower in the severe COVID group, despite having similar ovarian reserve as controls. Interestingly, a recent report shows that seminal parameters are altered after COVID-19 infection (Luay *et al.* 2022). Because in human cumulus cells TMPRSS2 has low expression levels, it is more difficult for the virus to infect those cells at later stages of folliculogenesis (Stanley *et al.* 2020). Therefore, if the lower oocyte maturation rate observed in severe COVID group depended directly on the viral infection, it would probably happen at earlier stages of follicular development on GCs.

Lower numbers of mature oocytes reduce the possibility to generate embryos. This may not be determining fertility outcomes at younger ages since the response to hormone stimulation is generally high (Polonio *et al.* 2020). Besides, estrogen expression is higher at younger ages and seems to have a protective effect against COVID-19 (Stelzig *et al.* 2020). However, at older ages, having less mature oocytes may be an issue because the total number of oocytes retrieved after stimulation is low and the rate of aneuploidy increases (Franasiak *et al.* 2014), making it more difficult to achieve healthy embryos for transfer. Interestingly, once transferable embryos are formed, COVID-19 infection does not significantly change pregnancy outcomes (Ovali 2020) or the probability of healthy newborns (Kyle *et al.* 2020).

Together, our results point to a potential role of long telomeres in follicle maturation. In support of this idea, the oocyte maturation rate positively correlated with TL of GCs in controls. Longer telomeres of GCs may favor follicular maturation by providing higher division potential to GCs, as observed in pig follicles (Russo *et al.* 2006). In addition, as discussed earlier, shorter telomeres of GCs are found in women with ovarian insufficiency (Butts *et al.* 2009, Xu *et al.* 2017). However, further work should be done to address this observation in depth.

In conclusion, our work suggests that SARS-CoV-2 does not alter the telomere pathway and fertility outcomes in COVID-19 patients, except in severe cases, in agreement with previous observations.

Taking into consideration that two different SARS-CoV viruses have arisen in a short period of time, 2003 and 2019 (Hodgens & Gupta 2022) and that in severe cases, the ovary could be susceptible to alterations, new perspectives in ART protocols might be considered for these patients if a new virus arose. Different studies support a dual trigger strategy (hCG and GnRH agonist) to increase oocyte maturation in patients who reported lower maturation rates in previous cycles (Fabris *et al.* 2017, Griffin *et al.* 2014). Another possible strategy for these patients is *in vitro* oocyte maturation (Chang *et al.* 2014), which is not routinely performed.

Regarding limitations, this work was an observational pilot study with a limited number of women, recruited before and during early establishment of the COVID-19 vaccination protocols in Spain.

Declaration of interest

The authors declare that there is no conflict of interest that could be perceived as prejudicing the impartiality of the research reported.

Funding

The Laboratory of Telomeres and Reproduction is supported by the Instituto de Salud Carlos III (Spanish Government) through PI20/00252 to E V; by CDTI and FEDER through IDI-20190160 and IDI-20181240 to J A G V; by Ferring COVID-19 grant in RM to E V; by FINOX through FORWARD 2018_6 to E V and J A G V; and by IVIRMA (2004-FIVI-041-MV; 1711-FIVI-111-MV; 1707-FIVI-084-MV; 1711-FIVI-112-MV). L C-S is supported by the Instituto de Salud Carlos III (Spanish Government) though FI19/00008 and European Union (ESF, 'Investing in your Future'). A M P is funded by the Spanish Ministry of Science, Innovation and Universities (FPU 18/02904). I C-O is funded by the Spanish Ministry of Science, Innovation and Universities (FPU 18/04068). S H participation was funded by the CP19/00141 grant from Instituto de Salud Carlos III and co-funded by European Union (ESF, 'Investing in your Future').

Author contribution statement

L C-S recruited patients and collected information about the COVID-19 symptoms, obtained and purified samples, performed all experiments, analyzed the results, did the statistical analysis, and participated in the manuscript writing. A M P analyzed and discussed results. I C-O recruited patients, obtained and analyzed fertility data. M M obtain TL data. S H discussed results, added new ideas to the study, and did critical revision of the manuscript. F B supervised and helped with the work of the IVF laboratory. He critically read the manuscript. J A G-V designed experiments, discussed results, did critical reading of the manuscript, and obtained funds for the laboratory. E V designed experiments; wrote the protocol for CEI approval; supervised experiments; discussed results; wrote the manuscript with L C-S; and obtained funds for the laboratory.

Acknowledgements

The authors would like to thank Nicolás Garrido (from IVI Foundation and The Health Research Institute La Fe) for counselling about statistical methods. Eva Loustau-Rodriguez for her assistance in surgery room with blood extraction.

AUTHOR COPY ONLY

María Testillano-González and Cristina Durán de la Torre for collecting GCs the day of follicular puncture.

References

Ackermann M, Verleden SE, Kuehnel M, Haverich A, Welte T, Laenger F, Vanstapel A, Werlein C, Stark H, Tzankov A *et al.* 2020 Pulmonary vascular endothelialitis, thrombosis, and angiogenesis in Covid-19. *New England Journal of Medicine* **383** 120–128. (https://doi.org/10.1056/NEJMoa2015432)

Allsopp RC, Vaziri H, Patterson C, Goldstein S, Younglai EV, Futcher AB, Greider CW & Harley CB 1992 Telomere length predicts replicative capacity of human fibroblasts. *PNAS* **89** 10114–10118. (https://doi.org/10.1073/pnas.89.21.10114)

Benetos A, Lai TP, Toupance S, Labat C, Verhulst S, Gautier S, Ungeheuer MN, Perret-Guillaume C, Levy D, Susser E *et al.* 2021 The nexus between telomere length and lymphocyte count in seniors hospitalized with COVID-19. *Journals of Gerontology: Series A, Biological Sciences and Medical Sciences* **76** e97–e101. (https://doi.org/10.1093/gerona/glab026)

Bentov Y, Beharier O, Moav-Zafrir A, Kabessa M, Godin M, Greenfield CS, Ketzinel-Gilad M, Ash Broder E, Holzer HEG, Wolf D *et al.* 2021 Ovarian follicular function is not altered by SARS-CoV-2 infection or BNT162b2 mRNA COVID-19 vaccination. *Human Reproduction* **36** 2506–2513. (https://doi.org/10.1093/humrep/deab182)

Blackburn EH 1991 Structure and function of telomeres. *Nature* **350** 569–573. (https://doi.org/10.1038/350569a0)

Butts S, Riethman H, Ratcliffe S, Shaunik A, Coutifaris C & Barnhart K 2009 Correlation of telomere length and telomerase activity with occult ovarian insufficiency. *Journal of Clinical Endocrinology and Metabolism* **94** 4835–4843. (https://doi.org/10.1210/jc.2008-2269)

Canela A, Vera E, Klatt P & Blasco MA 2007 High-throughput telomere length quantification by FISH and its application to human population studies. *PNAS* **104** 5300–5305. (https://doi.org/10.1073/pnas.0609367104)

Chang EM, Song HS, Lee DR, Lee WS & Yoon TK 2014 In vitro maturation of human oocytes: its role in infertility treatment and new possibilities. *Clinical and Experimental Reproductive Medicine* **41** 41–46. (https://doi.org/10.5653/cerm.2014.41.2.41)

Chico-Sordo L, Córdova-Oriz I, Polonio AM, S-Mellado LS, Medrano M, García-Velasco JA & Varela E 2021 Reproductive aging and telomeres: are women and men equally affected? *Mechanisms of Ageing and Development* **198** 111541. (https://doi.org/10.1016/j.mad.2021.111541)

Crinion RA & Hofstad MS 1972 Pathogenicity of four serotypes of avian infectious bronchitis virus for the oviduct of young chickens of various ages. *Avian Diseases* **16** 351–363. (https://doi.org/10.2307/1588800)

de Lange T 2005 Shelterin: the protein complex that shapes and safeguards human telomeres. *Genes and Development* **19** 2100–2110. (https://doi.org/10.1101/gad.1346005)

Donate LE & Blasco MA 2011 Telomeres in cancer and ageing. *Philosophical Transactions of the Royal Society of London: Series B, Biological Sciences* **366** 76–84. (https://doi.org/10.1098/rstb.2010.0291)

Dos Santos GA, Pimenta R, Viana NI, Guimaraes VR, Romao P, Candido P, De Camargo JA, Hatanaka DM, Queiroz PG, Teruya A *et al.* 2021 Shorter leukocyte telomere length is associated with severity of COVID-19 infection. *Biochemistry and Biophysics Reports* **27** 101056. (https://doi.org/10.1016/j.bbrep.2021.101056)

Erdel F, Kratz K, Willcox S, Griffith JD, Greene EC & De Lange T 2017 Telomere recognition and assembly mechanism of mammalian shelterin. *Cell Reports* **18** 41–53. (https://doi.org/10.1016/j.celrep.2016.12.005)

Fabris AM, Cruz M, Legidos V, Iglesias C, Munoz M & Garcia-Velasco JA 2017 Dual triggering with gonadotropin-releasing hormone agonist and standard dose human chorionic gonadotropin in patients with a high immature oocyte rate. *Reproductive Sciences* **24** 1221–1225. (https://doi.org/10.1177/1933719116682873)

Flores I, Canela A, Vera E, Tejera A, Cotsarelis G & Blasco MA 2008 The longest telomeres: a general signature of adult stem cell compartments. *Genes and Development* **22** 654–667. (https://doi.org/10.1101/gad.451008)

Franasiak JM, Forman EJ, Hong KH, Werner MD, Upham KM, Treff NR & Scott Jr RT 2014 The nature of aneuploidy with increasing age of the female partner: a review of 15,169 consecutive trophectoderm biopsies evaluated with comprehensive chromosomal screening. *Fertility and Sterility* **101** 656.e1–663.e1. (https://doi.org/10.1016/j.fertnstert.2013.11.004)

Griffin D, Feinn R, Engmann L, Nulsen J, Budinetz T & Benadiva C 2014 Dual trigger with gonadotropin-releasing hormone agonist and standard dose human chorionic gonadotropin to improve oocyte maturity rates. *Fertility and Sterility* **102** 405–409. (https://doi.org/10.1016/j.fertnstert.2014.04.028)

Hemann MT, Strong MA, Hao LY & Greider CW 2001 The shortest telomere, not average telomere length, is critical for cell viability and chromosome stability. *Cell* **107** 67–77. (https://doi.org/10.1016/s0092-8674(01)00504-9)

Hodgens A & Gupta V 2022 *Severe Acute Respiratory Syndrome*. Treasure Island (FL): StatPearls. (https://doi.org/10.1038/nm1143)

Hoffmann M, Kleine-Weber H, Schroeder S, Kruger N, Herrler T, Erichsen S, Schiergens TS, Herrler G, Wu NH, Nitsche A *et al.* 2020 SARS-CoV-2 cell entry depends on ACE2 and TMPRSS2 and is blocked by a clinically proven protease inhibitor. *Cell* **181** 271.e8–280.e8. (https://doi.org/10.1016/j.cell.2020.02.052)

Huang C, Wang Y, Li X, Ren L, Zhao J, Hu Y, Zhang L, Fan G, Xu J, Gu X *et al.* 2020 Clinical features of patients infected with 2019 novel coronavirus in Wuhan, China. *Lancet* **395** 497–506. (https://doi.org/10.1016/S0140-6736(20)30183-5)

Kashani KB 2020 Hypoxia in COVID-19: sign of severity or cause for poor outcomes. *Mayo Clinic Proceedings* **95** 1094–1096. (https://doi.org/10.1016/j.mayocp.2020.04.021)

Kohlrausch FB, Wang F, Chamani I & Keefe DL 2021 Telomere shortening and fusions: a link to aneuploidy in early human embryo development. *Obstetrical and Gynecological Survey* **76** 429–436. (https://doi.org/10.1097/OGX.0000000000000907)

Kyle MH, Glassman ME, Khan A, Fernandez CR, Hanft E, Emeruwa UN, Scripps T, Walzer L, Liao GV, Saslaw M *et al.* 2020 A review of newborn outcomes during the COVID-19 pandemic. *Seminars in Perinatology* **44** 151286. (https://doi.org/10.1016/j.semperi.2020.151286)

Lara-Molina EE, Franasiak JM, Marin D, Tao X, Diaz-Gimeno P, Florensa M, Martin M, Seli E & Pellicer A 2020 Cumulus cells have longer telomeres than leukocytes in reproductive-age women. *Fertility and Sterility* **113** 217–223. (https://doi.org/10.1016/j.fertnstert.2019.08.089)

Liu W & Zhu GJ 2003 Expression of telomerase in human ovarian luteinized granulosa cells and its relationship to ovarian function. *Zhonghua Fu Chan Ke Za Zhi* **38** 402–404.

Liu L, Bailey SM, Okuka M, Munoz P, Li C, Zhou L, Wu C, Czerwiec E, Sandler L, Seyfang A *et al.* 2007 Telomere lengthening early in development. *Nature Cell Biology* **9** 1436–1441. (https://doi.org/10.1038/ncb1664)

Lopez-Otin C, Blasco MA, Partridge L, Serrano M & Kroemer G 2013 The hallmarks of aging. *Cell* **153** 1194–1217. (https://doi.org/10.1016/j.cell.2013.05.039)

Luay A, Al-Kawaz U & Mohsin E 2022 O-253 impact of Covid-19 infection on male seminal and hormonal parameters. *Human Reproduction* **37** deac106.035. (https://doi.org/10.1093/humrep/deac106.035)

Ma X, Guan C, Chen R, Wang Y, Feng S, Wang R, Qu G, Zhao S, Wang F, Wang X *et al.* 2021 Pathological and molecular examinations of postmortem testis biopsies reveal SARS-CoV-2 infection in the testis and spermatogenesis damage in COVID-19 patients. *Cellular and Molecular Immunology* **18** 487–489. (https://doi.org/10.1038/s41423-020-00604-5)

Martinez P & Blasco MA 2017 Telomere-driven diseases and telomere-targeting therapies. *Journal of Cell Biology* **216** 875–887. (https://doi.org/10.1083/jcb.201610111)

Martinez P, Thanasoula M, Munoz P, Liao C, Tejera A, Mcnees C, Flores JM, Fernandez-Capetillo O, Tarsounas M & Blasco MA 2009 Increased telomere fragility and fusions resulting from TRF1 deficiency lead to degenerative pathologies and increased cancer in mice. *Genes and Development* **23** 2060–2075. (https://doi.org/10.1101/gad.543509)

Mongelli A, Barbi V, Gottardi Zamperla M, Atlante S, Forleo L, Nesta M, Massetti M, Pontecorvi A, Nanni S, Farsetti A *et al.* 2021 Evidence for biological age acceleration and telomere shortening in COVID-19 survivors. *International Journal of Molecular Sciences* **22** 6151. (https://doi.org/10.3390/ijms22116151)

AUTHOR COPY ONLY

Munoz-Lorente MA, Cano-Martin AC & Blasco MA 2019 Mice with hyper-long telomeres show less metabolic aging and longer lifespans. *Nature Communications* **10** 4723. (https://doi.org/10.1038/s41467-019-12664-x)

Olovnikov AM 1973 A theory of marginotomy. The incomplete copying of template margin in enzymic synthesis of polynucleotides and biological significance of the phenomenon. *Journal of Theoretical Biology* **41** 181–190. (https://doi.org/10.1016/0022-5193(73)90198-7)

Olsen KW, Castillo-Fernandez J, Zedeler A, Freiesleben NC, Bungum M, Chan AC, Cardona A, Perry JRB, Skouby SO, Borup R *et al.* 2020 A distinctive epigenetic ageing profile in human granulosa cells. *Human Reproduction* **35** 1332–1345. (https://doi.org/10.1093/humrep/deaa071)

Ovali F 2020 SARS-CoV-2 infection and the newborn. *Frontiers in Pediatrics* **8** 294. (https://doi.org/10.3389/fped.2020.00294)

Phan LT, Nguyen TV, Luong QC, Nguyen TV, Nguyen HT, Le HQ, Nguyen TT, Cao TM & Pham QD 2020 Importation and human-to-human transmission of a novel coronavirus in Vietnam. *New England Journal of Medicine* **382** 872–874. (https://doi.org/10.1056/NEJMc2001272)

Polonio AM, Chico-Sordo L, Cordova-Oriz I, Medrano M, Garcia-Velasco JA & Varela E 2020 Impact of ovarian aging in reproduction: from telomeres and mice models to ovarian rejuvenation. *Yale Journal of Biology and Medicine* **93** 561–569.

Prescott JC & Blackburn EH 2000 Telomerase RNA template mutations reveal sequence-specific requirements for the activation and repression of telomerase action at telomeres. *Molecular and Cellular Biology* **20** 2941–2948. (https://doi.org/10.1128/MCB.20.8.2941-2948.2000)

Rothe C, Schunk M, Sothmann P, Bretzel G, Froeschl G, Wallrauch C, Zimmer T, Thiel V, Janke C, Guggemos W *et al.* 2020 Transmission of 2019-nCoV infection from an asymptomatic contact in Germany. *New England Journal of Medicine* **382** 970–971. (https://doi.org/10.1056/NEJMc2001468)

Russo V, Berardinelli P, Martelli A, Di Giacinto O, Nardinocchi D, Fantasia D & Barboni B 2006 Expression of telomerase reverse transcriptase subunit (tert) and telomere sizing in pig ovarian follicles. *Journal of Histochemistry and Cytochemistry* **54** 443–455. (https://doi.org/10.1369/jhc.4A6603.2006)

Sanchez-Vazquez R, Guio-Carrion A, Zapatero-Gaviria A, Martinez P & Blasco MA 2021 Shorter telomere lengths in patients with severe COVID-19 disease. *Aging* **13** 1–15. (https://doi.org/10.18632/aging.202463)

Segars J, Katler Q, Mcqueen DB, Kotlyar A, Glenn T, Knight Z, Feinberg EC, Taylor HS, Toner JP, Kawwass JF *et al.* 2020. Prior and novel coronaviruses, coronavirus disease 2019 (COVID-19), and human reproduction: what is known?. *Fertility and Sterility* **113** 1140–1149. (https://doi.org/10.1016/j.fertnstert.2020.04.025)

Sfeir A, Kosiyatrakul ST, Hockemeyer D, Macrae SL, Karlseder J, Schildkraut CL & De Lange T 2009 Mammalian telomeres resemble fragile sites and require TRF1 for efficient replication. *Cell* **138** 90–103. (https://doi.org/10.1016/j.cell.2009.06.021)

Stanley KE, Thomas E, Leaver M & Wells D 2020 Coronavirus disease-19 and fertility: viral host entry protein expression in male and female reproductive tissues. *Fertility and Sterility* **114** 33–43. (https://doi.org/10.1016/j.fertnstert.2020.05.001)

Stelzig KE, Canepa-Escaro F, Schiliro M, Berdnikovs S, Prakash YS & Chiarella SE 2020 Estrogen regulates the expression of SARS-CoV-2 receptor ACE2 in differentiated airway epithelial cells. *American Journal of Physiology: Lung Cellular and Molecular Physiology* **318** L1280–L1281. (https://doi.org/10.1152/ajplung.00153.2020)

Tumpel S & Rudolph KL 2012 The role of telomere shortening in somatic stem cells and tissue aging: lessons from telomerase model systems. *Annals of the New York Academy of Sciences* **1266** 28–39. (https://doi.org/10.1111/j.1749-6632.2012.06547.x)

Varela E & Blasco MA 2010 2009 Nobel prize in physiology or medicine: telomeres and telomerase. *Oncogene* **29** 1561–1565. (https://doi.org/10.1038/onc.2010.15)

Varela E, Schneider RP, Ortega S & Blasco MA 2011 Different telomere-length dynamics at the inner cell mass versus established embryonic stem (ES) cells. *PNAS* **108** 15207–15212. (https://doi.org/10.1073/pnas.1105414108)

Varela E, Munoz-Lorente MA, Tejera AM, Ortega S & Blasco MA 2016 Generation of mice with longer and better preserved telomeres in the absence of genetic manipulations. *Nature Communications* **7** 11739. (https://doi.org/10.1038/ncomms11739)

Vera E, Bernardes De Jesus B, Foronda M, Flores JM & Blasco MA 2012 The rate of increase of short telomeres predicts longevity in mammals. *Cell Reports* **2** 732–737. (https://doi.org/10.1016/j.celrep.2012.08.023)

Wang W, Chen H, Li R, Ouyang N, Chen J, Huang L, Mai M, Zhang N, Zhang Q & Yang D 2014 Telomerase activity is more significant for predicting the outcome of IVF treatment than telomere length in granulosa cells. *Reproduction* **147** 649–657. (https://doi.org/10.1530/REP-13-0223)

Wang M, Yang Q, Ren X, Hu J, Li Z, Long R, Xi Q, Zhu L & Jin L 2021*a* Investigating the impact of asymptomatic or mild SARS-CoV-2 infection on female fertility and in vitro fertilization outcomes: a retrospective cohort study. *EClinicalMedicine* **38** 101013. (https://doi.org/10.1016/j.eclinm.2021.101013)

Wang Q, Codd V, Raisi-Estabragh Z, Musicha C, Bountziouka V, Kaptoge S, Allara E, Angelantonio ED, Butterworth AS, Wood AM *et al.* 2021*b* Shorter leukocyte telomere length is associated with adverse COVID-19 outcomes: a cohort study in UK Biobank. *EBiomedicine* **70** 103485. (https://doi.org/10.1016/j.ebiom.2021.103485)

Wu C, Chen X, Cai Y, Xia J, Zhou X, Xu S, Huang H, Zhang L, Zhou X, Du C *et al.* 2020 Risk factors associated with acute respiratory distress syndrome and death in patients with coronavirus disease 2019 pneumonia in Wuhan, China. *JAMA Internal Medicine* **180** 934–943. (https://doi.org/10.1001/jamainternmed.2020.0994)

Wu M, Ma L, Xue L, Zhu Q, Zhou S, Dai J, Yan W, Zhang J & Wang S 2021 Co-expression of the SARS-CoV-2 entry molecules ACE2 and TMPRSS2 in human ovaries: identification of cell types and trends with age. *Genomics* **113** 3449–3460. (https://doi.org/10.1016/j.ygeno.2021.08.012)

Xu X, Chen X, Zhang X, Liu Y, Wang Z, Wang P, Du Y, Qin Y & Chen ZJ 2017 Impaired telomere length and telomerase activity in peripheral blood leukocytes and granulosa cells in patients with biochemical primary ovarian insufficiency. *Human Reproduction* **32** 201–207. (https://doi.org/10.1093/humrep/dew283)

Zaim S, Chong JH, Sankaranarayanan V & Harky A 2020 COVID-19 and multiorgan response. *Current Problems in Cardiology* **45** 100618. (https://doi.org/10.1016/j.cpcardiol.2020.100618)

Received 11 July 2022
First decision 8 August 2022
Revised manuscript received 19 September 2022
Accepted 22 September 2022

International Journal of
Molecular Sciences

MDPI

Article

Identification of miR-30c-5p microRNA in Serum as a Candidate Biomarker to Diagnose Endometriosis

Lucía Chico-Sordo [1,†], Tamara Ruiz-Martínez [2,†], Mónica Toribio [3], Roberto González-Martín [1], Emanuela Spagnolo [2], Francisco Domínguez [1], Alicia Hernández [2,*] and Juan A. García-Velasco [1,3,4]

1 IVIRMA Global Research Alliance, IVI Foundation, Instituto de Investigación Sanitaria La Fe (IIS La Fe), 46026 Valencia, Spain; lucia.chico@ivirma.com (L.C.-S.); francisco.dominguez@ivirma.com (F.D.); juan.garcia.velasco@ivirma.com (J.A.G.-V.)
2 Gynaecology Department, La Paz University Hospital, 28046 Madrid, Spain
3 IVIRMA Global Research Alliance, IVIRMA Madrid, 28023 Madrid, Spain
4 School of Health Sciences, Medical Specialties and Public Health, Obstetrics and Gynecology Area, Rey Juan Carlos University Alcorcón, 28922 Madrid, Spain
* Correspondence: aliciahernandezg@gmail.com
† These authors contributed equally to this work.

Abstract: The diagnosis of endometriosis by laparoscopy is delayed until advanced stages. In recent years, microRNAs have emerged as novel biomarkers for different diseases. These molecules are small non-coding RNA sequences involved in the regulation of gene expression and can be detected in peripheral blood. Our aim was to identify candidate serum microRNAs associated with endometriosis and their role as minimally invasive biomarkers. Serum samples were obtained from 159 women, of whom 77 were diagnosed with endometriosis by laparoscopy and 82 were healthy women. First, a preliminary study identified 29 differentially expressed microRNAs between the two study groups. Next, nine of the differentially expressed microRNAs in the preliminary analysis were evaluated in a new cohort of 67 women with endometriosis and 72 healthy women. Upon validation by quantitative real-time PCR technique, the circulating level of miR-30c-5p was significantly higher in the endometriosis group compared with the healthy women group. The area under the curve value of miR-30c-5p was 0.8437, demonstrating its diagnostic potential even when serum samples registered an acceptable limit of hemolysis. Dysregulation of this microRNA was associated with molecular pathways related to cancer and neuronal processes. We concluded that miR-30c-5p is a potential minimally invasive biomarker of endometriosis, with higher expression in the group of women with endometriosis diagnosed by laparoscopy.

Keywords: endometriosis; biomarker; microRNAs; diagnosis; serum; miR-30c-5p

check for updates

Citation: Chico-Sordo, L.; Ruiz-Martínez, T.; Toribio, M.; González-Martín, R.; Spagnolo, E.; Domínguez, F.; Hernández, A.; García-Velasco, J.A. Identification of miR-30c-5p microRNA in Serum as a Candidate Biomarker to Diagnose Endometriosis. *Int. J. Mol. Sci.* **2024**, *25*, 1853. https://doi.org/10.3390/ijms25031853

Academic Editor: Alfonso Baldi

Received: 12 January 2024
Revised: 30 January 2024
Accepted: 1 February 2024
Published: 3 February 2024

Copyright: © 2024 by the authors. Licensee MDPI, Basel, Switzerland. This article is an open access article distributed under the terms and conditions of the Creative Commons Attribution (CC BY) license (https://creativecommons.org/licenses/by/4.0/).

1. Introduction

Endometriosis is a chronic estrogen-dependent inflammatory disease characterized by the presence of endometrial tissue outside the uterine cavity [1]. The etiology and pathophysiology of endometriosis are unknown, but different theories have been proposed so far to explain its origin [2].

Currently, despite its high prevalence, there is a diagnostic delay estimated between 6 and 10 years from the onset of symptoms to clinical diagnosis [3,4]. The identification of precise minimally or non-invasive diagnostic methods that allow early diagnosis of the disease would improve the quality of life of these women. Different factors and molecules such as cytokines, chemokines or oxidative stress indicators have been proposed as biomarkers in the last decades [5]. However, none of them have been accurately effective in detecting endometriosis [6]. One of the most used clinical markers of endometriosis is the elevated serum level of carcinogenic antigen 125 (CA-125) [7]. This glycoprotein, frequently used in the diagnosis of ovarian cancer, when used to diagnose endometriosis

increases the false positive results [8]. One of the main reasons why CA-125 fails as a diagnostic method is that its blood levels fluctuate across the menstrual cycle [9].

Recently, microRNAs (miRNAs) have emerged as potential biomarkers of disease because they are present in extracellular body fluids such as blood, saliva, urine or uterine fluid [10–13]. miRNAs are bound to protein complexes or contained in exosomes, which characterize them with a high stability in biofluids [14]. miRNAs are small non-coding RNA molecules (approximately 22 nucleotides) involved in multiple biological processes. These miRNAs play a role in regulating gene expression at a post-transcriptional level through transcriptional degradation or gene silencing [15,16]. These molecules stand out for their high stability [17]—an important criterion in the search for clinical biomarkers. In fact, the analysis of different miRNAs has been investigated as an important tool in the diagnosis, treatment and understanding of cancer [18–21], neurological disorders [22–24] and cardiovascular diseases [25–27].

The study of miRNAs as biomarkers of endometriosis has been performed in saliva [28], serum [29–31], plasma [32,33] and endometrial samples [34–36]. With the aim of identifying biomarkers of endometriosis, one of the most studied biofluids is blood because it is easy to obtain and reflects physiological and/or pathological conditions [37,38]. However, although many studies have shared the same objective and have evidenced differential expression of miRNAs in endometriosis compared with healthy women, the differences in study design and methodological issues imply that the results are not reproducible [39] and limits the potential diagnostic of miRNAs [40]. The main limitations of this type of study are the absence of quality controls in the RNA extraction and retro-transcription processes, the lack of sample hemolysis controls [31,33,41–43], the variability in the endogenous controls used in the normalization of miRNAs expression [44–47] and in the relative quantification method used in reverse transcription–quantitative polymerase chain reaction (RT-qPCR) [48].

Then, the main objective of this study was to evaluate the diagnostic ability of miRNAs present in serum as minimally invasive biomarkers of endometriosis. Following this objective, we identified serum miRNAs differentially expressed in endometriosis using a real-time PCR specific panel and validated a selection of these miRNAs in a novel cohort.

2. Results

2.1. Study Participant Characteristics

The characteristics of the patients are shown in Table 1, divided according to whether they were used in the preliminary study to identify differentially expressed miRNAs (n = 20) or in the subsequent validation of candidate miRNAs (n = 139). The study cohort used for the preliminary analysis (miRNA qPCR profiling) did not show statistically significant differences in age and body mass index (BMI) parameters. Regarding the cohort used in the miRNA qPCR validation, the mean age (±standard deviation) of controls and endometriosis patients was 31.7 ± 5.2 years and 37.5 ± 7.0 years, respectively. There was a significant difference in the parameter age ($p < 0.001$), making it necessary to correct the next results using this variable.

Table 1. Demographics and clinical characteristics of study participants.

	miRNA qPCR Profiling n **= 20**		**miRNA Real-Time qPCR Validation** n **= 139**	
Variable	**Control Group** n **= 10**	**Endometriosis Group** n **= 10**	**Control Group** n **= 72**	**Endometriosis Group** n **= 67**
Age ± SD (years)	32 ± 4.6	34.9 ± 4.0	31.7 ± 5.2	37.5 ± 7.0
Body Mass Index ± SD (kg/m^2)	22.5 ± 2.4	22.6 ± 3.2	24.1 ± 3.0	22.8 ± 3.1

Table 1. *Cont.*

Variable	miRNA qPCR Profiling $n = 20$		miRNA Real-Time qPCR Validation $n = 139$	
	Control Group $n = 10$	Endometriosis Group $n = 10$	Control Group $n = 72$	Endometriosis Group $n = 67$
ASRM stage, *n* (%)				
I	NA	0 (0)	NA	1 (1.5)
II	NA	4 (40)	NA	6 (9.0)
III	NA	4 (40)	NA	19 (28.3)
IV	NA	2 (20)	NA	41 (61.2)
Phase of menstrual cycle, *n* (%)				
Proliferative	10 (100)	0	49 (68.1)	0
Secretory	0	0	7 (9.7)	0
Unknown	0	10 (100)	16 (22.2)	67 (100)
Pain symptoms, *n* (%)				
Any pain symptoms	10 (100)	2 (20)	72 (100)	6 (8.9)
Dyspareunia	0	3 (30)	0	30 (44.7)
Dysmenorrhea	0	7 (70)	0	51 (76.1)
Dyschezia	0	3 (30)	0	22 (32.8)
Dysuria	0	1 (10)	0	9 (13.4)
Chronic pelvic pain	0	4 (40)	0	42 (62.6)
Infertility, *n* (%)				
Primary	0	3 (30)	0	28 (41.7)
Secondary	0	1 (10)	0	1 (1.4)
Unknown	0	5 (50)	0	23 (34.3)
Proven fertility (live birth)	10 (100)	1 (10)	72 (100)	15 (22.3)
Tumoral makers ± SD				
CA-125 (U/mL)	NA	32.4 ± 17.4	NA	185.3 ± 527.8
CA-19.9 (U/mL)	NA	28.1 ± 19.2	NA	94.99 ± 268.2
HE4 (pmol/l)	NA	-	NA	76.43 ± 31.05
Comorbidities, *n* (%)				
Hypothyroidism	0	0	2 (2.7)	11 (16.4)
Asthma	0	0	2 (2.7)	7 (10.4)
Migraine	0	0	1 (1.3)	4 (5.9)
Allergic rhinoconjunctivitis	0	0	1 (1.3)	3 (4.4)
Vitiligo	0	0	0	3 (4.4)
Hypertension	0	0	0	3 (4.4)
Depression	0	0	0	3 (4.4)
Fibromyalgia	0	0	0	2 (2.9)
Raynaud Syndrome	0	0	0	2 (2.9)
Other	0	1 (10)	4 (5.5)	8 (11.9)

Data are represented as mean ± standard deviation. NA—not applicable; ASRM—American Society for Reproductive Medicine. There is no tumor marker HE4 value for the endometriosis group used in miRNA qPCR profiling because only 1 of the 10 patients recorded this test result. The comorbidities with the highest frequency in our study cohort are listed. The "Other" comorbidities section includes inflammatory traits (celiac disease, Crohn's disease and multiple sclerosis), gastrointestinal features (chronic gastritis) and mental disorders (anxiety, ADHD, bipolar and personality disorders) based on McGrath et al.'s (2023) review [49].

2.2. Identification of Serum Levels of Circulating miRNAs in Case and Control Groups

In the preliminary analysis ($n = 20$) using a serum/plasma-specific miRNAs panel, 185 different miRNAs were tested. Out of these 185 miRNAs tested in the panel, 105 miRNAs were identified in all samples, with an average of 165 miRNAs detectable per sample. When comparing the endometriosis and control groups, 29 miRNAs were found to be differentially expressed using a cutoff of p-value < 0.05 (Table 2, upper). The miRNAs with a higher stability (stability value ≤ 0.004) were considered candidates for miRNA normalization (Table 2, medium). The constant level of spike-in assays and the non-statistically significant

differences of these controls indicated that extraction, reverse transcription and qPCR were successful (Table 2, lower).

Table 2. Differentially expressed miRNAs in serum, reference miRNA candidates and technical controls in qPCR profiling preliminary study.

Differentially Expressed miRNAs	Assay Catalog No.	*p*-Value	Fold Change
[miR-210-3p] *	YP00204333	0.005	−1.73
[miR-185-5p] *	YP00206037	0.006	−1.44
[miR-25-3p] *	YP00204361	0.007	−1.44
miR-660-5p *	YP00205911	0.007	−1.44
[miR-142-3p]	YP00204291	0.008	1.55
[miR-92a-3p] *	YP00204258	0.010	−1.37
miR-28-5p	YP00204322	0.010	1.85
let-7a-5p	YP00205727	0.010	1.35
miR-532-5p *	YP00204003	0.014	−1.43
miR-16-2-3p *	YP00204309	0.014	−1.43
[let-7c-5p]	YP00204767	0.015	1.41
miR-16-5p *	YO00205702	0.017	−1.44
miR-766-3p	YP00204499	0.019	1.73
miR-451a *	YP02119305	0.020	−1.70
miR-7-1-3p	YP00205888	0.023	2.24
miR-19b-3p *	YP00204450	0.023	−1.29
miR-132-3p	YP00206035	0.027	1.57
miR-192-5p *	YP00204099	0.029	−1.43
miR-215-5p *	YP00204598	0.030	−1.51
[miR-30c-5p]	YP00204783	0.031	1.33
let-7g-5p	YP00204565	0.031	1.13
miR-338-3p	YP00204719	0.034	1.58
miR-19a-3p *	YP00205862	0.034	−1.25
miR-140-3p *	YP00204304	0.037	−1.26
miR-30b-5p	YP00204765	0.039	1.29
miR-141-3p *	YP00204504	0.040	−1.73
let-7d-5p	YP00204124	0.046	1.36
[miR-342-3p] *	YP00205625	0.046	−1.49
miR-150-5p *	YP00204660	0.048	−1.69
Reference miRNA candidates	**Assay catalog no.**	**Stability value**	
miR-30e-5p	YP00204714	0.003	
miR-652-3p	YP00204387	0.003	
miR-29b-3p	YP00204679	0.004	
miR-21-5p	YP00204230	0.004	
miR-15b-5p	YP00204243	0.004	
miR-22-3p	YP00204606	0.004	
miR-107	YP00204468	0.004	
Technical controls (spike-ins)	**Assay catalog no.**	***p*-value**	
RNA isolation control			
UniSp2	YP00203950	0.796	
UniSp4	YP00203953	0.971	
UniSp5	YP00203955	0.218	
cDNA synthesis control			
UniSp6	YP00203954	0.684	
Interplate calibrator			
UniSp3	YP02119288	0.143	

* miRNAs down-regulated in the endometriosis group. [] indicates the miRNAs selected for further validation as endometriosis candidates in a new cohort, with the exception of miR-125b-5p, which was selected from the literature. Fold change calculated by 2nd derivate method.

2.3. Suitability of miR-30c-5p as Potential Endometriosis Biomarker

Of the 29 differentially expressed miRNAs in the serum-specific qPCR panel, 9 of them were validated in a larger population (n = 139). The miRNAs let-7c-5p and miR-210-3p were discarded because the quantification cycle (Cq) values were greater than 35 (detection threshold), indicating a low amount of these miRNAs in the reaction. miR-185-5p, miR-25-3p, miR-342-3p, miR-125b-5p, miR-142-3p and miR-92a-3p were not differentially expressed in women with endometriosis compared with control women (Figure 1a). However, miR-30c-5p was significantly higher in the endometriosis group (Figure 1b). No significant difference in the mean Cq values of miRNAs miR-30e-5p and miR-15b-5p was found between women with endometriosis and the control (p = 0.551) during the validation, so these miRNAs were used as reference miRNAs to standardize the results of the candidate miRNAs (Figure 1c). To assess the utility of miR-30c-5p in diagnosing endometriosis, we calculated the receiver operating characteristic (ROC) curve. The area under the curve (AUC) value of miR-30c-5p was 0.8437, with a sensitivity and specificity of 0.7793 and 0.9081, respectively (Figure 1d). In addition, the usefulness of miR-30c-5p as a serum biomarker of endometriosis, independently of the phase of the menstrual cycle, was confirmed by comparing its levels between different phases of the menstrual cycle in the group of healthy women (Figure A1).

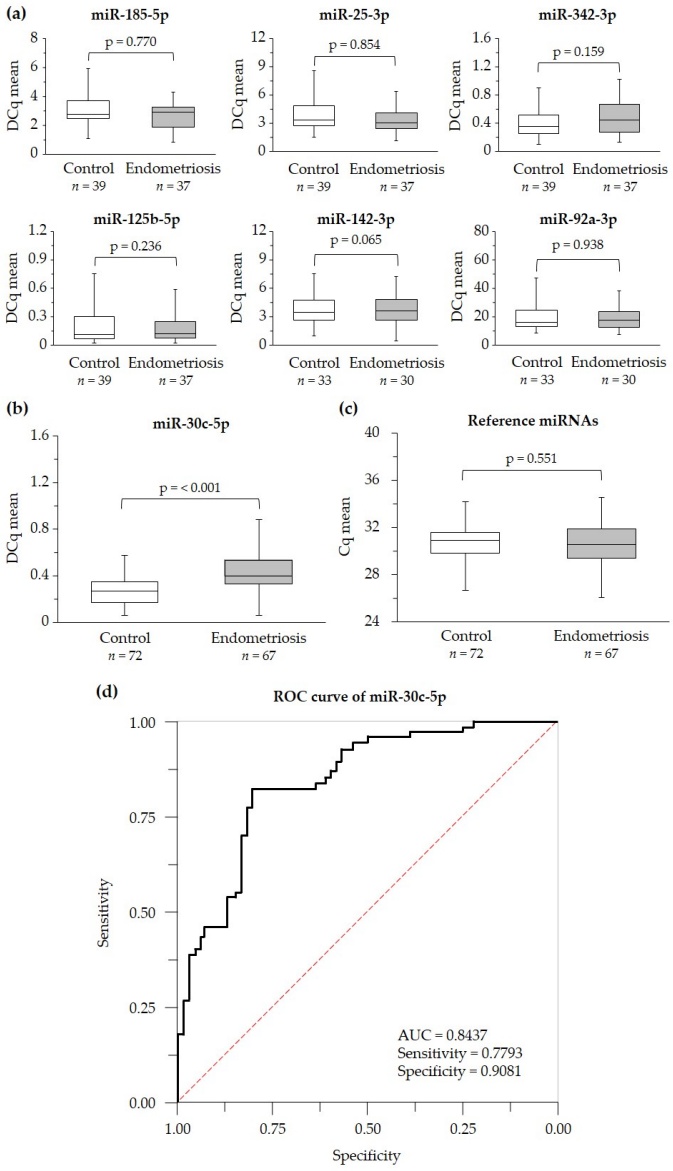


Figure 1. Serum expression of miRNAs in control and endometriosis groups in the validation cohort.

(**a**) Expression of miR-185-5p, miR-25-3p, miR-342-3p, miR-125b-5p, miR-142-3p and miR-92a-3p in the control and endometriosis groups. (**b**) Differential expression of miR-30c-5p between the control and endometriosis groups. (**c**) Mean value of the quantification cycle of the miRNAs chosen as endogenous (miR-30e-5p and miR-15b-5p) used in the normalization of the expression levels of candidate biomarker miRNAs. (**d**) Receiver operating characteristic curve (ROC) of serum miR-30c-5p obtained after adding the multivariate model with age. The corresponding area under the curve (AUC), sensitivity and specificity are indicated. Box plots were used to represent the levels of each miRNA (**a**,**b**) or the Cq mean (**c**). Data were plotted showing median and interquartile range. Results were compared using Student's *t*-test and were considered statistically significant when $p < 0.05$. *n* indicates the number of individuals analyzed. DCq indicates miRNA Cq values normalized to the mean Cq values of reference miRNAs. Cq indicates the quantification cycle of miRNA detection by quantitative PCR.

2.4. Serum miR-30c-5p Levels in Endometriosis Stages

To evaluate whether miR-30c-5p expression correlates with the stage of endometriosis, the levels of this miRNA in different stages were analyzed. Endometriosis stages I and II could not be analyzed because the sample size in these stages was small. The analysis of the expression levels of miR-30c-5p, based on the stage of the disease according to American Society of Reproductive Medicine (ASRM) classification, showed that this miRNA could distinguish stage III (Figure 2a) and IV (Figure 2b) from the control group. However, there was no statistically significant difference between stage III and IV (Figure 2c).

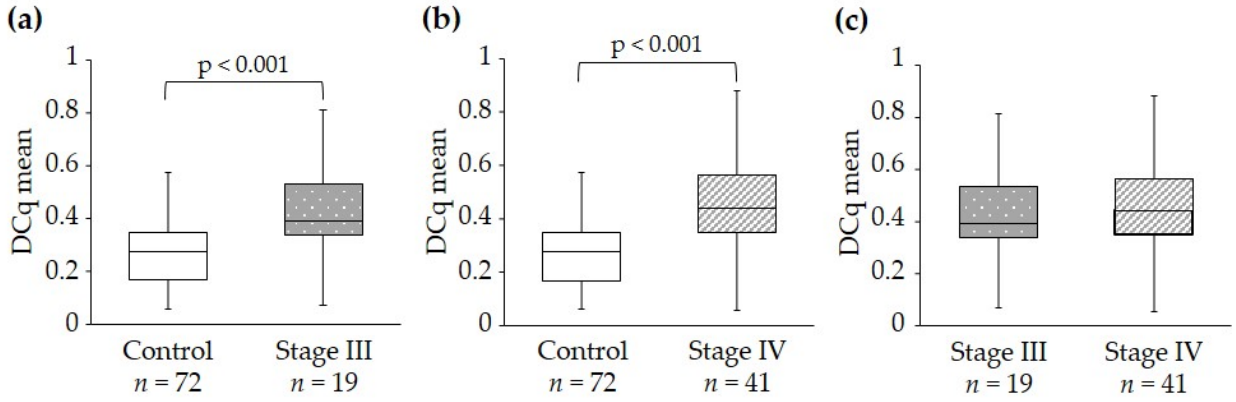


Figure 2. miR-30c-5p expression in different stages of endometriosis. (**a**) Expression of miR-30c-5p in the control group and patients with stage III endometriosis. (**b**) Comparison of miR-30c-5p expression between the control group and the stage IV endometriosis group. (**c**) Expression of miR-30c-5p in endometriosis subjects divided into stage III and IV. Endometriosis stage assignment was based on the ASRM classification. Box plots were used to represent miR-30c-5p levels after normalization with reference miRNAs. Data were plotted showing median and interquartile range. Results were compared using Student's *t*-test and were considered statistically significant when $p < 0.05$. *n* indicates the number of individuals analyzed. DCq indicates miRNA Cq values normalized to the mean Cq values of reference miRNAs.

2.5. The Impact of Hemolysis on Potential Diagnosis of miR-30c-5p

The level of hemolysis of the samples was variable, and this was assessed using the absorbance of hemoglobin at 414 nm (Supplementary Figure S1a,b) and delta Cq [(miR-23a-3p)–(miR-451a)] (Supplementary Figure S1c,d). Both methods of hemolysis assessment correlated with each other (Supplementary Figure S1e,f). However, there was no correlation between hemolysis, assessed by hemoglobin absorbance, and the miR-30c-5p value (Figure 3a). When hemolysis was measured using the delta Cq, there was a correlation between hemolysis levels and the value of the miRNA biomarker candidate (Figure 3b). After filtering for hemolysis, if delta Cq [(miR-23a-3p)–(miR-451a)] ≤ 9 the endometriosis group registered

higher miR-30c-5p compared with the control group (Figure 3c), and there was no correlation with hemolysis levels in the samples (Figure 3d). The AUC value of miR-30c-5p was 0.8095 when the criterion used to monitor hemolysis was delta Cq ≤ 9 (Figure 3e).

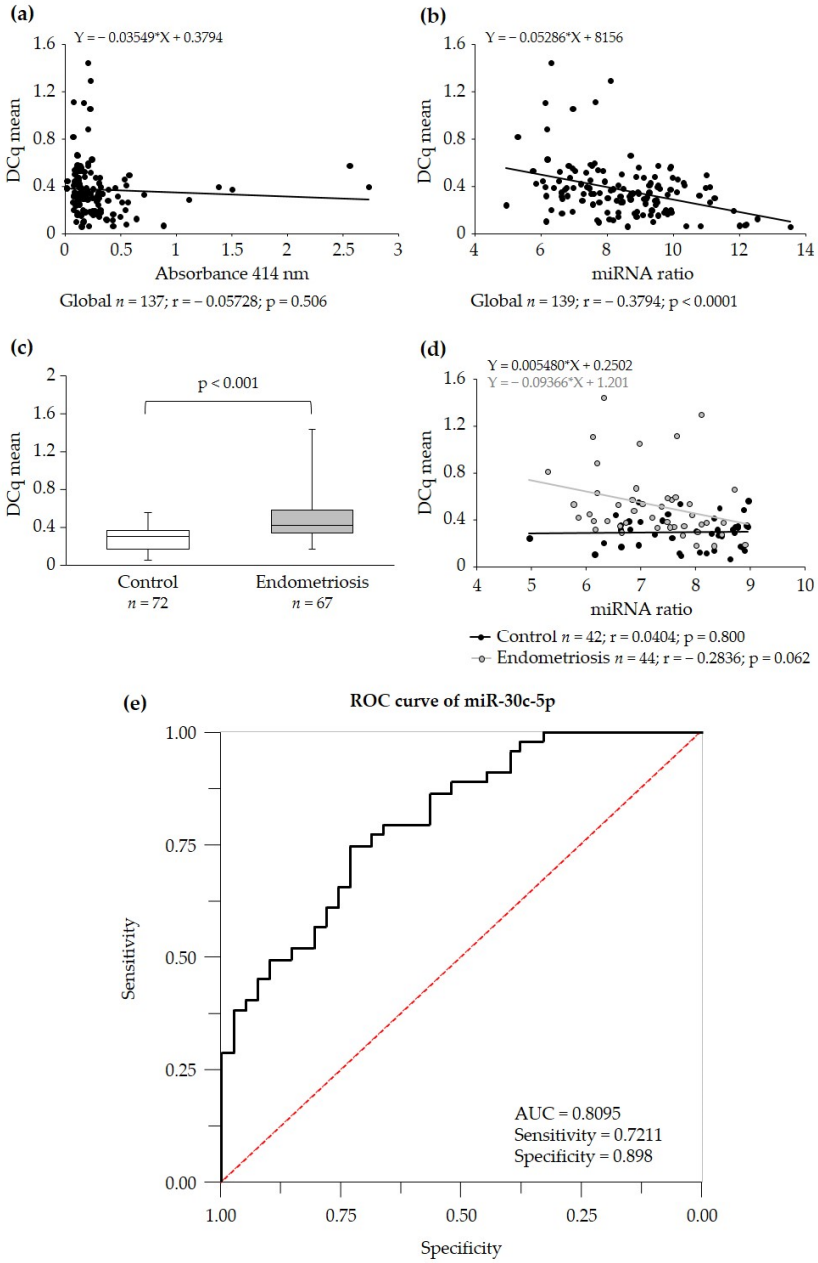


Figure 3. Variation of miR-30c-5p levels with the level of hemolysis. (**a**) Global correlation between hemoglobin absorbance and miR-30c-5p levels. (**b**) Global correlation between the delta Cq [(miR-23a-3p)–(miR-451a)] and miR-30c-5p levels. (**c**) Box plot of miR-30c-5p levels between the control and endometriosis groups, including samples with a delta Cq ≤ 9, excluding from the analysis those with a higher delta Cq. (**d**) Correlation between the delta Cq [(miR-23a-3p)–(miR-451a)] and miR-30c-5p levels in samples with a ratio ≤ 9, divided into controls (black) and women with endometriosis (grey). (**e**) Receiver operating characteristic curve (ROC) of serum miR-30c-5p when hemolysis delta Cq ≤ 9. The curve was obtained after adding the multivariate model with age. The corresponding area under the curve (AUC), sensitivity and specificity are indicated. r represents Pearson's correlation coefficient, and the equation of the line is indicated (a, b and d). Statistically significant data when $p > 0.05$. *n* represents the number of individuals analyzed. DCq indicates miRNA Cq values normalized to the mean Cq values of reference miRNAs.

2.6. Prediction of Target Genes and Functional Enrichment

A total of 1545 target genes were predicted for miR-30c-5p in the miRDB database (Supplementary Table S1). To unravel the biological impact in which miR-30c-5p may be involved, we evaluated the biological processes, cellular components and molecular functions using gene ontology and the Kyoto Encyclopedia of Genes and Genomes (KEGG) pathways related to these 1545 target genes.

After enrichment analysis, the miR-30c-5p target genes mainly belong to gene ontology biological processes related to neurogenesis and neuronal differentiation (Figure 4a, Supplementary Table S2) and gene ontology cellular components related to neurons and the endomembrane system (Figure 4a, Supplementary Table S3). Finally, gene ontology molecular functions related to the miR-30c-5p target genes include acting as kinases and DNA-binding proteins (Figure 4a, Supplementary Table S4).

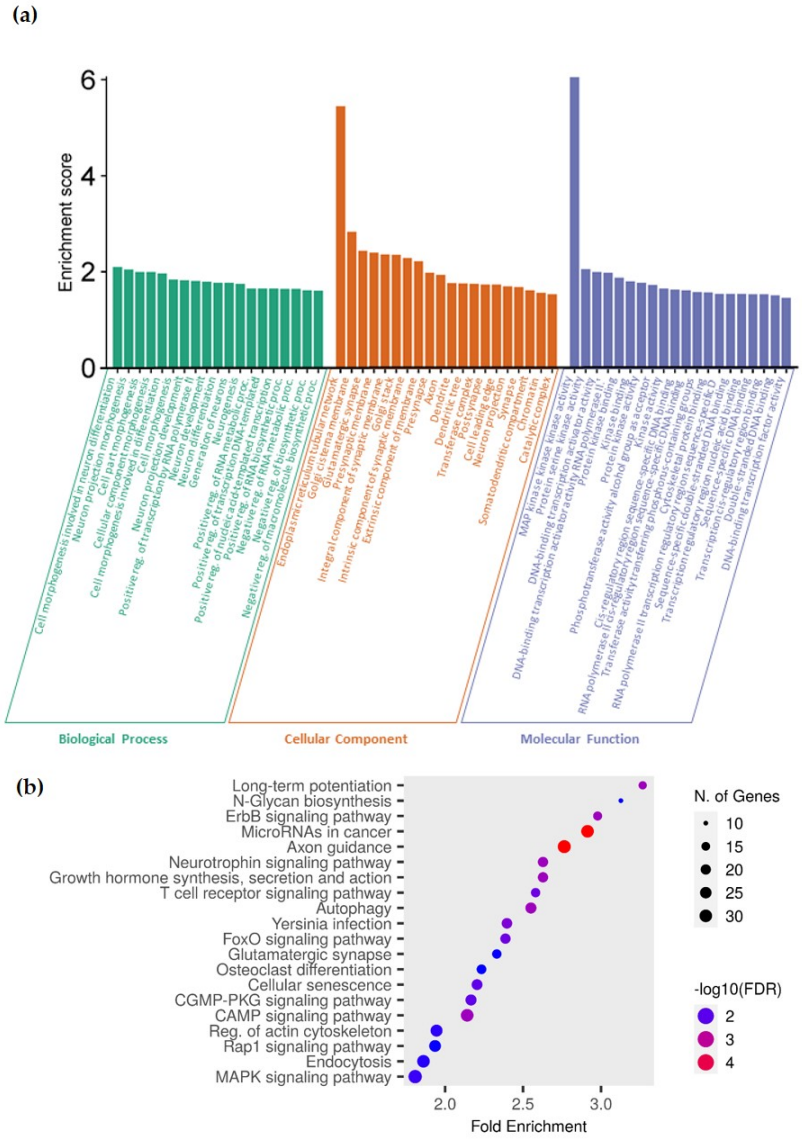


Figure 4. Functional enrichment of hsa-miR-30c-5p target genes. (**a**) Gene ontology function analysis histogram of miR-30c-5p target genes. Dark cyan represents top 20 gene ontology biological processes, sienna represents top 20 gene ontology cellular component and steel blue represents top 20 gene ontology molecular function. (**b**) Dot plot of KEGG pathways enriched in miR-30c-5p target genes. Fold enrichment represents the overrepresentation of genes from certain KEGG pathways, dot size is directly proportional to the number of genes involved in the pathway and color gradient represents the FDR.

Additionally, after evaluating the KEGG pathways for which these 1545 target genes are enriched, miRNAs in cancer and axon guidance pathways outstand, although KEGG pathways related to several signaling pathways and cellular processes such as autophagy and cellular senescence are also enriched (Figure 4b, Supplementary Table S5).

3. Discussion

Our results show the potential of miR-30c-5p as a biomarker of endometriosis in serum, maintaining its diagnostic potential even when there is an acceptable risk of hemolysis in blood samples.

The gold standard technique for the diagnosis of endometriosis is laparoscopy [50]. Despite its high diagnostic sensitivity and specificity, this technique is highly invasive and depends on the finding of lesions identifiable by the surgeon. In the last few years, the relentless search for a reliable and accurate diagnostic test for the early diagnosis of endometriosis has focused on the role of miRNAs. Despite the large number of studies on miRNAs as biomarkers, no validation studies have subsequently been carried out. A differential expression of miRNAs between women with endometriosis and healthy women has been evidenced in both plasma [32,33] and serum samples [29–31]. However, serum has certain advantages over plasma for several reasons. Firstly, the probability of contamination by platelets and erythrocytes is lower [51]. Secondly, the interference of the compounds used for serum collection with subsequent processes to quantify miRNAs such as reverse transcription and/or PCR is acceptable compared with the interference of those used for plasma collection [52]. In addition, in the case of performing a validation study from the clinic's sample repository, it is easier to perform it on serum as there is more availability [53].

There is great variability in the miRNAs reported as candidate biomarkers of endometriosis despite using the same type of sample (serum) and the same technique (RT-qPCR) for the quantification of miRNAs. Mainly, the difference is in the endogenous control used for data normalization [54] and in the applied equation [55]. A large number of studies use U6 small nuclear RNA (RNU6) to normalize the expression of miRNAs in serum [29–31,47,56–58]. However, its use in normalizing data for circulating serum cell-free miRNAs is not recommended because RNU6 has been shown to have high variability between samples [59,60]. In our study, the following two different methods were used for normalization of miRNA expression levels: normalization based on the overall mean of miRNAs detected in all samples and normalization using two reference miRNAs' mean with stable expression in both study groups. First, according to the results of the study by Mestdagh and coworkers, for the identification of differentially expressed miRNA candidates from a panel of 185 miRNAs, the mean of all expressed miRNAs was used as a normalization strategy [44]. Secondly, once the candidate miRNAs were identified in a discovery cohort, some of them were validated in a new cohort of patients; in this case, the mean of miR-30e-5p and miR-15b-5p was used for normalization, whose expression was equal in the control and endometriosis groups. The use of two or more reference miRNAs for normalization has been used in several studies in plasma [33,61,62], and their use is highly recommended in the Minimum Information for Publication of Quantitative Real-time PCR Experiments (MIQE) [55].

Preliminary analysis of a panel of 185 miRNAs with subjects from each of the groups allowed us to obtain not only endogenous miRNAs suitable for our study but also a list of differentially expressed miRNAs in the endometriosis group. From this panel, miRNA biomarker candidates were selected and quantified by RT-qPCR. Our results evidenced that not all differentially expressed miRNAs during the profiling maintain their diagnostic potential after validation in a new cohort, so validation is recommended. Consequently, it is assumed that there will be more miRNAs not included in this panel of 185 miRNAs that could be putative biomarkers for endometriosis. In our study, this specific serum/plasma panel was chosen for preliminary analysis because most of the miRNA biomarker candidates for endometriosis suggested in the previous literature were included. However, there

are other alternatives for preliminary analysis such as next-generation sequencing (NGS), which allows global miRNA screening, followed by subsequent validation by RT-qPCR, as in our study [33]. Further, miR-30c-5p would be a good cell-free serum biomarker for endometriosis because we found a statistically significant difference in its levels between women with endometriosis and control women, and it registered high sensitivity and specificity values. Previously, studies reported no difference in the expression levels of candidate miRNA biomarkers for endometriosis based on the phase of menstrual cycle in the control group [31,56]. Our biomarker candidate, miR-30c-5p, is unaltered by menstrual cycle phase when comparing the proliferative and secretory phase (even if we include subjects whose phase is unknown) in healthy women. The study by Wang and coworkers (2016) evidenced lower levels of miR-30c-5p in the serum of patients with endometriosis, whereas we observed the opposite trend. This difference could be due to either the method used in normalization, as our study used the mean of two stable endogenous miRNAs present in the samples versus their use of an exogenous synthetic miRNA (cel-miR-39) introduced prior to RNA extraction. Another explanation for our discrepancies could be that all endometriosis patients included were diagnosed at stage I/II [46]. Other studies have also reported lower expression levels of this miRNA in ectopic [63] and eutopic endometrium tissue samples [64], and decreased proliferation, adhesion, invasion and migration of endometrial stromal cells have been observed following miR-30c-5p upregulation [64]. However, in both studies, they used RNU6 as the internal reference gene for normalization. Furthermore, it is of great importance to specify which mature transcript was quantified, 5p or 3p [65,66]. Based on the sequence of the primer used, Chen and coworkers (2017) evaluated miR-30c-5p, while Zhang and coworkers (2022) quantified the miRNA precursor [63,64]. Both the precursor and mature miRNA can be quantified by RT-qPCR, although the levels may be different because the precursor undergoes faster degradation than the mature one [67].

In all other candidate miRNAs tested in the validation cohort, we found no statistically significant differences between the endometriosis and control groups, although these differences were detected in the profiling analysis. Previous studies have analyzed the potential of some of the proposed miRNAs as biomarkers of endometriosis, or as possible therapeutic targets. miR-342-3p and miR-125-5p were detected overexpressed in the serum of women with endometriosis [31,56]. Studies in plasma samples suggested miR-185-5p [68], miR-125b-5p [62] and miR-92a-3p [69,70] as good biomarkers of endometriosis. Other studies analyzed the effect of under- or overexpression of miR-185-5p [71], miR-142-3p [72,73] and miR-92a-3p [74] on the phenotype of eutopic and/or ectopic endometrial stromal cells, altering their properties and positioning them as future therapeutic alternatives. Another of the miRNAs recurrently suggested as an endometriosis biomarker is miR-451a [31,56,57]. This miRNA is highly expressed in erythrocytes; for this reason, it is used to test for the presence of hemolysis in serum and plasma samples [75–79]. Hemolysis is a major source of variation in these types of samples as it involves contamination with miRNAs from cells [41]. Although many hemolytic diseases exhibit increased levels of hemolysis in blood samples [80–82], the diagnostic potential of miR-451a in endometriosis is questionable because it could act as a confounding variable [83,84]. The levels of miR-451a and miR-23a-3p allowed us to calculate the delta Cq [(miR-23a-3p)–(miR-451a)] to assess the risk of hemolysis as an alternative to hemoglobin absorbance [41,85]. In our study, we analyzed the impact of hemolysis on the diagnostic potential of our candidate miRNA, miR-30c-5p. For this purpose, the hemolysis level of the samples from both study groups was similar, evaluated with both hemoglobin absorbance and miRNA delta Cq, which showed a positive correlation with each other. When we analyzed whether there was a correlation between the risk of hemolysis and the level of miR-30c-5p, its levels only showed a statistically significant correlation with the hemolysis delta Cq. In order to obtain hemolysis-free serum samples, certain precautions need to be taken during the extraction process [86]. In addition, there is a possibility that a sample first classified as non-hemolyzed may have hemolysis after measuring the hemoglobin absorbance or delta Cq [85]. This would involve obtaining a new

sample, with the inconvenience for the attending patient [87]. However, when only samples whose delta Cq $\leq$ 9 were taken into account, miR-30c-5p maintained differential expression between the control and endometriosis groups. Moreover, the variable hemolysis did not correlate with candidate miRNA levels, preserving its diagnostic potential.

Analysis of the molecular pathways in which miR-30c-5p is implicated according to the databases highlighted pathways related to cancer and neuronal processes. Previously, differential expression of miRNAs whose target genes were enriched in cancer-related pathways has been reported in patients with endometriosis [88]. In fact, studies on different types of cancer such as hepatocellular carcinoma [89], oral squamous cell carcinoma [90], gastric cancer [91], papillary thyroid carcinoma [92] or bladder cancer [93] have evidenced a lower expression of this miRNA in neoplastic tissues. In our study, women suffering from endometriosis showed increased serum miR-30c-5p expression. Molecular links exist between cancer and endometriosis, because the main cells involved in both pathologies are able to evade the apoptosis process, share characteristics with stem cells regarding division capacity and standout for a high angiogenic potential [94]. Endometriosis is a benign gynecological condition, although there are studies that relate it to an increased risk of some types of cancer such as ovarian cancer, breast cancer or endometrial cancer [95]. Studies on ovarian [96] or breast cancer [97], also estrogen-dependent conditions like endometriosis, showed that increased levels of miR-30c-5p inhibit tumor cell proliferation, migration and invasion. Therefore, the fact that this miRNA is elevated in patients with endometriosis as opposed to patients with ovarian or breast cancer could underline the differences between these two separate conditions. However, more studies are needed to further investigate the molecular mechanisms in which miR-30c-5p is involved in both endometriosis and different types of cancer to clarify its role in each of them. One of the potential molecular pathways that could be key in the role of miR-30c-5p in endometriosis and cancer is related to the TP53 (p53) gene. The presence of mutations in TP53, and consequently the elicitation of mutant p53 proteins, characterizes a large proportion of human tumors [98,99]. Studies in cancer have evidenced that there is a relationship between p53 and miR-30c, concluding that the reduced expression of miR-30c correlates with increased mutations in p53, which in turn increases tumor aggressiveness [100]. These results suggest that differences in miR-30c-5p levels, and consequently in molecular pathways regulated by this miRNA, could be associated with the activation or not of the cellular malignization process, which differentiates endometriosis from cancer [96,97,101–103]. Also, this miRNA could be used as a differential diagnostic tool between both pathologies.

Other miR-30c-5p-associated pathways are related to the processes of neuron formation and differentiation and axonal conduction. Recent studies suggested that endometriosis affects the central nervous system [104,105]. The unifying thread that links neural processes and endometriosis is the chronic pain experienced by patients [106,107]. This endometriosis-associated pain is considered a type of neuropathic pain [108–111]. In fact, one of the most studied genes has been the brain-derived neurotrophic factor (BDNF) [112], which has even been suggested as a neuronal biomarker for endometriosis diagnosis [113]. Tramullas and coworkers in their studies demonstrated a causal relationship of miR-30c-5p levels with nociception and neuropathic pain in rodents [114,115]. Furthermore, they suggested that this relationship was mediated by transforming growth factor-beta 1 (TGF-β1) [114], which was increased in endometriosis and was related to an increased migratory, invasive and colonizing potential of endometriotic cells [116].

Our study stands out for several strengths based on the normalization of the miRNA levels, the inclusion of quality controls in the methodology, the quantification of the variable hemolysis and the use of different cohorts for discovery and validation. Thanks to the preliminary analysis where numerous miRNAs were tested in a small population, both candidate disease biomarker miRNAs and endogenous miRNAs could be extracted. The method used for normalization was based on the previously published literature. The incorporation of spike-in markers in both RNA extraction, retrotranscription and quantification were helpful in monitoring the technique's efficiency. The variable hemolysis

was measured in two different ways, and its impact on the miRNA biomarker candidate was analyzed. Furthermore, serum levels of miR-30c-5p showed no differences between the phases of the menstrual cycle. Therefore, the use of miR-30c-5p as a mild or severe grade of endometriosis biomarker would be a reproducible technique in other laboratories, provided that its levels are normalized with endogenous miRNAs miR-30e-5p and miR-15b-5p, and the level of serum hemolysis measured by delta Cq [(miR-23a-3p)–(miR-451a)] does not exceed a value of 9. However, one of the main limitations of this study was that no cases of women with stage I endometriosis were included, and there were very few cases with stage II.

4. Materials and Methods

4.1. Study Population and Design

A total of 159 women, from La Paz University Hospital (LPUH) and IVIRMA Madrid, participated in this study, aged 22–55 years and with a BMI between 18.5 and 29.9 kg/m^2. Recruitment was carried out between March 2018 and January 2023. This study included women diagnosed with endometriosis after undergoing laparoscopic surgical exploration of the abdominal cavity and anatomopathological study of the lesions. The endometriosis stage was classified according to the ASRM revised classification. Women with endometriosis stages I, II, III and IV were recruited for the study. Patients treated with gonadotropin releasing hormone (GnRH) agonist or aromatase inhibitors in the last 3 months were excluded. The control group consisted of patients undergoing laparoscopic tubal ligation for contraception with the absence of endometriotic lesions from LPUH and healthy oocyte donor women from IVIRMA Madrid. These women had proven fertility at the time of sample collection as an inclusion criterion. Proven fertility was defined as at least one live birth and no history of non-progressive gestation. The exclusion criterion for the control group was the finding of endometriosis during laparoscopy. Women, from both study groups, were recruited at all phases of the menstrual cycle as this variable does not influence the serum levels of circulating miRNAs [56,57]. All patients provided written informed consent before being included in the study. Puerta de Hierro University Hospital and LPUH board (Madrid, Spain) approved the study protocol (1707-MAD-083-JG, approved in November 2017).

A preliminary real-time PCR panel analysis was performed in serum samples from women with confirmed endometriosis (n = 10) and women without endometriosis from the control group (n = 10) (Figure A2). A total of 185 miRNAs were evaluated in this miRNA qPCR serum profiling panel. From this preliminary analysis, 9 miRNAs with differential expression between the control and endometriosis groups and 2 serum miRNAs with stable expression in both groups to standardize the results were chosen for validation analysis. The miRNAs selected as biomarker candidates were validated by qPCR in a new cohort of women with endometriosis (n = 67) and women in the control group (n = 72) in two consecutive batches. The level of differentially expressed miRNAs in the validation was compared between the endometriosis stages, and the impact of hemolysis on their diagnostic potential was studied.

4.2. Serum Sample Collection

Blood samples (5 mL) were collected in sterile serum separator gel tubes (Sarstedt, Nümbrecht, Germany) by direct venipuncture prior to the procedure (laparoscopy or follicular puncture). The samples were immediately centrifuged at 3000× *g* for 10 min at room temperature. The serum was transferred to 2 mL tubes and stored at −80 °C until analysis.

4.3. miRNA qPCR Profiling

Serum samples from women with endometriosis (n = 10) and from the control group (n = 10) were analyzed using the miRNA Ready-to-Use PCR. A total of 185 miRNAs were evaluated by qPCR in serum using the miRCURY LNA SYBR Green master mix

(QIAGEN, Hilden, Germany). Amplification was performed with a LightCycler® 480 real-time PCR system (Roche, Mannheim, Germany) in 384-well plates. Amplification curves were analyzed using Roche LC 480 software for both Cq value determination and melting curve analysis. Normalization was performed based on the average of the assays detected in all samples (105 miRNAs), according to the following formula: normalized Cq (dCq) = global mean Cq − assay Cq (miRNA of interest). A higher value thus indicated that the miRNA was more abundant in the sample. The 2nd derivate method was used to analyze the relative changes in gene expression from expression profiling, obtaining the fold change.

4.4. RNA Extraction and cDNA Synthesis

The serum was thawed on ice and centrifuged at 3000× *g* for 5 min at 4 °C. Total RNA was extracted from 200 µL of serum using miRNeasy serum/plasma Advanced Kit (QIAGEN, Hilden, Germany) according to the manufacturer's instructions. In the first extraction step, RNA spike-in template mixture (UniSp2, UniSp4 and UniSp5) was added as an extraction control. RNA was eluted in 20 µL nuclease-free water. An amount of 7 µL of RNA was retrotranscribed using the First-Strand cDNA Synthesis kit (QIAGEN, Hilden, Germany) according to the manufacturer's guide on a Mastercycler® X50a (Eppendorf, Hamburg, Germany). To confirm that reverse transcription and amplification had occurred with equal efficiency in all samples, UniSp6 RNA spike-in template was added.

4.5. Selection of miRNA Biomarker Candidates of Endometriosis and Reference miRNAs

From the miRNAs analyzed in miRNA qPCR profiling and also based on the previous literature, miRNA biomarker candidates of endometriosis and reference miRNAs were selected. Then, nine differentially expressed miRNAs were selected as putative biomarkers (miR-185-5p, let-7c-5p, miR-30c-5p, miR-210-3p, miR-25-3p, miR-342-3p, miR-125b-5p, miR-142-3p and miR-92a-3p) and two miRNAs with stable expression in the control and endometriosis groups were selected as reference miRNAs (miR-30e-5p and miR-15b-5p). Endogenous miRNAs were chosen based on the stability value of miRNAs found in all samples. This value was calculated using NormFinder [117] software.

4.6. miRNA Real-Time qPCR Validation

The 9 miRNA biomarker candidates were validated in a larger number of patients in the endometriosis (n = 67) and the control group (n = 72). This experiment was performed in two consecutive rounds; for this reason, the sample size for the miRNAs evaluated was different. In the first round, miR-185-5p, let-7c-5p, miR-30c-5p, miR-210-3p, miR-25-3p, miR-342-3p and miR-125b-5p were analyzed. In the second round, miR-30c-5p, miR-142-3p and miR-92a-3p were analyzed, discarding miRNAs without differential expression of the first round. The miRNAs were quantified by real-time qPCR on a 7500 Fast System (Applied Biosystems) in 96-well plates using miRCURY LNA SYBR Green (QIAGEN, Hilden, Germany), according to the manufacturer's instructions. Primers (Table A1) for each miRNA were obtained from Qiagen. The Cq values of miRNAs in each subject were measured in duplicate, and the mean Cq value obtained was used in subsequent analyses. Quantification cycle values greater than 35 were considered to be below the detection level of the assay, and a UniSp3 interplate calibrator was used to calculate the calibration factor (mean plate UniSp3 Cq—mean global UniSp3 Cq). The miRNA Cq values were normalized, after interplate calibration, to the mean Cq values of two reference miRNAs. Relative expression for each miRNA in each sample was obtained using 2^{-dCq} ($2^{-(\text{Cq miRNA of interest} - \text{Cq reference miRNAs})}$).

4.7. Hemolysis Control

Hemolysis of serum samples was monitored by the following two methods: spectrophotometry and miRNA expression. By spectrophotometry, the absorbance of oxyhemoglobin was measured at λ= 414 nm using the NanoPhotometer N60 (Implent). The

other method used to identify sample hemolysis risk was based on the following two miRNAs: miR-23a-3p and miR-451a. Levels of miR-23a-3p are stable in serum and are not affected by hemolysis. However, miR-451a is enriched in erythrocytes and its levels are increased in serum when hemolysis occurs. During RT-qPCR, both miRNAs were measured in duplicate in each sample, and the delta Cq [(miR-23a-3p)–(miR-451a)] was calculated (mean miR-23a-3p Cq–mean miR-451 Cq).

4.8. miRNA Target Gene Prediction and Functional Enrichment Analysis

Target genes that could be under the modulation of the differentially expressed miRNA at validation, miR-30c-5p, were predicted employing the miRDB database [118,119]. Subsequently, functional annotation and graphical representation of the gene ontology biological processes, cellular component and molecular functions and KEGG pathways enriched for the previously predicted target genes were performed using the ShinyGO 0.77 tool [120] and the Bioinformatics (www.bioinformatics.com.cn, accessed on 29 January 2024) free online platform.

4.9. Statistical Analysis

Data were represented as mean ± standard deviation (SD) for age, and BMI of study participants and statistical analysis was performed with R software (version 4.0.3). For normalization of miRNA expression levels, the overall mean of all detected miRNAs (miRNA qPCR profiling) or the mean of two endogenous miRNAs (miRNA real-time qPCR validation) was used. In the preliminary analysis, miRNA expression was calculated as the 2nd derivative. During the validation phase, relative miRNA expression was calculated with the comparative Cq method based on Schmittgen and Livak (2008) [48]. The Student *t*-test was used to compare the study variables in the endometriosis and control groups, using a cutoff of p-value < 0.05. miRNAs with p-value < 0.05 were considered differentially expressed between the endometriosis and control groups. A multivariate model was applied with the variable age in the differentially expressed miRNAs. The AUC was calculated with the ROC curve for differentially expressed miRNAs between the endometriosis and control group. The ROC curves and AUCs were calculated with R software by adding the multivariate model with age. Pearson's correlation coefficient was used to examine the relationship between continuous variables. The variation of miR-30c-5p levels between the phases of the menstrual cycle was evaluated by ordinary one-way ANOVA test (when cases with unknown phase were taken into account) or by Student *t*-test (proliferative vs. secretory).

To assess the impact of hemolysis on the potential of miRNAs as biomarkers, candidate miRNA levels were evaluated between the endometriosis and control groups by Student *t*-test. This analysis was performed repeatedly, filtering by different delta Cq [(miR-23a-3p)–(miR-451a)] values.

5. Conclusions

In conclusion, serum levels of miRNAs are promising biomarkers of diseases such as endometriosis. Specifically, miR-30c-5p is postulated as a good candidate for a minimally invasive biomarker of endometriosis, allowing differentiation between healthy women and women with endometriosis in mild or advanced stages. However, to guarantee its diagnostic potential in serum, it is necessary to control the serum hemolysis. Future large-scale multicenter studies for the validation of the levels of this miRNA including women with both stage I and stage II endometriosis would be necessary. In addition, these studies could analyze the molecular pathways in which miR-30c-5p intervenes and its relationship with endometriosis, including other study groups such as women with different types of gynecological cancer, and in which the pain variable is quantified.

Supplementary Materials: The following supporting information can be downloaded at: https://www.mdpi.com/article/10.3390/ijms25031853/s1.

Author Contributions: Conceptualization, J.A.G.-V., A.H., F.D. and L.C.-S.; methodology, J.A.G.-V., F.D. and L.C.-S.; software, F.D., R.G.-M. and L.C.-S.; validation, L.C.-S., T.R.-M. and J.A.G.-V.; formal analysis, L.C.-S. and J.A.G.-V.; investigation, L.C.-S. and T.R.-M.; resources, M.T. and E.S.; data curation, L.C.-S.; writing—original draft preparation, L.C.-S.; writing—review and editing, J.A.G.-V., F.D., A.H., L.C.-S., T.R.-M. and E.S.; visualization, L.C.-S. and J.A.G.-V.; supervision, J.A.G.-V. and A.H.; project administration, J.A.G.-V. and A.H.; funding acquisition, J.A.G.-V. All authors have read and agreed to the published version of the manuscript.

Funding: This research was funded by the Instituto de Salud Carlos III (ISCIII) with the code PI20/01368, the Next Generation EU Fund, and Merck KGaA. L.C.-S. was supported by a predoctoral grant (PFIS FI19/00008) from the Instituto de Salud Carlos III (Spanish Government) and European Union (ESF, 'Investing in your Future'). R.G.-M. was supported by the Generalitat Valenciana (CIAPOT/2022/15).

Institutional Review Board Statement: The study was conducted in accordance with the Declaration of Helsinki, and approved by the Institutional Review Board (or Ethics Committee) of Puerta de Hierro University Hospital and LPUH board (Madrid, Spain) (protocol code 1707-MAD-083-JG, approved in November 2017).

Informed Consent Statement: Informed consent was obtained from all subjects involved in the study.

Data Availability Statement: The data supporting the findings of this study are available on request from the corresponding author.

Conflicts of Interest: The authors declare no conflicts of interest.

Appendix A

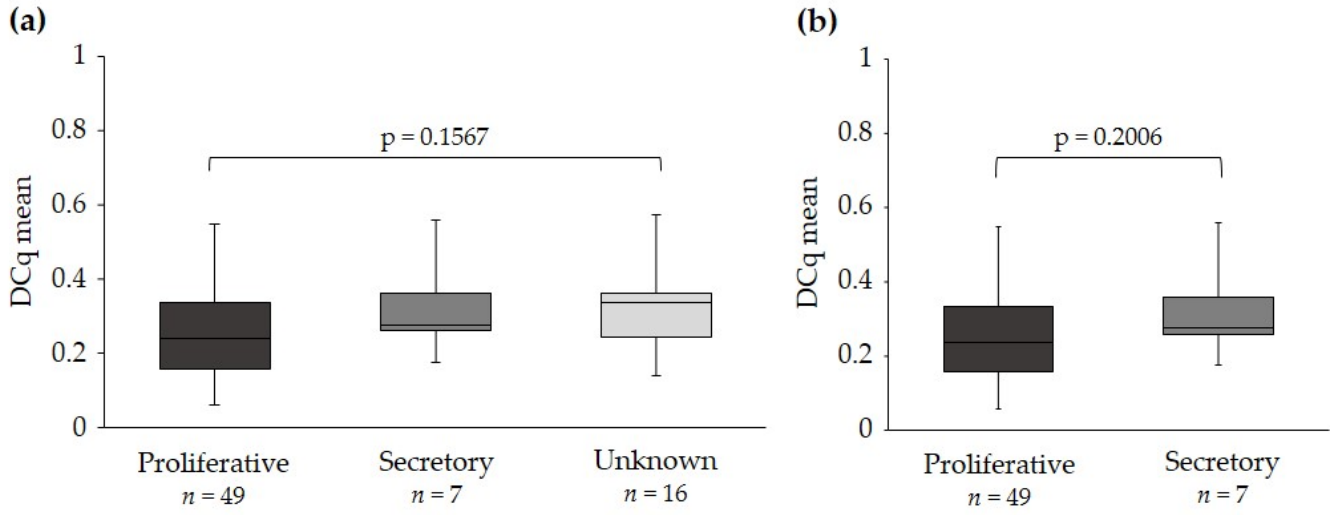


Figure A1. miR-30c-5p levels during phases of the menstrual cycle in healthy women. (**a**) Ordinary one-way ANOVA test to analyze miR-30c-5p levels in different phases of menstrual cycle in healthy women (control group), including subjects whose menstrual cycle phase was unknown at the time of sample collection. (**b**) Comparison of miR-30c-5p by Student's *t*-test between the proliferative and secretory phases of menstrual cycle. Box plots were used to represent miR-30c-5p levels after normalization with reference miRNAs. Data were plotted showing median and interquartile range. Results were considered statistically significant when $p < 0.05$. n indicates the number of individuals analyzed. DCq indicates miRNA Cq values normalized to the mean Cq values of reference miRNAs.

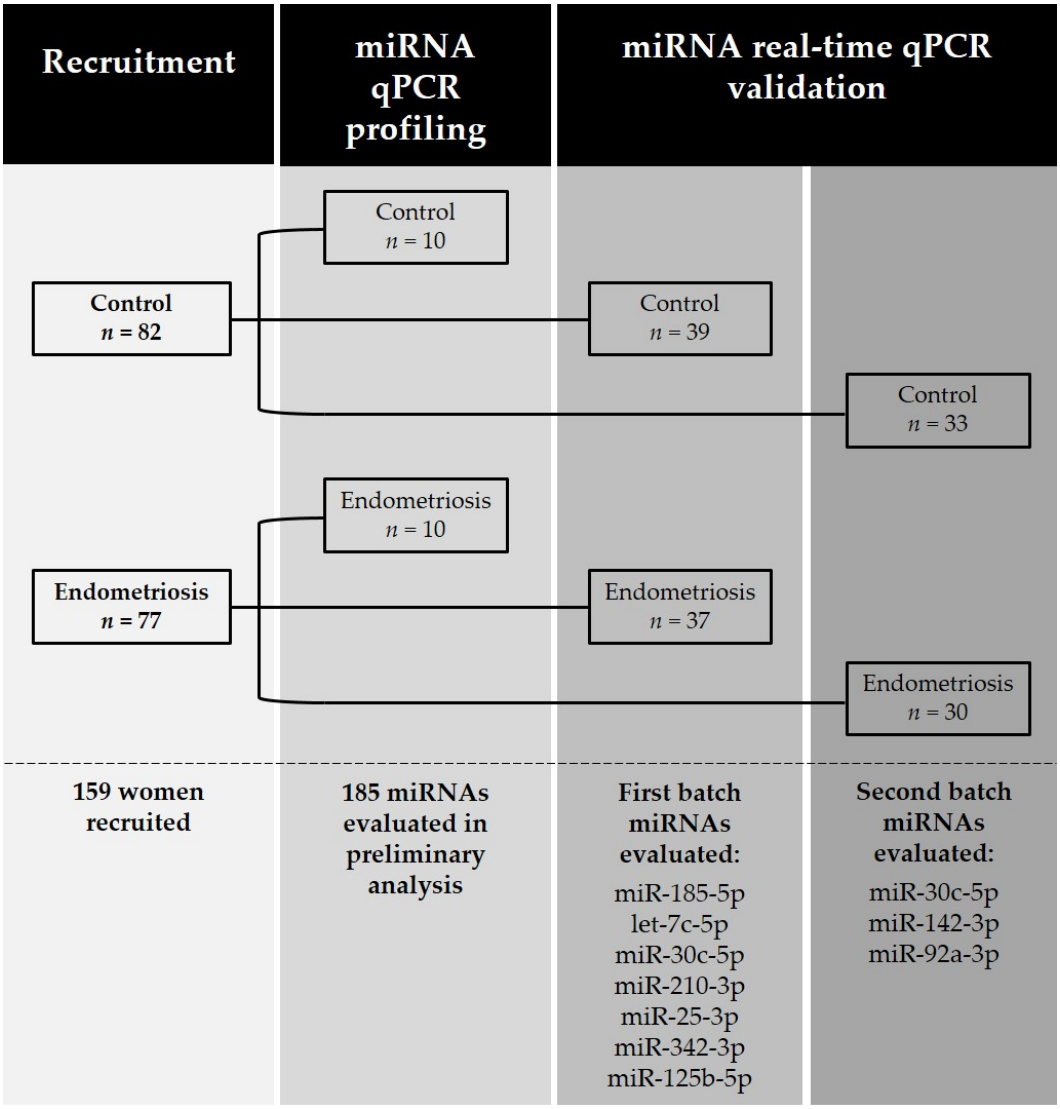


Figure A2. Diagram of the study design. Flow charts are shown for the endometriosis and control groups during recruitment, miRNA qPCR profiling and miRNA validation by qPCR. The sample size (n) analyzed in each phase of the study is specified.

Table A1. Sequence of the primers used for the validation study of miRNA candidates for endometriosis biomarkers in serum, miRNA candidates for endogenous and miRNA used for the technical control of hemolysis.

miRNA ID	Sequence (5′ > 3′)
miR-185-5p	UGGAGAGAAAGGCAGUUCCUGA
let-7c-5p	UGAGGUAGUAGGUUGUAUGGUU
miR-30c-5p	UGUAAACAUCCUACACUCUCAGC
miR-210-3p	CUGUGCGUGUGACAGCGGCUGA
miR-25-3p	CAUUGCACUUGUCUCGGUCUGA
miR-342-3p	UCUCACACAGAAAUCGCACCCGU
miR-125b-5p	UCCCUGAGACCCUAACUUGUGA
miR-142-3p	UGUAGUGUUUCCUACUUUAUGGA
miR-92a-3p	UAUUGCACUUGUCCCGGCCUGU
miR-30e-5p	UGUAAACAUCCUUGACUGGAAG
miR-15b-5p	UAGCAGCACAUCAUGGUUUACA
miR-451a	AAACCGUUACCAUUACUGAGUU
miR-23a-3p	AUCACAUUGCCAGGGAUUUCC

References

1. Saunders, P.T.; Horne, A.W. Endometriosis: Etiology, pathobiology, and therapeutic prospects. *Cell* **2021**, *184*, 2807–2824. [CrossRef] [PubMed]
2. Lamceva, J.; Uljanovs, R.; Strumfa, I. The main theories on the pathogenesis of endometriosis. *Int. J. Mol. Sci.* **2023**, *24*, 4254. [CrossRef]
3. Burney, R.O.; Giudice, L.C. Pathogenesis and pathophysiology of endometriosis. *Fertil. Steril.* **2012**, *98*, 511–519. [CrossRef]
4. Gruber, T.M.; Mechsner, S. Pathogenesis of endometriosis: The origin of pain and subfertility. *Cells* **2021**, *10*, 1381. [CrossRef] [PubMed]
5. Mahini, S.M.; Mortazavi, G.; Samare-Najaf, M.; Azadbakht, M.K.; Jamali, N. Non-invasive diagnosis of endometriosis: Immunologic and genetic markers. *Clin. Chim. Acta* **2022**, *538*, 70–86. [CrossRef] [PubMed]
6. Fassbender, A.; Vodolazkaia, A.; Saunders, P.; Lebovic, D.; Waelkens, E.; De Moor, B.; D'Hooghe, T. Biomarkers of endometriosis. *Fertil. Steril.* **2013**, *99*, 1135–1145. [CrossRef]
7. Mol, B.W.; Bayram, N.; Lijmer, J.G.; Wiegerinck, M.A.; Bongers, M.Y.; Van Der Veen, F.; Bossuyt, P.M. The performance of CA-125 measurement in the detection of endometriosis: A meta-analysis. *Fertil. Steril.* **1998**, *70*, 1101–1108. [CrossRef]
8. May, K.; Conduit-Hulbert, S.; Villar, J.; Kirtley, S.; Kennedy, S.; Becker, C. Peripheral biomarkers of endometriosis: A systematic review. *Hum. Reprod. Update* **2010**, *16*, 651–674. [CrossRef]
9. Kafali, H.; Artuc, H.; Demir, N. Use of CA125 fluctuation during the menstrual cycle as a tool in the clinical diagnosis of endometriosis; a preliminary report. *Eur. J. Obstet. Gynecol. Reprod. Biol.* **2004**, *116*, 85–88. [CrossRef]
10. Hanke, M.; Hoefig, K.; Merz, H.; Feller, A.C.; Kausch, I.; Jocham, D.; Warnecke, J.M.; Sczakiel, G. A robust methodology to study urine microRNA as tumor marker: microRNA-126 and microRNA-182 are related to urinary bladder cancer. *Urol. Oncol. Semin. Orig. Investig.* **2010**, *28*, 655–661. [CrossRef]
11. Mitchell, P.S.; Parkin, R.K.; Kroh, E.M.; Fritz, B.R.; Wyman, S.K.; Pogosova-Agadjanyan, E.L.; Peterson, A.; Noteboom, J.; O'Briant, K.C.; Allen, A. Circulating microRNAs as stable blood-based markers for cancer detection. *Proc. Natl. Acad. Sci. USA* **2008**, *105*, 10513–10518. [CrossRef]
12. Park, N.J.; Zhou, H.; Elashoff, D.; Henson, B.S.; Kastratovic, D.A.; Abemayor, E.; Wong, D.T. Salivary microRNA: Discovery, Characterization, and Clinical Utility for Oral Cancer DetectionSalivary microRNA. *Clin. Cancer Res.* **2009**, *15*, 5473–5477. [CrossRef]
13. von Grothusen, C.; Frisendahl, C.; Modhukur, V.; Lalitkumar, P.G.; Peters, M.; Faridani, O.R.; Salumets, A.; Boggavarapu, N.R.; Gemzell-Danielsson, K. Uterine fluid microRNAs are dysregulated in women with recurrent implantation failure. *Hum. Reprod.* **2022**, *37*, 734–746. [CrossRef]
14. Cheng, L.; Sharples, R.A.; Scicluna, B.J.; Hill, A.F. Exosomes provide a protective and enriched source of miRNA for biomarker profiling compared to intracellular and cell-free blood. *J. Extracell. Vesicles* **2014**, *3*, 23743. [CrossRef]
15. Bartel, D.P. MicroRNAs: Genomics, biogenesis, mechanism, and function. *Cell* **2004**, *116*, 281–297. [CrossRef]
16. Bushati, N.; Cohen, S.M. microRNA functions. *Annu. Rev. Cell Dev. Biol.* **2007**, *23*, 175–205. [CrossRef]
17. Li, J.; Smyth, P.; Flavin, R.; Cahill, S.; Denning, K.; Aherne, S.; Guenther, S.M.; O'Leary, J.J.; Sheils, O. Comparison of miRNA expression patterns using total RNA extracted from matched samples of formalin-fixed paraffin-embedded (FFPE) cells and snap frozen cells. *BMC Biotechnol.* **2007**, *7*, 36. [CrossRef] [PubMed]
18. Asakura, K.; Kadota, T.; Matsuzaki, J.; Yoshida, Y.; Yamamoto, Y.; Nakagawa, K.; Takizawa, S.; Aoki, Y.; Nakamura, E.; Miura, J. A miRNA-based diagnostic model predicts resectable lung cancer in humans with high accuracy. *Commun. Biol.* **2020**, *3*, 134. [CrossRef] [PubMed]
19. Cho, W.C.; Wong, C.F.; Li, K.P.; Fong, A.H.; Fung, K.Y.; Au, J.S. miR-145 as a Potential Biomarker and Therapeutic Target in Patients with Non-Small Cell Lung Cancer. *Int. J. Mol. Sci.* **2023**, *24*, 10022. [CrossRef] [PubMed]
20. Dar, G.M.; Agarwal, S.; Kumar, A.; Sharma, A.K.; Verma, R.; Sattar, R.S.A.; Ahmad, E.; Ali, A.; Mahajan, B.; Saluja, S.S. A non-invasive miRNA-based approach in early diagnosis and therapeutics of oral cancer. *Crit. Rev. Oncol./Hematol.* **2022**, *180*, 103850. [CrossRef] [PubMed]
21. Doghish, A.S.; Moustafa, H.A.M.; Elballal, M.S.; Sallam, A.-A.M.; El-Dakroury, W.A.; Mageed, S.S.A.; Elesawy, A.E.; Abdelmaksoud, N.M.; Shahin, R.K.; Midan, H.M. The potential role of miRNAs in the pathogenesis of testicular germ cell tumors-A Focus on signaling pathways interplay. *Pathol.-Res. Pract.* **2023**, *248*, 154611. [CrossRef]
22. Cheng, Y.-F.; Gu, X.-J.; Yang, T.-M.; Wei, Q.-Q.; Cao, B.; Zhang, Y.; Shang, H.-F.; Chen, Y.-P. Signature of miRNAs derived from the circulating exosomes of patients with amyotrophic lateral sclerosis. *Front. Aging Neurosci.* **2023**, *15*, 1106497. [CrossRef] [PubMed]
23. Lee, M.; Woo, J.; Kim, S.T.; Moon, M.; Kim, S.Y.; Cho, H.; Kim, S.; Kim, H.-K.; Park, J.-Y. MicroRNA super-resolution imaging in blood for Alzheimer's disease. *BMB Rep.* **2023**, *56*, 190–195. [CrossRef] [PubMed]
24. Zou, Y.F.; Wen, D.; Zhao, Q.; Shen, P.Y.; Shi, H.; Zhao, Q.; Chen, Y.X.; Zhang, W. Urinary MicroRNA-30c-5p and MicroRNA-192-5p as potential biomarkers of ischemia-reperfusion-induced kidney injury. *Exp. Biol. Med.* **2017**, *242*, 657–667. [CrossRef] [PubMed]
25. Benito, B.; García-Elías, A.; Ois, Á.; Tajes, M.; Vallès, E.; Ble, M.; Bisbe, L.Y.; Giralt-Steinhauer, E.; Rodríguez-Campello, A.; Capdevila, M.C. Plasma levels of miRNA-1-3p are associated with subclinical atrial fibrillation in patients with cryptogenic stroke. *Rev. Española De Cardiol. (Engl. Ed.)* **2022**, *75*, 717–726. [CrossRef] [PubMed]

26. Düzgün, Z.; Kayikçioğlu, L.M.; Aktan, Ç.; Bara, B.; Eroğlu, F.Z.; Yağmur, B.; Çetintaş, V.B.; Bayindir, M.; Nalbantgil, S.; Vardarli, A.T. Decreased circulating microRNA-21 and microRNA-143 are associated to pulmonary hypertension. *Turk. J. Med. Sci.* **2023**, *53*, 130–141. [CrossRef] [PubMed]
27. Huang, S.; Zhang, J.; Wan, H.; Wang, K.; Wu, J.; Cao, Y.; Hu, L.; Yu, Y.; Sun, H.; Yu, Y. Plasma extracellular vesicles microRNA-208b-3p and microRNA-143-3p as novel biomarkers for sudden cardiac death prediction in acute coronary syndrome. *Mol. Omics* **2023**, *19*, 262–273. [CrossRef] [PubMed]
28. Dabi, Y.; Suisse, S.; Puchar, A.; Delbos, L.; Poilblanc, M.; Descamps, P.; Haury, J.; Golfier, F.; Jornea, L.; Bouteiller, D. Endometriosis-associated infertility diagnosis based on saliva microRNA signatures. *Reprod. BioMed. Online* **2023**, *46*, 138–149. [CrossRef]
29. Cho, S.; Mutlu, L.; Grechukhina, O.; Taylor, H.S. Circulating microRNAs as potential biomarkers for endometriosis. *Fertil. Steril.* **2015**, *103*, 1252–1260.e1. [CrossRef]
30. Maged, A.M.; Deeb, W.S.; El Amir, A.; Zaki, S.S.; El Sawah, H.; Al Mohamady, M.; Metwally, A.A.; Katta, M.A. Diagnostic accuracy of serum miR-122 and miR-199a in women with endometriosis. *Int. J. Gynaecol. Obs.* **2018**, *141*, 14–19. [CrossRef]
31. Moustafa, S.; Burn, M.; Mamillapalli, R.; Nematian, S.; Flores, V.; Taylor, H.S. Accurate diagnosis of endometriosis using serum microRNAs. *Am. J. Obs. Gynecol.* **2020**, *223*, 557.e1–557.e11. [CrossRef]
32. Bashti, O.; Noruzinia, M.; Garshasbi, M.; Abtahi, M. miR-31 and miR-145 as Potential Non-Invasive Regulatory Biomarkers in Patients with Endometriosis. *Cell J.* **2018**, *20*, 84–89. [CrossRef]
33. Papari, E.; Noruzinia, M.; Kashani, L.; Foster, W.G. Identification of candidate microRNA markers of endometriosis with the use of next-generation sequencing and quantitative real-time polymerase chain reaction. *Fertil. Steril.* **2020**, *113*, 1232–1241. [CrossRef]
34. Braicu, O.-L.; Budisan, L.; Buiga, R.; Jurj, A.; Achimas-Cadariu, P.; Pop, L.A.; Braicu, C.; Irimie, A.; Berindan-Neagoe, I. miRNA expression profiling in formalin-fixed paraffin-embedded endometriosis and ovarian cancer samples. *OncoTargets Ther.* **2017**, *10*, 4225–4238. [CrossRef]
35. Ohlsson Teague, E.M.C.; Van der Hoek, K.H.; Van der Hoek, M.B.; Perry, N.; Wagaarachchi, P.; Robertson, S.A.; Print, C.G.; Hull, L.M. MicroRNA-regulated pathways associated with endometriosis. *Mol. Endocrinol.* **2009**, *23*, 265–275. [CrossRef]
36. Pan, Q.; Luo, X.; Toloubeydokhti, T.; Chegini, N. The expression profile of micro-RNA in endometrium and endometriosis and the influence of ovarian steroids on their expression. *Mol. Hum. Reprod.* **2007**, *13*, 797–806. [CrossRef]
37. Bayraktar, R.; Van Roosbroeck, K.; Calin, G.A. Cell-to-cell communication: microRNAs as hormones. *Mol. Oncol.* **2017**, *11*, 1673–1686. [CrossRef] [PubMed]
38. Thomou, T.; Mori, M.A.; Dreyfuss, J.M.; Konishi, M.; Sakaguchi, M.; Wolfrum, C.; Rao, T.N.; Winnay, J.N.; Garcia-Martin, R.; Grinspoon, S.K.; et al. Adipose-derived circulating miRNAs regulate gene expression in other tissues. *Nature* **2017**, *542*, 450–455. [CrossRef] [PubMed]
39. Nisenblat, V.; Bossuyt, P.M.; Shaikh, R.; Farquhar, C.; Jordan, V.; Scheffers, C.S.; Mol, B.W.J.; Johnson, N.; Hull, M.L.; Gynaecology, C.; et al. Blood biomarkers for the non-invasive diagnosis of endometriosis. *Cochrane Database Syst. Rev.* **1996**, *2006*, 5. [CrossRef] [PubMed]
40. Leonova, A.; Turpin, V.E.; Agarwal, S.K.; Leonardi, M.; Foster, W.G. A critical appraisal of the circulating levels of differentially expressed microRNA in endometriosisdagger. *Biol. Reprod.* **2021**, *105*, 1075–1085. [CrossRef] [PubMed]
41. Blondal, T.; Jensby Nielsen, S.; Baker, A.; Andreasen, D.; Mouritzen, P.; Wrang Teilum, M.; Dahlsveen, I.K. Assessing sample and miRNA profile quality in serum and plasma or other biofluids. *Methods* **2013**, *59*, S1–S6. [CrossRef]
42. Misir, S.; Hepokur, C.; Oksasoglu, B.; Yildiz, C.; Yanik, A.; Aliyazicioglu, Y.; Reproduction, H. Circulating serum miR-200c and miR-34a-5p as diagnostic biomarkers for endometriosis. *J. Gynecol. Obstet. Hum. Reprod.* **2021**, *50*, 102092. [CrossRef] [PubMed]
43. Zafari, N.; Tarafdari, A.M.; Izadi, P.; Noruzinia, M.; Yekaninejad, M.S.; Bahramy, A.; Mohebalian, A. A panel of plasma miRNAs 199b-3p, 224–225p and Let-7d-3p as non-invasive diagnostic biomarkers for endometriosis. *Reprod. Sci.* **2021**, *28*, 991–999. [CrossRef] [PubMed]
44. Mestdagh, P.; Van Vlierberghe, P.; De Weer, A.; Muth, D.; Westermann, F.; Speleman, F.; Vandesompele, J. A novel and universal method for microRNA RT-qPCR data normalization. *Genome Biol.* **2009**, *10*, R64. [CrossRef] [PubMed]
45. Wang, F.; Wang, H.; Jin, D.; Zhang, Y. Serum miR-17, IL-4, and IL-6 levels for diagnosis of endometriosis. *Medicine* **2018**, *97*, e10853. [CrossRef] [PubMed]
46. Wang, L.; Huang, W.; Ren, C.; Zhao, M.; Jiang, X.; Fang, X.; Xia, X. Analysis of Serum microRNA Profile by Solexa Sequencing in Women With Endometriosis. *Reprod. Sci.* **2016**, *23*, 1359–1370. [CrossRef] [PubMed]
47. Wang, W.T.; Zhao, Y.N.; Han, B.W.; Hong, S.J.; Chen, Y.Q. Circulating microRNAs identified in a genome-wide serum microRNA expression analysis as noninvasive biomarkers for endometriosis. *J. Clin. Endocrinol. Metab.* **2013**, *98*, 281–289. [CrossRef] [PubMed]
48. Schmittgen, T.D.; Livak, K.J. Analyzing real-time PCR data by the comparative C(T) method. *Nat. Protoc.* **2008**, *3*, 1101–1108. [CrossRef] [PubMed]
49. McGrath, I.M.; Montgomery, G.W.; Mortlock, S. Insights from Mendelian randomization and genetic correlation analyses into the relationship between endometriosis and its comorbidities. *Hum. Reprod. Update* **2023**, *29*, 655–674. [CrossRef]
50. Brosens, I. Diagnosis of endometriosis. *Semin. Reprod. Endocrinol.* **1997**, *15*, 229–233. [CrossRef]
51. McDonald, J.S.; Milosevic, D.; Reddi, H.V.; Grebe, S.K.; Algeciras-Schimnich, A. Analysis of circulating microRNA: Preanalytical and analytical challenges. *Clin. Chem.* **2011**, *57*, 833–840. [CrossRef] [PubMed]

52. Kroh, E.M.; Parkin, R.K.; Mitchell, P.S.; Tewari, M. Analysis of circulating microRNA biomarkers in plasma and serum using quantitative reverse transcription-PCR (qRT-PCR). *Methods* **2010**, *50*, 298–301. [CrossRef]
53. Kang, K.; Peng, X.; Luo, J.; Gou, D. Identification of circulating miRNA biomarkers based on global quantitative real-time PCR profiling. *J. Anim. Sci. Biotechnol.* **2012**, *3*, 4. [CrossRef] [PubMed]
54. Faraldi, M.; Gomarasca, M.; Sansoni, V.; Perego, S.; Banfi, G.; Lombardi, G. Normalization strategies differently affect circulating miRNA profile associated with the training status. *Sci. Rep.* **2019**, *9*, 1584. [CrossRef] [PubMed]
55. Bustin, S.A.; Benes, V.; Garson, J.A.; Hellemans, J.; Huggett, J.; Kubista, M.; Mueller, R.; Nolan, T.; Pfaffl, M.W.; Shipley, G.L.; et al. The MIQE guidelines: Minimum information for publication of quantitative real-time PCR experiments. *Clin. Chem.* **2009**, *55*, 611–622. [CrossRef]
56. Cosar, E.; Mamillapalli, R.; Ersoy, G.S.; Cho, S.; Seifer, B.; Taylor, H.S. Serum microRNAs as diagnostic markers of endometriosis: A comprehensive array-based analysis. *Fertil. Steril.* **2016**, *106*, 402–409. [CrossRef]
57. Nothnick, W.B.; Falcone, T.; Joshi, N.; Fazleabas, A.T.; Graham, A. Serum miR-451a Levels Are Significantly Elevated in Women With Endometriosis and Recapitulated in Baboons (*Papio anubis*) with Experimentally-Induced Disease. *Reprod. Sci.* **2017**, *24*, 1195–1202. [CrossRef]
58. Zhang, L.; Li, H.; Yuan, M.; Li, D.; Sun, C.; Wang, G. Serum exosomal microRNAs as potential circulating biomarkers for endometriosis. *Dis. Markers* **2020**, *2020*, 2456340. [CrossRef]
59. Qi, R.; Weiland, M.; Gao, X.-H.; Zhou, L.; Mi, Q.-S. Identification of endogenous normalizers for serum microRNAs by microarray profiling: U6 small nuclear RNA is not a reliable normalizer. *Hepatology* **2012**, *55*, 1640–1642. [CrossRef]
60. Wang, K.; Yuan, Y.; Cho, J.-H.; McClarty, S.; Baxter, D.; Galas, D.J. Comparing the MicroRNA spectrum between serum and plasma. *PLoS ONE* **2012**, *7*, e41561. [CrossRef]
61. Rekker, K.; Saare, M.; Roost, A.M.; Kaart, T.; Soritsa, D.; Karro, H.; Soritsa, A.; Simon, C.; Salumets, A.; Peters, M. Circulating miR-200-family micro-RNAs have altered plasma levels in patients with endometriosis and vary with blood collection time. *Fertil. Steril.* **2015**, *104*, 938–946.e2. [CrossRef]
62. Vanhie, A.; O, D.; Peterse, D.; Beckers, A.; Cuellar, A.; Fassbender, A.; Meuleman, C.; Mestdagh, P.; D'Hooghe, T. Plasma miRNAs as biomarkers for endometriosis. *Hum. Reprod.* **2019**, *34*, 1650–1660. [CrossRef]
63. Zhang, M.; Wang, X.; Xia, X.; Fang, X.; Zhang, T.; Huang, F. Endometrial epithelial cells-derived exosomes deliver microRNA-30c to block the BCL9/Wnt/CD44 signaling and inhibit cell invasion and migration in ovarian endometriosis. *Cell Death Discov.* **2022**, *8*, 151. [CrossRef]
64. Chen, X.; Jiang, Y.; Pan, D. miR-30c may serve a role in endometriosis by targeting plasminogen activator inhibitor-1. *Exp. Ther. Med.* **2017**, *14*, 4846–4852. [CrossRef]
65. Budak, H.; Bulut, R.; Kantar, M.; Alptekin, B. MicroRNA nomenclature and the need for a revised naming prescription. *Brief. Funct. Genom.* **2016**, *15*, 65–71. [CrossRef]
66. Desvignes, T.; Batzel, P.; Berezikov, E.; Eilbeck, K.; Eppig, J.T.; McAndrews, M.S.; Singer, A.; Postlethwait, J.H. miRNA nomenclature: A view incorporating genetic origins, biosynthetic pathways, and sequence variants. *Trends Genet.* **2015**, *31*, 613–626. [CrossRef] [PubMed]
67. Schmittgen, T.D.; Lee, E.J.; Jiang, J.; Sarkar, A.; Yang, L.; Elton, T.S.; Chen, C. Real-time PCR quantification of precursor and mature microRNA. *Methods* **2008**, *44*, 31–38. [CrossRef]
68. Razi, M.H.; Eftekhar, M.; Ghasemi, N.; Sheikhha, M.H.; Firoozabadi, A.D. Expression levels of circulatory mir-185-5p, vascular endothelial growth factor, and platelet-derived growth factor target genes in endometriosis. *Int. J. Reprod. Biomed. (IJRM)* **2020**, *18*, 347. [CrossRef]
69. Abo, C.; Biquard, L.; Girardet, L.; Chouzenoux, S.; Just, P.-A.; Chapron, C.; Vaiman, D.; Borghese, B. Unbiased In Silico Analysis of Gene Expression Pinpoints Circulating miRNAs Targeting KIAA1324, a New Gene Drastically Downregulated in Ovarian Endometriosis. *Biomedicines* **2022**, *10*, 2065. [CrossRef] [PubMed]
70. Bahramy, A.; Zafari, N.; Izadi, P.; Soleymani, F.; Kavousi, S.; Noruzinia, M. The role of miRNAs 340-5p, 92a-3p, and 381-3p in patients with endometriosis: A plasma and mesenchymal stem-like cell study. *BioMed Res. Int.* **2021**, *2021*, 5298006. [CrossRef] [PubMed]
71. Braza-Boïls, A.; Salloum-Asfar, S.; Marí-Alexandre, J.; Arroyo, A.B.; González-Conejero, R.; Barceló-Molina, M.; García-Oms, J.; Vicente, V.; Estellés, A.; Gilabert-Estellés, J.; et al. Peritoneal fluid modifies the microRNA expression profile in endometrial and endometriotic cells from women with endometriosis. *Hum. Reprod.* **2015**, *30*, 2292–2302. [CrossRef]
72. Börschel, C.S.; Stejskalova, A.; Schäfer, S.D.; Kiesel, L.; Götte, M. miR-142-3p reduces the size, migration, and contractility of endometrial and endometriotic stromal cells by targeting integrin-and Rho GTPase-related pathways that regulate cytoskeletal function. *Biomedicines* **2020**, *8*, 291. [CrossRef]
73. Ma, L.; Li, Z.; Li, W.; Ai, J.; Chen, X. MicroRNA-142-3p suppresses endometriosis by regulating KLF9-mediated autophagy *in vitro* and *in vivo*. *RNA Biol.* **2019**, *16*, 1733–1748. [CrossRef]
74. Zhu, J.; Xu, Z.; Wu, P.; Zeng, C.; Peng, C.; Zhou, Y.; Xue, Q.J.R.S. MicroRNA-92a-3p Inhibits Cell Proliferation and Invasion by Regulating the Transcription Factor 21/Steroidogenic Factor 1 Axis in Endometriosis. *Reprod. Sci.* **2023**, *30*, 2188–2197. [CrossRef] [PubMed]
75. Byon, J.C.; Papayannopoulou, T. MicroRNAs: Allies or Foes in erythropoiesis? *J. Cell. Physiol.* **2012**, *227*, 7–13. [CrossRef]

76. Masaki, S.; Ohtsuka, R.; Abe, Y.; Muta, K.; Umemura, T. Expression patterns of microRNAs 155 and 451 during normal human erythropoiesis. *Biochem. Biophys. Res. Commun.* **2007**, *364*, 509–514. [CrossRef] [PubMed]
77. Rasmussen, K.D.; O'Carroll, D. The Journal of the American Society of Hematology. The miR-144/451eGFP allele, a novel tool for resolving the erythroid potential of hematopoietic precursors. *Blood* **2011**, *118*, 2988–2992. [CrossRef]
78. Rasmussen, K.D.; Simmini, S.; Abreu-Goodger, C.; Bartonicek, N.; Di Giacomo, M.; Bilbao-Cortes, D.; Horos, R.; Von Lindern, M.; Enright, A.J.; O'Carroll, D. The miR-144/451 locus is required for erythroid homeostasis. *J. Exp. Med.* **2010**, *207*, 1351–1358. [CrossRef]
79. Zhan, M.; Miller, C.P.; Papayannopoulou, T.; Stamatoyannopoulos, G.; Song, C.-Z. MicroRNA expression dynamics during murine and human erythroid differentiation. *Exp. Hematol.* **2007**, *35*, 1015–1025. [CrossRef] [PubMed]
80. Bruchova, H.; Yoon, D.; Agarwal, A.M.; Mendell, J.; Prchal, J.T. Regulated expression of microRNAs in normal and polycythemia vera erythropoiesis. *Exp. Hematol.* **2007**, *35*, 1657–1667. [CrossRef]
81. Leecharoenkiat, K.; Tanaka, Y.; Harada, Y.; Chaichompoo, P.; Sarakul, O.; Abe, Y.; Smith, D.R.; Fucharoen, S.; Svasti, S.; Umemura, T. Plasma microRNA-451 as a novel hemolytic marker for β0-thalassemia/HbE disease. *Mol. Med. Rep.* **2017**, *15*, 2495–2502. [CrossRef]
82. Svasti, S.; Masaki, S.; Penglong, T.; Abe, Y.; Winichagoon, P.; Fucharoen, S.; Umemura, T. Expression of microRNA-451 in normal and thalassemic erythropoiesis. *Ann. Hematol.* **2010**, *89*, 953–958. [CrossRef] [PubMed]
83. Kirschner, M.B.; Edelman, J.J.B.; Kao, S.C.-H.; Vallely, M.P.; van Zandwijk, N.; Reid, G. The impact of hemolysis on cell-free microRNA biomarkers. *Front. Genet.* **2013**, *4*, 94. [CrossRef]
84. Pritchard, C.C.; Kroh, E.; Wood, B.; Arroyo, J.D.; Dougherty, K.J.; Miyaji, M.M.; Tait, J.F.; Tewari, M. Blood cell origin of circulating microRNAs: A cautionary note for cancer biomarker studies. *Cancer Prev. Res.* **2012**, *5*, 492–497. [CrossRef] [PubMed]
85. Shah, J.S.; Soon, P.S.; Marsh, D.J. Comparison of methodologies to detect low levels of hemolysis in serum for accurate assessment of serum microRNAs. *PLoS ONE* **2016**, *11*, e0153200. [CrossRef]
86. Simundic, A.-M.; Bölenius, K.; Cadamuro, J.; Church, S.; Cornes, M.P.; van Dongen-Lases, E.C.; Eker, P.; Erdeljanovic, T.; Grankvist, K.; Guimaraes, J.T.; et al. Joint EFLM-COLABIOCLI Recommendation for venous blood sampling: V 1.1, June 2018. *Clin. Chem. Lab. Med.* **2018**, *56*, 2015–2038. [CrossRef]
87. Lippi, G.; Von Meyer, A.; Cadamuro, J.; Simundic, A.-M. Blood sample quality. *Diagnosis* **2019**, *6*, 25–31. [CrossRef] [PubMed]
88. Gu, C.-L.; Zhang, Z.; Fan, W.-S.; Li, L.-A.; Ye, M.-X.; Zhang, Q.; Zhang, N.-N.; Li, Z.; Meng, Y.-G. Identification of MicroRNAs as potential biomarkers in ovarian endometriosis. *Reprod. Sci.* **2020**, *27*, 1715–1723. [CrossRef]
89. He, Z.; Tian, M.; Fu, X. Reduced expression of miR-30c-5p promotes hepatocellular carcinoma progression by targeting RAB32. *Mol. Ther. Nucleic Acids* **2021**, *26*, 603–612. [CrossRef]
90. Mehterov, N.; Vladimirov, B.; Sacconi, A.; Pulito, C.; Rucinski, M.; Blandino, G.; Sarafian, V. Salivary miR-30c-5p as Potential Biomarker for Detection of Oral Squamous Cell Carcinoma. *Biomedicines* **2021**, *9*, 1079. [CrossRef]
91. Cao, J.-M.; Li, G.-Z.; Han, M.; Xu, H.-L.; Huang, K.-M. MiR-30c-5p suppresses migration, invasion and epithelial to mesenchymal transition of gastric cancer via targeting MTA1. *Biomed. Pharmacother.* **2017**, *93*, 554–560. [CrossRef] [PubMed]
92. Zheng, T.; Zhou, Y.; Xu, X.; Qi, X.; Liu, J.; Pu, Y.; Zhang, S.; Gao, X.; Luo, X.; Li, M.; et al. MiR-30c-5p loss-induced PELI1 accumulation regulates cell proliferation and migration via activating PI3K/AKT pathway in papillary thyroid carcinoma. *J. Transl. Med.* **2022**, *20*, 20. [CrossRef] [PubMed]
93. Hao, Y.; Zhu, Y.; Sun, F.; Xu, D.; Wang, C. MicroRNA-30c-5p arrests bladder cancer G2/M phase and suppresses its progression by targeting PRC1-mediated blocking of CDK1/Cyclin B1 axis. *Cell. Signal.* **2023**, *110*, 110836. [CrossRef] [PubMed]
94. Pollacco, J.; Sacco, K.; Portelli, M.; Schembri-Wismayer, P.; Calleja-Agius, J. Molecular links between endometriosis and cancer. *Gynecol. Endocrinol.* **2012**, *28*, 577–581. [CrossRef] [PubMed]
95. Mogensen, J.B.; Kjær, S.K.; Mellemkjær, L.; Jensen, A. Endometriosis and risks for ovarian, endometrial and breast cancers: A nationwide cohort study. *Gynecol. Oncol.* **2016**, *143*, 87–92. [CrossRef] [PubMed]
96. Wang, D.; Wang, X.; Qiu, L.-W.; Peng, C.; Zhong, S.-P.; Ye, L. MicroRNA-30c inhibits metastasis of ovarian cancer by targeting metastasis-associated gene 1. *J. Cancer Res. Ther.* **2017**, *13*, 676–682. [CrossRef]
97. Pei, B.; Li, T.; Qian, Q.; Fan, W.; He, X.; Zhu, Y.; Xu, L. Downregulation of microRNA-30c-5p was responsible for cell migration and tumor metastasis via COTL1-mediated microfilament arrangement in breast cancer. *Gland. Surg.* **2020**, *9*, 747–758. [CrossRef]
98. Blagih, J.; Buck, M.D.; Vousden, K.H. p53, cancer and the immune response. *J. Cell Sci.* **2020**, *133*, jcs237453. [CrossRef]
99. Goh, A.M.; Coffill, C.R.; Lane, D.P. The role of mutant p53 in human cancer. *J. Pathol.* **2011**, *223*, 116–126. [CrossRef]
100. Lin, S.; Yu, L.; Song, X.; Bi, J.; Jiang, L.; Wang, Y.; He, M.; Xiao, Q.; Sun, M.; Olopade, O.I.; et al. Intrinsic adriamycin resistance in p53-mutated breast cancer is related to the miR-30c/FANCF/REV1-mediated DNA damage response. *Cell Death Dis.* **2019**, *10*, 666. [CrossRef]
101. Hu, S.; Zhang, J.; Fang, X.; Guo, G.; Dai, J.; Sheng, Z.; Li, D.; Chen, J.; Zhang, L.; Liu, C.; et al. Identification of microRNA hsa-miR-30c-5p as an inhibitory factor in the progression of hepatocellular carcinoma and investigation of its regulatory network via comprehensive analysis. *Bioengineered* **2021**, *12*, 7154–7166. [CrossRef] [PubMed]
102. Yuan, L.-Q.; Zhang, T.; Xu, L.; Han, H.; Liu, S.-H. miR-30c-5p inhibits glioma proliferation and invasion via targeting Bcl2. *Transl. Cancer Res.* **2021**, *10*, 337–348. [CrossRef] [PubMed]
103. Zhong, Z.; Xia, Y.; Wang, P.; Liu, B.; Chen, Y. Low expression of microRNA-30c promotes invasion by inducing epithelial mesenchymal transition in non-small cell lung cancer. *Mol. Med. Rep.* **2014**, *10*, 2575–2579. [CrossRef] [PubMed]

104. Bashir, S.T.; Redden, C.R.; Raj, K.; Arcanjo, R.B.; Stasiak, S.; Li, Q.; Steelman, A.J.; Nowak, R.A. Endometriosis leads to central nervous system-wide glial activation in a mouse model of endometriosis. *J. Neuroinflamm.* **2023**, *20*, 59. [CrossRef] [PubMed]
105. Castro, J.; Maddern, J.; Erickson, A.; Harrington, A.M.; Brierley, S.M. Peripheral and central neuroplasticity in a mouse model of endometriosis. *J. Neurochem.* **2023**. [CrossRef] [PubMed]
106. Coxon, L.; Wiech, K.; Vincent, K. Is There a Neuropathic-Like Component to Endometriosis-Associated Pain? Results From a Large Cohort Questionnaire Study. *Front. Pain Res.* **2021**, *2*, 743812. [CrossRef] [PubMed]
107. Taylor, H.S.; Kotlyar, A.M.; A Flores, V. Endometriosis is a chronic systemic disease: Clinical challenges and novel innovations. *Lancet* **2021**, *397*, 839–852. [CrossRef]
108. Ding, S.; Guo, X.; Zhu, L.; Wang, J.; Li, T.; Yu, Q.; Zhang, X. Macrophage-derived netrin-1 contributes to endometriosis- associated pain. *Ann. Transl. Med.* **2021**, *9*, 29. [CrossRef]
109. Ding, S.; Yu, Q.; Wang, J.; Zhu, L.; Li, T.; Guo, X.; Zhang, X. Activation of ATF3/AP-1 signaling pathway is required for P2X3-induced endometriosis pain. *Hum. Reprod.* **2020**, *35*, 1130–1144. [CrossRef]
110. Liu, Z.; Chen, S.; Qiu, C.; Sun, Y.; Li, W.; Jiang, J.; Zhang, J.-M. Fractalkine/CX3CR1 Contributes to Fractalkine/CX3CR1 contributes to endometriosis-induced neuropathic pain and mechanical hypersensitivity in rats. *Front. Cell. Neurosci.* **2018**, *12*, 495. [CrossRef]
111. Tang, Y.; Chen, Y.; Liu, R.; Li, W.; Hua, B.; Bao, Y. Wnt signaling pathways: A role in pain processing. *NeuroMol. Med.* **2022**, *24*, 233–249. [CrossRef]
112. Wang, S.; Duan, H.; Li, B.; Hong, W.; Li, X.; Wang, Y.; Guo, Z.C. BDNF and TrKB expression levels in patients with endometriosis and their associations with dysmenorrhoea. *J. Ovarian Res.* **2022**, *15*, 35. [CrossRef]
113. Dwiningsih, S.R.; Meilani, C.; Hadi, S. Brain Derived Neurotrophic Factor as a Non-invasive Biomarker for Detection of Endometriosis. *J. Reprod. Infertil.* **2022**, *23*, 207–212. [CrossRef]
114. Francés, R.; Mata-Garrido, J.; de la Fuente, R.; Carcelén, M.; Lafarga, M.; Berciano, M.T.; García, R.; Hurlé, M.A.; Tramullas, M. Identification of epigenetic interactions between MicroRNA-30c-5p and DNA methyltransferases in neuropathic pain. *Int. J. Mol. Sci.* **2022**, *23*, 13994. [CrossRef]
115. Tramullas, M.; Francés, R.; de la Fuente, R.; Velategui, S.; Carcelén, M.; García, R.; Llorca, J.; Hurlé, M.A. MicroRNA-30c-5p modulates neuropathic pain in rodents. *Sci. Transl. Med.* **2018**, *10*, eaao6299. [CrossRef]
116. Soni, U.K.; Chadchan, S.B.; Kumar, V.; Ubba, V.; Khan, M.T.A.; Vinod, B.S.V.; Konwar, R.; Bora, H.K.; Rath, S.K.; Sharma, S.; et al. A high level of TGF-B1 promotes endometriosis development via cell migration, adhesiveness, colonization, and invasiveness†. *Biol. Reprod.* **2019**, *100*, 917–938. [CrossRef] [PubMed]
117. Andersen, C.L.; Jensen, J.L.; Ørntoft, T.F. Normalization of real-time quantitative reverse transcription-PCR data: A model-based variance estimation approach to identify genes suited for normalization, applied to bladder and colon cancer data sets. *Cancer Res.* **2004**, *64*, 5245–5250. [CrossRef] [PubMed]
118. Chen, Y.; Wang, X. miRDB: An online database for prediction of functional microRNA targets. *Nucleic Acids Res.* **2019**, *48*, D127–D131. [CrossRef] [PubMed]
119. Liu, W.; Wang, X. Prediction of functional microRNA targets by integrative modeling of microRNA binding and target expression data. *Genome Biol.* **2019**, *20*, 18. [CrossRef] [PubMed]
120. Ge, S.X.; Jung, D.; Yao, R. ShinyGO: A graphical gene-set enrichment tool for animals and plants. *Bioinformatics* **2019**, *36*, 2628–2629. [CrossRef] [PubMed]

Disclaimer/Publisher's Note: The statements, opinions and data contained in all publications are solely those of the individual author(s) and contributor(s) and not of MDPI and/or the editor(s). MDPI and/or the editor(s) disclaim responsibility for any injury to people or property resulting from any ideas, methods, instructions or products referred to in the content.

International Journal of
Molecular Sciences

MDPI

Review

MicroRNAs as Biomarkers and Therapeutic Targets in Female Infertility

Lucía Chico-Sordo [1] and Juan A. García-Velasco [1,2,3,*]

[1] IVIRMA Global Research Alliance, IVI Foundation, Instituto de Investigación Sanitaria La Fe (IIS La Fe), 46026 Valencia, Spain; lucia.chico@ivirma.com
[2] IVIRMA Global Research Alliance, IVIRMA Madrid, 28023 Madrid, Spain
[3] School of Health Sciences, Medical Specialties and Public Health, Obstetrics and Gynecology Area, Rey Juan Carlos University Alcorcón, 28922 Madrid, Spain
* Correspondence: juan.garcia.velasco@ivirma.com

Abstract: The study of microRNAs (miRNAs) has emerged in recent decades as a key approach to understanding the pathophysiology of many diseases, exploring their potential role as biomarkers, and testing their use as future treatments. Not only have neurological, cardiovascular diseases, or cancer benefited from this research but also infertility. Female infertility, as a disease, involves alterations at multiple levels, such as ovarian and uterine alterations. This review compiles the latest studies published in humans that link female disorders that affect fertility with altered miRNA profiles. Studies on ovarian alterations, including diminished ovarian reserve (DOR), poor ovarian response to stimulation (POR), premature ovarian insufficiency (POI), and polycystic ovary syndrome (PCOS), are summarized and classified based on the expression and type of sample analyzed. Regarding uterine disorders, this review highlights upregulated and downregulated miRNAs primarily identified as biomarkers for endometriosis, adenomyosis, decreased endometrial receptivity, and implantation failure. However, despite the large number of studies in this field, the same limitations that reduce reproducibility are often observed. Therefore, at the end of this review, the main limitations of this type of study are described, as well as specific precautions or safety measures that should be considered when handling miRNAs.

Keywords: infertility; microRNA; ovarian alterations; uterine disorders

check for updates

Citation: Chico-Sordo, L.; García-Velasco, J.A. MicroRNAs as Biomarkers and Therapeutic Targets in Female Infertility. *Int. J. Mol. Sci.* **2024**, *25*, 12979. https://doi.org/10.3390/ijms252312979

Academic Editor: Giovanni Tossetta

Received: 14 November 2024
Revised: 1 December 2024
Accepted: 1 December 2024
Published: 3 December 2024

Copyright: © 2024 by the authors. Licensee MDPI, Basel, Switzerland. This article is an open access article distributed under the terms and conditions of the Creative Commons Attribution (CC BY) license (https://creativecommons.org/licenses/by/4.0/).

1. Introduction

Infertility is defined as the inability to achieve pregnancy after having regular unprotected sexual intercourse for 1 year. This condition affects millions worldwide, with a lifetime prevalence of 17.5% and 12.6% during the 12 months [1]. The origin of infertility can be in both male and female factors, with approximately 50% of the cases attributed to men [2]. Congenital bilateral absence of the vas deferens associated with mutations of the cystic fibrosis gene is one of the primary genetic origins [3], followed by varicocele as an acquired factor [4], and in another percentage of cases, the origin remains unknown. Focusing on women, infertility can be associated with endocrine [5], ovarian, or uterine alterations. However, in many cases, as in men, it is not possible to determine the infertility origin. Ultimately, conception and pregnancy take place in the woman, and disturbances at any of these levels may result in failure of conception or even miscarriage.

In many instances, assisted reproductive technologies (ARTs) are used to overcome infertility and conceive [6,7]. Establishing an accurate early diagnosis is crucial during this process. The origin of infertility and the available treatments will determine the prognosis when the infertility diagnosis is determined. For this reason, much of the research efforts in the field of ARTs are focused on (1) facilitating and accelerating the diagnosis of infertility, (2) providing a realistic prognosis, and (3) developing new therapies for this condition. In recent years, miRNAs have become promising molecules that could help achieve any

of the above mentioned objectives. Although this field of study is still in its very early stages, several researchers have explored the potential of miRNAs from different diseases or conditions. Given the invasiveness of diagnostic techniques, such as laparoscopy [8] or hysterectomy [9], used in women, many studies analyzing the role of miRNAs at the reproductive level focus on women, hence this literature review. However, despite a large number of published researches, specific considerations and precautions must be considered when dealing with miRNAs.

This literature review article summarizes the published preliminary studies in humans that postulate miRNAs as tools for the diagnosis, prognosis, and treatment of female reproductive disorders.

2. microRNAs

2.1. Identification and Biogenesis

Although not translated into proteins, some RNA molecules are functional and called non-coding RNA (ncRNA) [10]. These types of RNAs are classified according to their size. If it is more significant than 200 nucleotides, they are considered long non-coding RNAs (lncRNAs), while if it is smaller, they are classified as small non-coding RNAs (sncRNAs). Multiple types of sncRNAs exist as miRNAs or Piwi-interacting RNAs (piRNAs) [11]. Still, this review will focus on miRNAs because they are widely conserved molecules across species, and a single miRNA can exert its regulation on many different targets. They are RNA molecules of approximately 22 nucleotides that play a crucial role in regulating gene expression at the post-transcriptional level [12]. Its discovery dates back to 1993 in the organism *Caenorhabditis elegans* (*C. elegans*), when Lee et al. [13] demonstrated the existence of the *LIN-4* gene, which, after transcription, did not code for a protein but gave rise to two small RNA molecules. These small RNAs were complementary to the *LIN-14* gene mRNA in the 3′ untranslated region (UTR), and as a result of the interaction, a decrease in Lin-14 protein levels was observed [14]. Years later, Reinhart et al. (2000) [15], working on the same model organism, would reach the same conclusion by discovering a new *lethal-7* (*LET-7*) gene that showed a similar pattern.

Currently, multiple miRNAs have been identified, and their processing has been described in detail [16–18]. Although there are different post-transcriptional processing pathways, the majority of conserved miRNAs in all vertebrates originate from the canonical pathway explained below (Figure 1a) [19]. In general terms, RNA polymerase II (Pol II) transcribes the miRNA genes, generating a primary miRNA transcript (pri-miRNA) in the cell nucleus [20]. This pri-miRNA varies in size from hundreds of nucleotides to tens of kilobases and forms a stem-loop structure in which a hairpin and a base can be distinguished. The pri-miRNA is characterized by being polyadenylated and capped, and it can be spliced [21]. In the nucleus, it will undergo an initial processing by which the base part is cleaved, leaving only the hairpin miRNA precursor (pre-miRNA) of about 70 nucleotides. The machinery in charge of this first step in miRNA processing is the microprocessor complex formed by the RNase III enzyme Drosha and the double-stranded RNA-binding protein DiGeorge syndrome critical region gene 8 (DGCR8) [22]. Then, thanks to Exportin-5 [23–25], the pre-miRNAs will be transferred to the cell cytoplasm, where the next Dicer-mediated processing step will occur. Dicer is an RNase III enzyme that, after association with double-stranded RNA (dsRNA)-binding proteins, will cleave the stem-loop terminal region of pre-miRNA, generating a miRNA duplex. This duplex consists of a double strand of approximately 22 nucleotides. The dsRNA-binding proteins in human cells can be PKR activator protein (PACT) or transactivation response RNA-binding protein (TRBP) [26]. From the generated duplex, one of the strands will be bound to argonaute proteins (Ago) [27], the RNA-induced silencing complex (RISC) will be formed, and the other strand will be degraded [28].

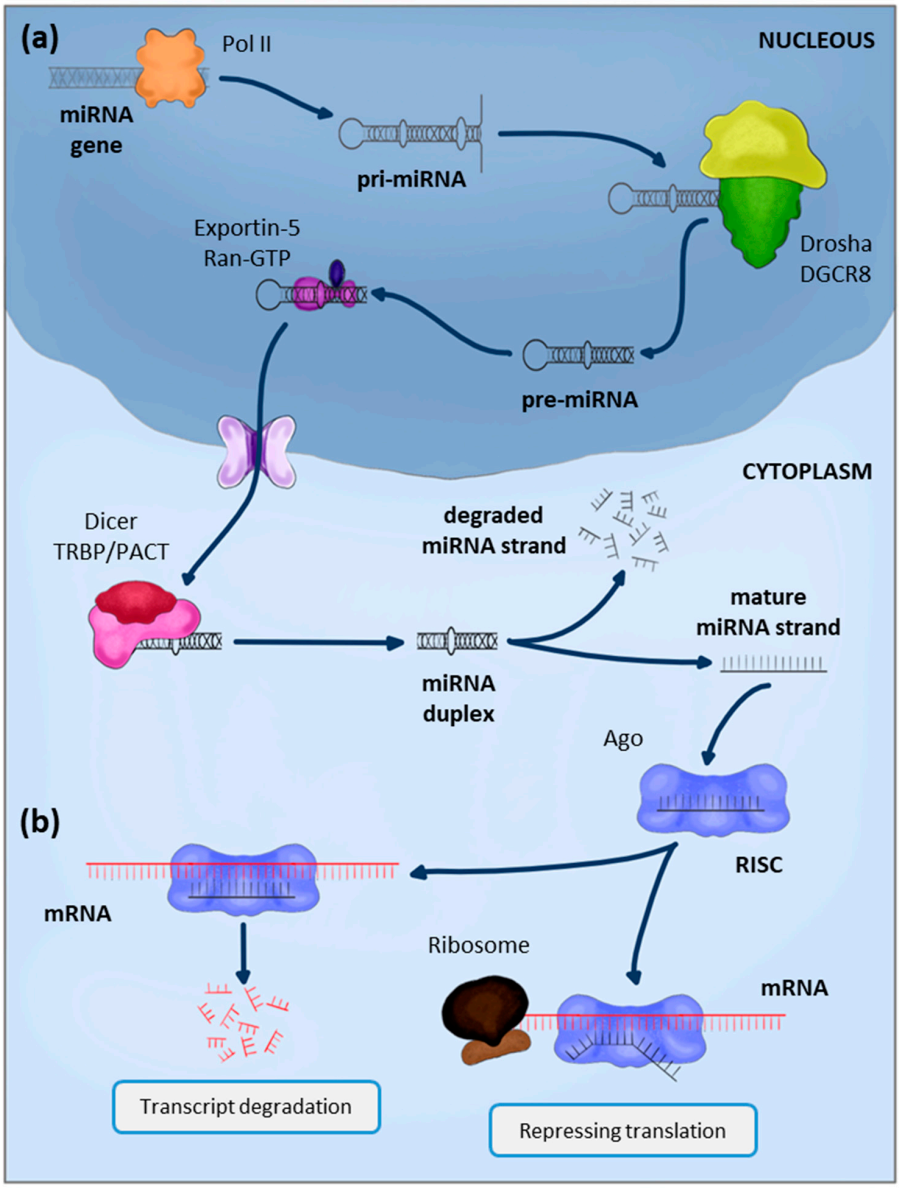


Figure 1. Biogenesis of miRNAs and their regulatory function of gene expression. (**a**) miRNAs obtention and maturation process. In the canonical pathway, RNA-polymerase II transcribes the miRNA gene; the initial transcript generated is called pri-miRNA. Then, thanks to the type III ribonuclease activity of Drosha, the double-stranded RNA will be recognized and removed from the poly-A tail, giving rise to the pre-miRNA. This pre-miRNA is exported from the cell nucleus to the cytoplasm bound to Exportin-5 via the RanGTP/RanGDP transport system. Once in the cytoplasm, another type III ribonuclease, Dicer, cleaves the stem-loop-terminal region and generates a double-stranded miRNA. One of the two strands that form the mature miRNA will be degraded (called the passenger strand) by the argonaute protein with endonuclease activity or RNases present in the cytoplasm. The other strand of the miRNA will remain bound to the argonaute protein to perform its function. (**b**) Gene silencing. Post-transcriptional regulation of the expression of different genes can occur in two ways. (**Left**) When the complementarity of bases between the miRNA and the target mRNA is total, the argonaute protein itself, with its endonuclease activity, will destroy the miRNA. (**Right**) However, if this complementarity is not total, the RISC complex will remain and impede the progress of the translation process.

By the process detailed above, canonical miRNAs are obtained. However, it is important to note the existence of miRNA isoforms called isomiRs. These small RNA molecules

differ from the canonical miRNAs in length, sequence, or both and sometimes even have a different function [29,30]. Their synthesis takes place using the same process as canonical miRNA synthesis. Alterations in the process, such as imprecise Drosha or Dicer excision, addition or deletion of nucleotides at the 5′ or 3′ ends, or inclusion of single nucleotide polymorphisms (SNPs), are the specific origin of isomiRs [31]. Therefore, their presence should be taken into account in studies on miRNAs as they may be missed in miRNA detection and expression methods [32].

2.2. Role in Biological Processes

The early findings about miRNAs mainly were attributed to the organism *C. elegans*, and these findings were further supported by research on the regulatory function of these molecules in *Drosophila* [33,34]. The primary function of miRNAs is to regulate gene expression by post-transcriptional gene silencing acting on messenger RNA (mRNA) [35,36]. Specifically, this is the process of RNA interference, a biological mechanism mainly mediated by small RNA molecules such as miRNAs and small interfering RNAs (siRNAs). For miRNA-mediated interference to occur, the miRNA, as a part of the RISC complex, must travel to its target mRNA and, through base complementarity, carry out its function (Figure 1b). Two regions are essential for the miRNA binding to target mRNA: the miRNA seed region and the 3′-UTR region of the mRNA. The miRNA seed region is between nucleotides 2 and 8 of the miRNA 5′ end [37]. The 3′-UTR region is an untranslated region of the mRNA localized at the 3′ end, also called the trailer sequence [38]. Total or partial base complementarity between the miRNA seed region and 3′-UTR mRNA can be used to characterize the phenomenon as translational repression or mRNA degradation [39,40]. In the first case, the direct and immediate degradation of mRNA will be induced and performed by Ago endonuclease activity [41,42]. If the base complementarity is partial, translation inhibition will be indirect since the RISC complex will stay attached to the mRNA, forming a spatial barrier that will stop the translation machinery from progressing [43].

Mature miRNAs mostly work in the cytoplasm of cells. However, recent studies have shown that these molecules can also act at the nuclear level [44]. Although the negative regulation of complementary target mRNAs is the main function at the cytosolic level, there are several ways in which this regulation can be executed at the nuclear level. Among these new approaches to miRNA-mediated regulation are the interaction between miRNAs and other ncRNAs as circular RNAs (circRNAs) [45,46] and the silencing of genes coding for proteins involved in the maturation process of the miRNAs themselves [47] or even indirectly involved in epigenetic modifications [48].

2.3. miRNA Availability

As explained above, miRNAs are synthesized in the cell nucleus and exported to the cytoplasm to complete their maturation process. Once the miRNAs have matured, they will mainly exert their function in the cytoplasm. However, it is important to mention that many miRNAs migrate out of the cell, having an important role as chemical messengers [49,50]. As a consequence of this migration, it is possible to identify miRNAs in body fluids such as blood [51], urine [52], saliva [53], follicular fluid [54], seminal fluid [55], and breast milk [56], among others. Furthermore, it has been observed that despite their ribonucleic acid nature, they are characterized by high stability in biofluids [57]. The reason is that miRNAs are not released in isolation; instead, they move and form vesicles or ribonucleoprotein complexes. Thanks to these bindings, the RNases present in biofluids cannot degrade them. Specifically, 90% of circulating miRNAs are bound to proteins such as AGO2 [58], GW182 [59], and HDL [51], while the remaining 10% travel inside exosomes or microvesicles [57,60].

2.4. miRNAs as a New Approach in Diagnosis and Treatment

After the last few years of study on miRNAs, it has been confirmed that these molecules play a fundamental role in the appearance or progression of diseases. While providing information on the molecular processes mediated by miRNAs that may be altered in

different conditions, all these studies also represent a major advance for diagnosing and treating diseases. One of the most promising roles for miRNAs is their use as biomarkers. Different researchers have explored these molecules in cancer [61–64], immunological [65] and neurological disorders [66–68], or even cardiovascular diseases [69–71]. Recently, miRNAs have also been evaluated as hopeful therapies using an analog or mimic [72] and inhibitors or antagonists [73] of the miRNA in question.

3. miRNAs and Infertility

The World Health Organization (WHO) classifies infertility as a disease [74]. Therefore, like many other pathologies mentioned above, miRNAs can also play a role in the diagnosis and treatment of infertility. However, infertility is a complex condition that involves the interaction of biological [75–77], emotional [78,79], anatomical or physical [80–84], and social factors [85–87]. In addition, infertility can have its origin in either the man or the woman. Specifically, infertility in women can be due to ovulatory disorders and uterine alterations, among others, as hormonal problems. The vast majority of published research on miRNAs and female infertility works with ovarian and endometrial samples, subsequently analyzing whether the miRNA expression pattern found in that type of sample is reflected in biofluids such as blood. For this reason, the latest research on miRNAs related to ovarian and uterine disorders will be discussed below.

3.1. Ovarian Alterations

One of the causes of female infertility is ovarian insufficiency. This concept includes poor ovarian response, premature ovarian insufficiency (also called premature ovarian failure, POF), and advanced maternal age. All these are characterized by reduced ovarian reserve, but the boundaries between these concepts are poorly defined [88]. Consequently, in many cases, the diagnosis is not clear since clinical features may overlap. This problem is directly reflected in the studies that analyze the relationship between miRNAs and the different situations of ovarian failure.

The following is a summary of research that has looked into the function and potential of miRNAs in cases of POI, POR, and DOR. Furthermore, a detailed discussion of PCOS, another extremely common ovarian condition, will be provided. Table 1 summarizes the miRNAs found to be altered in each ovarian disorder analyzed. They are classified by color depending on the nature of the sample studied.

Table 1. miRNAs differentially expressed in ovarian disorders.

	DOR	POR	POI	PCOS	
Upregulated	miR-128-3p [89] miR-6881-3p [90] miR-484 [91] miR-4463 [92] miR-342-3p [93] miR-483-3p [93] miR-625-3p [93] * miR-28-3p [94] * miR-155-5p [94] miR-29a-5p [94]	* miR-23a [95] * miR-21-5p [96] miR-15a-5p [97]	* miR-23a [98] miR-27a [98]	miR-33b [99] miR-142 [99] miR-1298-5p [100] miR-212-3p [101] miR-490-5p [101] miR-4643 [101] miR-3131 [102] miR-206 [102] miR-204-5p [102] miR-100-5p [102] miR-193a-5p [102] miR-381-3p [103] miR-199b-5p [103] * miR-93 [104] -3p [103] miR-361-3p [103] miR-127-3p [103]	miR-1238-3p [103] miR-382-5p [103] miR-425-3p [103] * miR-222 [105] * miR-146a [105] -5p [106] miR-30c [105] * miR-21-5p [107] * miR-23a-3p [107] miR-26a-5p [107] * miR-223 [104] miR-126-3p [106] miR-151a-5p [108] miR-488 [108]

Table 1. *Cont.*

	DOR	POR	POI	PCOS	
Downregulated	miR-221-3p [109] miR-16-5p [89] * miR-106a [110] miR-122-5p [93] miR-1246 [93] miR-130b-3p [93] * miR-21-5p [94]		miR-22-3p [111]	miR-423 [99] miR-647 [101] miR-539-5p [102] miR-650 [103] miR-663b [103] * miR-155 [112] miR-103-3p [107,113] miR-376a-3p [107,113] miR-19b-3p [107]	* miR-222-3p [107] miR-139-5p [113] * miR-28-3p [113] miR-320 [114] miR-20b-5p [106] * miR-106a-5p [106] miR-18a-3p [106] * miR-223-3p [108]

* indicates miRNAs that have been reported to be differentially expressed in several studies, either for the same or different conditions. More information can be found in Section 3.1.5. Differentially expressed miRNAs in follicular cells such as GCs or CCs are shown in blue. Those studied in FF appear in green, while those detected in blood (serum or plasma) are red. The miRNAs that combine both colors indicate that they have been detected in these two types of samples. DOR: diminished ovarian reserve; POR: poor ovarian response; POI: premature ovarian insufficiency; PCOS: polycystic ovarian syndrome.

3.1.1. Diminished Ovarian Reserve

Currently, there is no single accepted definition for the term DOR [115]. At the clinical level, it is mainly defined as a reduction in ovarian follicle number, a low ovarian response to stimulation, and a poorer oocyte quality [88]. Therefore, one of the key concepts is ovarian reserve, which can be assessed by the antral follicle count (AFC) or anti-müllerian hormone (AMH) level [116,117]. In most studies that examined the expression of miRNAs in DOR cases, the AMH and AFC were shown to differ between the DOR group and the control group. However, these differences in ovarian reserve markers are accompanied by statistically significant differences in the mean age of the groups. Although the concept of DOR only refers to a woman's ovarian reserve, it is important to mention that it is a normal physiological process linked to age and is very common in women in their mid-40s. However, when it appears in young women, it is a pathological condition [115].

An analysis of miRNAs in this patient profile has been conducted to comprehend the pathophysiology and physiology of DOR. Granulosa cells (GCs) and cumulus cells (CCs), which are ovarian follicle cells, have been the primary subjects of this kind of study. The main reason is that the decrease in oocyte competence in women with DOR could originate from abnormal regulation by the cells accompanying the oocyte in the environment of the antral follicle. The miRNAs miR-221-3p, which targets the gene *FOXO1* [109], and miR-106a, whose target is *ASK1* [110], showed reduced levels in DOR patients. In both studies, alteration in these miRNAs led to increased GCs or CCs apoptosis. The study by Woo et al. [89] also evidenced lower levels of miR-16-5p, triggering an increase in *MAPK* and *WNT3*, promoting elevated cell proliferation, differentiation, and apoptosis. The same study demonstrated higher levels of miR-128-3p, causing a decrease in *TGFBR1*, an alteration previously observed in older women. Consequently, the DOR profile would be similar to older women's profiles. MiR-6881-3p [90] and miR-484 [91], also with higher expression in DOR women, caused decreases in *SMAD4* and *YAP1*, respectively, increasing the levels of apoptosis of GCs. However, not only has the miRNA profile been studied in cells directly related to folliculogenesis, but miRNAs have also been evaluated in follicular fluid (FF). Since one of the primary roles of exosomes is cell-to-cell communication, the amounts of various miRNAs found in FF exosomes have been specifically examined. Among the most recent studies, Shen et al. [93] found a lower expression of miR-122-5p, miR-1246, and miR-130b-3p. The miRNAs miR-342-3p, miR-483-3p, and miR-625-3p were the most abundant FF exosomes from DOR patients. The fact that there were no statistically significant variations in the mean age of the DOR groups and the control group with normal ovarian reserve is a good aspect of this study. This fact cannot be stated in another study, the one carried out by Xie et al. [94], where despite finding downregulated miR-21-5p and upregulated miR-28-3p, miR-155-5p, and miR-29a-5p, the mean age between the study groups was statistically significant.

Each of the aforementioned research studies, which sought to elucidate the role of miRNAs in the etiology of DOR, proposes miRNAs as potential biomarkers for this condition. miRNAs as biomarkers would be an additional parameter, which, together with AMH and AFC values, would allow professionals to narrow down and diagnose this condition accurately. However, specific studies have focused on analyzing female blood samples with DOR, searching for non-invasive or minimally invasive biomarker candidate miRNAs. MiR-106a [110] and miR-4463 [92], the first decreased and the second increased in DOR patients, have been tested simultaneously in serum and follicular cell samples. The research by Abu-Halima et al. [118] did not focus on circulating miRNAs in serum or plasma but instead profiled miRNAs present in blood cells from women with lower AMH, normal AMH, and higher AMH.

3.1.2. Poor Ovarian Response

POR refers to a low number of competent oocytes retrieved after ovarian stimulation. This type of response to ovarian stimulation is mainly associated with maternal age over 40 years; it is typical in women with a previous history of cycle cancellation due to a low number of oocytes retrieved and a DOR [119,120].

Compared to research about DOR, fewer publications examine the expression profile of miRNAs in women with POR. However, many of the studies performed in DOR are executed during in vitro fertilization (IVF) treatments after ovarian stimulation. Once stimulation has been performed and oocytes are collected, GCs, CCs, or FF obtained during oocyte pick-up are used for miRNA analysis. Therefore, ovarian stimulation can influence the miRNA signature, and considering that DOR and POR conditions often overlap, it is difficult to determine whether these types of studies are exclusive to women with a DOR profile. The studies on POR women have been performed with the same objective as studies on DOR: to analyze the role of miRNAs in the etiology of this condition. These investigations have also been conducted in GCs, where an increase in miR-23a was evidenced. This is linked to an elevation of apoptosis in GCs, which results in follicular atresia by inhibiting *SIRT1*. The increase in apoptosis was evidenced by elevated Caspase-3 [95]. In CCs, the miRNA that recorded elevated levels in POR women was miR-21-5p, demonstrating independence concerning low estradiol levels [96]. The study by Zhang et al. [97] focused on FF, differentiated between younger and older POR women, and only in the younger group were high levels of miR-15a-5p detected. This upregulated miRNA promoted cell apoptosis by reducing *BCL2* levels.

Although studies on miRNAs that may play a role in the cause of POR are promising, to date, none have been explored as a treatment or biomarker per se. Currently, the clinical approach to POR cases is focused on obtaining a greater number of competent oocytes. To this end, smaller follicles, whose oocytes may also have compromised nuclear competence, are often aspirated during oocyte collection. From the point of view of miRNAs, and for clinical reassurance, there were no significant differences in the miRNA signature associated with oocyte maturation (miR-451 and miR-574) in FF from both small and large follicles [121]. The study showed that this strategy versus the POR condition does not imply a lower nuclear competence of the oocyte aspirated from the smaller follicles.

3.1.3. Premature Ovarian Insufficiency

As previously described, a loss in ovarian function is typical of advanced maternal age. Still, when it occurs before the age of 40, it refers to the term POI, also known as POF [122]. Clinically, the diagnosis is made when a woman presents menstrual irregularities, an increase in follicle-stimulating hormone (FSH), and low-level estrogen [123]. This alteration is represented in approximately 1% of the female population [124]. The main consequence of this ovarian activity decline is infertility [125]. Nonetheless, there are other consequences that negatively impact women's health, usually associated with menopause. Osteoporosis [126], cardiovascular disease [127], and sexual dysfunction [128], all of them linked to a decrease in estrogen production, accompany the symptomatology of POI. In

addition, the consequences on the psychological well-being of these women, like emotional distress, are devastating [129–131].

Respecting the etiology of POI, genetic causes [132,133], immunological alterations [134,135], metabolic disorders [136], and environmental toxins [137] have been identified. The induced POI by different agents as chemotherapeutic in animal models has made it possible to profile the miRNAs involved in this condition [138–142]. However, human studies are very difficult to carry out because follicular aspiration is not performed in many of these women due to cycle cancellation. After the cancellation of oocyte retrieval, collecting FF, GC, or CC samples for research is impossible. For this reason, many of the studies about POI are performed on blood. Recent plasma studies have studied miRNAs and the role of other ncRNAs, such as circRNA. They act as "molecular sponges", binding to and absorbing miRNAs and indirectly controlling the expression and function of the target mRNA [143]. A lower expression in circRNA_008901 and circRNA_403959 was observed in POI patients, suggesting these as biomarkers for this condition [144]. Other studies, following a more traditional experimental design, have focused on the direct search for miRNAs with altered expression in the blood of women with POI. These investigations have evidenced the importance of downregulated miR-22-3p [111] or the overexpression of miR-23a and miR-27a in women suffering from this condition [98]. Thanks to these types of studies that have suggested potential miRNAs that could directly affect the cause of POI, it has been possible to transfer the investigations from blood samples to cell cultures. The group of Nie et al. (2015) [145], based on their previous studies from blood samples [98], transfected primary cultures of GCs obtained from patients undergoing IVF techniques with miR-23a and miR-27a. Overexpression of these miRNAs showed that their increase caused a decrease in *SMAD5*, promoting apoptosis in human GCs. Studies with established cell lines, such as KGN cells (human granulosa-like tumor cells), complement those carried out with primary cultures. Co-transfection of these cells with miR-146b-5p and the lncRNA DLEU1 showed that there is indeed an interaction between the two so that DLEU1 promotes cell apoptosis by reducing the inhibitory effect of miRNA on cell apoptosis [146]. Not only are granulosa cells the direct target of these studies, but the clinical complexity of POI cases has led to the exploration of other cell types, such as Th17 [147]. These cells are a type of lymphocytes that activate the immune system, causing inflammation, whose activation is mediated by miR-326. The results recorded an increase in this miRNA in Th17 cells from patients with POF.

Previously, clinical management of POI cases was often limited to oocyte donation to increase pregnancy success rates. However, many new clinical approaches and promising therapies are now being implemented in this patient profile [148]. These new therapies also represent a promising front of study for miRNAs; profiling the differentially expressed miRNAs in POI patients under these treatments could provide important information on their role in the POI origin.

3.1.4. Polycystic Ovarian Syndrome

PCOS affects 4–20% of pre-menopausal women worldwide and is characterized by ovarian dysfunction, polycystic ovaries, and hyperandrogenism. Women with PCOS have reduced fertility [149]. However, this syndrome also involves other alterations, especially at the endocrine and metabolic levels [150]. These characteristics and manifestations include hirsutism, acne, obesity, and insulin resistance [151]. This variety in the alterations associated with PCOS complicates the study of the miRNAs differentially expressed in these patients since there is significant heterogeneity between studies [152].

MiRNAs in women with this profile have been investigated in blood samples, FF, GCs, and CCs. In blood, published studies have measured miRNA levels in both serum and plasma. With respect to serum studies, miR-222, miR-146a, miR-30c [105], miR-21-5p, miR-23a-3p, and miR-26a-5p [107] were upregulated in PCOS women, whereas miR-155 [112], miR-103-3p [107,113], miR-376a-3p [107,113], miR-19b-3p, miR-222-3p [107],

miR-139-5p, miR-28-3p [113], and miR-320 [114] were downregulated. In plasma, miR-93, miR-223 [104], miR-126-3p, miR-146a-5p [106], miR-151a-5p, and miR-4488 [108] were identified with higher expression in women with PCOS, whereas the levels of miR-20b-5p, miR-106a-5p, miR-18a-3p [106], and miR-223-3p [108] were lower. Among the studies on the expression profile of miRNAs in the FF of PCOS women, miR-539-5p [102], miR-650, and miR-663b [103] evidenced downregulation. MiR-3131, miR-206, miR-204-5p, miR-100-5p, miR-193a-5p [102], miR-381-3p, miR-199b-5p, miR-93-3p, miR-361-3p, miR-127-3p, miR-1238-3p, miR-382-5p, and miR-425-3p [103] recorded elevated levels in PCOS patients. One of the studies worked with FF and CCs found in both types of samples, and the same miRNAs were increased (miR-212-3p, miR-490-5p, and miR-4643) and downregulated (miR-647) [101]. Regarding GCs, Li et al. (2019) [99] determined by quantitative polymerase chain reaction (qPCR) that miR-33b and miR-142 expression was upregulated, whereas miR-423 was downregulated. However, in the study by Xu et al. (2023) [100], they went a step further, and after showing an increase in miR-1298-5p in GCs from PCOS patients, they transferred their study to cultured COV343 human ovarian granulosa cells to analyze their molecular role in this condition.

Despite the large number of studies on miRNAs and PCOS, the conclusions gained are conditioned by certain inherent characteristics of this condition. For this reason, it is necessary to define the PCOS study population clearly.

3.1.5. Overlapping miRNAs in Ovarian Alterations

After the analysis of the different miRNAs with differential expression in each ovarian disorder exposed, it can be observed that many of them have been identified in different alterations or even multiple times in the same disorder. MiR-106a was identified by its low expression in both blood and follicular cells in women with DOR [110]; its expression was also lower in PCOS blood, although in the study, it was specified that the miRNA identified was miR-106a-5p [106]. Something similar occurred with miR-155 [112] and miR-28-3p [113] downregulated in blood from PCOS women and upregulated in follicular fluid from DOR [94], although specifically, the first one was miR-155-5p [94]. Another miRNA with differential expression between DOR and PCOS was miR-21-5p; this miRNA recorded low expression in the FF of DOR [94] and high expression in the blood of PCOS [107]. In addition, this miRNA was upregulated in follicular ovarian cells of POR women [96]. The miRNA miR-23a showed elevated levels in POR women (in follicular cells) [95] and in the blood of POI [98] and PCOS cases; in the latter, it was miR-23a-3p [107].

The results within the group of women with PCOS are highly controversial. MiR-222 [105] and miR-223 [104] were upregulated in blood samples, whereas the specific miRNAs miR-222-3p [107] and miR-223-3p [108] registered low levels in the blood of these patients. Finally, both miR-146a [105] and miR-93 [104] were notable for their higher expression in blood samples from women with PCOS, although in the first case, both miR-146a and miR-146a-5p [106] were detected, and in the second case, it was miR-93-3p [103] that was also upregulated in the follicular fluid from these patients.

3.2. Uterine Alterations

Like the ovary, the uterus is an organ of great importance for fertility in the female reproductive system. This organ is formed by three layers, which, from the inside to the outside, are the endometrium, myometrium, and serosa [153]. Specifically, the endometrium is the most important one since its thickness varies cyclically in response to sex hormones during the menstrual cycle. Because the embryo will implant in the endometrium and the pregnancy will continue, the primary function of this tissue is associated with pregnancy. As in other tissues, miRNAs also have a regulatory role [154,155]. The endometrial miRNA profile can vary depending on the menstrual cycle phase [156,157], endometrial receptivity for embryo implantation [158–160], or in situations of implantation failure [161–163]. In addition, this profile may be altered by disorders closely linked to fertility, such as endometriosis or adenomyosis [164]. The miRNAs that were discovered to be changed in

endometriosis and adenomyosis are listed in Table 2. Depending on the type of sample examined, the miRNAs are categorized by color.

Table 2. miRNAs differentially expressed in endometriosis and adenomyosis.

	Endometriosis		Adenomyosis
Upregulated	miR-30a [165] miR-93 [165] miR-325 [166] miR-492 [166] miR-520e [166] * miR-145 [167] miR-122 [168]	miR-199a [168] miR-125b-5p [169] miR-150-5p [169] miR-342-3p [169] miR-451a [169] * miR-30c-5p [170]	miR-17 [171] miR-191 [172] miR-181b [172] * miR-145 [173]
Downregulated	miR-143 [165] miR-203a-3p [166] miR-126-5p [174] miR-202-3p [175] miR-424-5p [175] miR-449b-3p [175] miR-556-3p [175] miR-199a-3p [176] miR-143-3p [176] miR-340-5p [176]	* let-7b [169,177] -5p [176] miR-21-5p [176] miR-103a-3p [176] * miR-17-5p [176,178] * miR-20a-5p [176,178] miR-22 [178] miR-31 [167] miR-135a [177] miR-3613-5p [169]	miR-10b [172] miR-200c [172] let-7a [179] * miR-30c-5p [180] miR-183 [181]

* indicates miRNAs that have been reported to be differentially expressed in several studies, either for the same or different conditions. Differentially expressed miRNAs in endometrial tissue are shown in grey. Those studied in blood (serum or plasma) appear in red.

3.2.1. Endometriosis

Endometriosis is a disease characterized by endometrial tissue outside the uterine cavity. It is an estrogen-dependent chronic inflammatory disease [182,183]. It is estimated that endometriosis affects 10% of women of reproductive age [184]. Its symptoms include pelvic pain, menstrual irregularities, heavy bleeding, and pain during urination and sexual intercourse [185]. However, the symptomatology is somewhat generic, resulting in a 6–10 year delay in diagnosis. The reference technique for diagnosing this condition is laparoscopy, characterized by high diagnostic sensitivity and specificity. Invasiveness and dependence on the surgeon's judgment for identifying lesions are intrinsic to this technique [186]. This is why multiple studies have been carried out to explore the capacity of miRNAs as diagnostic biomarkers of endometriosis [187].

Numerous studies have been aimed at finding differentially expressed miRNAs in endometriosis. The latest publications work with samples obtained non-invasively, such as saliva [188]. One of the most explored samples in endometriosis is blood, obtained through a minimally invasive process. Studies on blood plasma, such as that by Papari et al. (2020) [176], showed low levels of miR-199a-3p, miR-143-3p, miR-340-5p, let-7b-5p, miR-21-5p, miR-103a-3p, miR-17-5p, and miR-20a-5p. These last two miRNAs were also detected as downregulated in women with endometriosis in the study by Jia et al. (2013) along with miR-22 [178]. However, in both studies, no differences were established regarding the stage of endometriosis severity, while Bashti et al. (2018) considered this criterion [167]. Among the miRNAs the last study detected as differentially expressed in women with endometriosis, miR-31 stands out for its lower expression and miR-145 for its higher expression. In blood serum samples, miR-122, miR-199a [168], miR-125b-5p, miR-150-5p, miR-342-3p, miR-451a [169], and miR-30c-5p [170] registered higher levels in samples from women with endometriosis. On the contrary, miR-135a [177], miR-3613-5p [169], and let-7b [169,177] showed lower levels.

Studies carried out directly with endometrial tissue samples showed that the levels of the same miRNA can vary depending on the location of the endometrial tissue [165,174,189]. This implies the importance of the type of sample in which the analysis is performed, where even the peritoneal fluid from this patient profile is of interest [190,191]. Among

the miRNAs that have been detected with a higher expression in endometrial tissue from women with endometriosis, miR-30a, miR-93 [165], miR-325, miR-492, miR-520e [166] stand out, while miR-143 [165], miR-203a-3p [166], miR-126-5p [174], miR-202-3p, miR-424-5p, miR-449b-3p, and miR-556-3p [175] registered lower levels.

Endometriosis and cancer share molecular characteristics because the cells involved in both pathologies can evade the apoptosis process; they are characterized by high proliferation and angiogenic potential [192]. For this reason, studies that focus on miRNA expressed in endometriosis and compare this condition with reproductive cancer would allow us to understand the differential processes between both [174].

3.2.2. Adenomyosis

Adenomyosis is a benign uterine disorder characterized by the presence of ectopic endometrium in the myometrial tissue and an increase in uterine volume. Invasion of the endometrial glands and stroma into the adjacent myometrium causes hyperplasia of smooth muscle cells, leading to anatomical distortion of the uterine cavity, local inflammation, altered estrogen metabolism, and dysregulation of genes involved in maternal–embryonic crosstalk [193,194]. This condition is estimated to affect 20–30% of women of reproductive age [195], and the symptomatology is similar to endometriosis cases [196]. These percentages are based on diagnosis using transvaginal ultrasound and magnetic resonance imaging [197]. However, the image characteristics of adenomyosis can be confused with those of other uterine diseases such as endometriosis, as explained above, uterine leiomyoma, or endometrial polyps, making clinical diagnosis difficult. For this reason, the reference technique for the definitive diagnosis of adenomyosis requires histological analysis of the uterus after hysterectomy [198]. The invasive nature of this technique hinders and delays diagnosis. As a result, several research studies have concentrated on identifying the profile of miRNAs that are differently expressed in adenomyosis.

Unlike endometriosis, where the profile of differentially expressed miRNAs has been extensively studied in biofluids, in adenomyosis, the vast majority of studies were performed in endometrial samples. These studies showed the following miRNAs overexpressed in eutopic and/or ectopic endometrium from women with adenomyosis: miR-17 [171], miR-191, miR-181b [172], and miR-145 [173]. Among the differentially downregulated miRNAs expressed, miR-10b, miR-200c [172], let-7a [179], miR-30c-5p [199], and miR-183 [181] stood out. However, these miRNA expression levels can be altered after the application of a treatment, such as high-intensity focused ultrasound, as observed with miR-191-5p, whose levels decreased after treatment [200]. Other studies, such as Juarez-Barber et al. (2023) [201], instead of studying miRNAs in the entire endometrial tissue, have focused on the extracellular vesicles that secrete endometrial organoids from women with adenomyosis whose maintenance in vitro is possible.

3.2.3. Receptivity Status and Implantation Failure

Both endometriosis and adenomyosis have high rates of infertility among their patients, mainly due to anatomical abnormalities present in their uterus [202]. In cases where surgery is not very aggressive, removal of the lesions allows pregnancy [203]. However, some women who do not suffer from any of these pathologies or ovarian disorders also have infertility. This may be due to problems linked to endometrial receptivity and embryo implantation failures.

For embryo implantation to take place, the moment in which the blastocyst-stage embryo attaches to the mother's endometrium, it is necessary for the endometrium to be in the mid-secretory phase (days 20–24 of the menstrual cycle, approximately 6-10 days after ovulation). This crucial moment of the endometrium is known as the implantation window [204,205]. Once the blastocyst attaches to the luminal epithelium of the endometrium, it invades the epithelial cell layer to enter the stromal compartment, leaving the embryo completely covered by the luminal epithelium [206]. Endometrial receptivity can be predicted by transvaginal ultrasound and hormonal analysis [207]. However, establishing

the miRNA expression profile during the implantation window would allow us to narrow down this optimal period. Ideally, achieving this objective with blood samples would be relevant since the endometrium would remain intact. Chen et al. (2023) [158] developed a predictive model based on the miRNA expression profile in blood to determine the implantation window of the endometrium. Other studies have worked in parallel on the endometrium and blood samples, finding similarities between miRNAs with expression linked to greater receptivity between both samples. An increase in miR-31 [160] or a decrease in miR-455-3p and miR-4423-3p [159] have been associated with the endometrial phase of greatest receptivity. Studies such as Di Pietro et al. (2018) [208] or Zhou et al. (2024) [209] in patients with chronic endometritis who present receptivity problems have shown elevated levels of miR-27a-3p and miR-124-3p in both endometrial tissue samples and serum. However, recent studies suggest that not only do miRNAs regulate the expression of genes important in endometrial receptivity but that there is cooperation between miRNAs and different isomiRs [210–212].

Even when the endometrium is most receptive, implantation failure can occur. Finding a cause has been the primary goal of studies on miRNAs implicated in implantation failure [213]. For the most part, these types of studies have recruited women with recurrent implantation failure (RIF), characterized by repeated embryo transfers without pregnancy (more than two attempts). Studies with this patient profile have been carried out in blood, endometrial tissue biopsies, and extracellular vesicles extracted from the endometrium. Zeng et al. (2021) [214] showed elevated levels of miR-6767-5p, miR-149-5p, and miR-4433b-5p and lower expression of miR-4511, miR-124-3p, miR-146-3p, miR-150-5p, miR-150-3p, miR-342-3p, and miR-874-3p in blood plasma and exosomes from it in women with RIF. Regarding extracellular vesicles originating from endometrial tissue, studies showed that miR-6131, miR-1246, and miR-218-5p were upregulated in women with RIF [163]. Among the upregulated miRNAs in endometrial tissue biopsies, miR-665 [162], miR-940, miR-144-3p [161], and miR-152-3p [159] stood out, while miR-20b-5p and miR-330-5p [161] were downregulated. However, there are discrepancies in miR-155-5p; for example, in the study by Chen et al. (2021) [161], its increase was associated with RIF, while in the study by Drissennek et al. (2022) [159], its levels were lower in the patient's profile.

4. Challenges and Precautions in miRNA Work

As demonstrated throughout this review, miRNAs are of great importance not only for disorders related to fertility but also for many other pathologies. They have a crucial role in the pathophysiology of illnesses because they are determinants in gene silencing at the post-transcriptional level. Due to the increase or decrease in their levels associated with certain conditions, they could be biomarkers of these pathologies. The promise of miRNAs as future therapeutics was further explored by research demonstrating that their effects might be reversed by changing their levels, particularly through transfection experiments using mimics and inhibitors [215,216]. However, in many of the studies analyzed throughout this article, certain limitations have marked the potential of such studies. Therefore, some specific aspects must be considered in the study design to ensure robust results and less confusion due to avoidable biases.

4.1. Definition of Study Population

Given that infertility is associated with an increase in maternal age [217], recruitment in both groups must be age-matched if the research objective is focused on a reproductive outcome. In this way, there will be a guarantee that there are no statistically significant differences between the mean age in case and control groups. For example, the differences in AMH or AFC values between study groups were statistically significant in studies that refer to ovarian alterations. When checking the age of both groups, this variable was also different. Given that the AMH [218] value and the AFC [219,220] decrease as age increases, comparing two groups whose age variable differs between them could imply that the differences found are not due to the pathology but the aging process.

Similarly, the timing of the sample collection that will be studied during the research is crucial. Women have hormonal fluctuations throughout the menstrual cycle [221], and these changes directly affect the ovarian and uterine levels. Studies where sample collection is not unified, both in the ovary and the uterus, could lead to comparing different cycle phases and, thus, incorrect results. In those cases where sample collection is carried out throughout the fertility treatment, unifying the time of sample collection and the ovarian stimulation protocol is of great importance.

4.2. miRNA Techniques

Massive sequencing methods using Next-Generation Sequencing (NGS), microarray technology, and qPCR are the principal methods for studying miRNAs [222]. In the first and second cases, the costs are increased. Using NGS, it is possible to detect both the expression and sequence of all the miRNAs present in a sample. This technique requires the extraction of high-quality RNA and the preparation of miRNA libraries. Microarray technology is based on probes and is gradually being displaced by NGS. These two technologies are very useful in developing a large profile of the miRNAs differentially expressed between different groups. However, it is necessary to verify these results subsequently using qPCR [223], which is the gold standard to date. Given that many of the studies are based on techniques such as NGS and microarray, and later qPCR, it is important to divide the study population into two groups: the discovery population intended for these massive techniques and the subsequent validation population for qPCR. Both populations must comprise patients with the same profile but not the same subjects. This will guarantee that the results have been verified with two different techniques and allow the budget to be adjusted if the sample size of higher-cost techniques such as NGS or microarrays is reduced.

Regardless of the technique used, it is necessary to normalize the values obtained. Seyednasrollah et al. (2015) compared eight software packages and pipelines used in normalization for RNA sequencing and concluded that the tool used can affect the outcome of data analysis [224]. In the case of massive sequencing techniques, the decision will depend on the software incorporated into the technology used. However, in the case of qPCR, there is significant controversy among the studies since many use the U6 non-coding small nuclear RNA (RNU6). The use of this RNA as endogenous for cellular or tissue samples is widely accepted, although it does not have the exact nature and composition as a miRNA. But its use is not recommended when the type of study sample is blood, whether plasma or serum, and the objective is to analyze the expression of circulating miRNAs [225]. Given that RNU6 is part of the cell nuclear, its presence would indicate cell rupture in these cases. For this reason, it is suggested that during the initial screening techniques, NGS or microarray, miRNAs that do not show differential expression between the groups are also selected for subsequent use as endogenous miRNAs to perform normalization in the qPCR [226].

A final note regarding the use of blood samples, both plasma and serum, is the monitoring of hemolysis in the samples since it is a source of significant variability in the profile of expressed miRNAs [227]. This can be checked by measuring the absorbance of the sample at 414 nm, the absorbance of hemoglobin, or by calculating delta Cq [(miR-23a-3p)–(miR-451a)]. By assessing these two miRNAs, the level of hemolysis of the samples can be determined since the levels of miR-23a-3p are stable in serum and plasma and are not affected by hemolysis, and miR-451a is highly expressed in erythrocytes [228].

Another common mistake in working with miRNAs is failing to specify whether the differentially expressed miRNA is 5p or 3p [229]. During the maturation process of miRNAs, the passenger strand is degraded, leaving the functional one that will travel attached to the argonaute proteins to its target mRNA. Depending on the cell type or tissue, both strands may be functional or only one, and the target mRNAs may vary. For this reason, it is important to specify which strand is associated with the studied pathology.

4.3. miRNAs as Therapy

Once the alteration in the levels of a particular miRNA has been evident in a specific pathology and its effect on its target mRNA has been determined, it can be used as a biomarker of the disease. Subsequent studies with this miRNA will focus on the transfection of the interest cells with a mimic and/or inhibitor of that miRNA to explore its potential use as therapy [215,216]. In this type of study, it is necessary to consider two main aspects: (1) a miRNA can have multiple target genes and (2) preventing degradation of the miRNA until it reaches its target mRNA. Therefore, to reduce the effect of miRNAs on other tissues, the route of administration of miRNAs must be monitored for the use of therapies. If it does not work, try developing delivery or vehicle systems like viral vectors [217] or nanoparticles [203] that ensure the miRNA reaches the intended organ, which will prevent the breaking down in the blood and even reduce adverse immune reactions to miRNA.

5. Conclusions

Numerous studies have shown that miRNAs are crucial for post-transcriptional regulation, even if they do not code for proteins. Because of their ability to inhibit specific mRNA targets, they are molecules of tremendous interest for understanding pathophysiology and for usage as biomarkers or future treatments. Thanks to this scientific review article, we hope to provide clarity on the studies performed to date in women that relate miRNA profiles and reproductive alterations, thus establishing a solid foundation on which to build future research. In addition, conducting multiple meta-analyses on miRNAs and female infertility disorders could offer several benefits, such as helping to generalize the findings, increasing statistical power, identifying consistent patterns, improving reproducibility, reducing biases, and strengthening the conclusions.

Funding: This research received no external funding.

Conflicts of Interest: The authors declare no conflicts of interest.

References

1. Cox, C.; Thoma, M.; Tchangalova, N.; Mburu, G.; Bornstein, M.; Johnson, C.; Kiarie, J. Infertility prevalence and the methods of estimation from 1990 to 2021: A systematic review and meta-analysis. *Hum. Reprod. Open* **2022**, *2022*, hoac051. [CrossRef] [PubMed]
2. Agarwal, A.; Baskaran, S.; Parekh, N.; Cho, C.-L.; Henkel, R.; Vij, S.; Arafa, M.; Selvam, M.K.P.; Shah, R. Male infertility. *Lancet* **2021**, *397*, 319–333. [CrossRef] [PubMed]
3. Salonia, A.; Rastrelli, G.; Hackett, G.; Seminara, S.B.; Huhtaniemi, I.T.; Rey, R.A.; Hellstrom, W.J.; Palmert, M.R.; Corona, G.; Dohle, G.R.; et al. Paediatric and adult-onset male hypogonadism. *Nat. Rev. Dis. Prim.* **2019**, *5*, 38. [CrossRef] [PubMed]
4. Damsgaard, J.; Joensen, U.N.; Carlsen, E.; Erenpreiss, J.; Jensen, M.B.; Matulevicius, V.; Zilaitiene, B.; Olesen, I.A.; Perheentupa, A.; Punab, M.; et al. Varicocele is associated with impaired semen quality and reproductive hormone levels: A study of 7035 healthy young men from six European countries. *Eur. Urol.* **2016**, *70*, 1019–1029. [CrossRef]
5. Concepción-Zavaleta, M.J.; Coronado-Arroyo, J.C.; Quiroz-Aldave, J.E.; Durand-Vásquez, M.d.C.; Ildefonso-Najarro, S.P.; Rafael-Robles, L.d.P.; Concepción-Urteaga, L.A.; Gamarra-Osorio, E.R.; Suárez-Rojas, J.; Paz-Ibarra, J. Endocrine factors associated with infertility in women: An updated review. *Expert Rev. Endocrinol. Metab.* **2023**, *18*, 399–417. [CrossRef]
6. Chiware, T.M.; Vermeulen, N.; Blondeel, K.; Farquharson, R.; Kiarie, J.; Lundin, K.; Matsaseng, T.C.; Ombelet, W.; Toskin, I. IVF and other ART in low-and middle-income countries: A systematic landscape analysis. *Hum. Reprod. Updat.* **2021**, *27*, 213–228. [CrossRef]
7. Choi, S.K.; Venetis, C.; Ledger, W.; Havard, A.; Harris, K.; Norman, R.J.; Jorm, L.R.; Chambers, G.M. Population-wide contribution of medically assisted reproductive technologies to overall births in Australia: Temporal trends and parental characteristics. *Hum. Reprod.* **2022**, *37*, 1047–1058. [CrossRef]
8. Bafort, C.; Beebeejaun, Y.; Tomassetti, C.; Bosteels, J.; Duffy, J.M. Laparoscopic surgery for endometriosis. *Cochrane Database Syst. Rev.* **2020**, *2020*, CD011031.
9. Bergholt, T.; Eriksen, L.; Berendt, N.; Jacobsen, M.; Hertz, J. Prevalence and risk factors of adenomyosis at hysterectomy. *Hum. Reprod.* **2001**, *16*, 2418–2421. [CrossRef]
10. Beermann, J.; Piccoli, M.-T.; Viereck, J.; Thum, T. Non-coding RNAs in development and disease: Background, mechanisms, and therapeutic approaches. *Physiol. Rev.* **2016**, *96*, 1297–1325. [CrossRef]
11. Stefani, G.; Slack, F.J. Small non-coding RNAs in animal development. *Nat. Rev. Mol. Cell Biol.* **2008**, *9*, 219–230. [CrossRef] [PubMed]

12. Bartel, D.P. MicroRNAs: Genomics, biogenesis, mechanism, and function. *Cell* **2004**, *116*, 281–297. [CrossRef] [PubMed]
13. Lee, R.C.; Feinbaum, R.L.; Ambros, V. The C. elegans heterochronic gene lin-4 encodes small RNAs with antisense complementarity to lin-14. *Cell* **1993**, *75*, 843–854. [CrossRef] [PubMed]
14. Wightman, B.; Ha, I.; Ruvkun, G. Posttranscriptional regulation of the heterochronic gene lin-14 by lin-4 mediates temporal pattern formation in C. elegans. *Cell* **1993**, *75*, 855–862. [CrossRef]
15. Reinhart, B.J.; Slack, F.J.; Basson, M.; Pasquinelli, A.E.; Bettinger, J.C.; Rougvie, A.E.; Horvitz, H.R.; Ruvkun, G. The 21-nucleotide let-7 RNA regulates developmental timing in Caenorhabditis elegans. *Nature* **2000**, *403*, 901–906. [CrossRef] [PubMed]
16. Berezikov, E.; Guryev, V.; van de Belt, J.; Wienholds, E.; Plasterk, R.H.; Cuppen, E. Phylogenetic shadowing and computational identification of human microRNA genes. *Cell* **2005**, *120*, 21–24. [CrossRef]
17. Friedman, R.C.; Farh, K.K.-H.; Burge, C.B.; Bartel, D.P. Most mammalian mRNAs are conserved targets of microRNAs. *Genome Res.* **2009**, *19*, 92–105. [CrossRef]
18. Lewis, B.P.; Shih, I.-h.; Jones-Rhoades, M.W.; Bartel, D.P.; Burge, C.B. Prediction of mammalian microRNA targets. *Cell* **2003**, *115*, 787–798. [CrossRef]
19. Shang, R.; Lee, S.; Senavirathne, G.; Lai, E.C. microRNAs in action: Biogenesis, function and regulation. *Nat. Rev. Genet.* **2023**, *24*, 816–833. [CrossRef]
20. Lee, Y.; Kim, M.; Han, J.; Yeom, K.H.; Lee, S.; Baek, S.H.; Kim, V.N. MicroRNA genes are transcribed by RNA polymerase II. *EMBO J.* **2004**, *23*, 4051–4060. [CrossRef]
21. Cai, X.; Hagedorn, C.H.; Cullen, B.R. Human microRNAs are processed from capped, polyadenylated transcripts that can also function as mRNAs. *RNA* **2004**, *10*, 1957–1966. [CrossRef] [PubMed]
22. Denli, A.M.; Tops, B.B.; Plasterk, R.H.; Ketting, R.F.; Hannon, G.J. Processing of primary microRNAs by the Microprocessor complex. *Nature* **2004**, *432*, 231–235. [CrossRef] [PubMed]
23. Bohnsack, M.T.; Czaplinski, K.; Görlich, D. Exportin 5 is a RanGTP-dependent dsRNA-binding protein that mediates nuclear export of pre-miRNAs. *Rna* **2004**, *10*, 185–191. [CrossRef]
24. Lund, E.; Guttinger, S.; Calado, A.; Dahlberg, J.E.; Kutay, U. Nuclear export of microRNA precursors. *Science* **2004**, *303*, 95–98. [CrossRef]
25. Yi, R.; Qin, Y.; Macara, I.G.; Cullen, B.R. Exportin-5 mediates the nuclear export of pre-microRNAs and short hairpin RNAs. *Genes Dev.* **2003**, *17*, 3011–3016. [CrossRef] [PubMed]
26. Lee, H.Y.; Zhou, K.; Smith, A.M.; Noland, C.L.; Doudna, J.A. Differential roles of human Dicer-binding proteins TRBP and PACT in small RNA processing. *Nucleic Acids Res.* **2013**, *41*, 6568–6576. [CrossRef]
27. Czech, B.; Hannon, G.J. Small RNA sorting: Matchmaking for Argonautes. *Nat. Rev. Genet.* **2011**, *12*, 19–31. [CrossRef]
28. Gregory, R.I.; Chendrimada, T.P.; Cooch, N.; Shiekhattar, R. Human RISC couples microRNA biogenesis and posttranscriptional gene silencing. *Cell* **2005**, *123*, 631–640. [CrossRef]
29. Morin, R.D.; O'Connor, M.D.; Griffith, M.; Kuchenbauer, F.; Delaney, A.; Prabhu, A.-L.; Zhao, Y.; McDonald, H.; Zeng, T.; Hirst, M.; et al. Application of massively parallel sequencing to microRNA profiling and discovery in human embryonic stem cells. *Genome Res.* **2008**, *18*, 610–621. [CrossRef]
30. Cloonan, N.; Wani, S.; Xu, Q.; Gu, J.; Lea, K.; Heater, S.; Barbacioru, C.; Steptoe, A.L.; Martin, H.C.; Nourbakhsh, E.; et al. MicroRNAs and their isomiRs function cooperatively to target common biological pathways. *Genome Biol.* **2011**, *12*, R126. [CrossRef]
31. Neilsen, C.T.; Goodall, G.J.; Bracken, C.P. IsomiRs–the overlooked repertoire in the dynamic microRNAome. *Trends Genet.* **2012**, *28*, 544–549. [CrossRef] [PubMed]
32. Ferre, A.; Santiago, L.; Sánchez-Herrero, J.F.; López-Rodrigo, O.; Sánchez-Curbelo, J.; Sumoy, L.; Bassas, L.; Larriba, S. 3′ IsomiR Species Composition Affects Reliable Quantification of miRNA/isomiR Variants by Poly (A) RT-qPCR: Impact on Small RNA-Seq Profiling Validation. *Int. J. Mol. Sci.* **2023**, *24*, 15436. [CrossRef] [PubMed]
33. Lai, E.C.; Burks, C.; Posakony, J.W. The K box, a conserved 3′ UTR sequence motif, negatively regulates accumulation of enhancer of split complex transcripts. *Development* **1998**, *125*, 4077–4088. [CrossRef]
34. Leviten, M.W.; Lai, E.C.; Posakony, J.W. The Drosophila gene Bearded encodes a novel small protein and shares 3′ UTR sequence motifs with multiple Enhancer of split complex genes. *Development* **1997**, *124*, 4039–4051. [CrossRef]
35. Catalanotto, C.; Cogoni, C.; Zardo, G. MicroRNA in control of gene expression: An overview of nuclear functions. *Int. J. Mol. Sci.* **2016**, *17*, 1712. [CrossRef]
36. Truesdell, S.; Mortensen, R.; Seo, M.; Schroeder, J.; Lee, J.; LeTonqueze, O.; Vasudevan, S. MicroRNA-mediated mRNA translation activation in quiescent cells and oocytes involves recruitment of a nuclear microRNP. *Sci. Rep.* **2012**, *2*, 842. [CrossRef] [PubMed]
37. Lewis, B.P.; Burge, C.B.; Bartel, D.P. Conserved seed pairing, often flanked by adenosines, indicates that thousands of human genes are microRNA targets. *Cell* **2005**, *120*, 15–20. [CrossRef]
38. Okamura, K.; Phillips, M.D.; Tyler, D.M.; Duan, H.; Chou, Y.-T.; Lai, E.C. The regulatory activity of microRNA* species has substantial influence on microRNA and 3′ UTR evolution. *Nat. Struct. Mol. Biol.* **2008**, *15*, 354–363. [CrossRef] [PubMed]
39. Filipowicz, W.; Bhattacharyya, S.N.; Sonenberg, N. Mechanisms of post-transcriptional regulation by microRNAs: Are the answers in sight? *Nat. Rev. Genet.* **2008**, *9*, 102–114. [CrossRef]
40. Selbach, M.; Schwanhäusser, B.; Thierfelder, N.; Fang, Z.; Khanin, R.; Rajewsky, N. Widespread changes in protein synthesis induced by microRNAs. *Nature* **2008**, *455*, 58–63. [CrossRef]

41. Baek, D.; Villén, J.; Shin, C.; Camargo, F.D.; Gygi, S.P.; Bartel, D.P. The impact of microRNAs on protein output. *Nature* **2008**, *455*, 64–71. [CrossRef] [PubMed]
42. Meister, G.; Landthaler, M.; Patkaniowska, A.; Dorsett, Y.; Teng, G.; Tuschl, T. Human Argonaute2 mediates RNA cleavage targeted by miRNAs and siRNAs. *Mol. Cell* **2004**, *15*, 185–197. [CrossRef] [PubMed]
43. Olsen, P.H.; Ambros, V. The lin-4 regulatory RNA controls developmental timing in Caenorhabditis elegans by blocking LIN-14 protein synthesis after the initiation of translation. *Dev. Biol.* **1999**, *216*, 671–680. [CrossRef]
44. Hwang, H.-W.; Wentzel, E.A.; Mendell, J.T. A hexanucleotide element directs microRNA nuclear import. *Science* **2007**, *315*, 97–100. [CrossRef]
45. Liang, H.; Zhang, J.; Zen, K.; Zhang, C.-Y.; Chen, X. Nuclear microRNAs and their unconventional role in regulating non-coding RNAs. *Protein Cell* **2013**, *4*, 325–330. [CrossRef]
46. Huang, Y. The novel regulatory role of lnc RNA-mi RNA-mRNA axis in cardiovascular diseases. *J. Cell. Mol. Med.* **2018**, *22*, 5768–5775. [CrossRef]
47. Kucherenko, M.M.; Shcherbata, H.R. miRNA targeting and alternative splicing in the stress response–events hosted by membraneless compartments. *J. Cell Sci.* **2018**, *131*, jcs202002. [CrossRef] [PubMed]
48. Braconi, C.; Kogure, T.; Valeri, N.; Huang, N.; Nuovo, G.; Costinean, S.; Negrini, M.; Miotto, E.; Croce, C.M.; Patel, T.J.O. microRNA-29 can regulate expression of the long non-coding RNA gene MEG3 in hepatocellular cancer. *Oncogene* **2011**, *30*, 4750–4756. [CrossRef]
49. Weber, J.A.; Baxter, D.H.; Zhang, S.; Huang, D.Y.; How Huang, K.; Jen Lee, M.; Galas, D.J.; Wang, K. The microRNA spectrum in 12 body fluids. *Clin. Chem.* **2010**, *56*, 1733–1741. [CrossRef]
50. Hanson, E.K.; Lubenow, H.; Ballantyne, J. Identification of forensically relevant body fluids using a panel of differentially expressed microRNAs. *Anal. Biochem.* **2009**, *387*, 303–314. [CrossRef]
51. Vickers, K.C.; Palmisano, B.T.; Shoucri, B.M.; Shamburek, R.D.; Remaley, A.T. MicroRNAs are transported in plasma and delivered to recipient cells by high-density lipoproteins. *Nat. Cell Biol.* **2011**, *13*, 423–433. [CrossRef] [PubMed]
52. Lin, J.-T.; Tsai, K.-W. Circulating miRNAs act as diagnostic biomarkers for bladder cancer in urine. *Int. J. Mol. Sci.* **2021**, *22*, 4278. [CrossRef] [PubMed]
53. Mehterov, N.; Vladimirov, B.; Sacconi, A.; Pulito, C.; Rucinski, M.; Blandino, G.; Sarafian, V. Salivary miR-30c-5p as Potential Biomarker for Detection of Oral Squamous Cell Carcinoma. *Biomedicines* **2021**, *9*, 1079. [CrossRef]
54. Sang, Q.; Yao, Z.; Wang, H.; Feng, R.; Wang, H.; Zhao, X.; Xing, Q.; Jin, L.; He, L.; Wu, L.; et al. Identification of microRNAs in human follicular fluid: Characterization of microRNAs that govern steroidogenesis in vitro and are associated with polycystic ovary syndrome in vivo. *J. Clin. Endocrinol. Metab.* **2013**, *98*, 3068–3079. [CrossRef] [PubMed]
55. Barceló, M.; Mata, A.; Bassas, L.; Larriba, S. Exosomal microRNAs in seminal plasma are markers of the origin of azoospermia and can predict the presence of sperm in testicular tissue. *Hum. Reprod.* **2018**, *33*, 1087–1098. [CrossRef]
56. Hicks, S.D.; Confair, A.; Warren, K.; Chandran, D. Levels of breast milk microRNAs and other non-coding RNAs are impacted by milk maturity and maternal diet. *Front. Immunol.* **2022**, *12*, 785217. [CrossRef]
57. Cheng, L.; Sharples, R.A.; Scicluna, B.J.; Hill, A.F. Exosomes provide a protective and enriched source of miRNA for biomarker profiling compared to intracellular and cell-free blood. *J. Extracell. Vesicles* **2014**, *3*, 23743. [CrossRef]
58. Arroyo, J.D.; Chevillet, J.R.; Kroh, E.M.; Ruf, I.K.; Pritchard, C.C.; Gibson, D.F.; Mitchell, P.S.; Bennett, C.F.; Pogosova-Agadjanyan, E.L.; Stirewalt, D.L.; et al. Argonaute2 complexes carry a population of circulating microRNAs independent of vesicles in human plasma. *Proc. Natl. Acad. Sci. USA* **2011**, *108*, 5003–5008. [CrossRef]
59. Yao, B.; La, L.B.; Chen, Y.C.; Chang, L.J.; Chan, E.K.L. Defining a new role of GW182 in maintaining miRNA stability. *Embo Rep.* **2012**, *13*, 1102–1108. [CrossRef]
60. Valadi, H.; Ekstrom, K.; Bossios, A.; Sjostrand, M.; Lee, J.J.; Lotvall, J.O. Exosome-mediated transfer of mRNAs and microRNAs is a novel mechanism of genetic exchange between cells. *Nat. Cell Biol.* **2007**, *9*, 654–659. [CrossRef]
61. Asakura, K.; Kadota, T.; Matsuzaki, J.; Yoshida, Y.; Yamamoto, Y.; Nakagawa, K.; Takizawa, S.; Aoki, Y.; Nakamura, E.; Miura, J.; et al. A miRNA-based diagnostic model predicts resectable lung cancer in humans with high accuracy. *Commun. Biol.* **2020**, *3*, 134. [CrossRef] [PubMed]
62. Cho, W.C.; Wong, C.F.; Li, K.P.; Fong, A.H.; Fung, K.Y.; Au, J.S. miR-145 as a potential biomarker and therapeutic target in patients with non-small cell lung cancer. *Int. J. Mol. Sci.* **2023**, *24*, 10022. [CrossRef] [PubMed]
63. Dar, G.M.; Agarwal, S.; Kumar, A.; Sharma, A.K.; Verma, R.; Sattar, R.S.A.; Ahmad, E.; Ali, A.; Mahajan, B.; Saluja, S.S.; et al. A non-invasive miRNA-based approach in early diagnosis and therapeutics of oral cancer. *Crit. Rev. Oncol. Hematol.* **2022**, *180*, 103850. [CrossRef] [PubMed]
64. Doghish, A.S.; Moustafa, H.A.M.; Elballal, M.S.; Sallam, A.-A.M.; El-Dakroury, W.A.; Mageed, S.S.A.; Elesawy, A.E.; Abdelmaksoud, N.M.; Shahin, R.K.; Midan, H.M.; et al. The potential role of miRNAs in the pathogenesis of testicular germ cell tumors—A Focus on signaling pathways interplay. *Pathol.-Res. Pract.* **2023**, *248*, 154611. [CrossRef] [PubMed]
65. Fan, Y.; Ji, Y.; Wang, X.; Hu, J.; Zhang, Q.; Xu, J.; Liu, W.; Wang, A. Relationship of miRNA-146a to systemic lupus erythematosus: A PRISMA-compliant meta-analysis. *Medicine* **2020**, *99*, e22444. [CrossRef]
66. Cheng, Y.-F.; Gu, X.-J.; Yang, T.-M.; Wei, Q.-Q.; Cao, B.; Zhang, Y.; Shang, H.-F.; Chen, Y.-P. Signature of miRNAs derived from the circulating exosomes of patients with amyotrophic lateral sclerosis. *Front. Aging Neurosci.* **2023**, *15*, 1106497. [CrossRef]

67. Lee, M.; Woo, J.; Kim, S.T.; Moon, M.; Kim, S.Y.; Cho, H.; Kim, S.; Kim, H.-K.; Park, J.-Y. MicroRNA super-resolution imaging in blood for Alzheimer's disease. *BMB Rep.* **2023**, *56*, 190. [CrossRef]
68. Zou, Y.-F.; Wen, D.; Zhao, Q.; Shen, P.-Y.; Shi, H.; Zhao, Q.; Chen, Y.-X.; Zhang, W. Urinary MicroRNA-30c-5p and MicroRNA-192-5p as potential biomarkers of ischemia–reperfusion-induced kidney injury. *Exp. Biol. Med.* **2017**, *242*, 657–667. [CrossRef]
69. Benito, B.; García-Elías, A.; Ois, Á.; Tajes, M.; Vallès, E.; Ble, M.; Bisbe, L.Y.; Giralt-Steinhauer, E.; Rodríguez-Campello, A.; Capdevila, M.C.; et al. Plasma levels of miRNA-1-3p are associated with subclinical atrial fibrillation in patients with cryptogenic stroke. *Rev. Espanola De Cardiol.* **2022**, *75*, 717–726. [CrossRef]
70. Düzgün, Z.; Kayikçioğlu, L.M.; Aktan, Ç.; Bara, B.; Eroğlu, F.Z.; Yağmur, B.; Çetintaş, V.B.; Bayindir, M.; Nalbantgil, S.; Vardarli, A.T. Decreased circulating microRNA-21 and microRNA-143 are associated to pulmonary hypertension. *Turk. J. Med Sci.* **2023**, *53*, 130–141. [CrossRef]
71. Huang, S.; Zhang, J.; Wan, H.; Wang, K.; Wu, J.; Cao, Y.; Hu, L.; Yu, Y.; Sun, H.; Yu, Y.; et al. Plasma extracellular vesicles microRNA-208b-3p and microRNA-143-3p as novel biomarkers for sudden cardiac death prediction in acute coronary syndrome. *Mol. Omics* **2023**, *19*, 262–273. [CrossRef]
72. Yang, J. Patisiran for the treatment of hereditary transthyretin-mediated amyloidosis. *Expert Rev. Clin. Pharmacol.* **2019**, *12*, 95–99. [CrossRef]
73. Gebert, L.F.; Rebhan, M.A.; Crivelli, S.E.; Denzler, R.; Stoffel, M.; Hall, J. Miravirsen (SPC3649) can inhibit the biogenesis of miR-122. *Nucleic Acids Res.* **2014**, *42*, 609–621. [CrossRef] [PubMed]
74. Zegers-Hochschild, F.; Adamson, G.D.; de Mouzon, J.; Ishihara, O.; Mansour, R.; Nygren, K.; Sullivan, E.; Vanderpoel, S. International Committee for Monitoring Assisted Reproductive Technology (ICMART) and the World Health Organization (WHO) revised glossary of ART terminology, 2009. *Fertil Steril* **2009**, *92*, 1520–1524. [CrossRef] [PubMed]
75. Edassery, S.L.; Shatavi, S.V.; Kunkel, J.P.; Hauer, C.; Brucker, C.; Penumatsa, K.; Yu, Y.; Dias, J.A.; Luborsky, J.L. Autoantigens in ovarian autoimmunity associated with unexplained infertility and premature ovarian failure. *Fertil. Steril.* **2010**, *94*, 2636–2641. [CrossRef] [PubMed]
76. Legro, R.S.; Strauss, J.F., III. Molecular progress in infertility: Polycystic ovary syndrome. *Fertil. Steril.* **2002**, *78*, 569–576. [CrossRef]
77. Monteleone, P.; Parrini, D.; Faviana, P.; Carletti, E.; Casarosa, E.; Uccelli, A.; Cela, V.; Genazzani, A.R.; Artini, P.G. Female infertility related to thyroid autoimmunity: The ovarian follicle hypothesis. *Am. J. Reprod. Immunol.* **2011**, *66*, 108–114. [CrossRef]
78. Abbey, A.; Halman, L.J.; Andrews, F.M. Psychosocial, treatment, and demographic predictors of the stress associated with infertility. *Fertil. Steril.* **1992**, *57*, 122–128. [CrossRef]
79. Ramezanzadeh, F.; Aghssa, M.M.; Abedinia, N.; Zayeri, F.; Khanafshar, N.; Shariat, M.; Jafarabadi, M. A survey of relationship between anxiety, depression and duration of infertility. *BMC Women's Health* **2004**, *4*, 9. [CrossRef]
80. David, A.; Carmil, D.; Bar-David, E.; Serr, D.M. Congenital absence of the vagina: Clinical and psychologic aspects. *Clin. Psychol. Asp.* **1975**, *46*, 407–409.
81. Broughton, D.E.; Moley, K.H. Obesity and female infertility: Potential mediators of obesity's impact. *Fertil. Steril.* **2017**, *107*, 840–847. [CrossRef] [PubMed]
82. Calanchini, M.; Aye, C.Y.; Orchard, E.; Baker, K.; Child, T.; Fabbri, A.; Mackillop, L.; Turner, H.E. Fertility issues and pregnancy outcomes in Turner syndrome. *Fertil. Steril.* **2020**, *114*, 144–154. [CrossRef] [PubMed]
83. Corroenne, R.; Legendre, G.; May-Panloup, P.; El Hachem, H.; Dreux, C.; Jeanneteau, P.; Boucret, L.; Ferré-L'Hotellier, V.; Descamps, P.; Bouet, P.-E. Surgical treatment of septate uterus in cases of primary infertility and before assisted reproductive technologies. *J. Gynecol. Obstet. Hum. Reprod.* **2018**, *47*, 413–418. [CrossRef]
84. Hammoud, A.O.; Gibson, M.; Peterson, C.M.; Meikle, A.W.; Carrell, D.T. Impact of male obesity on infertility: A critical review of the current literature. *Fertil. Steril.* **2008**, *90*, 897–904. [CrossRef]
85. Chico-Sordo, L.; Cordova-Oriz, I.; Polonio, A.M.; LS, S.M.; Medrano, M.; Garcia-Velasco, J.A.; Varela, E. Reproductive aging and telomeres: Are women and men equally affected? *Mech. Ageing Dev.* **2021**, *198*, 111541. [CrossRef]
86. Polis, C.B.; Cox, C.M.; Tunçalp, Ö.; McLain, A.C.; Thoma, M.E. Estimating infertility prevalence in low-to-middle-income countries: An application of a current duration approach to Demographic and Health Survey data. *Hum. Reprod.* **2017**, *32*, 1064–1074. [CrossRef]
87. Sharpe, R.M.; Franks, S. Environment, lifestyle and infertility—An inter-generational issue. *Nat. Med.* **2002**, *8* (Suppl. S10), S33–S40. [CrossRef]
88. Pastore, L.M.; Christianson, M.S.; Stelling, J.; Kearns, W.G.; Segars, J.H. Reproductive ovarian testing and the alphabet soup of diagnoses: DOR, POI, POF, POR, and FOR. *J. Assist. Reprod Genet.* **2018**, *35*, 17–23. [CrossRef] [PubMed]
89. Woo, I.; Christenson, L.K.; Gunewardena, S.; Ingles, S.A.; Thomas, S.; Ahmady, A.; Chung, K.; Bendikson, K.; Paulson, R.; McGinnis, L.K. Micro-RNAs involved in cellular proliferation have altered expression profiles in granulosa of young women with diminished ovarian reserve. *J. Assist. Reprod. Genet.* **2018**, *35*, 1777–1786. [CrossRef]
90. Ju, W.; Zhao, S.; Wu, H.; Yu, Y.; Li, Y.; Liu, D.; Lian, F.; Xiang, S. miR-6881-3p contributes to diminished ovarian reserve by regulating granulosa cell apoptosis by targeting SMAD4. *Reprod. Biol. Endocrinol.* **2024**, *22*, 17. [CrossRef]
91. Li, H.; Wang, X.; Mu, H.; Mei, Q.; Liu, Y.; Min, Z.; Zhang, L.; Su, P.; Xiang, W. Mir-484 contributes to diminished ovarian reserve by regulating granulosa cell function via YAP1-mediated mitochondrial function and apoptosis. *Int. J. Biol. Sci.* **2022**, *18*, 1008. [CrossRef] [PubMed]

92. Yazdanian, A.; Lotfi, M.; Montazeri, F.; Dashti, S.; Sheikhha, M.H. The possible regulatory role of miR-4463 and its target gene CYP19A1 on the ovarian response in the women with diminished ovarian reserve: A case-control study. *Int. J. Reprod. Biomed.* **2024**, *22*, 639. [CrossRef]
93. Shen, K.-Y.; Dai, X.-L.; Li, S.; Huang, F.; Chen, L.-Q.; Luo, P.; Qu, X.-L. Specific expression profile of follicular fluid-derived exosomal microRNAs in patients with diminished ovarian reserve. *BMC Med. Genom.* **2023**, *16*, 308. [CrossRef] [PubMed]
94. Xie, Y.; Chen, J.; Liu, K.; Huang, J.; Zeng, Y.; Gao, M.; Qian, Y.; Liu, L.; Tan, Y.; Nie, X. Differential expression of follicular fluid exosomal microRNA in women with diminished ovarian reserve. *J. Assist. Reprod. Genet.* **2024**, *41*, 1087–1096. [CrossRef] [PubMed]
95. Luo, H.; Han, Y.; Liu, J.; Zhang, Y. Identification of microRNAs in granulosa cells from patients with different levels of ovarian reserve function and the potential regulatory function of miR-23a in granulosa cell apoptosis. *Gene* **2019**, *686*, 250–260. [CrossRef]
96. Karakaya, C.; Guzeloglu-Kayisli, O.; Uyar, A.; Kallen, A.N.; Babayev, E.; Bozkurt, N.; Unsal, E.; Karabacak, O.; Seli, E. Poor ovarian response in women undergoing in vitro fertilization is associated with altered microRNA expression in cumulus cells. *Fertil. Steril.* **2015**, *103*, 1469–1476.e3. [CrossRef]
97. Zhang, K.; Zhong, W.; Li, W.-P.; Chen, Z.-J.; Zhang, C. miR-15a-5p levels correlate with poor ovarian response in human follicular fluid. *Reproduction* **2017**, *154*, 483–496. [CrossRef] [PubMed]
98. Yang, X.; Zhou, Y.; Peng, S.; Wu, L.; Lin, H.-Y.; Wang, S.; Wang, H. Differentially expressed plasma microRNAs in premature ovarian failure patients and the potential regulatory function of mir-23a in granulosa cell apoptosis. *Reproduction* **2012**, *144*, 235. [CrossRef]
99. Li, Y.; Xiang, Y.; Song, Y.; Wan, L.; Yu, G.; Tan, L. Dysregulated miR-142,-33b and-423 in granulosa cells target TGFBR1 and SMAD7: A possible role in polycystic ovary syndrome. *Mol. Hum. Reprod.* **2019**, *25*, 638–646. [CrossRef]
100. Xu, C.; Luo, M.; Liu, X.; Wei, T.; Zhou, Z.; Li, C.; He, Z.; Sui, H. MicroRNA-1298-5p in granulosa cells facilitates cell autophagy in polycystic ovary syndrome by suppressing glutathione-disulfide reductase. *Cell Tissue Res.* **2023**, *392*, 763–778. [CrossRef]
101. Rad, H.M.; Mowla, S.J.; Ramazanali, F.; Valojerdi, M.R. Characterization of altered microRNAs related to different phenotypes of polycystic ovarian syndrome (PCOS) in serum, follicular fluid, and cumulus cells. *Taiwan. J. Obstet. Gynecol.* **2022**, *61*, 768–779.
102. Yang, Y.; Lang, P.; Zhang, X.; Wu, X.; Cao, S.; Zhao, C.; Shen, R.; Ling, X.; Yang, Y.; Zhang, J. Molecular characterization of extracellular vesicles derived from follicular fluid of women with and without PCOS: Integrating analysis of differential miRNAs and proteins reveals vital molecules involving in PCOS. *J. Assist. Reprod. Genet.* **2023**, *40*, 537–552. [CrossRef] [PubMed]
103. Butler, A.E.; Ramachandran, V.; Hayat, S.; Dargham, S.R.; Cunningham, T.K.; Benurwar, M.; Sathyapalan, T.; Najafi-Shoushtari, S.H.; Atkin, S.L. Expression of microRNA in follicular fluid in women with and without PCOS. *Sci. Rep.* **2019**, *9*, 16306. [CrossRef]
104. Sathyapalan, T.; David, R.; Gooderham, N.J.; Atkin, S.L. Increased expression of circulating miRNA-93 in women with polycystic ovary syndrome may represent a novel, non-invasive biomarker for diagnosis. *Sci. Rep.* **2015**, *5*, 16890. [CrossRef] [PubMed]
105. Long, W.; Zhao, C.; Ji, C.; Ding, H.; Cui, Y.; Guo, X.; Shen, R.; Liu, J. Characterization of serum microRNAs profile of PCOS and identification of novel non-invasive biomarkers. *Cell. Physiol. Biochem.* **2014**, *33*, 1304–1315. [CrossRef]
106. Jiang, X.; Li, J.; Zhang, B.; Hu, J.; Ma, J.; Cui, L.; Chen, Z.-J. Differential expression profile of plasma exosomal microRNAs in women with polycystic ovary syndrome. *Fertil. Steril.* **2021**, *115*, 782–792. [CrossRef]
107. De Nardo Maffazioli, G.; Baracat, E.C.; Soares, J.M.; Carvalho, K.C.; Maciel, G.A.R. Evaluation of circulating microRNA profiles in Brazilian women with polycystic ovary syndrome: A preliminary study. *PLoS ONE* **2022**, *17*, e0275031. [CrossRef]
108. Liu, Y.; Shi, X.; Xu, B.; Wang, Z.; Chen, Y.; Deng, M. Differential expression of plasma-derived exosomal miRNAs in polycystic ovary syndrome as a circulating biomarker. *Biomed. Rep.* **2023**, *19*, 92. [CrossRef]
109. Wei, C.; Xiang, S.; Yu, Y.; Song, J.; Zheng, M.; Lian, F. miR-221-3p regulates apoptosis of ovarian granulosa cells via targeting FOXO1 in older women with diminished ovarian reserve (DOR). *Mol. Reprod. Dev.* **2021**, *88*, 251–260. [CrossRef]
110. Hong, L.; Peng, S.; Li, Y.; Fang, Y.; Wang, Q.; Klausen, C.; Yin, C.; Wang, S.; Leung, P.C.; Yang, X. miR-106a increases granulosa cell viability and is downregulated in women with diminished ovarian reserve. *J. Clin. Endocrinol. Metab.* **2018**, *103*, 2157–2166. [CrossRef]
111. Dang, Y.; Zhao, S.; Qin, Y.; Han, T.; Li, W.; Chen, Z.-J. MicroRNA-22-3p is down-regulated in the plasma of Han Chinese patients with premature ovarian failure. *Fertil. Steril.* **2015**, *103*, 802–807.e1. [CrossRef] [PubMed]
112. Arancio, W.; Calogero Amato, M.; Magliozzo, M.; Pizzolanti, G.; Vesco, R.; Giordano, C. Serum miRNAs in women affected by hyperandrogenic polycystic ovary syndrome: The potential role of miR-155 as a biomarker for monitoring the estroprogestinic treatment. *Gynecol. Endocrinol.* **2018**, *34*, 704–708. [CrossRef] [PubMed]
113. Udesen, P.B.; Sørensen, A.E.; Svendsen, R.; Frisk, N.L.; Hess, A.L.; Aziz, M.; Wissing, M.L.M.; Englund, A.L.M.; Dalgaard, L.T. Circulating miRNAs in women with polycystic ovary syndrome: A longitudinal cohort study. *Cells* **2023**, *12*, 983. [CrossRef] [PubMed]
114. Vogt, S.; Handke, D.; Behre, H.M.; Greither, T. Decreased Serum Levels of the Insulin Resistance-Related microRNA miR-320a in Patients with Polycystic Ovary Syndrome. *Curr. Issues Mol. Biol.* **2024**, *46*, 3379–3393. [CrossRef]
115. Testing and interpreting measures of ovarian reserve: A committee opinion. *Fertil. Steril.* **2020**, *114*, 1151–1157. [CrossRef]
116. La Marca, A.; Sunkara, S.K. Individualization of controlled ovarian stimulation in IVF using ovarian reserve markers: From theory to practice. *Hum. Reprod Update* **2014**, *20*, 124–140. [CrossRef]

117. Kedem, A.; Yung, Y.; Yerushalmi, G.M.; Haas, J.; Maman, E.; Hanochi, M.; Hemi, R.; Orvieto, R.; Dor, J.; Hourvitz, A. Anti Müllerian Hormone (AMH) level and expression in mural and cumulus cells in relation to age. *J. Ovarian Res.* **2014**, *7*, 113. [CrossRef]
118. Abu-Halima, M.; Becker, L.S.; Ayesh, B.M.; Baus, S.L.; Hamza, A.; Fischer, U.; Hammadeh, M.; Keller, A.; Meese, E. Characterization of micro-RNA in women with different ovarian reserve. *Sci. Rep.* **2021**, *11*, 13351. [CrossRef]
119. Papathanasiou, A. Implementing the ESHRE 'poor responder'criteria in research studies: Methodological implications. *Hum. Reprod.* **2014**, *29*, 1835–1838. [CrossRef]
120. Venetis, C.A.; Lottrup, G.; Nielsen, J.; Maroun, L.; Møller, L.; Yassin, M.; Leffers, H.; Skakkebæk, N.; Meyts, E.R.-D. The Bologna criteria for poor ovarian response: The good, the bad and the way forward. *Hum. Reprod.* **2014**, *29*, 1839–1841. [CrossRef]
121. Yagüe-Serrano, R.; Palomar, A.; Quiñonero, A.; Gómez, V.H.; de Los Santos, M.J.; Vidal, C.; Dominguez, F. Oocyte Competence, Embryological Outcomes and miRNA Signature of Different Sized Follicles from Poor Responder Patients. *Int. J. Mol. Sci.* **2024**, *25*, 10237. [CrossRef] [PubMed]
122. Welt, C.K. Primary ovarian insufficiency: A more accurate term for premature ovarian failure. *Clin. Endocrinol.* **2008**, *68*, 499–509. [CrossRef] [PubMed]
123. European Society for Human Reproduction and Embryology (ESHRE) Guideline Group on POI; Webber, L.; Davies, M.; Anderson, R.; Bartlett, J.; Braat, D.; Cartwright, B.; Cifkova, R.; de Muinck Keizer-Schrama, S.; Hogervorst, E.; et al. ESHRE Guideline: Management of women with premature ovarian insufficiency†. *Hum. Reprod.* **2016**, *31*, 926–937. [CrossRef]
124. Golezar, S.; Ramezani Tehrani, F.; Khazaei, S.; Ebadi, A.; Keshavarz, Z. The global prevalence of primary ovarian insufficiency and early menopause: A meta-analysis. *Climacteric* **2019**, *22*, 403–411. [CrossRef]
125. Nelson, L.M.; Covington, S.N.; Rebar, R.W. An update: Spontaneous premature ovarian failure is not an early menopause. *Fertil. Steril.* **2005**, *83*, 1327–1332. [CrossRef]
126. Szeliga, A.; Maciejewska-Jeske, M.; Męczekalski, B. Bone health and evaluation of bone mineral density in patients with premature ovarian insufficiency. *Menopausal Rev.* **2018**, *17*, 112–116. [CrossRef] [PubMed]
127. Roeters van Lennep, J.E.; Heida, K.Y.; Bots, M.L.; Hoek, A.; Collaborators of the Dutch Multidisciplinary Guideline Development Group on Cardiovascular Risk Management after Reproductive Disorders. Cardiovascular disease risk in women with premature ovarian insufficiency: A systematic review and meta-analysis. *Eur. J. Prev. Cardiol.* **2016**, *23*, 178–186. [CrossRef]
128. van Zwol-Janssens, C.; Pastoor, H.; Laven, J.S.; Louwers, Y.V.; Jiskoot, G. Sexual function in women with premature ovarian insufficiency (POI): Systematic review and meta-analysis. *Maturitas* **2024**, *184*, 107994. [CrossRef]
129. Mann, E.; Singer, D.; Pitkin, J.; Panay, N.; Hunter, M.S. Psychosocial adjustment in women with premature menopause: A cross-sectional survey. *Climacteric* **2012**, *15*, 481–489. [CrossRef]
130. Singer, D.; Mann, E.; Hunter, M.; Pitkin, J.; Panay, N. The silent grief: Psychosocial aspects of premature ovarian failure. *Climacteric* **2011**, *14*, 428–437. [CrossRef]
131. Deeks, A.; Gibson-Helm, M.; Teede, H.; Vincent, A. Premature menopause: A comprehensive understanding of psychosocial aspects. *Climacteric* **2011**, *14*, 565–572. [CrossRef] [PubMed]
132. Woad, K.J.; Watkins, W.J.; Prendergast, D.; Shelling, A.N.J.A.; Shelling, A.N. The genetic basis of premature ovarian failure. *Aust. New Zealand J. Obstet. Gynaecol.* **2006**, *46*, 242–244. [CrossRef] [PubMed]
133. Jiao, X.; Ke, H.; Qin, Y.; Chen, Z.-J. Molecular genetics of premature ovarian insufficiency. *Trends Endocrinol. Metab.* **2018**, *29*, 795–807. [CrossRef] [PubMed]
134. Maclaren, N.; Chen, Q.-Y.; Kukreja, A.; Marker, J.; Zhang, C.H.; Sun, Z.S. Autoimmune hypogonadism as part of an autoimmune polyglandular syndrome. *J. Soc. Gynecol. Investig.* **2001**, *8*, S52–S54. [CrossRef]
135. Coulam, C.B.; Ryan, R.J. Premature menopause: I. Etiology. *Am. J. Obstet. Gynecol.* **1979**, *133*, 639–643. [CrossRef]
136. Guo, X.; Zhu, Y.; Guo, L.; Qi, Y.; Liu, X.; Wang, J.; Zhang, J.; Cui, L.; Shi, Y.; Wang, Q.; et al. BCAA insufficiency leads to premature ovarian insufficiency via ceramide-induced elevation of ROS. *EMBO Mol. Med.* **2023**, *15*, e17450. [CrossRef]
137. Vabre, P.; Gatimel, N.; Moreau, J.; Gayrard, V.; Picard-Hagen, N.; Parinaud, J.; Léandri, R. Environmental pollutants, a possible etiology for premature ovarian insufficiency: A narrative review of animal and human data. *Environ. Health* **2017**, *16*, 37. [CrossRef]
138. Ai, A.; Xiong, Y.; Wu, B.; Lin, J.; Huang, Y.; Cao, Y.; Liu, T. Induction of miR-15a expression by tripterygium glycosides caused premature ovarian failure by suppressing the Hippo-YAP/TAZ signaling effector Lats1. *Gene* **2018**, *678*, 155–163. [CrossRef]
139. Kuang, H.; Han, D.; Xie, J.; Yan, Y.; Li, J.; Ge, P. Profiling of differentially expressed microRNAs in premature ovarian failure in an animal model. *Gynecol. Endocrinol.* **2014**, *30*, 57–61. [CrossRef]
140. Liu, T.; Liu, Y.; Huang, Y.; Chen, J.; Yu, Z.; Chen, C.; Lai, L. miR-15b induces premature ovarian failure in mice via inhibition of α-Klotho expression in ovarian granulosa cells. *Free. Radic. Biol. Med.* **2019**, *141*, 383–392. [CrossRef]
141. Zhang, X.; Zhang, R.; Hao, J.; Huang, X.; Liu, M.; Lv, M.; Su, C.; Mu, Y.L. miRNA-122-5p in POI ovarian-derived exosomes promotes granulosa cell apoptosis by regulating BCL9. *Cancer Med.* **2022**, *11*, 2414–2426. [CrossRef] [PubMed]
142. Zhao, H.; Gu, W.; Pan, W.; Zhang, H.; Shuai, L.; Diao, R.; Wang, L. miR-483-5p aggravates cisplatin-induced premature ovarian insufficiency in rats by targeting FKBP4. *Nan Fang Yi Ke Da Xue Xue Bao J. South. Med. Univ.* **2021**, *41*, 801–810.
143. Hansen, T.B.; Jensen, T.I.; Clausen, B.H.; Bramsen, J.B.; Finsen, B.; Damgaard, C.K.; Kjems, J. Natural RNA circles function as efficient microRNA sponges. *Nature* **2013**, *495*, 384–388. [CrossRef] [PubMed]

144. Wang, W.T.; Zhao, Y.N.; Han, B.W.; Hong, S.J.; Chen, Y.Q. Circulating microRNAs identified in a genome-wide serum microRNA expression analysis as noninvasive biomarkers for endometriosis. *J. Clin. Endocrinol. Metab.* **2013**, *98*, 281–289. [CrossRef]
145. Nie, M.; Yu, S.; Peng, S.; Fang, Y.; Wang, H.; Yang, X. miR-23a and miR-27a promote human granulosa cell apoptosis by targeting SMAD5. *Biol. Reprod.* **2015**, *93*, 98. [CrossRef]
146. Zheng, C.; Liu, S.; Qin, Z.; Zhang, X.; Song, Y. LncRNA DLEU1 is overexpressed in premature ovarian failure and sponges miR-146b-5p to increase granulosa cell apoptosis. *J. Ovarian Res.* **2021**, *14*, 151. [CrossRef]
147. Nouri, N.; Aghebati-Maleki, L.; Soltani-Zangbar, M.S.; Kamrani, A.; Mehdizadeh, A.; Danaii, S.; Heris, J.A.; Chakeri-Khiavi, F.; Yousefi, M. Analysis of Th17 cell population and expression of microRNA and factors related to Th17 in patients with premature ovarian failure. *J. Reprod. Immunol.* **2024**, *165*, 104290. [CrossRef]
148. Pellicer, N.; Cozzolino, M.; Diaz-García, C.; Galliano, D.; Cobo, A.; Pellicer, A.; Herraiz, S. Ovarian rescue in women with premature ovarian insufficiency: Facts and fiction. *Reprod. Biomed. Online* **2023**, *46*, 543–565. [CrossRef]
149. Escobar-Morreale, H.F. Polycystic ovary syndrome: Definition, aetiology, diagnosis and treatment. *Nat. Rev. Endocrinol.* **2018**, *14*, 270–284. [CrossRef]
150. Azziz, R. Polycystic ovary syndrome. *Obstet. Gynecol.* **2018**, *132*, 321–336. [CrossRef]
151. Witchel, S.F.; Oberfield, S.E.; Peña, A.S. Polycystic ovary syndrome: Pathophysiology, presentation, and treatment with emphasis on adolescent girls. *J. Endocr. Soc.* **2019**, *3*, 1545–1573. [CrossRef] [PubMed]
152. Nasser, J.S.; Altahoo, N.; Almosawi, S.; Alhermi, A.; Butler, A.E. The role of MicroRNA, long non-coding RNA and circular RNA in the pathogenesis of polycystic ovary syndrome: A literature review. *Int. J. Mol. Sci.* **2024**, *25*, 903. [CrossRef] [PubMed]
153. Rosner, J.; Samardzic, T.; Sarao, M.S. Physiology, Female Reproduction; 2019. Available online: https://europepmc.org/article/NBK/nbk537132 (accessed on 30 November 2024).
154. Altmäe, S.; Koel, M.; Võsa, U.; Adler, P.; Suhorutšenko, M.; Laisk-Podar, T.; Kukushkina, V.; Saare, M.; Velthut-Meikas, A.; Krjutškov, K. Meta-signature of human endometrial receptivity: A meta-analysis and validation study of transcriptomic biomarkers. *Sci. Rep.* **2017**, *7*, 10077. [CrossRef]
155. Kamalidehghan, B.; Habibi, M.; Afjeh, S.S.; Shoai, M.; Alidoost, S.; Almasi Ghale, R.; Eshghifar, N.; Pouresmaeili, F. The importance of small non-coding RNAs in human reproduction: A review article. *Appl. Clin. Genet.* **2020**, *13*, 1–11. [CrossRef]
156. Lamon, S.; Le Carré, J.; Petito, G.; Duong, H.P.; Luthi, F.; Hiam, D.; Léger, B. The effect of the menstrual cycle on the circulating microRNA pool in human plasma: A pilot study. *Hum. Reprod.* **2023**, *38*, 46–56. [CrossRef]
157. Rekker, K.; Saare, M.; Roost, A.M.; Salumets, A.; Peters, M. Circulating microRNA Profile throughout the menstrual cycle. *PLoS ONE* **2013**, *8*, e81166. [CrossRef] [PubMed]
158. Chen, M.J.; Hsu, A.; Lin, P.Y.; Chen, Y.L.; Wu, K.W.; Chen, K.C.; Wang, T.; Yi, Y.C.; Kung, H.F.; Chang, J.C.; et al. Development of a Predictive Model for Optimization of Embryo Transfer Timing Using Blood-Based microRNA Expression Profile. *Int. J. Mol. Sci.* **2023**, *25*, 76. [CrossRef]
159. Drissennek, L.; Baron, C.; Brouillet, S.; Entezami, F.; Hamamah, S.; Haouzi, D. Endometrial miRNome profile according to the receptivity status and implantation failure. *Hum. Fertil.* **2022**, *25*, 356–368. [CrossRef] [PubMed]
160. Kresowik, J.D.; Devor, E.J.; Van Voorhis, B.J.; Leslie, K.K. MicroRNA-31 is significantly elevated in both human endometrium and serum during the window of implantation: A potential biomarker for optimum receptivity. *Biol. Reprod.* **2014**, *91*, 17. [CrossRef]
161. Chen, C.H.; Lu, F.; Yang, W.J.; Yang, P.E.; Chen, W.M.; Kang, S.T.; Huang, Y.S.; Kao, Y.C.; Feng, C.T.; Chang, P.C.; et al. A novel platform for discovery of differentially expressed microRNAs in patients with repeated implantation failure. *Fertil. Steril.* **2021**, *116*, 181–188. [CrossRef]
162. Cho, S.H.; Kim, Y.M.; An, H.J.; Kim, J.H.; Kim, N.K. miR-665-Mediated Regulation of AHCYL2 and BVES Genes in Recurrent Implantation Failure. *Genes* **2024**, *15*, 244. [CrossRef] [PubMed]
163. Liu, C.; Wang, M.; Zhang, H.; Sui, C. Altered microRNA Profiles of Extracellular Vesicles Secreted by Endometrial Cells from Women with Recurrent Implantation Failure. *Reprod. Sci.* **2021**, *28*, 1945–1955. [CrossRef] [PubMed]
164. Devesa-Peiro, A.; Sebastian-Leon, P.; Garcia-Garcia, F.; Arnau, V.; Aleman, A.; Pellicer, A.; Diaz-Gimeno, P. Uterine disorders affecting female fertility: What are the molecular functions altered in endometrium? *Fertil. Steril.* **2020**, *113*, 1261–1274. [CrossRef] [PubMed]
165. Antonio, L.G.L.; Meola, J.; Rosa, E.S.A.; Nogueira, A.A.; Candido Dos Reis, F.J.; Poli-Neto, O.B.; Rosa-E-Silva, J.C. Altered Differential Expression of Genes and microRNAs Related to Adhesion and Apoptosis Pathways in Patients with Different Phenotypes of Endometriosis. *Int. J. Mol. Sci.* **2023**, *24*, 4434. [CrossRef]
166. Braicu, O.L.; Budisan, L.; Buiga, R.; Jurj, A.; Achimas-Cadariu, P.; Pop, L.A.; Braicu, C.; Irimie, A.; Berindan-Neagoe, I. miRNA expression profiling in formalin-fixed paraffin-embedded endometriosis and ovarian cancer samples. *OncoTargets Ther.* **2017**, *10*, 4225–4238. [CrossRef]
167. Bashti, O.; Noruzinia, M.; Garshasbi, M.; Abtahi, M. miR-31 and miR-145 as Potential Non-Invasive Regulatory Biomarkers in Patients with Endometriosis. *Cell J.* **2018**, *20*, 84–89. [CrossRef]
168. Maged, A.M.; Deeb, W.S.; El Amir, A.; Zaki, S.S.; El Sawah, H.; Al Mohamady, M.; Metwally, A.A.; Katta, M.A. Diagnostic accuracy of serum miR-122 and miR-199a in women with endometriosis. *Int. J. Gynaecol. Obstet.* **2018**, *141*, 14–19. [CrossRef]
169. Moustafa, S.; Burn, M.; Mamillapalli, R.; Nematian, S.; Flores, V.; Taylor, H.S. Accurate diagnosis of endometriosis using serum microRNAs. *Am. J. Obstet. Gynecol.* **2020**, *223*, 557 e1–557 e11. [CrossRef]

170. Chico-Sordo, L.; Ruiz-Martínez, T.; Toribio, M.; González-Martín, R.; Spagnolo, E.; Domínguez, F.; Hernández, A.; García-Velasco, J.A. Identification of miR-30c-5p microRNA in Serum as a Candidate Biomarker to Diagnose Endometriosis. *Int. J. Mol. Sci.* **2024**, *25*, 1853. [CrossRef]
171. Hu, H.; Li, H.; He, Y. MicroRNA-17 downregulates expression of the PTEN gene to promote the occurrence and development of adenomyosis. *Exp. Ther. Med.* **2017**, *14*, 3805–3811. [CrossRef]
172. Borisov, E.; Knyazeva, M.; Novak, V.; Zabegina, L.; Prisyazhnaya, T.; Karizkiy, A.; Berlev, I.; Malek, A. Analysis of Reciprocally Dysregulated miRNAs in Eutopic Endometrium Is a Promising Approach for Low Invasive Diagnostics of Adenomyosis. *Diagnostics* **2020**, *10*, 782. [CrossRef] [PubMed]
173. Zhang, Z.; Qin, Y.; Huang, J.; Wang, Y.; Zeng, L.; Wang, Y.; Zhuyun, F.; Wang, L. Oestrogen promotes the progression of adenomyosis by inhibiting CITED2 through miR-145. *Reprod. BioMedicine Online* **2024**, *49*, 104108. [CrossRef] [PubMed]
174. Meng, X.; Liu, J.; Wang, H.; Chen, P.; Wang, D. MicroRNA-126-5p downregulates BCAR3 expression to promote cell migration and invasion in endometriosis. *Mol. Cell. Endocrinol.* **2019**, *494*, 110486. [CrossRef] [PubMed]
175. Braza-Boïls, A.; Marí-Alexandre, J.; Gilabert, J.; Sánchez-Izquierdo, D.; España, F.; Estellés, A.; Gilabert-Estellés, J. MicroRNA expression profile in endometriosis: Its relation to angiogenesis and fibrinolytic factors. *Hum. Reprod.* **2014**, *29*, 978–988. [CrossRef]
176. Papari, E.; Noruzinia, M.; Kashani, L.; Foster, W.G. Identification of candidate microRNA markers of endometriosis with the use of next-generation sequencing and quantitative real-time polymerase chain reaction. *Fertil. Steril.* **2020**, *113*, 1232–1241. [CrossRef]
177. Cho, S.; Mutlu, L.; Grechukhina, O.; Taylor, H.S. Circulating microRNAs as potential biomarkers for endometriosis. *Fertil. Steril.* **2015**, *103*, 1252–1260. [CrossRef]
178. Jia, S.Z.; Yang, Y.; Lang, J.; Sun, P.; Leng, J. Plasma miR-17-5p, miR-20a and miR-22 are down-regulated in women with endometriosis. *Hum. Reprod.* **2013**, *28*, 322–330. [CrossRef] [PubMed]
179. Huang, J.-H.; Duan, H.; Wang, S.; Wang, Y.-Y.; Lv, C.-X. Upregulated microRNA let-7a accelerates apoptosis and inhibits proliferation in uterine junctional zone smooth muscle cells in adenomyosis under conditions of a normal activated hippo-YAP1 axis. *Reprod. Biol. Endocrinol.* **2021**, *19*, 81. [CrossRef]
180. Zhang, A.; Liu, X.; Wang, J.; Deng, K.; Wang, J. MiR-30c-5p Directly Targets MAPK1 to Regulate the Proliferation, Migration and Invasion of Adenomyotic Epithelial Cells in Adenomyosis. *Twin Res. Hum. Genet.* **2021**, *24*, 22–28. [CrossRef]
181. Wang, Y.; Chen, L. miR-183 inhibits the viability, migration and invasion of epithelium on adenomyosis via targeting MMP-9. *J. Gynecol. Obstet. Hum. Reprod.* **2022**, *51*, 102349. [CrossRef]
182. Saunders, P.T.K.; Horne, A.W. Endometriosis: Etiology, pathobiology, and therapeutic prospects. *Cell* **2021**, *184*, 2807–2824. [CrossRef] [PubMed]
183. Lamceva, J.; Uljanovs, R.; Strumfa, I. The Main Theories on the Pathogenesis of Endometriosis. *Int. J. Mol. Sci.* **2023**, *24*, 4254. [CrossRef] [PubMed]
184. Shan, J.; Li, D.J.; Wang, X.Q. Towards a Better Understanding of Endometriosis-Related Infertility: A Review on How Endometriosis Affects Endometrial Receptivity. *Biomolecules* **2023**, *13*, 430. [CrossRef]
185. Burney, R.O.; Giudice, L.C. Pathogenesis and pathophysiology of endometriosis. *Fertil. Steril.* **2012**, *98*, 511–519. [CrossRef]
186. Brosens, I. Diagnosis of endometriosis. *Semin. Reprod Endocrinol* **1997**, *15*, 229–233. [CrossRef] [PubMed]
187. Nothnick, W.B. MicroRNAs and Endometriosis: Distinguishing Drivers from Passengers in Disease Pathogenesis. *Semin. Reprod. Med.* **2017**, *35*, 173–180. [CrossRef]
188. Dabi, Y.; Suisse, S.; Puchar, A.; Delbos, L.; Poilblanc, M.; Descamps, P.; Haury, J.; Golfier, F.; Jornea, L.; Bouteiller, D.; et al. Endometriosis-associated infertility diagnosis based on saliva microRNA signatures. *Reprod. Biomed. Online* **2023**, *46*, 138–149. [CrossRef]
189. Ohlsson Teague, E.M.; Van der Hoek, K.H.; Van der Hoek, M.B.; Perry, N.; Wagaarachchi, P.; Robertson, S.A.; Print, C.G.; Hull, L.M. MicroRNA-regulated pathways associated with endometriosis. *Mol. Endocrinol.* **2009**, *23*, 265–275. [CrossRef]
190. Zhang, Z.; Li, H.; Zhao, Z.; Gao, B.; Meng, L.; Feng, X. miR-146b level and variants is associated with endometriosis related macrophages phenotype and plays a pivotal role in the endometriotic pain symptom. *Taiwan. J. Obstet. Gynecol.* **2019**, *58*, 401–408. [CrossRef]
191. Braza-Boils, A.; Salloum-Asfar, S.; Mari-Alexandre, J.; Arroyo, A.B.; Gonzalez-Conejero, R.; Barcelo-Molina, M.; Garcia-Oms, J.; Vicente, V.; Estelles, A.; Gilabert-Estellés, J.; et al. Peritoneal fluid modifies the microRNA expression profile in endometrial and endometriotic cells from women with endometriosis. *Hum. Reprod.* **2015**, *30*, 2292–2302. [CrossRef]
192. Pollacco, J.; Sacco, K.; Portelli, M.; Schembri-Wismayer, P.; Calleja-Agius, J. Molecular links between endometriosis and cancer. *Gynecol. Endocrinol.* **2012**, *28*, 577–581. [CrossRef] [PubMed]
193. Benagiano, G.; Brosens, I.; Habiba, M. Structural and molecular features of the endomyometrium in endometriosis and adenomyosis. *Hum. Reprod. Updat.* **2014**, *20*, 386–402. [CrossRef] [PubMed]
194. Guo, S.-W. The pathogenesis of adenomyosis vis-à-vis endometriosis. *J. Clin. Med.* **2020**, *9*, 485. [CrossRef]
195. García-Solares, J.; Donnez, J.; Donnez, O.; Dolmans, M.-M. Pathogenesis of uterine adenomyosis: Invagination or metaplasia? *Fertil. Steril.* **2018**, *109*, 371–379. [CrossRef]
196. Donnez, J.; Stratopoulou, C.A.; Dolmans, M.-M. Uterine adenomyosis: From disease pathogenesis to a new medical approach using GnRH antagonists. *Int. J. Environ. Res. Public Health* **2021**, *18*, 9941. [CrossRef]
197. Tellum, T.; Nygaard, S.; Lieng, M. Noninvasive diagnosis of adenomyosis: A structured review and meta-analysis of diagnostic accuracy in imaging. *J. Minim. Invasive Gynecol.* **2020**, *27*, 408–418. [CrossRef]

198. Bazot, M.; Cortez, A.; Darai, E.; Rouger, J.; Chopier, J.; Antoine, J.-M.; Uzan, S. Ultrasonography compared with magnetic resonance imaging for the diagnosis of adenomyosis: Correlation with histopathology. *Hum. Reprod.* **2001**, *16*, 2427–2433. [CrossRef]
199. Yuan, L.-Q.; Zhang, T.; Xu, L.; Han, H.; Liu, S.-H. miR-30c-5p inhibits glioma proliferation and invasion via targeting Bcl2. *Transl. Cancer Res.* **2021**, *10*, 337. [CrossRef]
200. Chen, W.-C.; Chang, T.-C.; Perera, L.; Cheng, M.-H.; Hong, J.-J.; Cheng, C.-M. Pilot study on the impact of HIFU treatment on miRNA profiles in vaginal secretions of uterine fibroids and adenomyosis patients. *Int. J. Hyperth.* **2024**, *41*, 2418426. [CrossRef]
201. Juárez-Barber, E.; Segura-Benítez, M.; Carbajo-García, M.C.; Bas-Rivas, A.; Faus, A.; Vidal, C.; Giles, J.; Labarta, E.; Pellicer, A.; Cervelló, I.; et al. Extracellular vesicles secreted by adenomyosis endometrial organoids contain miRNAs involved in embryo implantation and pregnancy. *Reprod. BioMedicine Online* **2023**, *46*, 470–481. [CrossRef]
202. Li, H.; Han, Y.; Cai, Y.; Su, X.; Tan, L. Clinical effects of laparoscopic surgery for the treatment of endometriosis and endometriosis-fertility: A retrospective study of 226 cases. *Front. Surg.* **2022**, *9*, 1049119. [CrossRef]
203. Tomassetti, C.; Geysenbergh, B.; Meuleman, C.; Timmerman, D.; Fieuws, S.; D'Hooghe, T. External validation of the endometriosis fertility index (EFI) staging system for predicting non-ART pregnancy after endometriosis surgery. *Hum. Reprod.* **2013**, *28*, 1280–1288. [CrossRef]
204. Achache, H.; Revel, A. Endometrial receptivity markers, the journey to successful embryo implantation. *Hum. Reprod. Update* **2006**, *12*, 731–746. [CrossRef]
205. Cakmak, H.; Taylor, H.S. Implantation failure: Molecular mechanisms and clinical treatment. *Hum. Reprod. Update* **2011**, *17*, 242–253. [CrossRef]
206. Kim, S.M.; Kim, J.S. A Review of Mechanisms of Implantation. *Dev. Reprod.* **2017**, *21*, 351–359. [CrossRef]
207. Craciunas, L.; Gallos, I.; Chu, J.; Bourne, T.; Quenby, S.; Brosens, J.J.; Coomarasamy, A. Conventional and modern markers of endometrial receptivity: A systematic review and meta-analysis. *Hum. Reprod. Update* **2019**, *25*, 202–223. [CrossRef]
208. Di Pietro, C.; Caruso, S.; Battaglia, R.; Iraci Sareri, M.; La Ferlita, A.; Strino, F.; Bonaventura, G.; Di Mauro, M.; Barcellona, M.L.; Perciavalle, V.; et al. MiR-27a-3p and miR-124-3p, upregulated in endometrium and serum from women affected by Chronic Endometritis, are new potential molecular markers of endometrial receptivity. *Am. J. Reprod. Immunol.* **2018**, *80*, e12858. [CrossRef]
209. Zhou, W.; Van Sinderen, M.; Rainczuk, K.; Menkhorst, E.; Sorby, K.; Osianlis, T.; Pangestu, M.; Santos, L.; Rombauts, L.; Rosello-Diez, A.; et al. Dysregulated miR-124-3p in endometrial epithelial cells reduces endometrial receptivity by altering polarity and adhesion. *Proc. Natl. Acad. Sci. USA* **2024**, *121*, e2401071121. [CrossRef]
210. Nikolova, M.; Naydenov, M.; Glogovitis, I.; Apostolov, A.; Saare, M.; Boggavarapu, N.; Salumets, A.; Baev, V.; Yahubyan, G. Coupling miR/isomiR and mRNA expression signatures unveils new molecular layers of endometrial receptivity. *Life* **2021**, *11*, 1391. [CrossRef]
211. Nikolova, M.; Naydenov, M.; Apostolov, A.; Glogovitis, I.; Saare, M.; Salumets, A.; Baev, V.; Yahubyan, G. Time-course analysis of endometrial miR/isomiR expression dynamics during hCG-primed menstrual-cycle phase transitions. In *Human Reproduction*; Oxford University Press: Oxford, UK, 2021; pp. 267–268.
212. Cao, Z.; Xu, B.; Wu, Y.; Luan, K.; Du, X. A comprehensive analysis of miRNA/isomiRs profile of hydrosalpinx patients with interventional ultrasound sclerotherapy. *PLoS ONE* **2022**, *17*, e0268328. [CrossRef]
213. Goharitaban, S.; Abedelahi, A.; Hamdi, K.; Khazaei, M.; Esmaeilivand, M.; Niknafs, B. Role of endometrial microRNAs in repeated implantation failure (mini-review). *Front. Cell Dev. Biol.* **2022**, *10*, 936173. [CrossRef]
214. Zeng, H.; Fu, Y.; Shen, L.; Quan, S. MicroRNA signatures in plasma and plasma exosome during window of implantation for implantation failure following in-vitro fertilization and embryo transfer. *Reprod. Biol. Endocrinol.* **2021**, *19*, 180. [CrossRef]
215. Khan, A.A.; Betel, D.; Miller, M.L.; Sander, C.; Leslie, C.S.; Marks, D.S. Transfection of small RNAs globally perturbs gene regulation by endogenous microRNAs. *Nat. Biotechnol.* **2009**, *27*, 549–555. [CrossRef]
216. Manikkath, J.; Jishnu, P.V.; Wich, P.R.; Manikkath, A.; Radhakrishnan, R. Nanoparticulate strategies for the delivery of miRNA mimics and inhibitors in anticancer therapy and its potential utility in oral submucous fibrosis. *Nanomedicine* **2022**, *17*, 181–195. [CrossRef]
217. Polonio, A.M.; Chico-Sordo, L.; Córdova-Oriz, I.; Medrano, M.; García-Velasco, J.A.; Varela, E. Focus: Sex & reproduction: Impact of ovarian aging in reproduction: From telomeres and mice models to ovarian rejuvenation. *Yale J. Biol. Med.* **2020**, *93*, 561.
218. de Vet, A.; Laven, J.S.; de Jong, F.H.; Themmen, A.P.; Fauser, B.C. Antimüllerian hormone serum levels: A putative marker for ovarian aging. *Fertil. Steril.* **2002**, *77*, 357–362. [CrossRef]
219. Broekmans, F.J.; Faddy, M.J.; Scheffer, G.; Velde, E.R.T. Antral follicle counts are related to age at natural fertility loss and age at menopause. *Menopause* **2004**, *11*, 607–614. [CrossRef]
220. Hansen, K.R.; Morris, J.L.; Thyer, A.C.; Soules, M.R. Reproductive aging and variability in the ovarian antral follicle count: Application in the clinical setting. *Fertil. Steril.* **2003**, *80*, 577–583. [CrossRef]
221. Speroff, L.; Vande Wiele, R.L. Regulation of the human menstrual cycle. *Am. J. Obstet. Gynecol.* **1971**, *109*, 234–247. [CrossRef]
222. Git, A.; Dvinge, H.; Salmon-Divon, M.; Osborne, M.; Kutter, C.; Hadfield, J.; Bertone, P.; Caldas, C. Systematic comparison of microarray profiling, real-time PCR, and next-generation sequencing technologies for measuring differential microRNA expression. *RNA* **2010**, *16*, 991–1006. [CrossRef]

223. Bustin, S.A.; Benes, V.; Garson, J.A.; Hellemans, J.; Huggett, J.; Kubista, M.; Mueller, R.; Nolan, T.; Pfaffl, M.W.; Shipley, G.L. *The MIQE Guidelines: M inimum I nformation for Publication of Q uantitative Real-Time PCR E xperiments*; Oxford University Press: Oxford, UK, 2009.
224. Seyednasrollah, F.; Laiho, A.; Elo, L.L. Comparison of software packages for detecting differential expression in RNA-seq studies. *Brief. Bioinform.* **2015**, *16*, 59–70. [CrossRef] [PubMed]
225. Qi, R.; Weiland, M.; Gao, X.H.; Zhou, L.; Mi, Q.-S. Identification of endogenous normalizers for serum microRNAs by microarray profiling: U6 small nuclear RNA is not a reliable normalizer. *Hepatology* **2012**, *55*, 1640–1642. [CrossRef] [PubMed]
226. Andersen, C.L.; Jensen, J.L.; Ørntoft, T.F. Normalization of real-time quantitative reverse transcription-PCR data: A model-based variance estimation approach to identify genes suited for normalization, applied to bladder and colon cancer data sets. *Cancer Res.* **2004**, *64*, 5245–5250. [CrossRef] [PubMed]
227. Blondal, T.; Nielsen, S.J.; Baker, A.; Andreasen, D.; Mouritzen, P.; Teilum, M.W.; Dahlsveen, I.K. Assessing sample and miRNA profile quality in serum and plasma or other biofluids. *Methods* **2013**, *59*, S1–S6. [CrossRef] [PubMed]
228. Shah, J.S.; Soon, P.S.; Marsh, D.J. Comparison of methodologies to detect low levels of hemolysis in serum for accurate assessment of serum microRNAs. *PLoS ONE* **2016**, *11*, e0153200. [CrossRef]
229. Mitra, R.; Lin, C.C.; Eischen, C.M.; Bandyopadhyay, S.; Zhao, Z. Concordant dysregulation of miR-5p and miR-3p arms of the same precursor microRNA may be a mechanism in inducing cell proliferation and tumorigenesis: A lung cancer study. *RNA* **2015**, *21*, 1055–1065. [CrossRef]

Disclaimer/Publisher's Note: The statements, opinions and data contained in all publications are solely those of the individual author(s) and contributor(s) and not of MDPI and/or the editor(s). MDPI and/or the editor(s) disclaim responsibility for any injury to people or property resulting from any ideas, methods, instructions or products referred to in the content.